

**The impacts of environmental
change on late Quaternary fossil
fauna at Cathedral Cave, eastern
Australia.**

By

Diana A. Fusco

Thesis

Submitted to Flinders University

for the degree of

Doctor of Philosophy

College of Science and Engineering

June 2021

Acknowledgement of Country

I would like to acknowledge that the research presented in this thesis was undertaken on the traditional lands of the Wiradjuri and Kaurna Nations. The Wiradjuri are the Traditional Custodians of the land on which the Wellington Caves are located. The Kaurna people are the Traditional Custodians of the land on which Flinders University has been built. Sovereignty has never been ceded, it always was and always will be, Aboriginal land. I pay respect to the Elders both past, present, and future.

To my children, Arin, Devin, and Ethan.

I did this for you.

Contents

List of figures	1
List of tables	3
Thesis summary	5
Declaration	7
Papers and manuscripts published during candidature	7
Acknowledgements	8
Introduction to the thesis	11
Preface	11
Context of the thesis and research progression.....	12
Thesis style	14
Statement of Authorship.....	14
1 Literature review	1
1.1 Understanding the past to conserve the future: The potential of palaeoecology and cave deposits.....	1
1.2 Environmental change during the late Quaternary	5
1.2.1 The global Quaternary climate	5
1.2.2 Understudied and underestimated: The palaeoclimate of MIS 4	7
1.2.3 The variable palaeoclimate of MIS 3.....	9
1.2.4 The glacial palaeoclimate of MIS 2.....	9
1.2.5 Climate amelioration during MIS 1	11
1.2.6 Anthropogenic Driven Environmental Change	11
1.3 The palaeontology of Wellington Caves, with a focus on Cathedral Cave.....	14
1.3.1 1829–1900	15
1.3.2 1901–1980	17
1.3.3 1981–present.....	18
1.4 Aims	20
2 Chapter 2: Study site and methods	21
2.1 Site Description	21
2.1.1 Physiographical setting	21
2.1.2 Geological setting	21
2.1.3 Description and genesis of Cathedral Cave.....	25
2.2 Excavation	29
2.2.1 Site selection.....	29
2.2.2 Site preparation.....	29

2.2.3	Excavation and sediment processing	31
2.3	Collection curation.....	35
2.4	Quantitative analysis.....	35
3	Chapter 3: Characterising the depositional environment of the late Quaternary fossiliferous infills of Cathedral Cave through sedimentary and taphonomic analyses.	37
3.1	Abstract	37
3.2	Introduction: caves as windows to the past.....	38
3.2.1	Characterising sediment infills.....	39
3.2.2	Taphonomy and bias in the fossil record	41
3.2.3	Taphonomy of Cathedral Cave.....	43
3.2.4	The complex stratigraphy of the Wellington Caves deposits.....	44
3.2.5	The confusing chronology of the Wellington Caves	46
3.3	Aims of this chapter	49
3.4	Methods and Materials.....	50
3.4.1	Stratigraphy	50
3.4.2	Sediment characterisation and petrography	50
3.4.3	Chronology.....	54
3.4.4	Radiocarbon dating.....	54
3.4.5	Optically Stimulated Luminescence Dating.....	55
3.4.6	Bayesian Depth Model.....	57
3.4.7	Taphonomy.....	58
3.4.8	Curation.....	58
3.5	Results	59
3.5.1	Stratigraphy	59
3.5.2	Description of stratigraphic layers.....	63
3.5.3	Grain size analysis	71
3.5.4	Geochemistry.....	74
3.5.5	Radiocarbon dating.....	77
3.5.6	Optically Stimulated Luminescence	78
3.5.7	Bayesian age-depth modelling.....	84
3.5.8	Assembling the chronology.....	85
3.5.9	Taphonomy.....	88
3.6	Discussion.....	92
3.6.1	Stratigraphic units.....	92
3.6.2	Entry point and source of the Cathedral Cave sediment infill	93

3.6.3	Geochemistry.....	95
3.6.4	Origin of indurated sediments	96
3.6.5	A new chronology for Cathedral Cave	97
3.6.6	Integrity of the stratigraphic sequence.....	99
3.6.7	The challenges of ¹⁴ C dating at Cathedral Cave.....	101
3.6.8	Taphonomic signal.....	103
3.6.9	Accumulation agents.....	104
3.6.10	A story of deposition.....	105
3.7	Conclusion.....	106
4	Chapter 4: Systematic palaeontology of Cathedral Cave, Wellington Caves.....	108
4.1	Abstract.....	108
4.2	Introduction	108
4.3	Aims of this chapter.....	109
4.4	Methods.....	111
4.4.1	Curation.....	111
4.4.2	Identifications	111
4.4.3	Nomenclature.....	112
4.4.4	Format of the systematics section.....	113
4.4.5	Equipment	114
4.4.6	Abbreviations.....	114
4.5	Results	115
4.5.1	Identifications and assemblage composition.....	115
4.5.2	Systematics.....	116
4.6	Discussion: Australia’s richest Pleistocene mammal assemblage.....	161
4.7	Conclusion.....	162
5	Chapter 5: Tracking mammalian faunal change through the late Quaternary of central-eastern Australia	163
5.1	Abstract	163
5.2	Introduction—using the past to predict the future.....	164
5.2.1	Ecosystem response to disturbance.....	164
5.2.2	Ecological resilience	165
5.2.3	Australian vertebrate palaeoecology.....	167
5.2.4	Mammal extinctions and Australia’s late Quaternary fossil record	167
5.2.5	Vertebrate responses to changing environments in the Australian Pleistocene fossil record	173
5.3	Aims.....	176

5.4	Methods and materials	177
5.4.1	Quantitative units.....	177
5.4.2	K-means clustering	177
5.4.3	Rarefaction, richness, diversity, and abundance.....	177
5.4.4	Taphonomy.....	179
5.4.5	Taxonomic Habitat Index.....	179
5.4.6	Mammal trajectories	180
5.4.7	Megafauna chronology.....	181
5.5	Results	182
5.5.1	Relative abundance	182
5.5.2	Layer partitioning	184
5.5.3	Rarefaction, richness, diversity and abundance.....	184
5.5.4	Taphonomy.....	187
5.5.5	Taxonomic Habitat Index.....	187
5.5.6	Mammal Trajectories	188
5.6	Discussion.....	198
5.6.1	Accumulation agency.....	198
5.6.2	Faunal responses to environmental change.....	198
5.6.2.2	<i>MIS 4–MIS 3 transition</i>	204
5.6.3	Megafaunal extinction implications.....	209
5.7	Conclusion.....	213
6	Chapter 6: General discussion and overview.....	215
6.1	Introduction and aims.....	215
6.2	The chronology and sedimentology of Cathedral Cave.....	215
6.3	The fossil fauna of Cathedral Cave.....	216
6.4	Tracking mammalian faunal change.....	218
6.4.1	Megafaunal trends.....	219
6.5	Conservation implications.....	220
6.5.1	Small mammal resilience to environmental change	221
6.5.2	Pre-European Mammalian baseline	221
6.5.3	Implications for a vulnerable native rodent.....	222
6.6	Future directions	223
6.6.1	Extending the record.....	223
6.6.2	Future approaches	224
6.6.3	Unresolved and cryptic taxa.....	225

6.6.4	The non-mammalian fossil fauna	225
6.7	Revisiting Australia’s palaeoecological record	226
6.8	Conclusions	227
7	Appendices	228
7.1	Appendix A: Supplementary to Chapter 2	228
7.1.1	Origin of the disturbed sediments.....	228
7.1.2	Engineering schematics.....	228
7.2	Appendix B: Supplementary to Chapter 3	233
7.2.1	Rbacon settings for Bayesian age-depth model.....	238
7.2.2	Bayesian age depth models	239
7.2.3	Sedimentology data.....	244
7.3	Appendix C: Supplementary to Chapter 4	245
7.4	Appendix D: Supplementary to Chapter 5	247
8	References	275

List of figures

Figure 1.1. Temperature curve for the last 130 ka, showing temperature change.....	6
Figure 1.2. Selected proxies from marine core MD03-2607 over the 55 – 75 ka	8
Figure 1.3. Survey of Cathedral Cave showing the location of Shaft 1 and Shaft 2	16
Figure 1.4. Palate and dentition of <i>Palorchestes azael</i> (F.120488) unearthed in.....	17
Figure 1.5. The UNSW excavation circa 1982.....	19
Figure 2.1. Location of Wellington Caves in relation to Australia’s climate zones.....	23
Figure 2.2. The main cave area at Wellington Caves.	25
Figure 2.3. Location of Wellington Caves in relation to the Bell and Macquarie Rivers.....	26
Figure 2.4. Map of the Main and Well chambers of Cathedral Cave	27
Figure 2.5. A sketch by Thomas L. Mitchell showing the floor of Cathedral Cave.....	28
Figure 2.6. Variable groundwater levels in Cathedral Cave	29
Figure 2.7. Top-down views of a) initial quadrature configuration in dark grey	31
Figure 2.8. Photographs from Cathedral Cave excavation.....	33
Figure 2.9. Excavation equipment a) gantry system set up over the excavation.....	34
Figure 2.10. Sediment processing a) poorly disassociated sediments	35
Figure 3.1. Depiction of relationships of recognised stratigraphic units	46
Figure 3.2. Radiocarbon ages and stratigraphy of UNSW excavation	49
Figure 3.3. Powers grain roundness scale following Powers (1953).....	53
Figure 3.4. Stylised curves showing mesokurtic, leptokurtic and platykurtic distributions ...	54
Figure 3.5. Stratigraphic section of Cathedral Cave	62
Figure 3.6. East wall of excavation showing a) boundaries between the <i>in situ</i> sediment	63
Figure 3.7. North wall of the excavation showing a) layers 1 – 7 and 9) top of layer 9.....	67
Figure 3.8. Images from petrographic slides of Cathedral Cave sediments.....	68
Figure 3.9. Cracks visible in the top of layer 11. North wall is top of page.	70
Figure 3.10. Sediment morphology a) cross section of lithified sediments of layer 11.....	71
Figure 3.11. Ternary diagram for Cathedral Cave samples	73
Figure 3.12. a) Relationships between the three oxide groups present.....	76
Figure 3.13. Single-grain OSL D_e distributions for the Cathedral Cave samples	83
Figure 3.14. Bayesian age-depth model (Model2) for 425 cm of the Cathedral Cave	86
Figure 3.15. Stratigraphic diagram of the west, north and east wall of Cathedral Cave.....	88
Figure 3.16. Articulated and associated faunal remains a) Elapidae gen. et sp. indet.	90
Figure 3.17. Taphonomic bone modifications a) <i>Thylacoleo carnifex</i> left and right	91

Figure 3.18. The main chamber of Cathedral Cave showing the Altar formation	95
Figure 3.19. Right dentary of sub-adult <i>Palorchestes azael</i>	105
Figure 4.1. Associated remains of <i>Megalibgwilia ramsayi</i> a) proximal R femur	118
Figure 4.2. Dasyuromorphs a) <i>Dasyurus</i> sp. indet., cranium (CCW3034)	122
Figure 4.3. Dasyuromorphs a) <i>Dasyuroides byrnei</i> , maxillae with M1–3 (CCW2212).....	125
Figure 4.4. Peramelemorphs a) <i>Chaeropus ecaudatus</i> , R M2 (CCW3384).....	128
Figure 4.5. Remains of a) <i>Thylacoleo carnifex</i> , P2 (CCW2983).....	134
Figure 4.6. Macropodiformes a) <i>Potorous tridactylus</i> , juvenile R dentary (CCW3662)	141
Figure 4.7. Macropodids a) <i>Macropus giganteus</i> , R dentary (CCW2941)	146
Figure 4.8. Murids. <i>Notomys</i> sp. indet. a) R maxilla (CCW3377), b) lateral view	154
Figure 4.9. <i>Rattus</i> sp. cf. <i>R. tunneyi</i> a) L maxilla (CCW144), R dentary	156
Figure 4.10. Unresolved murids. a) Muridae sp. 1, R maxilla (CCW1258)	159
Figure 5.1. A selection of Australian Pleistocene fossil sites.....	169
Figure 5.2. Chronological chart showing the temporal span of fossil localities	175
Figure 5.3. Rarefaction curves generated for individual spits by layers (a–f).....	186
Figure 5.4. Biodiversity curves for mammal taxa including a) Richness (S).....	187
Figure 5.5. Bodyweight of taxa recovered from each stratigraphic partition.....	188
Figure 5.6. Taxonomic Habitat Index showing taxa associated with arid, semi-arid.....	189
Figure 5.7. Relative abundance trends and trajectories for mammalian taxonomic.....	193
Figure 5.8. Relative abundance trends and trajectories for mammalian taxonomic.....	197
Figure 5.9. Presence and absence of extinct megafaunal species showing Ra%.	198
Figure 5.10. Relative abundances of mammal guilds, in which taxonomic units	200
Figure 5.11. Megafauna of Cathedral Cave and other non-mammalian taxa of interest	212
Figure 7.1. Bayesian age-depth model (Model1) for 425 cm.....	240
Figure 7.2. Bayesian age-depth model (Model3) for 425 cm.....	240

List of tables

Table 3.1. Chemical composition of soils and bedrock surrounding Cathedral Cave.....	41
Table 3.2. Assigned ages for other fossil bearing sites in the Wellington Caves.....	48
Table 3.3. Geometric (modified) Folk and Ward (1957) graphical measures.....	53
Table 3.4. Grainsize analysis and sediment statistics for Cathedral Cave sediment	74
Table 3.5. X-ray fluorescence analysis of major oxide composition (%wt).	77
Table 3.6. Radiocarbon data for charcoal samples from Cathedral Cave samples.....	79
Table 3.7. Summary of environmental dose rates, D_e values and final ages.....	82
Table 3.8. Bone yield, NISP, MNI and notes for each stratigraphic layer.....	92
Table 3.9. Associated and articulated elements from Cathedral Cave.....	92
Table 4.1. List of Cathedral Cave fauna compiled from Dawson and Augee (1997).....	111
Table 4.2. Molar dimensions for <i>Sarcophilus lanianus</i> maxilla (CCW2496).....	120
Table 4.3. Cranial and dental measurements in mm for <i>Vombatus</i> fossils	130
Table 4.4. Measurements of M1 (mm) of several <i>Notomys</i> species.	148
Table 5.1. Australian Megafaunal taxa with post 65 ka dates (youngest given).....	170
Table 5.2. Relative abundance of taxonomic units in the Cathedral Cave assemblage.....	183
Table 5.3. Modern and prehistoric vegetation groups for the Binjang region	204
Table 7.1. Radiocarbon dates obtained from charcoal from sediments excavated.....	234
Table 7.2. Pearson's correlation coefficient (r) for XRF analysis	235
Table 7.3. XRD analysis of %wt of crystalline structures in the Cathedral Cave.....	236
Table 7.4. XRF analysis of the elemental composition of the Cathedral Cave.....	237
Table 7.5. Eigenvalues for Principal Components Analysis in Figure 3.12b.....	238
Table 7.6. Bone samples from the 1982-86 UNSW excavation submitted for AMS.....	238
Table 7.7. Charcoal samples from the FU excavation submitted for AMS radiocarbon.....	238
Table 7.8. Charcoal samples submitted for AMS radiocarbon dating at ANSTO.....	239
Table 7.9. Bayesian age-depth modelled ages. Showing depth by cm, minimum age.....	241
Table 7.10. Reassignment of sedimentary layers that were detailed in field notebooks.....	245
Table 7.11 Sediment samples used for grain size.	245
Table 7.12. Comparative specimens.	246
Table 7.13. Fossil fauna of Cathedral Cave by spit and layer, quantified using MNI.....	248
Table 7.14 Spit concatenation.....	263
Table 7.15, Partitioning logic for layers 10, 13 and 14 showing 5, 4, 3 and 2 clusters.....	266
Table 7.16. Ecological table for the Cathedral Cave fauna.....	267

Table 7.17. Weighted habitat scores for Taxonomic Habitat Index	271
Table 7.18 Cumulative habitat score and Taxonomic Habitat Index.....	274
Table 7.19. Data used for biodiversity curves showing species richness (<i>S</i>).....	275

Thesis summary

The late Pleistocene in Australia was marked by the loss of >90% of large terrestrial vertebrate species and the formation of modern faunal assemblages. The relative roles that humans, who arrived on the continent c. 60,000 years ago, and climatic change played in shaping observed patterns have long been debated. Rich empirical datasets that allow for changes in the proportional representation of species to be tracked through time are critical for resolving the relative effects of these two drivers. These also hold great potential for informing on how modern ecosystems may respond in the future to changing climates and intensifying anthropogenic pressures. Such records, however, are rare. Here I investigate faunal responses to environmental change through the Cathedral Cave deposit in the Wellington Caves system of central-eastern Australia. This is the stratigraphically deepest late Pleistocene vertebrate sequence in Australia. This study is the first to track changes in faunal assemblages through the late Pleistocene in central-eastern Australia, and the highest resolution palaeoecological study of its type yet undertaken in Australia. Excavation of the deposit to a depth of 4.2 m revealed 13 sedimentary layers, the distinctiveness of which were supported by sedimentary and geochemical data. Radiocarbon dating of charcoal clasts and optically stimulated luminescence dating of sediments reveals that the cave was accumulating fossils and sediments between 65.8 and 43.2 thousand years (ka) ago, during the megafaunal extinction interval. A hypothesised roof entrance, now hidden by a large stalagmite, was open during this period, acted as a pitfall trap for larger species and an entry for roosting owls, which contributed most of the remains of smaller species. This was followed by a hiatus of 37 ka during which the roof entrance closed. Deposition reinitiated during the mid-Holocene, at 5.8 ka and continued at least until 0.81 ka when the roof entrance closed again. This chronology refutes earlier published ages that indicated the deposit had accumulated through the Last Glacial Maximum.

Fossils were identified by comparing them to known osteological material and published descriptions. At least 69 species of terrestrial mammals have now been identified from the deposit, 66 of which were collected during this study. Cathedral Cave thus contains the most diverse late Pleistocene mammal deposit in Australia. Species relative abundance, richness, diversity and evenness trajectories revealed a typically temperate faunal community with incursions of some xeric taxa during drier periods. The relative proportions of the temperate and xeric groups fluctuated subtly in response to drier, cooler conditions that were in effect in

the middle of MIS 4, 65 ka ago. This was accompanied by reduced richness, diversity and evenness values. During MIS 3, the community underwent greater restructuring, with faunal changes consistent with drying conditions 50.6–44.7 ka ago. This interval is not associated with any identified regional climatic changes but postdates the regional arrival of humans. Faunal turnover among the small-medium bodied mammals remained low during MIS 3, with most displaying changes in their relative abundances, rather than extirpation or extinction.

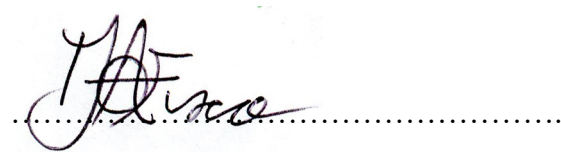
By contrast, most of the 11 extinct megafaunal mammal species vanished from the record by 50–45 ka ago with just two persisting until at least 43.2 ka ago. This timeline aligns better with human mediated extinction than with known climatic changes and small mammal responses. The timing and nature of observed patterns fits better with that reported from comparable southern Australian records rather than from fossil sites above or near the Tropic of Capricorn, the latter which lack the resolution available in the southern and Cathedral Cave records.

The incongruity of response trends shown by the large and smaller bodied species suggests that each was subject to different drivers, or, that they were affected unequally by the same drivers. These findings point to the complexity that is implicit in natural systems and highlights gaps in our understanding of community responses to environmental change. This study clarifies the temporal range of nine megafaunal taxa and demonstrates for them a probable overlap with humans. For four of these taxa, Cathedral Cave provides their first, and only, dated occurrence. These data exemplify the large gaps that remain in the Australian fossil record and highlights the inadequacy of current extinction chronologies from which extinction causes are being inferred.

Declaration

I certify that this thesis:

1. does not incorporate without acknowledgement any material previously submitted for a degree or diploma in any university; and
2. to the best of my knowledge and belief it does not contain any material previously published or written by another person except where due reference is made in the text.



Diana A. Fusco

Date. 29th April 2021

Papers and manuscripts published during candidature

Fusco, D. A., M. C. McDowell, G. Medlin, and G. J. Prideaux. 2017. Fossils reveal late Holocene diversity and post-European decline of the terrestrial mammals of the Murray–Darling Depression. *Wildlife Research* 44:60-71.

Fusco, D. A., M. C. McDowell, and G. J. Prideaux. 2016. Late Holocene mammal fauna from southern Australia reveals rapid species declines post-European settlement: implications for conservation biology *The Holocene* 26:699-708.

Grealy, A. C., M. C. McDowell, R. P. Scofield, D. C. Murray, D. A. Fusco, J. Haile, G. J. Prideaux, and M. Bunce. 2015. A critical evaluation of how ancient DNA bulk bone metabarcoding complements traditional morphological analysis of fossil assemblages. *Quaternary Science Reviews* 128:37-47.

Pearson, S., S. Tobe, D. Fusco, C. Bull, and M. Gardner. 2015. Piles of scats for piles of DNA: deriving DNA of lizards from their faeces. *Australian Journal of Zoology* 62:507-514.

Acknowledgements

A PhD is a journey, and I am indebted to all those who travelled with me.

First and foremost, I would like to thank my principal supervisor Professor Gavin Prideaux for his excellent guidance, trust, encouragement, and for creating the opportunity to work on such an incredible project. I also thank my associate supervisor Dr Trevor Worthy for his sage advice and mentorship. Both have contributed not only to this thesis, but also to my evolution as a scientist. This journey would have been much harder without having such a supportive and generous supervisory team.

I am grateful to all of my colleagues at Flinders Palaeontology, past and present, for their camaraderie, mentoring and practical assistance. There were times that I questioned whether I belonged, but my lab-mates always made me feel welcome and valued. I feel fortunate to have undertaken this PhD in such a collegial research group. I would especially like to thank Aaron Camens, who probably doesn't even realise how important his encouragement and friendship has been over the last few years. Aaron and Althea Walker-Hallam provided delicious, precooked meals when I was unable to fend for myself. Likewise, I want to thank my office-buddy Elen Shute for her friendship, pragmatic idealism, help with bird things, and company on long thesis-relief walks in Belair National Park. Kailah Thorn for her irrepressible enthusiasm, good times, and assistance with the reptiles. Carey Burke for technical support in the lab and during field work. My office-mates past and present, including Brian Choo, Alice Clement, Rachel Correll, and Warren Handley, the latter ended up easily beating me to the finish line. I extend my gratitude to colleagues Ben Arman, Sam Arman, Aidan Couzens, Grant Gully, Ellen Mather, Timothée Niederer, Lisa Nink, Cassy Petho, Elen Shute, Kailah Thorn, and Jacob van Zoelen who along with some of the others already mentioned above, enthusiastically participated in field work at Wellington. Lisa especially, who gave up months of her time to help on most of the Wellington trips.

I thank the volunteers, students, and staff who assisted with field work, wet-screening, fossil preparation, and sorting. There are too many to list here — I counted well over 100 individuals — but this project would not have been possible without their input. This includes Lauren Alexander, Uschi Artym, Sue Double, Riley Foley, Haydn Geraldine, Paige Greenhalgh, Roger Matthews, Sean Moore, Andy Phillips, Nathan Phillips, Craig Winston,

members of the fantastic Flinders University Palaeontology Society and Youth at the Zoo (Taronga Western Plains Zoo).

I would like to extend my gratitude to the staff at the Wellington Caves and the Dubbo Regional Council for their interest, assistance, and for making the space for us to undertake this project — especially Jodie Anderson, Michelle Tonkins and Ian Eddison. Ian, I apologise for the muddy boot prints. Mike Augee and Lyndall Dawson for their generosity and willingness to share Cathedral Cave with me. Thanks also to Michelle Baumann at the University of New South Wales who facilitated our use of the research station at Wellington.

This thesis has benefited from the advice and contribution of a number of people. My collaborators Lee Arnold, Geraldine Jacobson, Vladimir Levchenko and Gavin Prideaux. Michael Tyler had been looking at the frogs prior to his passing in March 2020 — he will be greatly missed. Alex Baynes helped me come to terms with the Wellington rodents. Michael Archer and Kenny Travouillon discussed dasyurids and peramelids with me. Andy Baker and Armstrong Osbourne generously shared their knowledge of geology, sedimentology, and geochemistry. Henri Garon worked on the initial OSL samples. Fiona Petchey at the Waikato Radiocarbon Dating Laboratory provided radiocarbon dating services. Keith Cook gave us an amazing 3D look at the caves. Heather Burke identified archaeological glassware. Paige Standen-Burrows made my excel spreadsheet fancier. David Stemmer, Graham Medlin, and Mary-Anne Binnie provided access to the Mammal, Sub-Fossil, and Palaeontology collections at the South Australian Museum. Matthew McCurry and Sandy Ingleby provided access to the Palaeontology and Mammal collections at the Australian Museum. Tim Ziegler from Museums Victoria facilitated specimen loans and waxed lyrical about giant echidnas with me. I would also like to especially thank Matthew McDowell, who gave me a good grounding in all things palaeoecological and started me on this journey — I still believe I won the earworm competition though.

Financial support for this project has come from a range of sources. This work was backed by an Australian Research Council Discovery Project grant (DP150100264 to Gavin Prideaux) and grants from the Australian Institute of Nuclear Science and Engineering (ALNGRA14514 and AP10991 to Gavin Prideaux). I owe a raft of gratitude to Keith and Anita Cook from the MAXIM foundation for their genuine interest in this project and generous support. Other funding was received in the form of an Australian Government Research Training Program Scholarship, Soroptimists Adelaide Esther Bright Travel Grant,

Royal Society of South Australia small research grant, Flinders University Student Association development grant and a Flinders University Elaine Martin Fund Travel Grant.

I would like to thank my family and friends who were ever a source of encouragement and support. I look forward to all those post-thesis catch-ups we've been talking about. I also thank Pedro, my thesis-support-dog and the *goodest boi* ever. To my children, Arin, Devin, and Ethan, thank you for your understanding and patience. To my partner Grant Gully, I am fortunate to have been able to take this journey with my best friend by my side.

Lastly, I would like to respectfully acknowledge the animals that lived and died in the Wellington Caves to become part of the fossil assemblage used in this study. This thesis is their story.

Introduction to the thesis

Preface

The Wellington Caves are, undoubtedly, Australia's most historically significant palaeontological locality. In 1830, fossils from the Wellington Caves gave the scientific world its first glimpse in to the prehistory of Australia's fauna (Lang, 1831). These fossils quickly came to the attention of surveyor-general of New South Wales, Major Thomas Mitchell (later Sir Thomas Livingstone Mitchell), who had been searching Australian caves for fossils since his arrival in Australia in 1827 (Dunkley, 2016). Mitchell's interest in cave fossil assemblages was likely a result of his acquaintance with Reverend William Buckland and his diluvial theories (Buckland, 1824; Foster, 1936; Dugan, 1980). Buckland's diluvial geology held that the Earth's short history was punctuated by sudden violent catastrophic events that periodically wiped entire assemblages of species off the face of the earth (Buckland, 1824; Anderson, 1926; Dugan, 1980). In *Reliquiae Diluvianae* (1824) Buckland had concluded that caves in Europe that contained the remains of species no longer present in Europe, provided evidence for a universal deluge *sc.* the biblical flood. It was presumed that Australian fossils would yield a similar discontinuous fauna, thus confirming the universality of the deluge.

Indigenous people had been on country for millennia, but to the rest of the world, Australia was still a new and unexplored place. Its fauna was strange, unlike anything previously known, and its extinct fauna was even stranger. It is not surprising that the Wellington Caves fossils sparked global interest and many of the early specimens (and replicas) were sent to Paris, England and Scotland to be studied by icons of science including Robert Jameson, Georges Cuvier, Joseph Pentland, William Clift and Richard Owen (Dawson, 1985). The fossils from Wellington Caves were identified as belonging to extinct marsupials, as well as to species that still occupied Australia at the time. This demonstrated that Australia had maintained a closely related assemblage of marsupials over a long period of time. The continuity of Australian fauna presented a challenge to catastrophic hypotheses, adding to a growing body of evidence that supported the theory of uniformitarianism and thus opening the way for the development and acceptance of new scientific ideas. Indeed, Dugan (1980) proposes that the Wellington Cave fossils led to the development of Darwin's 1837 "Law of Succession of Types".

The significance of Wellington Caves runs deeper than its history. Wellington Caves holds an aggregated palaeontological archive of the last 4 million years, including the early Pliocene to the Holocene. Fossils from Wellington Caves have typically been collected from: The Big Sink (Pliocene (Dawson, 1995)), Mitchell Cave (Pleistocene (Dawson et al., 1999)), Cathedral Cave (late Pleistocene and Holocene (Dawson and Augee, 1997)) and locations within Phosphate Mine that include Koppa's Pool (early Pliocene (Nipperess, 2002)) and Bone Cave (early Pleistocene (Dawson, 1982a)). Although large quantities of fossils have been collected from these caves since at least 1830, provenance, chronology and stratigraphic context is commonly lacking. Overall, surprisingly little has been published on the Wellington Caves fauna following the early spate of interest in its extinct megafauna and the locality remains underutilised and poorly understood. However, what these earlier collections did reveal was the inordinate capacity of Wellington Caves for investigating fundamental questions regarding the late Quaternary fauna of Australia and the environment in which it existed.

Context of the thesis and research progression

The overarching aim of the research presented in this thesis was to investigate how the late Pleistocene fauna in central-eastern Australia responded to changes in its environment. This thesis documents the collection and analysis of fossiliferous infill sediments from Cathedral Cave in the Wellington Caves system, central-eastern New South Wales. The sediments, and the fossils they contain, were collected during an excavation that was planned and undertaken as part of this study. The primary focus is the terrestrial mammal assemblage, but implications from other taxa, i.e., reptiles, and birds, are considered where relevant.

In chapter 1, I examine the utility of cave fossil deposits as a source of information to guide modern ecology and conservation. I then review the timing and dynamics of environmental changes that were likely to have impacted on Australia's fauna during the late Quaternary and consider this in the context of global climate records. Because regional climates are better defined by local records, I then focus on records from the temperate, subtropical and semi-arid zones of south-east and east Australia given that the Wellington Caves is located near the junction of these climatic zones. Following this, I shift the focus of the literature review to the study location and detail the palaeontological work that has been undertaken there over the last 190 years. The European history of the Wellington Caves has been well documented

previously (e.g., Lane and Richards, 1963; Dawson, 1999, 2000; Dunkley, 2016) and so I include only a brief historical account.

In Chapter 2, I include a description of the study site and general methodology relevant to all data chapters. Specific methodology is included within chapters 3–5 as relevant.

In Chapter 3, I briefly review studies of cave infill sediments and introduce previous work revealing the complex stratigraphy of the Wellington Caves. In this chapter, I present new radiocarbon and OSL ages, construct a chronology, and investigate the stratigraphy and taphonomy of the fossiliferous infill sediments of Cathedral Cave. This chapter details the temporal and depositional backdrop upon which the faunal changes will be projected in chapter 5.

In Chapter 4, I detail the systematic palaeontology of the fauna collected during this excavation.

In Chapter 5, the focus is on the use of the Cathedral Cave vertebrate fossil assemblage as an indicator of the effects of environmental changes that occurred in central eastern Australia during the late Quaternary. I firstly discuss the ecological concepts of resilience and disturbance. I then review what the fossil record has so far revealed about the responses of terrestrial vertebrates to late Quaternary environmental changes. The focus is on Australian palaeontological studies, but I incorporate a global perspective. Following the introduction, I undertake a palaeoecological analysis of the Cathedral Cave fossil mammals. In the analysis, I highlight changes in both the taxonomic composition of the assemblage and in the relative abundance trajectories of species and ecological guilds. These changes are placed within the chronological framework that was established in chapter three of this thesis and interpreted within other published palaeoecological archives. I then discuss what the identified trends reveal about faunal responses to environmental change in the late Quaternary, and what these trends mean for megafaunal extinction theories.

Chapter 6 is the general discussion for the thesis. A synthesis of the data chapters is already presented in for Chapter 5, where I interpret faunal trends within the framework set out by the chronology and sedimentology of Chapter 3 and using the systematic palaeontology detailed in Chapter 5. I briefly address each chapter, how its aims were met, limitation and directions for future research.

The appendices present additional data and information that I did not consider essential to understanding the chapters that precede it.

Thesis style

All cited references in thesis chapters are included in a single bibliography following the appendices.

The Wellington Caves are located in the Wellington Valley, near the town of Wellington. The area is called ‘Binjang’ by the Wiradjuri traditional owners, meaning ‘beautiful valley’.

Acknowledging the unacceptable damage that colonisation has inflicted on Australia’s First Nations people, I respectfully refer to the general region around the Wellington Caves as Binjang throughout this thesis.

Throughout the scientific and popular literature on the late Quaternary, the term ‘megafauna’ is often used to broadly refer to the suite of large-bodied taxa that became extinct during this interval. The definition of what constitutes megafauna is fluid, ranging from species with body mass estimates of >45 kg (Roberts et al., 2001; Galetti et al., 2018) to >30 kg or >130 % of the body mass of their closest extant relatives (Prideaux et al., 2007a). In this thesis, I define Australian megafauna as the suite of large (>45 kg) mammals that went extinct during the late Pleistocene, but also include the large extinct Pleistocene echidna *Megalibgwilia ramsayi*, which had an estimated body mass of around 10 kg (Helgen et al., 2012) as its extinction occurred in the same timeframe as the larger megafauna.

Statement of Authorship

This thesis was completed without the use of any professional editing services.

Chapter 1. I undertook and wrote the literature review and prepared all figures.

Chapter 2. I was responsible for ascertaining the appropriate methodology, in discussion with Gavin Prideaux. I wrote the text and prepared all figures for this chapter.

Chapter 3. I led the excavation, collected samples, undertook grain-size analysis, analysed the stratigraphy and taphonomy, synthesised and interpreted the chronological data, wrote R scripts, prepared most of the figures, and wrote the text; Lee Arnold prepared and analysed optically stimulated luminescence samples, assisted with interpretation, provided XRF and XRD data, supplied methodology, and produced Figure 3.13 and data for Table 3.7. Vladimir

Levchenko and Geraldine Jacobsen prepared and analysed radiocarbon samples as well as offering insight into the radiocarbon results. Gavin Prideaux conceived the project, guided the excavation, collected samples, and edited chapter drafts. All authors viewed the final draft.

Chapter 4. I stabilised and prepared the majority of the fossils, with some assistance from laboratory staff and volunteers; identified and catalogued the majority of the fossils; and wrote systematic diagnoses. Gavin Prideaux identified many of the macropodid fossils; checked my macropodid identifications; wrote systematic diagnoses for the macropodids and edited chapter drafts.

Chapter 5. I analysed and interpreted the data, wrote R scripts, prepared all figures and drafted the chapter.

Gavin Prideaux and Trevor Worthy read all chapter drafts and offered comment and feedback.

1 Literature review

1.1 Understanding the past to conserve the future: The potential of palaeoecology and cave deposits

Earth's ecosystems are changing rapidly due to the persistent and far-reaching effects of *Homo sapiens* (Hughes, 2000; Parmesan, 2006; Hoegh-Guldberg et al., 2007; Dirzo et al., 2014). The global assessment report on biodiversity and ecosystem services by the Intergovernmental Science-Policy Platform on Biodiversity and Ecosystem Services (IPBES) details that the extent and condition of the earth's ecosystems have declined by an average of 47 % from their estimated natural baselines. Globally, 75 % of terrestrial ecosystems are significantly altered, to a point where ecological and evolutionary processes are affected. An estimated 25 % of the world's animals and plants are threatened by extinction and this number is drawn only from groups that have been sufficiently studied (Díaz et al., 2020). In Australia, at least 100 endemic floral and faunal species have become extinct since Europeans colonised the continent in 1788. This includes one fish, four frogs, three reptiles, nine birds and 34 mammal species (Woinarski et al., 2019). Extinctions often have multiple drivers and these recent losses in Australia are overwhelming due to human agency, predominantly the introduction of invasive species and predators, habitat loss due to changing land use, overharvesting, transport of pathogens between ecosystems, and anthropogenic climate change (Woinarski et al., 2019).

Under the 2015 Paris Agreement, global temperature rise is targeted to be held at no greater than 1.5–2 °C by 2030. However, if we remain on current emission trajectories, a rise in the order of 3.2 °C is predicted (Christensen and Olhoff, 2019). The impact of these changes are being observed in biological systems across the world (Parmesan and Yohe, 2003; Parmesan, 2006; Pecl et al., 2017), including terrestrial, marine and freshwater ecosystems in Australia (Hughes et al., 2017; Hoffmann et al., 2019). The Australian climate has warmed >1 °C in the last 110 years, with most of this increase occurring since 1950 (BOM 2018). Also on the rise are extreme weather events, sea levels, ocean acidification, drought conditions and fire weather, as well as rainfall decreases across the south-west and south-east of the continent (BOM 2018). In 2016, Australia confirmed the extinction of *Melomys rubicola* (Bramble Cay Melomys), the first mammal extinction solely attributed to anthropogenically driven climate change (Gynther et al., 2016).

With climate driven extinctions predicted to increase in the near future (Thomas et al., 2004), and with anthropogenic pressures increasing, the extinction of the Bramble Cay Melomys may be the tip of a rapidly melting iceberg. Clearly, anthropogenic environmental change poses the largest single threat to the future of biodiversity on this planet (Froyd and Willis, 2008; Birks, 2012), and without prompt mitigation, will test our management strategies and capabilities.

On many fronts, we are ill-prepared to meet the challenge. Predicting how biota will respond to future environmental changes will require a sound knowledge of how it has countered disturbances in the past. Our understanding of responses that a changing environment is likely to provoke from individual species and ecosystems is deficient (Blois and Hadley, 2009; Nogués-Bravo et al., 2018). Our knowledge of ecosystem processes has been assembled mostly on research within highly disturbed ecosystems and using short-term (<5 yr) timeframes that cannot capture long term ecological processes (Willis et al., 2010; Rull, 2014; Seddon et al., 2014; Kidwell, 2015). Recent work has shown that short-term trends, identified in ecological studies of forest biomes, were not reliable predictors of long-term resilience (Morel and Nogué, 2019), highlighting the need to apply both ecological and palaeoecological perspectives to conservation management.

Palaeoecology is the study of long-term relationships between past organisms and the environments in which they lived (Birks and Birks, 1980). Palaeoecology enables us to peel back layers of time and observe ancient ecosystems via fossils and archives left behind even after the ecosystem is long gone. Analogues of the past can be used to understand modern ecosystems and forecast how ecosystem processes might be altered by current and future environmental change. Thus, palaeoecology is a critical addition to the conservation toolbox, improving our ability to predict, mitigate and manage for the impending biological response (Fordham et al., 2020).

Palaeoecology uses biological and geological evidence to reconstruct and investigate past ecosystems, thus enabling ecological theory and processes to be explored over geological timescales (Louys et al., 2009a; Birks, 2019). In this way, palaeoecology provides long-term perspectives on interactions between organisms and their environment. At the core of palaeoecology lie two assumptions. The first is the principle of uniformitarianism: processes that took place in the geological past are the same as those observed today (Hutton, 1788; Lyell, 1830). That is, modern-day processes provide reliable analogies for the past, even if

the rates of change and the nature of interactions may differ markedly. Secondly, palaeoecology assumes that fossil assemblages reflect real ecological communities, thereby providing accurate insights into the ecosystem or interval under investigation. This second assumption is often validated by a high degree of fidelity between palaeoecological proxies (Louys, 2012). For example, mammal turnover events during the middle Pleistocene Climatic Transition in northern East Asia coincided with vegetation changes inferred from pollen (Zhou et al., 2018).

Studies in palaeoecology draw on a wide range of proxies to reconstruct and understand past environments. Pollen and phytoliths, representing past vegetation communities, are often found in sediments that have accumulated in caves and waterbodies (Navarro et al., 2001; Chase et al., 2012; McCarroll et al., 2017). Charcoal can record local and regional fire histories (Prideaux et al., 2010; Mooney et al., 2012; McCarroll et al., 2017). Stable isotopes obtained from carbonate materials that includes cave speleothems, shells, and corals, can reveal environmental conditions at the time of formation (Ayliffe and Veeh, 1988; Wang et al., 2001; Balakrishnan and Yapp, 2004; Lopes et al., 2013; Lone et al., 2014). Ancient DNA from sediments, bones and middens compliments morphological and palynological data (Murray et al., 2012; Murray et al., 2013; Haouchar et al., 2014). Fossil remains of animals can provide insights into ecosystem structures and interactions, as well as being a proxy for climatic and habitat conditions (Macken et al., 2012).

However, using faunas as proxies for environmental conditions comes with caveats. Environmental conditions at any given point in space and time would never be optimal for every species within the local community (Lyman, 2017). Some are likely to be living at the edge of their tolerances. For example, some North American plant taxa are known to have persisted in small populations for >10 thousand years (ka) outside of their core bioclimatic habit (Pearson, 2006). Additionally, a species niche may evolve over time (Holt, 2009), and so the modern niches occupied by species, which are habitually used to inform habitat preferences and environmental envelopes, may not wholly reflect the past ecologies of those species. This is well documented in several modern Australian species that have undergone post-colonisation range reductions or expansions (McDowell et al., 2012; Fusco et al., 2016; Cooke, 2020). Using multiple proxies is the best way to provide the most robust interpretations of palaeoenvironments (Louys et al., 2009b). In this thesis, I focus on changes in the species composition of vertebrate fossil assemblages, and the relative abundance

trajectories of taxonomic units or defined ecological groups, as indicating the effects of environmental changes.

Examples of the contributions of palaeoecology to conservation include: assessments of ecosystem thresholds and resilience (Macken and Reed, 2014; Spanbauer et al., 2016; Calder and Shuman, 2019); impacts of disturbance and response to environmental change (Blois and Hadley, 2009; Blois et al., 2010; Macken et al., 2012); establishing baseline reference conditions (McDowell and Medlin, 2010; Fusco et al., 2017a; Medina et al., 2020); identifying candidates for translocations and reintroductions (Archer et al., 2019; Westaway et al., 2019; Grealy et al., 2020), identifying refugia (Mosblech et al., 2011); evaluating natural variation (Macken et al., 2012); determining ecological niches and biogeography (Fusco et al., 2016; Jarvie et al., 2021); identifying species at risk as well as timing and mode of extinctions (Saltr   et al., 2016; Saltr   et al., 2019). Although there has historically been some disconnect between palaeontologists and conservation ecologists (Grace et al., 2019), the utility of palaeoecological data is being better recognised. For example, the International Union for Conservation of Nature is in the process of defining metrics for a Green Status of Species to be adopted alongside the Red List of Threatened Species (Ak  akaya et al., 2018). The Green Status will show how close a species is to its “fully recovered state” and includes measuring recovery against pre-human impact baselines.

Cave infill deposits, as archives of biotic and abiotic matter, present an opportunity to view the past and study the interactions between antecedent fauna and environments across geological timescales. Fossil deposits containing the required faunal and temporal resolution for palaeoecological studies are uncommon and studies of this type in Australia have been mostly limited to caves in the south, south-east and south-west of the continent (e.g., Prideaux et al., 2007b; Prideaux et al., 2007a; Prideaux et al., 2010; Macken et al., 2012; McDowell, 2013) with some sampling having occurred in the north-east (Hocknull, 2005; Hocknull et al., 2007). Some palaeoecologists attempt to get around the issue of resolution by combining fossil records from multiple sites (e.g., Hocknull, 2005; Hocknull et al., 2007; Price et al., 2019; Hocknull et al., 2020). However, combining a number of low resolution fossil sites can introduce its own set of limitations. Each site may be subject to unique biases in its fossil record, and the temporal coverage can be variable.

Cathedral Cave is an ideal location for palaeoecological studies. Its location in central-east Australia links palaeoecological studies investigating patterns of faunal response in south and

north-east Australia (e.g., Hocknull et al., 2007; Prideaux et al., 2007a; Macken et al., 2012; Macken and Reed, 2014; Hocknull et al., 2020). Thereby, testing patterns across geographical clines and in different biomes. The cave's proximity to the boundary of three modern climate zones, the temperate, semi-arid and subtropical zones, indicates a potential to capture changes in its faunal assemblage driven by fluctuating biomes associated with late Quaternary climate shifts. Earlier palaeontological excavations in Cathedral Cave detail a rich, late Quaternary vertebrate fossil assemblage (Dawson and Augee, 1997), but were not able to adequately resolve the chronology or provide robust palaeoecological interpretations. Inclusive of other fossil localities at Wellington Caves, Cathedral Cave is part of a 4 million year (Ma) archive of Australia's fauna and environment.

The usefulness of the earlier collections from Cathedral Cave and the Wellington Caves in general is limited by poor documentation of specimen provenance (Dawson, 1985), lack of curation, the incompleteness of collections and especially the absent or insufficient stratigraphic and chronological controls. New collections are required to further interrogate these sites.

1.2 Environmental change during the late Quaternary

1.2.1 The global Quaternary climate

The Quaternary Period (last 2.6 Ma) has been characterised by cyclical climatic fluctuations termed glacial–interglacial cycles, during which glaciers advanced and retreated across North America, Europe and Asia (Clark and Mix, 2002; Clark et al., 2009). In the Southern Hemisphere, glacial cycles occurred within a trend of increasing aridity, which had begun with the onset of seasonality after 14 Ma (Kershaw et al., 1994; Byrne, 2008). During the early Pleistocene, glacial cycles occurred in 41 ka intervals, increasing in both amplitude and length to 100 ka intervals following the middle Pleistocene Climatic Transition 1.2 Ma ago (McClymont et al., 2013; Miller et al., 2020). Major glacial events were separated by warmer interglacials and punctuated by stadials (colder, minor glacial advances) and interstadials (warmer, temporary glacial retreats). The end of the Pleistocene, and transition to the Holocene at 11.65 ka ago is marked by glacial retreat and increasing temperatures and precipitation. Climatic oscillations of the late Quaternary are captured in diverse records, including ice cores (GRIP Greenland Ice-core Project Members, 1993; Petit et al., 1999; Augustin et al., 2004; Jouzel et al., 2007), deep sea sediment cores (Gingele et al., 2004; Lisiecki and Raymo, 2005; De Deckker et al., 2019), faunal assemblages (Blois et al., 2010;

Macken et al., 2012; De Deckker et al., 2018b; De Deckker et al., 2018a), calcite speleothems (Ayliffe and Veeh, 1988; Ayliffe et al., 2008), and pollen and lake sediments (Black et al., 2006; De Deckker et al., 2018a; Kemp et al., 2019).

Some of the best characterised palaeoclimatological records derive from deep sea cores and ice cores. Marine Isotope Stages (MIS) are derived from the $^{18}\text{O} / ^{16}\text{O}$ ratio of foraminifera remains in marine sediments over the past 6 Ma. This isotopic ratio is influenced by ocean temperature and geochemistry, which are in turn affected by global ice volume, providing a proxy for temperature (Lisiecki and Raymo, 2005). Higher concentrations of foraminiferal ^{18}O in deep sea cores denote colder periods and lower concentrations warmer conditions. Relevant to this research are the last four Marine Isotope Stages, MIS 1 to MIS 4 (Figure 1.1).

Bubbles of air trapped in the ancient ice cores from Greenland and the Antarctic show a tight coupling between atmospheric CO_2 concentrations and temperature through the past 800 ka (Petit et al., 1999; Augustin et al., 2004). The ice cores are well dated and can be correlated to other climatic proxies as well as to each other (Blunier and Brook, 2001; Lisiecki and Raymo, 2005; Cai et al., 2006), thereby providing a reliable chronologically controlled long-term record of palaeoclimates. The high resolution of the ice core records has captured abrupt millennial scale Dansgaard–Oeschger cycles and Antarctic Isotopic Maximum events.

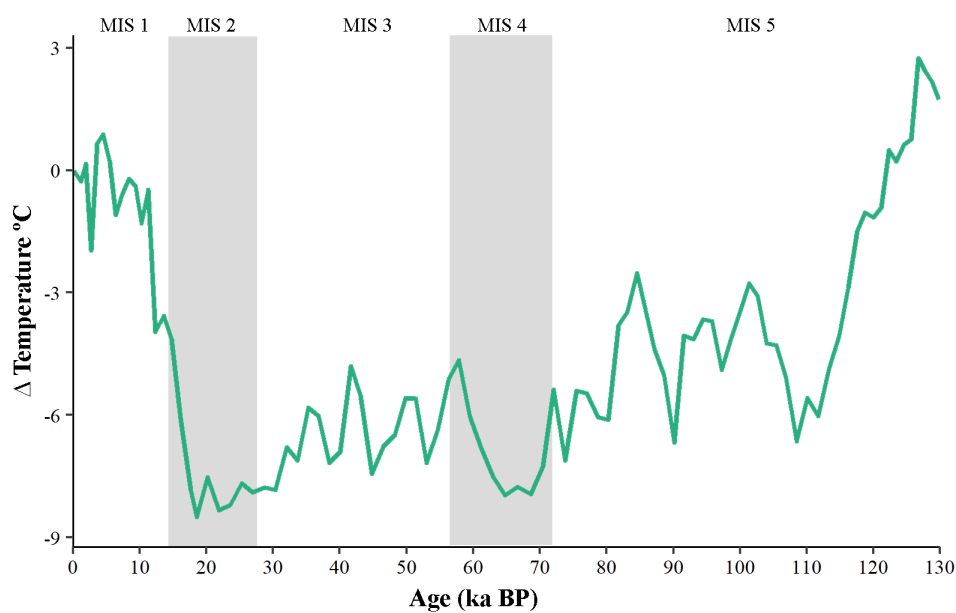


Figure 1.1. Temperature curve for the last 130 ka, showing temperature change from modern ($^{\circ}\text{C}$) based on the Vostok ice core CO_2 record (Petit et al., 1999). Also showing Marine Isotope Stages 1–5.

Dansgaard–Oeschger cycles are periods of rapid Northern Hemisphere climate change that commence with accelerated warming of 8–16 $^{\circ}\text{C}$ within a few decades. The warming is followed by gradual cooling

over several centuries and culminating in a rapid return to cold stadial conditions (Huber et al., 2006). At least twenty-five DO cycles are recognised since MIS 5, 130 ka ago, with 19 having occurred since the onset of MIS 4, 71 ka ago (Wolff et al., 2010). Dansgaard–Oeschger cycles over the last glacial cycle correspond to Antarctic Isotope Maxima events recorded in Antarctic ice cores, although there are some significant differences. Antarctic temperature variations show less pronounced, more gradual warming (1–3 °C) and cooling events over the same period (Johnsen et al., 1972; Blunier et al., 1998; EPICA Community Members 2006). The Greenland and Antarctic events are anti-phase and have been described as a “bipolar seesaw” (Broecker, 1998), with the south warming as stadial conditions occur in the north and cooling as soon as Dansgaard–Oeschger warming sets in (EPICA Community Members 2006; Wolff et al., 2010). However, both regions are cooling at the same time, during the gradual cooling phase (Steig and Alley, 2002).

Although the signature of DO events has been detected in marine and terrestrial records (e.g., Turney et al., 2004; Itambi et al., 2009; Liang et al., 2019), evidence of terrestrial vertebrate responses to millennial-scale variability associated with abrupt climatic events is rare, mostly due to resolution of the vertebrate record, but not absent. Dansgaard–Oeschger and Heinrich Events, during which large quantities of ice are discharged into the North Atlantic, have driven faunal turnover among small mammal communities of the Italian Peninsula (Berto et al., 2019). In south-west France, rapid climatic change through the late Quaternary appeared to influence the composition of local rodent assemblages, but regionally, these assemblages remained stable with little faunal turnover (Royer et al., 2016). Rapid climate changes associated with Dansgaard–Oeschger events were strongly associated with regional replacement or extinction of major genetic clades or species of Holarctic megafauna (Cooper et al., 2015). These studies demonstrate that millennial-scale events warrant consideration when evaluating the influence of climate changes on vertebrate faunal assemblages. However, most vertebrate fossil assemblages lack the resolution and chronological controls necessary to detect such fine scale changes.

1.2.2 Understudied and underestimated: The palaeoclimate of MIS 4

The climate of MIS 4 (71–59 ka ago) is relatively understudied in the Australasian region, as the majority of continuous palaeoenvironmental records do not extend beyond the last glacial maximum (LGM) (Cadd et al., 2018; De Deckker et al., 2019; Kemp et al., 2020). Recent work has suggested that MIS 4 conditions in Australia were almost as cool as MIS 2, with

glacial conditions peaking at 65 ka ago, as evident in the MD03-2607 marine core record, taken from offshore South Australia (De Deckker et al., 2019; Figure 1.2). Within it, changes in aeolian dust flux, terrestrial vegetation types, sea-surface temperatures and foraminiferal assemblages correlate with a shift toward, and a return from, glacial conditions during MIS 4 (De Deckker et al., 2019).

Exposure dating of moraines indicates that glaciation in the Snowy Mountains was more extensive during MIS 4 than during the LGM (Barrows et al., 2001). These shifts correlate with a drop in global sea-levels, that reached a low-stand of ~100 m at 64.2 ka (Grant et al., 2012). Ice core archives from Antarctica tell a parallel story with temperatures decreasing and

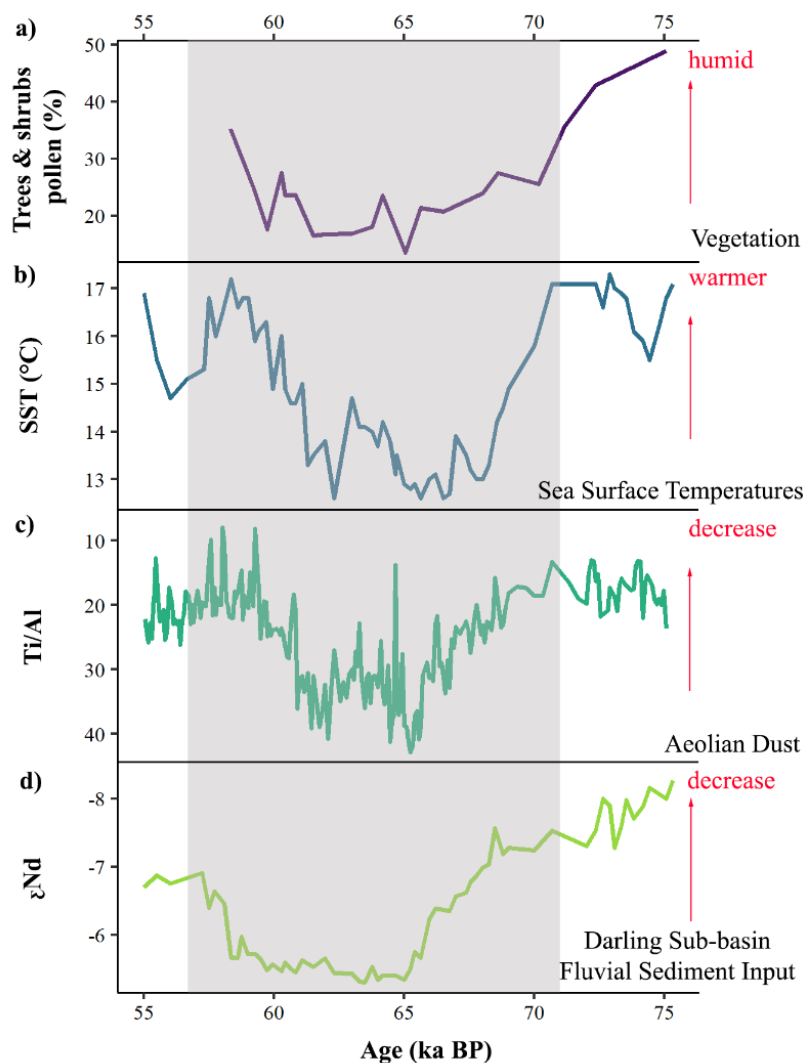


Figure 1.2. Selected proxies from marine core MD03-2607 over the 55–75 ka period (De Deckker et al., 2019). a) Vegetation based on relative abundance of pollen originating from trees and shrubs. b) Sea Surface Temperatures based on alkenone thermometry. c) Aeolian dust input based on trace metal analyses by XRF core scanning. d) Fluvial discharge based on ϵNd signature. Grey band represents MIS4.

then rising, while dust flux follows an inverse pattern (Stenni et al., 2010; Bereiter et al., 2012). However, climatic variability across Australia is evident, with the $\delta^{18}\text{O}$ record of emu eggshell from Lake Eyre, the Darling Lakes and Port Augusta in central Australia, showing an increase of moisture from 71 ka that is related to point-potential evapotranspiration (Miller and Fogel, 2016). Dry conditions had returned to these lakes by 65.2 ka. Lake Mega-Frome, in the middle latitudes of south-central Australia, was full at around 65 ka (Cohen et al., 2012). Core MD03-2607 reveals an increase in fluvial discharge from the Darling River catchment that peaks

at 63.5 ka (De Deckker et al., 2019). These records indicate that central Australia was wet at around 65 ka. During MIS 4 – 2, the East Australian Current migrated north, resulting in lower sea surface temperatures in the Tasman Sea (Kawagata, 2001) and probably reduced rainfall in the temperate and sub-tropical areas of the east coast. The Welsby Lagoon record, in sub-tropical south-east Australia, captures a shift to drier conditions between MIS 5 to MIS 3 (Cadd et al., 2018).

1.2.3 The variable palaeoclimate of MIS 3

The MIS 3 interstadial (57–30 ka ago) was marked by an increase in the number of Dansgaard-Oeschger events (Wolff et al., 2010). A synthesis of 40 Australian hydroclimatic records found between 57 to 49 ka ago, the climate was spatially variable across the continent becoming largely wet from ~49 to 40 ka ago and then increasingly dry for the remainder of MIS 3 (Kemp et al., 2019). At the end of MIS 3, water availability across the continent was reduced by an average of 30% compared to modern values and most of the sites recorded their driest conditions. Sites influenced by south-westerly winds were wetter from 50 to 40 ka ago, whereas those influenced by the Australian monsoon commenced drying from 48 ka ago to the end of MIS 3. Spatial variability of climates was most evident during the early part of MIS 3. Central Australia experienced predominantly wet conditions between 57 to 50 ka ago while the climate was spatially variable in the eastern third of Australia. Drying commenced in north-east Australia in the period between 50 to 45 ka ago while climates were generally moist in south-central and south-east Australia. The south-east remained mildly wet between 45-40 ka ago as central Australia became more arid. Widespread aridification set in across most of the continent between 40 to 29 ka ago, with MIS 3 aridity peaking between 35 and 29 ka ago leading in to MIS 2 (Kemp et al., 2019, and references therein).

It has been recently hypothesised that widespread global environmental change was triggered 42 ka ago by a weakening of the Earth's geomagnetic field immediately preceding the Laschamps Excursion (Cooper et al., 2021). However, evidence for major environmental changes at 42 ka is currently lacking.

1.2.4 The glacial palaeoclimate of MIS 2

The frequency of DO events reduced through MIS 2 (Wolff et al., 2010) which commenced 29 ka ago. During the early glacial period (30–22 ka ago), glaciers in the Northern Hemisphere began to expand, locking up vast amounts of water and increasing the amount of reflected solar radiation. The ice sheets reached their maximum extent during the LGM (22–

18 ka ago) at which time sea levels were 120 m lower than present levels (Yokoyama et al., 2000) and temperatures across Australia reduced (Williams et al., 2009; Petherick et al., 2013). The present day coastal regions of Australia would have experienced drier conditions than today, due to being located further inland and away from the maritime source of moist air (Williams et al., 2009). Sea ice in the Southern Ocean expanded, forcing oceanic fronts north and resulting in an influx of cold water along the south-east and south-west coasts of Australia (Petherick et al., 2013). Sea levels rose rapidly after 19 ka ago, reaching present levels by 6.5 ka ago (Yokoyama et al., 2000; Petherick et al., 2013).

The subtropical zone experienced cooler and drier conditions, being more similar to the climate of the modern temperate zone than the tropical zone (Petherick et al., 2013). In tropical Australia, mean annual temperatures were 3–7 °C cooler and summer precipitation decreased by at least 30%. This is consistent with a weakened summer monsoon due to a northward placement of the Intertropical Convergence Zone (ITCZ) (Williams et al., 2009). Deglaciation commenced after 18 ka ago as temperatures and precipitation rose and by 14 ka ago, the summer monsoon had been restored over north-west Australia (Williams et al., 2009).

In Australia's temperate zone, the climate was relatively cool and dry through the early glacial period, with these conditions intensifying across the LGM, at which time temperatures were up to 8° C cooler in mainland south-east Australia (Williams et al., 2009; Petherick et al., 2013). Aeolian dust flux in marine cores show that wind-borne dust across temperate and tropical Australia in the LGM was three times that of Holocene dust flux (Hesse and McTainsh, 2003). Winter rainfall across much of southern Australia was reduced, although episodes of extreme flood events are evident in the fluvial record (Williams et al., 2009). Responding to the cooler and drier climate, grasslands expanded along with an increase in open vegetation habitats (Harle, 1997; Petherick et al., 2013). In the postglacial period, between 18 – 16 ka ago, ice retreated rapidly from the Snowy Mountains and Tasmania as temperatures and rainfall increased (Petherick et al., 2013, and references therein). These changing conditions are evident in the pollen record, with a return of trees and a reduction of herbs and shrubs.

Fluvial, lake and speleothem records for the Murrumbidgee, Brachina Gorge, Lake Mungo and Lake Urana in the southern Australian semi-arid zone and Naracoorte Caves on the edge of the semi-arid zone, are contradictory (Hesse et al., 2004, and references therein). Hesse et

al. (2004) suggested that if not due to the behaviour of the proxies themselves, the inconsistencies could indicate a greater gradient of effective moisture across south-east Australia than today. Perhaps due to a greater gradient in evaporation and/or a stronger runoff gradient. With active dunes and dust entrapment from a sparsely vegetated landscape, yet with enhanced runoff from the highlands feeding large rivers in the Murray Darling Basin, Hesse et al. (2004) concluded that the LGM landscape of inland south-east Australia has no modern analogue.

1.2.5 Climate amelioration during MIS 1

MIS 1 commenced 14 ka ago, with climate amelioration across the Pleistocene-Holocene transition that was reflected in fluvial, faunal and vegetation changes across Australia (Kershaw, 1995). In the seasonally wet monsoon tropics of north-east Queensland, pollen records from Lynch's Crater, Lake Euramoo and an offshore marine core are in general agreement that conditions were wetter across the Pleistocene-Holocene boundary, with a brief return to drier conditions sometime around 11.6 to 9.5 ka ago (Williams et al., 2009, and references therein).

In the temperate region, the pollen record shows warmer, wetter postglacial conditions briefly reversed to more open vegetation, indicating a drier, colder climate between 12.5 to 10.9 ka ago. This was followed by an increase in winter rainfall and temperatures through southern Australia, resulting in more closed vegetation types as sclerophyll woodland and rainforest expanded (Williams et al., 2009; Petherick et al., 2013). Williams et al. (2009) suggested the increase in winter rainfall is associated with southward displacement of the westerlies as sea surface temperatures increased around Antarctica and the winter pack ice and Antarctic Convergence Zone retreated to the south. After 6 ka ago, the climate is variable, possibly influenced by the onset of El Niño/Southern Oscillation (Petherick et al., 2013).

1.2.6 Anthropogenic Driven Environmental Change

The first pulse of human activity in Australia commenced arguably at least 65 ka ago, with the arrival of the First Australians (Clarkson et al., 2017; O'Connell et al., 2018). The next major pulse followed the arrival of Europeans in 1788. Both events modified the ecological landscape of Australia through altered fire regimes, introduced species, increased harvesting, habitat removal and changed land use practices. Establishing pre-historical anthropogenic impacts on ecosystems can be complex, and Australian palaeontology has focused much attention on debating human or climate focused hypotheses for the late Pleistocene extinction

of the continent's megafauna (Ayliffe et al., 2001; Roberts et al., 2001; Johnson, 2005; Miller et al., 2005; Wroe and Field, 2006; Prideaux et al., 2007b; Prideaux et al., 2007a; Fillios et al., 2010; Prideaux et al., 2010; Price et al., 2011; Bird et al., 2013; Cohen et al., 2015; Saltré et al., 2016; Van Der Kaars et al., 2017; Saltré et al., 2019). The debate has become highly politicised, with ardent supporters in both camps. Untangling the relative impacts of both drivers in Australia is compounded by the patchy resolution of the late Quaternary fossil record, and our still incomplete understanding of when humans entered and expanded across the continent (Prideaux, 2007; Saltré et al., 2016). I address the status of this debate in Australian palaeontology in more detail in chapter 5.

Elsewhere across the globe, opinion is also divided. In North America, although still controversial, more evidence points toward harvesting by humans as the primary cause of the megafauna extinctions that occurred there during the terminal Pleistocene and Holocene (e.g., Koch and Barnosky, 2006; Barnosky, 2008; Perry et al., 2014; Sandom et al., 2014; Cooper et al., 2015). A palaeoecological study on a high-resolution late Quaternary mammal assemblage from Porcupine Cave, Colorado found that changes in the climate, in the form of variations in species composition and species richness, were first evident in the smaller mammals, and at lower trophic levels (Barnosky et al., 2004b). The effect of contemporary environmental changes, attributed to anthropogenic impacts, instead occurred from top down at the highest trophic levels and affected larger mammals first.

Despite a poorly dated fossil record, both human impacts and rapid climate change have been implicated in megafaunal extinctions in South America (Barnosky and Lindsey, 2010; Metcalf et al., 2016). More recently, it has been proposed that a bolide impact in southern Chile 12.8 ka ago may have been at least partially responsible for the disappearance of the region's megafauna (Pino et al., 2019). Investigations in Southeast Asia were unable to pinpoint an extinction cause until more recently, when megafaunal extinctions were linked to the replacement of grassland environments with rainforests to which megafaunal taxa were unable to adapt (Louys et al., 2007; Louys and Roberts, 2020). Still, despite highlighting the ability of *Homo sapiens* to thrive in rainforest environments, the potential impacts of a thriving population of modern humans on the megafaunal species were not considered in the conclusion.

In Eurasia, early hominins were present sporadically on the landscape from some 1.4 Ma ago (Bar-Yosef and Belfer-Cohen, 2001). There, megafaunal extinctions in the late Pleistocene

follow a staggered chronology amid individualistic shifts in distributions and population densities that are linked to climatic and vegetational shifts (Pushkina and Raia, 2008; Stuart and Lister, 2012). The addition of modern humans in the late Pleistocene as predators and ecosystem engineers likely exacerbated these impacts (Pushkina and Raia, 2008). The case for human agency is strong in New Zealand, where megafauna vanished within a few hundred years of low-density human occupancy (Holdaway and Jacomb, 2000; Perry et al., 2014), thus showing that high human population densities are not a prerequisite for megafauna extinction (Holdaway et al., 2014). In Madagascar, humans have been implicated in two pulses of megafaunal extinctions that commenced after the arrival of humans 2.5 ka ago (Crowley, 2010). Harvesting by humans and, to a lesser degree, Holocene aridity, are given as the cause of the second pulse at around 1 ka ago. Humans and megafauna evolved side-by-side in Africa, with the continent still retaining a substantial suite of large-bodied taxa. The first indication of above-normal rates of extinction in Africa were contemporaneous with increased carnivory being adopted by *Homo erectus* (see Sandom et al., 2014; Malhi et al., 2016). An alternative view proposes that taxa associated with grassland habitats were disproportionately affected, thus pointing the finger at a reduction in suitable grassland habitats rather than humans (Faith, 2014).

Arguably, the balance of evidence falls in favour of human impacts, including predation, commensal animals and landscape changes, being more significant in the global extinctions of the Pleistocene megafauna than climatic impacts (Koch and Barnosky, 2006; Sandom et al., 2014; Araujo et al., 2017). Nonetheless, extinctions usually have multiple drivers, and on several continents, megafauna extinction pulses only occurred at times when human presence and climatic changes overlapped. It is unsurprising then that a synergistic explanation is often invoked (Nogués-Bravo et al., 2008; Prescott et al., 2012; Metcalf et al., 2016).

There is little evidence recording the impacts of human arrival in Australia on non-megafauna species. In some regions, evidence suggests that firestick farming modified the boundaries of vegetation associations and created a mosaic of habitat at different stages of regeneration, which favoured some mammal species over others (Bowman, 1998; Bliege Bird et al., 2008; Griffiths and Brook, 2014). Human activity, including the introduction of the dingo has been implicated in the mainland extinction of at least three species: *Thylacinus cynocephalus*, *Sarcophilus harrisii* and *Gallinula mortierii* (see Johnson and Wroe, 2003;

Fillios et al., 2012; Roberts, 2014; White et al., 2018). Harvesting pressure probably altered both the composition and abundances of faunal communities (Kohen, 1995).

The impact of fire on Australian biota, during the late Quaternary, is equally unclear. Fire history is commonly reconstructed by quantifying charcoal particles present in sediments that have accumulated in anoxic sediments in swamps and lakes (Singh et al., 1981; Black et al., 2006; Mooney et al., 2012). This usually occurs alongside palynological analyses of pollen, thus showing how fire has impacted on vegetation types, or how vegetation types have impacted on fire regimes. Pre-historic anthropogenic fire regimes have been correlated to dramatic changes in regional vegetation and climate (Bowman, 1998). An analysis of 70 Australian charcoal records found an increase in the climate-controlled trajectory of fires during the Late Pleistocene, and particularly around 40 ka ago. The increase was attributed to human contribution, due to the absence of major environmental change (Kershaw et al., 2002), but this interpretation has been challenged. A synthesis of 224 charcoal sites from across Australasia showed that an increase in the level of biomass burning around 50 ka ago was consistent with global patterns of increased biomass burning across climate warming events and decreases during cool phases. Therefore, the composite charcoal record did not support a fundamental shift in fire regimes in Australia at this time (Mooney et al., 2012).

Establishing European impacts in Australia is simplified by a distinct signature of vegetation changes (Bickford et al., 2008) and faunal turnover having occurred rapidly following settlement (Burbidge et al., 2009; Bilney et al., 2010; Woinarski et al., 2015a). Faunal turnover is evident in stratified fossil deposits of appropriate age and a growing body of data is showing that extirpations and extinctions occurred at the European boundary at a much greater rate than thought earlier (McDowell and Medlin, 2010; McDowell et al., 2012; Fusco et al., 2017a). A major peak in fire activity is correlated to the time of European arrival in Australia, although in recent decades, this has reduced to a level similar to that of the early Holocene (Kershaw et al., 2002; Mooney et al., 2012).

1.3 The palaeontology of Wellington Caves, with a focus on Cathedral Cave.

Cathedral Cave in the Wellington Caves complex features in the early literature under several names including Mosman's Cave (Earle, 1826), The Great Cave, The Large Cave, The Large Cavern (Mitchell, 1838), The Main Cave and Cave No. 4 (Ramsay, 1882). The Wiradjuri

people knew of the cave system well prior to its “discovery” by Europeans sometime around 1828 (Lang, 1830; Lane and Richards, 1963), but there is little in the way of written or published records detailing their use of the caves. Thus, this portion of the thesis includes the colonial history of Cathedral Cave, while acknowledging that the cave has a deeper pre-colonial history and significance to the Wiradjuri Nation. A full site description is included in Chapter 2.

1.3.1 1829–1900

Following the 1829 collection of fossils from the Wellington Caves (Lang, 1830), Major Thomas Mitchell dug at least three pits in Cathedral Cave during the 1830–1831 exploration and survey of the cave system. In *Three expeditions into the interior of Eastern Australia*, Mitchell (1838) briefly describes sinking a pit of a “great depth” approximately 125 feet from the entrance that yielded a few kangaroo bone fragments. Another pit, several feet deep, was excavated in the main cavern, possibly near the foot of the Altar, and a further pit was sunk in the lower chamber. No bones were found in the latter two holes and Mitchell turned his attention to Breccia Cave (now called Mitchell Cave), where ample specimens were obtained. Fossils collected during Mitchell’s expedition were deposited in the Museum of the Geological Society of London and later transferred to the British Museum of Natural History (Lane and Richards, 1963), now the Natural History Museum, London. Unfortunately, the provenance of many of these fossils is inexact, recorded simply as ‘Wellington Caves’ or ‘Wellington Valley’.

Mitchell Cave remained the focus of most of the early fossil collecting at the caves, with substantial collections made in 1866 and 1869 by Gerard Krefft, Curator and Secretary of the Australian Museum. The lack of scientific interest in Cathedral Cave, when compared to Mitchell Cave, was undoubtedly due to the predominantly modern fauna in the former, which did not hold the same appeal as novel extinct species. Of Cathedral Cave, a report by Dr A. M. Thomson, communicated by Krefft to the Colonial Secretary states:

“Though a few fragments of bone have been found in the Great Cave, no discovery of importance has yet been made there” (Krefft, 1882 p.12).

In 1881, Edward P. Ramsay, the Curator of the Australian Museum, led an expedition to the caves. Ramsay recorded fossils of *Diprotodon*, *Protemnodon*, *Macropus*, *Halmaturus*), rodents, birds, *Thylacinus*, *Phascolomys* and *Thylacoleo* from a series of shafts in Cathedral

Cave, including No. 1 C. IV at the entrance to the large chamber and No. 2. C. IV at the base of the Altar (Ramsay, 1882). Only the locations of these two shafts were recorded on published maps (Figure 1.3).

Specimens excavated during the Krefft and Ramsay expeditions comprise part of what is referred to as the “Old Collection” in the Australian Museum register. Like Mitchell’s earlier collections, many of these specimens lack associated provenance data, severely limiting the utility of these collections. Some of the museum specimens have been flagged as potentially mislabelled, based on preservation characteristics (Dawson, 1985). This includes specimens labelled ‘Wellington Caves’ that may have other origins, and specimens attributed to other sites that have probably come from the Wellington Caves. However, preservation within the system varies, even within the same bone units, and similar preservation is known from other fossil sites nearby, thus preservation characteristics alone cannot be used to determine provenance for Wellington Caves fossils (Dawson, 1985).

In 1884, the vicinity of the caves was declared a natural reserve and organised tours of Cathedral Cave commenced. The first keeper of the caves, George Sibbald, actively collected fossils over the next 25 years (Dawson, 1985). In 1891, Sibbald unearthed the palate and associated dentition of *Palorchestes azael* in Cathedral Cave (Figure 1.4), a species that had,

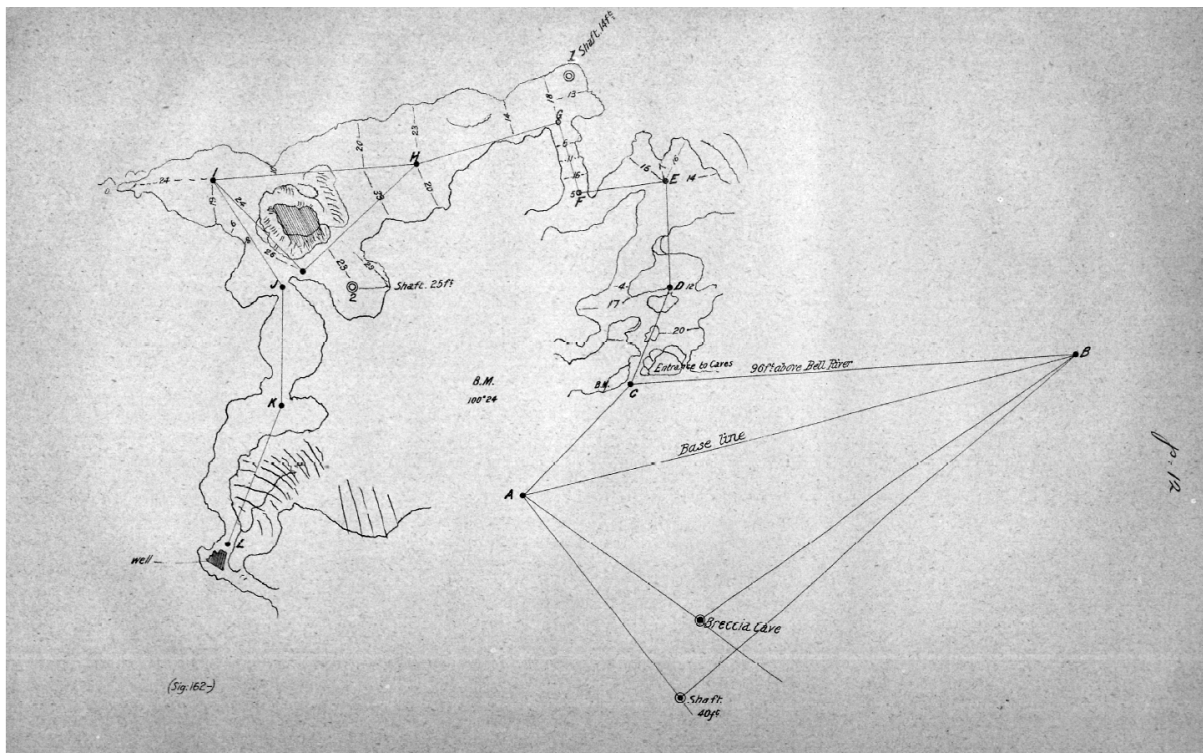


Figure 1.3. Survey of Cathedral Cave showing the location of Shaft 1 and Shaft 2 (Krefft, 1882).

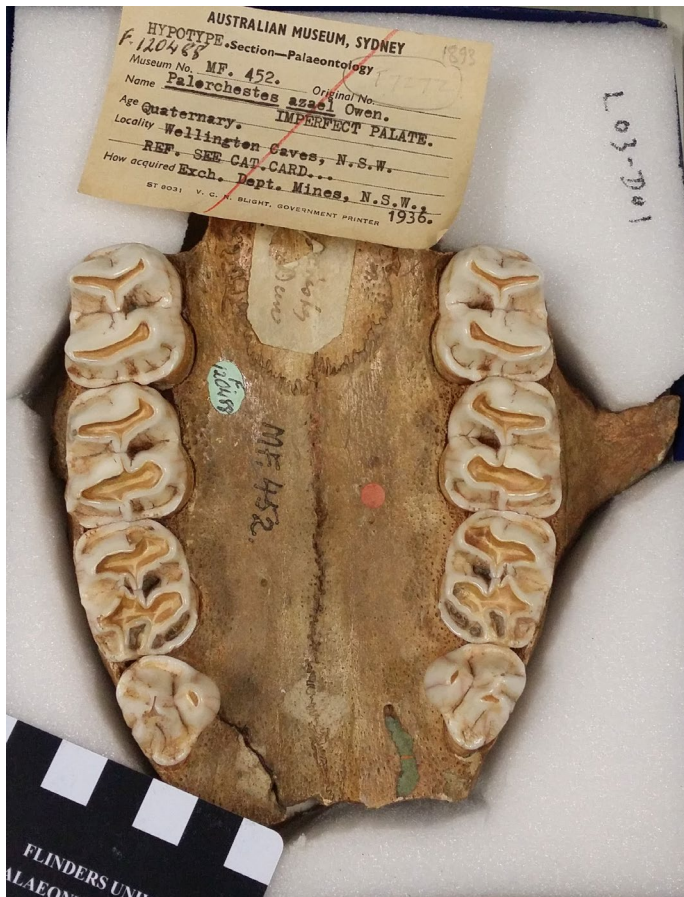


Figure 1.4. Palate and dentition of *Palorchestes azael* (F.120488) unearthed in Cathedral Cave by G. Sibbald in 1891. Figured in Dun (1893). Photo: D. Fusco

until then, been known only from a single specimen from Victoria (Dun, 1893; Lane and Richards, 1963). The exact provenance of the specimen is ambiguous. Dun reported that it originated from the bone bed of No. 4 Cave but then recounts that the Superintendent of Caves, Mr. W. S. Leigh, identified the specimen as coming from "... practically the same level as others from which previous supplies of marsupial remains have been obtained, and is a small chamber leading off from the larger caves". This could be a fundamentally poor description of Cathedral Cave, possibly lost in the retelling, or it could be a reference to the *P. azael* specimen being collected from one of the small chambers leading off

from the larger chambers of Cathedral Cave. Tellingly, the early survey map of Cathedral Cave shows the entrance marked as "entrance to caves" (Figure 1.3), perhaps indicating that early explorers of the caves initially considered this to be the entrance to a series of caves, or a cave system. The preservation of this fossil is not typical of those that have been interred in the Cathedral Cave sediments.

1.3.2 1901–1980

By 1909, fossil collection for scientific research had all but ceased at Wellington Caves. Between 1913 and 1917, the New South Wales Phosphate Company excavated mine passages through a sediment-filled cave that was later informally named Marradhal Cave, meaning 'long ago' in the Wiradjuri language (Dawson, 1999). The mine passages, referred to as the Phosphate Mine, allowed unprecedented access to the bone beds and a deeper understanding of the cave sediments (Dawson, 1985; Osborne, 1997). New interest was ignited in the collections, resulting in the sorting and study of the Old Collections and several new collections were made from the Phosphate Mine passages (Anderson, 1926, 1929; Dehm

and Schroder, 1941; Augee et al., 1986; Augee, 1997). Numerous fossils were collected from Bone Cave, a natural cavity within the infill sediments of Marradhah Cave that is intersected by Phosphate Mine passages (Dawson, 1982a). In 1926, fossils from Cathedral Cave were sent to the Australian Museum by J Harvey Truman, having been collected during the installation of electric lights (Lane and Richards, 1963).

1.3.3 1981–present

In 1982, researchers from the University of New South Wales (UNSW) began a four year excavation of the main chamber of Cathedral Cave (Figure 1.5), as part of a larger study that included the Big Sink (Dawson, 1999), the Phosphate Mine and Bone Cave (Dawson, 1982a). Eighteen mammal taxa were collected from Big Sink and faunal biocorrelation implied that the Big Sink Local Fauna has a Pliocene origin (Dawson et al., 1999). Within the Phosphate Mine, fossils have been collected from numerous localities that encompass several stratigraphic and chronological units. These localities include Bone Cave (Dawson, 1982a), Shaft Cave (Augee et al., 1986), Koppa’s Pool (Nipperess, 2002) and South Shaft (Bell, 2004). The largest and most extensively studied Phosphate Mine collection originates from Bone Cave and is the subject of an unpublished PhD thesis (Dawson, 1982a). Dating has so far been biochronological, placing a Pleistocene age on most of the Phosphate Mine localities and an early Pliocene age on Koppa’s Pool. The biochronological age for the Mitchell Cave fauna is Pleistocene (Dawson et al., 1999). As well as the leading study on the sediments and vertebrate fauna of Cathedral Cave (Dawson and Augee, 1997), two unpublished Honours



Figure 1.5. The UNSW excavation circa 1982. Photograph supplied by L. Dawson.

theses investigated aspects of the excavation. Blanford (1985) focused on the fossil rodent fauna and Hodge (1991) investigated the bandicoot fauna and sedimentology.

The UNSW excavation reached a depth of 7.5 m from the top of the sediment floor and at this depth, had not reached the bottom of the

sediment infill in the cave. The excavation pit measured 2 x 1 m and was divided into 8 horizontal quadrats. Sediments were excavated in variable depth spits of 10 – 20 cm, dependant on the character of the sediments exposed (Dawson, 1985). How much of the excavated sediment was processed and analysed, and how much was unprocessed and used as backfill in the excavation is unclear. M. Augee stated that one quarter of the sediment was processed and that large and obvious fossils were removed from the unprocessed sediment when observed (M. Augee pers coms). Field notes kept by L. Dawson indicate that not all sediment was processed until after spit 46. Sediment samples for the uppermost metre were inadvertently lost or destroyed, preventing a sedimentological analysis for this phase (Hodge, 1991).

Three phases of accumulation were identified with each characterised by distinct changes in sedimentology, faunal composition and taphonomy (Blanford, 1985; Hodge, 1991; Dawson and Augee, 1997). These were termed either, as the lower, middle and upper units (Hodge (1991), or phases 1–3 (Dawson and Augee (1997). In this thesis, I use the latter stratigraphic terminology when referring to the UNSW excavation. Radiocarbon dates were obtained for all three phases, ranging from 35.2 to 2.54 ka. Although the dates show a general trend of youngest to oldest with increasing depth, some dates are not sequential and concerns about potential contamination were raised (Dawson and Augee, 1997). A further red flag is that these dates show megafaunal species persisted in the Binjang region at least until the LGM, a suggestion that is incompatible with most other studies that investigate the timing of extinction (e.g., Roberts et al., 2001; Prideaux et al., 2010; Saltré et al., 2019). The limitations of the UNSW chronology are discussed further in Chapter 3.

Authors of studies associated with the UNSW excavation generally agree that the sediments, stratigraphy and vertebrate faunal record indicate that phase 1 sediments accumulated during a warmer and wetter interval than those of the next-youngest interval, phase 2, during which aridity increased with the onset of the LGM (Blanford, 1985; Hodge, 1991; Dawson and Augee, 1997). Phase 3 saw a return of a tree-dominated environment, although some xeric taxa remained, suggesting a complexity of habitats in Binjang. However, these studies did not analyse relative abundance trends within sedimentary units, despite the existence of adequate sample sizes to achieve this.

The UNSW excavation uncovered a diverse and abundant fossil fauna and was the first palaeontological work in the caves to report faunal change within a framework that imposed

some form of stratigraphic and chronological control (Dawson and Augee, 1997). However, by the 2010s it had become evident that the use of a more refined, multifaceted approach, including the application of different dating methods, held great potential for extracting more palaeoecological information from the rich Cathedral Cave archive. Moreover, understanding of Australia's Pleistocene environments and climate have advanced significantly over the last decade (e.g., Petherick et al., 2013; De Deckker et al., 2018b; De Deckker et al., 2019; Kemp et al., 2019; De Deckker et al., 2020; Kemp et al., 2020). Therefore, providing a more robust backdrop against which faunal trends can be interpreted. This formed the fundamental premise for the present study: how did terrestrial mammals represented in the Cathedral Cave record respond to a changing environment through the late Quaternary.

1.4 Aims

Specifically, the research aimed to:

1. Establish the depositional history and chronology of the cave infill deposit.
2. Determine the impacts of environmental change on the late Quaternary mammal fauna of central-eastern Australia.

To achieve these aims, it was necessary to:

1. Plan and execute a palaeontological excavation in Cathedral Cave.
2. Interpret the stratigraphy and depositional history of the Cathedral Cave deposit using sedimentary and geochemical data.
3. Test and update the prior chronology for Cathedral Cave with a new series of ages, using radiocarbon dating and optically stimulated luminescence dating.
4. Establish the species composition of the fossil assemblage by means of a systematic palaeontology approach.
5. Interpret changes in the composition of the faunal assemblage in relation to the depositional history and revised chronology of the deposit, in the context of other published palaeoenvironmental and fauna records.
6. Examine contemporary conservation implications of the Cathedral Cave fossil record.

2 Chapter 2: Study site and methods

2.1 Site Description

2.1.1 Physiographical setting

The Wellington Caves are situated in the 155-hectare Wellington Caves Reserve, approximately 6 km south of the town of Wellington, in the Central West region of eastern New South Wales (Figure 2.1). The caves lie in the traditional lands of the Wiradjuri people.

Near the caves, the landscape has been heavily developed for tourism and agriculture. Remaining native vegetation adjacent to the caves consists mostly of open woodlands of black cypress, white cypress, kurrajong, silky oak and remnant white and yellow box gum with a groundcover of mostly native grass (Jex et al., 2012). The region supports a variety of remnant vegetation communities that are mostly open forest and woodland with shrubby or grassy understorey (Taylor et al., 2015).

Wellington is in the temperate climatic zone of the Australian Bureau of Meteorology climate classification (Figure 2.1). It shows some seasonal variation in monthly precipitation, ranging from a high of 64.5 mm in January to a low of 40.3 mm in June. Mean annual rainfall recorded at the Wellington Research Centre between 1946 and 2005 was 619.6 mm. Temperature regimes show strong seasonality with January recording the highest mean maximum and minimum temperatures (31.2–17.5 °C) and July recording the lowest mean maximum and mean minimum temperatures (14.1–3.4 °C). The mean annual maximum and minimum temperatures are 28.8 °C and 10.5 °C, respectively (Australian Bureau of Meteorology, http://bom.gov.au/climate/averages/tables/cw_065035.shtml).

2.1.2 Geological setting

The Wellington Caves have developed in the Middle Devonian Garra Formation (Strusz, 1965) in the valley of the Bell River. The caves have formed in two north–south running ridges of a massive limestone outcrop at an elevation of 318 m above sea level (Figure 2.2). Around 700 m west of the caves, the Bell River flows at an elevation of 300 m above sea level (Cuthbert et al., 2014a; Figure 2.3).

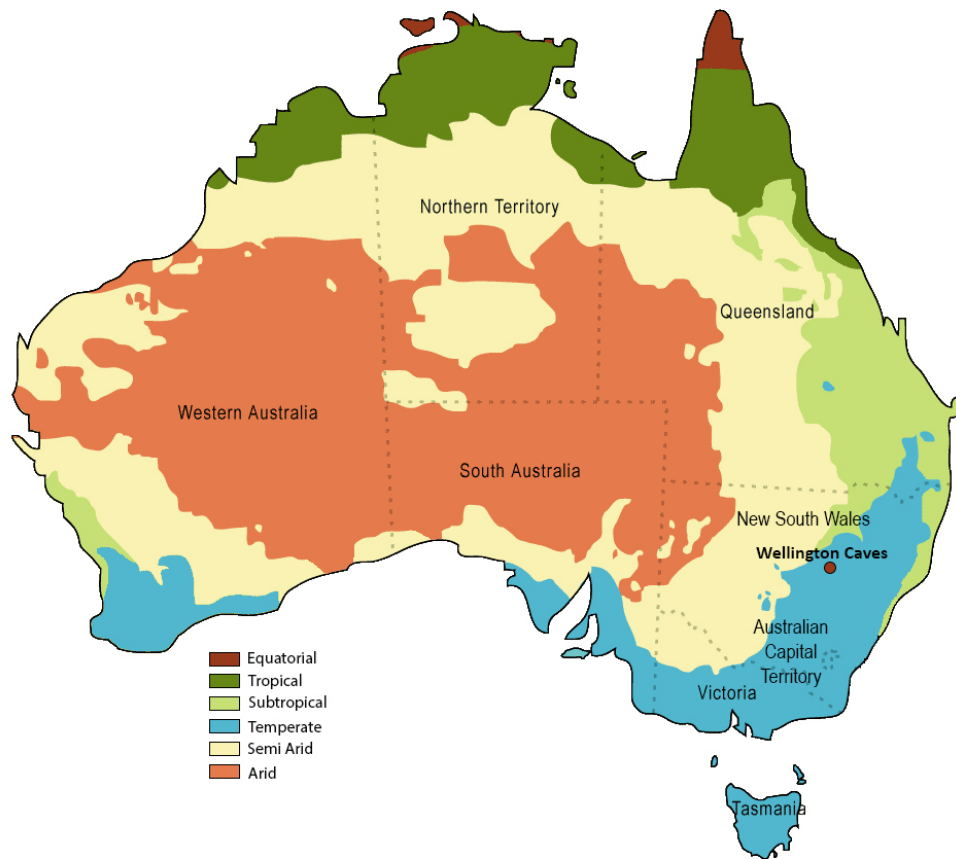


Figure 2.1. Location of Wellington Caves in relation to Australia’s climate zones. Adapted from the Australian Bureau of Meteorology climate classification, a modification of Köppen’s classification http://bom.gov.au/iwk/climate_zones/map_1.shtml.

The Bell River is a north flowing tributary of the Macquarie River and part of the Murray–Darling Drainage System.

Around 80 entrances are known in the Wellington Caves reserve (Figure 2.2). Most are only a few metres in depth or length. Some may be part of a large cave system separated by sediment filled chambers (Osborne, 2007). Nearly all caves have formed at the boundary between massive lime-mudstone and thinly bedded limestone facies (Osborne, 1984, 2001). Two sets of faults run across the strike of the limestone that have led the development of some cave sections (Osborne, 2001, 2010).

Initially, the caves were argued to have been developed through fluvial activity (Colditz, 1942; Frank, 1971; Francis, 1973). However, it has since been proposed that many have a hypogene origin (Osborne, 2010), where groundwater moves upward through the rock as a result of heat, density or pressure. Hypogene caves are prone to filling with accumulated sediment when open to the surface, as they lack effective exits through which sediment can be removed (Osborne, 2010). The sediment infills can be excavated by meteoric processes,

slumping, falling into lower cave levels or by further hypogene speleogenesis. Such processes are evident in the complex stratigraphy of the Wellington Caves, suggesting repeated episodes of filling, excavation and refilling (Osborne, 2010).

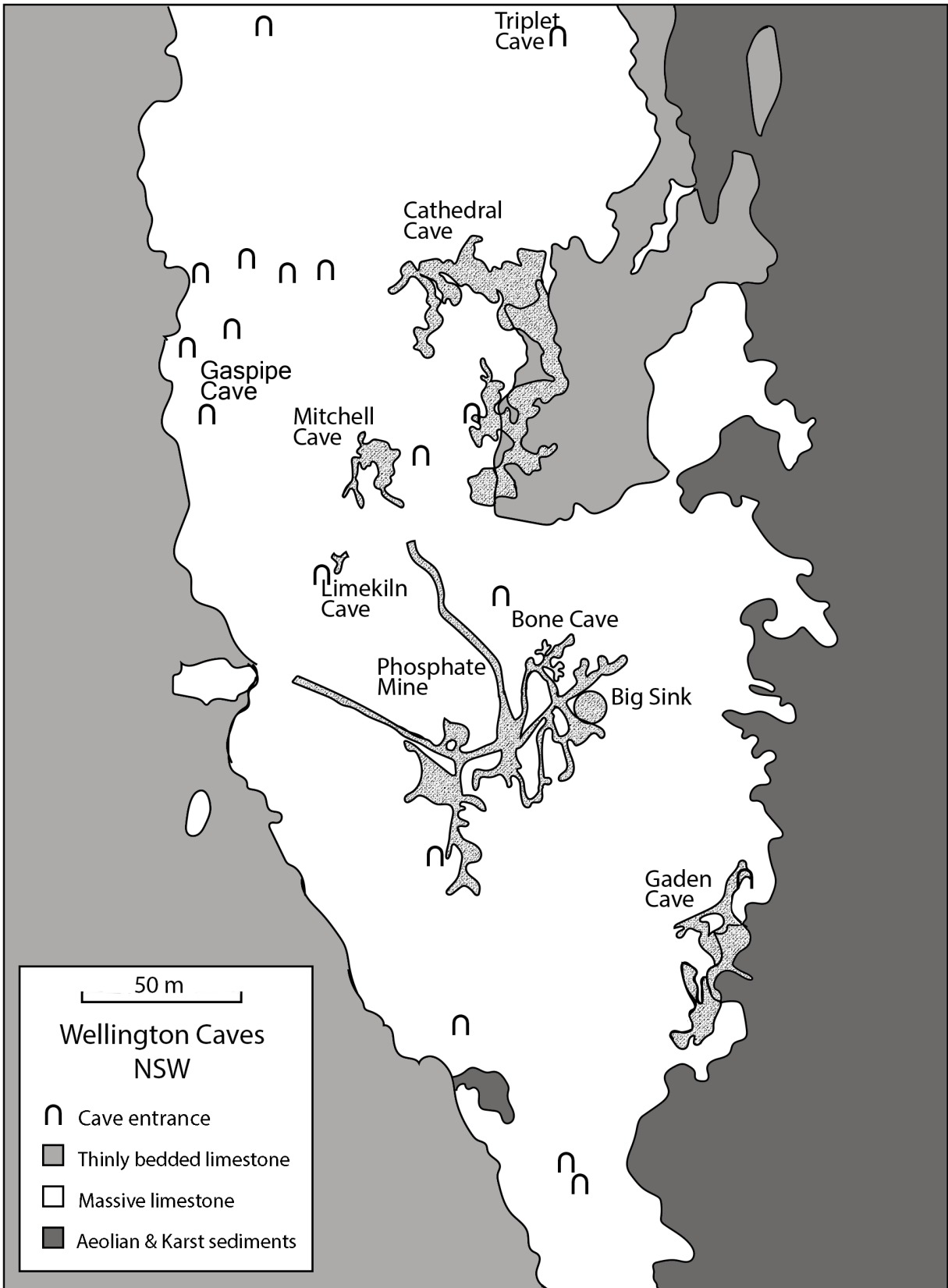


Figure 2.2. The main cave area at Wellington Caves, redrafted after Figure 3 of Osborne (2007), based on dgps mapping by A. Osborne and Brett Scott. Included with permission John Wiley and Sons. North is top of page.

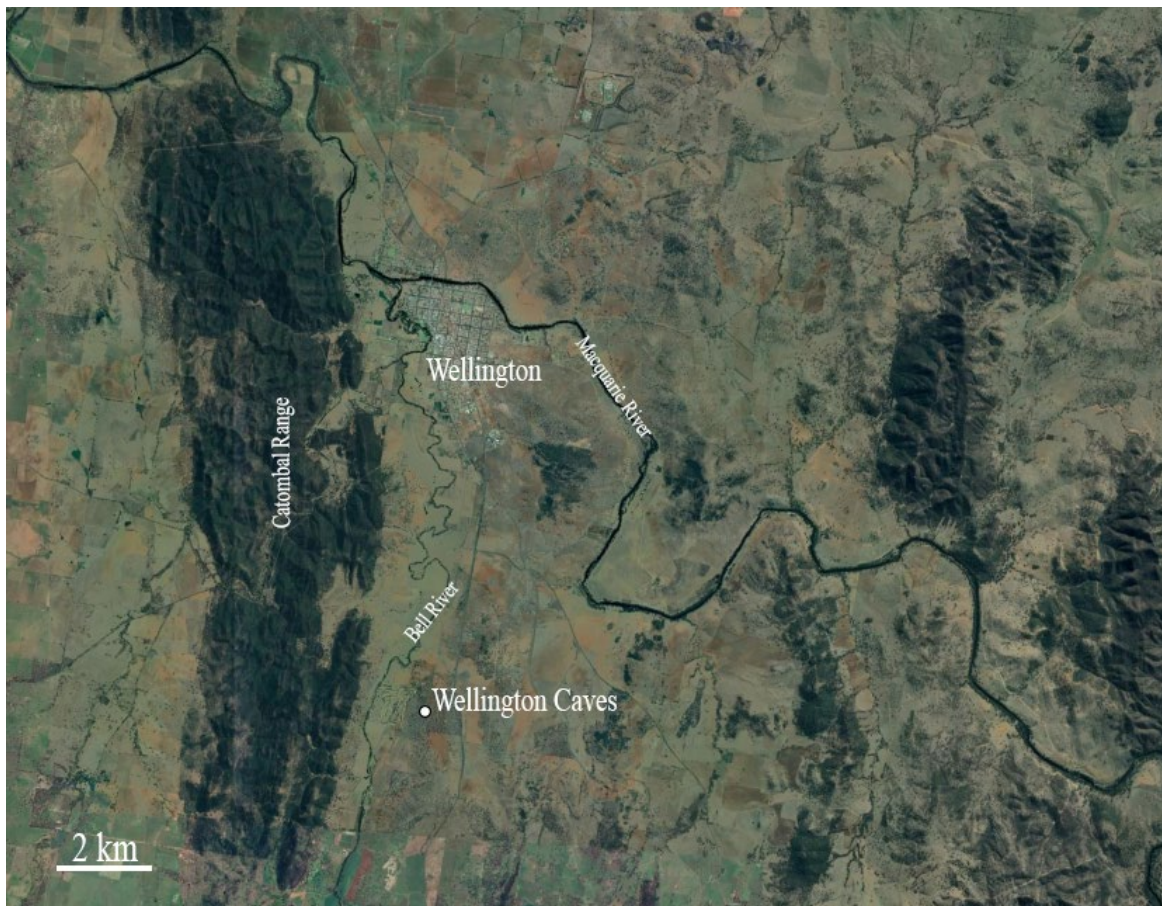


Figure 2.3. Location of Wellington Caves in relation to the Bell and Macquarie Rivers. Image adapted from Google Earth, retrieved 13th April 2021. North is top of page.

2.1.3 Description and genesis of Cathedral Cave

Cathedral Cave (ASF 2WE-1/WE-8) is the largest natural cave in the Wellington Caves system and is in regular use as a tourist cave (Figure 2.4). The cave has been comprehensively mapped (Osborne, 2007) and is also the subject of ongoing hydrological drip monitoring, infiltration and groundwater studies (Jex et al., 2012; Cuthbert et al., 2014a; Cuthbert et al., 2014b; Rutledge et al., 2014; Rau et al., 2015; Baker et al., 2016; Markowska et al., 2016; McDonough et al., 2016; Keshavarzi et al., 2017; Markowska et al., 2020).

Cathedral Cave consists of a series of interconnected chambers that were formerly isolated cavities (Osborne, 2007, 2010). Entrance to the cave is via a passage that slopes steeply downwards for around 40 m before opening into a large main chamber 45 m long and 20–25 m wide and with a maximum height of 14 m (Figure 2.4). The main chamber was initially thought to have developed along the unconformable boundary between massive lime-mudstone and tightly folded, thinly bedded limestone (Osborne, 2001) but it has since been established that the chamber has developed along a fault (Osborne, 2010).

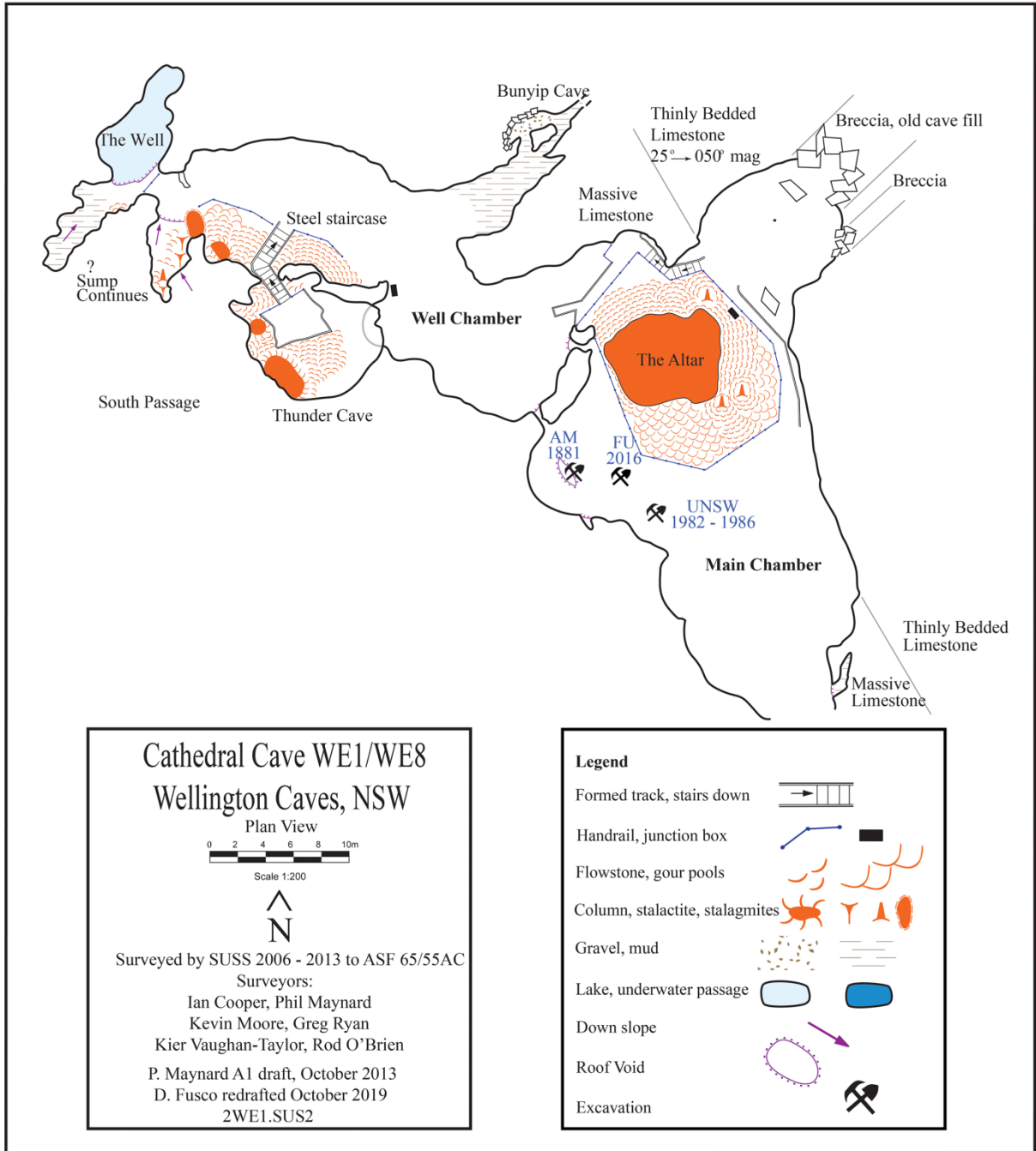


Figure 2.4. Map of the Main and Well chambers of Cathedral Cave, Wellington Caves. Modified and reproduced with permission after SUSS 2006 to also show tourism infrastructure and locations of key fossil excavations.

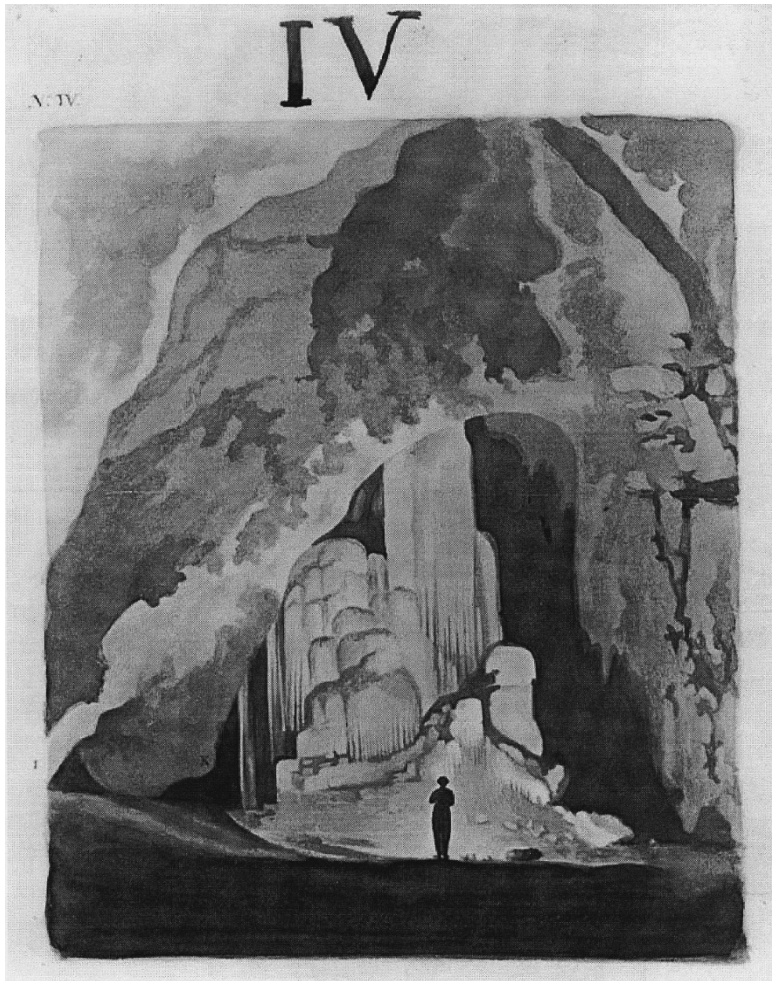


Figure 2.5. A sketch by Thomas L. Mitchell showing the floor of Cathedral Cave rising to the south. "Large Cavern at Wellington Valley, NSW." Sepia sketch, c1830/1838? from T. L. Mitchell, *Three Expeditions into the Interior of Eastern Australia*. 2nd ed.

A large stalagmite column, the Altar, dominates the northern end of the main chamber, reaching from the sediment floor to the roof, directly below the fault line. The Main Chamber is partially filled with sediment. The limestone floor is 3 m below the sediment at the entrance of the Main Chamber and 10.6 m deep at the base of the Altar (Ramsay, 1882). The sediment floor is heavily compacted, and has been artificially levelled, using soil of unknown provenance to facilitate tourism (Appendix A pg. 228). Thomas Mitchell described an even floor of dry reddish dust and talus cones located under lateral crevices (Mitchell, 1838). A sketch by

Mitchell shows the original cave floor rising along the cave wall, to the south of the Altar (Figure 2.5).

A second chamber is entered north of the Altar, with a floor 3.5 m lower than that of Main Chamber (Figure 2.4). This chamber extends for 30 m before terminating at a vertical drop of 6–7 metres into a sump known as the Well. The Well is connected to the groundwater table and water levels within it vary, dependent on groundwater recharge (Keshavarzi et al., 2017). During high recharge, Cathedral Cave is prone to flooding (Figure 2.6), with the most extensive historical flood event recorded in 1956, when water in the Well Chamber rose to 1 m above the sediment floor (Dawson and Augee, 1997).

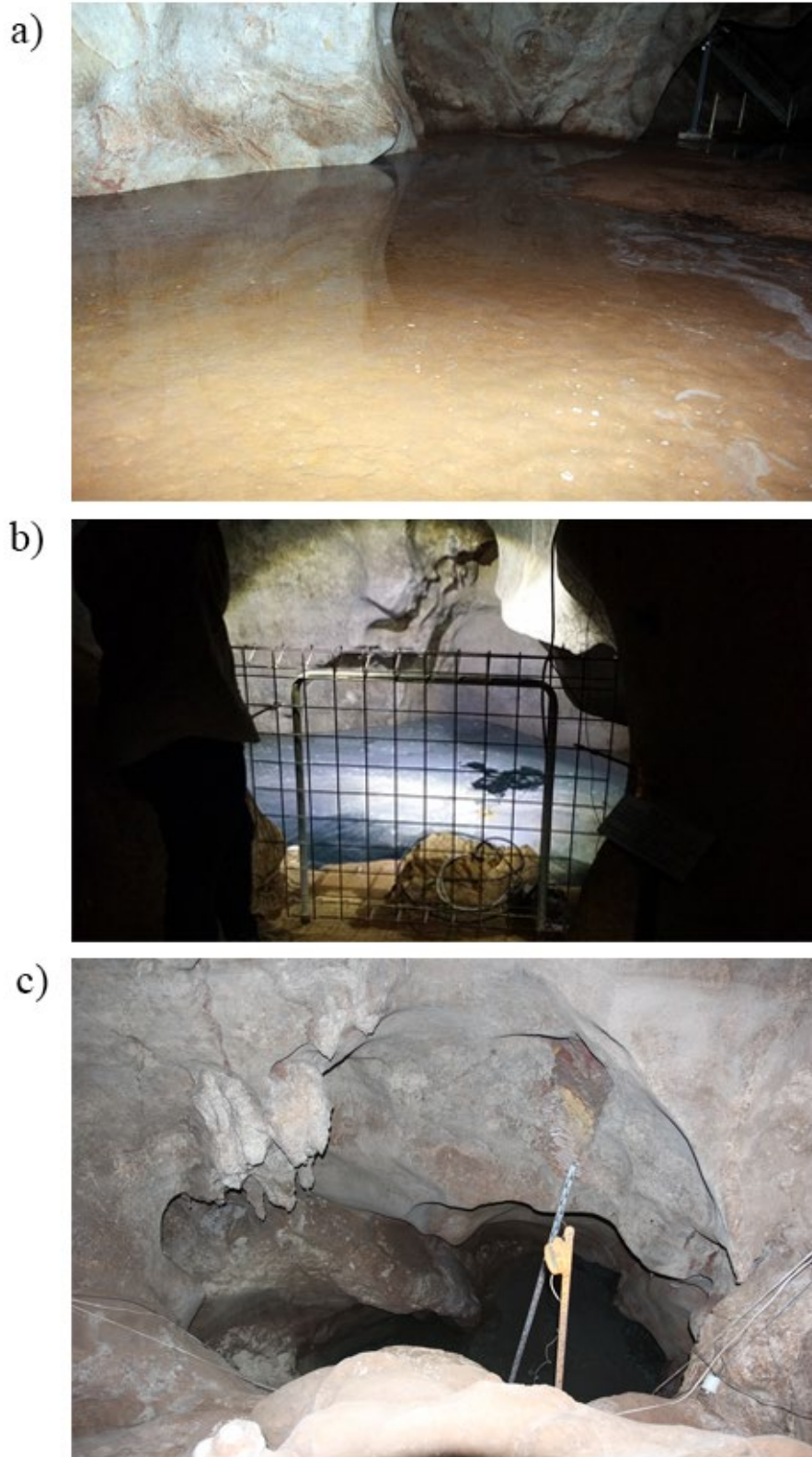


Figure 2.6. Variable groundwater levels in Cathedral Cave. Excavations by Flinders University in September 2016 occurred during widespread flooding in New South Wales. a) During this wet period, groundwater inundated the second chamber of Cathedral Cave; b) High groundwater levels in the Well during the September 2016 field trip prior to flooding of the second chamber; c) The Well was completely dry during drought conditions in April 2019. Photographs: D. Fusco

2.2 Excavation

2.2.1 Site selection

Potential excavation locations were limited to those offering minimal disruption to cave tourism. After considering cave geomorphology, we decided to locate the Flinders University (FU) excavation, to the south-west of the Altar, between the backfilled 1982–1986 University of New South Wales (UNSW) excavation and the 1881 Australian Museum (AM) shaft No. 2. C. IV (Ramsay, 1882; Dawson and Augee, 1997; Figure 2.4). The FU excavation site is located below and between two former openings in the cave roof. Both openings are now closed to the surface. One opening is not visible but is hypothesised to be above the Altar and the entry point of the fossiliferous sediment infill (Dawson & Augee, 1997; Osbourne, 2007). The second opening is a chimney located to the west of the Altar, inventoried as G123 (Osbourne, 2003). G123 has been open to the surface in the distant past, and possibly more recently (A. Osbourne, pers. comms).

2.2.2 Site preparation

A 2 x 2 m grid was established on the sediment floor of the Main Chamber and divided into four equal 1 m x 1 m quadrats labelled A, B, C and D (Figure 2.7a–d). Points of interest were surveyed using a Leica TCR705 total station digital theodolite until the survey prism could no longer be sighted above the lip of the excavation at 4 m depth. A datum (tape measure) was attached to a bolt drilled into the cave roof overhanging the pit. Most of the depth measurements were taken from this datum. The distance between the datum and the surface of the sediment floor was 166 cm at the centre of the north wall of the excavation pit. All measurements used in this thesis have been converted to cm depth below the surface of the sediment floor (i.e., datum depth minus 166 cm), unless stated otherwise. The side of the excavation closest to the Altar is referred to in this thesis as the north wall although it is not true north.

In the early stages of the excavation, the north-west corner of the pit intersected a small collapse feature in the sediments. This compromised the integrity of the surrounding stratigraphy, complicated the logistics of the excavation, and was deemed likely to be problematic during the future installation of wall shoring (Figure 2.7e). To circumvent these problems, the excavation was moved 0.5 m east, effectively reducing the size of quadrats A and C to 0.5 m x 1 m each.

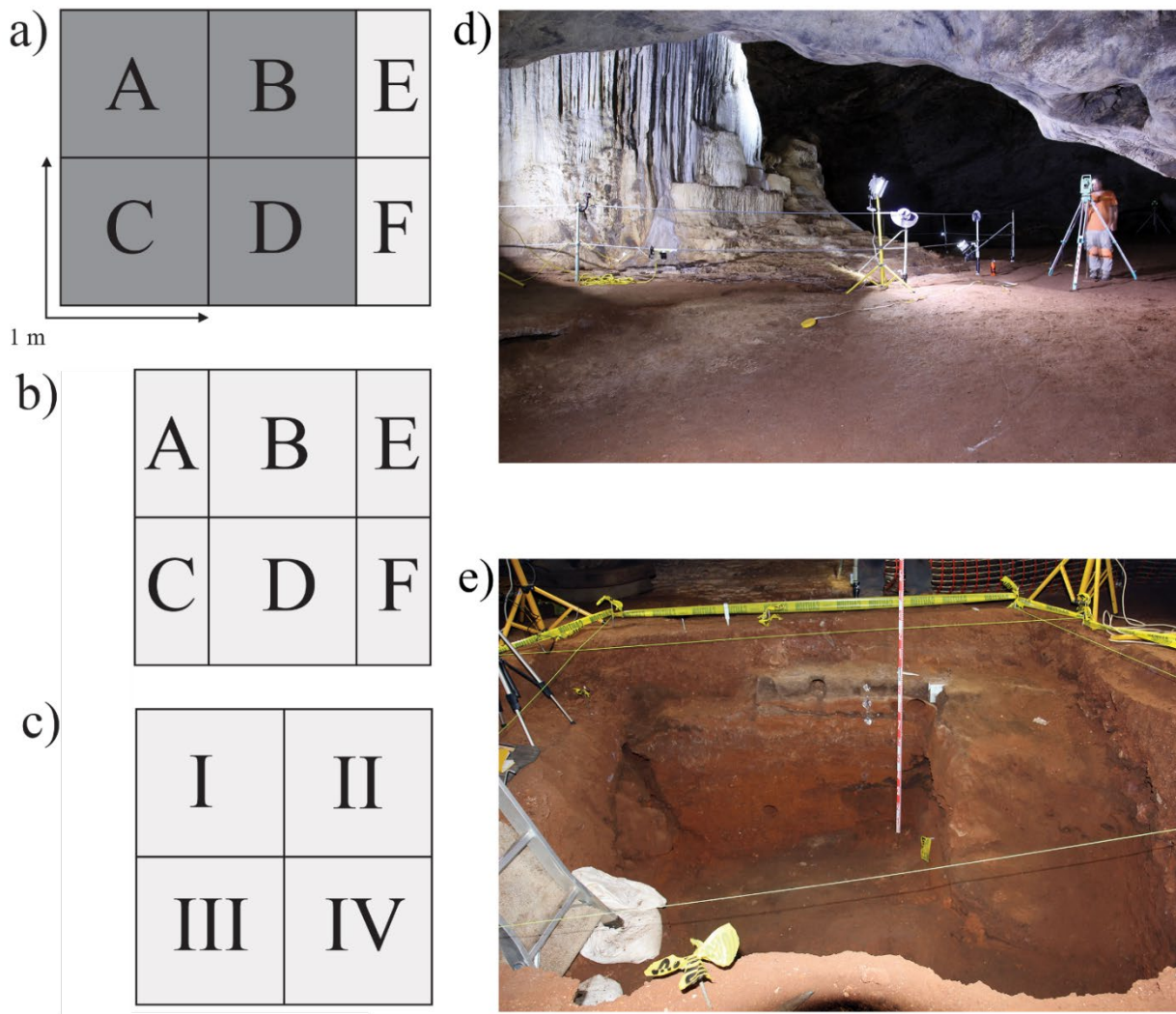


Figure 2.7. Top-down views of a) initial quadrat configuration in dark grey. Quadrats added later as a result of moving the pit boundaries in light grey; b) quadrat configuration after moving pit boundaries; c) quadrat configuration after 355 cm. d) cave floor prior to excavation, Total Station above plaque marking the UNSW excavation; e) Excavation showing collapse in north-west corner of quadrat A and commencement of boundary extension on the eastern wall. Photographs: D. Fusco

Two additional 0.5 x 1 m quadrats (E and F) were appended to the east wall of the excavation to maintain the original excavation dimensions (Figure 2.7b). The now abandoned half of quadrats A and C were backfilled during the installation of shoring. Equal sized quadrats of 1 x 1 m were re-instated at 355 cm once a level floor was reached. From there on, the quadrats were relabelled I, II, III and IV (Figure 2.7c). Several samples from the new quadrat II were erroneously labelled as coming from quadrat E until this was corrected at a depth of 375 cm. When encountered, these samples are considered synonymous with II.

The depth of the excavation, and the intention of the caves management team to leave the excavation open as a feature in the cave, necessitated the installation of custom designed shoring to protect against pit collapses. Engineers from Barnson Pty Ltd, Dubbo NSW, were engaged to design and supply shoring in consultation with Gavin Prideaux, Grant Gully and me (Appendix A pg. 228). Shoring was installed progressively in 0.5 m sections added to the

base of the shoring as the excavation deepened (Figure 2.8a–b). A gantry system was set up over the top of the excavation to enable the safe movement of sediment, equipment and people in and out of the pit (Figure 2.9a). A wet-screening station to process excavated sediment was set up adjacent to the caves (Figure 2.9b).

2.2.3 Excavation and sediment processing

Excavation progressed in 5 cm deep horizontal spits when possible, although constrained by sedimentary layers, that were numbered sequentially. Most sediments were able to be removed using standard excavation tools, e.g., trowels and dental picks. However, a hammer drill and jack hammer were required to remove heavily cemented sediments. Spit depth is variable in these sections due to cemented slabs breaking unevenly. Where this has occurred, spit depth is recorded as a range e.g., 430–435+ or by the date of collection. Labels for all samples followed the format of “location (CCW) | quadrat | stratigraphic layer | datum depth (cm) | date collected | collector’s initials”. Charcoal, pollen, and sediment samples were collected during the excavation for further analysis. The pollen data is not included in this thesis as the data is preliminary and will be further analysed by Kale Sniderman at the University of Melbourne as part of future work at Cathedral Cave.

Excavating in wet, extremely sticky clay-rich sediments that ranged from friable to cemented posed some challenges. Small fossils were rarely visible during excavation and were easily damaged when trying to remove them from the sediments. The most successful recovery method was found to be removing bulk sediments containing the small fossils. Excavated sediments were then wet screened through 0.5 mm mesh screens to concentrate the bone bearing sediment. Sediment disassociation was poor due to the high clay content (Figure 2.10a). After transportation to Flinders University, the sediments were dehydrated in an industrial oven at 50 °C and then soaked in water overnight prior to a second wet-screen treatment. Clay disassociation during the second wet screening was much improved after baking and resoaking. Allowing the sediment to dry off naturally only moderately improved disassociation. This is assumed to be due to moisture retention inside lumps of clay that had otherwise dried on the outside.

CaCO₃-indurated sediments did not respond favourably to wet screening and so were subjected to 10 % acetic acid digestion to release the fossils. An acid-lab was built at Flinders University to handle the large volumes of indurated sediments (Figure 2.10b).

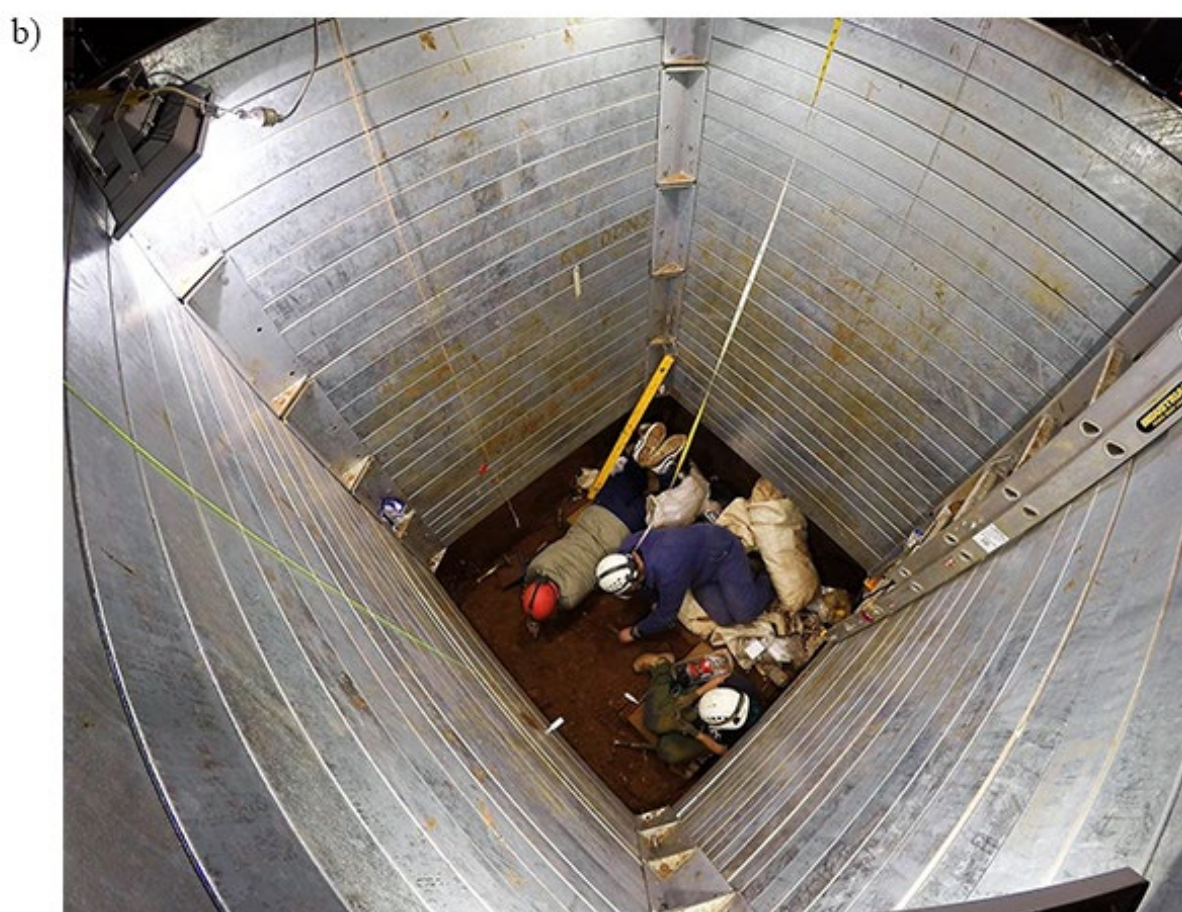
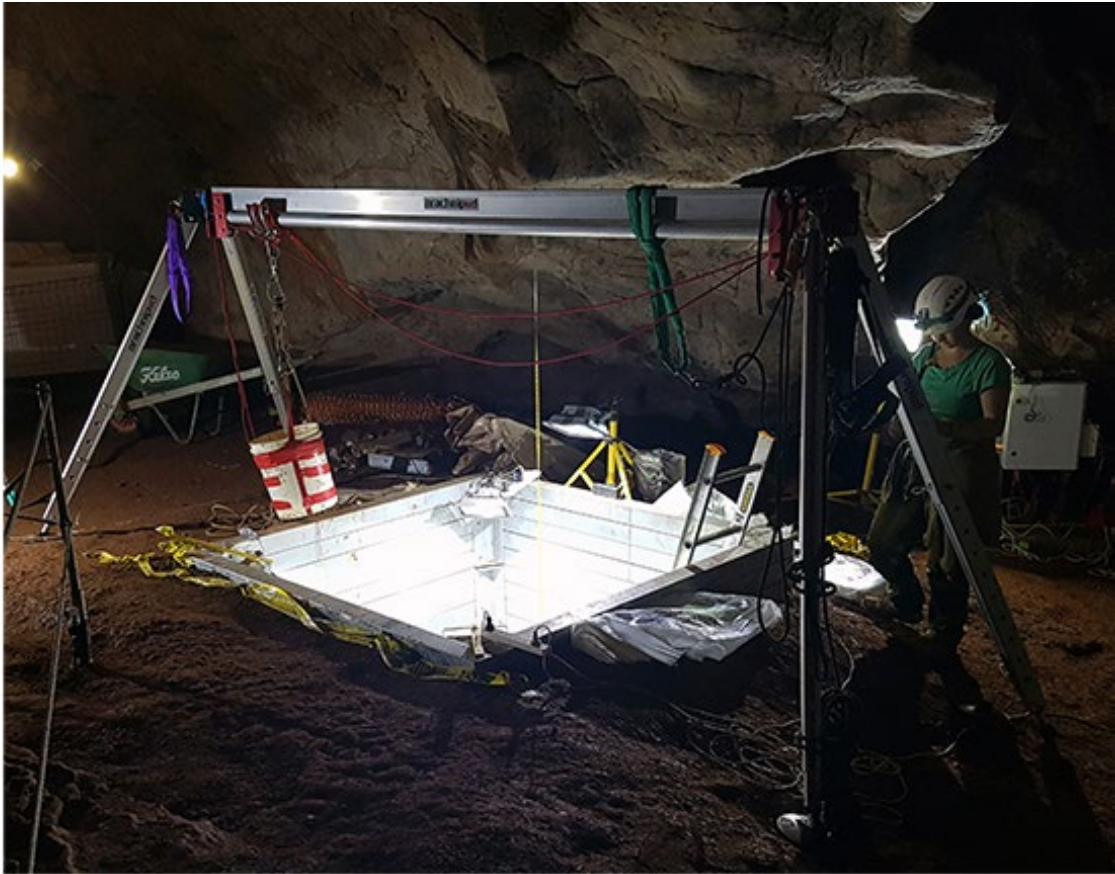


Figure 2.8. Photographs from Cathedral Cave excavation showing a) C. Burke and G. Prideaux installing the first tier of shoring during the September 2016 field trip; b) Excavation during January 2017 at ~4 m deep with 3.5 m of shoring installed with A. Couzens, M. McDowell and D. Fusco excavating. Photographs: D. Fusco.

a)



b)



Figure 2.9. Excavation equipment a) gantry system set up over the excavation; b) wet-screen station on site at Wellington Caves.

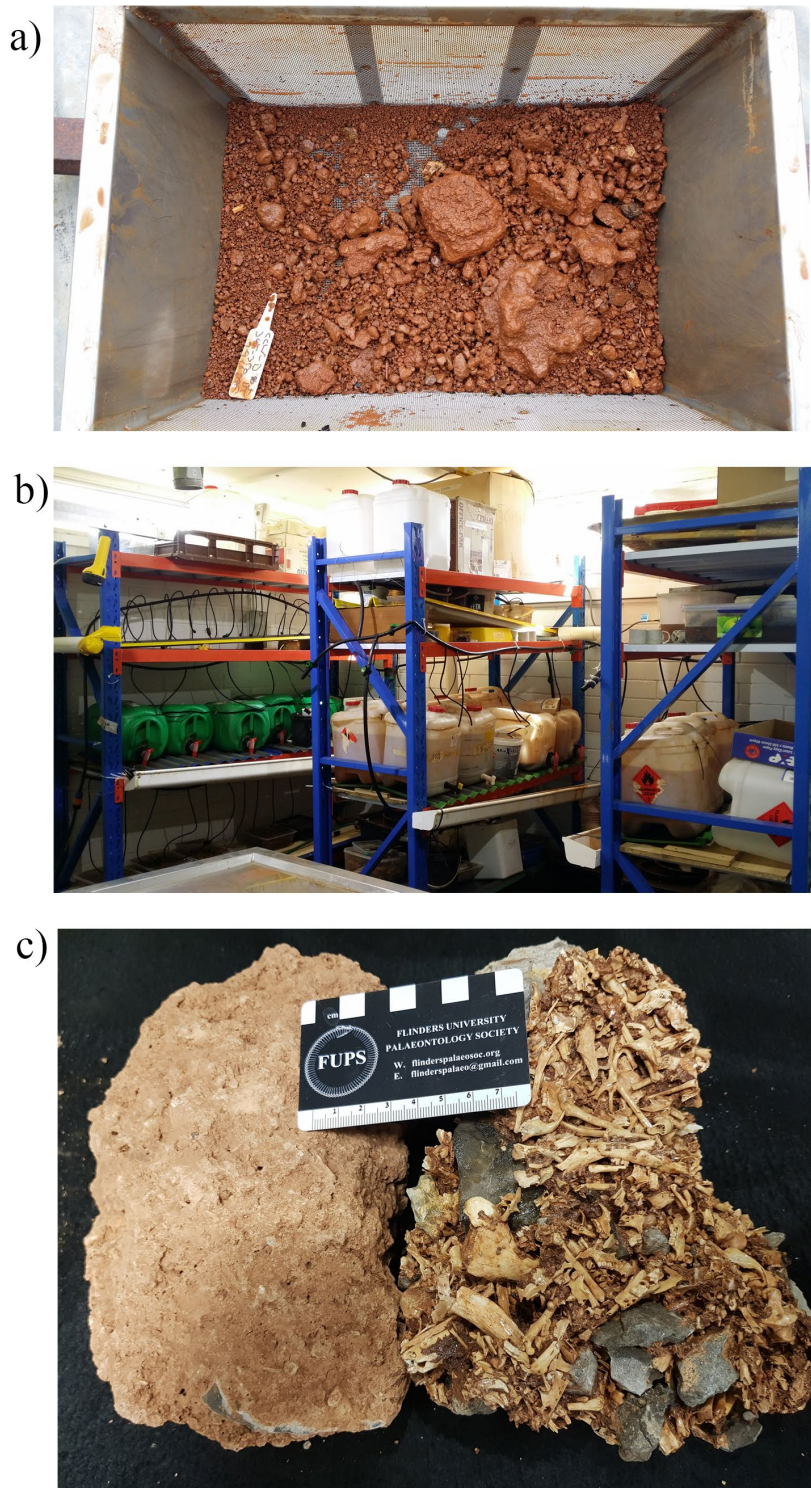


Figure 2.10. Sediment processing a) poorly disassociated sediments after first wet-screening; b) acid digestion lab. Breccia and cemented sediments undergo acid digestion in the plastic containers. Dripper system used to rinse the treated sediments with an overflow system directing water to a sediment trap; c) untreated block of indurated sediment on right compared to indurated sediment block undergoing acid treatment on right.

Blocks of indurated sediment were immersed in the acid solution for up to 24 hours, then rinsed with slow running water via a drip and overflow system for three days, or, until acetate crystals stopped forming on drying surfaces of the fossils. The block was examined, and fossils treated with a solution of paraloid B-72 and acetone for protection (Figure 2.10c). The acid digestion treatment was repeated until the fossils were released from the matrix, or, in some cases, treatment was stopped when the fossil was deemed to be at risk of damage by over exposure to the acid solution.

Concentrated bone bearing matrix was sorted for identifiable vertebrate remains. Fossils were consolidated by application of a solution of Paraloid B-72 and acetone when necessary.

Initially, quadrats A, B and E (I and II) were selected for inclusion in this study (Figure 2.7). These quadrats contained the most complete representation of the upper layers and were not as subject to disturbance by infill sediments as C, D and F (II and IV). However, after processing the bulk of the material for quadrats A, B and E, the sheer volume of material excavated and the laborious processing required, necessitated scaling back to analysing a single quadrat. Quadrat II was selected as the most complete sedimentary record. Because faunal remains were less abundant in the upper layers, faunal remains from quadrats A, B and E were included to increase sample size for layers 1–10. All unprocessed sediments are currently stored in the Flinders Palaeontology collection.

2.3 Collection curation

All identified fossils were assigned an interim reference number, prefixed by CCW, pending registration into the Palaeontology collection of the Australian Museum whither specimens will be transferred when the study is completed. Specimens that have been published as part of other studies have been assigned Australian Museum collection numbers and these are used preferentially to the interim reference numbers when available. A collection of specimens from the UNSW excavation (mostly small mammals) were deposited with Flinders University by Michael Augee. These will eventually join other specimens from the UNSW excavation that have already been deposited in the Australian Museum. Fossils from the UNSW excavation have not been used in this study.

An unregistered collection that included 20 boxes of mostly small mammals, was given to the Australian Museum by W. D. L. Ride in 2004, flagged as “the Augee Collection from Cathedral Cave, Wellington Caves”. I examined this material and found that the provenance is incorrect. The labelling format is inconsistent with the UNSW collection, and neither the preservation nor species assemblage are typical of Cathedral Cave or the Wellington Caves. One of the more obvious deviations is *Pseudomys oralis*. This rodent is the most abundant in the material returned by Ride but it is rare at Wellington Caves. I propose this material originates from either Jenolan or Wombeyan Caves, two localities from which Ride was known to have collected.

2.4 Quantitative analysis

Identified specimens were entered into an Excel spreadsheet with accompanying stratigraphic data, elements, field numbers and notes. Number of Identified Specimens (NISP) and

Minimum Number of Individuals (MNI) were used to quantify specimens. NISP is a simple count of all identified elements, and MNI is a count of the most numerous single element belonging to each taxonomic unit. I use MNI for the faunal analysis as NISP has a tendency to overestimate abundances (Marshall and Pilgram, 1993).

Quantitative and statistical analysis was performed in R statistical software V 3.6.1 (R Core Team 2019), using the R packages tidyverse 1.3.0 (Wickham et al., 2019), ggplot2 3.3.2 (Wickham, 2016), ggpubr 0.4.0 (Kassambara, 2020), vegan 2.5-6 (Oksanen et al., 2019), directlabels 2020.6.17 (Hocking, 2020), reshape2 1.4.4 (Wickham, 2007), data.table (Dowle et al., 2019), and PAST 4.03 (Hammer et al., 2001). All plots use viridis v 0.5.1 (Garnier, 2018) colour ramps to accommodate readers with diverse colour vision.

3 Chapter 3: Characterising the depositional environment of the late Quaternary fossiliferous infills of Cathedral Cave through sedimentary and taphonomic analyses

Diana A. Fusco¹, Lee J. Arnold², Vladimir Levchenko³, Geraldine Jacobson³, Gavin J. Prideaux¹

¹ College of Science and Engineering, Flinders University, Bedford Park, South Australia.

² School of Physical Sciences, Environment Institute, and Institute for Photonics and Advanced Sensing (IPAS), University of Adelaide, North Terrace Campus, Adelaide, SA, 5005, Australia

3.1 Abstract

Reconstructions of the depositional environmental record of a cave deposit provides the necessary framework for their interpretation. Cathedral Cave, in the Wellington Caves system, NSW, is a terrestrial vertebrate fossil locality of significant scientific and historical importance. Earlier palaeontological work in Cathedral Cave did not exploit its palaeoenvironmental archives and was not able to confidently determine the temporal span of deposits. Here we present results from a study stemming from new excavation of the upper 4.2 m of the Cathedral Cave deposit that provides new context for this fossil locality. This work employs Optically Stimulated Luminescence and AMS Radiocarbon dating to establish a robust chronology for the locality alongside observations of the stratigraphy, petrography, sedimentology, geochemistry, and taphonomy. These methods contribute to building a depositional scenario for the cave infill.

Thirteen sedimentary layers and sub layers belonging to two stratigraphic units are identified. Unit 2 is reached at a depth of 50 cm from the surface of the cave sediment floor and has accumulated during the late Pleistocene, between 65.8 ± 5.0 and 43.2 ± 2.7 ka. A hypothesised entrance in the roof above the Altar, a large speleothem, was open during this period, and is the source of most of the fossiliferous sediments. This entrance also acted as a pitfall trap, admitting large species as well as the owls and/or their food remains that comprise much of the smaller species in the deposit. The cave underwent repeated wet and dry phases, driven by the infiltration of meteoric waters, resulting in alternating horizons of

indurated sediments, dirty flowstones, and less consolidated sediments. This was followed by a hiatus of up to 37.4 ka as a result of the roof entrance closing, halting accumulation.

Deposition of unit 1 was initiated during the mid to late Holocene, at around 5.8 ± 0.4 ka and continued at least until 0.81 ± 0.6 ka. Most unit 1 layers have accumulated during a period of closure or extreme restriction of the roof entrance and comprise sediments derived from both bat excrement and the natural weathering of the limestone host rock exposed on cave walls and roof. The uppermost sediments are reworked from past palaeontological excavations and or tourist development.

We show that the study of deposits in Cathedral Cave has the capacity to elucidate biotic responses to the changing late Quaternary environments for this little-known region of eastern Australia especially during the critical time period between 55–43 ka that brackets the late Pleistocene Australian megafauna extinction window.

3.2 Introduction: caves as windows to the past

Cave infill deposits form as a result of accumulation of sediments from both allochthonous and autochthonous sources (Baird, 1991). Allochthonous, or those that are sourced externally, derive from erosional processes on the surface, after which the sediments may wash or fall into the cave. Autochthonous sediments are derived from within the cave itself, largely from weathering of the cave surfaces or the contribution of organic material from cave users. For example, bat or bird guano may contribute organic matter to cave soils. Both autochthonous and allochthonous sediments can then be transported by in-cave erosional processes and can form extensive infill deposits (Baird, 1991; Lowe and Walker, 2014). Cave accumulations accrue sequentially through time and can incorporate fossils of plants and animals in a depositional environment that is largely protected from external weathering processes (Lowe and Walker, 2014). Due to these properties, cave infills can contain a rich legacy of palaeoenvironmental archives. Furthermore, the physical and chemical properties of sediments are important to determine provenance, diagenesis, transport mode and energy and environmental conditions at the time of deposition (Forbes and Bestland, 2006; Forbes et al., 2007; Macken et al., 2011; McDowell et al., 2013). Infill deposits in caves provide the largest and most diverse collections of Australian Pleistocene vertebrate faunas and so are well-studied (e.g., Wells et al., 1984; Hocknull et al., 2007; Prideaux et al., 2007b; Prideaux et al., 2007a; Prideaux et al., 2010; Macken et al., 2012; McDowell, 2013; McDowell et al., 2013; Jankowski et al., 2016).

3.2.1 Characterising sediment infills

There has been a broad range of studies of late Quaternary infill deposits in Australian caves aimed at better understanding the timing, environment and conditions under which these deposits accumulated (e.g., Osborne, 1982; Moriarty et al., 2000; Kiernan et al., 2001; Kos, 2001; Turney et al., 2001b; Forbes and Bestland, 2006; Forbes et al., 2007; Darrénougué et al., 2009; Macken et al., 2011; McDowell et al., 2013). These types of investigations are useful to provide a framework and context for palaeoecological interpretations of vertebrate fossil assemblages. For example, at Grant Hall, in the Naracoorte Caves, the composition of the vertebrate fossil assemblage, indicated that there were well-forested woodlands with dense understorey occurring in the proximity of the cave 125 ka ago, across the peak of the last glacial (Fraser and Wells, 2006). This contradicted local speleothem records, that showed conditions had been relatively dry across the same time period (Ayliffe and Veeh, 1988). Further work on the cave infills provided a better understanding of their stratigraphy and age, finding that the deposit had accumulated rapidly across the end of the last interglacial rather than at the peak, which better fit the vegetation signal indicated by the fossil taxa and aligned with the local speleothem records (Macken et al., 2011; Macken et al., 2012).

Common approaches to characterising cave fills include analyses of grain morphology and size, geochemical and mineralogical properties of sediments, as well as isotopes. None of these approaches have been systematically applied to sediments in Cathedral Cave at Wellington. To date, investigations of the cave's sediments have been limited to the UNSW excavation where they received brief consideration in an unpublished Honours thesis (Hodge, 1991) and were the subject of qualitative descriptions (Dawson and Augee, 1997). Both studies lacked detailed descriptions for the top metre of the UNSW excavation, as these samples were either lost or destroyed, and thus not available for analysis (Hodge, 1991).

Useful physical characteristics of sediment include colour, and grain morphology and size. Sediment colour is most valuable in the field to distinguish distinct depositional events and to some degree, allowing a quick appraisal and comparison of the composition of the sediments. Grain morphology focuses on the shape and detectable wear on grain surfaces. These characters indicate modes of sediment transport, diagenesis that occurs during lithification, and the depositional environment (Brown and Wells, 2000; Macken et al., 2011). Grain size analysis, or granulometry, determines the frequency and distribution of different sized particles within a sedimentary column. It is most useful to classify and describe a sediment

type and establish the environment and energy associated with transport at the time of deposition (López, 2017).

Geochemistry uses X-ray fluorescence (XRF) and X-ray diffraction (XRD) to determine the composition of bulk sediment samples. XRF measures the abundance of major and trace elements based on the emission of X-ray fluorescence, whereas XRD measures the abundance of crystalline materials. Both are commonly used alongside Loss On Ignition (LOI) analysis, a simple method using ignition to estimate the content of organic matter (Heiri et al., 2001). Geochemical analysis is generally applied in caves to determine the provenance of sediments and investigate diagenesis (e.g., Forbes and Bestland, 2006; Forbes et al., 2007). In Cathedral Cave, XRF analysis of drip water samples have been used to investigate short-term water infiltration (Rutledge et al., 2014), but geochemical analysis has not been applied to Cathedral Cave fossiliferous sediments.

As part of water infiltration studies at Cathedral Cave, Rutledge et al. (2014) used XRF analysis to fingerprint the chemical composition of exogenous soils surrounding Cathedral Cave and the limestone bedrock, providing a useful comparison for the cave-fill sediments (Table 3.1). The oxides Al_2O_3 , SiO_2 and Fe_2O_3 emerged as soil signatures whereas CaO is a signature of the limestone within which the caves at Wellington have formed. K_2O was detected in low abundance in soils but was below detectable levels in the limestone (Table 3.1), thus it too may be a signature of soil. At the Naracoorte Caves in south-east Australia, the abundance of SO_3 , CaO and P_2O_5 , alongside LOI, has been used to identify infill sediments derived from accumulations of bat guano (Forbes and Bestland, 2006).

Table 3.1. Chemical composition of soils and bedrock surrounding Cathedral Cave, Wellington Cave as determined by XRF analysis and LOI (Rutledge et al., 2014).

<i>XRF analysis</i>	Soil wt%	Bedrock wt%
Na₂O	0.2	0.01
MgO	0.57	0.33
Al₂O₃	13.33	0.07
SiO₂	52.84	0.11
P₂O₅	0.26	BLD
K₂O	1.73	BLD
CaO	2.19	57.49
Fe₂O₃	7.02	0.13
LOI	20.63	43.16

3.2.2 Taphonomy and bias in the fossil record

Variations in the modes and agents of accumulation can introduce biases to assemblages of animal remains that affect how accurately they represent the then-living faunal community (Baird, 1991). Understanding bias is critical for making appropriate inferences about a faunal community from a fossil assemblage. For example, components of an assemblage may be filtered by the size or shape of a cave entrance or their climbing ability (Andrews, 1990) or biased by the activity period and preferred prey body-size range of predators using the cave (Andrews and Nesbit-Evans, 1983). Assemblages that have accumulated as the result of predation by owls illustrate this point well. Modern owl-accumulated assemblages have been shown to accurately reflect both species richness and relative abundance of small mammal faunas present in the community being sampled by the owl (Terry, 2010). Yet such assemblages entirely neglect sections of the community such as diurnally active species or larger elements of the faunal community (Andrews, 1990; Worthy, 2001). Larger species within a faunal community are more likely to be sampled by falling into a cave through a roof entrance or transported into the cave by mammalian predators or water.

Gravity-induced, pitfall death-trap assemblages are attritional rather than catastrophic, so juveniles and older individuals are generally well represented (Baird, 1991). Abundance of elements mostly reflects skeletal frequency unless secondary transport has taken place. Bones can display smooth spiral or greenstick fracturing, indicating that breakage has occurred when the bone is fresh, probably a result of the fall into the cave. Taxa are chiefly terrestrial foragers and, in the case of birds, usually those incapable of vertical flight (Baird, 1991). Kangaroos are a diverse and abundant component of the terrestrial herbivore guild and are particularly susceptible to pitfall trapping because of their bipedal hopping form of locomotion (Reed, 2006).

In a predator-accumulated assemblage, bones will show damage that is consistent with the mode of dispatching, devouring, and digesting prey. Bite marks, chewed ends and digestive corrosion are sometimes evident on bones (Baird, 1991). Bone that has passed through the digestive tract of a mammalian predator is normally highly fragmented due to being masticated prior to ingestion and corroded by digestive acids (Andrews and Nesbit-Evans, 1983; Andrews, 1990). Rodents inflict distinct gnawing damage to bone, with preference given to old bone rather than fresh (Andrews, 1990). Owls (Strigiformes) and raptors (Falconiformes) are known to contribute to bone assemblages (Andrews, 1990; Baird, 1991).

Other diurnal birds of prey (Accipitriformes) are rare contributors and are not discussed further here. Owls are a common accumulator of small-mammal remains, following ejection of a gastric pellet of undigested fur, feathers and bones of their prey (Bilney, 2012). Owl-accumulated assemblages feature a higher proportion of complete bones, milder digestive erosion than that typical of diurnal birds of prey, as well as a high occurrence of nocturnal prey species as fits their activity times (Andrews, 1990; Worthy, 2001). The higher levels of bone damage is due to Strigiformes swallowing entire prey, or their decapitated heads, whole, whereas diurnal raptors tear their prey apart before ingesting a mouthful at a time (Dodson and Wexlar, 1979; Andrews, 1990; Kusmer, 1990). Tytonid owls (barn owls) more commonly contribute to cave fossil assemblages as they often roost in caves, whereas diurnal raptors tend to nest in trees or overhangs (Baird, 1991). *Ninox novaeseelandiae* (Boobook) is a small, nocturnally active owl which sometimes roosts in caves. It preys on invertebrates and small vertebrate prey (Baird, 1991; McNabb, 2002), leaving a distinct signature of smaller bodied prey and invertebrate remains (Fusco, 2014). A further difference between avian and mammalian predators is that there is a direct relationship between avian predators and their prey species, whereas mammalian predators can consume species from a greater range of sizes (Andrews and Nesbit-Evans, 1983; Andrews, 1990; Baird, 1991).

The carnivorous *Macroderma gigas* (ghost bat) is an accumulator of fossil deposits at Riversleigh, north-west Queensland (Boles, 1999) and at the Wellington Caves in the Cathedral Cave deposit (Dawson and Augee, 1997). *Macroderma gigas* takes prey within a size range of 6 – 60 g and preference is shown toward smaller prey <35 g (Nguyen et al., 2016). Quarry is often carried back to the bat's roost to devour. The dentition of *M. gigas* is well adapted to fracturing and crushing bone and endoskeletons (Freeman, 1998) but their feeding behaviour is variable. Small mammals are wholly devoured, although portions are often dropped (Kulzer et al., 1984) whereas the skulls, legs and tails of larger mammals are discarded. Avian prey are partially consumed, with *M. gigas* discarding the feathers, legs and quills and inflicting severe damage on the pectoral region (Boles, 1999). Accordingly, an assemblage accumulated by *M. gigas* includes highly fragmented mammal remains, whereas the distal elements of bird limbs are frequently undamaged (Nguyen et al., 2016).

Not all animal remains in an assemblage are allochthonous. In a cave, some remains result from the natural death of animals that forage, shelter, nest or roost in caves. In these

instances, juvenile members are present, as associated skeletons with little damage, and elements reflect skeletal frequency (Baird, 1991).

Secondary modifications of bones can occur in a cave environment. Water-transported bones may show evidence of abrasion due to tumbling or the impact of water-transported stones and sediment (Fernández-Jalvo and Andrews, 2003). Water-transported bones are dispersed according to their hydrodynamic qualities (Voorhies, 1969; Behrensmeyer, 1978). Remains can be trampled and dispersed by other animals that have fallen into or use the cave.

Trampled bones show surface modifications that include scratches, scrapes, cuts and gouges as well as smooth and stepped breakage patterns characteristic of older bones in which collagen has degraded (Lyman, 1994; Kos, 2003a). Termites are known to feed on bone and show preference for fresh bone and may travel many tens of metres into the dark zone to access a skeleton (Reed, 2006). Boreholes and surface pitting are commonly seen on termite-damaged bones (Backwell et al., 2012).

If bones are exposed to open-air elements prior to burial, weathering can take place. Weathering occurs in predictable stages, initially with cracking parallel to the collagen fibres and mosaic cracking of articular surfaces, followed by flaking, fibrous surface texture and splintering before finally falling apart *in situ* (Behrensmeyer, 1978). However, similar modifications can occur in burial environments (Kos, 2003b). Bone flaking in a burial environment is feasibly due to small-scale fluid interactions with bone surfaces causing delamination of the outer layer of compact bone. Cracking and splitting of bone also occur during burial (Kos, 2003b; Reed, 2006), probably due to repeated episodes of wetting and drying.

3.2.3 Taphonomy of Cathedral Cave

Dawson and Augee (1997) found that the Cathedral Cave fossil deposit was the result of complex sources and multiple accumulation agents acting at various times. Fossils include taxa from a wide range of body sizes, although the focus was largely on the mammals (Chapter 4). Sizes ranged from the 12 g *Acrobates pygmaeus* (feathertail glider) to *Thylacoleo carnifex* and *Procoptodon oreas*, both estimated to weigh up to 100 kg (Johnson, 2006; Arman and Prideaux, 2016). The latter two are the largest mammals identified that were represented by more than just fragments of tooth enamel. The assemblage was heavily biased toward small vertebrates, with at least 85 % of the taxa present in each stratigraphic unit having adult body weights that do not exceed 1.5 kg. Overall, taxa greater than 1.5 kgs

were uncommon and those that did not belong to carnivores or scavengers were fragmented remains of juvenile individuals. Dawson and Augee (1997) concluded that the small taxa in the assemblage accumulated largely as the result of predation by owls and *M. gigas*. Larger taxa entered the cave via gravity induced pitfall-trapping, although they hypothesised that any entrances open to the surface were probably too small to admit larger animals as anything other than already fragmented bones.

The relative contribution of accumulation agents and modes varied between each of the recognised depositional phases (Dawson and Augee, 1997). Phase 1 contained a higher proportion of well-preserved, less fragmented bone and some associated and intact remains of larger animals that indicated attritional pitfall accumulation. Some bones had been gnawed, but the predator was not identified. The small-mammal bones were highly fragmented and were attributed as prey remains from *M. gigas*, which was abundant in phase 1 (Dawson and Augee, 1997). In phase 2, no skeletal associations were identified. Fragmented bones showed indications of weathering prior to their deposition and large taxa were typically present only as isolated teeth or cranial fragments of juveniles (Dawson and Augee, 1997). These were interpreted as a high level of disturbance, prompting the hypothesis that the phase 2 accumulation was via redeposition of bones and sediments from another deposit i.e., an entrance facies deposit above the Altar (Hodge, 1991; Dawson and Augee, 1997). Owls were identified as the primary accumulator of small mammals in phase 2 as the degree of fragmentation did not implicate *M. gigas*, nor was this species present. Phase 3 fossils were highly fragmented and in low density. Large taxa are represented only by isolated teeth leading to the proposal that the entrance above the Altar must have been inactive during this time (Dawson and Augee, 1997). No accumulation agents were identified for phase 3.

3.2.4 The complex stratigraphy of the Wellington Caves deposits

Cave-infill deposits can have complex histories featuring multiple depositional and erosional processes that have the potential to modify the temporal and spatial relationships of stratigraphic sequences (Osborne, 1984; Curnoe et al., 2019). Lateral facies changes, unconformities and stratigraphic reversals have been identified in multiple stratigraphic sequences exposed in the Phosphate Mine and Big Sink localities at the Wellington Caves (Osborne, 1982, 1984). Stratigraphy of sediments within the various caves at the Wellington Caves reveals two sedimentary units common to the cave complex, the Pleistocene aged Mitchell Cave beds, that includes the Upper Red Unit present in Cathedral Cave, and the

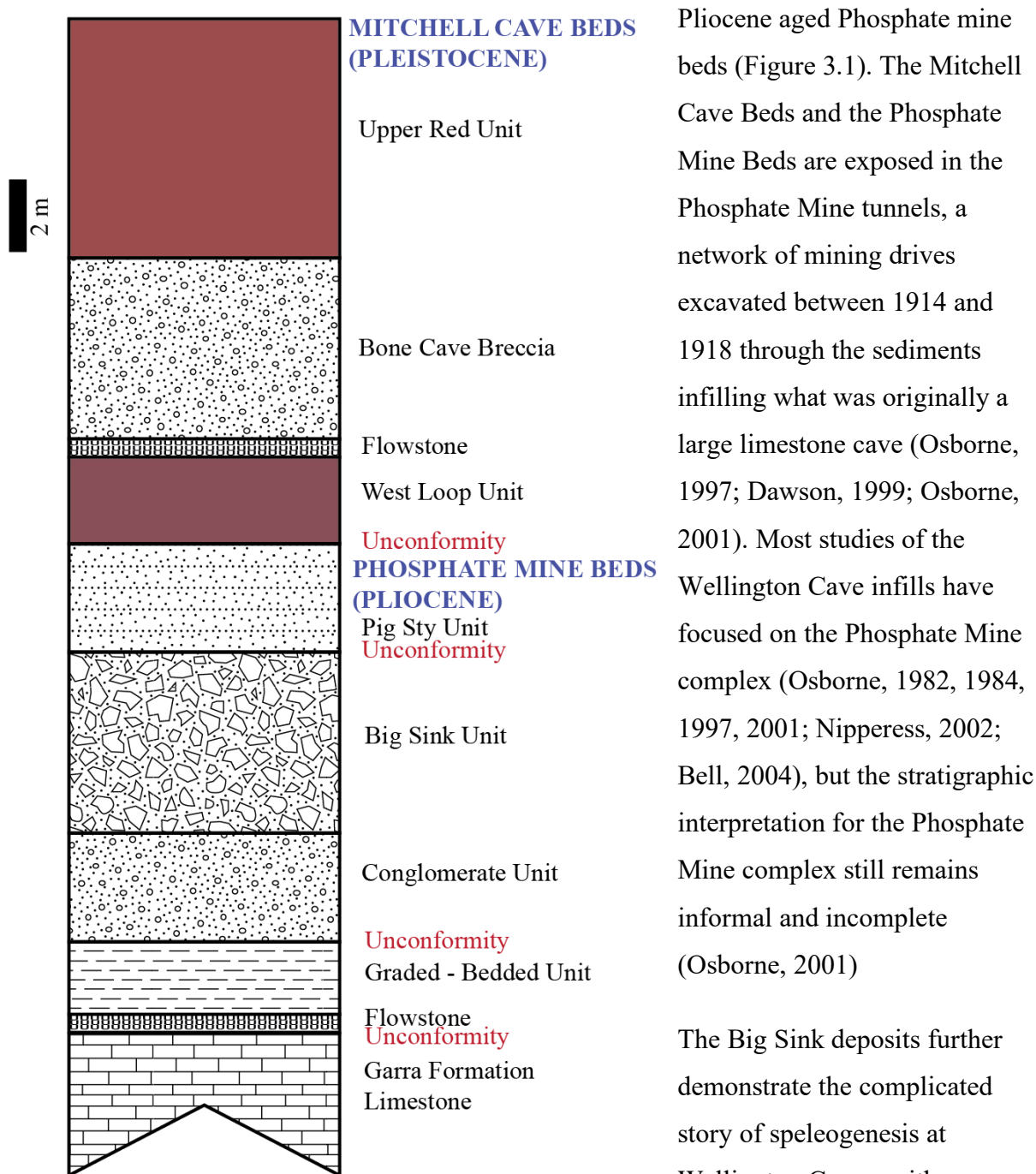


Figure 3.1. Depiction of relationships of recognised stratigraphic units within Phosphate Mine East following Osborne (2001) and Bell (2004). 2 m scale bar applies to units only. The Upper Red Unit, present in Cathedral Cave, is shown here in the Mitchell Cave Beds.

Pliocene aged Phosphate mine beds (Figure 3.1). The Mitchell Cave Beds and the Phosphate Mine Beds are exposed in the Phosphate Mine tunnels, a network of mining drives excavated between 1914 and 1918 through the sediments infilling what was originally a large limestone cave (Osborne, 1997; Dawson, 1999; Osborne, 2001). Most studies of the Wellington Cave infills have focused on the Phosphate Mine complex (Osborne, 1982, 1984, 1997, 2001; Nipperess, 2002; Bell, 2004), but the stratigraphic interpretation for the Phosphate Mine complex still remains informal and incomplete (Osborne, 2001)

The Big Sink deposits further demonstrate the complicated story of speleogenesis at Wellington Caves, with multiple cycles of accumulation and erosion of sediments resulting in a complex

stratigraphy. An unconformity in the east wall of the Big Sink exposes a stratigraphic reversal. Here, the Pliocene Phosphate Mine Beds overlie the younger Pleistocene Mitchell Cave Beds due to an erosional infill (Osborne, 1997). Such complexity has not been noted in the sediment floor of Cathedral Cave (Dawson and Augee, 1997), however, its infill sediments have received little attention to date. Hodge (1991) concluded that the Cathedral

Cave sediments were composed primarily of clastic sediments from the surface which have washed in due to rainfall, sheeting and gullyng on the surface.

3.2.5 The confusing chronology of the Wellington Caves

Dating of cave fills allows the sedimentary history and any contained assemblages to be placed within a temporal framework and correlated to other dated faunal and palaeoenvironmental records. Dating methods commonly used in Quaternary cave deposits are AMS radiocarbon dating of ^{14}C held in charcoal and bone (e.g., Dawson and Augee, 1997; Forbes et al., 2007), optically stimulated luminescence (OSL) dating of quartz minerals (e.g., Prideaux et al., 2007a; Darrénougué et al., 2009), electron spin resonance dating of tooth enamel (Goede and Bada, 1985), palaeomagnetic dating of sediments (Musgrave and Webb, 2007), and Uranium-Thorium (U-series) dating of secondary calcium carbonate deposits — usually speleothems such as flowstone, stalagmites and stalactites (e.g., Brown and Wells, 2000; McDowell et al., 2013). At Wellington Caves, most ages assigned to the fossil deposits have been based on faunal biocorrelation (Table 3.2). Cathedral Cave is the exception, with ^{14}C ages from charcoal dating the assemblage (Dawson, 1985). Otherwise, geochronological methods have been only sparsely applied, and with limited success (Table 3.2). Thus, the ages of the Wellington Caves fossil localities remain unclear. Our understanding of the relationships between these fossil deposits, and their relationship to other Australian fossil localities, will benefit from attempts to determine more robust chronologies with updated dating technologies. Eleven ^{14}C dates were acquired on charcoal during the UNSW excavation (Dawson and Augee, 1997; Appendix B Table 7.1). Although sometimes transposed, the dates show an overall trend of increasing age with depth (Figure 3.2), indicating that the sediments had accumulated over the last 33.8 ka, incorporating the Last Glacial Maximum and the Holocene. The dating irregularities, on non-sequential dates, were purported to be due to one or more of contamination during handling and pre-treatment of small, pooled charcoal samples, undetected lateral facies changes, and variable transport of material within the cave (Dawson and Augee, 1997). This resulted in the Cathedral Cave ages being assigned a quality rating of C, or extremely unreliable, in the FosSahul database of Australian late Quaternary fossil occurrences (Peters et al., 2019).

Pooled charcoal samples are not ideal candidates for radiocarbon dating as ages are time-averaged across the sample. Even though charcoal is a useful material for dating, it is extremely sensitive to contamination by younger and older exogenous ^{14}C that can result in

anomalous ages (Adams and Ringer, 2004; Lee et al., 2011; Wood et al., 2012; Becerra-Valdivia et al., 2020). The effect increases disproportionately with age and an addition of just 1% modern carbon to an infinitely old sample (>50 ka) can produce a measured age of 37 ka (Higham et al., 2009). Contamination can occur *in situ* by humic/humin acids created by the breakdown of organic materials in the soil profile and transported in percolation water, breakdown of the charcoal itself (Becerra-Valdivia et al., 2020), or through poor storage and handling of samples.

The association of extinct megafauna species with young dates further decreases confidence in the Cathedral Cave ages. For example, *Procoptodon oreas* was identified in spits 34 – 38 that yielded a ¹⁴C age of 14.3 ka (Dawson and Augee, 1997). This timeline is not supported by other proposed dates for Australian megafaunal extinction (Roberts et al., 2001; Rodríguez-Rey et al., 2016; Peters et al., 2019). A more parsimonious explanation is that extinct megafaunal species in the deposit suggest that it is at least 42 ka old. Evidently, the chronology of Cathedral Cave requires a revision, which would facilitate reinterpretation of the cave’s fossil deposit and the prevailing environmental conditions.

Table 3.2. Assigned ages for other fossil bearing sites in the Wellington Caves. * indicates unpublished dates.

Location	Assigned age	References and notes
Big Sink LF	early Pliocene	Dawson et al. (1999) — biocorrelation based on affinities to Chinchilla LF from south-east QLD and Bow LF from north-east NSW.
Koppa's Pool LF (PM)	early Pliocene	Nipperess (2002)* — biocorrelation - U-series date of 0.3 Ma discounted due to perceived diagenesis of rodent molar enamel sampled.
	early Pliocene	Bell (2004)* — biocorrelation, synonymised with Big Sink LF, Conglomerate unit and Pig Sty unit.
Loopy LF (PM)	early Pleistocene	Bell (2004)* — biocorrelation and stratigraphic data - palaeomagnetic date of 0.3 Ma discounted due to undisclosed issues with palaeomagnetic dating in karst settings.
Pig Sty unit	early Pleistocene	Osborne (2001) — stratigraphy.
	early Pliocene	Bell (2004)* — biocorrelation, synonymised with Big Sink LF, Conglomerate unit and Koppa's Pool LF.
Bone Cave (PM)	128 ka	Dawson (1985) — biocorrelation and incorporating observations from other palaeoenvironmental studies.
	late Pliocene / early Pleistocene	Dawson (1995) — biocorrelation.
	<272 +/- 4ka	Fischer (1997) as cited in Nipperess (2002) — U-series age of flowstone underlying the Bone Cave breccia unit.
	Unpublished palaeomagnetic ages	(Hesse et al., 1999) as cited in Nipperess (2002) — Bone Cave breccia unit may be a mixed, partially reworked non-contemporaneous assemblage.
Mitchell Cave	128 ka	Dawson (1985) — biocorrelation and incorporating observations from other palaeoenvironmental studies.
Cathedral Cave	(lower levels) 128 ka	Dawson (1985) — biocorrelation and incorporating observations from other palaeoenvironmental studies.
	33.8 - 2.54 ka	Dawson and Augee (1997) — ¹⁴ C dating.

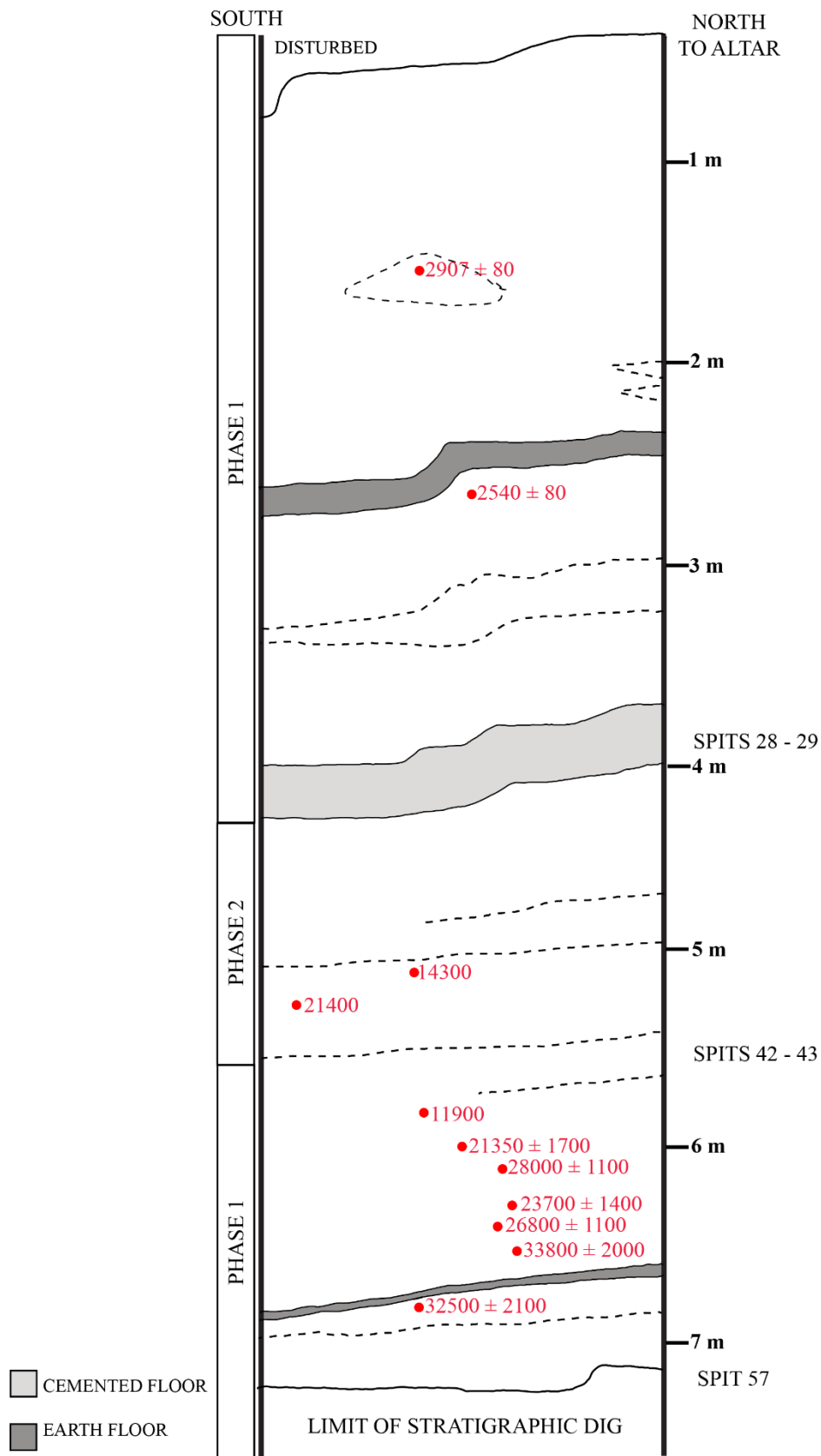


Figure 3.2. Radiocarbon ages and stratigraphy of UNSW excavation based on Blanford (1985); Dawson and Augée (1997). Cemented floor refers to indurated sediments, no description was provided for the earth floors.

3.3 Aims of this chapter

As shown earlier, the depositional environment of Cathedral Cave is not adequately understood. In this chapter, we establish the chronology, stratigraphy, and depositional environment of the Cathedral Cave deposit (to 4.2 m). The following aims will be addressed in this study:

1. Interpret the stratigraphy and depositional history of Cathedral Cave using sedimentary and geochemical data.
2. Test and update the prior chronology for Cathedral Cave with a new series of ages, using radiocarbon dating and optically stimulated luminescence dating.
3. Seek taphonomic evidence to assess the previously hypothesised taphonomic agents

To meet these aims, we examine the stratigraphy, sedimentology, geochemical composition of the sediments and taphonomy of the faunal material and place these within a chronological framework. This framework is built using two absolute dating methods, AMS radiocarbon dating (^{14}C) of charcoal and optically stimulated luminescence (OSL) dating of quartz grains contained in the sediments. The findings of this study are compared with previous work in Cathedral Cave (Dawson and Augee, 1997). We then synthesise the findings of these multiple evidence sources to reconstruct the conditions under which the sediment infill of Cathedral Cave was deposited.

3.4 Methods and Materials

See Chapter 2 for general methods, including site description, excavation procedure, sediment processing and curation.

3.4.1 Stratigraphy

Sedimentary layers were identified during excavation based on texture, colour and cementation and numbered sequentially with Layer 1 at the surface. Stratigraphy was recorded in sections prior to the excavation walls being concealed by the installation of shoring.

3.4.2 Sediment characterisation and petrography

Bulk sediment samples of every sedimentary layer were collected from cleaned exposures of the excavation walls for analysis. Twenty subsamples from the bulk samples (one per bulk sample) were selected for analysis for both sediment characterisation and XRF / XRD analyses. Selection was based on obtaining coverage for all layers. XRD and XRF analyses were undertaken on the same samples. Due to different sampling strategies used between workers, depth was not recorded for some sediment samples taken as part of the OSL sampling program, however, it has been possible to accurately reconstruct the depths using photographs and fieldnotes. The physical properties of sediment colour, grain size and grain morphology are analysed in this study. For consistency, dried sediments from bulk samples are compared against the Munsell soil colour charts (Munsell, 1994), a scheme that encompasses hue (relation to yellow, red, green, blue and purple), value (lightness) and chroma (strength or departure from a neutral of the same lightness). Because sand-sized grains, that were not clay and silt aggregates, were sparse, sediment samples were washed through a fine screen of undetermined gauge to remove fine particles, then the target grains (usually quartz) were removed from the concentrate under magnification and examined. Powers Roundness scale was used to describe grain morphology (Powers, 1953; Figure 3.3).

Sediment samples used for grain size analysis were dried and weighed. Characterisation of grain size was made using a Malvern Mastersizer 2000 laser diffraction particle analyser. During laser diffraction, a laser beam is passed through particles (e.g., sediment grains) and the diffraction patterns used to calculate the geometric dimensions of a particle. The angle of the diffracted light is inversely proportional to the size of the particle and its intensity is a measure of the quantity of particles in the optical path with a specific cross-sectional area (Di Stefano et al., 2010). The Mastersizer 1000 is unable to process particles >1mm, thus, all

samples were screened through a 1 mm mesh with the >1 mm particles removed and then dried and weighed. Aggregates formed of silt and clay aggregates were the primary components of the >1 mm fraction. The <1 mm particle concentrate was treated with 10% HCl in distilled water to remove carbonates. HCl treatment continued until effervescence ceased. After overnight settling, the solution containing the dissolved carbonates, was removed via pipette. The samples were washed in distilled water, settled overnight prior to removal of the residue containing solution via pipette, dried and weighed again. Dried samples were hydrated with distilled water prior to laser diffraction at which time it was noted that aggregates of fine material had formed during drying. These proved resistant to breakdown by hydration, requiring a second screening through >1 mm mesh.

During laser diffraction, an average of six replicates were generated for each sample. Grain size analysis was undertaken using GRADISTATv8 (Blott and Pye, 2001), using the Folk and Ward (1957) method for sorting, skewness and kurtosis (Table 3.3). Sorting (σ_G) describes the distribution of grain size, e.g., poorly sorted indicates that grain sizes are mixed. The degree of sorting is useful for describing sediments as well as suggesting the transport mode and energy responsible for depositing the sediment. Skewness (Sk_G) depicts the lack of symmetry of the frequency of distribution; using the Folk and Ward graphical measures, Sk_G indicates whether the distribution is skewed towards fine or coarse particles. Kurtosis (K_G) measures the degree of asymmetry in the frequency distribution, e.g., if a sample is platykurtic, or has negative K_G values, it has a wider peak and thinner tails than a normal distribution. Leptokurtic distribution implies positive K_G values and is associated with a tall, thin peak and wider tails. Mesokurtic represents normal distribution (Figure 3.4). Sediment plinths to be used for thin sections were scribed from the walls of the excavation for layers 2, 4, 8, 9 and 10. Plinths were plastic wrapped to retain moisture then plaster jacketed to retain structure prior to removal from the wall. Thin sections were prepared by Adelaide Petrographic Laboratories in Stepney, South Australia, and examined under plain and cross-polarised magnification.

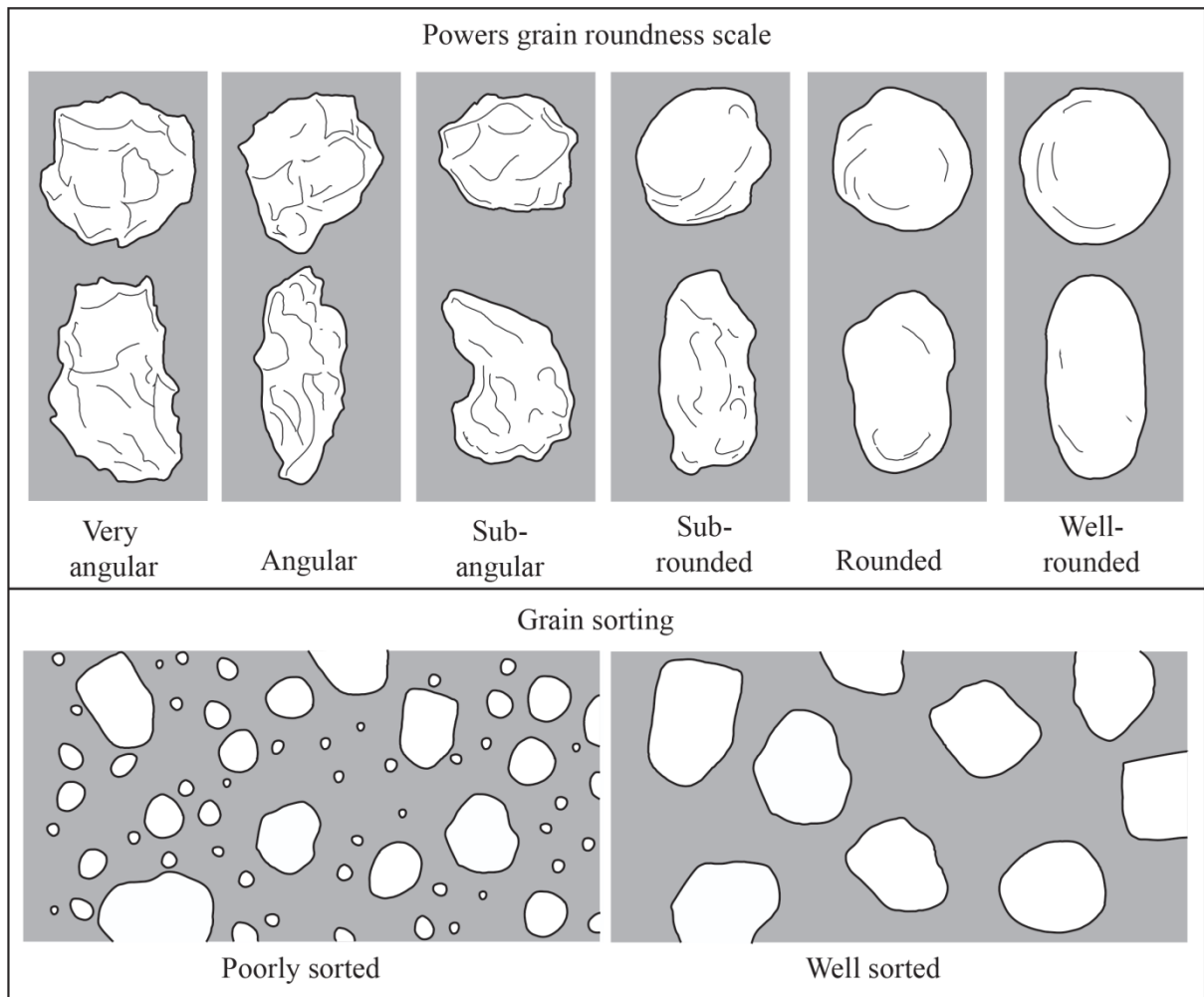


Figure 3.3. Powers grain roundness scale following Powers (1953) and an overview of grain sorting classes.

Table 3.3. Geometric (modified) Folk and Ward (1957) graphical measures.

Sorting (σ_G)		Skewness (Sk_G)		Kurtosis (K_G)	
Very well sorted	<1.27	Very fine skewed	-0.3 to -1.0	Very platykurtic	<0.67
Well sorted	1.27–1.41	Fine skewed	-0.1 to -0.3	Platykurtic	0.67–0.90
Moderately well sorted	1.41–1.62	Symmetrical	-0.1 to +0.1	Mesokurtic	0.90–1.11
Moderately sorted	1.62–2.00	Coarse skewed	+0.1 to +0.3	Leptokurtic	1.11–1.50
Poorly sorted	2.00–4.00	Very coarse skewed	+0.3 to +1.0	Very leptokurtic	1.50–3.00
Very poorly sorted	4.00–16.00			Extremely leptokurtic	>3.00
Extremely poorly sorted	>16.00				

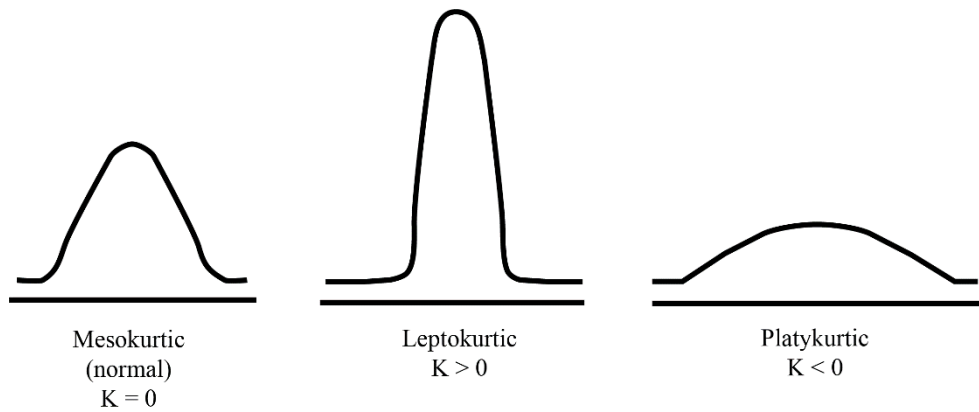


Figure 3.4. Stylised curves showing mesokurtic, leptokurtic and platykurtic distributions.

Samples for XRF, XRD and LOI analysis were submitted to the University of Wollongong by LJA. XRF reported on the %Wt abundance of 11 major oxides; Na₂O (sodium oxide), MgO (magnesium oxide), Al₂O₃ (aluminium oxide), SiO₂ (silicon dioxide), P₂O₅ (phosphorus pentoxide), SO₃ (sulphur trioxide), K₂O (potassium oxide), CaO (calcium oxide), TiO₂ (titanium dioxide), MnO (manganese (II) oxide), Fe₂O₃ (iron(III) oxide), and LOI. The abundance of 33 minor elements were reported in ppm: Cl (chlorine), V (vanadium), Cr (chromium), Co (cobalt), Ni (nickel), Cu (copper), Zn (zinc), Ga (gallium), Ge (germanium), As (arsenic), Se (selenium), Br (bromine), Rb (rubidium), Sr (strontium), Y (yttrium), Zr (zirconium), Nb (niobium), Mo (molybdenum), Cd (cadmium), Sn (tin), Sb (antimony), Cs (cesium), Ba (barium), La (lanthanum), Ce (cerium), Hf (hafnium), Ta (tantalum), W (tungsten), Hg (mercury), Pb (lead), Bi (bismuth), Th (thorium), and U (uranium).

XRD analysis measured the %Wt abundance of 20 crystalline structures: quartz, albite, albite-Ca low An16, albite-Ca low An28, labradorite, orthoclase, microcline, calcite, aragonite, high mag calcite, hematite, kaolinite, chlorite, illite, mixed-layer illite-smectite, ankerite, siderite, gypsum, goethite and muscovite. Sediment samples were submitted for XRD analysis on two separate occasions as the excavation progressed. On the second occasion, proportions of La, Ce, ankerite, siderite, gypsum, goethite and muscovite were not recorded, therefore, these abundances are only reported for layers 1–9. Abundance of elements of V, Cr, Co and Ni are probably due to contamination from a Cr-steel crushing vessel used during preparation for XRF analysis, as identified by workers at the University of Wollongong that

processed the sample and have not been included in this analysis. Samples from disturbed layers were reported but are not included in this analysis.

Only the major oxides were found useful for the purposes of this thesis and are reported in this chapter. Minor elements and crystalline structures are included in Appendix B Table 7.3, Table 7.4) but are not reported in this chapter. Exceptions to this are quartz and calcite, which are included where relevant in sedimentological descriptions.

Pearson's Correlation Coefficient (r) was used to test for linear relationships between oxides, quartz and calcite. The chemical composition of the excavated sediments is compared with that of sediments surrounding Cathedral Cave and the limestone bedrock (Table 3.1).

3.4.3 Chronology

The chronology of the sediments in Cathedral Cave was constructed using all available chronological data. These data include OSL and charcoal ages from the FU excavation and previously published charcoal ages (Dawson and Augee, 1997).

3.4.4 Radiocarbon dating

To test the existing chronology for Cathedral Cave (Dawson and Augee, 1997), AMS radiocarbon dating was attempted on bone samples from the UNSW excavation (Appendix B Table 7.6). Samples were selected based on general preservation, choosing better preserved bones that appeared to be more likely to have retained collagen and these were sent to the Australian Nuclear Science and Technology Organisation (Fink et al., 2004). Collagen was extracted from the bone samples using a modified Longin technique (Longin, 1971), then purified via ultrafiltration (Brown et al., 1988; Higham et al., 2006). The ratio of carbon and nitrogen content (N%) of the bones was determined to assess the collagen content and thereby suitability of bones for AMS radiocarbon dating (DeNiro and Weiner, 1988; Van Klinken, 1999).

Charcoal samples were primarily collected *in situ* during excavation of the Flinders University pit and were not pooled. The charcoal was usually of small quantities, often wet and appeared highly degraded. Later, it was discovered that a small number of charcoal samples had been collected during wet screening of sediments when it was observed floating to the top of the screens. It was not possible retrospectively to differentiate between samples collected *in situ* and those collected during wet screening as they had all been placed in the

same repository. It is possible that some of the wet-screen samples pooled more than one charcoal fragment from within a 5 cm spit.

Samples were selected for AMS radiocarbon dating based on weight of sample and stratigraphic provenance. Preference was given to samples that did not originate in quadrats C, D, F, III and IV due to the potential for contamination from the adjacent backfill sediments that probably originate from the 1881 excavation. However, some samples from quadrat IV were selected when samples from other quadrats were not available. When depth of charcoal samples was recorded by a range i.e., spit depth, rather than absolute location, depth is given as the deepest extent of the spit depth range e.g., 210–215 cm is reported as 215 cm in this thesis.

Charcoal samples collected during the early stages of the FU excavation were submitted for AMS radiocarbon dating at the University of Waikato Radiocarbon Dating Laboratory in 2016 (Appendix B Table 7.7). Samples were cleaned using acid-base-acid (ABA) pre-treatment cleaning procedure. Samples were washed in hot HCl, rinsed and treated with multiple hot NaOH washes, remaining NaOH insoluble fraction was treated with hot HCl, filtered, rinsed and dried and converted to CO₂. AMS radiocarbon measurements were made on these samples by the contracted AMS provider using Waikato's standard measurement procedures (Waikato University, 2017). Radiocarbon ages were calibrated using OxCal v4.2.4 (Bronk Ramsey, 2013) and the SHCal13 atmospheric curve (Hogg et al., 2013). Charcoal samples collected in the later stages of the excavation were submitted to the Australian Nuclear Science and Technology Organisation (ANSTO) for AMS radiocarbon dating (Appendix B Table 7.8). These samples were pre-treated and cleaned using standard ANSTO ABA procedure. All conventional radiocarbon ages (yrsBP) were calibrated to calendar ages (CalBP) using the SHCal13 Southern Hemisphere calibration curve (Hogg et al., 2013) using OxCal 4.3 (Bronk Ramsey, 2009).

3.4.5 Optically Stimulated Luminescence Dating

OSL samples were taken from cleaned exposure faces using PVC or metal tubes, which were immediately sealed in opaque plastic containers upon extraction. Quartz grains were processed under safe (dim red) light conditions at the University of Adelaide's Prescott Environmental Luminescence Laboratory using standard preparation procedures (Aitken, 1985, 1998), including a 48% hydrofluoric acid etch (40 minutes) to remove the alpha-irradiated outer layers of the quartz extracts.

OSL measurements were made using the experimental apparatus described by Arnold et al. (2016). For equivalent dose (D_e) evaluation, quartz grains with a diameter of 212–250 μm were measured in aluminium discs drilled with an array of $300 \times 300 \mu\text{m}$ holes to ensure true single-grain resolution (Arnold et al., 2012a). Individual D_e values were determined using a single-aliquot regenerative-dose procedure (Murray and Wintle, 2000) with a regenerative dose preheat of 260 °C for 10 s and a test dose preheat of 160 °C for 10s. Between 500 and 700 single-grain D_e measurements were made for each sample with individual D_e values being included in the final age calculation if they satisfied a series of standard and widely tested quality-assurance criteria as detailed in Arnold et al. (2013); Arnold et al. (2016). Sensitivity-corrected dose-response curves were constructed using the first 0.08 s of each OSL stimulation after subtracting a mean background count obtained from the last 0.25 s of the signal.

Environmental dose rates were estimated using a combination of *in situ* field gamma spectrometry and low level beta counting or high-resolution gamma spectrometry, taking into account cosmic ray contributions (Prescott and Hutton, 1994), an assumed minor internal alpha dose rate (Bowler et al., 2003), beta-dose attenuation and long-term water content. Beta and gamma dose rates of samples CC16-5, CC16-8, CC16-9 and CC16-10 were determined using high-resolution gamma spectrometry. Gamma spectrometry measurements could not be undertaken *in situ* on these samples during sample collection. Gamma dose rates of all samples except CC16-5, CC16-8, CC16-9 and CC16-10 were calculated from *in situ* measurements made at each sample position with a NaI:Tl detector, using the ‘energy windows’ approach (Arnold et al., 2012b). Beta dose rates of all samples except CC16-5, CC16-8, CC16-9 and CC16-10 were calculated on dried and powdered sediment samples using a Risø GM-25-5 low-level beta counter (Bøtter-Jensen and Mejdahl, 1988). Cosmic-ray dose rates were calculated using the approach of Prescott and Hutton (1994) and assigned a relative uncertainty of $\pm 10 \%$. Long-term water content is expressed as % of dry mass of mineral fraction, with an assigned relative uncertainty of $\pm 10 \%$.

Overdispersion values estimate the relative standard deviation from a central D_e value in context of a statistical estimate of errors of the individual D_e values in the dataset.

Overdispersion values (%) were calculated using the central age model (CAM) of Galbraith et al. (1999). Three age models were used to calculate the sample averaged D_e value for each sample. MAM-3 is the 3-parameter minimum age model of Galbraith et al. (1999). MAM-4

is the 4-parameter minimum age model of Galbraith et al. (1999). MAM-3_{UL} is the unlogged 3-parameter minimum age model of Arnold et al. (2009), suitable for near zero or negative aged grains. MAM-3, MAM-3_{UL} and MAM-4 D_e estimates were calculated after adding, in quadrature, a relative error of 20 % to each individual D_e measurement error to approximate the underlying dose overdispersion observed in the single-grain dose-recovery tests. The decision between using the MAM-3_(UL) or MAM-4_(UL) for each sample has been made on statistical grounds using the maximum log likelihood score.

3.4.6 Bayesian Depth Model

Bayesian age-depth modelling applies Bayesian statistics to produce an age-depth model that is constrained by the stratigraphic and chronological ordering of dates (Blaauw and Christen, 2011). The model is further informed using prior knowledge, in this instance, priors consist of sediment accumulation rates and a hiatus in accumulation. Bayesian age-depth models were constructed in R statistical software using the rbacon package (Blaauw and Christen, 2018). After considering the ages obtained from OSL and radiocarbon, a hiatus of a maximum of 34.5 ka was set at a depth of 87 cm. The sediment accumulation rate was estimated as 67 yr / cm above a depth of 87 cm and 79 yr / cm below 87 cm. All settings used in the model are given in Appendix B pg. 238.

Model_1 incorporated all 14 OSL ages and five radiocarbon ages (WK43563, WK43564, OZW071, OZW072 and OZW075). Thirteen radiocarbon dates were excluded from this model due to returning infinite dates ($n = 5$), probably originating from backfill sediments ($n = 2$), or having been flagged as less robust during pre-treatment and analysis ($n = 3$)

Model_2 included all 14 OSL dates and two radiocarbon dates (WK43563 and WK43564). All other radiocarbon ages were excluded for the reasons outlined above in Model_1, additionally, OZW071, OZW072 and OZW075 were excluded after considering that these have given finite ages at depths below which other charcoal samples had returned infinite ages. WK43563 and WK43564 were retained as no issues impacting confidence of these ages has been identified. These samples are relatively young and thus less prone to errors caused by contamination of older samples. Additionally, these ages align with OSL ages for Unit 1, adding further confidence.

Model_3 uses all 14 OSL ages. All radiocarbon ages were excluded for the reasons outlined in Model_1 and Model_2. The remaining two radiocarbon ages for samples WK43563 and WK43564 were excluded for consistency.

3.4.7 Taphonomy

It has previously been established that the Cathedral Cave palaeofaunal assemblage has accumulated via pitfall trapping and the predatory action of owls and *Macroderma gigas* (Dawson and Augee (1997). The purpose here is to refine the taphonomic reinterpretation of the site. Bones were examined for taphonomic modifications that may assist in the interpretation of the assemblage, including associated or articulated elements, bite marks, termite damage and evidence of weathering. Weathering on larger bones was assessed against a six-stage system of weathering developed for taxa with an adult body mass <5kg (Behrensmeyer, 1978).

3.4.8 Curation

All identified fossils used in this thesis were assigned an interim reference number, prefixed by CCW, pending curatorial assignment at the Australian Museum. All specimens used in this chapter are presently held in the palaeontology research laboratories at Flinders University and will be transferred to the Australian Museum when no longer required. Specimens published as part of other studies have been assigned AM collection numbers and these are used preferentially to interim CCW reference numbers when available.

3.5 Results

3.5.1 Stratigraphy

The sediments in Cathedral Cave were excavated to a depth of 420 cm in the FU excavation during four field trips between 2016 and 2017 (Figure 3.5). An additional field trip in April 2019 reached ~500 cm. Data from the 2019 field trip is not included in this thesis as it is surplus to the aims of this thesis and would require substantial additional time to analyse. Some key specimens and observations from the 2019 field trip are referred to when relevant.

Twenty stratigraphic layers and sublayers were initially distinguished chiefly by sediment colour, level of induration and texture. Subsequently, this was reduced to 13 layers by excluding sedimentary changes that are recognised as secondary infills, and also by combining layers subsequently recognised as representing a single, distinct stratigraphic layer (Appendix B Table 7.10).

The uppermost layer of sediment lacked any evidence of grain sorting and contained post-European anthropogenic artefacts including small pieces of glass, bits of metal and a musket bullet. This is consistent with European artifacts encountered in the top metre of sediment in the UNSW excavation (Dawson and Augee, 1997). These sediments are rich in the remains of both extant and extinct fauna, but the disturbance and lack of provenance severely limits the value of this layer for scientific analysis. These sediments probably derive from an admixture of those derived from excavations for tourism development of the cave and of the earlier fossil excavations. No further analysis was undertaken on this layer and it is hereafter referred to in this thesis as “disturbed sediments”. A brief discussion on the origin of these disturbed sediments is included in Appendix A pg. 228.

During the initial stages of the excavation, a second unit of reworked sediment was encountered. The reworked sediments are not well consolidated, mottled and contain multiple inclusions with very little fossil material. Initially, these sediments covered a significant proportion of the excavation area (Figure 3.6a) although this decreased with depth. The boundary of the mottled sediment with the undisturbed sediments is straight and clearly does not belong to a natural cave feature. This was confirmed by the recovery of post-European artefacts, including an undamaged amber glass bottle at a depth of 3 m, timber and a rusted metal peg. The bottle is typical of an 1870s – 1880s alcoholic spirits container (H. Burke, pers coms). The reworked sediments are interpreted as those backfilling a previous

excavation, possibly part of the 1881 AM excavation (Ramsay, 1882). Alternatively, it could be one of Mitchell's unmapped trenches (Mitchell, 1838). At a depth of 4.2 m, the trench was still evident but had thinned considerably. At a depth of 5 m, obtained during the April 2019 field trip, the excavation had either reached the bottom of the old trench, or no longer intersected it. Sediments from the old trench are referred to as 'backfill sediments' in this thesis and are easily distinguished from *in situ* sediments (Figure 3.6b).

Several small soil pipes intruded into *in-situ* sediment. These are mostly small, localised intrusions and easily distinguished from *in-situ* sediments by being rich in charcoal and darkly coloured. Only the largest soil pipes are noted on the stratigraphic diagram as holes (Figure 3.5). Samples from soil pipe sediments are labelled as BT (black tube) and the depth. Soil pipe samples were not analysed as part of this study.

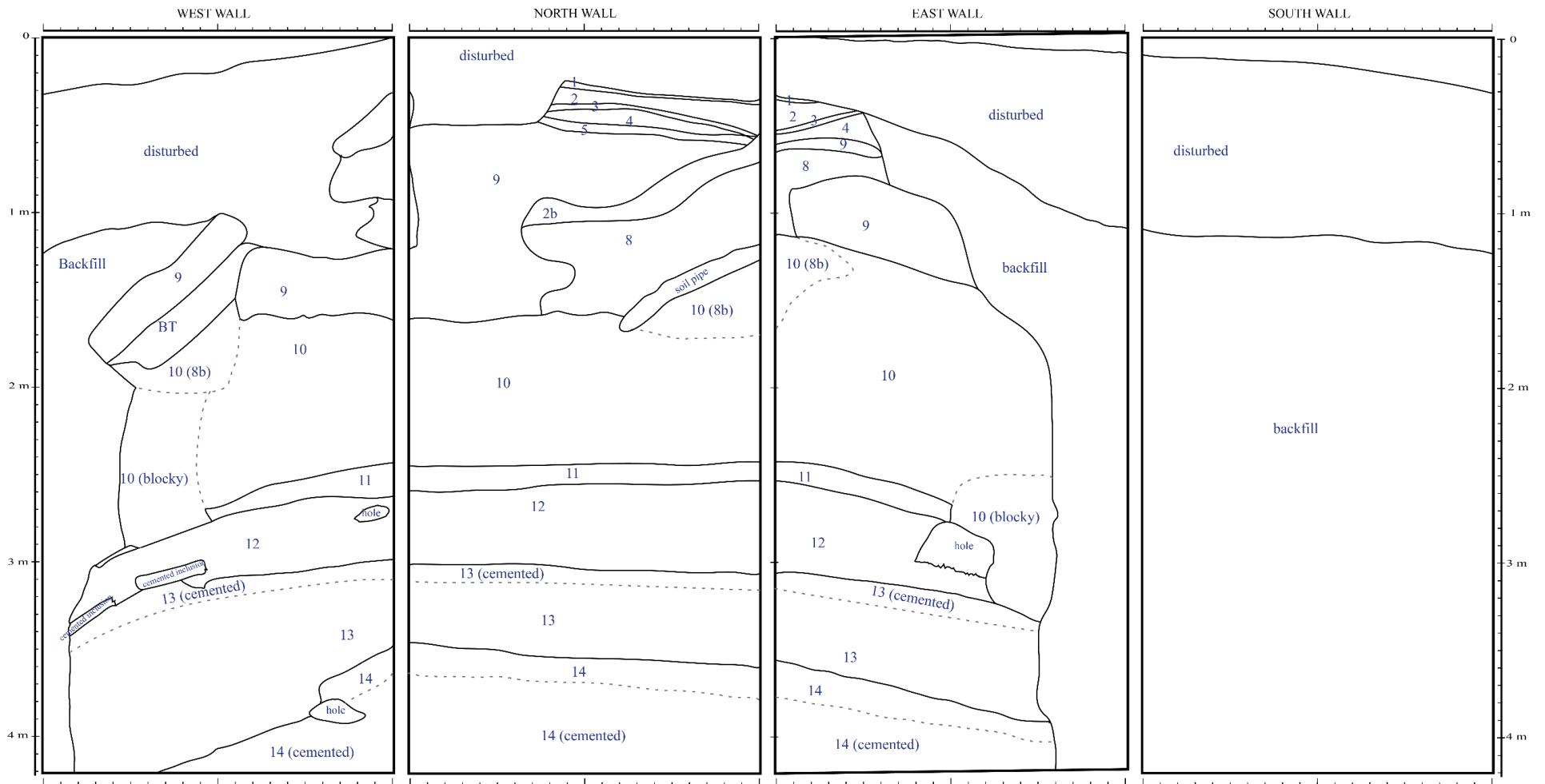


Figure 3.5. Stratigraphic section of Cathedral Cave. Dashed lines indicate former boundaries of combined layers.



Figure 3.6. East wall of excavation showing a) boundaries between the *in situ* sediment layers on the left and the disturbed and backfill on the right; b) easily defined boundary between *in situ* sediment on left and backfill on right.

3.5.2 Description of stratigraphic layers

All strata in the excavation are truncated by disturbed or backfill sediments on their southern margin (Figure 3.5). The area of layers 1–8 were substantially truncated and as a result, the degree of dip was unable to be determined for these layers. From layer 9 and below, all strata in the FU excavation dip approximately 20° from north to south, away from the Altar more evenly so on the east wall. A description of the sediment samples is included in Appendix B Table 7.11.

Layer 1, directly below the disturbed layer, is friable brown (7.5YR 4/4) very coarse silt of a fairly uniform 2-cm thickness (Figure 3.5; Figure 3.7a). Sand-sized grains are rare and sub-angular. Viewed under magnification, the layer contains abundant organic material including insect carapaces and wood/charcoal, as well as flakes of carbonate material. Purple clay clasts, up to a few mm in diameter, appear to be derived from palaeoclasts such as those visible in the chimney G123 and on the roof of Cathedral Cave near the Altar.

Layer 2 is friable dark brown (7.5 YR 3/3) coarse silt of variable thickness that reaches a maximum of around 20 cm (Figure 3.5; Figure 3.7a). Sand-sized grains are mostly quartz and range from angular to rounded, with the majority characterised by sub-angular morphology. Petrographic analysis reveals microlaminations and aggregates of silt and clay as well as numerous wood / charcoal particles (Figure 3.8a).

Layer 2b is brown (7.5 4/4) coarse silt of a maximum thickness of 20 cm. Layer 2b caps layer 8 and with it, forms a stratigraphic reversal, cutting through layers 3, 4 and 5, as visible on the north and east walls (Figure 3.5; Figure 3.7a). There is no visible distinction between layer 2 and layer 2b, with the latter appearing to be an intrusion of layer 2 that has excavated into underlying sediments via a fissure. Sand-sized grains are predominately sub-rounded quartz, although morphology ranges from sub-angular to rounded. The sediments contain microlaminations (Figure 3.8b).

Layer 3 is friable pink (7.5YR 7/4) very coarse silt approximately 2-cm thick (Figure 3.5; Figure 3.7a). Sand sized grains are infrequent in the sample and ranged from angular to rounded, but most are best described as sub-angular quartz. The thin section for layer 3 was unsuccessful, possibly due to layer 3 lensing out in the section of the plinth that was processed for thin section. Magnification showed that sediments are comprised mostly of pale coloured aggregates. This layer is conspicuous in being visibly unlike other layers

encountered in the excavation. In both the north and east wall, layer 3 slopes down toward the north-east corner of the pit, highlighting a depression that has formed above the void where layer 2b and 8 intrude.

Layer 4 is reddish brown (5 YR 4/4) friable coarse silt with a thickness of around 13 cm (Figure 3.5; Figure 3.7a). Sand sized grains are sub-angular to sub-rounded. Magnification showed the sediments consist of mostly of silt and clay aggregates within a silt and clay matrix. The petrographic slides show evidence of microlaminations in some isolated sections; the direction of the lamination varies, indicating that these sediments have undergone displacement, probably during collection or preparation of the petrographic slide (Figure 3.8c).

Layer 5 is composed of dark reddish grey (5 YR 4/2) medium silt with a maximum thickness of ~5 cm (Figure 3.5; Figure 3.7a). Sand-sized grain morphology ranges from sub-angular to rounded, with most being sub-angular. Magnification revealed numerous silt and clay aggregates and very large pebble sized clay coated aggregates comprising of manganese and an unidentified carbonate material. Small carbonate crystals have formed on the clay coating of some of the large pebble sized aggregates.

Layer 8 is yellowish red (5 YR 4/6) medium silt with a maximum thickness of 55 cm (Figure 3.5). Layer 8 is capped by layer 2b, underlain by a charcoal rich soil pipe, and intrudes into layer 9. Layer 2b and 8 are interpreted as infilling an erosional feature. The source of layer 8 is unknown, but it may represent a fissure fill. Sand sized grains are sub-angular to rounded, with most being sub-angular. In thin section, layer 8 contains less silt and clay aggregates than overlying layers, but the silt and clay matrix contain a higher proportion of clay sized grains. Some bone is associated with spar and adhesions of calcite cement, as identified by its extreme birefringence, creamy white interference colour, and presence of birefringent dust on extinction (Figure 3.8d).

Layer 9 is yellowish red (5 YR 5/8) interbedded dirty flowstone with a maximum thickness of around 1100 mm (Figure 3.5; Figure 3.7a). Unconsolidated sediments from this layer contain medium to coarse silt sized particles. The top of layer 9 is capped by a well cemented dirty flowstone of varying thickness that contains a shallow basin in quadrat B (Figure 3.7b), probably the result of a continuous water drip. The capping is partially underlain by the

intrusion of layer 2b. Sand sized grains were not able to be isolated from the layer 9 sediment sample, for all particles in this size range are aggregates or bone fragments.

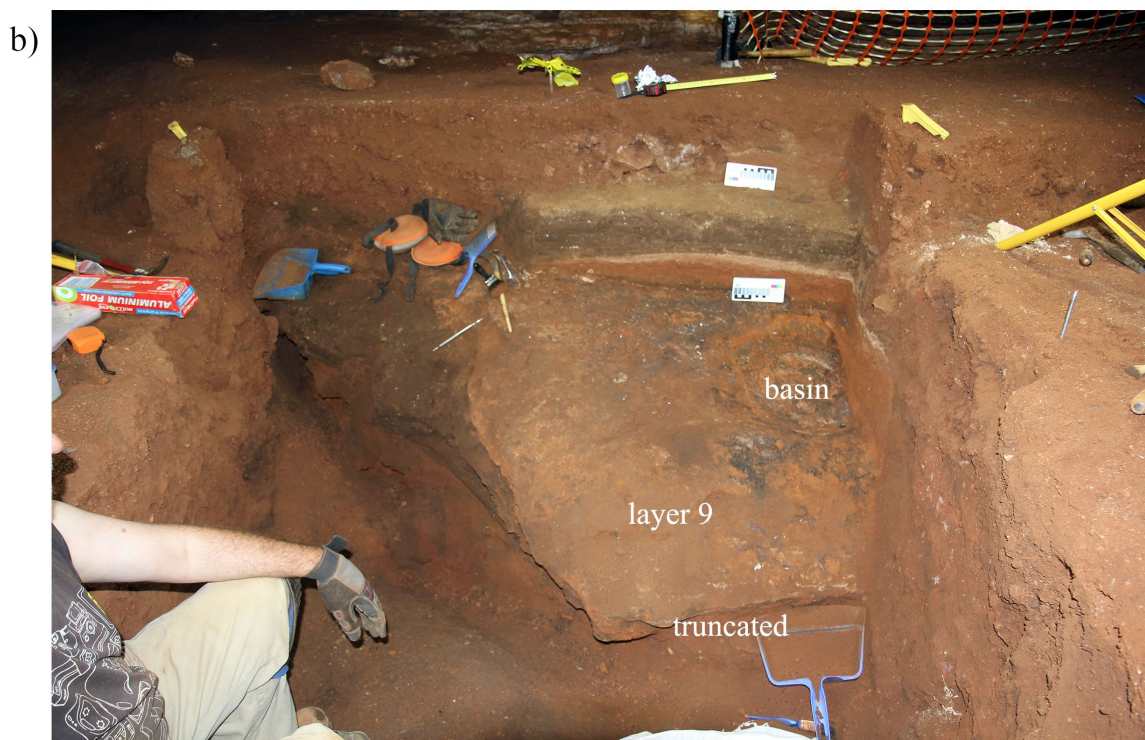
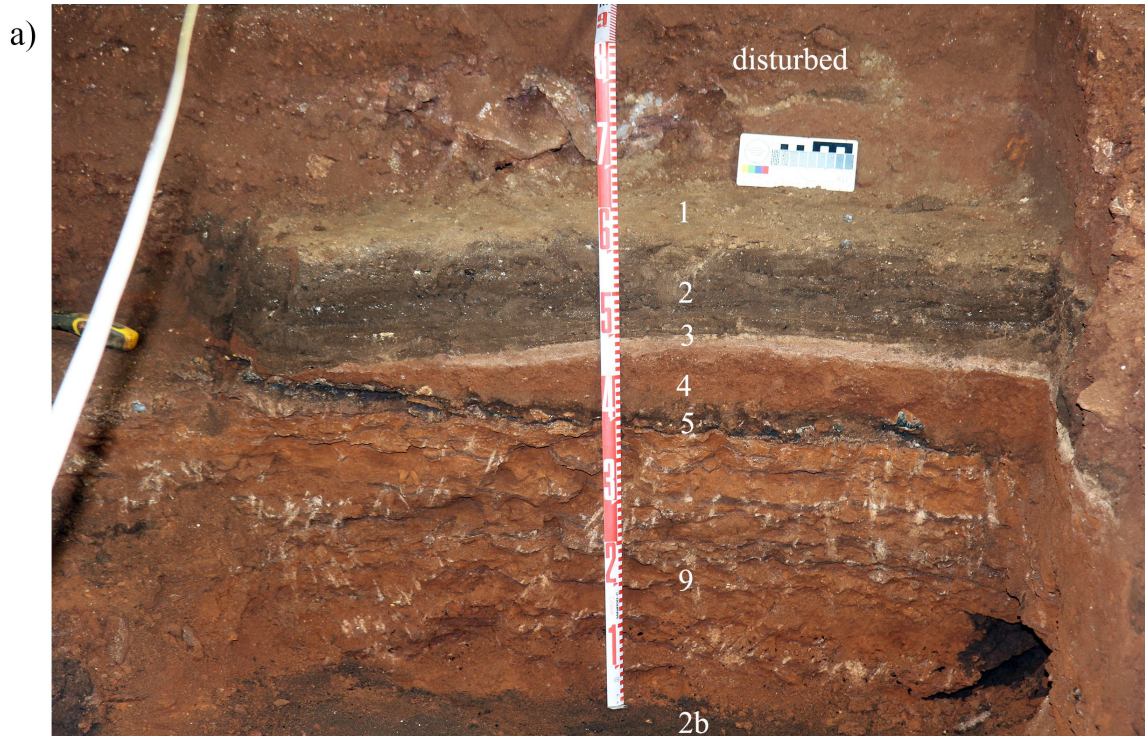


Figure 3.7. North wall of the excavation showing a) layers 1 – 7 and 9; b) top of layer 9 showing shallow basin. Sharp edge shows where layer is truncated by backfill sediments. Black squares on scale bar card represent 1cm.

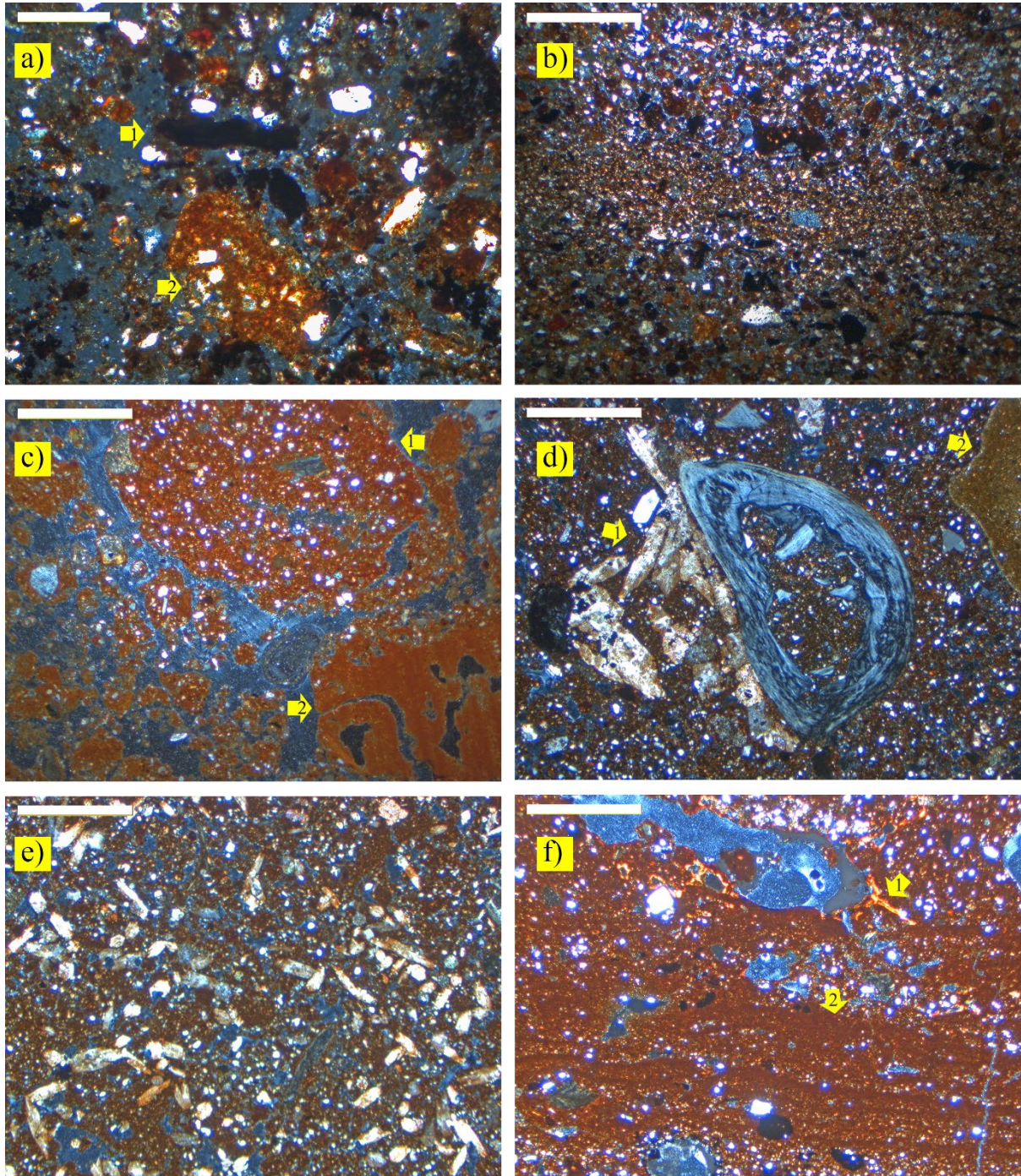


Figure 3.8. Images from petrographic slides of Cathedral Cave sediments – scale for a) is 200 μm , all others 1 mm, a – c under plain light, d – f under cross polarised light. a) charcoal (1) and silt / clay aggregates (2) in layer 2; b) microlaminations within silt-clay matrix of layer 2; c) large silt-clay aggregate (1) and displaced microlamination (2) in layer 4; d) carbonate spar (1) associated with bone and limestone fragment (2) in layer 8; e) carbonate spar in silt-clay matrix in layer 9; f) plasmic fabric (1) and microlaminations (2) in layer 10.

Petrographic analysis of layer 9 shows a dense silt and clay matrix, with some silt and clay aggregates and bone fragments. Bones frequently have calcite cement associated with the external and internal surfaces. Calcite spar is abundant in the matrix (Figure 3.8e). Bones embedded in the flowstone were oriented in a north-south direction following the slope away from the Altar.

Layer 10 is dark red (2.5 YR 4/8) and composed of coarse silt and fine sand (Figure 3.5). The layer has a maximum thickness of 1300 mm. Sand size grains are angular to sub-rounded, with most being sub-angular. A petrographic slide taken from the upper portion of layer 10 comprises of a dense silt and clay matrix that largely lacks the silt and clay aggregates that characterise some of the overlying layers in the sequence (Figure 3.8f). Calcite spar and cement is present but infrequent and far lower than observed in layer 9. Bones viewed on thin section do not have associated calcite cement as in layer 9. Localised lamination of silt and clay particles is evident, and some pores are bordered by plasmic fabric created by the arrangement of uniformly oriented, optically anisotropic clay particles, this is sometimes referred to as “bright clay. These features are interpreted here as being water escape features.

Layer 11 is yellowish red (5 YR 5/8) lithified dirty flowstone that reaches a maximum thickness of around 15 cm deep (Figure 3.5). Large cracks run through the top face of this layer (Figure 3.9). The layer comprises of several distinct horizons, the first is a capping of heavily cemented silt and clay, followed by a horizon of cave pearls embedded in indurated silt and clay matrix (Figure 3.10a–b). Voids filled or bordered with spar indicate that this layer has undergone diagenesis. Cave pearls are formed by deposition of calcium carbonate in concentric layers around a nucleus (Jones, 2009). Formation of cave pearls occurs in basins and pools where water agitation, usually a drip, prevents the formations attaching to the substrate as they form. However, there is no evidence of a suitable basin or depression within the excavation boundary, signifying that the cave pearls have been transported downslope from the original site of formation. Directly below the cave pearls lies a dark manganese band, and below this, more lithified silt and clay. A small band of higher quality flowstone ~1 cm thick is located in the north-west corner of the pit. Very little evidence of fossil material was observed in this layer, and the high level of lithification proved problematic for retrieval. The lithified sediments were unable to be sufficiently broken down with a 10 % acetic acid dilution and higher dilutions would potentially damage any fossil material, thus acid digestion was discontinued.



Figure 3.9. Cracks visible in the top of layer 11. North wall is top of page.

Layer 12 is yellowish red (5 YR 4/6) with very fine sand and very coarse silt sized particles (Figure 3.5). The layer has a maximum thickness of around 50 cm. and encompasses small clasts of dirty flowstone. Sand sized grains are sub-angular to sub-rounded, with most having sub-angular morphology.

Layer 13 is dark red (2.5 YR 4/6) medium silt with a maximum thickness of around 55 cm (Figure 3.5). The top ~30 cm of layer 13 is heavily cemented with limestone clasts up to 30 cm in size. The clasts are mostly thinly bedded limestone rather than massive limestone. Cemented sections of layer 13 often broke along uneven horizontal planes, creating slabs of variable thickness when leverage was applied (Figure 3.10c). Calcite cemented pebble and sand sized aggregates are frequent. Quartz grains show sub-angular to sub-rounded morphology.

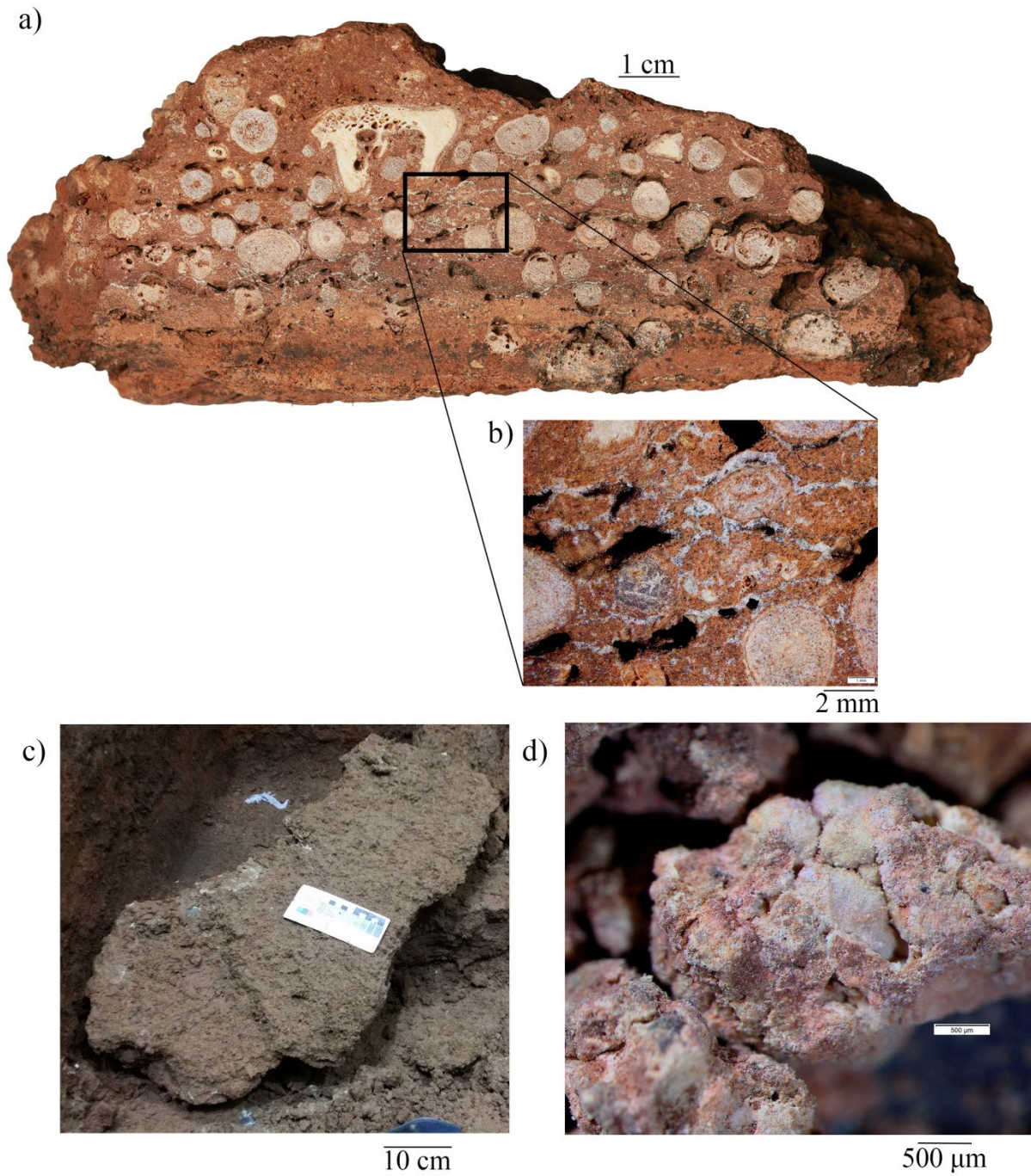


Figure 3.10. Sediment morphology a) cross section of lithified sediments of layer 11, including cave pearls and fossil; b) magnified view of cross section of layer 11 showing spar in voids; c) uneven slabs of layer 13; d) aggregates of layer 14.

Layer 14 is composed mostly of yellowish red (5 YR 5/6) medium to coarse silt (Figure 3.5). Sample CC17-SB, taken from the less cemented sediment at the top of layer 14 differs in colour, being reddish brown (5YR 4/4). By January 2017, layer 14 had been excavated to a thickness of 75 cm but its extent remains to be determined (Figure 3.5). Layer 14 sediments are largely cemented bone breccia, however, the top ~15 cm of layer 14 is less cemented. The level of cementation exceeds that of layer 13. Boulder sized limestone clasts are common up to 30 cm in size. Under magnification the less cemented sediments are comprised almost entirely of aggregates of silt and clay (Figure 3.10d). Grain morphology is sub-angular to sub-rounded, but quartz grains are rare. However, locating grains was difficult due to the high levels of aggregation.

3.5.3 Grain size analysis

Laser diffraction particle size analysis (Figure 3.11; Table 3.4) showed that the Cathedral Cave sediments are composed primarily of silt (69.3–23.5 %) with varying amounts of clay sized particles (27.4–8.8 %). Sand sized particles are also present (12.2–10.9 %). However, when viewed under magnification, the sediments include very little sand, thus, the abundance of sand sized particles is probably a result of the silt and clay aggregates that are prominent throughout the Cathedral Cave sediments. The majority of samples showed bimodal and trimodal distribution (Table 3.4), revealing that the sorting, skewness and kurtosis statistics for the multimodal samples are not reliable as these statistics are generally applied to unimodal distributions (see Blott and Pye, 2001). The uppermost sample from each of layers 9 and 10 showed trimodal distribution, in contrast to the mode of other samples from these layers which were bimodal (layer 9) and unimodal (layer 10). All sediment samples returned high standard deviation (σ_G) values indicating that the sediments throughout the excavation are very poorly sorted ($\sigma_G = 4.00$ – 16.00) to poorly sorted ($\sigma_G = 2.00$ – 4.00). Skewness (Sk_G) values show that particle size in most samples is very fine skewed ($Sk_G = -0.3$ – -1.0) to fine skewed ($Sk_G = -0.1$ – -0.3). A single sample in layer 12 is symmetrical ($Sk_G = -0.1$ – 0.1). Kurtosis (K_G) values show broad variation, with values ranging between very platykurtic and very leptokurtic (Table 3.4).

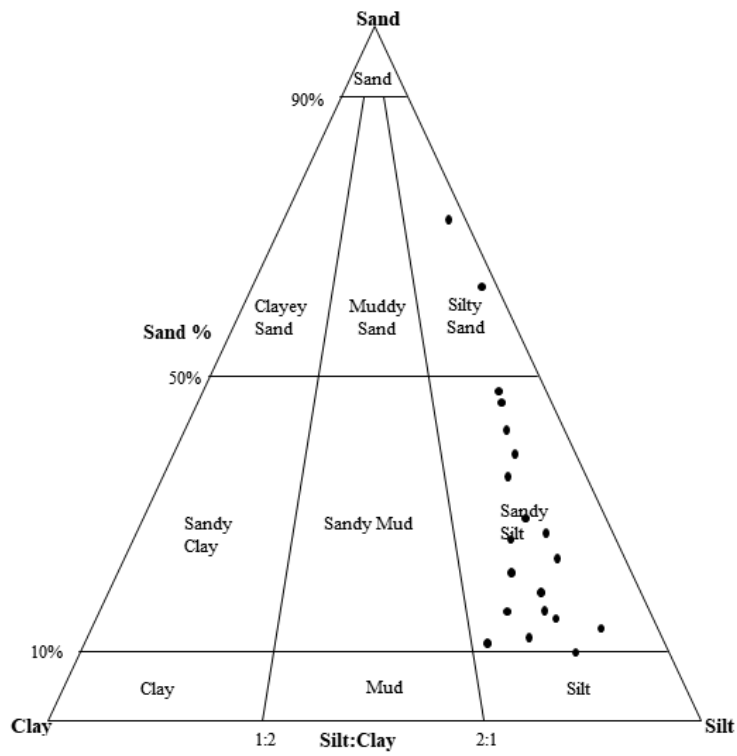


Figure 3.11. Ternary diagram for Cathedral Cave samples, showing the majority of sample falling within the range of Sandy Silt or Silty Sand despite very little sand being evident in the sediments.

Table 3.4. Grainsize analysis and sediment statistics for Cathedral Cave sediment samples

Sample	Layer	\bar{x}	σ_G	Sk_G	K_G	Mode 1	Mode 2	Mode 3	D10	D50	D90	Sand	Silt	Clay
		μm				μm			μm			%		
CC16-S3	1	37.14	7.74	-0.16	0.82	475.06	84.48	3	2.16	45.41	436.12	43.3	47.9	8.8
CC16-S4	2	21.46	4.35	-0.51	1.08	53.3	1.89		1.87	36.12	91.51	24.5	65	10.4
CC16-S12	2b	23.39	6.14	-0.11	1.14	37.74	475.1		1.91	27.56	330.05	28.3	61.5	10.2
CC16-SA	3	46.7	6.61	-0.23	0.9	75.29	377.35		2.82	59.65	396.52	48.9	43.9	7.2
CC16-S6	4	29.38	4.85	-0.47	1.07	75.29			2.13	47.38	140.59	39.8	50.8	9.4
CC16-S7	5	13.08	4.43	-0.36	0.88	33.63			1.31	19.01	64.89	10.9	74.7	14.4
CC16-S10	8	13.48	5.16	-0.28	0.82	37.74	1.69		1.24	19.45	87.25	17	66.9	16.1
CC16-S8	9	15.13	4.79	-0.47	0.87	42.34	1.06	3	1.22	25.77	74.64	45.8	69.3	14.9
CC16-S11	9	15.66	5.2	-0.42	0.87	42.34	0.95		1.16	26.12	88.25	19.7	65	15.3
CC16-S23a	9	11.12	5.23	-0.33	0.71	42.34	1.19		0.97	16.78	69.61	13	66.5	20.5
CC16-S20	10	16.66	5.94	-0.34	0.78	67.1	3	1.19	1.13	25.97	118.13	27.4	56.4	16.2
CC16-S28	10	126.51	3.69	-0.26	1.2	168.56			20.12	140.32	478.2	73.9	23.5	2.5
CC16-S34	10	18.35	3.74	-0.35	1.07	37.74			2.28	24.46	73.59	14.4	77	8.6
CC17-S2	12	45.62	4.23	-0.38	1.61	67.1			3.21	58.78	185.22	47.3	45.1	7.6
CC17-S4	12	93.63	3.27	-0.05	1.24	75.29			21.15	88.62	384.56	64.2	33.5	2.3
CC17-S6	13	11.74	5.8	-0.4	0.7	47.51	0.95	6.71	0.84	20.35	78.01	16.9	61.1	22
CC17-S10	13	7.96	5.98	-0.15	0.66	47.51	0.84	3.36	0.69	9.66	68.2	12.2	60.4	27.4
CC17-SB	14	24.8	5.16	-0.55	1.13	67.1	0.95		1.5	46.07	120.52	36.5	51.5	12
CC17-12	14	15.12	5.75	-0.47	0.77	53.3	1.06		1.01	28.87	93.49	22.6	58.9	18.5
CC17-S15	14	22.6	4.85	-0.55	1.18	59.81	1.06		1.47	41.26	103.47	30.4	57.2	12.4

3.5.4 Geochemistry

The abundance of major oxides show variation throughout the Cathedral Cave stratigraphic sequence (Table 3.5). The strongest variations are found in SiO₂ which accounts for 31.52–60.02 %wt of the sample, Al₂O₃ (9.7–15.02 %wt), P₂O₅ (1.07–6.75 %wt), SO₃ (0.04–5.0 %wt), CaO (2.5–23.83 %wt) and Fe₂O₃ (3.61–6.99 %wt). Minor variation occurs in the lesser occurring oxides Na₂O (0.67–2.88 %wt), MgO (0.45–0.77 %wt), K₂O (1.22–1.85 %wt), TiO₂ (0.51–1.12 %wt) and MnO (0.04–0.60 %wt). Total organic carbon content varies from 9.15–26.68 %wt as revealed by Loss On Ignition (LOI) scores (Table 3.5). The most abundant oxide, SiO₂ shows strong a strong positive linear relationship with TiO₂ ($r = 0.96$), Fe₂O₃ ($r = 0.94$), Al₂O₃ ($r = 0.91$) and K₂O ($r = 0.77$), a strong negative linear relationship with CaO ($r = 0.80$) and LOI ($r = 0.95$) and a moderate negative relationship with Na₂O ($r = -0.56$) and SO₃ ($r = -0.56$) (Appendix B Table 7.2). This trend is emulated through most of the major oxides, with SiO₂, Fe₂O₃, Al₂O₃, K₂O and TiO₂ having significant positive linear relationships and mostly significant negative linear relationships with CaO, Na₂O, P₂O₅, SO₃ and LOI. Na₂O and SO₃ have a strong positive linear relationship to each other ($r = 0.82$) and strong to moderately positive linear relationships to P₂O₅ ($r = 0.96$ and 0.66 respectively) and a moderately positive relationship with CaO ($r = 0.50$ and 0.55 respectively). CaO has a moderately positive linear relationship with LOI ($r = 0.68$) but does not show a significant linear relationship with Na₂O, SO₃ or P₂O₅ ($r = 0.08$, 0.05 and -0.03 respectively).

Three distinct oxide signals are evident within the Cathedral Cave sediments. Group one is SiO₂, TiO₂, Fe₂O₃, Al₂O₃ and K₂O, group two includes Na₂O, P₂O₅ and SO₃ and CaO is the sole member of a third grouping. The relative abundances of the three groups are visualised in Figure 3.12a. LOI has a strong negative linear relationship to group 1 oxides ($r = -0.7$ – -0.95), a strong to weak positive linear relationship to group 2 oxides ($r = 0.36$ – 0.55) and a moderate positive linear relationship to CaO ($r = 0.68$). Quartz has a strong positive relationship to group one oxides ($r = 0.76$ – 0.89), a weak negative linear relationship to group 2 oxides ($r = -0.06$ – -0.15) and a strong negative relationship to CaO ($r = -0.89$). Calcite has a moderate negative relationship to group 1 oxides ($r = -0.48$ – -0.61), a weak negative linear relationship to group 2 oxides ($r = -0.28$ – -0.41), a strong positive relationship to CaO ($r = 0.92$) and a strong negative relationship to quartz ($r = -0.79$).

It is notable that XRD analysis reports gypsum abundance in layer 3 at 15.7 %, well above the 4.8 % average reported for layers 1 – 9 (Appendix B; Table 7.2).

The relationships between geochemical composition and stratigraphic layers are best summarised in a principal component plot (Figure 3.12b). Sediment samples from layers 4, 8, 9, 10, 12 and 14 plot near quartz and group 1 oxides on the plot, samples from layers 1, 2, 2b and 3 associate strongest with group 2 oxides. The sample from layer 5 plots between group 2 and group 3 oxides. Samples from layers 9, 13 and 14 are associated with group 3 oxides and calcite. Eigenvalues indicate that PC1 explains 53.86 % of the variation, PC2 explains 29.56 % of the variation and PC axis 3–13 explain 16.58 % of variation overall (Appendix B Table 7.5; Figure 3.12b).

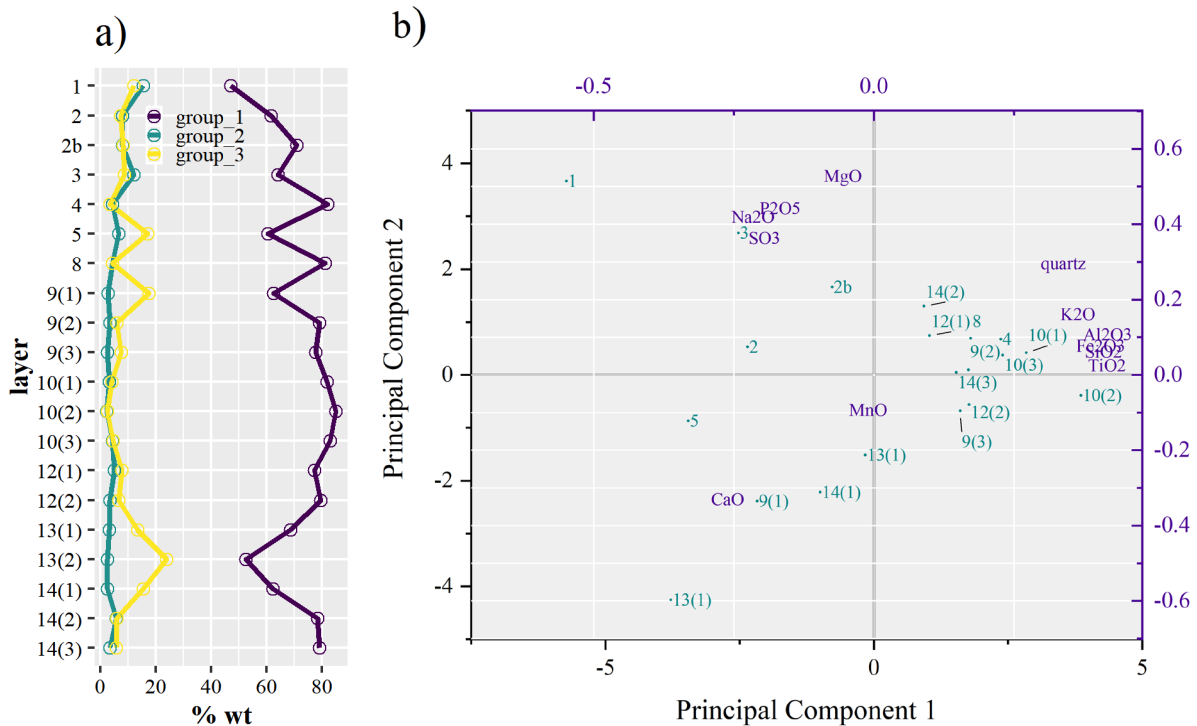


Figure 3.12. a) Relationships between the three oxide groups present in the Cathedral Cave sediments. See text for detail of group membership; b) Principal Component plot showing the relationships between major oxides, quartz, calcite and individual layers.

Table 3.5. X-ray fluorescence analysis of major oxide composition (%wt) of Cathedral Cave sediments and XRD analysis of quartz and calcite crystalline structures (%wt).

Field #	Layer	Na ₂ O	MgO	Al ₂ O ₃	SiO ₂	P ₂ O ₅	SO ₃	K ₂ O	CaO	TiO ₂	MnO	Fe ₂ O ₃	LOI	Quartz	Calcite
%wt															
CC16-S3	1	2.88	0.77	9.75	31.52	6.75	5	1.5	11.94	0.51	0.08	3.61	26.68	42.7	0.7
CC16-S4	2	1.66	0.59	10.27	44.61	3.64	2.01	1.42	7.22	0.69	0.16	4.42	23.75	50.7	0.6
CC16-S9	2b	1.76	0.68	12.22	50.63	5.28	0.13	1.6	8.23	0.84	0.19	5.47	13.55	52.5	0.8
CC16-S5	3	2.13	0.69	11	46.02	4.09	5.2	1.4	8.65	0.77	0.06	4.91	15.71	56.7	0.2
CC16-S6	4	1.03	0.58	14.65	58.22	2.29	0.44	1.79	3.37	0.98	0.04	6.32	10.48	58.7	0
CC16-S7	5	1.74	0.62	9.43	43.49	4.02	0.31	1.22	17.1	0.66	0.6	5.5	16.1	41.5	28.4
CC16-S10	8	1.08	0.63	14.22	57.95	2.65	0.06	1.74	4.26	0.98	0.15	6.17	10.01	54.1	0.2
CC16-S8	9	0.91	0.54	9.79	46.09	1.28	0.04	1.26	17.5	0.77	0.1	4.41	18.26	44.7	31
CC16-S11	9	0.88	0.61	14.24	56.21	1.81	0.06	1.74	6.01	0.96	0.1	5.93	11.49	55	6.4
CC 16-S23a	9	0.67	0.56	13.31	55.79	1.25	0.05	1.73	7.56	0.93	0.04	5.9	12.11	53.3	13.9
CC 16-S20	10	0.79	0.61	14.6	57.64	1.78	0.05	1.77	3.98	1.04	0.25	6.69	10.26	64.5	1.2
CC 16-S28	10	0.53	0.52	15.02	60.02	1.07	0.04	1.85	2.5	1.12	0.2	6.99	10.71	63.8	0.5
CC 16-S34	10	1.01	0.59	14.57	58.75	2.61	0.05	1.77	4.51	1.06	0.18	6.78	9.43	53.4	0
CC 17-S2	12	1.2	0.65	13.19	55.22	2.99	0.08	1.62	7.78	0.96	0.21	6.1	10.88	59.7	5.4
CC 17-S4	12	0.8	0.55	13.48	56.92	1.96	0.04	1.59	6.63	0.99	0.21	6.58	11.38	57	7.8
CC 17-S6	13	0.8	0.53	12.35	48.54	1.73	0.04	1.53	13.43	0.84	0.19	5.33	15.83	52.5	24.4
CC 17-S10	13	0.71	0.45	9.7	36.93	1.23	0.05	1.33	23.83	0.63	0.15	3.93	22.76	24.2	50.1
CC 17-SB	14	0.7	0.52	11.34	43.87	1.13	0.04	1.63	15.33	0.75	0.17	4.66	17.45	45.8	30.4
CC 17-S12	14	1.39	0.64	12.71	56.93	3.66	0.08	1.69	5.8	0.86	0.16	6.05	9.15	62.8	0
CC 17-S15	14	0.89	0.61	13.15	57.18	1.9	0.06	1.66	5.67	0.97	0.12	6.09	11.16	54.7	4.3
Average:		1.18	0.6	12.45	51.13	2.66	0.69	1.59	9.06	0.86	0.17	5.59	14.36	52.4	10.3

3.5.5 Radiocarbon dating

The fifteen bone samples from the UNSW excavation that were submitted to ANSTO for AMS radiocarbon dating were highly degraded and contained insufficient collagen to be dated (F. Bertuch pers coms). These samples were not subject to further analysis. The unsuccessful samples had been collected at depths between 2–3.7 m in the UNSW excavation (Appendix B Table 7.6).

Charcoal samples from the FU excavation provided a range of calibrated ages between 864 ± 38 to $>52,000$ calBP (Table 3.6). However, confidence in some of the samples is limited. The charcoal samples submitted to ANSTO were degraded and of low quantity, which caused difficulties during preparation.

WK43563 and WK4364, from layer 2 and 2b, place these layers in the late Holocene with ages of 864 ± 38 and 1777 ± 31 CalBP respectively (Table 3.6). No issues are reported with these samples and these dates are here considered robust.

OZW084 and OZW085 were collected from the boundary of the backfill sediments and are unlikely to be *in situ*. This is further supported by young radiocarbon ages of 2886 ± 49 and 2444 ± 89 respectively (Table 3.6). Both samples are not considered further in this thesis.

Three of the four charcoal samples from layer 10, OZW076, OZW078 and OZW079, yielded infinite ages $>52,000$ CalBP. The remaining sample for layer 10 OZW077 was dated at $38,072 \pm 813$ CalBP (Table 3.6). However, just 30 micrograms of carbon that remained after the cleaning phase of preparation. To retain this small amount of carbon, cleaning was prematurely concluded. Accordingly, this date is treated with very limited confidence. No issues were reported for the samples that returned infinite ages.

OZW071 from layer 12 yielded an age of $44,613 \pm 419$ CalBP (Table 3.6). This age is younger than the infinite ages shown in layer 10. No issues were reported during preparation of this sample.

Two charcoal samples were collected in layer. 13. OZW072 provided an age of $45,912 \pm 416$ CalBP and OZW081 gave an infinite age $>52,000$ CalBP (Table 3.6). The age for OZW081 is flagged as being less robust due to the size and deterioration of the sample.

Four charcoal samples were collected from layer 14. OZW073 provided an infinite age >52,000 CalBP. The three remaining samples returned finite ages. OZW074 returned an age of $42,668 \pm 406$ CalBP, however, like sample OZW077 from layer 10, this sample was small, resulting in incomplete cleaning during preparation and has been flagged as deserving very low confidence. Two other samples from layer 14, OZW083 and OZW075 returned finite ages of $49,713 \pm 1241$ and $47,892 \pm 470$ CalBP respectively (Table 3.6). The age of OZW083 was flagged as being less robust due to the nature of the charcoal sample.

Table 3.6. Radiocarbon data for charcoal samples from Cathedral Cave samples submitted for AMS radiocarbon dating, showing $\delta^{13}\text{C}$ values, percent Modern Carbon (pMC), conventional radiocarbon age (yrsBP) and calibrated calendar age (CalBP) all with 1σ error. * = values assumed as measured value is not available; nr = not recorded.

Lab Code	Layer	Depth (cm)	$\delta^{13}\text{C}$ per mil	pMC 1σ error (F ¹⁴ C%)	yrsBP 1σ error	CalBP 1σ error
Wk43563	2	22	nr	88.2 ± 0.2	1013 ± 20	864 ± 38
Wk43564	2b	85	nr	79.1 ± 0.2	1882 ± 20	1777 ± 31
OZW076	10	204	-22.4	0.16 ± 0.03	>52,000	>52,000
OZW077	10	204	-25.0*	1.49 ± 0.11	$33,800 \pm 620$	$38,072 \pm 813$
OZW078	10	239	-23.5 ± 0.1	0.12 ± 0.02	>52,000	>52,000
OZW079	10	254	-23.8 ± 0.1	0.07 ± 0.01	>52,000	>52,000
OZW071	12	269	-25.0*	0.57 ± 0.03	$41,140 \pm 440$	$44,612 \pm 419$
OZW084	Backfill	289	-25.3 ± 0.1	70.28 ± 0.25	2830 ± 30	2886 ± 49
OZW072	13	334	-22.3 ± 0.4	0.47 ± 0.03	$42,680 \pm 420$	$45,912 \pm 416$
OZW081	13	344	-19.2	0.12 ± 0.03	>52,000	>52,000
OZW085	Backfill	364	-24.5 ± 0.1	73.84 ± 0.26	2430 ± 30	2444 ± 89
OZW073	14	364	-21.8 ± 0.4	0.12 ± 0.02	>52,000	>52,000
OZW074	14	374	-25.0*	0.8 ± 0.06	$38,650 \pm 560$	$42,668 \pm 406$
OZW083	14	404	-25.0*	0.22 ± 0.03	$48,510 \pm 980$	$49,713 \pm 1241$
OZW075	14	404	-22.3 ± 0.1	0.24 ± 0.01	$47,850 \pm 470$	$47,892 \pm 470$

3.5.6

Optically Stimulated Luminescence

The ages obtained from the fourteen OSL samples are presented in Table 3.7 with equivalent dose distributions (D_e) shown graphically in Figure 3.13. All OSL samples are characterised by heterogenous equivalent dose distributions (D_e) with a considerable portion of the measured D_e values falling outside of the weighted mean burial dose 2σ ranges and displaying distinct leading-edges of low D_e values or tails of higher D_e values (Table 3.7; Figure 3.13). Overdispersion values are high throughout the samples and range from 35 – 153 % (Table 3.7). These values are above those which are generally reported for well-bleached and unmixed single-grain datasets at 2σ e.g., Arnold and Roberts (2009) report a global average of 20 ± 1 %. These values exceed the overdispersion values of 15 – 20 % obtained

for the single-grain dose recovery tests of the Cathedral Cave samples. Maximum D_e values are recorded in the four samples taken from layers 2, 4 and 8 (Table 3.7).

Overall, the D_e characteristics of the Cathedral Cave samples suggest there has been some entrainment of grains from predeposited cave sediments during the transportation of largely well-bleached, externally derived sediments through the closed cave (e.g., Arnold et al., 2019). Accordingly, the minimum age models (MAM) of Galbraith et al. (1999) and Arnold et al. (2009) have been used to determine the final burial dose estimates.

Sample CC16-1 from layer 2 yielded an OSL age of 0.81 ± 0.06 ka using the MAM-3 age model (Table 3.7). A high overdispersion value of 153 ± 10 % was based on 121 D_e measurements, taken from 500 grains, that passed the SAR rejection criteria (Figure 3.13a).

Sample CC16-2 from layer 4 yielded an OSL age of 4.0 ± 0.6 ka using the MAM-3 age model (Table 3.7). The overdispersion value for layer 2 is high, at 111 ± 8 %, determined from 108 D_e measurements from 500 grains (Figure 3.13b).

Two OSL samples were analysed from layer 8. CC16-3 yielded an age of 3.4 ± 0.6 ka using the MAM-3 age model (Table 3.7). A high overdispersion value of 116 ± 8 % was calculated on 101 D_e measurements from 500 grains (Figure 3.13c). An age of 5.8 ± 0.4 ka was measured for sample CC16-5 using the MAM-4 age model (Table 3.7). An overdispersion value of 103 ± 7 % was calculated on 119 D_e measurements from 500 grains (Figure 3.13d).

Two samples were analysed from layer 9. CC16-4 yielded an age of 43.2 ± 2.7 ka using the MAM-4 age model (Table 3.7). The overdispersion value for this sample is 41 ± 3 %, this is less than that of overlying layers, but is still above the global average of 20 ± 1 % reported by Arnold and Roberts (2009). This value was based on 121 D_e measurements from 500 grains (Figure 3.13e). CC16-6 provided an age of 45.1 ± 3.2 ka using the MAM-3 age model (Table 3.7). An overdispersion value of 37 ± 3 % is measured on 127 D_e measurements from 500 grains (Figure 3.13f).

Three samples were analysed from layer 10. CC16-7 yielded an age of 44.7 ± 4.6 ka using the MAM-3 age model (Table 3.7). An overdispersion value of 38 ± 4 % was obtained from 96 D_e measurements taken from 500 grains (Figure 3.13g). CC16-8b yielded an age of 50.6 ± 3.7 ka using the MAM-4 age model (Table 3.7). An overdispersion value of 39 ± 3 % was based on 115 D_e measurements from 600 grains (Figure 3.13h). CC16-9b yielded an age of

50.3 ± 5.3 ka using the MAM-3 age model (Table 3.7) and had an overdispersion value of 35 ± 3 % calculated on 121 D_e measurements from 600 grains (Figure 3.13i).

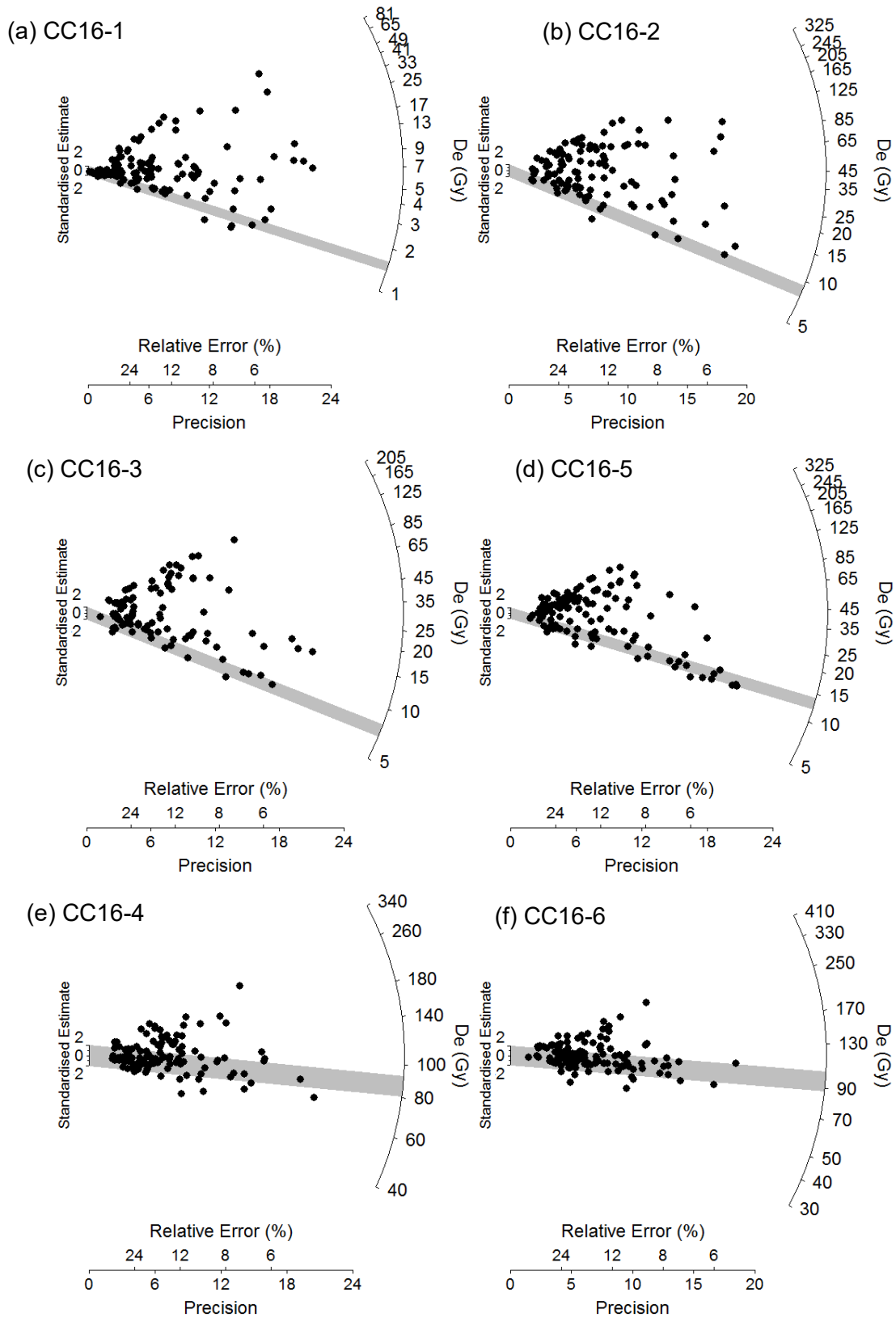
Two samples were analysed from layer 12. CC16-10 yielded an age of 56.5 ± 5.5 ka using the MAM-3 age model (Table 3.7). CC17-11 returned an age of 61.2 ± 4.0 ka using the MAM-4 age model (Table 3.7). Overdispersion values of 36 ± 3 and 39 ± 3 % (respectively) were obtained from 99 and 118 D_e measurements from 600 grains for each sample (Figure 3.13j–k).

Sample CC17-12, collected from layer 13, yielded an age of 68.2 ± 5.0 ka using the MAM-3 age model (Table 3.7). An overdispersion value of 38 ± 3 % was gained from 121 D_e measurements from 600 grains (Figure 3.13m). A second sample was taken from a section of layer 13 in quadrat I that on initial inspection was assessed as potentially containing admixed material from layer 12. This sample, CC17-14, yielded an age of 61.8 ± 4.7 ka using the MAM-4 age model (Table 3.7). The overdispersion value at 41 ± 4 % (Figure 3.13l) was not considered to be significantly elevated, when compared to contiguous layers, suggesting no admixture between these two layers. The overdispersion value was generated from 94 D_e measurements from 700 grains.

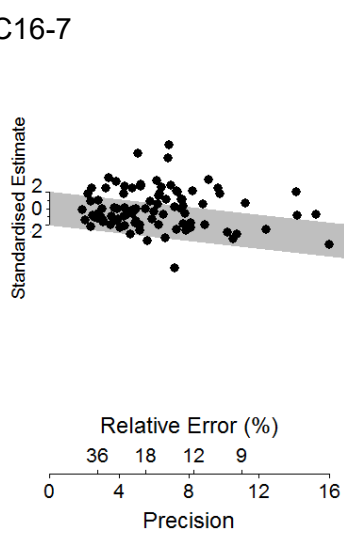
Sample CC17-13 from layer 14 yielded an age of 65.1 ± 4.4 ka using the MAM-3 age model (Table 3.7). The overdispersion value of 15 ± 3 % was calculated on 110 D_e measurements from 600 grains (Figure 3.13n). This age is younger than that given for layer 13 but is still within range given the overlap of ± age uncertainties. However, a second age of 82.2 ± 5.2 ka using a CAM age model (Galbraith et al., 1999) is also statistically supported. We elect to take a conservative approach and present the MAM-3 modelled age in this thesis. Future analysis of further samples will determine which model is the most accurate and further clarify this age.

Table 3.7. Summary of environmental dose rates, D_e values and final ages for Cathedral Cave OSL dating samples. ^a Specific activities and radionuclide concentrations have been converted to dose rates using conversion factors given in Guérin et al. (2011), making allowance for beta-dose attenuation (Mejdahl, 1979; Brennan, 2003); ^b Mean \pm total uncertainty (68% confidence interval), calculated as quadratic sum of the random and systematic uncertainties. ^c Includes internal dose rate of 0.03 Gy/ka with assigned relative uncertainty of $\pm 30\%$, based on intrinsic ^{238}U and ^{232}Th contents published by Mejdahl (1987), Bowler et al. (2003), Jacobs et al. (2006), and Pawley et al. (2008), and an α -value of 0.04 ± 0.01 (Rees-Jones, 1995; Rees-Jones and Tite, 1997). ^d Number of D_e measurements that passed SAR rejection criteria and were used for D_e determination / total number of grains analysed. ^e Age model selection: The CC samples are interpreted as being heterogeneously bleached on the basis of D_e distribution characteristics, high overdispersion values, and complex geomorphic contexts. The choice of whether to use the MAM-3_(UL) or MAM-4_(UL) for each sample has been made on statistical grounds using maximum log likelihood score criterion as outlined by Arnold et al. (2009). ^f Total uncertainty includes systematic component of $\pm 2\%$ associated with laboratory beta-source calibration

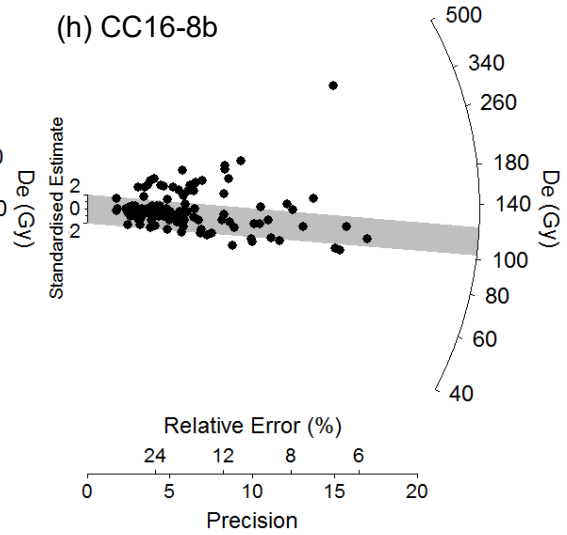
Sample name	Layer	Depth (cm)	Water content	Environmental dose rate (Gy/ka)				Equivalent dose (D_e) data				
				Beta dose rate ^a	Gamma dose rate	Cosmic dose rate	Total dose rate ^{b,c}	No. of grains ^d	Over-dispersion (%)	Age model ^e	D_e (Gy) ^b	OSL age (ka) ^{b,f}
CC16-1	2	7	21 \pm 2	1.11 \pm 0.06	0.74 \pm 0.03	0.01 \pm 0.01	1.89 \pm 0.09	121 / 500	153 \pm 10	MAM-3	1.5 \pm 0.1	0.81 \pm
CC16-2	4	18	18 \pm 2	1.32 \pm 0.07	0.79 \pm 0.03	0.01 \pm 0.01	2.15 \pm 0.10	108 / 500	111 \pm 8	MAM-3	8.7 \pm 1.2	4.0 \pm 0.6
CC16-3	8	68	21 \pm 2	1.31 \pm 0.07	0.89 \pm 0.03	0.01 \pm 0.01	2.25 \pm 0.11	101 / 500	116 \pm 8	MAM-3	7.6 \pm 1.2	3.4 \pm 0.6
CC16-5	8	86	23 \pm 2	1.25 \pm 0.07	0.97 \pm 0.04	0.01 \pm 0.01	2.26 \pm 0.13	119 / 500	103 \pm 7	MAM-4	13.1 \pm 0.6	5.8 \pm 0.4
CC16-4	9	87	22 \pm 2	1.14 \pm 0.06	0.82 \pm 0.03	0.01 \pm 0.01	2.00 \pm 0.10	121 / 500	41 \pm 3	MAM-4	86.3 \pm 3.0	43.2 \pm 2.7
CC16-6	9	95	27 \pm 3	1.22 \pm 0.06	0.86 \pm 0.03	0.01 \pm 0.01	2.12 \pm 0.11	127 / 500	37 \pm 3	MAM-3	95.7 \pm 4.3	45.1 \pm 3.2
CC16-7	10	152	24 \pm 2	1.26 \pm 0.06	0.97 \pm 0.03	0.01 \pm 0.01	2.27 \pm 0.11	96 / 500	38 \pm 4	MAM-3	101.7 \pm	44.7 \pm 4.6
CC16-8b	10	220	29 \pm 3	1.20 \pm 0.07	0.97 \pm 0.05	0.01 \pm 0.01	2.21 \pm 0.13	115 / 600	39 \pm 3	MAM-4	111.7 \pm	50.6 \pm 3.7
CC16-9b	10	256	22 \pm 2	1.29 \pm 0.08	1.02 \pm 0.05	0.01 \pm 0.01	2.36 \pm 0.14	121 / 600	35 \pm 3	MAM-3	118.6 \pm	50.3 \pm 5.3
CC16-10	12	270	24 \pm 2	1.24 \pm 0.08	0.99 \pm 0.05	0.01 \pm 0.01	2.28 \pm 0.14	99 / 600	36 \pm 3	MAM-3	128.6 \pm	56.5 \pm 5.5
CC17-11	12	298	21 \pm 2	1.12 \pm 0.06	0.83 \pm 0.03	0.01 \pm 0.01	2.00 \pm 0.10	118 / 600	39 \pm 3	MAM-4	122.1 \pm	61.2 \pm 4.0
CC17-14	12/13	369	14 \pm 1	1.10 \pm 0.06	0.82 \pm 0.03	0.01 \pm 0.01	1.96 \pm 0.10	94 / 700	41 \pm 4	MAM-4	121.0 \pm	61.8 \pm 4.7
CC17-12	13	358	15 \pm 2	0.94 \pm 0.05	0.74 \pm 0.03	0.01 \pm 0.01	1.72 \pm 0.08	121 / 600	38 \pm 3	MAM-3	117.1 \pm	68.2 \pm 5.0
CC17-13	14	400	26 \pm 3	0.85 \pm 0.04	0.67 \pm 0.02	0.01 \pm 0.01	1.56 \pm 0.07	110 / 600	35 \pm 3	MAM-3	101.3 \pm	65.1 \pm 4.4



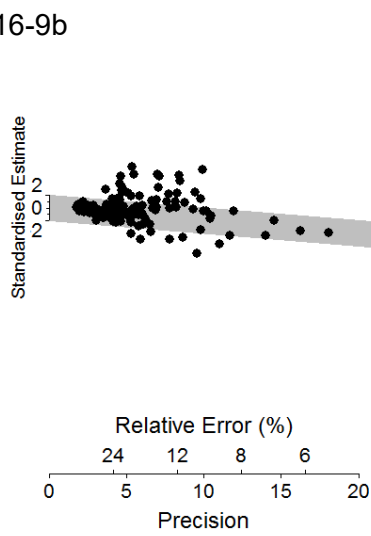
(g) CC16-7



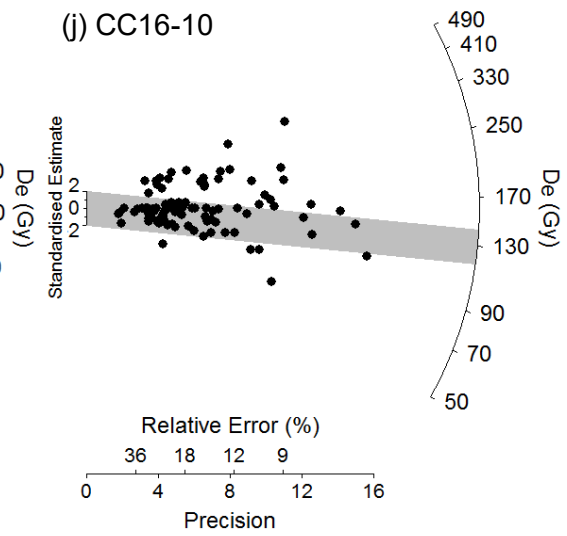
(h) CC16-8b



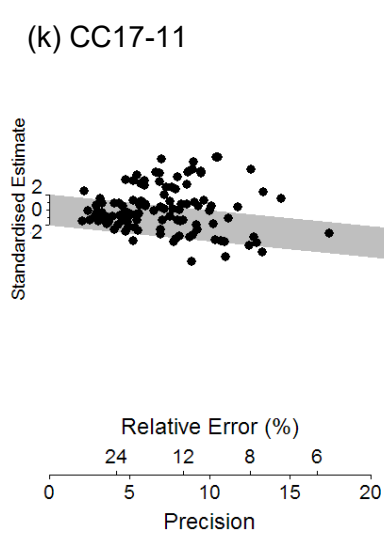
(i) CC16-9b



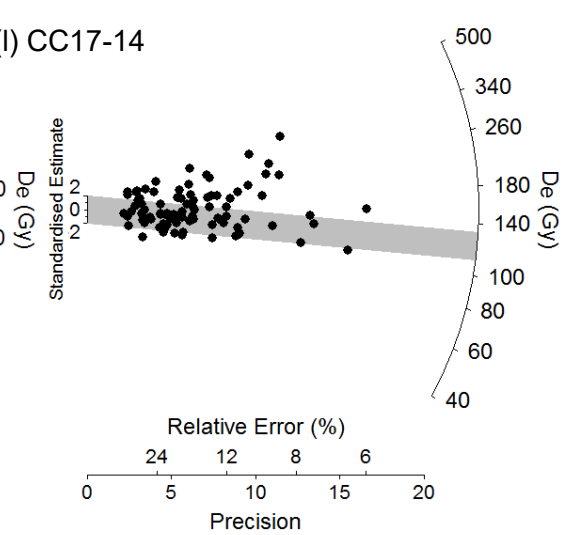
(j) CC16-10



(k) CC17-11



(l) CC17-14



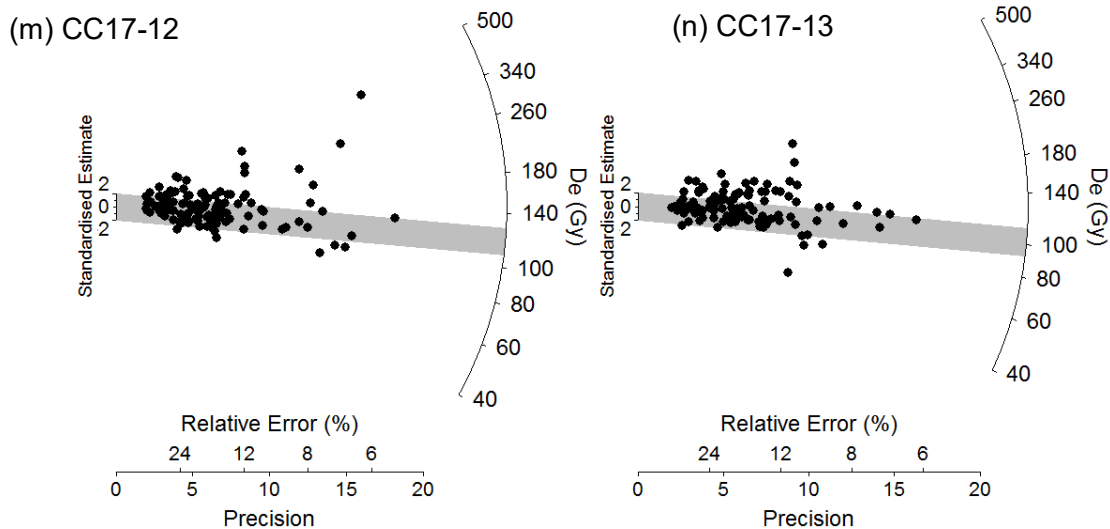


Figure 3.13 Single-grain OSL D_e distributions for the Cathedral Cave samples, shown as radial plots. The grey bands are centred on the D_e values used for the age calculations, which were derived using either the 3-parameter minimum age model, 4-parameter minimum age model or unlogged 3-parameter minimum age model (Galbraith et al., 1999; Arnold et al., 2009). Points outside of the grey bar represent the scatter within the dataset, in an idealised situation, 95% of points should fall within the grey bar if all values are consistent with each other at 2 standard error.

3.5.7 Bayesian age-depth modelling

Bayesian age-depth models were built for three potential scenarios using different combinations of chronological data. The rationale behind the selection of included ages is detailed after the discussion of the models.

Model1 includes all 14 OSL ages and five radiocarbon ages. This model was poorly resolved with only 63% of ages overlapping 95 % confidence ranges and with a mean confidence range of 3421 yr (minimum 390 yr at 22 cm and a maximum of 5048 yr at 425 cm (Appendix B Figure 7.1).

Model2, on which our chronology is based, incorporated all 14 OSL dates and two radiocarbon dates. This model resolved with 88 % the ages falling within 95 % confidence ranges and a mean 95 % confidence range of 5342 yrs (minimum 335 yrs at 22 cm, maximum 6912 yr at 423 cm (Figure 3.14). The output ages for this model are given in Appendix B Table 7.9. According to this model, at 4.2 m, the sediments are aged 65.8 ka.

Model3 was built exclusively using the OSL dataset (Appendix B Figure 7.2). This model was well resolved with 93% of the dates captured within 95 % confidence ranges. Mean 95% confidence ranges are 5400 yr (minimum 347 yr at 9 cm, maximum 6979 yr at 425 cm)

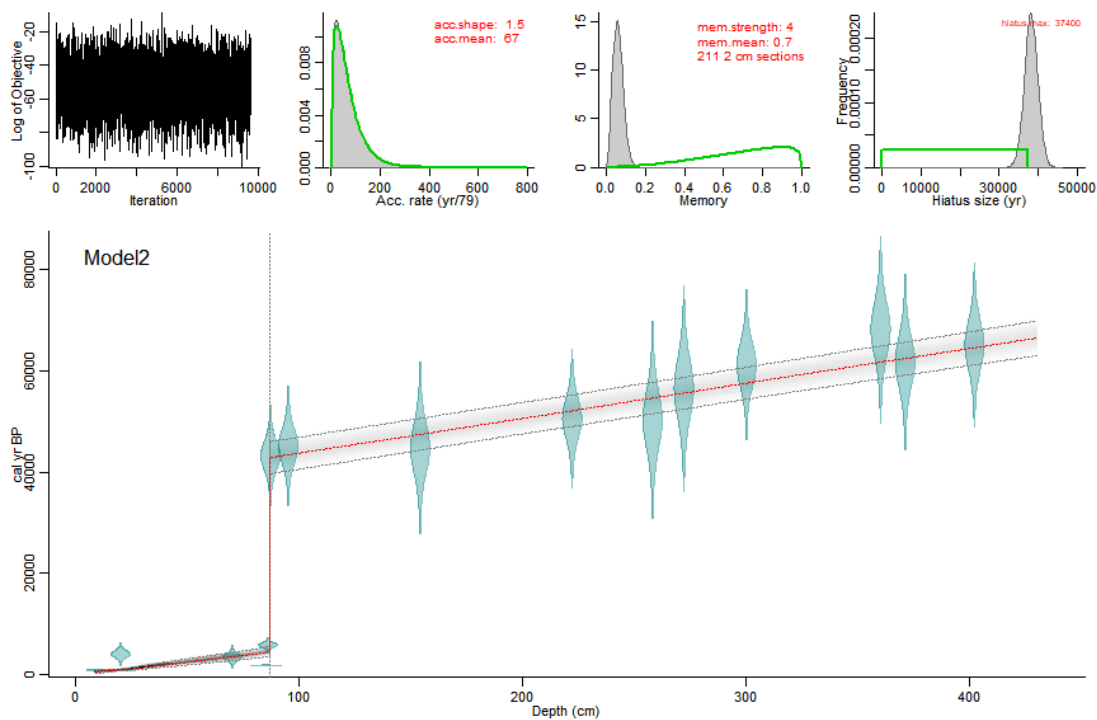


Figure 3.14. Bayesian age-depth model (Model2) for 425 cm of the Cathedral Cave deposit using fourteen OSL dates and two AMS radiocarbon dates.

3.5.8 Assembling the chronology

The entire available chronological dataset was considered in the construction of this chronology. These data include OSL and charcoal ages from the FU excavation and previously published charcoal ages (Dawson and Augee, 1997). After assessing the confidence in each age, all fourteen OSL ages were retained for the final analysis alongside two radiocarbon ages generated by the FU excavation that were deemed to be robust.

The OSL ages are treated with confidence in this study. Despite having relatively high overdispersion values (Table 3.7), the OSL ages are stratigraphically consistent and increase with depth. A single age inversion occurs in layer 13 where one sample has a measured age that is older than the two ages positioned below it in the stratigraphic column. These ages fall within overlapping 1σ error ranges and so are not statistically significantly different (Table 3.7). Overdispersion values were highest in layers 2, 4 and 8. Layers 2 and 4 are thin and photographs of the remaining OSL sample holes suggest there is potential for admixing of sediment from contiguous layers. Layer 8 appears to be a fill, thus, high overdispersion values due to sediment mixing, are not unexpected. Infinite radiocarbon ages (>52 ka) are not included in the modelled age scenario but bear relevance in showing that the age of the

charcoal sample exceeds the maximum bounds of radiocarbon dating. This allows a minimum age of 52 ka to be assigned to these samples. All other AMS radiocarbon ages are excluded from the chronology. Of the measured ages of samples collected during the FU excavation, several were rejected on prior knowledge, after being identified as problematic during pre-treatment or were thought to have been collected from reworked sediments at the edge of the old fill sediments in quadrat IV and had returned outlier ages (Figure 3.15). Of the five remaining FU charcoal samples, three returned finite ages from depths below at which infinite charcoal ages were obtained, and these ages did not agree with the OSL data. Two gave Holocene ages that were broadly in agreement with OSL data. An age-depth model that included all OSL and the five remaining charcoal ages resolved poorly with just 63 % of the ages captured within the 95 % confidence range (Appendix B Figure 7.1). A model based exclusively on OSL dates was well resolved and captured 93 % of ages (Appendix B Figure 7.2). However, no issues were identified that warranted exclusion of the two Holocene charcoal ages, and so these were retained in the final model (Figure 3.14). Adding to the argument in favour of their inclusion, these two ages agree with OSL data from Unit 1, and being late Holocene aged, the samples are less prone to accuracy issues arising from contamination and degradation as can occur with older samples (see Becerra-Valdivia et al., 2020). The resultant model is well-resolved and captures 88 % of ages within 95 % confidence bounds (Figure 3.14).

The ages underlying the former chronology for Cathedral Cave were not incorporated in the revised chronology for several reasons outlined here. The radiocarbon ages published by Dawson and Augee (1997) do not agree with the OSL ages or bear any parallel to the radiocarbon ages generated by this study. Ages generated by the UNSW study are considerably younger than the OSL ages, including ages of 2590 ± 80 yrs BP at 2.7 m deep and 14300 ± 730 yrs BP at 5.1 m deep. Confidence in the UNSW age sequence is further eroded by numerous age inversions (Figure 3.2), the use of pooled samples, as well as the potential contamination that may have occurred, an issue raised by (Dawson and Augee, 1997). Figure 3.15 shows the ages used in Model2 of the Bayesian age-depth modelling mapped on to the stratigraphic sequence of Cathedral Cave. A review of the challenges of ^{14}C dating at Cathedral Cave is included later in the discussion.

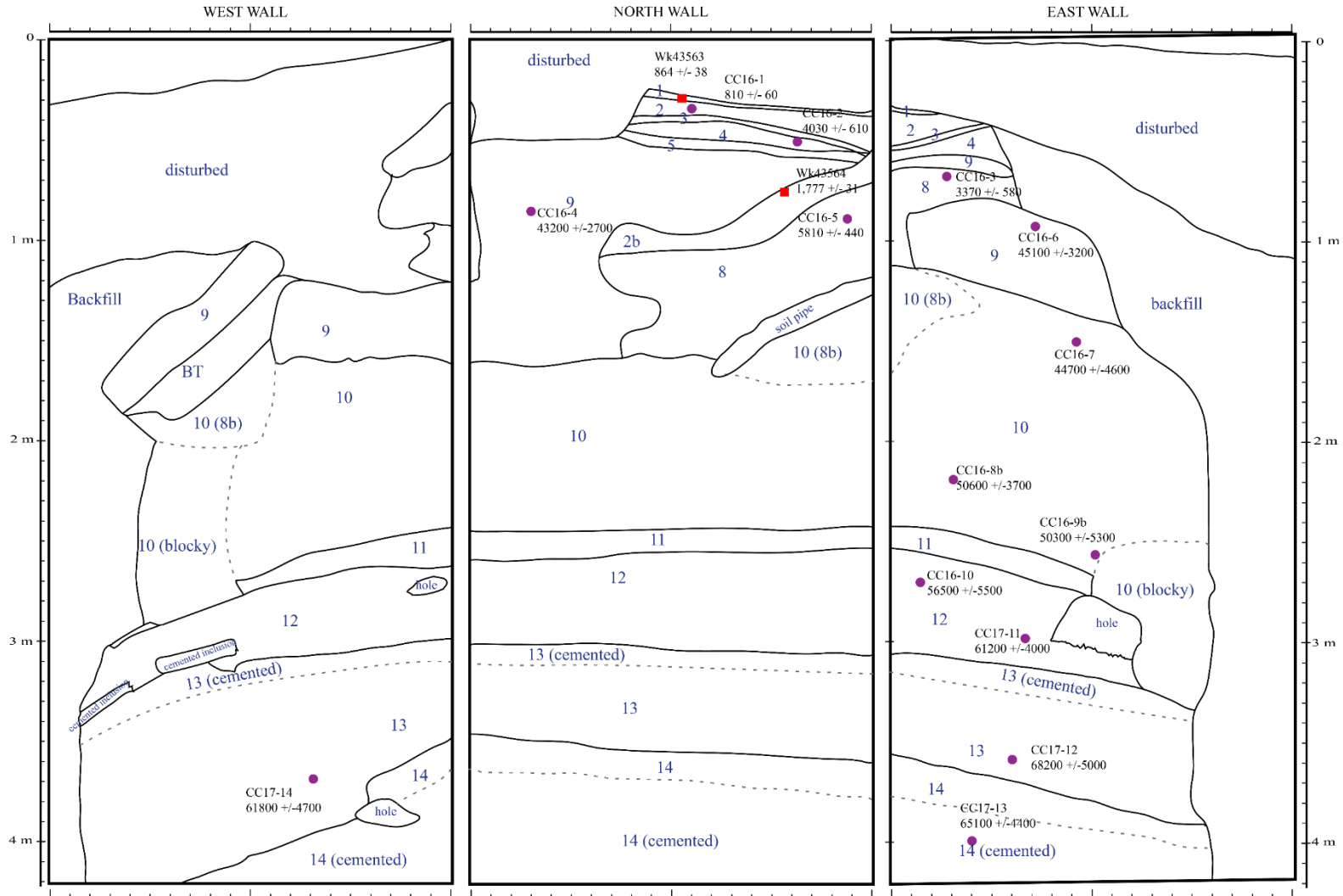


Figure 3.15. Stratigraphic diagram of the west, north and east wall of Cathedral Cave with sample sites marked for AMS radiocarbon ages (red square) and Optically Stimulated Luminescence ages (violet circle) used in the final Bayesian age-depth model

3.5.9 Taphonomy

Associated or articulated elements from individuals were recovered from layers 8, 10, 13 and 14 (Figure 3.16; Table 3.9). Associated remains were also encountered during the April 2019 field trip, the most significant being a partial associated *Thylacoleo carnifex* at a depth of ~5 m. The tibiae of this individual have been recovered and show cracking features seen in other large bones in Cathedral Cave (Figure 3.17a). Cracks, parallel or sub-parallel to the direction of collagen fibres, were evident on many of the larger bones (Figure 3.17a–c). These modifications compare to stage 1 of bone weathering as defined by Behrensmeyer (1978) using an open air environment. Examples of these modifications are shown in. Termite damage was observed on a single macropodid tibia collected from the top of layer 13 (Figure 3.17b). Rodent gnaw marks were evident on some of the larger bones (Figure 3.17d), but no other evidence of mammalian predation was observed. The April 2019 field trip also yielded remains of *Tyto novaehollandiae*, one of the taxa probably responsible for the accumulation of small mammal remains, at a depth of 4.5 m (Appendix D Table 7.13).

Bone yield varied throughout the excavated layers. Layers 1–8 had low to moderate amounts of diagnostic bone and in general, non-diagnostic bone was quite fragmentary. Larger species were represented almost exclusively by fragmentary and isolated molars. Bone yield increased in layers 9 – 14 (excluding layer 11 which was not processed). These layers gave moderate to high bone yield (Table 3.8) and larger species were represented by more complete elements. Layer 9 is an exception to the higher yield layers, with larger species represented entirely by isolated or fragmented molars (Table 3.8).

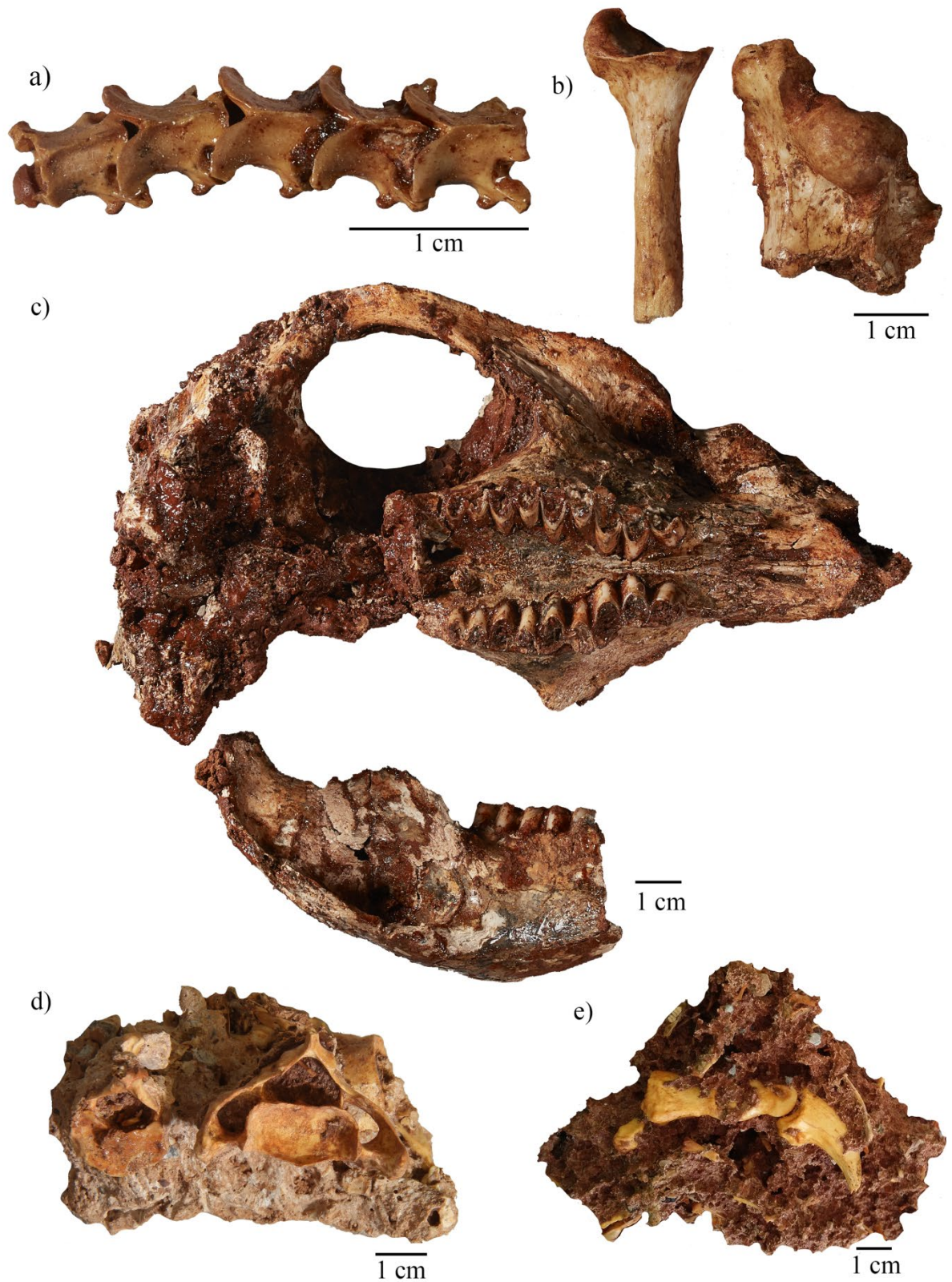


Figure 3.16. Articulated and associated faunal remains a) Elapidae gen. et sp. indet., five articulated vertebrae (CCW2339); b) *Megalibgwilia ramsayi*, associated left distal humerus and left proximal radius (CCW3095); c) *Vombatus ursinus*, associated right dentary and cranium (CCW2433); d) *Megalibgwilia ramsayi*, associated thoracic and cervical vertebrae *in situ* (CCW5033); e) *Baringa* sp. nov. 1, articulated proximal, medial and distal phalanges and digit V (CCW4862).

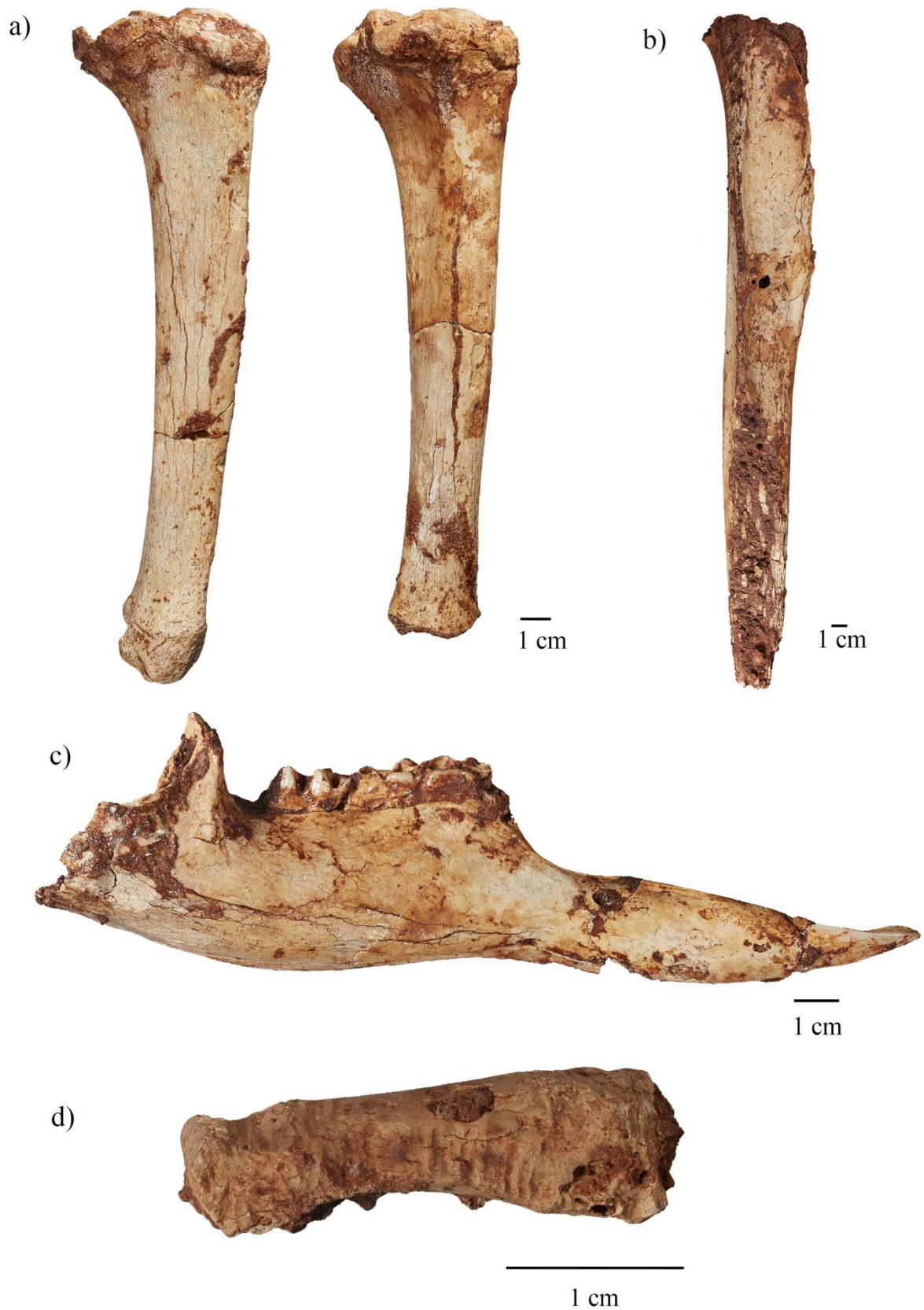


Figure 3.17. Taphonomic bone modifications a) *Thylacoleo carnifex* left and right tibiae (CCW5009, CCW5008) showing longitudinal cracking; b) *Protetnodon* sp. cf. *brehus*, left tibia with termite damage (CCW4938); c) *Macropus giganteus/titan/ferragus*, left dentary showing cracks aligned with collagen fibres (CCW2949); d) Macropodidae gen. et sp. indet., phalanx showing gnaw marks typical of rodents (CCW3514).

Table 3.8. Bone yield, NISP, MNI and notes for each stratigraphic layer of the Cathedral Cave deposit.

Layer	Bone yield	NISP	MNI	Notes
1	extremely low	2	2	Only two diagnostic elements of a rodent and a microchiropteran recovered
2	low	64	36	No medium or large taxa
2b	moderate	327	200	Mostly isolated teeth and fragmented bones – except for numerous well-preserved microchiropteran remains
3	extremely low	1	1	Single potoroine molar recovered
4	low	39	26	Larger mammals represented by n = 3 isolated and fragmentary molars
5	low	17	13	Mostly small mammals, single larger macropodid isolated tooth
8	moderate	200	331	Medium to large mammals represented only by isolated and often fragmentary molars.
9	high	674	351	Bones extremely fragmented <i>in situ</i> and medium to large mammals represented by mostly isolated and / or fragmented molars. Small mammal postcranial bones largely oriented north-south, parallel to the slope
10	high	9246	3339	All size classes present
11	nil	0	0	Unable to process this layer due to lithification, very little bone observed, none recovered
12	moderate	258	162	All size classes present
13	high	2443	949	All size classes present
14	high	6282	2190	All size classes present

Table 3.9. Associated and articulated elements from Cathedral Cave. 2433, 2339, 4862, 5033 and 3095 are shown in Figure 3.16.

Quad rat	Layer	Depth	Identification	Elements	Field #
B	8	256-261	<i>Microchiroptera</i> gen. et sp. indet.	Associated three radii, two humeri, one femur, various small bone including six metatarsals	CCW332
III	10	415	<i>Vombatus ursinus</i>	Associated right dentary and cranium	CCW2433
II	13	470-475	<i>Lagorchestes leporides</i>	Associated left and right maxillae	CCW2303
II	13	475-480	Elapidae gen. et sp. indet.	Five articulated vertebrae	CCW2339
II	13	505-510	Elapidae gen. et sp. indet.	Three associated vertebrae	CCW2629
II	13	505-520	<i>Baringa</i> sp. nov. 1	Articulated proximal, medial and distal phalanges and digit V (manus)	CCW4862
II	13	505-520	Macropodidae gen. et sp. indet.	Articulated calcaneus and pes bones	CCW3670
II	14	560-565	cf. <i>Macropus giganteus/titan/ferragus</i>	Associated left metatarsal IV, left metatarsal V	CCW2971
II	14	530-545+	<i>Megalibgwilia ramsayi</i>	Associated cervical and thoracic vertebrae	CCW5033
II	14	560-565+	<i>Megalibgwilia ramsayi</i>	Associated left distal humerus and left proximal radius	CCW3095

3.6 Discussion

3.6.1 Stratigraphic units

The infill sediments of Cathedral Cave are composed primarily of silty clays derived from exogenous sources (Figure 3.11; Figure 3.8). The sedimentary sequence can be broadly categorised into three stratigraphic and chronological units separated by age and observations of the sedimentology, geochemistry, stratigraphy and taphonomy. The *in-situ* sediments are capped by the disturbed and old fill sediments which comprise the disturbed unit (Figure 3.6). Unit 1 incorporates the mid to late Holocene aged layers (1–8) that have their origins in the upper 50 cm of the excavation (Figure 3.7; Figure 3.15). Unit 1 sediments are characterised by low bone yields (Table 3.8), and larger fauna is represented by mostly fragmented and isolated teeth. The colour and texture of layers in unit 1 are visually conspicuous in often deviating away from the red hues that dominate unit 2. This makes their absence in sedimentary descriptions by Dawson and Augee (1997) noteworthy. The UNSW excavation describes the top metre of sediment as being extensively disturbed and the top 1.5 m as mottled grey loamy textured silt (Dawson and Augee, 1997). This description is comparable to that of the old fill sediments encountered in the FU excavation but could also be characteristic of reworked soils involving Unit 1 sediments (Figure 3.6). It is plausible that the unit 1 layers were not present in the locality of the UNSW excavation, having been disturbed by earlier anthropogenic activity, perhaps in the process of backfilling the historic trench. Unfortunately sediment samples from the upper section of the NSW excavation were lost or destroyed (Dawson and Augee, 1997) and not available for comparison.

Unit 1 and unit 2 are separated by an unconformity marking a temporal hiatus of around 37.4 ka that includes late MIS 3, the entire MIS 2 and the early Holocene. Unit 2 begins at a depth of 50 cm and encompasses the Upper Pleistocene layers 9–14 (Figure 3.15). The lower boundary of unit 2 has not yet been determined, although observations during the April 2019 field trip indicate that this boundary probably occurs at around 5 m deep. Layers in unit 2 are characterised by having a greater homogeneity of sediments and sediment colour, more numerous limestone inclusions, higher bone yield (Table 3.8), and increased representation of larger elements of extinct and larger species that include Pleistocene megafauna species.

The units do not wholly align with the phases described by Dawson and Augee (1997). A comparison of the stratigraphic columns places unit 1 in the upper portion of phase 3, the youngest of the three phases that was recorded to extend from the base of the disturbed

sediments to a depth of ~3 m. (Figure 3.2; Figure 3.5). Phase 2 occurred at a depth of 3–5 m deep in the UNSW excavation, whereas the upper boundary for unit 2, described here, commences far higher in the sequence, at a depth of just 50 cm. Phase 1 is not relevant to the findings of this study because it occurs deeper than the 4.2 m excavation depth featured in this thesis.

3.6.2 Entry point and source of the Cathedral Cave sediment infill

Stratigraphy (Figure 3.5), geochemistry (Figure 3.12) and taphonomy (Table 3.8) indicate the entry point and source of the sediment exposed in the FU excavation in Cathedral Cave.

Sedimentary layers of unit 2 dip away from the Altar with a north-south slope of around 20 °. We concur with earlier findings that this is characteristic of the distal fan of a talus cone with the apex in approximate vertical alignment with the Altar, consistent with an entry point above the Altar (Dawson and Augee, 1997). Our stratigraphy does not indicate that the chimney G123 (Osborne, 2003) contributed an additional source of material to the deposit. We find that unit 2, the bulk of the excavated deposit, accumulated via sediment, animals and animal remains entering the cavern via a roof entrance located above the Altar formation. In unit 1, the same evidence lines point to this entrance being either closed or highly restricted and sedimentation has been primarily as the result of the activity of bats and the natural weathering of the limestone of the cave. There is no entrance visible in the roof above the Altar as can be assessed from the floor now. Viewed from inside the chamber, the Altar obstructs the view of the roof; on the land surface above the cave, the area is partially covered by old tanks and vegetation and there is no indication of a former entrance to the cave.

The Altar clearly incorporates calcite coated debris (large boulders and broken cave decorations); it may have formed over the top of a talus cone, consistent with the roof entrance hypothesis (Figure 3.18). The deposition of flowstone on top of the debris cone shows that there is focused drainage occurring from the surface, as would be expected if there were a route through the rock from the surface. Layers 9 and 11 are comprised of poor-quality flowstone (Figure 3.7), indicating that calcites were actively being deposited at the time that these layers accumulated. Transported cave pearls in layer 11 suggest there were basins or depressions such as shallow rimstone pools occurring further upslope towards the location of the modern Altar formation, perhaps similar to the rimstone basins that surround the skirt of the Altar today (Figure 3.10). Thus, the same cave processes that resulted in the formation of the Altar have evidently been active in the past. The cave contains examples where stalagmites appear to have formed on talus cones. The first is a shell of dirty flowstone formation that has formed on a now extinct talus cone on the western side of the passage leading to the main chamber of Cathedral Cave. A second analogue can be found in an unused entrance to the cave (Figure 2.4) where a flowstone shell is all that remains of a cone structure, the underlying sediment now entirely eroded away. Coring of the formation may shed more light on its structure and formation. Given the potential palaeoclimatic data that



Figure 3.18. The main chamber of Cathedral Cave showing the Altar formation. FU excavation site on left. Photo: D. Fusco.

calcites can provide (e.g., Xia et al., 2001; McDermott, 2004; Markowska et al., 2020), coring the Altar could prove valuable for climatic reconstructions of the Wellington region.

3.6.3 Geochemistry

Three distinct oxide groups in the Cathedral Cave sediments can be considered signatures of different cavern soil sources. Group 1 oxides (SiO_2 , TiO_2 , Fe_2O_3 , Al_2O_3 and K_2O) are abundant through all of the sediment layers in Cathedral Cave (Table 3.5), and are characteristic of the surface sediments surrounding Cathedral Cave (Rutledge et al., 2014). These have been used as signatures of allogenic soil in studies of cave infill sediments (Forbes and Bestland, 2006; Forbes et al., 2007). Quartz, the most common mineral in clastic rocks and soils, increases in layers where group one oxides dominate (Table 3.5). These data show that the clastic soils surrounding Cathedral Cave have been the primary contributor to the infill sediments.

A second group of oxides (Na_2O , P_2O_5 and SO_3) is associated with accumulations of bat guano (Hutchinson, 1950; Forbes and Bestland, 2006; Forbes et al., 2007). Group 2 oxides are present in all Cathedral Cave sediment samples, but to varying degrees (Figure 3.12). They are elevated in Unit 1 layers (excluding layer 8) where they are associated with high organic content and a lower proportion of group 1 oxides (Figure 3.12). We interpret this as representing periods of restriction or closure of the roof entrance, when the contribution of bat guano increased, relative to allogenic soil inputs. Microchiropteran remains are present throughout the assemblage, and are well represented in unit 1, confirming their presence in the cavern at the time (Table 3.8; Table 7.13). Invertebrate remains, abundant in layers 1–2b, are probably remnants of bat prey or detritivorous invertebrates associated with guano (Moulds, 2004).

The sole member of the third oxide group, CaO , can be derived from breakdown of the limestone host rock by frittering of the cave roof and walls (Forbes and Bestland, 2006; Forbes et al., 2007; Rutledge et al., 2014). Carbonates can also be deposited by water that has percolated through limestone. In the Cathedral Cave sediments, CaO is highest in most unit 1 layers and the uppermost samples of layers 9, 13 and 14 (Table 3.5). Most of these samples have elevated CaCO_3 (calcite), a possible source of the CaO . However, layers 1, 2b and 3, do not show elevated calcite, thus the CaO could be derived from other sources. Layer 3 is conspicuously different to other layers in the sedimentary sequence, and it has a comparatively high gypsum content, suggesting it may be evaporative. Layer 4 diverges from others in unit 1, having a signal more in line with allogenic soil inputs, rather than bat guano

and autochthonous materials (Table 3.5). Layer 4 is not extensive and could represent a time when the roof entrance was restricted but not completely closed. Layer 8 has an allogenic soil signature (Table 3.5), however, the localised and intrusive nature of these sediments suggests that they are derived primarily from cavern soils (perhaps layer 4), rather than fresh infill. The varied function of the roof entrance is further demonstrated by taphonomic evidence lines that are discussed later below.

3.6.4 Origin of indurated sediments

The indurated sediments in Cathedral Cave offer some insight into local environmental conditions. (Dawson and Augee, 1997) hypothesised that the indurated “floors” that feature through the sedimentary sequence are the result of saturation by carbonate rich rising groundwater, followed by drying periods. Given the hypothesis regarding hypogene speleogenesis (Osborne, 2007), the rising groundwater explanation is reasonable but is equally explained by rising epigenic waters which better fits the relationship between rainfall and changes in the elevation of the sump water. However, the height of the water table in Cathedral Cave over the last 70 ka is unknown. The cave sediments are mostly homogenous clays and silt, and in a rising groundwater scenario, these sediments could be hypothesised to become saturated, and then indurated, in a relatively uniform and predictable manner. We observed that sediments upslope, toward the north wall of the excavation, tended to be more heavily indurated, as could be expected by being nearer to the source of carbonate saturated water responsible for depositing the Altar flowstone. Differences in the indurated sediments described in this study, and comparisons with indurated sediments described previously (Dawson and Augee, 1997) also show local variation. Meteoric waters sinking through the vadose zone, followed by drying periods, gives an alternative theory for the origin of the cemented sediments.

The soils above Cathedral Cave are mostly thin (<1 m in depth) and contain little capacity for water storage (Jex et al., 2012). Today, the Altar is hydrologically active after heavy or prolonged precipitation events, however, these effects are short lived. September 2016 recorded the highest September rainfall on record for NSW, during which carbonate enriched water flowed down the Altar and breached the skirt to run across the sediment floor. The Well Chamber also flooded. The increase of hydrological activity ceased within just weeks of the heavy rainfall (I. Eddison, pers. coms.).

A petrographic slide from the upper portion of layer 10 shows that this layer consists mostly of coarse silt with some fine sand, perhaps indicating increased aeolian activity on the surface (Figure 3.8). The sediments of layer 10 contain water escape features, suggesting some low volume hydrological activity occurred in the cave. However, these features can form either in original voids in the sediment, or later, during diagenetic dissolution of grains after deposition (Retallack, 1990).

3.6.5 A new chronology for Cathedral Cave

Our chronology (Figure 3.15) differs to the previously published ages for Cathedral Cave that showed accumulation occurring through the terminal Pleistocene into the Holocene, between 32.5–2.95 ky ago (Dawson and Augee, 1997). Within this interpretation, the assemblage accumulated as interstadial conditions of late MIS 3 shifted to glacial conditions in MIS 2, and then through the onset of the modern climate in MIS 1. Our data from the 4.2 m deep excavation refutes this picture, revealing two episodes of deposition separated by a hiatus of 37.4 ka. We demonstrate that the first episode of deposition occurred during the late Pleistocene 65.8 ± 5.0 – 43.2 ± 2.7 ka ago in a global climate that was shifting from colder, drier glacial conditions of MIS 4 to warmer and wetter conditions during MIS 3 (De Deckker et al., 2019; Kemp et al., 2019). At least six Dansgaard-Oeschger climate events are included in this interval (Huber et al., 2006). The second episode took place during MIS 1, between 5.8 ± 0.4 to 0.81 ± 0.06 ka ago, after the onset of contemporary climate conditions in the mid to late Holocene (Figure 3.15). The deposit was not accumulating through MIS 2, contrary to earlier interpretations of the deposit that placed the LGM as the climatic backdrop (Dawson and Augee, 1997).

There is some inversion of the OSL ages, but this is not considered problematic as all ages overlap within \pm uncertainties of adjacent ages (Table 3.7). The most considerable inversion occurs between layers 13 and 14. Layer 14 has an OSL age of 65.1 ± 4.4 ka, layer 13 has two OSL ages of 61.8 ± 4.7 ka and 68.2 ± 5.0 ka. We have considered three scenarios in the absence of evidence of reworking. The first two scenarios are built on the overlap of the \pm age uncertainties. The first scenario is that the 68.2 ka age in layer 13 is younger and lies between 65.1 ka to 61.8 ka as suggested by the adjacent OSL ages. The second scenario is that layer 14 is older than the 68.2 ka obtained from layer 13. The third scenario involves the statistical models behind the OSL ages and considers that layer 14 may be substantially older than 65.1 ka. The 65.1 ka age uses a Minimum Age Model (Galbraith et al., 1999; Arnold et

al., 2009), the same model used for the majority of other OSL dates in this study. However, a second age for the same OSL sample of 82.2 ± 5.2 ka using a Centre Age Model (Galbraith et al., 1999) was also statistically supported. The first scenario is best matched by our Bayesian age depth model which indicates that the sediments at 4.2 m deep are aged 65.8 ka model (Table 7.9; Figure 3.14). Awaiting analysis of additional samples to clarify these dates, we elect to submit the ages that use the Minimum Age Model ages in this thesis to preserve a consistency for the OSL data set. In doing so, we assign an overall age range of 61.8–65.8 ka to layers 13 and 14, in line with our Bayesian age depth model.

Palaeoecological archives in the sediments from Cathedral Cave inform on a period of substantial climatic change in Australia, and one that is still sparsely sampled in the literature (De Deckker et al., 2019). Importantly, these Cathedral Cave sediments document the critical time period 55–45 ka ago, that includes the late Pleistocene Australian megafauna extinctions and the earliest known occurrences of humans in inland NSW (Roberts et al., 2001; Bowler et al., 2003; Cupper and Duncan, 2006). Cathedral Cave can now be considered among a small number of late Pleistocene fossil sites that provide a stratigraphically and chronologically constrained faunal record through the megafauna extinction window. Comparable localities are Tight Entrance Cave, Kudjal Yolgah Cave (Jankowski et al., 2016) and Devil’s Lair (Roberts et al., 2001; Turney et al., 2001a), in south-west Australia, Wet Cave (Pate et al., 2002) at Naracoorte Caves in south-east Australia and South Walkers Creek in east Queensland (Hocknull et al., 2020). Of these locations, Tight Entrance Cave offers the most comparable record, where the mammalian fauna has been tracked over a 100 ka period that includes the appearance of humans on the landscape (Prideaux et al., 2010). Kudjal Yolgah Cave accumulated between 80 – 41 ka ago (Jankowski et al., 2016), but does not contain adequate faunal resolution to track abundance trends through time. Devil’s Lair holds a faunal record from 55 to 13.5 ka ago (Turney et al., 2001a). However, these sites are geographically distant from Wellington Caves, and likely to be influenced by different regional environmental conditions. Wet Cave provides a geographically closer analogue, although the record here starts at 45 ka ago (Pate et al., 2002; Macken et al., 2013; Macken and Reed, 2014), barely overlapping with that of Cathedral Cave. The South Walkers Creek locality is an amalgamation of four sites located along a 600 m stretch of Walker Creek that are dated between 65 – 40 kya (Hocknull et al., 2020) but these sites do not contain adequate stratigraphic or faunal resolution to track trends through that interval of time.

Assuming a consistent sedimentation rate and no further significant hiatus, the entire of the Cathedral Cave deposit (to 10.5 m deep) could hypothetically stretch back at least 120 ka and include MIS 5, the last major interglacial period prior to the Holocene. If this holds true, the record between Cathedral Cave and Mitchell Cave would be more or less continuous if based on the biocorrelated minimum age of 128 ka assigned to the latter (Dawson, 1985), which in itself requires revision. However, because cave sedimentation is often event driven (Gunn, 2004), further dating is necessary to test this hypothesis.

3.6.6 Integrity of the stratigraphic sequence

The stratigraphy exposed within the FU excavation of Cathedral Cave (excluding disturbed and backfill sediments) is interpreted here, as it shows that layers within the deposit have largely accumulated consecutively through time. With the exception of the infill by layers 2b and 8 (discussed below), the deposit was evidently little disturbed prior to the exploration and use of the cave by European colonists, when the disturbed and backfill sediments were added to the deposit. However, this does not confirm that accumulation has occurred at a constant rate through time, as sedimentation in caves is frequently event driven. Events such as water pulses and collapse of upper chambers can deposit large amounts of sediments in a relatively short time (Gunn, 2004). We identify a single stratigraphic reversal where layers 2b and 8 intrude into layer 9, probably the result of unit 1 sediments filling a void caused by internal erosion (Figure 3.7a). The OSL ages for layer 8 suggest that it is broadly contemporaneous with layer 4 (Table 3.7) and these layers also share similar geochemical signatures (Figure 3.12). An osteoderm from the large extinct Pleistocene skink *Tiliqua frangens* (Thorn, 2019) in layer 8 and a fragment of a molar of *Diprotodontidae* sp. indet., in layer 2b (Appendix D Table 7.13) are the only extinct Pleistocene species in unit 1 and are probably reworked. A tooth fragment of *Macroderma gigas* (Appendix D Table 7.13) is the sole element of this species recorded in the FU excavation and recorded only at depths >6.5 m by (Dawson and Augee, 1997). This is also probably reworked.

Minor intrusive soil pipes occur occasionally through the excavation (Figure 3.5). These are localised and consist of darkly coloured, sometimes mottled, charcoal-rich sediments. The source of the soil pipes has not been established by this study, but we hypothesise that the soil pipes are the result of exogenous surface sediments washing into the cave after rains following fire events. Wildfires increase surface runoff and erosion by the removal of vegetation and by altering the hydrological properties of soil. Fires create a layer of ash and

sediment that is easily eroded and transported (Dragovich and Morris, 2002; Cawson et al., 2012). After being washed into Cathedral Cave, the charcoal-rich sediments have filled cracks or internal erosion voids caused by water seepage. Further work on the soil pipes in Cathedral Cave, and the microcharcoal record in the infill sediments, could prove useful in establishing the timing of local fire events and investigating the effect of climate and anthropogenic influences on local fire regimes. Given the catastrophic bushfires that decimated large parts of Australia during 2019 – 2020, and the certainty that events like this will continue to modify our climate (Dowdy et al., 2019), there is much to be gained in enhancing our understanding of the intensity, frequency, causes and impacts of past fire regimes.

A further question to address when discussing the integrity of the stratigraphic sequence is the suggestion that sediments in the UNSW phase 2 (3–5 m), have been reworked as a unit from a primary accumulation above the Altar (Dawson and Augee, 1997). This idea was founded on the appearance of limestone boulders and rocks in the sediments, bones being highly fragmented, purported (but undetailed) bone weathering, and the complete absence of any associated skeletal elements. Articulated, and associated elements were collected from comparable depths during the FU excavation (Figure 3.16; Table 3.9) and there are numerous instances of probable associations. Examples include multiple elements from uncommon taxa emerging from the same spit, which are most parsimoniously interpreted as originating from the same individual but were not adjacent to one another. Such levels of association and articulation do not suggest major disturbance. However, unconsolidated sediments can subside either gradually or rapidly into cavities from solution pipes, often as a result of water action (Gunn, 2004). D_e distributions from the OSL samples suggest some capture of older grains within younger sediments (Figure 3.13). Although we cannot rule mass redeposition out entirely without further sedimentological and micromorphological analyses, the fact that age increases steadily with depth (Figure 3.15) and there is no lithological evidence of substantial reworking augurs against the likelihood of this scenario.

Bone modifications were cited as further evidence for reworking (Dawson and Augee, 1997). The modifications were not described in any detail but were ascribed to pre-weathering prior to deposition. We note that some larger bones from the FU excavation show splitting that is parallel or subparallel to the direction of collagen fibres (Figure 3.16a–c). These modifications were assessed to be at the equivalent of bone weathering stage 1

(Behrensmeyer, 1978). However, these stages are modelled on open-air environments rather than caves, where conditions can be humid, moist, and the burial environment can be alkaline. We find that these modifications are the result of deterioration that has occurred in the cave, rather than pre-weathering before burial. Hydrological regimes exert a major influence over bone diagenesis, particularly if attack by microorganisms has already increased bone porosity, making it more susceptible to modification by fluids (Behrensmeyer, 1978; Mayer et al., 2020). These regimes are most damaging to bone tissues when variations occur, e.g., repeated wetting and drying rather than continual submersion. Swelling and shrinking stresses causes cracking at both macroscopic and microscopic scales (Pokines et al., 2018; Mayer et al., 2020). Alkaline soil environments, like those usually found in limestone caves, further weakens bones by corrosion after burial (Fernandez-Jalvo and Andrews, 1992; Kos, 2003b). These modifications would leave bones more vulnerable to fragmentation and could partially explain some of the fragmentation seen in the Cathedral Cave assemblage that cannot be attributed to excavation damage.

Termite boreholes were identified on the distal portion of a tibia of *Protemnodon* sp. cf. *brehus* in layer 13, close to the contact with layer 12 (Figure 3.16b). This is the sole example of termite damage, but it is unlikely to be unique. Modifications such as those described would make bones more vulnerable to further damage and fragmentation caused by swelling, shrinking or movement and transport of the sediments in which they are buried.

3.6.7 The challenges of ^{14}C dating at Cathedral Cave

All attempts to apply ^{14}C dating at Cathedral Cave have generated uncertain radiocarbon results, leaving the question to be addressed - why has radiocarbon dating been problematic here?

Our attempt to use ^{14}C dating on bone material from the UNSW excavation failed. Bone was highly degraded and lacked sufficient collagen for radiocarbon dating. This is unsurprising, as our chronology reveals that the bones (and some of the charcoal samples) are substantially older than previously held. For our charcoal dates, we consider three additional sources of error that could contribute to inconsistent results. These are; the vertical movement of charcoal (Archer, 1974), *in-situ* contamination (Bronk Ramsey, 2008; Higham et al., 2009) and, efficacy of pre-treatment methods (Higham, 2011; Deviese et al., 2018; Becerra-Valdivia et al., 2020).

Outside of the soil pipes and disturbed/backfill sediments, which we avoided collecting from, no indication of vertical charcoal movement was identified in the FU excavation. Cracks are evident in layer 11 (Figure 3.9), but these are shallow and do not breach other layers. A scenario in which the finite ^{14}C ages in layer 13 and 14 are accurate and aligned with OSL dates would require charcoal to have undergone vertical movement from layers 9 or 10. This is a distance of at least 2 m and is unlikely given the lack of stratigraphical evidence to support this.

Contamination *in situ* with younger ^{14}C is a parsimonious explanation. As discussed in the introduction to this chapter, charcoal samples are exceedingly susceptible to contamination by older or younger ^{14}C , and older samples are disproportionately affected (Becerra-Valdivia et al., 2020). Contamination of an infinitely aged charcoal sample with <1% modern carbon would reproduce ages in line with those yielded by the charcoal in this study (Bronk Ramsey, 2008; Higham et al., 2009). Humic acid is a common source of contamination, a partially soluble organic macromolecule distributed in soils, sediments, and water. Humic acid forms as a result of the decay of vegetable and natural residues, or even as a decay product of the charcoal itself (Becerra-Valdivia et al., 2020). Removal of humic acid occurs during the pre-treatment of charcoal and samples prior to radiocarbon dating. However, not all pre-treatment methods are equally as efficient at removing contaminants.

Both Acid Base Acid (ABA) and Acid-Base-Wet Oxidation (ABOx) are commonly used to pre-treat charcoal for ^{14}C dating (Higham, 2011; Becerra-Valdivia et al., 2020). Pre-treatment using ABA is less aggressive but less efficient than ABOx at cleaning samples. For this reason, ABA is usually satisfactory for younger samples but may not be sufficient for Pleistocene aged or heavily contaminated samples (Higham, 2011; Deviese et al., 2018). Our charcoal samples underwent ABA pre-treatment as they were highly degraded and too small for ABOx.

Dawson and Augee (1997) explained ^{14}C irregularities in their radiocarbon ages as potentially arising from contamination during handling, the pre-treatment of small pooled samples, lateral facies changes and variable transport mechanisms. In light of our stratigraphic findings, it has to be considered that some UNSW samples may have been unknowingly collected from intrusive sediments e.g., the charcoal rich soil pipes, as these do not appear to have been recognised. The close proximity of the two excavation sites suggests it is feasible that soil pipes also intruded on the UNSW excavation site.

This study casts doubts on the effectiveness of AMS radiocarbon dating of Cathedral Cave. However, it is important to acknowledge that there is no evidence that conclusively supports a scenario where the three finite ages in layers 13 and 14 are contaminated or have not undergone vertical movement. Rather, these are hypotheses and the charcoal ages in question have been excluded from the analysis on the balance. Ideally, other dating methods can be applied to Cathedral Cave, e.g., U-series or ESR, to seek consensus. This work has been started, with several carbonate samples already submitted for U-series dating and an intention of attempting ESR dating of quartz grains and tooth enamel and infrared stimulated luminescence dating of feldspars in the near future. These findings demonstrate that there is great value in using multiple methods to revisit the chronology of other Pleistocene-aged palaeontological sites, where the ages are reliant on single dating methods or where improved methods may give a refined chronology.

3.6.8 Taphonomic signal

The taphonomic signal provides two key pieces of evidence for the Cathedral Cave story that have not been reviewed in other sections of this discussion. It supports the varied restriction of the roof entrance suggested by Dawson and Auger (1997) and provides further clarity on the accumulation mode and agents.

In unit 1, bone yield varies from extremely low to moderate and the mammalian assemblage from this unit is mostly small sized taxa. Medium to large mammals are almost entirely known by isolated and often fragmented molars, and large mammals are almost absent from layers 1–3 (Table 3.8). This is consistent with a closed or restricted roof entrance filtering larger taxa. Although the quantity of sediment available to excavate was substantially less in unit 1, bone yield for layers 1 and 3 is still low (MNI = 3), supporting the suggestion that the roof entrance may have been completely closed at this time. Small mammal remains in unit 1 layers (other than bats), indicate that owls were active, although not to the extent seen in unit 2. Unlike bats that use echolocation, owls require at least some light to navigate (Dice, 1945; Martin, 1986). We think it is unlikely that owls would have gained access to the chamber from the two other known entrances, due to having to navigate 100s of metres in darkness. Instead, we suggest that the roof entrance was at least partially open during the time that layers 2, 4 and 5 were deposited.

Unit 2 differs in having mostly moderate to high bone yield, medium and large mammals in higher abundance and less isolated and fragmented remains. In layers 12, 13 and 14, bones

are less fragmented and complete or near complete elements of large mammals are present. This is consistent with open roof pitfall trapping scenario. The largest taxon recovered is a sub-adult dentary of *Palorchestes azael* in layer 14 (Figure 3.19). This species reaches an estimated adult body weight of >1000 kg (Richards et al., 2019).

In layers 9 and 10, large and medium sized mammals are represented mostly by isolated and fragmented molars (although slightly less so in layer 10) despite the bone yield being high. This could reflect increasing stages of restriction of the roof entrance prior to its complete closure during the 37.4 ka hiatus that followed the accumulation of this layer. Alternatively, it could be due to a decrease in the larger sized mammals in the landscape.



Figure 3.19. Figure 3.20. Right dentary of sub-adult *Palorchestes azael*.

3.6.9 Accumulation agents

Accumulation of the faunal remains in the Cathedral Cave has previously been found to be the result of pitfall entrapment (via the roof entrance) as well as the feeding behaviour of predatory owls and *Macroderma gigas* (Dawson and Augee, 1997). *Macroderma gigas* is not discussed here as the FU excavation has not reached a depth equivalent where *M. gigas* is reported by Dawson and Augee (1997). Our data supports the findings of Dawson and Augee (1997) in that the assemblage is characteristic of accumulation by both owls and pitfall trapping. It features both isolated and associated/articulated elements of larger species that have accumulated via pitfall entrapment (Table 3.9; Figure 3.16; Figure 3.17), and the numerous remains of small mammals >100 g, consistent with the prey remains of owls

(Andrews, 1990; Baird, 1991). *Tyto* owls have been identified amongst the remains (Appendix D Table 7.13). Bone modifications attributable to mammalian predators are not featured in the assemblage, which likely reflects unsuitability of the main chamber for denning. The only bite marks noted occur on larger bones as distinct closely-spaced, near-parallel, often paired grooves that are typical of rodent gnawing (Camens and Carey, 2013; Figure 3.17d). Thus, the larger predators present in the assemblage will be there as a consequence of the pitfall entrance in the cave roof, rather than the death of autochthonous cave inhabitants.

3.6.10 A story of deposition

At 65.8 ka ago, the roof entrance above the Altar was active through the relatively cold, dry climatic conditions that were in effect during MIS 4 (De Deckker et al., 2019). On the surface above the cave, the entrance acted as a pitfall trap, sending unwary members of the local faunal community plunging to their instant or eventual deaths on the cave floor below. The entrance was large enough that some of the bigger members of the faunal community became victims, including *Procoptodon goliah* and *Protemnodon brehus*, taxa that weigh in at 250 and 100 kg respectively. Most of the smaller taxa found their way into the cave as the prey of owls that roosted in the cave, or perhaps more likely, in a nook in the roof entrance itself. After capturing and swallowing their prey, the owls regurgitated pellets containing the undigestible fur, feathers, and bones of their prey. Bats frequented the cave. Between 65.8 – 65.1 ka, two periods of significant precipitation occurred and resulted in meteoric waters infiltrating the chamber. Carbonate rich water saturated sediments as the fluid sank through the vadose zone. These sediments later became cemented by carbonates as conditions became drier.

The roof entrance remained open through the transition into MIS 3, at a time when the Australian climate was shifting toward warmer and wetter conditions (Kemp et al., 2019). The remains of fauna continued to accumulate, as either pitfall victims or owl prey. Bats remained active in the cave. During early to mid MIS 3, the cave was hydrologically active. Cave pearls and dirty flowstones formed on the floor and the roof entrance remained open. Between 50.6 to 44.7 ka ago, conditions were drier and less meteoric water entered the cave. The roof entrance stayed open, and the remains of animals continued to accumulate below. Some larger animals are present, but not in great quantities. This may be due to restriction of

the roof entrance or reduced abundance of these animals in the faunal community. Owls and bats remained active.

By the middle of MIS 3, the cave was hydrologically active again with interbedded dirty flowstones forming through cyclical water activity as sediment continued accumulating through the roof entrance. During wetter periods in the cave, enough water flowed across the floor to orient bones in the direction of the slope. By 43.2 ka ago, fewer larger animals fell into the cave, but owls and bats continued to be active. The reduction in larger animals could be due to increasing restriction of the roof entrance, leading up to its complete closure sometime after 43.2 ka. The roof entrance remained closed for the next 37.4 ka, and accumulation ceased in the main chamber, as did owl and bat activity. During the closure of the roof entrance, conditions on the surface became colder and dryer through MIS 2 and then modern climate commenced into MIS 1. The roof entrance opened again, although probably highly restricted, during the mid to late Holocene. Bats and owls had access to the chamber, but owl activity was low. By the late Holocene, the roof entrance closed and remained so to present times. Bats were present in the main chamber, but the activity of owls had reduced substantially. There was little input from external sediment sources, although the high incidence of charcoal indicates fire activity on the surface during the late Holocene. For the most part, the main chamber of Cathedral Cave remained mostly silent and undisturbed through much of the late Holocene, at least, until its exploration and subsequent development by Europeans commencing sometime in the 1820s.

3.7 Conclusion

This study bolsters our understanding of the chronology and history of sediment infilling in Cathedral Cave, thereby providing a robust framework against which palaeoenvironmental and faunal trends can be interpreted against. The revised chronology significantly changes our understanding of the timing of the accumulation of the Cathedral Cave assemblage and enables us to revise the climatic framework used in previous interpretations. Our revised chronology, framed around OSL and charcoal ages, shows that the sediment infills of Cathedral Cave (to 4.2 m deep) accumulated mostly during MIS 4 and MIS 3, between $65.8 \pm 5.0 - 43.2 \pm 2.7$ ka ago. This is followed by a significant hiatus in the order of 37.5 ka during which the roof entrance above the Altar was closed and the cave did not actively accumulate sediment or fossils. Accumulation reinitiated in MIS 1, between $5.8 \pm 0.4 - 0.81 \pm 0.06$ ka ago but the roof entrance remained restricted during this time. Twelve individual stratigraphic

layers were identified, belonging to two defined stratigraphic units, on either side of the hiatus, that are broadly separated by age, fauna, and accumulation mode.

We identify Cathedral Cave as one of just four cave fossil localities in Australia that have stratigraphically and chronologically controlled infill records that include the probable arrival of humans, the megafauna extinction window, and the period directly preceding the arrival of Europeans. Cathedral Cave is the sole locality of this type in central-eastern Australia. With just 4.2 m of the 10.7 m sediment floor excavated, further excavation in Cathedral Cave has the exceptional potential to provide a record that stretches back at least through MIS 5.

4 Chapter 4: Systematic palaeontology of Cathedral Cave, Wellington Caves

Diana A. Fusco & Gavin J. Prideaux

College of Science and Engineering, Flinders University, Bedford Park, South
Australia

4.1 Abstract.

Determining the evolutionary relationships of animals contained in a fossil assemblage is a critical step for palaeoecological analysis. During earlier studies in Cathedral Cave, the species composition of the assemblage was not adequately resolved, thus limiting palaeoecological interpretations. By comparing fossils to known osteological material and published descriptions, we find that the Cathedral Cave sediments contain a diverse and rich fossil assemblage. This assemblage includes at least 69 species of terrestrial mammals, 66 of which were collected during this study. Eleven of the mammals collected belong to the suite of extinct late Pleistocene megafauna. Cathedral Cave therefore contains the richest assemblage of Australia's late Pleistocene mammals collected from a single location.

4.2 Introduction

Nearly 200 years ago, Wellington Caves was where European colonisers first encountered fossils of Australian extinct marsupials (Lang, 1830). A number of collections have been made from fossil localities at the caves during this time, including from Cathedral Cave (see Chapter 1). However, these were mostly exploratory or opportunistic. The first methodical collection from Cathedral Cave did not occur until the excavations by the University of New South Wales between 1982 – 1986 (Dawson and Augee, 1997).

Prior to the Flinders University excavations, the fossil remains of at least 41 marsupial taxa, two bats, ten different rodents and five snails had been identified from Cathedral Cave (Dun, 1893; Flannery and Szalay, 1982; Blanford, 1985; Hodge, 1991; Dawson and Augee, 1997). The fauna was considered to be typical of other late Pleistocene and Holocene faunas of east and south-east Australia. Many of the taxa recognised in these earlier studies were not identified confidently to species level (Table 4.1) and the non-mammalian vertebrates have

been largely overlooked, thereby not providing a full picture of the species richness of the fossil deposit.

The UNSW excavation collection is substantial, incorporating a sample with a Minimum Number of Individuals (MNI) of 1894 (Dawson and Augee, 1997). However, its utility for palaeoecological research is now limited by its lack of completeness and samples from spits have been combined. Therefore, it was necessary to make a new collection from the sediments of Cathedral Cave, to provide the resolution and context required for this study

4.3 Aims of this chapter

In this chapter, we establish the mammalian species composition of the Cathedral Cave fossil assemblage, focusing nearly exclusively on specimens collected during the FU excavation.

The following aims will be addressed in this chapter:

1. Identify the fossil remains collected by the FU excavation, whenever possible.
2. Review additional taxa reported during the UNSW excavation.
3. Compile a list of the fossil mammals known from Cathedral Cave.

To meet these aims, we compare the Cathedral Cave fossils with voucher specimens held at the South Australian Museum, Flinders University, Australian Museum and Museum Victoria and published descriptions.

Table 4.1. List of Cathedral Cave fauna compiled from Dawson and Augee (1997), Blanford (1985), Hodge (1991), Flannery and Szalay (1982) and Dun (1893). X indicates presence, except for *Palorchestes azael* and *Bohra paulae* which were not collected by the UNSW excavation; *indicates megafauna species; ? indicates species presence unknown for this phase. Taxon names have been updated to conform with current nomenclature. *Dasyuroides* sp. indet. is given by Dawson and Augee (1997) as ‘?Dasyuroides sp.’ and *Notamacropus* sp. nov. as *Macropus* cf. *rankeni*.

Family	Species	P1	P2	P3	Family	Species	P1	P2	P3	
Dasyuridae	<i>Dasyuroides</i> sp. indet.	X	X		Macropodidae	<i>Notamacropus</i> sp. nov.	X			
	<i>Dasyurus geoffroii</i>	X	X	X		<i>Osphranter altus</i>	X	X		
	<i>Dasyurus hallucatus</i>		X			<i>Macropus ferragus</i> *		X		
	<i>Dasyurus viverrinus</i>	X	X			<i>Macropus giganteus</i>			X	
	<i>Sarcophilus harrisi</i>	X				<i>Macropus titan</i> *	X	X		
	<i>Antechinus</i> sp. cf. <i>A. flavipes</i>	X	X			<i>Osphranter</i> sp. indet.			X	
	<i>Phascogale calura</i>	X				<i>Onychogalea</i> sp. indet.	X			
	<i>Phascogale tapoatafa</i>	X	X			<i>Petrogale</i> sp. indet.	X	X		
	<i>Sminthopsis crassicaudata</i>	X	X			<i>Thylogale</i> sp. indet.	X	X	X	
	<i>Sminthopsis murina</i>	X	X	X		Muridae	<i>Conilurus albipes</i>	X	X	X
<i>Sminthopsis</i> sp. 1	X			<i>Mastacomys fuscus</i>	X		X	X		
Thylacinidae	<i>Thylacinus cynocephalus</i>	X	X		<i>Notomys</i> sp. indet.		X		?	
	Peramelidae	<i>Isoodon obesulus</i>	X	X	X		<i>Pseudomys australis</i>	X	X	?
		<i>Perameles</i> sp. cf. <i>P. gunnii</i>	X	X	X		<i>Pseudomys gracilicaudatus</i>	X	X	?
<i>Perameles nasuta</i>		X	X	X	<i>Pseudomys novaehollandiae</i>		X	X	?	
Thylacoleonidae	<i>Thylacoleo carnifex</i> *	X	X		<i>Pseudomys</i> sp. indet.				?	
	Phascolarctidae	<i>Phascolarctos</i> sp. indet.	X				<i>Hydromys chrysogaster</i>	X		?
Vombatidae		<i>Vombatus</i> sp. indet.	X	X	X		<i>Rattus</i> sp. cf. <i>R. lutreolus</i>			?
	Diprotodontidae	<i>Diprotodon</i> sp. indet.*	X	X			<i>Rattus</i> sp. indet.			?
		<i>Palorchestes azael</i> *	NA	NA	NA	<i>Muridae</i> sp. indet.			?	
Petauridae	<i>Petaurus</i> sp. cf. <i>P. breviceps</i>	X	X	X	Chiroptera	<i>Macroderma gigas</i>	X			
Pseudocheiridae	<i>Pseudocheirus</i> sp. indet.	X	X	X		<i>Microchiroptera</i> sp. indet.	X	X	X	
Acrobatidae	<i>Acrobates pygmaeus</i>	X			Squamata	<i>Varanus</i> sp. indet.	X	X		
Phalangeridae	<i>Trichosurus vulpecula</i>	X	X			<i>Tiliqua</i> sp. indet.		X		
Potoroidae	<i>Aepyprymnus rufescens</i>	X	X	X		<i>Squamata</i> sp. indet.	X	X	X	
	<i>Bettongia</i> sp. indet.	X			Aves	<i>Aves</i> sp. indet.	X	X		
	<i>Potorous tridactylus</i>	X	X			Gastropoda	Charopidae sp. indet.	X		
Macropodidae	<i>Protomnodon</i> sp. indet*.	X	X		<i>Elsothera</i> sp. indet.			X		
	<i>Procoptodon oreas</i> *	X	X		<i>Galidistes</i> sp. indet.			X	X	
	<i>Bohra paulae</i>	NA	NA	NA	<i>Glyptopupoides egregia</i>				X	
	<i>Notamacropus</i> sp. cf. <i>N. agilis</i>	X	X		<i>Nevistitis aridorum</i>			X	X	
	<i>Notamacropus</i> sp. cf. <i>N. dorsalis</i>	X	X							

4.4 Methods

4.4.1 Curation

All identified fossils reported in this thesis were assigned an interim reference number, prefixed by CCW, pending curation at the Australian Museum (AM). All specimens used in this chapter are presently held in the palaeontology research laboratories at Flinders University (FU) in South Australia. A large portion of the UNSW collection are also held at FU following transfer from the previous caretaker, M. Augee. All specimens will be transferred to the AM when no longer required. Specimens published as part of other studies have been assigned AM collection numbers and these are used preferentially to interim reference numbers when available.

4.4.2 Identifications

We identified fossil remains whenever possible, by means of comparisons with specimens held at the South Australian Museum, Flinders University, Australian Museum and Museum Victoria (Appendix C Table 7.12) and augmented with published descriptions. For rodents, figures and descriptions included in Watts and Aslin (1981) were useful for seeking characters to compare and narrow down potential candidates. Archer (1976, 1981) provided many of the dasyurid characters, and work by Van Dyck (1982a); Baker and Van Dyck (2013); and Baker et al. (2015) was especially valuable for distinguishing between species of *Antechinus*. Characters for bats are taken from Martinez (2010).

Cranial bones and teeth were used preferentially, but not exclusively, for identification, as these are the most informative for mammals and are the most commonly preserved. Isolated rodent molars and incisors were numerous and deemed surplus to the better-preserved cranial material, except in the rare case where they indicated a species otherwise not represented in a spit. Non-mammalian taxa recovered from the excavation includes birds, reptiles, amphibians, gastropods, and a small number of fish remains (Appendix D Table 7.13). These taxa are not the focus of this investigation, although we refer to some specimens when relevant.

In addition to the fossils collected in this study, key fossils from the UNSW collection were reviewed to further clarify the taxonomic composition of the Cathedral Cave fauna by checking the identity of species not encountered in our excavation or those deemed rare or

possibly misidentified. A specimen register for the UNSW excavation was supplied by M. Augee.

4.4.3 Nomenclature

Nomenclature for modern mammals follows Jackson and Groves (2015) as the most current taxonomic source for contemporary Australian mammals. An exception to this is for the order Chiroptera, where we retain the traditional Suborders of Megachiroptera and Microchiroptera (Dobson, 1875) rather than the current Suborders Yinpterochiroptera and Yangochiroptera (Springer et al., 2001). Only a small number of the small bat fossils have been identified so far and retaining the traditional suborders enables the relative abundances of these to be analysed as a single taxonomic unit, Microchiroptera sp. indet. Nomenclature for extinct macropodids follows Prideaux (2004) and Prideaux and Warburton (2010); that of all others follow published literature.

Where identification is uncertain or incomplete, we use open nomenclature qualifiers to indicate five levels of confidence in the identification.

- 1) Definite attribution to described species (e.g., *Pseudomys australis*);
- 2) Referable to genus but insufficient diagnostic features to identify to species level (sp. indet.);
- 3) Definite attribution to undescribed species (sp. nov.);
- 4) Distinct morphotype requiring further investigation or attribution to possible undescribed species (sp. 1, etc);
- 5) Attribution to probable described species (sp. cf.).

We do not differentiate closely related giant Pleistocene forms from modern taxa that are often separated from each other primarily on size but are poorly delineated taxonomically (for examples see: Dawson, 1982b; 1983; Dawson and Flannery, 1985). Thus, we consider *Macropus titan* and *M. ferragus* to be conspecific with *M. giganteus*, as we do *Sarcophilus harrisii* with *S. lanarius*, *Osphranter robustus* with *O. altus*, and *Notamacropus siva* / *N. agilis siva* with *N. agilis*. Most of the fossils assigned to the genus *Perameles* are isolated molars or edentulous cranial material. Both *P. nasuta* and *P. gunnii* have been confirmed as present in the assemblage, but most fossils belonging to *Perameles* have not been identified to species due to time constraints. As it is not possible to perform a trajectory analysis on

isolated identifications, all *Perameles* specimens are referred to here as *P. nasuta / gunnii*, enabling analysis of the relative abundances of this taxonomic unit. *Dasyurus geoffroii* and *D. viverrinus* are morphologically similar species (Archer, 1976). Identifications for these two species are sometimes based on size and geographic distribution alone (Dawson and Augee, 1997), if a rationale is given at all. Given that molar size and geographic distribution can vary through time, I have taken a conservative approach, referring relevant *Dasyurus* specimens to *D. geoffroii / viverrinus* pending further work.

4.4.4 Format of the systematics section

For taxa that are highly abundant, we only refer to exemplar specimens in descriptions and diagnoses. Occasionally we refer to exemplar specimens from non-target quadrats, if they have been essential to the identification. We give MNI and NISP only for specimens used in the analysis in Chapter 5. Preliminary work has revealed at least three species of bats, we provide diagnostic characters for these, but because they are already quantified within *Microchiroptera* spp. we do not provide individual MNI or NISP.

To assist with locating specimens, provenance is supplied as depth below datum as this is how the specimens are labelled and stored.

Tooth type is indicated as: I, incisor; C, canine; P, premolar; dP, deciduous premolar; M, molar; and are numbered by order of placement. Upper and lower teeth are denoted by upper and lower case characters respectively, and 'x' is used to indicate uncertain tooth position. For example, M1 denotes the first upper molar and p3 indicates the third lower premolar. Dental nomenclature follows Lockett (1993) for marsupials, in which the dental formula is P1-3 and M1-4; Musser (1981) for rodents and Menu and Popelard (1987) for bats. All taxa included here are described elsewhere in other publications, therefore, we limit descriptions of the fossil taxa to characters used in their identification.

Because mammals are the focus of this study, species level identifications have not yet been attempted on the majority of the bird, reptile, and frog specimens from the target quadrats. The non-mammalian fauna identified so far from this collection is included in Appendix D Table 7.13.

4.4.5 Equipment

Photographs of the specimens in this chapter were taken using a Visionary Digital LK imaging system (Dun, Inc.) with Canon EOS 5DsR camera using Zerene Stacker 1.04 software. Measurements to 0.01 mm were taken using Mitutoyo digital callipers.

4.4.6 Abbreviations

ant anterior

caud caudal

cran cranial

dist distal

L left

MNI Minimum Number of Individuals

NISP Number of Identified Specimens

pos posterior

prox proximal

Q quadrat

R right

St stylar cusp

4.5 Results

4.5.1 Identifications and assemblage composition

Identifications were assigned to a total of 21,212 individual specimens resulting in an MNI of 6871 (Appendix D Table 7.13). Mammals were overwhelmingly dominant, making up 94.3 % of all individuals identified. The rest of the vertebrate assemblage comprised reptiles, (3.5 %), birds (1.5 %), frogs (0.7 %) and fish (0.03 %).

Eighteen mammalian families (plus Order Chiroptera) were identified in the assemblage. Rodents were by far the most abundant, comprising 79.9 % of specimens identified to at least family level. The balance of the mammal assemblage is composed of taxa from the families Dasyuridae (8.7 %), Peramelidae (4.1 %), Macropodidae (3.7 %), Potoroidae (1.7%) and Chiroptera (1.3 %), with the remaining 1.85 % made up of the families Petauridae, Vombatidae, Phalangeridae, Chaeropodidae, Burramyidae, Pseudocheiridae, Thylacinidae, Diprotodontidae, Acrobatidae, Tachyglossidae, Thylacoleonidae, Thylacomyidae and Palorchestidae.

Seventy-three unique taxonomic units were identified within the mammal assemblage, incorporating at least 66 species. This number is probably underestimate of the true species richness of the sample as the morphotypes may contain distinct species, and several taxonomic units could contain multiple species

Reviewing taxa previously reported in Cathedral Cave by Dawson and Augee (1997) was complicated by the UNSW sample being incomplete and lacking curation. I was unable to locate the sole specimen referred to *Dasyurus* sp. cf. *D. hallucatus*, instead, finding an empty ziplock bag labelled “CC.36 A + B WC 148 *Dasyurus* cf *hallucatus*”. I was likewise unable to locate specimens referred to *Sminthopsis* sp. 1., and this taxon was not recorded in the UNSW specimen register or described in any publication. I have therefore removed these two taxa from the faunal list for Cathedral Cave.

Review of the UNSW specimens resulted in corrections to a few species identifications included in Dawson and Augee (1997). Fossils assigned to *Macropus rankeni*, #1724–1728 in the UNSW specimen register have been reidentified as *Congruus kitcheneri*. Specimens labelled *Thylogale* sp. indet. have been reidentified as belonging to *Congruus kitcheneri*, *Osphranter* sp. indet. and *Protemnodon* sp. indet.

Prior to the FU excavation, at least 44 fossil mammals had been recorded from Cathedral Cave (Dun, 1893; Flannery and Szalay, 1982; Blanford, 1985; Hodge, 1991; Dawson and Augee, 1997). *Phascolarctos cinereus*, *Procoptodon oreas* and *Bohra paulae* were not represented in the FU excavation sample. Including them brings the total number of mammal species so far collected from fossil deposits in the Main Chamber deposit to at least 69.

The excavation has also so far yielded nearly 300 fossil bones belonging to reptiles, 67 belonging to frogs and over 200 ascribed to birds (Appendix D Table 7.13). The bulk of these are unidentified or superficially identified.

4.5.2 Systematics

Order MONOTREMATA Bonaparte, 1832

Family TACHYGLOSSIDAE Gill, 1872

Megalibgwilia ramsayi (Owen, 1884)

Megalibgwilia

MATERIAL: MNI = 2, NISP = 10. CCW4985, Q II, layer 14, 535–540+, proximal R femur (Figure 4.1a), proximal L tibia (Figure 4.1b), proximal R tibia (Figure 4.1c), proximal R fibula (Figure 4.1d), vertebra, axis (Figure 4.1e–f), associated CCW5003, Layer 14, Q II, 535–540+, cervical vertebra, thoracic vertebra, associated (Figure 3.16d). CCW3095, Layer 14, Q II, 560–565+, distal L humerus, proximal L radius, associated (Figure 3.16b).

REMARKS: The fossils belong to an echidna larger and more robust than modern *Tachyglossus aculeatus*. CCW3095 includes a distal portion of a left humerus retaining the trochlea, capitulum and ectepicondyle, but missing the entepicondyle (Figure 3.16b). The humerus compares well with AM F86749, from Darling Downs, QLD, and AM F10948, the holotype of *M. ramsayi*, which was collected from Mitchell Cave. The latter is missing much of the ectepicondyle. CCW4985 includes proximal left and right tibiae and a proximal left femur (Figure 4.1a–c). The femur of *M. ramsayi* differs from those of other tachyglossids in having low, broad trochanters that are equidistant from the femoral head. It is further distinguished by its hindlimb proportions, with the tibia being longer than the femur (Murray, 1978). Despite the damage to CCW4985, it appears that both tibiae would exceed the length

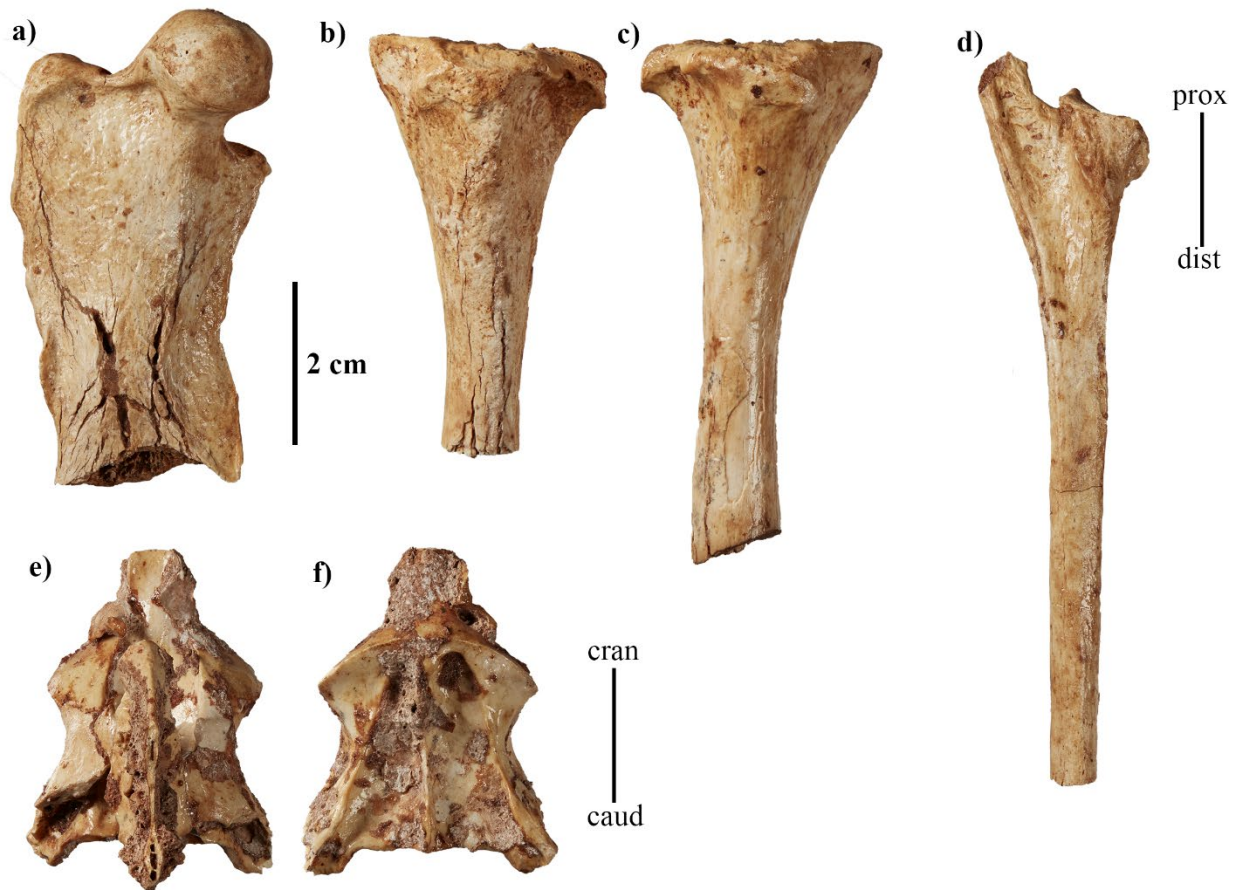


Figure 4.1. Associated remains of *Megalibgwilia ramsayi* a) proximal R femur; b) proximal L tibia; c) proximal R tibia; d) proximal R fibula; e–f) dorsal and ventral view of axis (CCW4985).

of the femur. Other large Tachyglossidae fossils in layer 14 are also referred to *M. ramsayi*, based primarily on association.

Tachyglossus aculeatus (Shaw, 1792)

Short-beaked Echidna

MATERIAL: MNI = 2, NISP = 2. CCW827, Q II, Layer 12, 415–420 cm, distal ungual phalanx. CCW2521, Q III, Layer 13, 500–515 cm, distal ungual phalanx.

REMARKS: Indistinguishable from modern specimens of *T. aculeatus*.

Order DASYUROMORPHIA Gill, 1872

Family DASYURIDAE Goldfuss, 1820

Dasyurus geoffroii Gould, 1841 or *Dasyurus viverrinus* (Shaw, 1800)

Western Quoll or Eastern Quoll

MATERIAL: MNI = 141, NISP = 650. Exemplars only. CCW2513, Q II, layer 14, 515–520 cm, 4 L maxillae, 4 R maxillae, 2 L dentaries, cranium, 10 isolated teeth. CCW3034, Q II, layer 14, 560–565 cm, cranium with detached maxillae (Figure 4.2a). CCW2574, Q I, 14, 570–575, damaged cranium, R dentary.

REMARKS: *Dasyurus* is separated from most other Australian dasyurids by: having a larger body size; two premolars (the third premolar is lost); no paraconid on m1; relatively uncrowded premolars (Archer, 1976). It is separated from *Sarcophilus* by: having narrower, more elongated, less crowded premolars; less bulbous molars; a higher, better developed talonid on m1–4 (Archer, 1976). *Dasyurus* fossils from Cathedral Cave are predominantly isolated molars or damaged dentaries and maxillae that do not preserve the features, in most cases, required to make a confident identification (Archer, 1976; Van Dyck, 1987; Wroe and Mackness, 1998). For example, *D. geoffroii* is alone among species of *Dasyurus* in having a small diastema between I1 and I2 but premaxilla are rarely preserved. CCW3034 does include the premaxilla and shows no visible diastema between the alveoli for I1 and I2, suggestive of *D. viverrinus*. However, the molar shape and size relative to the cranium compares better to *D. geoffroii*. More work is required to confidently assign the Cathedral Cave specimens to species. *Dasyurus maculatus* is able to be separated by its more bulbous and larger molars (Archer, 1976). However, the other two taxa are less distinct, and a conservative approach is taken here in assigning fossils that are not *D. maculatus* to *D. geoffroii* / *viverrinus*, pending future work.

Dasyurus maculatus (Kerr, 1792)

Spotted-tailed Quoll

MATERIAL: MNI = 5, NISP = 7. CCW4849, layer 13, 500–505 cm, R M1. CCW2807, Q II, layer 14, 535–540 cm, cranium, R dentary. CCW855, Q III, layer 14, 555–560 cm, cranium (Figure 4.2b). CCW4850, Q II, layer 14, 560–565 cm, partial L M1, R M1, C¹. CCW3829, Q II, layer 14, 575–580 cm, L dentary.

REMARKS: See remarks for *Dasyurus geoffroii* / *viverrinus*.

Sarcophilus laniarius Owen, 1838

Tasmanian Devil

MATERIAL: MNI = 2, NISP = 2. CCW4973, Q E, layer 10, 340–345 cm, isolated incisor. CCW2496, Q II, layer 14, Q II, 560–565cm, R maxillary fragment with M1–2 (Figure 4.2c).

REMARKS: A right maxillary fragment with molar measurements comparable to *S. laniarius* from mid Pleistocene deposits at Wellington Caves and from the Manning Karst in northern NSW (Table 4.2).

Table 4.2. Molar dimensions for *Sarcophilus laniarius* maxilla (CCW2496) compared with other specimens from Wellington Caves and the Manning Karst. Measurements are in mm.

Molar measurements	Cathedral Cave (CCW2496)	Wellington Caves (Dawson, 1985)	Manning Karst (Price et al., 2019)
M1 length	14.35*	12.3 (11.3–13.4)	11.5
M1 width	10.5	10.0 (8.3–10.9)	10.3
M2 length	15.58	13.7 (12.5–16.0)	15.4
M2 width	11.25*	11.0 (9.8–13.2)	11

Antechinus sp. cf. *A. agilis* Dickman et al., 1998

Agile Antechinus

MATERIAL: MNI = 1, NISP = 1. CCW2742, II, 13, 520–525 cm, L dentary with M3–4 (Figure 4.2e).

REMARKS: *Antechinus* are small dasyurids separated from other similar sized dasyurids by having: a markedly reduced, two rooted p3; a crowded premolar row; metacristids that are not transverse to the long axis of the tooth row (Archer, 1976). CCW2724 is a posterior portion of a dentary with moderate wear to the remaining molars. An entoconid is visible on M3, although the wear makes it difficult to assess the degree of development. The metacristids on the upper molars are not transverse to the long axis of the tooth row. This, along with its size, place this fossil in the genus *Antechinus*. The molars being smaller than those of *A. flavipes* (but larger than for *Sminthopsis crassicaudata*) accords better with *A. agilis*, a species that is known from eastern Australia. Also see remarks for *A. flavipes*.

Antechinus flavipes Waterhouse, 1838

Yellow-footed Antechinus

MATERIAL: MNI = 79, NISP = 154. Exemplars only. CCW2475 Q II, layer 13, 495–500 cm, 3 L dentaries, 1 R dentary (Figure 4.2d). CCW2657, Q II, layer 13, 505–520 cm, L maxilla, 5 R maxillae, 4 L dentaries, 3 R dentaries. CCW2701, Q II, layer 14, 520–525 cm, 2 R maxillae, 4 L dentaries, 2 R dentaries. CCW2836, Q II, layer 14, 535–540 cm, 5 L maxillae, 4 R maxillae, 6 L dentaries, 15 R dentaries. CCW3032, Q II, layer 14, 560–565 cm, 2 L maxillae, 2 R maxillae, L dentary.

REMARKS: Four species of *Antechinus* are known from central-eastern New South Wales today. *Antechinus flavipes* is separated from *A. agilis* by its larger size. From *A. stuartii* by: possessing a shorter molar row, larger entoconids and a wider talonid on m1–4 (Van Dyck, 1982a). From *A. mimetes* by having: a diastema separating I1 and I2; a strongly developed buccal and lingual cingulum on C1; more crowded premolars; no StC on M1–4; less developed entoconids on m1–4 (Baker and Van Dyck, 2013; Baker et al., 2015).

Phascogale calura Gould, 1884

Red-tailed Phascogale

MATERIAL: MNI = 1, NISP = 1. CCW3518, Q II, layer 12, 455–560 cm, L maxilla with M1–2.

REMARKS: The genus *Phascogale* is distinguished from other dasyurids in having: three premolars with well-developed cingula on the premolars and molars; I1 is procumbent; *StB* is distinct on M1; anterior cingulum is complete on M1–4; c1 is premolariform; p1–4 are wide with subrounded outline, the third premolars are higher than the second premolars, m1 has a well-developed protoconid; posterior cingulid on m1–4 is not interrupted prior to meeting the hypoconulid (Archer, 1976). Of the three members of the genus *Phascogale*, only *P. calura* and *P. tapoatafa* have distributions that include eastern Australia (Short and Hide, 2012; Aplin et al., 2015). *Phascogale calura* is the most diminutive of the three *Phascogale* species and easily distinguished by size.

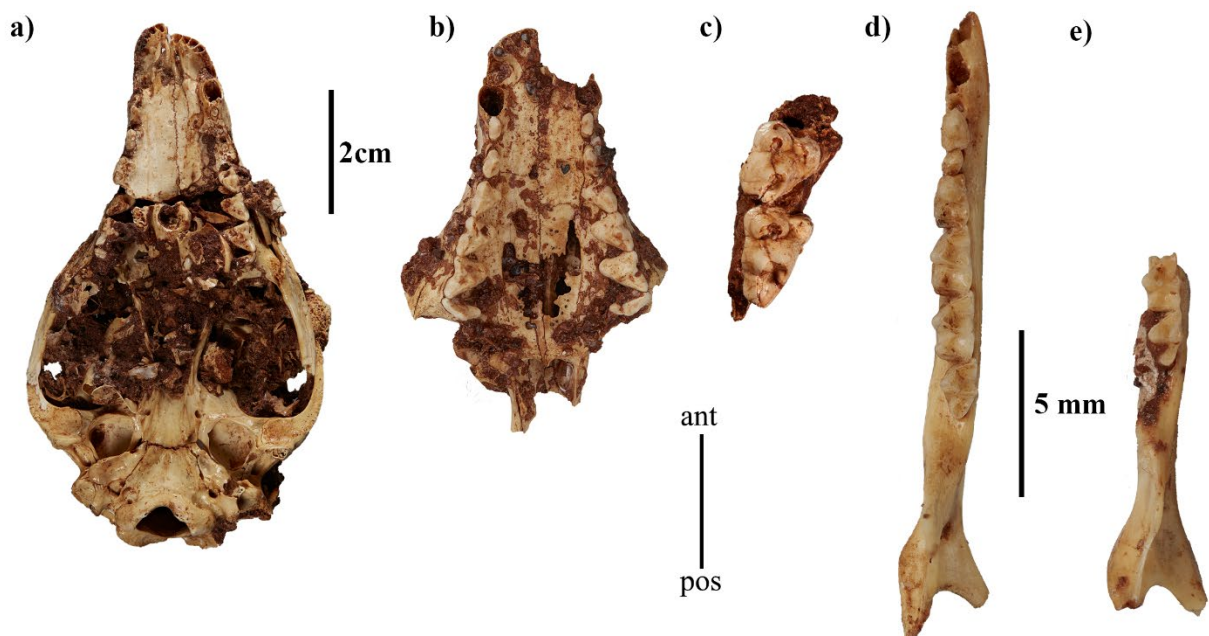


Figure 4.2. Dasyuromorphs a) *Dasyurus* sp. indet., cranium (CCW3034); b) *D. maculatus*, partial cranium (CCW885); c) *Sarcophilus lanarius*, R maxillary fragment with M1–2 (CCW2496); d) *Antechinus flavipes*, L dentary (CCW2475); e) *Antechinus* sp. cf. *A. agilis*, L partial dentary with M3–4 (CCW2742). 2 cm scale applies to a–c, 5 mm scale applies to d–e.

Phascogale tapoatafa (Meyer, 1793)

Brush-tailed Phascogale

MATERIAL: MNI = 11, NISP = 25. Exemplars only. CCW2655, Q II, layer 13, 505–520, R maxilla. CCW3793, Q II, layer 13, 510–515 cm, R dentary. CCW2868, Q II, layer 14, 515–520 cm, R maxilla fragment, L dentary, L mx. CCW2702, Q II, layer 14, 520–525 cm, L maxilla fragment, L M2. CCW2749, Q II, layer 14, 525–530 cm, R maxilla.

REMARKS: See notes for *Phascogale calura*. *Phascogale tapoatafa* is the largest member of this genus. Indistinguishable from modern specimens of *P. tapoatafa*.

Sminthopsis crassicaudata (Gould, 1844)

Fat-tailed Dunnart

MATERIAL: MNI = 72, NISP = 147. Exemplars only: CCW2698, Q II, layer 14, 520–525 cm, 2 L maxillae, R maxilla, 2 R dentaries, L dentary. CCW2747, Q II, layer 14, 525–530 cm, L dentary. CCW3209, Q II, layer 14, 560–565 cm, L maxilla.

REMARKS: The genus *Sminthopsis* includes 21 modern species, two of which are known to inhabit the Binjang region today; *S. murina* and *S. crassicaudata*. A further species, *S. macroura*, inhabits the more arid regions to the north-west and *S. leucopus* is known from southern coastal regions. *Sminthopsis* is differentiated from other genera of small dasyurids by a combination of characters that include having: no posterior cingulum on the upper molars; the third premolars are only slightly reduced or subequal in size to the second premolars; I4 with a longer crown than I2; metacristids and hypocristids are transverse to the long axis of the tooth row (Archer, 1976, 1981). *Sminthopsis crassicaudata* is distinguished from other entoconid bearing species of *Sminthopsis* (*S. macroura*, *S. virginiae*, and *S. douglasi*) by the hypocristid being connected to the prominent entoconid on M1–3 (Archer, 1976, 1981).

Sminthopsis murina (Waterhouse, 1838)

Common Dunnart

MATERIAL: MNI 67, NISP = 125. Exemplars only. CCW3795, Q II, layer 13, 510–515 cm, L dentary. CCW2873, Q II, layer 14, 515–520 cm, 2 L maxillae, 4 R maxillae, 7 L dentaries, 6 R dentaries. CCW2699, Q II, layer 14, 520–525, L maxilla, R maxilla, 2 L dentaries, R dentary. CCW3030, Q II, layer 14, 560–565 cm, 2 L dentaries.

REMARKS: *Sminthopsis murina* lacks an entoconid on m1–4 and the palate bears interdental fenestrae, but the latter are not as numerous as in *S. crassicaudata*, see Archer (1976).

Dasyuroides byrnei (Spencer 1896)

Kowari

MATERIAL: MNI = 14, NISP = 37. Exemplars only. CCW1658, layer 10, Q E, 335–340 cm, R dentary fragment with M1 (Figure 4.3b) and isolated R M1, R M3, L M2, R m3, L m2, L m3. CCW1105, layer 10, Q B, 345–350 cm, L maxillary fragment with M3–4 and isolated L m3. CCW4848, Q II, layer 14, 515–520 cm, R M3. CCW2212, layer 14, Q I, 570–580 cm, R maxillary fragment with M1–3 and isolated R m2 (Figure 4.3a).

REMARKS: Material of *Dasyuroides byrnei* collected in the FU excavation is mostly fragmentary, therefore, better preserved fossils collected by UNSW that were referred to “?*Dasyuroides* sp.” have been included to refine identification (Dawson and Augee, 1997). This taxon is distinguished from all other members of Dasyuridae in possessing a combination of the following characters: enlarged canines; P3 greatly reduced compared to P2; lacking posterior cingula on M1–4; weakly developed anterior cingula on M1; StB not distinct on M1; complete buccal cingula on p2 and m1–3 (no examples of p1 available); weakly developed paraconid on m1 (Archer, 1976).

Family THYLACINIDAE Bonaparte, 1838

Thylacinus cynocephalus (Harris, 1808)

Thylacine

MATERIAL: MNI = 5, NISP = 6. CCW2154, layer 12, Q II, 430–435 cm, isolated C1. CCW2908, layer 14, Q II, 515–520 cm, R m4 (Figure 4.3d). CCW2743, layer 14, Q II, 520–525 cm, RC1. CCW4859, Q I, layer 14, 530–535 cm, R M3. CCW1329, layer 14, Q II, 560–565 cm, R calcaneus (Figure 4.3c), R distal fibula (CCW1329).

REMARKS: Indistinguishable from modern specimens of *Thylacinus cynocephalus*

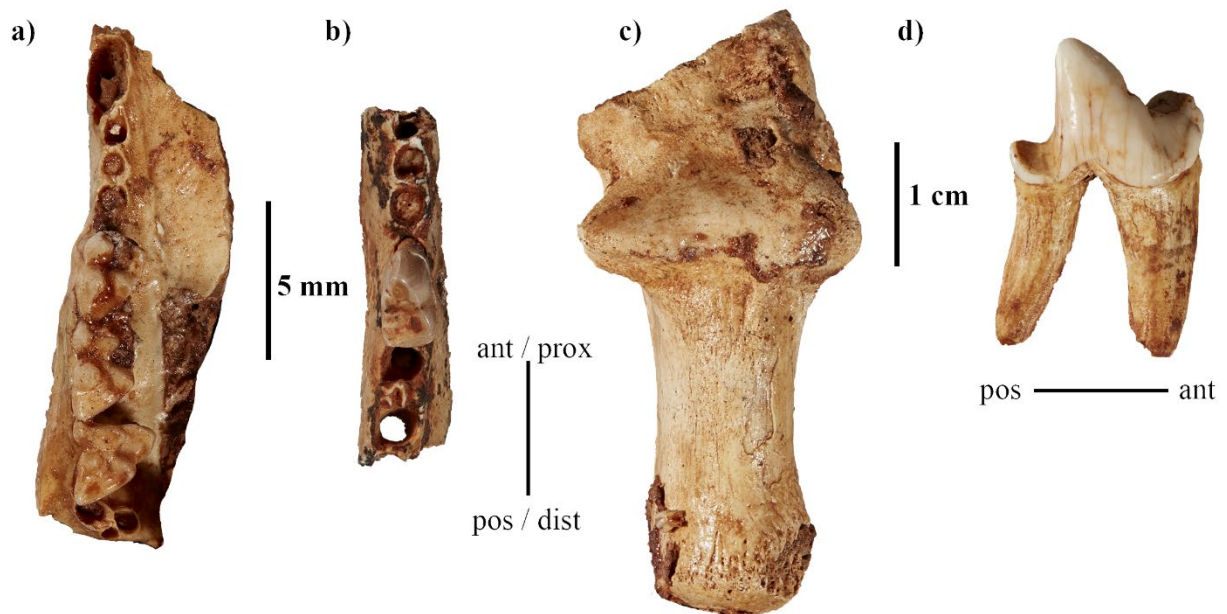


Figure 4.3. Dasyuromorphs a) *Dasyuroides byrnei*, maxillae with M1–3 (CCW2212); b) *D. byrnei*, dentary fragment with m1 (CCW1658); c) *Thylacinus cynocephalus*, R calcaneus (CCW1329); d) *T. cynocephalus*, R m4 (CCW2743). 5 mm scale applies to a–b, 1 cm scale applies to c–d.

Order PERAMELEMORPHIA Ameghino, 1889

Family CHAEROPODIDAE Gill, 1872

Chaeropus ecaudatus (Ogilby, 1838)

Pig-footed Bandicoot

MATERIAL: MNI = 10, NISP 20. CCW64, layer 5, Q B, 210–215 cm, L Mx. CCW1193, layer 10, Q B, 315–320 cm, R M1. CCW2085, Q A, layer 10, 325–330, R M1, L mx. CCW4047, Q A, layer 10, 335–340 cm, L M1, L M3, R m1. CCW3299, layer 10, Q B, 340–345, R M2, R M3, wear stages indicate not the same individual. CCW1691, layer 10, Q B, 345–350 cm, L M3, L m2, R M2, R Mx. CCW1692, layer 10, Q E, 350–355 cm, L M1, L M2, R M2, L M4. CCW2132, layer 10, Q II, 365–370 cm, L M1, L Mx. CCW3384, layer 10, Q II, 375–380 cm, R M2 (Figure 4.4a).

REMARKS: The extinct genus *Chaeropus* is distinct among peramelemorphs in having; high crowned teeth, with this height achieved by increasing the width of the tooth at an angle, rather than producing taller cusps; a prominent crest running buccally across the talon between the paracone and metacone, from the junction of the postprotocrista and the premetaconule (Travouillon, 2016). Additional characters that distinguish it from other peramelemorphs include; centrocrista ending on the lingual side of Mx; enamel on mx descends partially along the buccal side of the roots, but not to the same extent of *Isoodon*. Three species of *Chaeropus* are known from Pleistocene fossil records. *Chaeropus baynesi* is known from a single fossil locality of late Pliocene to early Pleistocene age in south-west NSW (Travouillon, 2016). *Chaeropus yirratji* has recent records from central Australia and Pleistocene fossils are known from north-east QLD (Travouillon et al., 2019). Fossil and modern records of *C. ecaudatus* stem from south-east, south-west and west of Australia. *Chaeropus ecaudatus* differs from *C. baynesi* in being higher crowned and from *C. yirratji*, in having a reduced metaconule on M1–3 that gives its molars a more triangular shape; StD absent on M1; distinctly larger metacone on M4; continuous paracristid on m1 (Travouillon et al., 2019).

Family PERAMELIDAE Gray, 1825

Isoodon obesulus (Shaw, 1797)

Southern Brown Bandicoot

REFERRED MATERIAL: MNI = 103, NISP = 954. Exemplars only. CCW2588, Q I, layer 13, 505-520 cm, cranium (Figure 4.4c). CCW2856, Q II, layer 14, 515–520 cm, 3 L maxillae, 9 R maxillae, 3 L dentaries, 3 R dentaries, 33 isolated teeth.

REMARKS: Indistinguishable from modern specimens of *Isoodon obesulus*. Differentiated from *I. auratus* in being larger and having a complete anterior cingulum on M2.

Perameles nasuta Geoffroy, 1804 or *Perameles gunnii* Gray, 1838

Southern Long-nosed Bandicoot or Eastern Barred Bandicoot

REFERRED MATERIAL: MNI = 139, NISP = 1870, NISP = 141. Exemplars only. CCW2049, Q II, layer 10, 380–385 cm, edentulous R dentary. CCW2855, Q II, layer 14, 515–520 cm, 3 L maxillae, 9 R maxillae, 15 L dentaries, 10 R dentaries 128 isolated teeth. CCCW2805, Q II, layer 14, 535–540, 11 L maxillae, 9 R maxillae, 12 L dentaries, 9 R dentaries.

REMARKS: Both *Perameles nasuta* and *Perameles gunnii* have been identified in the Cathedral Cave material, with *P. nasuta* being the most numerous (Hodge, 1991). However, the bulk of the fossils belonging to *Perameles* are isolated teeth and edentulous dentaries or maxillae that requires further work to identify the species for.

Family THYLACOMYIDAE Bensley, 1903

Macrotis lagotis (Reid, 1837)

Greater Bilby

REFERRED MATERIAL: MNI = 3, NISP = 6. CCW1934, Q E, layer 10, 345–350 cm, LMx missing posterior half. CCW3322, Q B, layer 10, 350–355 cm, mx, R m3. CCW1974, Q II, layer 10, 360–365, 2 m1/2, L M3? (Figure 4.4b).

REMARKS: *Macrotis* is easily recognised amongst peramelemorphs in having molars with bulbous cusps and square crowns. Other distinguishing characters are: absent hypocone, lingually placed metacone, absent anterior cingulum on upper molars; absent paraconid and broad anterior cingulid on lower molars (Long, 2002). *Macrotis lagotis* can be separated from *M. leucura* by the formers larger size.

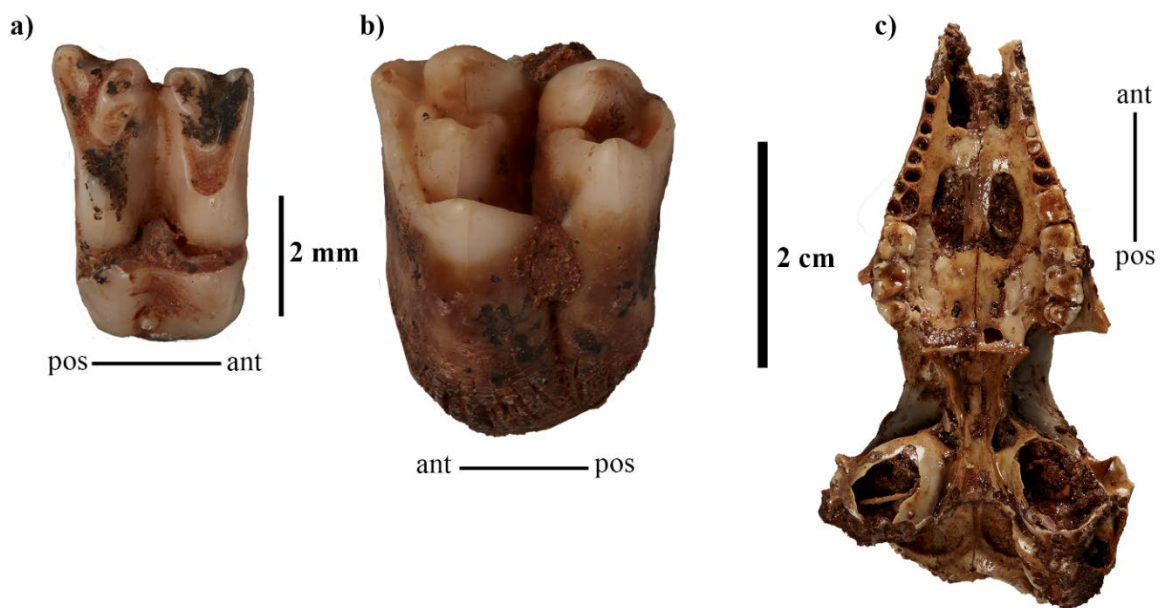


Figure 4.4. Peramelemorphs a) *Chaeropus ecaudatus*, R M2 (CCW3384); b) *Macrotis lagotis*, L M3? (CCW1974); c) *Isoodon obesulus*, cranium (CCW2588). 2 mm scale applies to a–b, 2 cm scale refers to c.

Order DIPROTODONTIA Owen, 1877

Family VOMBATIDAE Burnet, 1830

Vombatus sp. cf. *V. ursinus* (Shaw, 1800)

Bare-nosed Wombat

REFERRED MATERIAL: MNI = 16, NISP = 23. Exemplars only. CCW2433, Q III, layer 10, 415 cm, cranium with associated R dentary (Figure 3.16c). CCW2618, Q I, layer 13, 480–485 cm, L dentary. CCW3647, Q II, layer 13, 495–500, L dentary. CCW2799, Q III, layer 13,

505–510 cm, partial cranium including attached L and R maxillae, broken at premaxillary suture.

REMARKS: Species of *Vombatus* are distinguished from *Lasiorhinus* by numerous characters, those that are relevant to the material recovered in this excavation include: having narrower palate width between the posterior lobe of the left and right M1; a deep and large masseteric canal; anterolingual groove on upper premolars; a lack of inward curvature on the antero-buccal aspect of the fore lobe of the molars; more acute angularity of the apices of the lobes of m1–4; a sharper transition from lingual to lateral faces of m1–4; sharper transition from lateral to buccal faces of m1–4 (Merrilees, 1967; Dawson, 1983). *Vombatus ursinus* and *Vombatus mitchellii* are the sole Pleistocene species in the genus *Vombatus* known from eastern Australia; a third species, *Vombatus hacketti*, is known only from south-west Australia (Dawson, 1983; Louys, 2015). CCW2443 includes a cranium and associated R dentary. The cranium is missing much of the cranial vault and the right zygomatic arch but has complete rows of left and right cheek teeth. The dentary is missing the superior portion of the ramus and the anterior portion beyond m2 (Figure 3.16c). The length of the ectalveolar plate (Owen, 1872) and the length of the upper tooth row falls within the range of *V. mitchellii* (Table 4.3). The anterior palate is very restricted, with the distance between the posterior lobes of M1 within the range for *V. ursinus* rather than *V. mitchellii* (Table 4.3). The fossil has undergone post-depositional dorsolateral distortion; it is possible that the anterior palate has been compressed and artificially decreased the distance between the first molars. CCW2799 is a partial cranium with L M2–3 *in situ*. The ectalveolar plate length and length of the anterior palate place CCW2799 within the range for *V. mitchellii*, although the length of the upper tooth row falls within the range for both *V. mitchellii* and *V. ursinus* (Table 4.3). CCW3647 and CCW2618 are left dentaries with complete rows of cheekteeth. The toothrow lengths of both fossils fit within the range of *V. ursinus* but cannot be compared to *V. mitchellii* as there are not lower toothrow measurements available for this taxon due to a lack of complete dentary material (Dawson, 1983). These measurements place the *Vombatus* fossils from the FU excavation between the size range of *V. ursinus* and *V. mitchellii*.

The first fossil wombat material from the Wellington Caves was originally described as *Phascolomys mitchellii* by Richard Owen in 1838. This was later reduced to a subspecies of *V. ursinus* by Dawson (1983), who noted that there was little difference between modern samples of *V. ursinus*, other than the ectalveolar plate length. The subspecies level was

assigned to these fossils in an attempt to demarcate a topotypical sample of *Vombatus* from Wellington Caves (Dawson, 1983). During the UNSW excavation of Cathedral Cave, wombat fossils were referred to *Vombatus* sp. (Dawson and Augee, 1997). Elevation of *V. mitchellii* by Louys (2015) is based on statistical significance of the three cranial measurements and the addition of a partial cranium from the Pliocene Chinchilla Sands in south-east Queensland. The Chinchilla specimen grouped with *V. mitchellii* from Wellington Caves and displayed additional cranial characters that were seen to differ from modern *V. ursinus*. These characters are a circular fossa in the area between the maxillary process and the lateral margin of the tooth row, bulbous ectalveolar plate and lateral extension of the root of the zygomatic. The bulbous ectalveolar plate holds true on CCW2799 but less so on CCW2443; the fossa near the maxillary process is best described as ovoid in shape on both these specimens and is the same shape as the fossa on a compared cranium of modern *V. ursinus* (FUR212). To the best of our knowledge, *V. ursinus* and *V. mitchellii* have not been identified together in the same temporal and geographic space. The discrepancy between these specimens, over time and geographical distance, suggests that they represent a morphological cline of the same taxon. We elect to assign the Cathedral Cave specimens to *Vombatus* sp. cf. *V. ursinus*, due to their affinities with modern *V. ursinus*, pending future work.

Table 4.3. Cranial and dental measurements in mm for *Vombatus* fossils from Wellington Caves (Dawson, 1983), Chinchilla (Louys, 2015) and modern *V. ursinus*. Some measurements are presented as a range, indicated by –.

	Ectoalveolar length		Upper cheek teeth (alveoli)		Palate length between M ¹ – M ¹	Lower teeth row
	L	R	L	R		L
CCW2433	14.32		52.8	52.61	4.55	
CCW2779	14.17	14.25	46.99	46.71	6.24	
CCW3647						48.44
CCW2618						46.52
<i>V. ursinus</i>	11.0–13.5		43–50		4.5–7.6	45.5–54.5
<i>V. mitchellii</i> (Wellington Caves)	14.5–17		44.5–54.5		5.85–7.3	
<i>V. mitchellii</i> (Chinchilla)	14–16.1		53.2–53.5		7.4	

Family DIPROTODONTIDAE Gill 1872

Diprotodontidae gen. et. sp. indet.

REFERRED MATERIAL: MNI = 5, NISP = 5. CCW167, Q A, layer 2b, 252–257 cm, fragment of tooth enamel. CCW325, Q B, layer 8, 256–261 cm, fragment of tooth enamel. CCW443, Q A, layer 9, 280–295 cm, fragment of tooth enamel. CCW2958, Q II, layer 14, 530–540 cm, fragment of tooth enamel. CCW2964, Q IV, layer 14, 560–565 cm, fragment of tooth enamel.

REMARKS: All three fossils are too fragmentary to identify to genus or species level, but their size and enamel thickness clearly aligns them with the Diprotodontidae rather than the following.

Family PALORCHESTIDAE Gill 1872

Palorchestes azael Owen 1874

Palorchestes

REFERRED MATERIAL: MNI = 1, NISP = 1. CCW844, Q II, layer 14, 570–575, Li₁. CCW5032, Q IV, layer 14, 585–590 cm, juvenile L dentary with complete row of cheek teeth and unerupted m4 (Figure 3.19).

REMARKS: *Palorchestes* is easily recognised by its high crowned subrectangular, bilophodont molars. The lower molars have high, crescent shaped lophids; a deep, V-shaped interlophid valley; high, divided midlink (Woods, 1958). *Palorchestes azael* is the largest and most common of the two *Palorchestes* species at Wellington Caves and can be separated from *P. parvus* by size. *Palorchestes parvus* has been identified in older assemblages at Wellington (Dawson, 1985), but not in Cathedral Cave. CCW5032 was recovered during the April 2019 field trip, at a stratigraphic level below that included in the faunal analysis.

Family THYLACOLEONIDAE Gill, 1872

Thylacoleo carnifex Owen, 1859

Thylacoleo

REFERRED MATERIAL: MNI = 2, NISP = 2. CCW947, Q B, layer 10, 340–345 cm, P2 (Figure 4.5a). CCW2983, Q II, layer 14, 560–565 cm, R proximal femur.

REMARKS: The proximal femur CCW2983 has a large, hemispherical femoral head; a well-developed greater trochanter and a deep trochanteric fossa (Finch and Freedman, 1988). The premolar is single rooted, with a thick enamel crown and textured dentine. Identification of the premolar was made after comparisons with photographs of museum specimens as access to the specimens was not possible due to covid restrictions. The best match was with a P2.

Family BURRAMYIDAE Broom, 1898

Cercartetus nanus (Desmarest, 1817)

Eastern Pygmy-possum

REFERRED MATERIAL: MNI = 7, NISP = 7. CCW3310, Q B, layer 10, 345–350 cm, isolated L M2. CCW3326, Q B, layer 10, 350–355 cm, R dentary. CCW2411, Q II, layer 13, 485–490 cm, L dentary. CCW2640, Q II, layer 13, 505–510 cm, L dentary. CCW3661, Q II, layer 13, 500–505 cm, L maxilla. CCW3661, Q II, layer 14, 520–525, R maxilla. CCW2752, Q II, layer 14, 525–530 cm, L dentary.

REMARKS: *Cercartetus nanus* is separated from other members of its genus by combination of: its larger size; a distinctly bifid P3 that is larger than that of *C. lepidus*; a triangular p3; three molars.

Family PETAURIDAE Bonaparte, 1832

Petaurus breviceps (Waterhouse, 1838)

Sugar Glider

REFERRED MATERIAL: MNI = 32, NISP = 54. Exemplars only. CCW2389, Q II, layer 13, 480–495 cm, R dentary. CCW2529, Q II, layer 13, 500–505, R maxilla, 2 L dentaries, R

dentary, L i1. CCW2937, Q I, layer 13, 510–520 cm, cranium (Figure 4.5b). CCW2797, Q II, layer 14, 535–540 cm, 2 L maxillae, 3 R dentaries, 2 isolated molars.

REMARKS: *Petaurus breviceps* is differentiated from *P. norfolcensis* by its smaller third premolar and from *P. australis* by its smaller size; smaller third premolar; lack of metaconid on m1; squarer occlusal outline of M2 (Archer, 1984). A fourth Australian species, *P. agilis*, is smaller than *P. breviceps* and has a restricted distribution in coastal northern Queensland.

Family PSEUDOCHEIRIDAE Winge, 1893

Pseudocheirus peregrinus (Boddaert, 1785)

Eastern Ring-tailed Possum

REFERRED MATERIAL: MNI = 7, NISP = 14. CCW4975, Q E, layer 10, 335–340, R i1. CCW2412, Q II, layer 13, 485–490, isolated R m1, L p3. CCW3608, Q II, layer 13, 490–495, R m2. CCW2866, Q II, layer 14, 515–520 cm, L maxilla with M2–3. CCW2834, Q II, layer 14, 535–540, L M4, R M4, L m1, L m2, R M1, R M2, R M3, R M4. CCW3070, Q I, layer 14, 570–575 cm, isolated L Mx.

REMARKS: Within Australian pseudocheirids, only *Pseudocheirus peregrinus* and *Petauroides volans* have modern ranges that are not restricted to the north or south-west of the continent. *Pseudocheirus peregrinus* is differentiated from *Pet. volans* by lacking distinct posterolingual crests that originate at the paracone and metacone of M1–4 (Archer, 1984); in lacking a posterolingual protocristid and by the protocristid connecting with the metastylid on m1–4 (McDowell, 2002).

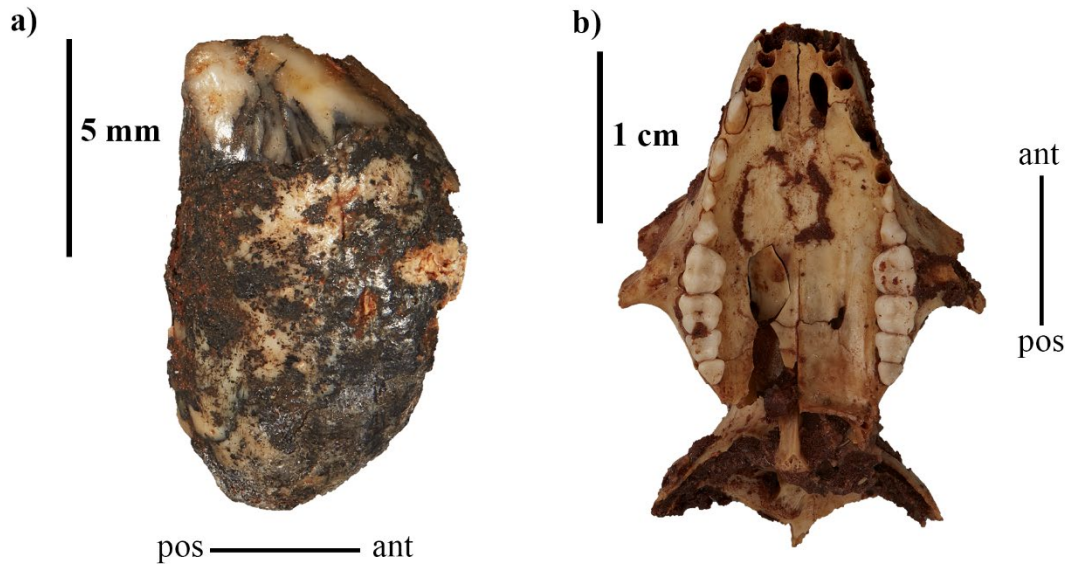


Figure 4.5. Remains of a) *Thylacoleo carnifex*, P2 (CCW2983); b) *Petaurus breviceps*, cranium (CCW2937).

Family ACROBATIDAE Aplin, 1987

Acrobates pygmaeus (Shaw, 1794)

Narrow-toed Feather-tailed Glider

REFERRED MATERIAL: MNI = 4, NISP = 5. CCW3550, Q II, layer 13, 470–475, R dentary. CCW2614, Q II, layer 13, 500–505, 2 L dentaries. CCW2641, Q II, layer 13, 505–510, R maxillae, L dentary.

REMARKS: *Acrobates pygmaeus* is recognisable among other small phalangeriforms by having: double rooted P2–3; in the second premolar being as large as, or larger than, the third premolar (Archer et al., 1997).

Family PHALANGERIDAE Thomas, 1888

Trichosurus vulpecula (Kerr, 1792)

Common Brush-tailed Possum

REFERRED MATERIAL: MNI = 15, NISP = 18. Exemplars only. CCW327, Q B, layer 8, 256–261 cm, L premaxilla. CCW365, Q B, layer 8, 261–266 cm, R maxilla. CCW2603, Q II, layer 13, 500–515, L maxilla. CCW3646, Q III, layer 14, 575–580 cm, cranium, L dentary. REMARKS: Indistinguishable from modern *T. vulpecula* presently in the area. A cranium from Q III, layer 14, 5775–580 cm is notably large, being comparable to larger modern specimens collected from Tasmania (Correll et al., 2016).

Family POTOROIDAE Gray, 1821

Aepyprymnus rufescens (Gray, 1837)

Rufous Bettong

REFERRED MATERIAL: Exemplars only. MNI = 45, NISP = 110. CCW4712, Q II, layer 12, 440–445 cm, partial cranium, cranium. CCW2332, unit II, layer 13, 475–480 cm, L maxilla, 2 L dentaries, R dentary, L calcaneus with cuneiform complex.

REMARKS: Indistinguishable from modern *Aepyprymnus rufescens*. P3 is tall, narrow, with seven vertical ridges and a serrated edge. The molars are bunodont and differ from *Potorous* and *Bettongia* in being larger and having a less symmetrical occlusal outline.

Bettongia gaimardi (Desmarest, 1822)

Eastern Bettong

REFERRED MATERIAL: MNI = 6, NISP = 6. CCW1772, Q E, layer 10, 345–350 cm, L M4. CCW3300, Q B, layer 10, 350–355 cm, R m3. CCW4899, Q II layer 12, 450–455, RM₃. CCW2306, Q II, layer 13, 470–474 cm, 2 L dentaries. CCW4709, Q II, layer 13, 505–510 cm, R m1.

REMARKS: Species of *Bettongia* are differentiated from other potoroids by: large, blade-like third premolars 7–11 vertical ridges; upper molars with buccal crests that are better developed than the lingual crests; lower molars with lingual crests that are better developed than buccal crests. Of the six modern species of *Bettongia*, *B. gaimardi*, *B. lesueur* and *B. penicillata* have distributions that include central-east or south-east Australia. *B. gaimardi* is

separated from other species of recently extant *Bettongia* by possessing larger molars with less of a size gradient between M1 and M4; P3 is broad compared to *B. lesueur* and does not flex outward as it does in *B. penicillata*.

Bettongia lesueur (Quoy & Gaimard, 1824)

Boodie / Burrowing Bettong

REFERRED MATERIAL: MNI =26, NISP = 54. Exemplars only. CCW8, Q B, layer 2, 183–188 cm, L maxilla with M2. CCW3364, Q E, layer 10, 360–365 cm, L M1, L M2, L p3, L m2, L m3, R I1. CCW2564, Q II, layer 13, 500–505 cm, R maxilla, R dentary, isolated R Mx.

REMARKS: *Bettongia lesueur* is separated from other species of *Bettongia* in having: a molar size gradient that is greater only in *B. anhydra*; a curved upper molar row; P3 is proportionally narrower and more elongate with a straighter crest.

Genus *Potorous* Desmarest, 1804

Potorous tridactylus (Kerr, 1792)

Long-nosed Potoroo

REFERRED MATERIAL: MNI = 21, NISP = 41. Exemplars only. CCW3619, Q II, layer 13, 500–505 cm, R maxilla, isolated L M1, R M1, R dp3. CCW5023, Q II, layer 13, 505–510, juvenile R maxilla. CCW3662, Q II, L 14, 520–525 cm, juvenile R dentary (Figure 4.6a). CCW2830, Q II, layer 14, 535–540 cm, L dentary, R dentary, 7 isolated molars.

REMARKS: Members of the genus *Potorous* are distinguished by their bunolophodont molars that are longer than they are wide (cf. *Bettongia*); P3 has 3 – 5 vertical ridges with the anterior and posterior ridges being wider. *Potorous tridactylus* is the only modern species of *Potorous* to have a distribution that is not restricted to coastal or near-coastal regions. Indistinguishable from modern specimens of *P. tridactylus*.

Family MACROPODIDAE Gray, 1821

Subfamily STHENURINAE Glauert, 1926

Sthenurus andersoni Marcus, 1962

REFERRED MATERIAL: MNI = 4, NISP = 4. CCW1212, Q B, layer 10, 315–320 cm, R dp2 loph. CCW4971, Q E, layer 9, 280–285 cm, posterior half L Mx. CCW2305, Q II, layer 13, 470–475 cm, L I1. CCW4707, Q II, layer 14, 570–575 cm, anterior half of R m2 (Figure 4.6b).

REMARKS: Species of *Sthenurus* are distinguished from other sthenurines by their higher crowned teeth and broadened I1. These specimens have been attributed to *Sthenurus andersoni* based on their small size and the presence of a few, very fine enamel crenulations on the anterior faces of the molar lochs (Prideaux, 2004).

Sthenurus atlas (Owen, 1838)

REFERRED MATERIAL: MNI = 1, NISP = 1. CCW843, Q II, layer 14, 560–565, m3 (Figure 4.6e).

REMARKS: Larger than *S. andersoni* and marked by its distinctive paracristid morphology, where the posterior portion is oriented decidedly anterolingually and the anterior portion is reduced to a cusp (Prideaux, 2004).

Simosthenurus pales De Vis, 1895

REFERRED MATERIAL: MNI = 2, NISP = 2. CCW1626, Q II, layer 12, 440–445 cm, L P3. CCW837, Q II, layer 13, 460–465, R p3 (Figure 4.6c).

REMARKS: P3 and p3 are larger and higher crowned than in all other species of *Simosthenurus*. The P3 has a strong, high transverse ridge that separates the anterior and longitudinal basins and lacks a well-developed transverse ridge separating the posterior and longitudinal basins (Prideaux, 2004). The p3 bears a very prominent anteriormost cuspule of

main crest and the long buccal crest terminates adjacent to short ridgelet directed posteriorly along tooth midline from anteriormost cuspule (Prideaux, 2004).

Procoptodon goliah (Owen, 1845)

REFERRED MATERIAL: MNI = 3, NISP = 3. CCW1733, Q E, layer 8, 260–265 cm, L Mx. CCW1326, Q E, layer 10, 360–365 cm, Mx (Figure 4.6d). CCW4577, Q I, layer 10, 395–400 cm, M2 fragment.

REMARKS: Species of *Procoptodon* are distinguished from other sthenurines by having molars with very high, coarse cristae, and a mesocrista that is united with the posterior portion of the postprotocrista to form a ‘midlink’ (Prideaux, 2004). The upper molars of *P. goliah* differ from those of *P. rapha* by being more bulbous and larger relative to the size of the maxilla.

Subfamily MACROPODINAE Gray, 1821

Baringa sp. nov. 1

REFERRED MATERIAL: MNI = 3, NISP = 5. CCW4931, Q A, layer 10, 335–340 cm, medial phalanx of manual digit I. CCW2125, Q II, layer 10, 385–390 cm, LI¹. CCW4862, Q II, layer 13, 505–520, proximal, medial and distal phalanges of digit V (manus) collected in articulation (Figure 3.16e).

REMARKS: This macropodine species is currently being described based largely on material from the Nullarbor caves and Lake Callabonna (Warburton and Prideaux, in prep.). It is distinguished by several highly unique craniodental and limb attributes (G. Prideaux, pers. comm., February 2021).

Congruus kitcheneri (Flannery, 1989)

REFERRED MATERIAL: MNI = 10, NISP = 13. CCW973, Q B, layer 10, 325–330 cm, L m4. CCW4976, Q B, layer 10, 345–350 cm, L dP2. CCW4979, Q E, layer 10, 350–355 cm, L

M2, posterior fragment, L I1 fragment. CCW4948, Q II, layer 12, 435–440 cm, R m2 anterior loph. CCW4944, Q II, layer 12, 450–455 cm, L M4. CCW2326, Q II, layer 13, 470–475 cm, R i1. CCW4563 Q II, layer 13, 510–520 cm, juvenile L dentary, L calcaneus. CCW2489, Q IV, layer 13, 520–530 cm, R calcaneus (Figure 4.6h). CCW5017, Q II, layer 14, 535–540 cm, isolated R p3, L I1. CCW2575, Q I, layer 14, 535–540 cm, juvenile R dentary (Figure 4.6i). CCW1615, Q II, layer 14, 560–565, juvenile L dentary including m1–3.

REMARKS: Morphologically, the molars of *Congruus kitcheneri* are most similar to those of the species of *Thylogale* and *Protemnodon*, and are intermediate in size between the two (Warburton and Prideaux, 2021). The lophids and lower-molar enamel are distinctly thinner in *C. kitcheneri* than in species of *Protemnodon*, and the p3 is relatively shorter and wider than in species of both *Thylogale* and *Protemnodon*. Its dentary is more elongate and gracile than that of any other macropodine genus known from the Quaternary. The calcaneus is robust and broad posteriorly compared to other macropodines of similar size and is most similar in shape to that of the species of *Thylogale*.

Genus *Petrogale* Gray, 1837

Petrogale sp. indet.

Rock-Wallaby

REFERRED MATERIAL: MNI = 1, NISP = 2. CCW2494, Q II, layer 13, 470–475 cm, L maxilla, L calcaneus.

REMARKS: *Petrogale* is most similar in upper molar morphology to *Thylogale*, but is distinguished by having thicker lophids with more curved crests. The calcaneus is characterised by an elongate tuber and a talar articulation that is narrow relative to its length.

Protemnodon brehus Owen, 1874

REFERRED MATERIAL: MNI = 6, NISP = 9. CCW3207, Q B, layer 10, 325–330, L m2. CCW2308, Q II, layer 13, 470–475, juvenile R femur. CCW2514, Q I, layer 13, 475 – 480 cm, L dentary, L I1 (Figure 4.6g). CCW2973, Q II, layer 13, 485–490, metatarsal IV.

CCW2520, Q III, L 13, 500 – 515 cm, L M2 (Figure 4.6f). CCW2653, Q II, layer 13, 505–520, metatarsal V, distal pedal phalanx V.

REMARKS: This species of macropodine is currently under revision as part of a PhD by Isaac Kerr at Flinders University, based largely on material from Lake Callabonna, Laena's Breath Cave, Green Waterhole Cave and Mount Cripps. It is distinguished from other species of *Protemnodon* by several osteological characters (I. Kerr, pers. comm., February 2021).

Lagorchestes leporides (Gould, 1841)

Eastern Hare-wallaby

REFERRED MATERIAL: MNI = 12, NISP = 13. Exemplars only. CCW329, Q B, layer 8, 256–261 cm, L m4. CCW81, Q B, layer 9, 340–345 cm, isolated R dP2. CCW4958, Q B, layer 10, 350–355 cm, isolated R M1. CCW2252, Q II, layer 12, 445–450 cm, isolated L P3. CCW2303, Q II, layer 13, 470–475 cm, associated L and R maxillae. CCW2960, Q II, layer 14, 560–565 cm, cranium.

REMARKS: Among Quaternary macropodins, species of *Lagorchestes* are similar in size only to those of *Onychogalea*, but differ by having longer, blade-like premolars and upper molars that lack a strongly developed postprotocrista and retain a postprotocrista. Within *Lagorchestes*, *L. leporides* is intermediate in size between the central Australian *L. hirsutus* and northern tropical *L. conspicillatus*.



Figure 4.6. Macropodiformes a) *Potorous tridactylus*, juvenile R dentary (CCW3662); b) *Sthenurus andersoni*, anterior half of R m2 (CCW4704); c) *Simosthenurus pales*, R p3 (CCW837); d) *Procoptodon goliah*, Mx (CCW1326); e) *Sthenurus atlas*, m3 (CCW843); f) *Protamnodon brehus*, L M2 (CCW2520) g) *Protamnodon brehus*, L dentary (CCW2514); h) *Congruus kitcheneri*, R calcaneus (CCW2489); i) *Congruus kitcheneri*, juvenile L dentary (CCW2575). 1 cm scale applies to a–f, 2 cm scale applies to g–i.

Macropus giganteus Shaw, 1790

Eastern Grey Kangaroo

REFERRED MATERIAL: MNI = 35, NISP = 82. Exemplars only. CCW2490, Q II, layer 13, 480–485, R maxilla, L dentary, L M1, L I1, L P3, R calcaneus, partial R calcaneus, proximal tibia epiphysis. CCW2582 Q II, layer 14, 515–530, R dentary with dp2–3. CCW2941, Q I, layer 14, 525–530 cm, R dentary (Figure 4.7a). CCW2922, Q II, layer 14, 535 – 540 cm, L maxilla, 2 R maxillae, L dentary, 5 R dentaries, L I2, L I3, L dP3, R I1, R I2, R I3, L dp2, L dp3, 2 L i1, 3 R i1, 2 R dp2, R dp3, R m1, calcaneus, distal tibia epiphysis. CCW2902, Q II, layer 14, 570–575 cm, L maxilla, R dentary.

REMARKS: Large, high crowned macropodin with high molar links distinguished from species of *Osphranter* by kinked cristid obliqua and paracristid on lower molars, and upper molars with a kinked postprotocrista and distinct preprotocrista (forelink). The calcaneus is elongate but more robust than in species of *Osphranter*. There are no known osteological grounds upon which *M. giganteus* and *M. fuliginosus* may be distinguished.

Notamacropus agilis (Gould, 1842)

Agile Wallaby

REFERRED MATERIAL: MNI = 14, NISP = 25. Exemplars only. CCW3004, Q II, layer 13, 480–485, proximal R metatarsal IV (large). CCW2950, Q II, layer 14, 535–540, L P3, 2 L M2, R P3, L p3, posterior portion L m2, 2 R m1, R m3, R mx, L mx, proximal metatarsal IV, R ilium fragment. CCW4918, Q II, layer 14, 560–565, R dentary. CCW2578, Q II, layer 14, 570–575, R dentary.

REMARKS: Species of *Notamacropus* share extensive similarities with those of *Osphranter* and *Macropus* in dental and skeletal morphology but are typically much smaller. Dentally, they exhibit no molar progression and lower molars possess a distinct posthypocristid. The referred specimens are indistinguishable from modern specimens of *N. agilis*, the largest extant species in the genus.

Notamacropus dorsalis (Gray, 1837)

Black-striped Wallaby

REFERRED MATERIAL: MNI = 14, NISP = 23. Exemplars only. CCW1873, Q E, layer 4, 205–210, M1. CCW2169, Q II, layer 12, 435–440, partial L M2, 2 L dp3, posterior portion L m2, anterior portion L m2, R m3. CCW2051, Q II, layer 12, 445–450 cm, R maxilla with dp2. CCW3066, Q II, layer 14, 570–575, R dP3.

REMARKS: Intermediate-sized species of *Notamacropus*, most similar to *N. parryi*, but distinguished by having larger premolars and a procumbent i1.

Notamacropus parma (Waterhouse, 1846)

Parma Wallaby

REFERRED MATERIAL: MNI = 33, NISP = 68. CCW789, Q II, layer 10, 370–375 cm, R maxilla, R M2. CCW5029, Q II, layer 13, 470–475 cm, R maxilla, L dentary, L I1. CCW3562, Q II, layer 13, 475–480, 2 R maxillae, 2 R dentaries. CCW3023, Q II, layer 14, 560–565, L dentary, R dentary, cranium, L I3, R dp3. CCW4936, Q I, layer 14, 635 – 640, cranium (Figure 4.7b).

REMARKS: *Notamacropus parma* is distinctly the smallest extant species in the genus.

Notamacropus parryi (Bennett, 1835)

Whip-tailed Wallaby

REFERRED MATERIAL: MNI = 4, NISP = 3. CCW1577, Q E, layer 10, 370–375 cm, isolated L M4. CCW3403, Q II, layer 12, 430–435, isolated posterior portion R dp3. CCW4922, Q I, layer 13, 505–510, R maxilla. CCW2956, Q II, layer 14, 535–540 cm, partial R dentary with i1.

REMARKS: Moderately large species of *Notamacropus* with reduced premolars and a distinctly upturned i1, reminiscent of that seen in species of *Petrogale*.

Onychogalea frenata (Gould, 1840)

Bridled Nail-tailed Wallaby

REFERRED MATERIAL: MNI = 9, NISP = 11. Exemplars only. CCW448, Q B, layer 8, 284–289 cm, L dp3. CCW1621, Q B, layer 9, 251–256, L dP3. CCW991, Q B, layer 10, 325–330 cm, R M4. CCW3319, Q B, layer 10, 350–355 cm, L m2. CCW2358, Q II, layer 10, 405–410, R M2. CCW4956, Q II, layer 12, 420–425, R maxilla fragment with P3.

REMARKS: Species of *Onychogalea* are distinguished from those of other genera by having a deep superficial masseter origin on the jugal with a distinctly projected orbital rim. The premolars are highly reduced to a bicuspid morphology. *Onychogalea frenata* is intermediate in size between *O. lunata* and *O. unguifera*.

Onychogalea lunata (Gould, 1840)

Crescent Nail-tailed Wallaby

REFERRED MATERIAL: MNI = 3, NISP = 3. CCW414, Q A, layer 8, 275–285 cm, L M2. CCW4935, Q E, layer 10, 305–310, R Mx. CCW741, Q B, layer 10, 340–345 cm, L P3.

REMARKS: Distinguished from *O. frenata* by its smaller size.

Osphranter robustus (Gould, 1840)

Wallaroo

REFERRED MATERIAL: MNI = 11, NISP = 17. Exemplars only. CCW4972, Q II, layer 10, 360–365 cm, isolated R P3. CCW4597, Q II, layer 14, 530–535 cm, R maxilla. CCW4921, Q II, layer 14, 535–540 cm, 2 R dentaries, 2 R I3, R M1, L m1. CCW4952, Q II, layer 14, 570–575 cm, L I1.

REMARKS: Species of *Osphranter* are distinguished from species of the similarly sized and closely related *Macropus* by possessing a shorter I3, a blade-like as opposed to bi- or tri-cuspid P3, and upper molars with a shelf-like postmetaconulecrista, which forms a distinct pocket on the posterior molar face. *Osphranter robustus* is distinguished from *O. rufus* by having a longer I3 and larger P3, a slight preprotocrista (forelink) and a slightly kinked paracristid and cristid obliqua.

Osphranter rufus (Desmarest, 1822)

Red Kangaroo

REFERRED MATERIAL: MNI = 2, NISP = 2. CCW4913, Q E, layer 9, 285–290 cm, juvenile L premaxilla with I1. CCW2580, Q I, layer 14, 560–565, R M4.

REMARKS: *Osphranter rufus* is distinguished from *O. robustus* by having a shorter, smaller I3 and P3, no preprotocrista, and a paracristid and cristid obliqua that curve toward the midline of the lower molar with no inflection.

Wallabia bicolor (Desmarest, 1804)

Swamp Wallaby

REFERRED MATERIAL: MNI = 2, NISP = 2. CCW1618, Q E, layer 10, 370–375 cm, R M3. CCW4900, Q II, layer 10, 385–390, isolated R P3.

REMARKS: Similar in size to *Notamacropus agilis*, but distinguished by having the main P3 crest composed of multiple cusps, and molars that are shorter for their width with a slight postparacrista.

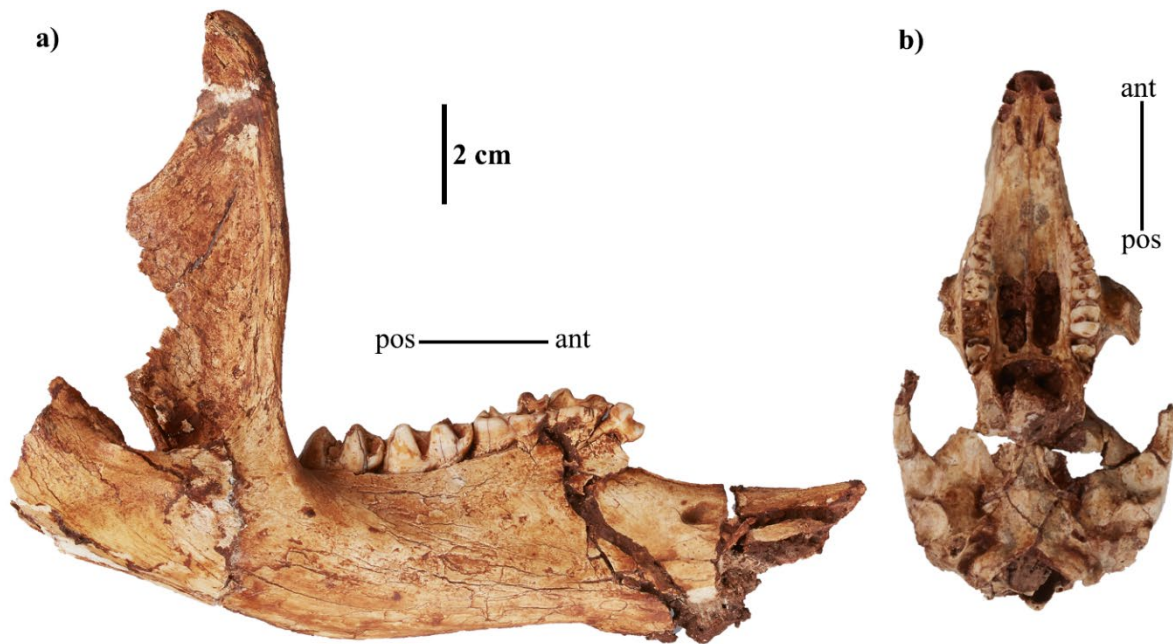


Figure 4.7. Macropodids a) *Macropus giganteus*, R dentary (CCW2941); b) *Notamacropus parma*, cranium (CCW4936).

Order RODENTIA Bowdich, 1821

Family MURIDAE Illiger, 1811

Conilurus albipes (Lichtenstein, 1829)

White-footed Rabbit-rat

REFERRED MATERIAL: MNI = 159, NISP = 415. Exemplars only. CCW2791, Q II, layer 13, 535–540, 29 L dentaries, 22 R dentaries, 25 L maxillae, 26 R maxillae, cranium.

REMARKS: The recently extinct *Conilurus albipes* is recognised by: its large size; upright, well defined molar cusps and well-developed T7 on M1–2; the anterior edge of the zygomatic arch is straight; the anterior palatal foramen is broad, short and rounded at the posterior terminus. On the dentary, M1 have a large posterior accessory cusp; the coronoid process is small and low, ending well below the articular process; the deep masseter scar does not intrude on the mental foramen.

Hydromys chrysogaster Geoffroy, 1804

Rakali / Water Rat

REFERRED MATERIAL: MNI = 2, NISP = 2, CCW1771, Q E, layer 10, 345–350 cm, isolated R m2. CCW5000, Q II, layer 13, 500–515 cm, isolated L m1.

REMARKS: *Hydromys chrysogaster* is the only known member of its genus in Australia. The dentition of *H. chrysogaster* is distinct in consisting of two molars, rather than three, a trait not shared with any other Australian rodents. The first molars are elongate, with deep basins on the occlusal surface.

Mastacomys fuscus Thomas, 1882

Tooarrana / Broad-Toothed Rat

REFERRED MATERIAL: MNI = 45, NISP = 101. Exemplars only. CCW1670, Q E, layer 10, 335–340 cm, 1 L maxilla, 3 R maxillae, 2 L dentaries, 3 R dentaries, isolated R M3. CCW3053, Q II, layer 14, 570–575 cm, 6 L maxillae, 5 L maxillae, 3 L dentaries, 6 R dentaries.

REMARKS: *Mastacomys fuscus* is the sole member of its genus. It is recognised by its large, broad molars, with distinctly formed columnar cusps. The upper molars have a strong posterior slope, whereas the lower molars have a strong anterior slope. The zygomatic plate is short and comparatively narrow, with a curved anterior edge. The anterior palatal foramen terminates in a sharp point. The dentary is robust, with a short diastema and the coronoid process ends above the articular process.

Notomys Lesson, 1842

Notomys sp. indet.

Hopping Mouse

REFERRED MATERIAL: MNI = 174, NISP = 339, Exemplars only. CCW1673, Q E, layer 10, 335–340 cm, 23 L maxillae, 17 R maxillae, 18 L dentaries, 24 R dentaries. CCW4989, Q E, layer 10, 345–350 cm, 10 L maxillae, 22 R maxillae, 18 L dentaries, 13 R dentaries. CCW3377, Q E, layer 10, 360 – 365 cm, 3 R maxillae, 6 L maxillae, 5 L dentaries, 4 R dentaries (Figure 4.8a). CCW2859, Q II, layer 14, 9.2.17 (515–520 cm), 1 R maxilla. CCW3303, Q B, layer 10, 340 – 345 cm, 3 L maxillae, 1 R maxilla, 6 L dentaries, 14 R dentaries (Figure 4.8a–c).

REMARKS: Specimens of *Notomys* sp. indet. are unable to be determined beyond genus. The Cathedral Cave specimens differ from *N. mitchellii*, *N. alexis* and *N. fuscus* by possessing a longer, rounder, open angle of the concave posterior edge of the zygomatic plate thus resulting in a wider distance between the edge of the maxillary alveolar process and the zygomatic arch. Measurements of the M1 are smaller than those of the holotypes of *N. mordax* but within range of those for *N. mitchellii* (Table 4.4). The zygomatic arch was poorly preserved in most specimens, except CCW2850 that retains this feature and shows a wide expansion of anterodorsal region of the zygomatic arch. Molars are low crowned (compared to *P. australis*) and upright (compared to *P. gracilicaudatus*). M3 is reduced and the outline is relatively round (compared to *P. fieldi* which is more triangular in outline). When viewed in occlusal view, there is no obvious ‘step’ down where the maxillary alveolar process meets the palatine. The anterior palatal foramen tapers in on the buccal edge prior to terminating. Buccal surface of maxillary alveolar process is flat and tall dorsoventrally. Maxillary alveolar process and palatine are curved dorsoventrally. On M1, T2 is posteriorly placed, T3 is highly reduced. On the dentary, the deep masseter scar projects over the mental foramen. The lophs of the lower molars are straight.

Table 4.4. Measurements of M1 (mm) of several *Notomys* species.

Species	M ¹ L x W	Specimen #	
<i>Notomys</i> sp. indet.	2.82 x 1.78	CCW2850	Cathedral Cave
<i>Notomys mordax</i>	3.3 x 2.2	1846.4.4.65	(Mahoney, 1977)
<i>Notomys mitchellii</i>	2.9 x 1.9	C2530	(Mahoney, 1977)
	2.5 x 1.7	C15019	

Pseudomys australis J Gray, 1832

Palyoora / Plains Mouse

REFERRED MATERIAL: MNI = 2688, NISP = 7989. Exemplars only. CCW317, Q A, layer 8, 256–261 cm, 1 cranium, 6 R maxillae, 6 L maxillae, 2 L dentaries. CCCW1214, Q B, layer 10, 315–320 cm, 148 L maxillae, 143 R maxillae, 79 L dentaries, 80 R dentaries. CCW2663, Q II, layer 13, 505–520, 3 crania, 23 L maxillae, 30 R maxillae, 39 L dentaries, 38 R dentaries. CCW3062, Q II, layer 14, 570–575 cm, 115 L maxillae, 85 R maxillae, 136 L dentaries, 151 R dentaries, cranium (Figure 4.8d–e).

REMARKS: A large species of *Pseudomys*. The anterior spine on the zygomatic plate is well developed, and the anterior edge of the zygomatic plate curves posteriorly but is more symmetrical than *Notomys*. The anterior palatal foramen is long, and wide with an acute curve at the posterior terminus; the buccal edge of the anterior palatal foramen is straight. The palatine is recessed, more so toward the anterior palatal foramen. Molars are high crowned molars with tall and upright cusps. On the first loph of M1, T1 is posterior to T2 and T3 is reduced but present. A T1 bis is intermittently present on M1 in various stages of development. On the second loph of M1, T4 is posterior to T5 and T6 is moderately well developed. On the dentary, the deep masseter scar terminates at the mental foramen and often intrudes (but not to the extent of *Notomys*). The ascending ramus commences rising at the middle of m2 and is gently sloped. The coronoid process is straight and rises to a height that is equal to that of the articular process. A posterior accessory cusp is present on m1 and m2: this cusp becomes continuous with the buccal cusps on worn molars.

Pseudomys desertor Troughton, 1932

Desert Mouse

REFERRED MATERIAL: MNI = 87, NISP = 210. Exemplar only. CCW1631, Q E, layer 9, 280–285 cm, 1 cranium, 1 L maxilla, 1 R maxilla. CCW1677, Q E, layer 7, 335–340 cm, 6 L maxillae, 7 R maxillae, 3 L dentaries, 8 R dentaries (Figure 4.8f). CCW4012, Q E, layer 10, 345–350 cm, 8 L maxillae, 8 R maxillae, 8 L dentaries, 6 R dentaries. CCW1042, Q B, layer 10, 350–355, 2 L dentaries, 2 R dentaries, 2 L maxillae, 2 R maxillae (Figure 4.8g–h)

CCW1295, Q E, layer 10, 350–355 cm, 8 L maxillae, 6 R maxillae, 5 L dentaries, 5 R dentaries.

REMARKS: A medium sized species of *Pseudomys*. The anterior edge of the zygomatic plate is straight (compared to *P. australis*) sometimes with a slight curve. The anterior palatal foramen is short and pinches to a point at the posterior terminus. The upper molar cusps are posteriorly sloped. M1 is without an accessory cusp. The dentary has a short diastema, a well-developed deep-masseter scar and the ascending ramus is tall. The anterior face of the incisors is flat and chisel shaped. On the wedge-shaped M1, placement of the buccal cusps is posterior to the lingual cusps, therefore a line drawn between the lochs is angled more posteriorly than *P. gracilicaudatus*. An additional lingual root on m1 is visible on some specimens. The posterior loph of m1 is usually wider than the anterior loph of m2. The protoconid on m2 does not protrude as prominently as for *P. gracilicaudatus*.

cf. *Pseudomys fumeus* Brazenor, 1934

Smokey Mouse

REFERRED MATERIAL: MNI = 1, NISP = 1. CCW1376, Q E, layer 10, 310–315 cm, 1 L maxillae (Figure 4.8i).

REMARKS: A small *Pseudomys* species that is larger than *P. novaehollandiae*. CCW1376 is a broken maxilla with M1–3 intact but is missing most of the zygomatic region. The anterior edge of the remaining zygomatic plate is straight and broad. The anterior palatal foramen is broad and tapers to a wide rounded posterior terminus that ends in line with the anterior root of M1. There is no stepdown where the maxillary bone meets the palatine. The molars appear buccolingually compressed when compared to the size of the maxillary bone, but not to the same extent as modern specimens from the SA Museum or fossil specimens from Naracoorte Caves. More material is required to confirm the identity of this taxon.

Pseudomys gouldii (Waterhouse, 1839)

Gould's Mouse

REFERRED MATERIAL: MNI = 2, NISP = 2. CCW1918, Q E, layer 2b, 235–240, 1 R dentary (Figure 4.8k). CCW1678, Q E, layer 10, 335–340, 1 R maxillae (Figure 4.8j).

REMARKS: A medium sized *Pseudomys* species. Both specimens are fragmentary and have only M1 intact. CCW1678 has an expanded zygomatic arch, but only moderately so. The anterior edge of the zygomatic plate is damaged, but the remaining portion suggests it is curved. The anterior palatal foramen is broad, terminating in an open angled point level with the second lingual root on M1. The M1 has a well-defined anterior accessory cusp, a feature that separates *P. gouldii* from *P. australis* (Watts and Aslin, 1981). The M1 has a rounded outline and the lophs are only moderately posteriorly inclined. CCW1918 is the anterior portion of a dentary, broken just posterior to m1. The deep masseter scar is poorly developed and terminates at the mental foramen. The m1 is barrel shaped and the lophs are slightly inclined to the anterior.

Pseudomys gracilicaudatus (Gould, 1845)

Eastern Chestnut Mouse

REFERRED MATERIAL: MNI = 99, NISP = 201. Exemplars only. CCW2444, Q II, layer 13, 490–495 cm, 1 cranium, 1 L maxilla, 3 R maxillae, 3 L dentaries. CCW3635, Q II, layer 13, 500–505 cm, 1 cranium, 7 L maxillae, 8 R maxillae, 10 L dentaries, 3 R dentaries. CCW3802, Q II, layer 13, 510–520 cm, 1 cranium, 1 R maxilla, 2 R dentaries. CCW2813, Q II, layer 14, 535–540 cm, 3 L maxillae, 3 R maxillae, 18 L dentaries, 10 R dentaries (Figure 4.8l–m). CCW3056, Q II, layer 14, 570–575 cm, 1 cranium, 2 R maxillae, 1 R dentary.

REMARKS: A medium sized *Pseudomys* species. The anterior edge of the zygomatic plate is asymmetrically curved, and the zygomatic arch is moderately expanded. The anterior palatal foramen is broad, with a rounded terminus that ends level with the second lingual root of M1. The upper molar cusps are posteriorly inclined. M1 features a defined anterior accessory cusp. The dentary has a short diastema, a well-developed deep masseter scar and the ascending ramus is tall but rises at an angle that is not as acute as *P. desertor*. The anterior face of the incisor is slightly rounded, compared to *P. desertor*, and the crown wears to a rounded wedge. On the wedge-shaped M1, a line drawn between the lophs is angled less posteriorly than *P. desertor*. The posterior loph of m1 is usually narrower than the anterior loph of m2 due to the prominently protruding protoconid on the three rooted m2.

Pseudomys novaehollandiae (Waterhouse, 1843)

New Holland Mouse

REFERRED MATERIAL: MNI = 281, NISP = 643. Exemplars only. CCW1197, Q B, layer 10, 315–320 cm, 4 L maxillae, 2 R maxillae, 6 L dentaries, 7 R dentaries. CCW2240, Q II, layer 12, 440–445 cm, 3 R maxillae, 3 R dentaries. CCW2665, Q II, layer 13, 505–520 cm, 1 cranium, 7 L maxillae, 5 R maxillae, 11 L maxillae, 15 R maxillae. CCW2601, Q II, layer 13, 500–515 cm, 1 cranium, 1 L maxilla, 3 R maxillae, 3 L dentaries, 5 R dentaries. CCW2522, Q II, layer 13, 490–495 cm, 2 L maxillae, 10 L dentaries, 6 R dentaries (Figure 4.8n–p).

REMARKS: A small *Pseudomys* species. The anterior edge of the zygomatic plate is straight and without a spike. The anterior palatal foramen is broad, and the posterior terminus is well-rounded. This species has an intermittently present anterior cingular cusp on M1. The upper molar lophs are posteriorly inclined. The dentary diastema is relatively long (compared to *P. desertor*) and the ramus ascends at a wide and open angle. The distal terminus of the deep masseter scar is well developed and ends above the mental foramen, but rarely intrudes. The i1 is pointed and slender. The lower molar lophs are anteriorly inclined, m1 is elongate with a posterior loph that is often narrower than the anterior loph of m2.

Pseudomys oralis Thomas, 1921

Hastings River Mouse

REFERRED MATERIAL: MNI = 12, NISP = 27. Exemplars only. CCW2534, Q II, layer 13, 500–505 cm, 1 R maxilla, 1 L dentary, 2 R dentaries. CCW2665, Q II, layer 13, 505–520 cm, 1 L dentary, 1 R dentary. CCW2676, Q II, layer 13, 520–525 cm, 1 L dentary. CCW4024, Q II, layer 14, 9.2.17 (515–520 cm), 3 L maxillae, 2 R maxillae, 1 L dentary, 4 R dentaries. CCW2715, Q II, layer 14, 520–525 cm, 1 L maxilla, 1 R maxilla. CCW2819, Q II, layer 14, 535–540 cm, 3 L maxillae, 2 R maxillae, 2 L dentaries, 1 R dentary (Figure 4.8q–r).

REMARKS: A large species of *Pseudomys*. This species has superficial similarities to *P. australis* and is of comparable size, thus many of the characters here are compared to *P. australis*. The anterior edge of the zygomatic plate is straight and does not develop a spine.

The anterior palatal foramen is wide, tapers toward the posterior terminus and often terminates anterior to, or equal to, the anterior of m1. The palate is slightly arched. The upper molars are large, with tall upright cusps, and are deeply set in the maxillary bone. The first root on M1 is more buccally inclined than in *P. australis* and the alveolus for the lingual root is reniform in cross-section (this is ovate shaped in *P. australis*). All specimens examined had four roots on M2. On the dentary, the deep masseter scar terminates prior to meeting the mental foramen. The area between the articular and angular processes is symmetrically curved. In occlusal view, the crown of the upper molars wears flat, whereas in *P. australis*, the earlier stages of wear are focused on the longitudinal centre of the molar and form a deep furrow. The m3 has retained T9 which when subjected to wear, forms a wide basin with T8.

Rattus fuscipes (Waterhouse, 1839)

Bush Rat

REFERRED MATERIAL: MNI = 1, NISP = 1. CCW200, Q A, layer 2b, 257–262 cm, 1 R dentary (Figure 4.9e).

REMARKS: A small species of *Rattus*. CCW200 is a damaged dentary with m1–2 intact. The dentary, and molars, are proportionally smaller to other *Rattus* identified in this deposit. The deep masseter is mostly missing on this specimen, but it terminates prior to meeting the mental foramen. The M1 has four roots and the occlusal outline is a rounded wedge. The m1 has a well-developed posterior accessory cusp.



Figure 4.8. Murids. *Notomys* sp. indet. a) R maxilla (CCW3377), b) lateral view L maxilla (CCW3303), c) L dentary (CCW3303); *Pseudomys australis* d) L dentary (CCW3062), e) L maxilla (CCW3062); *P. desertor* f) L maxilla (CCW1677), g) R dentary (CCW1042), h) lateral view L dentary (CCW1042); cf. *P. fumeus* i) L maxilla (CCW1376); *P. gouldii* j) R maxilla (CCW1678), k) R dentary (CCW1918); *P. gracilicaudatus* l) L maxilla (CCW2818), m) L dentary (CCW2818); *P. novaehollandiae* n) L maxilla (CCW2522), L dentary (CCW2522), lateral view L dentary (CCW2522); *P. oralis* q) L dentary (CCW2819), L maxilla (CCW2819).

Rattus sp. cf. *R. lutreolus* (Gray, 1841)

Swamp Rat

REFERRED MATERIAL: MNI = 42, NISP = 53. Exemplars only. CCW2372, Q II, layer 13, 480–484 cm, 1 cranium, 1 L maxilla. CCW2535, Q II, layer 13, 500–505 cm, 2 L maxillae, 1 L dentary, 2 R dentary, 1 cranium. CCW3669, Q II, layer 13, 505–520 cm, 1 cranium, 1 R maxilla, 1 L dentary. CCW2815, Q II, layer 14, 535 – 540 cm, 4 L maxillae, 3 R maxillae (Figure 4.9c). CCW3052, Q II, layer 14, 570–575, 1 cranium, 1 L dentary, 2 R dentaries. CCW3843, Q II, layer 14, 575–580 cm, 2 R dentaries (Figure 4.9d).

REMARKS: A large species of *Rattus*. The cranium has conspicuous supraorbital ridges (Watts and Aslin, 1981); the zygomatic arch is slightly expanded; and the edge of the zygomatic plate is straight. The anterior palatal foramen is narrow, curved and tapers to a tight point at the posterior terminus. The shape of the anterior palatal foramen, the large and wide molars and the broad incisors distinguish *R. lutreolus* from other native *Rattus* (Watts and Aslin, 1981). The dentary is robust, with a well-developed deep masseter scar. The m1 is wedge shaped and does not possess a posterior accessory cusp.

Rattus sp. cf. *R. tunneyi* (Thomas, 1904)

Pale Field Rat

REFERRED MATERIAL: MNI = 11, NISP = 13. Exemplars only. CCW12, Q B, layer 2, 183–188 cm, 2 R maxillae. CCW144, Q A, layer 2b, 247–252 cm, 1 R maxilla (Figure 4.9a). CCW241 (Figure 4.9b), Q A, layer 2b, 265–270 cm, 1 L dentary. CCW1448, Q E, layer 10, 320–325 cm, 1 R maxilla. CCW2425, Q II, layer 13, 485–490 cm, 2 L dentaries. CCW3037, Q II, layer 14, 560–565 cm, 1 R maxilla.

REMARKS: Large species of *Rattus*, comparable in size to *R. lutreolus*. Although there is some variation of characters between individuals, and no complete specimens were recovered, after extensive comparisons with museum specimens, *R. sp. cf. tunneyi* was assessed to be the best match for specimens possessing various combinations of the characters listed here. The anterior edge of the zygomatic plate is straight, with a moderately

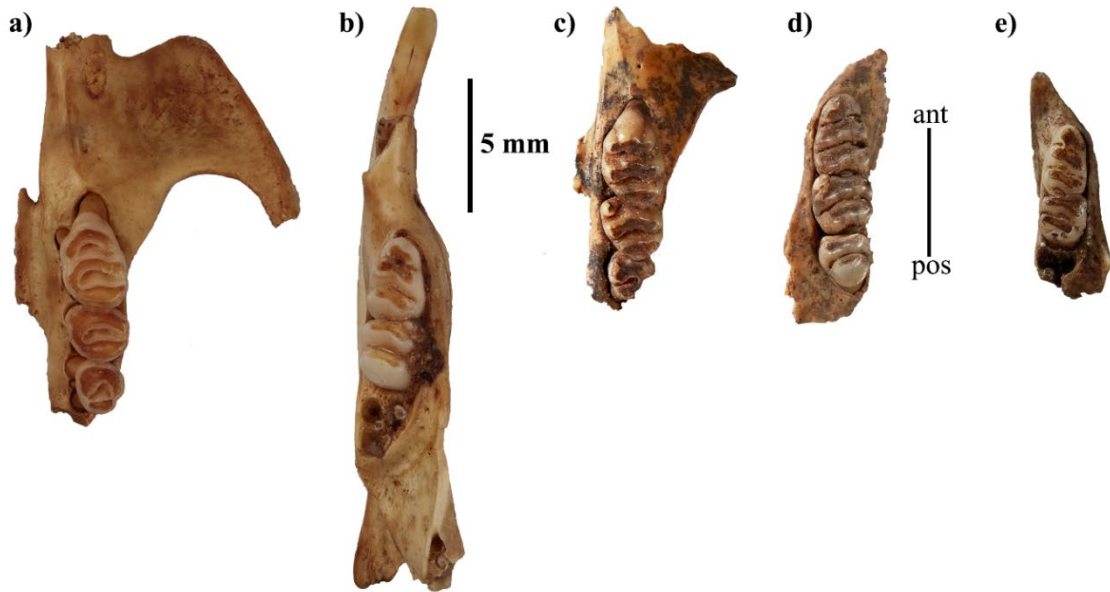


Figure 4.9. *Rattus* sp. cf. *R. tunneyi* a) L maxilla (CCW144), R dentary (CCW241); *R. sp. cf. R. lutreolus* c) L maxilla (CCW2815), d) R dentary (CCW3843); *R. fuscipes* e) R dentary CCW200).

expanded zygomatic arch. The anterior palatal foramen is wider than in *R. lutreolus* and the posterior terminus is rounded. On the M1, T1 and T3 are well developed and distinct from T2. On the dentary, the deep masseter scar is well developed and terminates just prior to the mental foramen. The m1 is wedge shaped and possesses a posterior accessory cusp.

Murinae sp. 1

REFERRED MATERIAL: MNI = 2, NISP = 2. CCW2116, Q B, layer 10, 305–310, L maxilla (Figure 4.10b). CCW1258, Q B, layer 10, 330–335 cm, R maxilla (Figure 4.10a).

REMARKS: CCW2116 belongs to a medium sized murine, smaller than *Pseudomys australis* but larger than *P. novaehollandiae*. The zygomatic plate is broad, and the margin of the anterior palatal foramen is straight, with a rounded posterior terminus. The M1 is narrow, with a poorly developed T3 not easily distinguished from T2. CCW1258 is morphologically similar to CCW2116, but the molars are more worn.

Murinae sp. 2

REFERRED MATERIAL: MNI = 1, NISP = 1. CCW1981 Q II, layer 10, 360–365 cm, edentulous R maxilla (Figure 4.10c).

REMARKS: CCW1981 belongs to a small murine that shares many similarities to *Pseudomys novaehollandiae* but differs in having a broad zygomatic plate and the posterior terminus of the anterior palatal foramen is pointed.

Murinae sp. 3

REFERRED MATERIAL: MNI = 1, NISP = 1. CCW4988 Q A, layer 2b, 257–262 cm, L maxilla with M1–3 (Figure 4.10d).

REMARKS: CCW4988 belongs to a medium sized murine that is larger than *P. gracilicaudatus* or *P. desertor*. The lophs are posteriorly inclined and the molars are low crowned and wide, appearing rounded in shape. T3 is poorly developed on M1 and on M2–3, T1 is well developed and distinctly separate from the first loph. The anterior palatal foramen is wide, with an open curve at the posterior terminus.

Murinae sp. 4

REFERRED MATERIAL: MNI = 1, NISP = 1. CCW5025 Q B, layer 10, 310–315 cm, L dentary with m1 (Figure 4.10e).

REMARKS: CCW1981 is a small murine, that is larger than *Pseudomys novaehollandiae* and smaller than *P. desertor*. The m1 is worn, but even in its worn state, it appears high-crowned and comparatively wider than *P. novaehollandiae*. The alveolus for the incisor is large, suggesting a broad incisor.

Murinae sp. 5

REFERRED MATERIAL: MNI = 1, NISP = 1. CCW3615 Q II, layer 13, 500–505 cm, L partial maxilla with M1 (Figure 4.10f).

REMARKS: CCW3615 has features suggestive of *Pseudomys oralis* (see remarks for *P. oralis*), including upright, high-crowned cusps on M1 that create an occlusal outline that is less elongate than *P. australis* and the anterior palatal foramen terminates just prior to the

second anterior root of M1. It differs to *P. oralis* in possessing an additional lingual root on M1. This individual may simply represent a variant of *P. oralis*.

Murinae sp. 6

REFERRED MATERIAL: MNI = 1, NISP = 1. CCW1603 Q E, layer 10, 315–320 cm, L dentary with m1 (Figure 4.10g).

REMARKS: CCW1603 is fragmentary with few characters that may enable identification of this fossil. The m1 is larger than *Pseudomys novaehollandiae* but smaller than *P. desertor*.

Murinae sp. 7

REFERRED MATERIAL: MNI = 1, NISP = 1. CCW2677 Q II, layer 13, 520–525 cm, cranium (Figure 4.10h).

REMARKS: The cranium shares affinities with that of *Pseudomys australis* except the anterior palatal foramen is narrow at the posterior terminus and the tooth row and molars are smaller. The molars are in an advanced stage of wear.

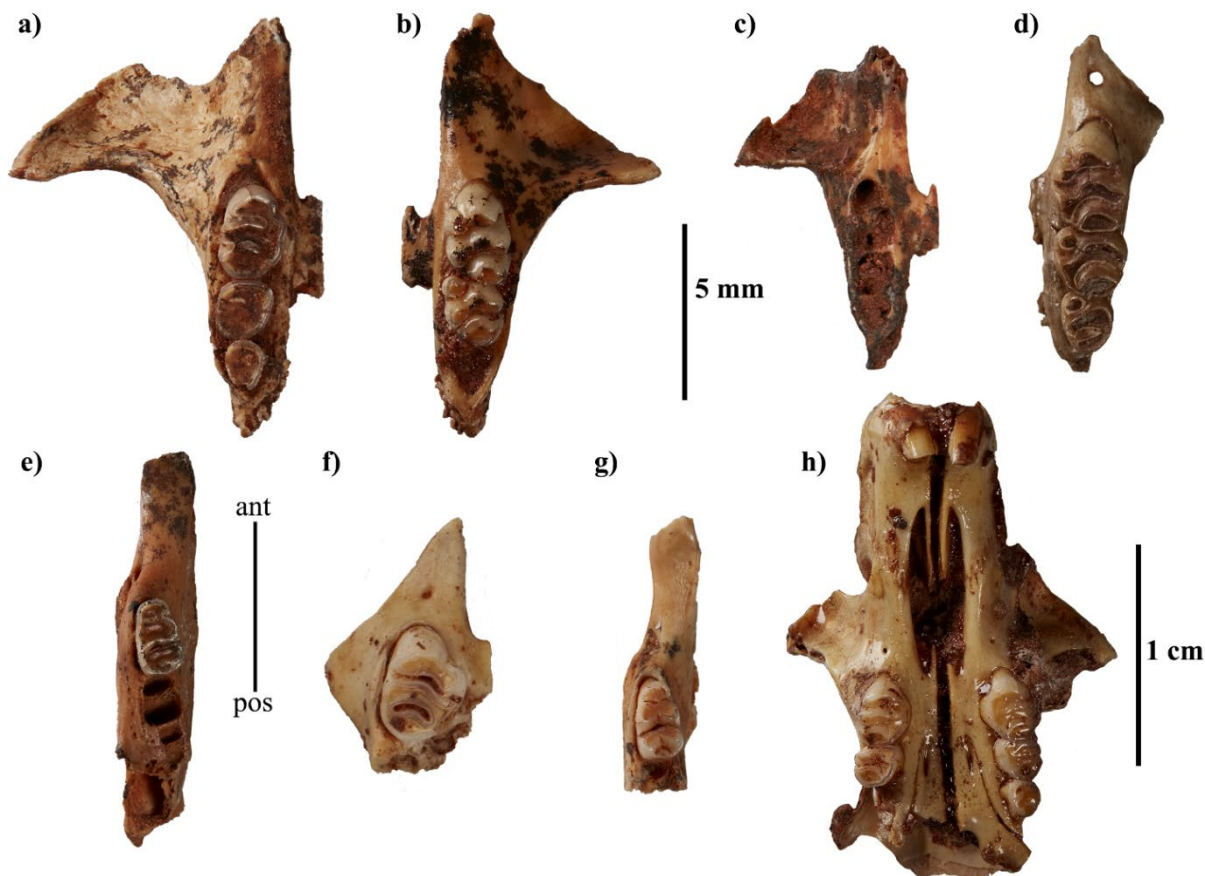


Figure 4.10. Unresolved murids. a) Muridae sp. 1, R maxilla (CCW1258); b) Muridae sp. 1, L maxilla (CCW2116); c) Muridae sp. 2, R maxilla (CCW981); d) Muridae sp. 3 L maxilla (CCW4988); e) Muridae sp. 4, L dentary (CCW5025); f) Muridae sp. 5, R maxilla (CCW3615); g) Muridae sp. 6, L dentary (CCW1603); h) Muridae sp. 7, splanchnocranium (CCW2677).

Order CHIROPTERA Blumenbach, 1779

Suborder MEGACHIROPTERA Dobson, 1875

Family MEGADERMATIDAE Allen 1864

Macroderma gigas (Dobson, 1880)

Ghost Bat

REFERRED MATERIAL: MNI = 1, NISP = 1. CCW193, Q A, layer 2b, 257–262 cm., L c1.

REMARKS: Large canine with inflated cingulum around the base that compares to modern specimens of *M. gigas*.

Suborder MICROCHIROPTERA Dobson 1875

Microchiroptera spp.

REFERRED MATERIAL: MNI = 84, NISP = 207. Exemplars only. CCW92, Q B, layer 2b, 236–241 cm, 1 L maxilla, 2 R maxillae, 2 L dentaries, 2 R dentaries. CCW1641, Q E, layer 10, 280–285 cm, 1 L dentary, 1 R dentary. CCW2171, CCW2842, Q II, layer 14, 535–540 cm, 3 L maxillae, 5 R dentaries, 8 L dentaries, miscellaneous postcranial. CCW3416, Q II, layer 12, 425–430 cm, 1 L maxilla, 1 L dentary.

REMARKS: The NISP given here is for all microchiropterans identified in the deposit and includes those species recorded below.

Family RHINOLOPHIDAE J. Gray 1825]

Rhinolophus megaphylus Gray. 1834

Eastern Horseshoe-bat

REFERRED MATERIAL: CCW93, Q A, layer 2b, 257–262 cm, 1 R maxilla, 1 L dentary. CCW127, Q A, layer 2b, 265–280 cm, 1 cranium, 1 L maxilla, 1 R maxilla, 2 L dentaries. CCW161, Q A, layer 2b, 275–280 cm, 1 R dentary.

REMARKS: Diagnostic characters taken from Martinez (2010): Rostrum is dorsally inflated into a prominent dome; dental formula is I1/2 C1/1 P2/3 M3/3; C1 is robust, simple and lacks cingula; P2 is small; P4 and M1 have a well-developed heel; M1-2 have an open protofossa and lack a hypocone; metastyle of M3 is absent or poorly developed; M3 is not reduced, with five cusps and three commissures; c1 is not as robust as C1; p3 is highly reduced; all lower molars are nyctalodont with a deep postfossa that is enclosed by a “wavy” entocristid; well-developed talonid on m3.

Family VERSPERTILIONIDAE J. Gray, 1821

Chalinolobus gouldii (Gray, 1841)

Gould's Wattled Bat

REFERRED MATERIAL: CCW2527, Q II, layer 13, 490–495 cm, 1 R dentary.

REMARKS: The dentary is small, compact and with an exceedingly low ramus that curves ventrally between the coronoid and articular processes. The dentary is missing ix, c1, p2 and m3, but retains dental characters for *C. gouldii* given by Martinez (2010). These characters are: alveoli indicate two premolars, with p2 being much smaller than p4; p4 with well-developed basal cingulum that swells into a small anterolingual cusplet; lower molars are myotodont with a well-developed hypoconulid and basal cingula; alveolar spacing of m3 does not suggest it is highly reduced.

Family MINIOPTERIDAE Dobson, 1875

Miniopterus orianae Thomas, 1922

Large Bent-wing Bat

REFERRED MATERIAL: CCW1916, Q E, layer 7, 235–240 cm, 1 L dentary, 1 R dentary. CCW2841, Q II, layer 14, 535–540 cm, 1 L maxilla, 4 L dentaries, 7 R dentaries.

REMARKS: Several subspecies have been defined within *M. orianae*, with some suggestions that these warrant elevation to species (Jackson and Groves, 2015). Here we retain only *M. orianae* due to the taxonomic instability and lack of osteological studies of these subspecies. Characters for *M. orianae* are given under *M. shreibersii* by Martinez (2010), predating the recognition of *M. orianae* for Australian miniopterids that had previously been included within *M. shreibersii* (Jackson and Groves, 2015). *Miniopterus orianae* is separated from other Australian microbats by the following characters: dental formula of I2/3 C1/1 P2/3 M3/3; slender, conical C1 with continuous and straight basal cingulum; P2 is three rooted and large; P4 is large and wide; posterolingual heel on M1 is well developed; well-developed hypocone on M1–2; inflated posterolingual cingulum at the base of the hypocone on M2; three commissures on M3; lower molars are nyctalodont; p2–3 are equal in size; p4 slender and high; protoconid taller than hypoconid in m1–3; m3 is not reduced.

4.6 Discussion: Australia's richest Pleistocene mammal assemblage

With at least 69 mammal species now identified, Cathedral Cave has Australia's richest Pleistocene fossil mammal assemblage. Second to Cathedral Cave, the Main Fossil Chamber of Victoria Fossil Cave at Naracoorte, south-east Australia, has yielded the remains of 65 mammalian species (Reed and Bourne, 2000; 2009). The true species richness of Cathedral Cave could increase further following identification of the rodent morphotypes and further work on taxonomic units that might contain multiple species. Most of these taxa have been identified in 4.2 m of sediments that have accumulated over just 30 ka (Figure 3.15).

Therefore, the deposit lends itself to analyses of an exceptional resolution.

Deposits that have accumulated over extended periods of time are mostly thought to have had greater opportunity to sample a larger portion of the local fauna (Staff and Powell, 1988). For example, the Riversleigh World Heritage fossil area in north-west Queensland spans around 25 Ma and has produced over 200 mammal species (Archer et al., 1989; Price, 2012). At Cathedral Cave, the richness of the assemblage cannot be attributed to an extended period of accumulation. Instead, it is best explained by the cave's proximity to the boundaries of the modern temperate, semi-arid and sub-tropical climate zones (Figure 2.1). Boundaries of these biomes have expanded and contracted through time in response to the changing late Quaternary climate (Kershaw, 1995). Cathedral Cave is well located to capture these shifts, sampling species from each of these biomes as boundaries moved and environmental conditions changed in Binjang. Even so, this is not suggesting that the boundary of these climatic zones presents a sharp border between ecological community *a* and ecological community *b*. Nor does this boundary represent a sharp change in species assemblages. Rather, we view these boundaries as ecotones, or gradients of change in which ecological transitions between the biomes is gradual.

The deposit is not only speciose, but also exceptionally fossiliferous, having yielded more than 21,000 identifiable fossils from the targeted quadrats so far. The fossils belong mostly to mammals, with numerous small taxa, including rodents. Rodents are especially useful for palaeoecological analyses as many have strict ecological requirements (Fernández-García et al., 2016; Piñero and Agustí, 2020). Therefore, the deposits of Cathedral Cave hold great potential to elucidate changes in the composition of its vertebrate fossil fauna in response to changing environmental conditions. This assemblage is analysed in the following chapters, in which changes in the assemblage composition and relative abundances of species is

investigated in the context of the chronological and sedimentological framework established in Chapter 3.

4.7 Conclusion

Cathedral Cave's proximity to the junction of several modern climate zones leaves it "sensitive" to changing climatic conditions. The densely fossiliferous deposit has yielded the richest Pleistocene mammal assemblage yet known in Australia. The deposit has accumulated over a relatively short period of time compared to other species rich deposits in Australia. By nature of its location and the richness of its fossil deposits, Cathedral Cave is an ideal place to investigate faunal response to changing environments.

5 Chapter 5: Tracking mammalian faunal change through the late Quaternary of central-eastern Australia

5.1 Abstract

Fossil assemblages have long been used to explore how animals, populations and ecosystems respond to changes in their environment. Cathedral Cave, in the Wellington Caves system, NSW, is a terrestrial vertebrate fossil locality of significant historical and scientific importance. Fossils have been collected from Cathedral Cave since at least 1831, yet only a single published study has focused on exploring faunal change through time. Here I present results from a study of the fossil mammals collected from a new excavation of the upper 4.2 m of the Cathedral Cave deposit. This chapter uses the newly established chronology given in Chapter 3, to place changes in the occurrence of fossil mammals of Cathedral Cave in context with other palaeoenvironmental records from mid MIS 4 to mid MIS 3 (68.2 and 43.2 ka ago) and late MIS 1 (5.8–0.81 ka ago).

Using fossils from the assemblage, change in the mammal assemblage through time is characterised by the trajectories of species composition, relative abundance, species richness, and biodiversity metrics (Shannon's diversity index H' , Simpson's index of diversity 1-D, and Pielou's index of Equitability J). These reveal that the late Pleistocene mammal community of Binjang was typical of a temperate open forest and woodland community with xeric adapted taxa increasing in abundance during drier periods. Subtle fluctuations in the relative proportions of each group characterises the response to cold and dry conditions that were in effect at 65 ka ago during MIS 4. At this time, the community also underwent a reduction in its richness, diversity, and evenness. Restructuring of the community was greater during MIS 3, with changes to the assemblage composition suggesting that Binjang had become drier between 50.6–44.7 ka. No suitable regional palaeoenvironmental records exist for this time period. At this time, faunal turnover among within the small-medium bodied mammals was minimal, with all but the more mesic adapted species surviving locally beyond the Pleistocene. Loss among the megafaunal species was high, with few persisting into the Holocene. The data does not support a solely climate-driven extinction model and suggests response and extinction trends in eastern Australia more closely follow those found in fossil sites of southern Australia than those that lie above, or closer to, the Tropic of Capricorn. The latter sites lack the resolution of their southern counterparts.

Importantly, Cathedral Cave is one of a very restricted number of fossil sites that includes a record of both megafauna and small mammals leading up to, and through, the proposed megafaunal extinction window during MIS 3. This has enabled refinement of the temporal range of nine megafaunal taxa and demonstrated for them a potential temporal overlap with humans. For four of these taxa, this represents their first, and only, dated occurrence.

5.2 Introduction—using the past to predict the future

It has never been more critical than now to be able to predict the future states of ecological systems, and how they might respond to current and future environmental changes. Human driven environmental changes are affecting ecosystems across the globe, and are arguably the largest, and most immediate threat facing the Earth's ecosystems (Parmesan, 2006; Hoegh-Guldberg et al., 2007; Dirzo et al., 2014). When combined with reliable chronological controls, the fossil record is a valuable data-source for understanding how these systems responded to past environmental change (Rull, 2010; Willis et al., 2010; Rowe and Terry, 2014; Grace et al., 2019; Fordham et al., 2020).

5.2.1 Ecosystem response to disturbance

An ecosystem disturbance occurs when a habitat occupied by a population, community, or ecosystem, is subjected to potentially damaging biotic or abiotic forces or events that can cause mortality and changes in the spatial patterning of ecosystems (Lake, 2000). Disturbance has long been recognised as having a major influence in shaping the structure of ecosystems and biotic communities (Connell, 1978). Disturbances are categorised into two types (pulse and press) that are broadly defined by the duration of the disturbance event (Bender et al., 1984; Glasby and Underwood, 1996). Pulse disturbances (e.g., extreme weather events, fire and flood) are short-term disturbances that cause a rapid change in diversity, and from which an ecosystem is usually able to recover. The ability to measure and detect pulse disturbances is dependent on the resolution of the record being assessed (Davies et al., 2018). The required resolution is rarely, if ever, available in long-term vertebrate fossil record, and the nature of pulse events that result in fossilisation can mean that these records are discontinuous temporally or geographically, without longer-term context. For example, the rich fossil bed of Lake Callabonna in northern South Australia, may capture the remains of megafaunal species that perished during a singular drying event (A. Camens, pers coms.), but the record lacks the long-term context required to assess faunal resilience. Press disturbances are long-term, and continue at a similar intensity following their onset, e.g., climatic changes, land use

conversion (Bender et al., 1984; Glasby and Underwood, 1996). Time-series analysis of fossil assemblages are well suited to capturing press disturbance (e.g., Prideaux et al., 2007b; Prideaux et al., 2007a; Blois et al., 2010; Prideaux et al., 2010; Macken et al., 2012; McDowell, 2013; Macken and Reed, 2014).

5.2.2 Ecological resilience

Ecological resilience is defined variously in the literature (for discussion of this see: Newton, 2016; Davies et al., 2018) but broadly refers to the ability of an ecosystem to renew or reassemble itself when subject to disturbances (Holling, 1973; Elmqvist et al., 2003; Ives and Carpenter, 2007). It differs to engineered resilience, which instead describes how rapidly an ecosystem can return to its equilibrium state (Pimm, 1994; Holling, 1996; Davies et al., 2018). Engineered resilience requires a baseline, and thus assumes a single equilibrium state, this assumption may fail to capture the true complexity and dynamic nature of ecosystems (Gunderson and Pritchard, 2012 as cited in ; Baho et al., 2017). Ecological resilience (hereafter referred to as resilience) consists of three component processes: resistance, recovery and reorganisation (Falk et al., 2019). Resistance, sometimes called persistence, is a measure of the ability of individuals or structures to endure relatively unchanged through a disturbance and return to the pre-disturbance state (Halpern, 1988; Lake, 2013; Falk et al., 2019). When the effects of a disturbance exceed the ability of individuals to resist, the population level process of recovery kicks in. Recovery entails the renewal of the pre-disturbance population through recruitment or colonisation (Falk et al., 2019). The third process, reorganisation, is invoked after the failure of resistance and recovery. The ecosystem then reorganises into an alternative state that may be transitory or stable, but is different from its pre-disturbance state (Beisner et al., 2003). Thus, changes in the abundance and distribution of species through time can be, but are not always, a precursor to ecosystem shifts (Macken and Reed, 2014; Clements and Ozgul, 2018). Ecosystems are not static, and the ability to change and adapt is a key factor in their continued function and resilience (Falk and Millar, 2016).

Complex and diverse responses to environmental change is an integral part of ecosystem resilience (Elmqvist et al., 2003; Wittebolle et al., 2009) and should be expected to be encountered in palaeoecological studies. At the Naracoorte Caves in south-east Australia, fossil taxa with similar modern ecological preferences did not necessarily follow parallel relative abundance trajectories through the MIS 5–MIS 4 transition (Macken et al., 2012).

Nor did taxa necessarily follow a consistent trend through comparable climatic changes during the MIS 9–8 transition in Cathedral Cave at Naracoorte (Prideaux et al., 2007a; Macken et al., 2012).

How biota responds to a disturbance determines how resilient an ecosystem is to that mode and magnitude of disturbance. When conditions within an ecosystem breach the tolerance levels of the biotic occupants, then there are three primary responses that can be adopted. These responses can be effected in isolation or in combination and the magnitude and direction of the response is dependent on a range of factors that includes temporal scale, rate and extent of environmental change, availability of alternative habitat, life history, and dispersal ability (Graham et al., 1996; Gienapp et al., 2008; Schloss et al., 2012). Biota can respond by persisting *in situ* via acclimatisation or adapting via genetic evolution, by tracking suitable conditions by dispersal and migration or, if these fail, by becoming extinct in the ecosystem (Davis et al., 2005; Parmesan, 2006). Eurytopic species, those able to tolerate a wide range of conditions, should be less sensitive to environmental changes than stenotopic species that have a narrow range of tolerances (Vegas-Vilarrúbia et al., 2011). Dispersal and migration are key processes for evading unsuitable conditions and enabling organisms to track their preferred environmental envelopes through time and space (Chen et al., 2011). Both dispersal and migration can lead to local extinction in the original area of occupancy if conditions there are no longer viable. Extinction, migration and dispersal can be observed as changes in the taxonomic composition of a fossil assemblage (e.g., Hocknull, 2005; Prideaux et al., 2007a; Prideaux et al., 2010; Macken et al., 2012; Macken and Reed, 2014).

Disturbance and stress is sometimes implied in palaeoecological studies by observations of taxonomic restructuring of the assemblage, changes in species richness and the relative abundance of individuals within specific taxa or guilds (e.g., Prideaux et al., 2007a; Blois et al., 2010; Prideaux et al., 2010; Macken et al., 2012; Macken and Reed, 2014). Diversity metrics are frequently used to explore the effects of disturbance on contemporary and ancient faunal communities (e.g., Barnosky et al., 2004b; Blois et al., 2010; Macken et al., 2012; McDowell, 2013). Species richness is the most basic measure of biodiversity, measuring the number of species present in a defined area (Whittaker, 1972) and in the palaeontological context, is limited to a specific time interval. Species richness is tied to critical ecosystem attributes that includes habitat disturbance, productivity and habitat heterogeneity (Hadly and Barnosky, 2009). Changes in species richness can therefore indicate that fundamental

ecosystem changes have occurred. Evenness is also commonly used as a measure of relative dominance within the distribution of abundance among taxonomic units (Pielou, 1966). A community that includes one or more highly dominant taxa can be vulnerable to change if the change does not favour the dominant species, therefore, evenness can be a predictor of community stability under environmental stress (Wittebolle et al., 2009). Shannon's index (H') and Simpson's index (1-D) are also commonly used. Both take richness and evenness into account (Shannon, 1948; Simpson, 1949).

5.2.3 Australian vertebrate palaeoecology

Although numerous Pleistocene vertebrate deposits are known in Australia (Figure 5.1), most are poorly dated, temporally limited, or underexplored (Hocknull et al., 2007; Prideaux, 2007; Hocknull et al., 2020). Few hold the taxonomic diversity and resolution required to extract useful patterns in community structure and abundance trajectories for detailed palaeoecological studies. Coverage across much of the continent is poor, with more fossil localities known from the southern margins of Australia than elsewhere (Figure 5.1). In Australia, the spotlight has long been held on extinct megafaunal taxa, with an overriding focus on attempting to explain the disappearance of these charismatic species during the late Pleistocene (Roberts et al., 2001). There are some notable exceptions where the smaller fauna has been analysed (e.g., Hocknull et al., 2007; Prideaux et al., 2007a; Prideaux et al., 2010; Macken et al., 2012; McDowell, 2013; Macken and Reed, 2014; Price et al., 2019), but for the main, the non-megafaunal record remains relatively underexploited, despite their known potential as indicators of environmental change (e.g., Fernández, 2006).

5.2.4 Mammal extinctions and Australia's late Quaternary fossil record

The cause of the megafaunal extinctions is the most contentious question in Australian palaeontology. The debate centres on three primary explanations for the disappearance of most of Australia's megafaunal species by ~40 ka ago: anthropogenic impacts, climate change, or the synergistic effects of both. As examined in the literature review (Chapter 1), similar debates take place overseas, but globally, and notwithstanding some geographical variation, and some disagreement, the balance of evidence currently points towards human agency as the most significant driver of the extinctions (Barnosky et al., 2004a; Koch and Barnosky, 2006; Sandom et al., 2014; Araujo et al., 2017). In Australia, however, there is no such agreement. The anthropogenic impact hypothesis points to harvesting by humans or modifications to natural fire regimes, vegetation communities and trophic dynamics as the

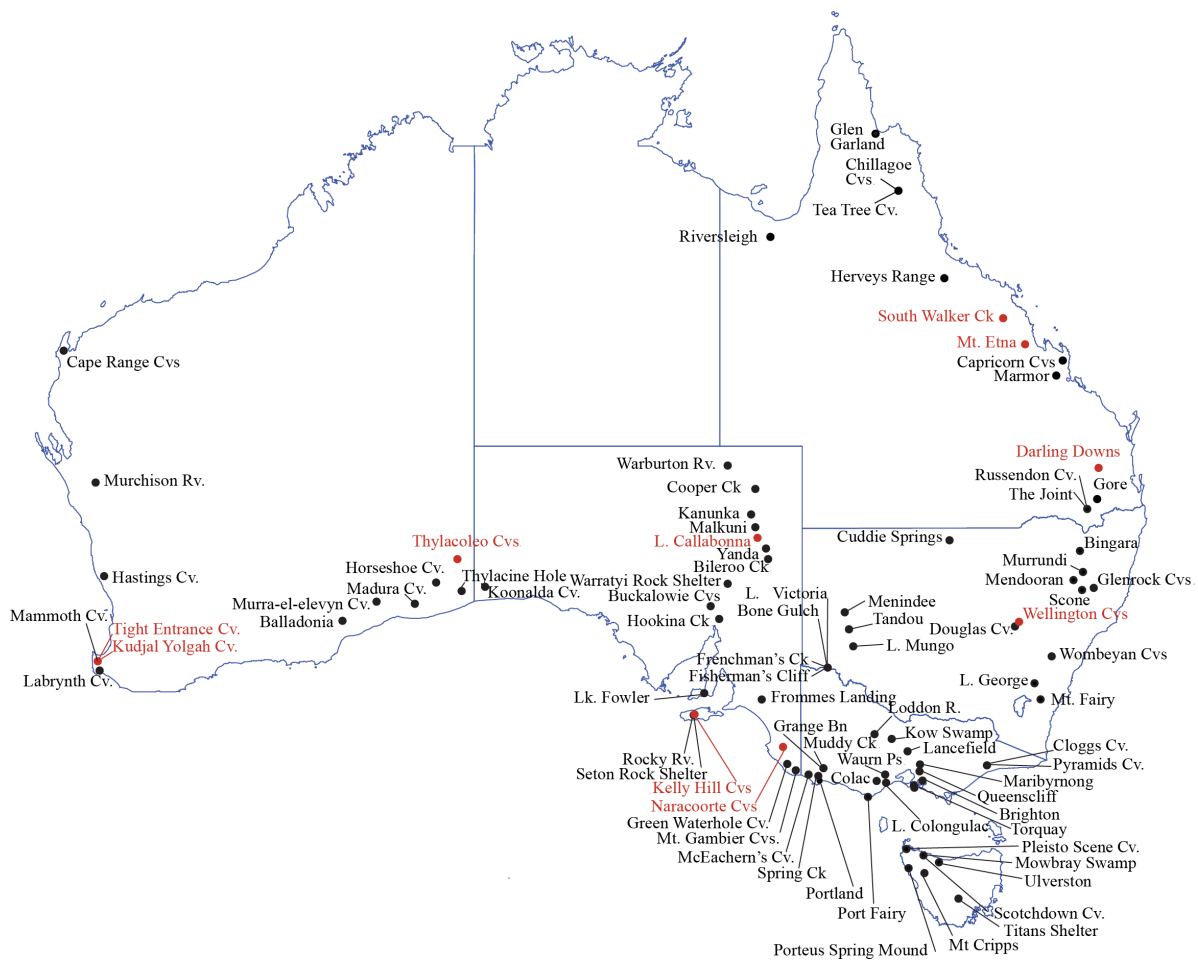


Figure 5.1. A selection of Australian Pleistocene fossil sites following Archer and Hand (1984). Locations discussed in this thesis are in red.

main driver in the megafauna extinctions (e.g., Burney and Flannery, 2005; Miller et al., 2005; Brook et al., 2007; Miller and Fogel, 2016). The “overkill” hypothesis argues that naive megafauna were harvested by people and disappeared from the landscape rapidly (Flannery, 1990; Flannery, 1994), or by attritional loss (Johnson, 2002; Saltré et al., 2016). This argument emphasises the temporal overlap between humans and megafauna in Australia (e.g., Roberts et al., 2001; Turney et al., 2008; Jankowski et al., 2016; Saltré et al., 2016), finding that most of the extinctions occurred within a 51.2–39.8 ka ago extinction window (Roberts et al., 2001). The period of overlap and the timing of the extinction peak are controversial (Wroe and Field, 2006; Field et al., 2008; Price, 2012; Wroe et al., 2013). It has been argued that only a small number of megafaunal species persisted into MIS3 and that extinctions were staggered and had been occurring long before humans arrived (Wroe and Field, 2006; Field et al., 2008; Wroe et al., 2013). Those that did survive are then purported to have shared a long overlap with humans, which has been suggested to therefore refute the overkill hypothesis.

Table 5.1. Australian Megafaunal taxa with post 65 ka dates (youngest given) from FosSahul 2.0 dataset (Peters et al., 2019) with A or A* rated dates. ¹ Hamm et al. (2016); ² Miller et al. (2016); ³ Roberts et al. (2001); ⁴ Turney et al. (2008); ⁵ Grün et al. (2008); ⁶ Prideaux et al. (2010); ⁷ Jankowski et al. (2016). Earlier dates of 31.1 ka for *D. optatum* and *Z. trilobus* at Lancefield Swamp have been assigned an A rating in FosSahul 2.0, but the age for this site has been pushed back to > 45 ka (Dortch et al., 2016).

Species	Age
<i>Diprotodon optatum</i> ¹	43.8
<i>Genyornis newtoni</i> (eggshell) ²	39.5
<i>Macropus ferragus</i> ³	52
<i>Megalibgwilia ramsayi</i> ^{4,3}	56 / 63
<i>Metasthenurus newtonae</i> ⁴	56
<i>Palorchestes azael</i> ⁴	56
<i>Phascolonus gigas</i> ³	52
<i>Procoptodon browneorum</i> ⁷	41.4
<i>Procoptodon gilli</i> ⁵	41
<i>Procoptodon goliah</i> ³	52
<i>Protomnodon anak</i> ⁴	56
<i>Protomnodon brehus</i> ³	52
<i>Protomnodon roechus</i> ⁶	44.9
<i>Simosthenurus occidentalis</i> ⁶	43
<i>Simosthenurus pales</i> ⁶	44.9
<i>Thylacoleo carnifex</i> ⁶	44.9
<i>Wonambi naracoortensis</i> ³	63
<i>Zaglossus hacketti</i> ³	63
<i>Zygomaturus trilobus</i> ³	42.2

However, more recent palaeontological and archaeological evidence has shown that the number of megafaunal species that persisted until humans appeared on the landscape have been historically underestimated (Prideaux et al., 2007a; Macken et al., 2012; Jankowski et al., 2016). For example, it was previously thought that just four out of 20 megafaunal species known at Naracoorte at 130 ka survived beyond this time (Wroe and Field, 2006) but a later small excavation in Grant Hall at Naracoorte raised this to minimally eight megafaunal taxa (Macken et al., 2012).

It is now thought that Aboriginal occupation of Australia occurred earlier than previously held.

Madjedbebe in northern Australia is an indigenous rock shelter site dated to 65

ka (Clarkson et al., 2017). Extending the range of human occupation to 65 ka ago brings 19 reliably dated extinct megafaunal taxa into a potential overlap with humans (Table 5.1). If a conservative approach to human arrival dates is adopted, at least 9 of these taxa persisted until 45 ka ago. At least four additional megafaunal taxa have been reported at South Walker Creek (Hocknull et al., 2020). Although ostensibly held to contain the youngest megafauna remains, the ages for the South Walker Creek sites are a mean age that is derived from multiple dates and the taxonomy has not yet been fully resolved. Future discoveries and improved multi-proxy dating techniques will likely increase the number of megafauna shown to overlap with humans. Still, Madjedbebe stands alone in Australia, with no other confirmed archaeological sites of comparable antiquity. The Madjedbebe dates are not without challengers (O'Connell et al., 2018). Therefore, the 65 ka ago arrival date may not be broadly applicable across the rest of the continent. People were present in the arid interior by 49 ka

ago at Warraty rock shelter in the Flinders Ranges (Hamm et al., 2016; Figure 5.1), had reached Willandra Lakes in south-west New South Wales by 46 ka ago (Bowler et al., 2003; Westaway et al., 2017; Figure 5.1), and were at the Menindee Lakes in far western New South Wales by 45 ka ago (Copper and Duncan, 2006; Figure 5.1). The question is not whether there was an overlap between humans and some megafaunal taxa, but, rather, how long the overlap was, in which regions overlap occurred, and which species were concurrent with humans. Across Australia, the equivalent of one dated archaeological site exists per 4,000 km², and in some poorly sampled areas, this number can be as low as 1 per 10,000 km² (Williams et al., 2015). The earliest human populations probably inhabited the coastal fringes, on what is now the submerged continental shelf (Hiscock, 2007). The sparse archaeological record leaves us without a clear chronology of arrival and migration useful for pinpointing when humans arrived on the landscape regionally, thus defining a starting point for potential human impacts.

Opponents of the overkill hypothesis frequently cite a lack of sites showing clear interactions between humans and megafauna (Wroe et al., 2004; Wroe and Field, 2006); Warraty rock shelter is the only reliably dated archaeological site that preserves megafaunal remains alongside cultural artefacts (Hamm et al., 2016). The remains were transported to the site by people (Hamm et al., 2016), but are without butchery marks, or any evidence of human modification. Nonetheless, megafauna and humans clearly overlapped in space and time, so it would be naïve to posit that humans would not have been able to, or chose not to, exploit the largest, slowest moving 95% of larger vertebrate species.

The blitzkrieg hypothesis, *sensu* Flannery (1990), evokes mass-harvesting and rapid extinction of megafauna, however, a demographic population model using *Diprotodon optatum* showed that even low levels of harvesting could have been sufficient to drive *D. optatum* to extinction within a few centuries (Brook and Johnson, 2006). This theory may also apply, though, to other large-bodied megafaunal species with slow life histories. Sites purported to contain late persisting megafauna have been held as evidence against the overkill model (Wroe and Field, 2006; Field et al., 2008; Wroe et al., 2013). The argument follows that a substantial overlap indicates that megafauna and humans lived side by side, implying that harvesting was either non-existent or sustainable and thus refuting the blitzkrieg hypothesis (Wroe et al., 2004; Trueman et al., 2005). However, revision of these sites formerly used to argue for late persisting megafauna (Cuddie Springs, Lancefield,

Cloggs Cave and Seton Rock Shelter), has found each to be either older, or contain significant chronostratigraphic issues that have yet to be resolved (for discussion see David et al., 2021).

The climate extinction hypothesis focuses on escalating aridity and climatic variability as the primary cause of megafaunal extinctions (e.g., Wroe and Field, 2006; Price et al., 2011; Wroe et al., 2013; Hocknull et al., 2020). Recently, it was proposed that extinctions followed sustained drying of the hydroclimate across the drainage basins of the eastern half of the continent (Hocknull et al., 2020). Even more recently, a reversal in the Earth's magnetic field 42 ka ago was purported to have caused global upheaval, ultimately resulting in the mass extinction of Australia's megafauna (Cooper et al., 2021). However, evidence supporting widespread environmental change at 42 ka ago is scant.

As discussed in chapter 1, glacial–interglacial cycles were set against a backdrop of increasing aridity and seasonality, which had its onset in the later Miocene (Kershaw et al., 1994; Byrne, 2008). Through the early Pleistocene, glacial cycles followed ~41 ka intervals, before increasing in amplitude and length to ~100 ka intervals after the middle Pleistocene Climatic Transition (McClymont et al., 2013). Terrestrial palaeoclimate records for Australia are sparse, but global records show that the last glacial cycle was marked by elevated climatic variability (Wolff et al., 2010). Increased climatic variability has been cited as a cause for the megafaunal extinctions (Wroe et al., 2013). This is supported by recent work finding that short term climatic changes, imposed on long-term trends in the same direction can substantially increase extinction risk (Mathes et al., 2021).

However, when the sum of empirical evidence for later Pleistocene climatic change is appraised as a whole, any clear linkages to megafaunal extinctions are lacking. The number of well-studied palaeoenvironmental records is increasing, although they remain few across much of Australia (e.g., De Deckker et al., 2018b; De Deckker et al., 2019; Kemp et al., 2019; De Deckker et al., 2020), this is especially so for terrestrial records. Records that show millennial-scale climate variability are exceedingly rare in Australia (Turney et al., 2004). Some promoters argue that the extinction chronologies show a staggered attrition of megafaunal taxa over the last 400 ka, with few megafaunal species surviving the MIS 6 Penultimate Glacial Maximum (PGM) at 140 ka ago (Wroe and Field, 2006; Wroe et al., 2013). More likely, these data suffer from the Signor-Lips effect; species become extinct after their most recent evidence in the fossil record (Signor et al., 1982). No doubt some

attenuation has occurred through time, but having survived through multiple glacial and interglacial cycles, megafauna that were extant post MIS 6 were likely to be adapted to aridity (Prideaux et al., 2007b; Prideaux et al., 2007a; Prideaux et al., 2010; Macken et al., 2012; Saltr e et al., 2016) or were able to persist in and then expand from refugia (Byrne, 2008). It can be inferred by their persistence that the megafauna should have been able to survive ongoing climate cycles of similar amplitude. However, recent evidence suggests the severity of the glacial conditions of MIS 4 may have been underestimated (De Deckker et al., 2019) and MIS 3 saw an increase in the number of Dansgaard-Oeschger events (Wolff et al., 2010). Thus, the last glacial cycle through to the MIS 3 extinctions included two cold glacial periods followed by an increasingly variable climate. It is theoretically feasible that this combination of events could have negatively impacted megafaunal taxa, but evidence for this is lacking.

A review of hydroclimate records through MIS 3 found that climates across Australia were spatially discordant (Kemp et al., 2019), and so it is difficult to picture climate change being solely able to drive a simultaneous continent wide extinction. Nor does the climate model offer a satisfactory explanation for why the largest and slowest moving of Australia's terrestrial animals were disproportionately affected. A claim that small-medium animals were similarly affected (Wroe et al., 2013) is poorly supported. Only a handful of extinctions within Australia's small-medium mammals are thought to have occurred between the late Pleistocene and colonisation by Europeans. These include *Perameles sobbei* (see Price, 2002), *Conilurus capricornensis* (see Cramb and Hocknull, 2010), *Antechinus putes* (in Van Dyck, 1982b; Price et al., 2009) and the mainland extinctions of *Sarcophilus harrisii* and *Thylacinus cynocephalus* during the Holocene (White et al., 2018). For the first three, the timing of extinction is unclear; all are known from single localities, suggesting a narrow distribution and increased extinction risk. It is true that extinction risk is known to scale with body size, due to a combination of intrinsic and extrinsic traits that include slower life histories, smaller population densities, and disproportionate exploitation by humans (Johnson, 2002; Jerolimski and Peres, 2003; Cardillo et al., 2005). This still does not explain the selectivity of the late Pleistocene extinctions. Different environmental drivers may have size-specific impacts. For example, climate change was found to have a bottom-up effect in a fossil mammal community from western USA, first impacting small mammals at lower trophic levels first (Barnosky et al., 2004b). Anthropogenic impacts occurred from the top down, affecting larger mammals at the higher trophic level first.

The synergistic model amalgamates two competing hypotheses, and so it suffers from the same uncertainties and lack of direct evidence. More recently, the extinction question has been tackled using big data approaches, however, these models are reliant on the same uncertain occurrence chronologies (Peters et al., 2019; Saltré et al., 2019; Bradshaw et al., 2021). It is clear that improving our understanding of the late Pleistocene extinctions will benefit from the revision of existing sites, such as Wellington Caves, as well as investigations that focus on newer or lesser-known localities. Given the intensity of the debate, far more direct evidence will be required before any current hypothesis reaches general acceptance. Understanding the causes and effects of these extinctions is not simply a matter of discourse. It has real applications to predict trends and prepare for future landscapes in which, continuing with current trajectories trends, large mammals are increasingly depauperate (Wolfe and Broughton, 2021).

Small mammals also have a part to play in understanding the megafaunal extinctions, due to their usefulness as indicators of ecological change (Fernández, 2006; Rowe and Terry, 2014; Fernández-García et al., 2016). Small mammals are numerous enough in some fossil assemblages (particularly owl accumulated assemblages) to track the presence and abundances of individual species and functional guilds through time. The resolution of the small mammal record is unmatched by megafaunal species that are usually less well represented. By following the responses of the small mammals, we may infer how the megafaunal species might have also met the changing late Pleistocene environments.

5.2.5 Vertebrate responses to changing environments in the Australian Pleistocene fossil record

Below I review insights that the Australian Pleistocene fossil record has provided into terrestrial vertebrate responses to changing environments. Included sites are grouped by modern climate associations partially to aid readability and partially in recognition that responses are likely to be geographically diverse. Studies discussed here are restricted to those in which comparable palaeoecological inferences have been reported.

5.2.5.1 Temperate Australia

More late Quaternary fossil sites are known from the temperate region than from any other climate zone (Figure 5.1; Figure 5.2). The Naracoorte Caves (Figure 5.1) offers a rich and diverse fossil record and has been the subject of several studies looking at responses to climate change (McDowell, 2002; Prideaux et al., 2007a; Macken et al., 2012; Macken and

Reed, 2014). During the middle Pleistocene, populations of some mammalian taxa at Naracoorte fluctuated between glacial–interglacial cycles, but the taxonomic composition remained largely stable for 500 ka prior to the late Pleistocene extinctions (Prideaux et al., 2007a). Larger species declined temporarily during a dry interval 270–220 ka ago, but these recovered and persisted into the late Pleistocene. Small mammals followed a similar pattern of declining richness through the MIS 5–MIS 4 transition (Macken et al., 2012). However, some declines were temporary, with taxa reappearing in MIS 3 and younger assemblages at Naracoorte (McDowell, 2002; Macken et al., 2012). Through MIS 2, the small mammal assemblages showed little change through the Last Glacial Maximum (LGM), but exhibited restructuring during and after deglaciation (Macken et al., 2012). Some taxa indicated complex and individualistic responses, even between ecologically similar species and across comparable climatic changes (Macken et al., 2012).

At Kelly Hill Caves, on South Australia’s, Kangaroo Island, (Figure 5.1), the mammalian response during the LGM is comparable to that observed at Naracoorte. The richness of small mammals at Kelly Hill remained consistent through the LGM, but changes in the abundance of ecologically diverse species indicated community rearrangement had occurred in response to the changing climate (McDowell, 2013). Species richness remained stable on Kangaroo Island until <1 ka ago and probably until the arrival of Europeans (Adams et al., 2016). Tight Entrance Cave, south Western Australia (Figure 5.1), contains one of the most comprehensive palaeoecological records of Pleistocene Australia. The assemblage contains a diverse late Pleistocene mammal community, accompanied by $\delta^{13}\text{C} / \delta^{18}\text{O}$ records from the shells of land-snails that were present in the sediments (Prideaux et al., 2010). These record a

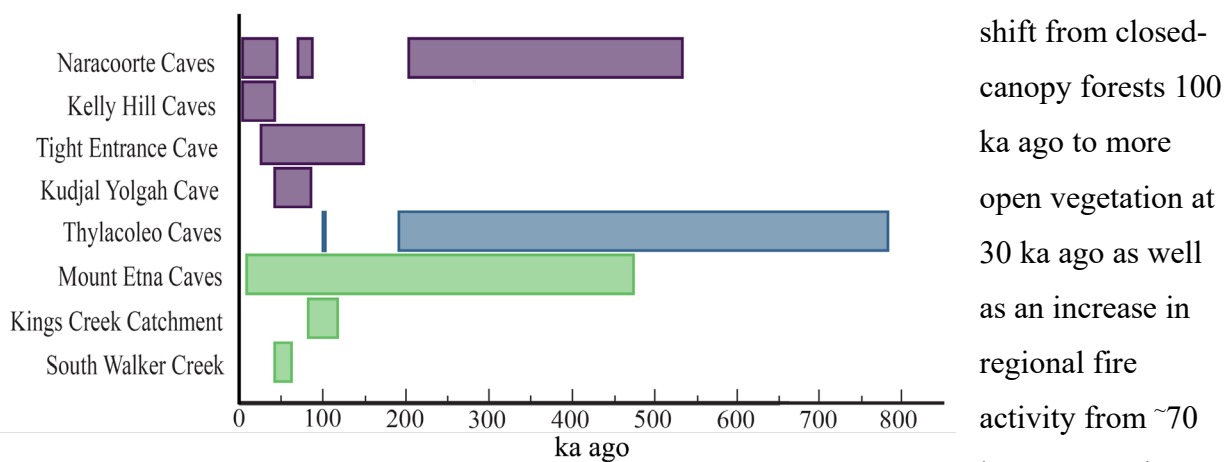


Figure 5.2. Chronological chart showing the temporal span of fossil localities discussed in this section. Temperate zone = purple; semi-arid zone = blue, tropical or subtropical = green. Mount Etna Caves, Kings Creek Catchment and South Walker Creek are composite records that include multiple sites and may contain time-gaps in the record

shift from closed-canopy forests 100 ka ago to more open vegetation at 30 ka ago as well as an increase in regional fire activity from ~70 ka ago. Species richness of larger mammals declined

after 104 ka ago but the most conspicuous decline (from 12 to 6 species), occurred sometime between 70 and 37 ka ago. Small mammal richness remained effectively stable through 100 ka, leading up to the earliest evidence of humans in the region at 49 ka ago (Turney et al., 2001a; Prideaux et al., 2010). The mammalian fauna was mostly unchanged by glacial conditions toward the end of the Penultimate Glacial Maximum and remained so until the loss of most of the region's larger species between 50 and 40 ka ago. These losses occurred during a drier phase, but well prior to LGM aridity and coincide with evidence for human presence in the region (Prideaux et al., 2010). At nearby Kudjal Yolghah Cave (Figure 5.1), several megafaunal species persisted into the late Pleistocene and vanished after the arrival of humans (Roberts et al., 2001; Jankowski et al., 2016). Both studies point toward the mammals being adapted to aridity, having survived the Penultimate Glacial Maximum, and so should not have been largely affected by less-dramatic climatic conditions during MIS 4–MIS 3.

5.2.5.2 Arid and semi-arid Australia

There are few late Pleistocene fossil sites in the arid and semi-arid zone of Australia, and only a small number have been the subject of palaeoecological analyses (Figure 5.1). The Thylacoleo Caves, on the Nullarbor Plain of central-south Australia, contain middle Pleistocene fossil assemblages (Prideaux et al., 2007b; Figure 5.1; Figure 5.2). Around half of the mammal species identified in the caves are known to have persisted through several Pleistocene glacial–interglacial cycles and have local Holocene records. The timing of extinctions could not be established, but species that did not survive to the Holocene were adapted to aridity and considered unlikely to have been impacted by drier conditions (Prideaux et al., 2007b).

5.2.5.3 Tropical and subtropical Australia

Tropical and subtropical fossil assemblages that lie above the Tropic of Capricorn in north-east Australia show trends that differ from those elsewhere on the continent, suggesting that these faunas were more heavily impacted by Quaternary climatic cycles than their more southern counterparts. However, these sites do not offer a faunal record of similar resolution to those from other regions such as Naracoorte Caves, Wellington Caves and sites from south-west Western Australia. A composite record of fossil assemblages from the Mount Etna region in central-east Queensland (Figure 5.1) has been interpreted as revealing faunal stability through several glacial cycles, until 80 % of the mammal species were replaced by

xeric taxa between 280 and 205 ka ago (Hocknull, 2005; Hocknull et al., 2007; Price, 2012). Palaeoenvironmental records show increasing climatic variability and weaker northern monsoons at this time (Kershaw et al., 2003; Kawamura et al., 2006). A similar loss of 65 % of the small to medium mammals occurred sometime after 205–107 ka ago, when the xeric taxa were replaced with an essentially modern and more mesic fauna (Hocknull et al., 2007). However, the Mount Etna record incorporates a substantial timeframe, thus it would be expected to see a greater attenuation of faunal assemblages over this time. At South Walker Creek in north-east QLD (Figure 5.1), pooled fossils from four collection sites are purported to show the staggered extinction of megafaunal taxa in response to a drying hydroclimate and environmental change (Hocknull et al., 2020). In the youngest South Walker Creek site, megafauna are purported to have persisted until 40.9 ka ago. The assigned age for this site is a weighted mean derived from 24 OSL and US-ESR ages that span nearly 38 ka (68.6–30.7 ka ago) and might be better viewed as a range rather than a single representative age.

Fossils have been collected from several sites in the Kings Creek Catchment, Darling Downs, south-east Queensland (Figure 5.1). These sites show a stepwise decrease in taxonomic diversity between 120–83 ka ago, held to be consistent with climate driven extirpation of the region's megafauna (Price and Webb, 2006; Price et al., 2011). The small-bodied fauna of Darling Downs has also been studied (Price, 2004), but taphonomic and dating limitations have restricted palaeoecological studies to broad palaeoenvironmental interpretations on habitat types existing at the time of fossil accumulation.

5.3 Aims

Despite a number of studies investigating how Australian terrestrial mammals were impacted by the environmental changes through the late Quaternary, there are many gaps in our knowledge. Suitable faunal records are constrained to the south and north-east margins of the continent, with these geographic regions so far revealing different responses and resolution. Cathedral Cave offers a high-resolution faunal record that lies intermediate to these other records from the north and south of the continent. Alongside the revised chronology and stratigraphy presented in Chapter 4, Cathedral Cave contains great potential to record the changing environments at the nexus of xeric and mesic climate zones in Australia's middle latitudes.

In this chapter, I present research pertaining to the overarching objectives of this thesis, to investigate how late Pleistocene environmental changes impacted on the mammalian fauna of central-eastern Australia. I aim to:

1. Establish the impacts of environmental change on the late Pleistocene mammalian fauna of central-eastern Australia.
2. Determine how the mammalian component of the assemblage responded to these changes and assess the implications for megafauna extinction hypotheses.

5.4 Methods and materials

5.4.1 Quantitative units

The MNI of each taxonomic unit from each stratigraphic partition were transformed to a percentage of Relative abundance (Ra%).

$$\text{Ra}\% = \text{MNI}_{\text{species}} / \text{MNI}_{\text{total}} \times 100$$

To aid readability, spits have been assigned numbers. On occasion, volunteers recorded spit depths incorrectly e.g., 402–407 cm instead of 400–405. Where this has occurred, spits have been combined as detailed in Appendix D Table 7.14.

5.4.2 K-means clustering

K-means clustering used Ra% of the mammalian taxonomic units in each layer to look for similarity-based clusters to define sublayer partitions and homogenise sample size across layers with differential yield. K-means clustering applies Euclidian distance to numeric values and is useful to show groups of samples with similar characteristics (Krishna and Murty, 1999; Hill et al., 2013).

5.4.3 Rarefaction, richness, diversity, and abundance

5.4.3.1 Rarefaction

Rarefaction curves were used to assess sample coverage and to correct for sample size in our assessment of species richness (Gotelli and Colwell, 2001). Rarefaction curves used MNI values for mammalian taxonomic units across spits, layers, and partitioned sublayers.

5.4.3.2 Richness

Species richness (S) is the number of species present in a defined space at a given time interval (Magurran, 1988). It is strongly mediated by sample size (Gotelli and Colwell, 2001). In this thesis, species richness uses unique taxonomic units per sedimentary partition. For example, if *Sthenurus* sp. indet. appears in a layer that is otherwise devoid of *Sthenurus* species, then it is included in species richness analyses as it represents a unique taxonomic unit for that layer. I use S as a measure of total species richness prior to correction by rarefaction, and E as a measure of expected species richness that has been corrected for sample size via rarefaction. The initial S and E trajectories were seen to closely mimic the relative abundance trajectory of *Pseudomys australis*. To assess if the dominance of *P. australis* was driving the results, the analysis was also run after removing *P. australis* from the dataset. This did not alter the overall trend but had a smoothing effect on the amplitude of peaks and troughs in the trajectory. Because the overall trend was unchanged, *P. australis* was retained to minimise deviation from the true assemblage composition.

5.4.3.3 Diversity

Biodiversity indices were generated for the mammal assemblage across layers and sublayers using MNI. Diversity is described by richness (S and E), total MNI, Shannon's diversity index (H'), equitability (J) and Simpson index 1-D. Correlations between these indices are expected as they essentially measure slightly different aspects of the same phenomenon.

The Shannon's diversity index (H') (Shannon, 1948) takes into account species richness and relative abundances. H' is given as,

$$H' = -p_i \ln p_i$$

where p_i is the proportion of species i relative to S (n_i/n). The log to species relative abundance means that weighting is slightly reduced for more abundant species. This makes H' useful when attempting to quantify diversity for communities with low evenness (that are dominated by a few abundant species). If only a single taxon is present in the sample, then $H' = 0$. The value of H' increases as richness and evenness increase. Values for ecological data are usually between 1.5 and 3.5 and rarely exceed 4.0 (Kent and Coker, 1992).

Equitability (J) (Pielou, 1966) is an index of evenness, the distribution of abundance among taxonomic units in a sample. J is normalised for species richness and is given as,

$$J = H'/H_{max}$$

where $H_{max} = \ln S$. Equitability values range from 0–1 and increases with increasing evenness.

Simpson's Index of Diversity (1-D) (Simpson, 1949) describes the probability of two random individuals in a sample belonging to the same taxonomic unit. The formula for D is given as,

$$D = \sum_i \left(\frac{n^i}{n} \right)^2$$

and 1-D is expressed as the reverse. The given values range from 0–1 with increasing values indicating increasing diversity.

5.4.4 Taphonomy

Earlier work established that the fossils accumulated via pitfall trapping and the predatory action of owls in phase 2, with the addition of a third contributor, the carnivorous bat *Macroderma gigas*, in phase 1 (Dawson and Augee (1997). Phase 1 lies below the equivalent depth reached by the FU excavation, and the almost complete absence of remains of *M. gigas* removes it as a potential contributor for the fossils used in this study (Appendix D Table 7.13) To assess the consistency of accumulation agents, and determine potential accumulation bias, the Cathedral Cave mammals are plotted through time by adult bodyweight. Weight partitions of ≤ 500 g and >500 g were selected to differentiate between taxa that are likely to have been accumulated as prey of owls and those that fell victim to pitfall entrapment. *Tyto novaehollandiae*, the largest cave roosting owl recorded regionally, prefers prey up to a weight of 500 g (Kavanagh, 2002b). Adult body weights are derived from literature sources given in Appendix D Table 7.16. When weight has been given as a range, I use the minimum adult weight in acknowledgement that owls commonly prey on juveniles that would not have reached a maximum adult weight (Andrews, 1990).

5.4.5 Taxonomic Habitat Index

The Taxonomic Habitat Index (THI) combines the preferred habitats associated with taxonomic units to generate a cumulative index showing the relative number of habitats represented by the sum of the taxa sampled by the assemblage (Evans et al., 1981; Andrews, 1990). Using THI allows each taxonomic unit to be assigned to multiple habitats by assigning a score, as a proportion of one, for each taxonomic unit to each of the habitat classes. The score is weighted toward the importance of each habitat class to each taxonomic unit. Scores in each stratigraphic partition are summed for each habitat type. The cumulative habitat score is then divided by S for that partition to give the Taxonomic Habitat Index score. A further advantage to using THI is that because it is calculated on S , it is decoupled from relative abundance trajectories and avoids domination or skewing by dominant species, as can occur with trajectories calculated on relative abundances.

The fossil assemblage includes multiple extinct species for which habitat preferences are poorly established, so I apply THI to Köppen climate classes adapted for Australia (Stern et al., 2000). The five main classes, desert (arid), grassland (semi-arid), temperate, sub-tropical and tropical are based on regional precipitation and temperature patterns. For species with extant relatives, or recently extinct species with reasonably well-established distributions this score is proportioned on their known habitats as distributed on Atlas of Living Australia (<https://www.ala.org.au/>) and taking records of prior distributions into account. However, it is acknowledged that the historical distribution of species may not be a completely accurate representation of their prehistoric distributions prior to anthropogenic impacts (Fusco et al., 2016). For extinct species, these scores are assigned based on their known distribution.

5.4.6 Mammal trajectories

To correct for taphonomic bias, the assemblage was analysed in weight partitions of ≤ 500 g or >500 g. Ra% was calculated for each of these groups independently. *Pseudomys australis* was by far the most dominant species within the smaller body-size group, and its abundance concealed trends for other taxonomic units. Therefore, Ra% for the small mammals was calculated both with and without *P. australis*. Thus, the Ra% for *P. australis* represents its abundance across the entire ≤ 500 g group, whereas the trajectories for other small mammals have been calculated after the removal of *P. australis*. Where Ra% is too low to generate a meaningful trajectory, Ra% is plotted on presence / absence grids.

Ecological traits and preferences for each of the taxonomic units are detailed in Appendix D Table 7.16 with references provided. In the analysis, I do not include lesser habitat

associations that are not relevant to the environments expected to be present in Binjang during the late Pleistocene and Holocene. For example, I do not anticipate that the region included coastal swamps, alpine heath or tropical moist forests, and so these habitat associations are omitted from our analysis. Relative abundances were tracked through stratigraphic layers to assess any changes that occurred in these trajectories through time.

5.4.7 Megafauna chronology

To compare the temporal ranges of the megafaunal species found in Cathedral Cave, I interrogated the data in the FosSahul 2.0 dataset, (Peters et al., 2019). Here, reliable is defined as those dates given a quality rating of A* or A using the quality rating criteria established by Rodríguez-Rey et al. (2015). Some of these ages may be considerably older than previously published last-occurrence dates published in earlier versions of FosSahul (e.g., Roberts et al., 2001; Wroe and Field, 2006; Saltré et al., 2016). Dates rated B and C are considered unreliable (Rodríguez-Rey et al., 2016; Peters et al., 2019).

5.5 Results

5.5.1 Relative abundance

The Cathedral Cave assemblage consists of seventy-three taxonomic units including at least 66 named species (Table 5.2). *Pseudomys australis* was the most dominant species in the assemblage, accounting for between 20.2 % and 75.3 % of taxa present in each sublayer or layer and making up 57 % of the overall assemblage.

Table 5.2. Relative abundance of taxonomic units in the Cathedral Cave assemblage (including *Pseudomys australis*). Relative abundances of the partitioned size classes that have been calculated after the removal of *P. australis*, and used in relative abundance trajectories, are included in Appendix D Table 7.13.

species	layer:	1–8	9	10a	10b	10c	10d	12	13a	13b	13c	14a	14b	14c	Σ
Tachyglossidae															
<i>Tachyglossus aculeatus</i>		-	-	-	-	-	-	0.8	-	0.5		-	-	-	0.04
<i>Megalibgwilia ramsayi</i>		-	-	-	-	-	-	-	-	-	-	-	0.2	0.2	0.04
Dasyuridae															
<i>Dasyurus geoffroii</i> / <i>viverrinus</i>		4.8	3.8	6	3.1	3.6	2.9	5.9	2.1	1.8	2	1.9	1.3	1.3	3
<i>Dasyurus maculatus</i>		-	-	-	-	-	-	-	-	0.5	-	-	0.4	0.4	0.11
<i>Sarcophilus lanianus</i>		-	-	-	-	0.2	-	-	-	-	-	-	-	0.2	0.04
<i>Antechinus flavipes</i>		1.5	0.0	0.8	0.3	0.2	0.6	0.8	4.3	4.6	5.3	2.7	2.9	1.3	1.68
<i>Phascogale tapoatafa</i>		-	-	-	0.3	0.2	-	-	0.4	0.9	0.8	0.5	0.2	-	0.23
<i>Sminthopsis crassicaudata</i>		1.1	2.2	3.2	2.6	2.3	2.1	-	2.6	0.9	0.4	0.7	-	0.2	1.53
<i>Sminthopsis murina</i>		0.7	1.1	2	1.1	0.9	0.6	1.7	0.9	3.7	2.9	2.2	1.9	0.4	1.42
cf. <i>Dasyuroides byrnei</i>		-	1.1	-	0.3	0.5	0.9	-	-	-	0.4	0.2	-	0.4	0.3
Dasyuridae sp. 3		-	-	-	-	-	-	-	-	-	0.4	-	-	-	0.2
Dasyuridae sp. 4		-	-	-	-	-	-	0.8	-	-	-	-	-	-	0.01
Thylacinidae															
<i>Thylacinus cynocephalus</i>		-	-	-	-	-	-	0.8	-	-	-	0.5	0.2	0.2	0.11
Chaeropodidae															
<i>Chaeropus ecaudatus</i>		0.4	-	0.2	0.3	0.7	0.6	-	-	-	-	-	-	-	0.21
Peramelidae															
<i>Isoodon obesulus</i>		4.8	2.7	2.4	0.7	0.7	2.1	4.2	3.9	2.3	4.1	3.6	2.3	0.5	2.19
<i>Perameles gunnii</i> / <i>nasuta</i>		5.9	5.5	2.6	0.5	0.5	2.9	5.9	5.2	4.1	4.9	4.4	2.7	2.4	2.95
Thylacomyidae															
<i>Macrotis lagotis</i>		-	-	-	-	0.4	0.3	-	-	-	-	-	-	-	0.06
Vombatidae															
<i>Vombatus ursinus</i>		1.1	1.1	-	-	0.2	0.3	0.8	1.7	0.9	0.4	-	0.2	-	0.34
Diprotodontidae															
Diprotodontidae gen. et sp. indet.		0.7	0.5	-	-	-	-	-	-	-	-	-	0.2	0.2	0.11
Palorchestidae															
<i>Palorchestes azael</i>		-	-	-	-	-	-	-	-	-	-	-	-	0.2	0.02
Thylacoleonidae															
<i>Thylacoleo carnifex</i>		-	-	-	-	0.2	-	-	-	-	-	-	-	0.2	0.04
Burramyidae															

species	layer:	1–8	9	10a	10b	10c	10d	12	13a	13b	13c	14a	14b	14c	Σ
<i>Cercartetus nanus</i>		-	-	-	-	0.4	-	-	0.4	0.5	0.4	0.2	0.2	-	0.15
Petauridae															
<i>Petaurus breviceps</i>		0.4	0.5	-	0.5	0.4	0.9	1.7	2.6	0.9	2	1	0.6	-	0.68
Pseudocheiridae															
<i>Pseudocheirus peregrinus</i>		0.4	-	-	0.2	-	-	-	0.9	-	-	0.2	0.2	0.2	0.15
Acrobatidae															
<i>Acrobates pygmaeus</i>		-	-	-	-	-	-	-	0.4	0.9	0.4	-	-	-	0.08
Phalangeridae															
<i>Trichosurus vulpecula</i>		3.3	0.5	-	0.2	-	0.3	-	-	0.5	0.4	-	-	0.2	0.32
Potoroidae															
<i>Aepyprymnus rufescens</i>		4.5	0.0	0.6	0.3	0.5	2.1	9.2	1.7	0.5	0.0	0.2	0.2	0.0	0.96
<i>Bettongia gaimardi</i>		-	-	-	-	0.4	-	0.8	0.9	-	0.4	-	-	-	0.13
<i>Bettongia lesueur</i>		2.2	0.5	0.8	0.7	0.5	1.8	0.8	-	0.5	-	-	-	-	0.55
<i>Potorous tridactylus</i>		1.9	-	0.2	-	0.2	0.3	1.7	0.9	0.5	0.4	0.5	0.4	0.5	0.45
Macropodidae															
<i>Sthenurus andersoni</i>		-	0.5	0.2	-	-	-	-	0.4	-	-	-	-	0.2	0.08
<i>Sthenurus atlas</i>		-	-	-	-	-	-	-	-	-	-	-	-	0.2	0.02
<i>Simosthenurus pales</i>		-	-	-	-	-	-	0.8	0.4	-	-	-	-	-	0.04
<i>Procoptodon goliah</i>		0.4	-	-	-	-	0.6	-	-	-	-	-	-	-	0.06
<i>Congruus kitcheneri</i>		-	-	-	0.2	0.4	-	1.7	0.4	-	0.8	-	0.2	0.2	0.21
<i>Protomnodon brehus</i>		-	-	-	0.2	-	-	-	1.3	0.5	0.4	-	-	-	0.13
<i>Baringa</i> sp. nov. 1		-	-	-	0.2	-	0.3	-	-	-	0.4	-	-	-	0.06
<i>Petrogale</i> sp. indet.		-	-	-	-	-	-	-	0.4	-	-	-	-	-	0.02
<i>Lagorchestes leporides</i>		1.9	0.5	0.4	-	0.2	-	0.8	0.4	-	-	-	-	0.2	0.25
<i>Macropus giganteus</i>		0.7	-	0.2	0.2	0.4	0.9	4.2	3.4	-	-	1.2	1.3	0.4	0.74
<i>Notamacropus agilis</i>		-	-	0.2	-	-	0.9	2.5	1.3	-	-	-	0.4	0.4	0.3
<i>Notamacropus dorsalis</i>		0.7	-	-	-	-	0.9	4.2	0.9	-	-	-	0.2	0.2	0.3
<i>Notamacropus parma</i>		0.7	-	-	0.2	0.4	1.8	7.6	2.6	0.9	0.4	-	0.2	0.5	0.7
<i>Notamacropus parryi</i>		-	-	-	-	-	0.3	0.8	-	-	0.4	-	0.2	-	0.08
<i>Onychogalea frenata</i>		1.1	0.5	-	0.3	0.2	0.3	0.8	-	-	-	-	-	-	0.19
<i>Onychogalea lunata</i>		0.4	-	0.2	-	0.2	-	-	-	-	-	-	-	-	0.06
<i>Wallabia bicolor</i>		-	-	-	-	-	0.6	-	-	-	-	-	-	-	0.04
<i>Osphranter robustus</i>		-	-	-	-	0.2	0.3	1.7	0.4	-	-	0.2	0.6	0.4	0.23
<i>Osphranter rufus</i>		-	0.5	-	-	-	-	-	-	-	-	-	-	0.2	0.02
Muridae															
<i>Conilurus albipes</i>		3.3	2.2	0.4	0.8	0.9	2.3	4.2	6.9	6.9	8.6	4.1	6.5	3.8	3.38
<i>Hydromys chrysogaster</i>		-	-	-	-	0.2	-	-	-	-	0.5	-	-	-	0.04
<i>Mastacomys fuscus</i>		1.1	-	1.6	1.6	0.4	0.3	-	0.4	-	0.8	0.2	0.8	2.4	0.96
<i>Notomys</i> sp. indet.		4.8	6.6	4.2	7.3	9.9	5.9	2.5	0.4	-	0.4	0.2	-	0.4	3.7
<i>Pseudomys australis</i>		30.1	61.5	65.7	70.3	67.7	56.6	20.2	25.3	37.7	35.9	53.5	59.7	$\frac{75.3}{3}$	57.12
<i>Pseudomys desertor</i>		1.5	3.8	2.4	4.4	4.1	4.1	-	-	-	-	-	-	-	1.85
cf. <i>Pseudomys fumeus</i>		-	-	0.2	-	-	-	-	-	-	-	-	-	-	0.04
<i>Pseudomys gouldii</i>		0.4	-	-	0.2	-	-	-	-	-	-	-	-	-	0.04
<i>Pseudomys gracilicaudatus</i>		1.1	-	-	-	-	-	-	8.6	6.8	6.6	5.1	4	0.9	2.1
<i>Pseudomys novaehollandiae</i>		3	1.6	4.2	2.3	1.4	4.1	5.9	13.3	18.8	13.5	12.6	6.3	3.5	5.97
<i>Pseudomys oralis</i>		-	-	-	-	-	-	-	-	0.9	0.8	1.2	0.6	-	0.25

species	layer:	1–8	9	10a	10b	10c	10d	12	13a	13b	13c	14a	14b	14c	Σ
<i>Rattus fuscipes</i>		0.4	-	-	-	-	-	-	-	-	-	-	-	-	0.02
<i>Rattus</i> sp. cf. <i>R. lutreolus</i>		-	-	-	-	-	-	0.8	1.7	2.3	2.4	1.7	2.7	1.1	0.89
<i>Rattus</i> sp. cf. <i>R. tunneyi</i>		2.6	-	-	0.2	-	-	-	0.9	-	-	-	-	0.2	0.23
Murinae sp. 1		-	-	0.2	0.2	-	-	-	-	-	-	-	-	-	0.04
Murinae sp. 2		-	-	-	-	-	0.3	-	-	-	-	-	-	-	0.02
Murinae sp. 3		0.4	-	-	-	-	-	-	-	-	-	-	-	-	0.02
Murinae sp. 4		-	-	0.2	-	-	-	-	-	-	-	-	-	-	0.02
Murinae sp. 5		-	-	-	-	-	-	-	-	0.5	-	-	-	-	0.02
Murinae sp. 6		-	-	0.2	-	-	-	-	-	-	-	-	-	-	0.02
Murinae sp. 7		-	-	-	-	-	-	-	-	-	0.4	-	-	-	0.02
Chiroptera															
<i>Macroderma gigas</i>		0.4	-	-	-	-	-	-	-	-	-	-	-	-	0.02
Microchiroptera spp. (inc. <i>Rhinolophus megaphyllus</i> , <i>Miniopterus schreibersii</i> & Microchiroptera gen. et. sp. indet.)		11.2	2.2	0.4	0.3	0.5	1.2	5	1.7	0.9	2	1	1.9	0.9	1.7

5.5.2 Layer partitioning

K-means clustering was used to assess if spits within the higher yielding layers (10, 13 and 14) formed clusters based on taxonomic similarity that could be used for partitions. K-means clustering of spits in layer 10 at five, three, four and two clusters levels, did not result in meaningful clusters with comparable sample sizes (Appendix D Table 7.15). Similarly, informative clusters were not identified in layer 14 at the four, three or two cluster level. Therefore, partitioning of the spits in most extensive and better sampled layers 10, 13, and 14, focused on achieving comparable sample sizes in each partition (Appendix D Table 7.14).

5.5.3 Rarefaction, richness, diversity and abundance

5.5.3.1 Rarefaction

Rarefaction curves for individual spits (Figure 5.3a–f), layers (Figure 5.3g) and partitioned sublayers in layers 10, 13 and 14 (Figure 5.3h), were not asymptotic, indicating that additional sampling would detect additional species. Sample coverage in layers 10, 13 and 14 is more comprehensive than in 1–8, 9 and 12 (Figure 5.3).

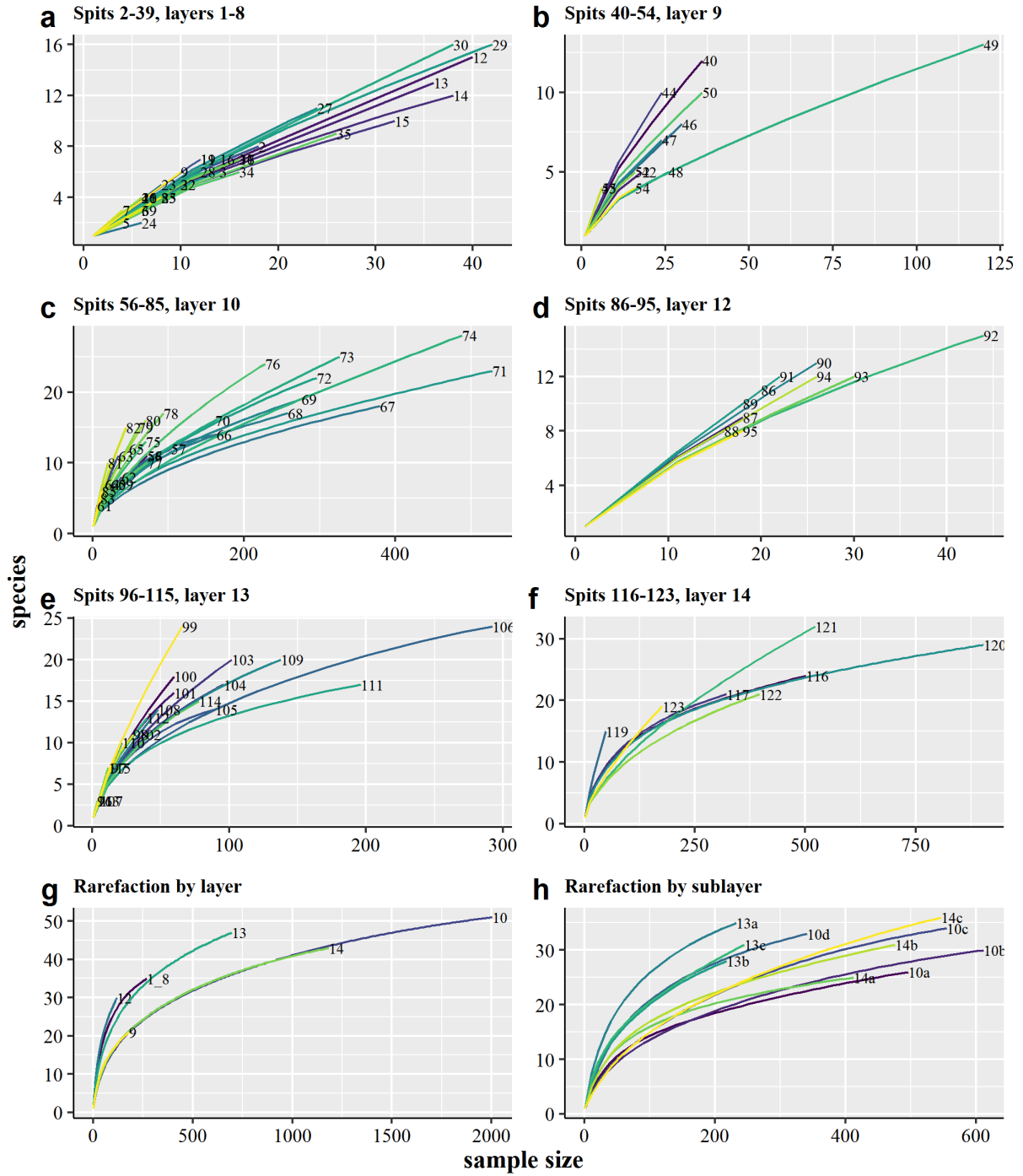


Figure 5.3. Rarefaction curves generated for a–f) individual spits by layers, excluding spits where MNI < 2; g) by layers; h) by partitioned sublayers.

5.5.3.2 Richness

Expected mammalian species richness (E), corrected by rarefaction to the smallest sample size of 119 in layer 12 (Figure 5.4a, Appendix D Table 7.19), increases through layers 14 and 13 ($E = 15-26$) and peaks in layer 12 ($E = 28$). After layer 12, E decreases, reaching lows in sublayers 10a and 10b ($E = 14$), before recovering in layers 9 and 1–8 ($E = 17-26$). E diverges from actual species richness (S) in sublayers 14c and layers 1–8 with these showing higher richness ($S = 36$ and 35 respectively). E declines rapidly from layer 12 into sublayer 10d, whereas S continues increasing until decreasing until sublayer 10b, after which it declines until layers 1–8. Simpson (1-D), Shannon (H') and Equitability (J) diversity and evenness indices follow close trends across sublayers and layers. All indices increase from sublayer 14c, with Shannon H' peaking in sublayer 13a and Simpson 1-D and Equitability J peaking in layer 12 (Figure 5.4b). After a decrease into layer 10, all indices show an increase into sublayer 10a, and reach levels nearly on par with layer 12 in layers 1–8. I caution that Shannon H' returns a value that lies within 0–5, whereas both Simpson 1-D and Equitability J return values between 0–1, thus, trends are compared between indices rather than values.

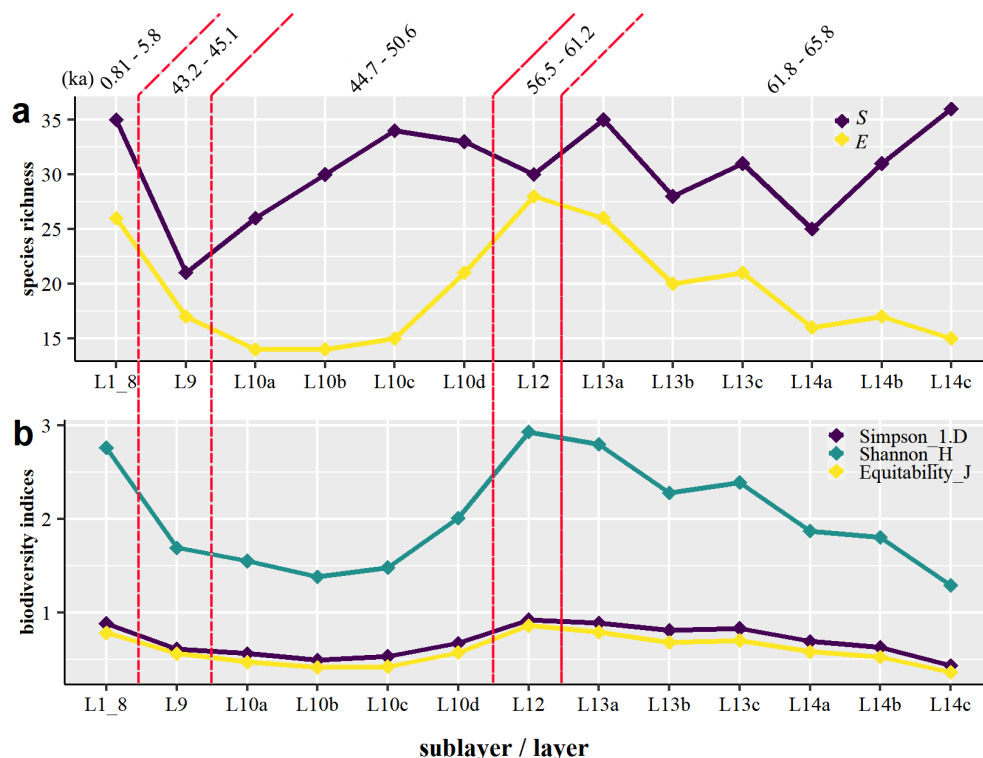


Figure 5.4. Biodiversity curves for mammal taxa including a) Richness (S) and expected richness corrected by rarefaction (E) on the smallest sample size of 119. b) Biodiversity and evenness curves generated with Simpson Index of Diversity (1-D), Shannon diversity Index (H') and Equitability (J). Age range across the top represents ka (thousands of years) ago.

5.5.4 Taphonomy

The Cathedral Cave mammal assemblage is dominated by taxa with a maximum adult bodyweight ≤ 500 g (Figure 5.5). These taxa make up over half of all identified specimens in all layers and sublayers (54–95 %). This number decreases in sublayer 13a (71 %), layer 12 (54 %) and layers 1–8 (75 %). Otherwise, the size classes remained relatively consistent in Cathedral Cave.

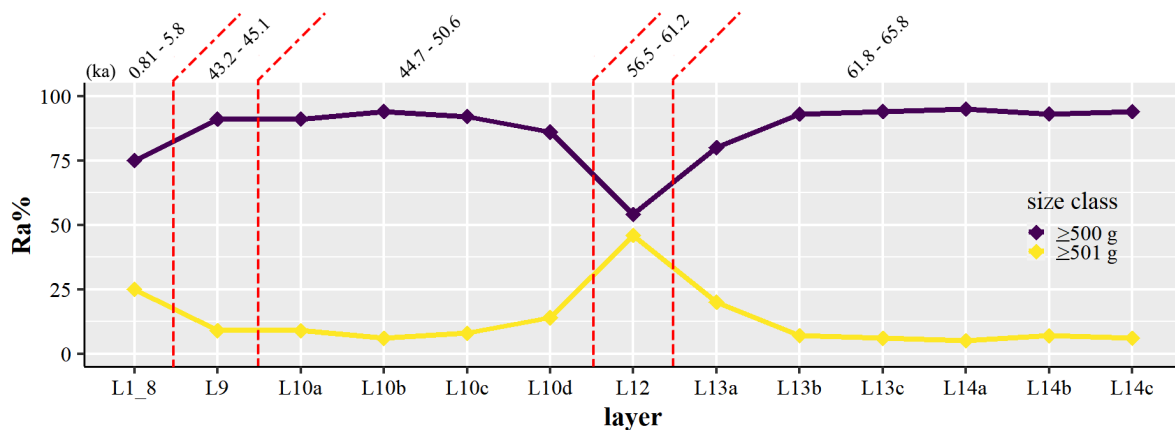


Figure 5.5. Bodyweight of taxa recovered from each stratigraphic partition in the Cathedral Cave excavation, shown as Relative abundance (Ra%). Age range across the top represents ka (thousands of years) ago.

5.5.5 Taxonomic Habitat Index

The Taxonomic Habitat Index (THI) shows clear dominance of taxa associated with temperate climates through the sequence (Figure 5.6). THI values increase for temperate zone taxa from sublayer 14c and decline into layers 9–1 after a peak in sublayer 13b. Temperate zone taxa decline in layer 9, when compared to sublayer 10a, however, the decline is of a similar magnitude to the sawtooth trajectory followed by this group during layer 10. Overall, there is a higher prevalence of taxa associated with temperate zones through layers 14 and 13.

Species associated with sub-tropical and tropical zones follow a similar trend in being more prevalent in layers 14, 13 and 1–8 than elsewhere (Figure 5.6). However, the trajectory for sub-tropical taxa peaks in sublayer 14b, whereas the peak occurs in sublayer 13a for tropical zone taxa. None of the Cathedral Cave taxa are solely associated either tropical or sub-tropical climatic zones, and only *Notamacropus parryi* and *N. dorsalis* have strong modern associations with either of these zones.

Taxa known from the semi-arid zone are less common through layers 14, 13, and 1–8. The trajectory shows a decline from sublayer 14c, recovery in sublayer 13c and then a further

decline in sublayer 13b (Figure 5.6). In sublayer 13a, the THI reveals an increase in taxa that associate with semi-arid zone habitats that continues through to layer 10. On the other side of the accumulation hiatus, in layers 1–8, these taxa appear in lower numbers. Taxa associated with the arid zone follow a similar trend to those from the semi-arid zone, with an overall increase from sublayer 14c to layer 9 (Figure 5.6). These taxa are at their lowest in layer 14b and show a reduction in layer 1–8. Several species in the assemblage have strong associations with the arid or semi-arid zone than with the temperate zone (*Osphranter rufus*, *Chaeropus ecaudatus*, *Bettongia lesueur*, *Notomys* sp., *Pseudomys australis*, *Pseudomys desertor*), and one (*Dasyuroides byrnei*), is known only from the arid and semi-arid regions.

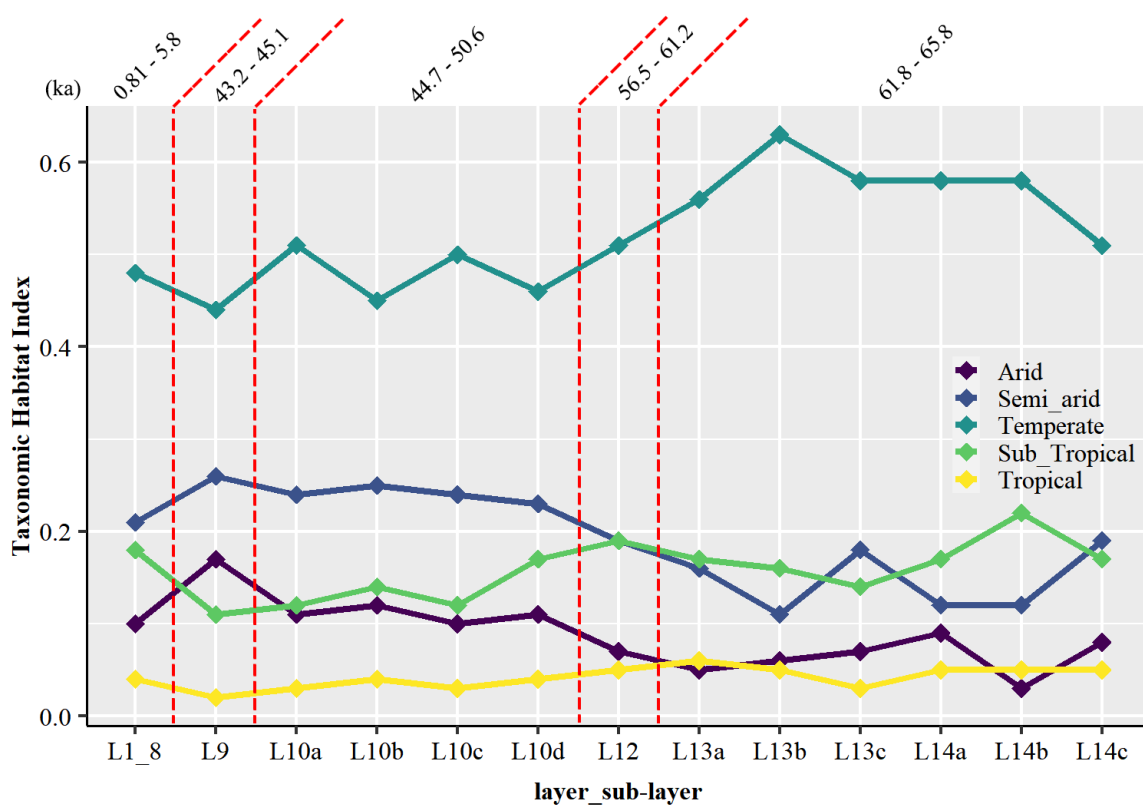


Figure 5.6. Taxonomic Habitat Index showing taxa associated with arid, semi-arid, temperate, sub-tropical and tropical climate classes defined by Köppen climate classes adapted for Australia (Stern et al., 2000)

5.5.6 Mammal Trajectories

5.5.6.1 ≤ 500 g mammals

Thirty-six taxonomic units were assigned to the ≤ 500 g size class (). Several of these taxa were present infrequently and / or in abundances too low to generate useful trajectories.

These taxa are presented on a heat map showing presence / absence and Ra% (Figure 5.7a).

Dasyuroides byrnei, today known from gibber plains and grasslands (Appendix D Table 7.16), is present in layers 14, 13, 10, and 9. It reaches its maximum abundance in layer 9

(3.70 Ra%, \bar{x} 1.04 Ra%). The aquatic rodent *Hydromys chrysogaster* is uncommon in the assemblage, appearing twice, in sublayers 13b (0.82 Ra%) and 10c (0.74 Ra%). *Macroderma gigas* is represented by a single canine in layers 1–8 (0.82 Ra%) but this specimen is likely not *in situ*, but incorporated from overlying disturbed sediments, which contain material from deeper layers. The record for cf. *Pseudomys fumeus*, *Pseudomys gouldii*, *Rattus fuscipes* and *Rattus* sp. cf. *R. tunneyi* is sparse. A single fossil is assigned to cf. *Pseudomys fumeus* in layer 10a (0.79 Ra%). This species is today known from dry ridgeline forest and occasionally wetter gullies (Appendix D Table 7.16). *Pseudomys gouldii* appears in sublayers 10b (0.68 Ra%) and layers 1–8 (0.82 Ra%). *Rattus fuscipes* is now known from dense, temperate habitats, it is only present in layers 1–8 (0.82 Ra%) *Rattus* sp. cf. *R. tunneyi* appears sporadically in sublayers 14c, 13a, 10b and layers 1–8 (\bar{x} 0.69 Ra%). Its preferred modern habitat is tall grasslands, often associated with waterways (Appendix D Table 7.16). Little useful information can be gleaned from the murids and dasyurids that have not been resolved to species (Figure 5.7a). None of these are common in the assemblage (1.02–0.68 Ra%).

Antechinus flavipes, *Conilurus albipes*, *Pseudomys gracilicaudatus*, *Pseudomys novaehollandiae*, *Pseudomys oralis* and *Rattus* sp. cf. *R. lutreolus* are at their most abundant in layers 14 and 13, before declining to their lowest abundances into layer 10 (Figure 5.7b). Modern habitat associations for these taxa comprise of open forest or woodland with heath or grassy understorey (Appendix D Table 7.16). *Antechinus flavipes* is common in the assemblage (\bar{x} 4.69 Ra%) but is more abundant in layers 14 and 13 (9.15–6.3 Ra%) than in layers 12–1 (3.30–0.00 Ra%). The extinct arboreal rodent *Conilurus albipes* is common through most layers and sublayers (\bar{x} 10.30 Ra%) but is more abundant through layers 14–12 (21.00–9.88 Ra%) than in layers 10–1 (8.1–1.5 Ra%). *Conilurus albipes* initially decreases through layer 14 (21.00–9.88 Ra%), then shows a non-linear increase through layer 13 (14.79–12.29 Ra%). *Pseudomys gracilicaudatus* is common in layers 14–13 (15.74–5.00 Ra%) but does not appear again until layers 8–1 (2.47 Ra%). *Pseudomys novaehollandiae* is common throughout the assemblage (\bar{x} 5.4 Ra%) but is more abundant through layers 14–13 (22.60–18.63 Ra%) than elsewhere in the excavation (17.50–5.55 Ra%). In layers 14–13, *Pseudomys novaehollandiae* begins to increase above sublayer 14b. *Pseudomys oralis* is only present in layers 14–13 (2.90–1.40 Ra%, \bar{x} 0.60 Ra%). *Rattus* sp. cf. *R. lutreolus* appears only in layers 14–12 (8.07–2.50 Ra%, \bar{x} 2.47 Ra%). The latter four taxa are all associated with relatively more mesic habitats (Appendix D Table 7.16). All taxa, excluding *C. albipes* and *P. novaehollandiae*, initially increase in abundance from sublayer 14c.

Several taxa with more xeric habitat associations, show an inverse trajectory to those featured earlier (Figure 5.7b–c). *Chaeropus ecaudatus*, *Notomys* sp. indet., and *Pseudomys desertor* are currently associated with arid or semi-arid habitats (Appendix D Table 7.16) and all reach their highest relative abundances in layer 10. *Chaeropus ecaudatus* is uncommon (\bar{x} 0.61 Ra%) being present in layer 10 (2.9–0.79 Ra%) and also in layers 1–8, where it is represented by a single isolated molar (0.82 Ra%). *Notomys* sp. indet. is common in the assemblage (\bar{x} 11.76 Ra%). Although present intermittently through layers 14 and 13 (2.00–0.58 Ra%), *Notomys* sp. indet. shows a dramatic increase through layers 12 and 9 (40.74–7.5 Ra%), before declining in layers 1–8 (10.74 Ra%). *Pseudomys desertor* is absent in layers 14–12 but mimics the trajectory for *Notomys* sp. indet. in layers 10–1 (18.36–3.30 Ra%), albeit in lower relative abundance (\bar{x} 5.80 Ra%). *Sminthopsis crassicaudata* (\bar{x} 4.61 Ra%) shows up intermittently through layers 14 and 13 (4.72–0.00 Ra%) but increases in layer 10 (12.69–7.14 Ra%) before decreasing through layers 9–1 (7.40–2.47 Ra%). *Sminthopsis crassicaudata* is not strictly limited to arid or semi-arid habitats, however, its modern distribution includes more xeric habitats than *S. murina*, the other species of *Sminthopsis* identified in this assemblage (Appendix D Table 7.16).

Mastacomys fuscus (\bar{x} 2.29 Ra%) shows a steep decline from sublayer 14c (13.00 Ra%) and then follows a non-linear intermittent trajectory (2.48–0.00 Ra%) through to sublayer 10c. After this, it shows a brief increase through sublayers 10b and 10a (6.80–6.34 Ra%) (Figure 5.7d). *Mastacomys fuscus* prefers mesic habitats, including swamps or sedgeland, with proximity to watercourses (Appendix D Table 7.16). It now has a disjunct distribution in high altitude regions, but its fossil record shows that it was formerly much more widespread (Fusco et al., 2016). *Isoodon obesulus* and *Perameles gunnii* / *nasuta* share a broadly similar trend. Both are common in the assemblage (*I. obesulus* \bar{x} 7.04 Ra%, *P. gunnii* / *nasuta* \bar{x} 10.06 Ra%) and their relative abundances peak in layer 12 (*I. obesulus* 12.50 Ra%, *P. gunnii* / *nasuta* 17.50 Ra%). These trajectories diverge at two points. In sublayer 14c, *I. obesulus* is at its lowest abundance for in layers 14–13 (3.00 Ra%), whereas *P. gunnii* / *nasuta* is at its highest abundance for these layers (13.00 Ra%). In layer 10, both taxa reach their lowest abundance in sublayer 10c (*I. obesulus* 2.72 Ra%, *P. gunnii* / *nasuta* 2.04 Ra%). *Isoodon obesulus* shows a modest increase from layer 9 (9.25 Ra%) into layers 8–1 (10.74 Ra%), while *P. gunnii* / *nasuta* reaches its highest abundance in layer 9 (18.51 Ra%) before declining in layers 8–1 (12.22 Ra%). *Isoodon obesulus* prefers habitats that are more mesic than *P. gunnii* / *nasuta* (Appendix D Table 7.16). *Sminthopsis murina* follows a non-linear

trajectory through the excavation (\bar{x} 4.20 Ra%), reaching its highest relative abundance (7.93 Ra%) in sublayer 10a and its lowest in layers 8–1 (1.65 Ra%).

Petaurus breviceps is present throughout the excavation (\bar{x} 2.17 Ra%), excluding sublayers 14c and 10a (Figure 5.7e). The abundance of *P. breviceps* peaks in sublayer 13a (1.72 Ra%) and layer 12 (5.00 Ra%). *Acrobates pygmaeus* appears only in layer 13, where it peaks in sublayer 13b (1.63 Ra%, \bar{x} 0.24 Ra%). *Cercartetus nanus* (\bar{x} 0.38 Ra%) and *Phascogale tapoatafa* (\bar{x} 0.59 Ra%) are intermittently present through the assemblage. Both reach their highest abundance in sublayer 13b (*Ct. nanus* 0.82 Ra%, *Ph. tapoatafa* 1.63 Ra%). Neither are present in 14c or layer 12 (Figure 5.7e). All four of these taxa require a reasonable density of suitable trees (or shrubs) on the landscape with *Acrobates pygmaeus* today is most commonly found in tall eucalypt forest (Appendix D Table 7.16).

Pseudomys australis (Figure 5.7f) is the most common taxon in the assemblage (\bar{x} 57.06 Ra%) and shows a steep decline from a peak in sublayer 14c (80.46 Ra%), to its lowest abundance, in sublayer 13a (31.72 Ra%). Sublayer 13a appears to be a pivot point for this taxon, with abundances recovering through layer 10 and remaining high through layers 10 and 9 (74.56–66.32 Ra%). The abundance of *P. australis* is lower in layers 8–1 (40.09 Ra%). Today, *P. australis* is associated with a range of semi-arid and arid habitats that includes open grasslands and gibber plains (Watts and Aslin, 1981; Medlin, 2008). However, its fossil record shows that it formerly occupied a broader variety of biomes, and morphological variability in attributed fossils has led to some speculation that fossil occurrences of *P. australis* could represent multiple species or subspecies (McDowell, 2013; Fusco et al., 2016). In Cathedral Cave, *Pseudomys australis* follows a trajectory that is consistent with other arid and semi-arid taxa. Therefore, I consider its relative abundance trajectory to be a valid ecological signal, with higher abundances indicating a drier, more open environment.

Microchiroptera spp. (Figure 5.7g) are present throughout the excavation (\bar{x} 5.97 Ra%), but peak in layer 12 (15.00 Ra%) and layers 8–1 (24.79 Ra%). Some of the bat remains in the assemblage could be owl prey, but bats are autochthonous in Cathedral Cave and so their numbers are essentially decoupled from those of other allochthonous small mammals. The number of bats in the assemblage has not increased in layer 12, rather, their numbers have remained more or less stable as the taxa in the ≤ 500 size class reduced.

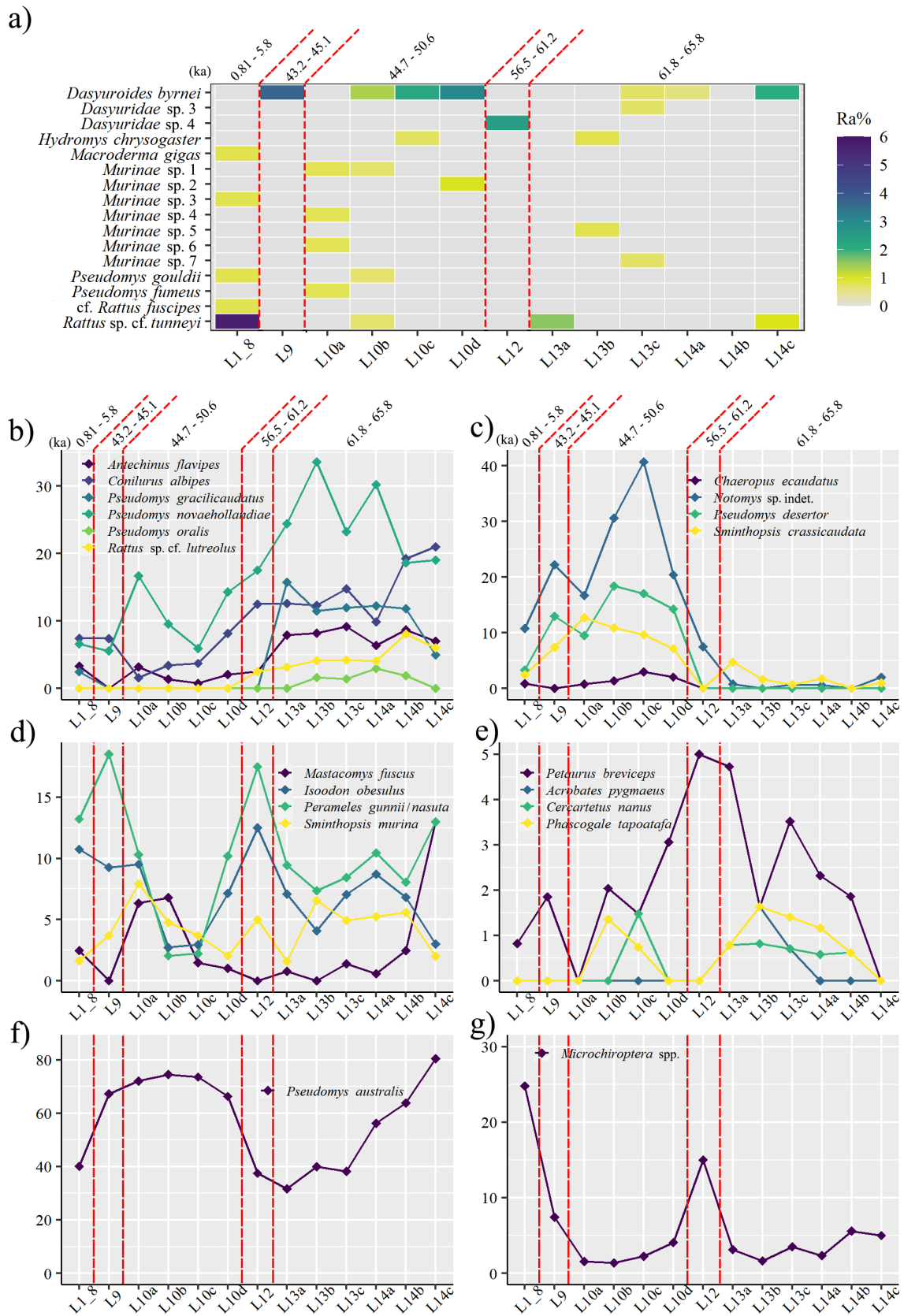


Figure 5.7. Relative abundance trends and trajectories for mammalian taxonomic units with adult bodyweight ≤ 500 g. a) Presence absence and Ra% of fauna that do not generate useful trajectories and are best interpreted by their presence / absence. The y axis shows taxonomic units and the x axis shows layers and sublayers. b-f) Ra% trajectories grouped by general trend similarities.

5.5.6.2 >500 g mammals

Thirty-six taxonomic units were assigned to the >500 g grouping (Figure 5.8; Figure 5.8a; Figure 5.9). Several taxa that are currently associated with open forest and woodland with grassy understorey (Appendix D Table 7.16) appear intermittently in the assemblage (Figure 5.8a). *Bettongia gaimardi* appears intermittently between 13c and 10c (\bar{x} 1.32 Ra%); *Petrogale* sp. indet. is only found in 13a (2.12 Ra%); *Thylacinus cynocephalus* is present only in layers 14 and 12 (\bar{x} 1.37 Ra%); *Vombatus ursinus* is common and present through every layer of the excavation, but not in all sublayers (\bar{x} 4.21 Ra%). *Wallabia bicolor* appears only in sublayer 10d (4.00 Ra%). Today, this species is found in forests and woodlands with dense vegetation (Appendix D Table 7.16). *Onychogalea lunata* appears intermittently through layers 10 to 1 only (\bar{x} 0.46 Ra%). The now extinct *O. lunata* was known from thick scrub and dense thickets as well as woodlands and open timbered country (Appendix D Table 7.16). Its distribution included arid and temperate regions (Woinarski et al., 2015b). The modern habitat niche of *Notamacropus parryi* has xeric associations, being an inhabitant of open forest with grassy understorey and dry savannah (Appendix D Table 7.16). It is intermittently present in sediments below sublayer 10d (\bar{x} 1.05 Ra%) but peaks in sublayer 13c (6.66 Ra%).

Today, *Sarcophilus laniarius* frequents open dry eucalypt forests as well as grassy woodlands (Appendix D Table 7.16). This taxon has been identified in sublayers 14c (2.85 Ra%) and 10c (2.27 Ra%). Modern populations of the arboreal taxa *Pseudocheirus peregrinus* and *Trichosurus vulpecula* prefer eucalyptus forest (Appendix D Table 7.16). Both appear intermittently through the excavation (*Ps. peregrinus* \bar{x} 1.52 Ra%, *T. vulpecula* \bar{x} 3.13 Ra%) (Figure 5.8a). *Macrotis lagotis*, today restricted to grass and shrublands (Appendix D Table 7.16), appears only in sublayers 10d and 10c (2.00 and 4.54 Ra% respectively). *Osphranter rufus* is now found in open arid and semi-arid environments (Appendix D Table 7.16). This taxon appears only in sublayer 14c (0.70 Ra%) and layer 9 (6.25 Ra%). *Tachyglossus aculeatus* was identified in 13 (6.66 Ra%) and 13c (1.81 Ra%), but provides little useful ecological information given its broad habitat associations and widespread distribution (Appendix D Table 7.16). *Tachyglossus aculeatus* has the broadest distribution of any Australian mammal and remains extant in the region today. Therefore, its absence in most layers is undoubtedly taphonomic.

Several taxa show a non-linear trend of higher abundances in layers 14–13 (Figure 5.8b). Three of these, *Potorous tridactylus*, *Dasyurus maculatus* and *Macropus giganteus* are today associated with woodland, forest and sclerophyll forest (Appendix D Table 7.16). *Potorous tridactylus* is common in the assemblage (\bar{x} 4.63 Ra%) but is more abundant through layers 14–13 (10.00–4.2 Ra%) than in layers 12–9 (3.63–0.00 Ra%). *Dasyurus maculatus* is only present intermittently in layers 14–13 (6.66–5.71 Ra%). *Macropus giganteus* is common in the assemblage (\bar{x} 7.30 Ra%), but is more abundant, although intermittently, in layers 14 and 13 (19.35–0.00 Ra%) than in layers 12–1 (9.09–0.00 Ra%). *Osphranter robustus* has broad habitat associations across much of Australia, bar some of the southern and northern extremities of the continent (Appendix D Table 7.16). This taxon is common in the assemblage (\bar{x} 7.30 Ra%) and is most abundant in sublayer 14b (9.67 Ra%).

Species with open habitat preferences are more abundant in sediments younger than sublayer 13a (Figure 5.8c). *Bettongia lesueur*, now inhabits open forests with grassy or heath understorey (Appendix D Table 7.16) and is common in the assemblage (\bar{x} 4.87 Ra%), but other than a single appearance in sublayer 13b (6.66 Ra%), does not appear in layers 14–13. *Lagorchestes leporides* became extinct in the 19th century but was recorded from open plains and grassland habitats (Appendix D Table 7.16). This species is uncommon in the assemblage (2.10 Ra%) but is absent for much of layers 14 and 13, appearing only in sublayers 14c (2.85 Ra%) and 13a (2.12 Ra%). *Onychogalea frenata*, which is today associated with tall acacia shrubland and grassy woodland (Appendix D Table 7.16), is absent from layers 14 through 12 (\bar{x} 1.74 Ra%).

Several taxa peak in abundance in layer 12 (Figure 5.8d). Modern populations of *Aepyprymnus rufescens* show preference for open forests and woodlands with sparse or grassy understorey (Appendix D Table 7.16). Common in the assemblage (\bar{x} 7.29 Ra%), the trajectory of *A. rufescens* peaks in layer 12 (20.00 Ra%). Today, *Notamacropus agilis* is associated with both open woodland and grassland habitats (Appendix D Table 7.16). It is uncommon and infrequent in the assemblage (\bar{x} 2.48 Ra%). *Notamacropus dorsalis* now frequents forests with dense shrub and open forest with dense acacia (Appendix D Table 7.16). The species is present infrequently in the assemblage (\bar{x} 2.18 Ra%), but peaks in layer 12 (9.09 Ra%). *Notamacropus parma* (\bar{x} 6.41 Ra%) is more abundant in layers 14–12 (16.36–0.00 Ra%) than in layers 10–1 (12.76–0.00 Ra%). This taxon is today associated with

more mesic, northern habitats, but it is occasionally found in dry sclerophyll forest (Appendix D Table 7.16).

The combined taxonomic unit incorporating *Dasyurus geoffroii* and *D. viverrinus* is common in the assemblage (\bar{x} 31.95 Ra%; Figure 5.8e). This taxon peaks in sublayer 14a (40.00 Ra%) and again in sublayer 10a (68.18 Ra%). However, *D. geoffroii* and *D. viverrinus* have differing habitat preferences and distribution (Appendix D Table 7.16), thus it is difficult to ascertain useful palaeoecological inferences from their combined trajectory.

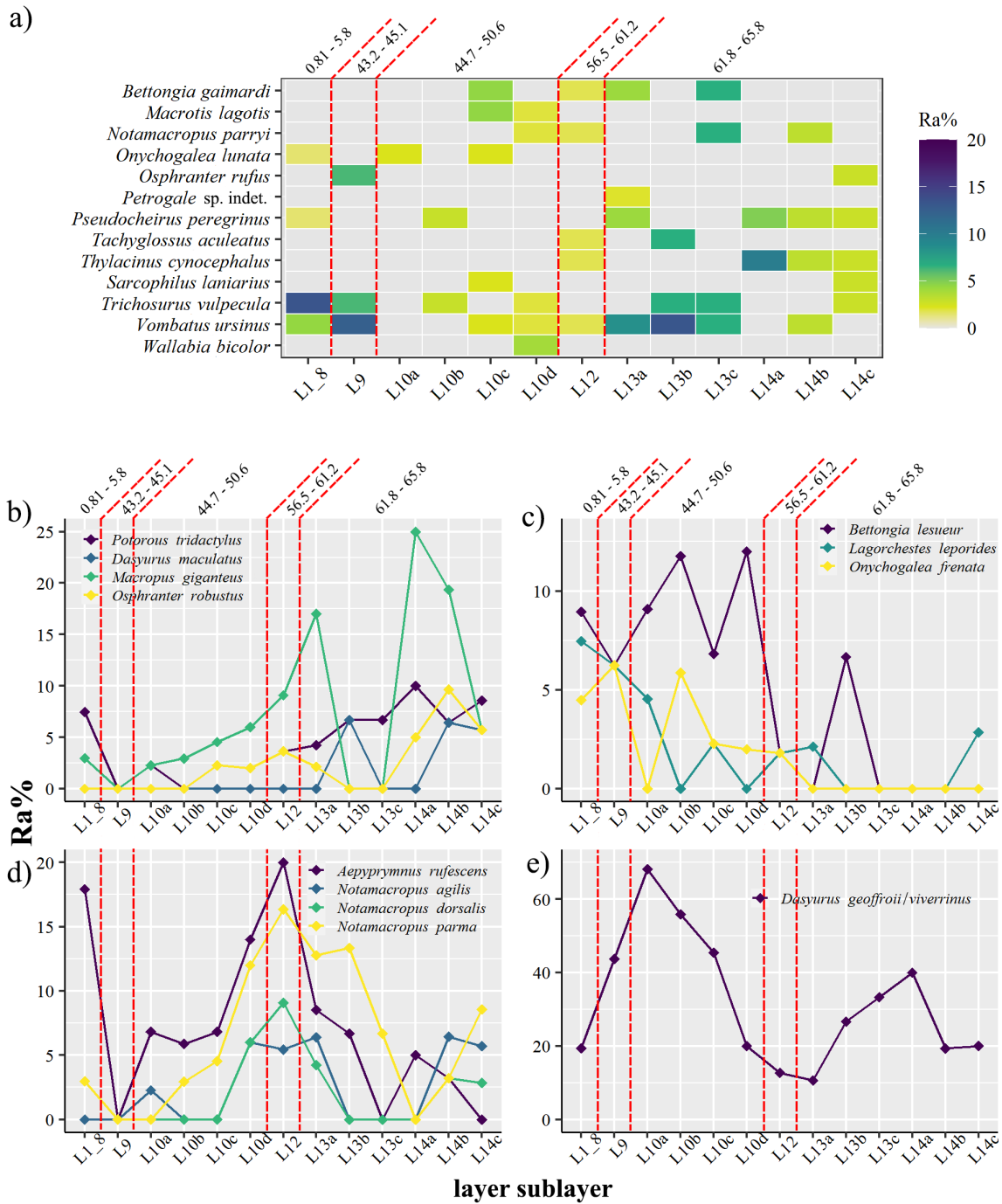


Figure 5.8. Relative abundance trends and trajectories for mammalian taxonomic units with adult bodyweight > 500 g. a) Presence absence and Ra% of fauna that do not generate useful trajectories and are best interpreted by their presence / absence. The y axis shows taxonomic units and the x axis shows layers and sublayers. b-e) Ra% trajectories grouped by general trend similarities. The y axis, showing Ra% is scaled to the maximum value in each plot and x axis shows layers and sublayers.

5.5.6.3 Extinct megafauna

Eleven extinct megafaunal taxa were identified in the assemblage (Figure 5.9). They are generally present in low abundances. *Congruus kitcheneri* is the most prevalent megafaunal taxon (\bar{x} 2.51 Ra% in the >500 g grouping), while *Palorchestes azael* and *Sthenurus atlas* are the rarest (both \bar{x} 0.21 Ra%).

All but one of these taxa, *Procoptodon goliah*, is present in layers 14 and 13. Megafaunal species richness is highest in sublayer 14c ($S = 7$) with most other layers containing just two or three taxa (\bar{x} $S = 2.3$). *Megalibgwilia ramsayi* and *Palorchestes azael* appear only in sublayers 14c–14b, and in sublayer 14c, respectively. In layer 12, just two taxa, *Congruus kitcheneri* and *Simosthenurus pales* are present. Layer 10 includes six megafaunal taxa, while layer 9 and layers 8–1 include two species each. Apparent species turnover between sublayers is generally high due to the intermittent appearance of most of these taxa, which is due to their very low sample sizes. Molar fragments of Diprotodontidae gen. et. sp. indet. and *Procoptodon goliah* in layers 8 and 2b are unlikely to be *in situ*; both layers are erosional fills that contain reworked material.

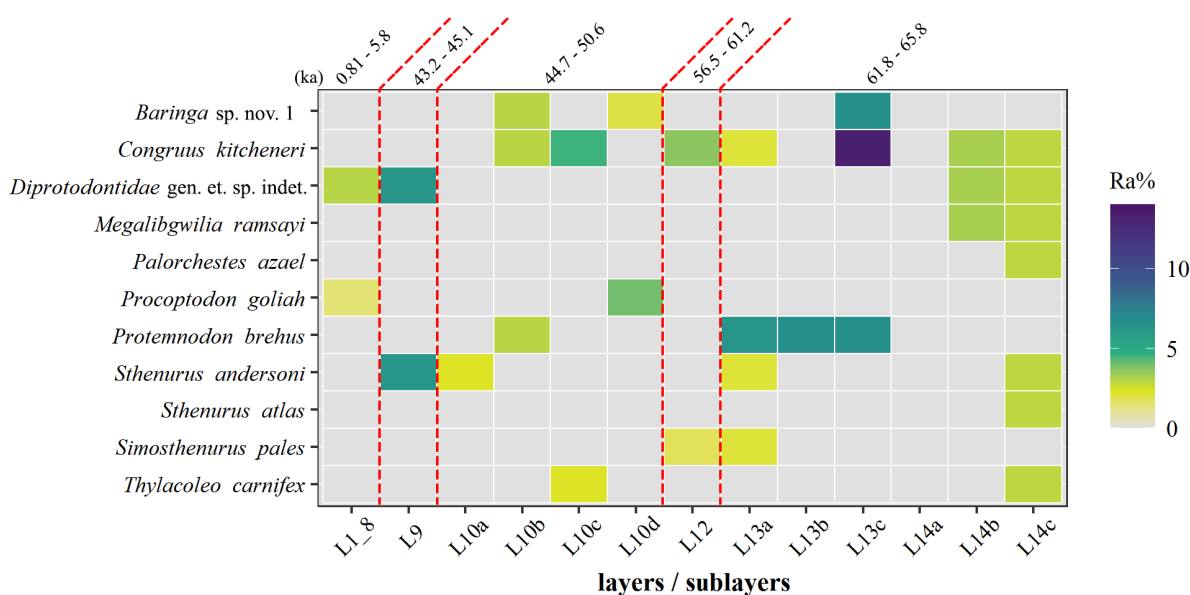


Figure 5.9. Presence and absence of extinct megafaunal species showing Ra%.

5.6 Discussion

5.6.1 Accumulation agency

My findings support the hypothesis that the vertebrate fossils in the Cathedral Cave sediment have accumulated by pitfall entrapment, and the predatory actions of owls as per previous work at the site (Dawson and Augee, 1997). Generally, taxa less than 500 g were attributed to owl predation, with some exceptions (bats) and those over 500 g to pitfall. The relative contributions of both accumulation modes have been overall consistent through the period of deposition, except during the transition between MIS 4–MIS 3 (Figure 5.5). The reduction in smaller mammal frequency implies that owls were contributing fewer prey remains to the assemblage. The reduced owl activity could be due to multiple factors including a change to cave morphology making it less suitable for roosting owls, lower prey availability or, a change to vegetation structures in the vicinity of the cave. Tytonid Owls, including *Tyto novaehollandiae* and *T. delicatula* represented in this fauna, prefer hunting in open areas (Kavanagh, 2002b) and faunal trends (discussed later) suggests a closing of the vegetation in the vicinity of the cave at this time. Thus, the latter offers the strongest explanation for changes in the relative abundances of size classes of the Cathedral Cave assemblage.

5.6.2 Faunal responses to environmental change

5.6.2.1 Mid MIS 4

The portion of the Cathedral Cave fossil record investigated here commences at 65.8 ka ago (Figure 3.15), corresponding to a glacial peak, which preceded increased precipitation and warmer temperatures for the remainder of MIS 4 (Barrows et al., 2001; De Deckker et al., 2019; De Deckker et al., 2020). The Binjang mammal community responded with an increase in the number of taxa associated with temperate climate zones after the mid MIS 4 glacial peak. A drop in the number of temperate zone species, indicating colder and drier conditions, is evident in sublayer 13a at around 61.8 ka ago, prior to the transition into MIS 3 (Figure 5.6). Palaeoenvironmental records do not show a corresponding dry and cold phase near 61.8 ka ago. For example, aeolian dust flux at the core site of MD03-2607 had decreased to near pre-MIS 4 levels and fluvial discharge from the Darling Sub-basin showed only minor reduction from 65 ka ago (De Deckker et al., 2019). Lake levels in central Australia indicate that the interior remained wet through most of MIS 4 (Miller and Fogel, 2016; De Deckker et al., 2019; De Deckker et al., 2020). Therefore, the drier conditions at 61.8 ka ago, indicated by the species composition of the fossil assemblage, probably represents regional conditions.

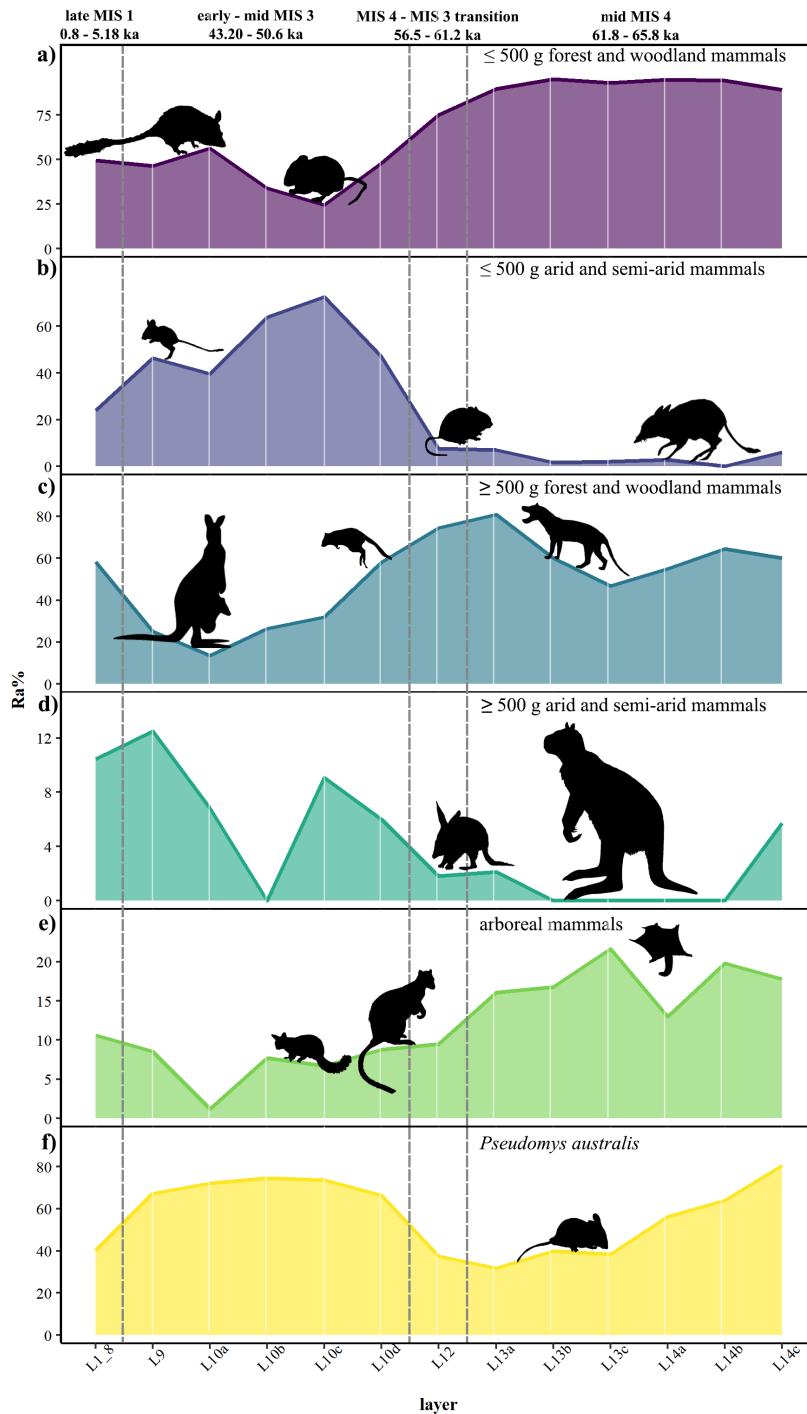


Figure 5.10. Relative abundances of mammal guilds, in which taxonomic units are assigned a single habitat association (either forest and woodland or arid and semi-arid). Taxonomic units with broad or inconclusive habitat associations have not been included. a) small mammals associated with forest or woodland with grassy or heath understorey. Ra% is calculated on relative abundance within the ≤ 500 g class after removal of *P. australis*. b) small mammals associated with arid or semi-arid habitats. Ra% is calculated on relative abundance within the ≤ 500 g class after removal of *P. australis*. c) large mammals associated with forest or woodland habitats with grassy or heath understorey. Ra% is calculated on relative abundance within the ≥ 500 g class. d) large mammals associated with arid or semi-arid habitats. Ra% is calculated on relative abundance within the ≥ 500 g class. e) Ra% of arboreal mammals, calculated after removal of *P. australis* but prior to division into size classes. f) *Pseudomys australis*. Ra% calculated prior to subdivision into size classes.

Such spatial variability is evident in hydrological records through MIS 3 (Kemp et al., 2019).

Biodiversity measurements, including species richness, diversity, and evenness, are low in sublayer 14c; evidently the glacial peak of MIS 4 did challenge the resilience of the mammal community, but recovery followed (Figure 5.4). Decreases in species richness in response to aridity have been recorded previously in late and mid Pleistocene small-mammal assemblages of the Naracoorte Caves (Macken et al., 2012) and in North America (Grayson, 1998;

Barnosky et al., 2004b). Therefore, reduced species richness in sublayer 14c, during the most glacial conditions of MIS 4, is not unexpected. However, declines in species richness have been

recorded in response to climatic warming over the Pleistocene to Holocene transition in North America (Blois et al., 2010) and to both LGM aridity and Holocene warming in south-west Europe (López-García et al., 2013). Thus, if these patterns are assumed to be solely due to climatic changes, then decreasing species richness appears to represent restructuring of mammal communities in response to changing environments, regardless of the direction of change.

Increasing biodiversity values for much of the remainder of MIS 4 shows that these impacts were not permanent, and the mammal community underwent a period of recovery through the remainder of layers 14 and 13 (Figure 5.4). As community evenness confers stability under environmental stress (Wittebolle et al., 2009; Blois et al., 2010), the evenness apparent in the assemblage at 61.8 ka ago characterises a community likely to have a high level of resistance to change (Figure 5.4). In contrast, small mammal communities at Naracoorte were stable during the LGM, but underwent significant variability in relative abundances and species richness within a few thousand years of warming that followed deglaciation (Macken and Reed, 2014).

During mid MIS 4, the local environment favoured species that show a preference for open forests and woodlands, with heath or grassy understorey (Figure 5.10a, 54c; Appendix D Table 7.16). The combined relative abundance of these small forest and woodland mammals is lower in sublayer 14c and then increases as aridity decreases (Figure 5.10a). This trend is marked for *P. novaehollandiae*, *P. gracilicaudatus*, *P. oralis* and *R. sp. cf. R. lutreolus* (Figure 5.7b), four species that today occupy relatively mesic habitats (Fox, 2008b; Kemper and Wilson, 2008; Townley, 2008; Woinarski et al., 2014) and are likely to be sensitive to drying conditions. *Pseudomys oralis* makes its final appearance in sublayer 13b (Figure 5.7b)

Mastacomys fuscus is also associated with more mesic environments, but the abundance peak of this species in sublayer 14c (Figure 5.7d) at first seems to contradict the evidence that sublayer 14c accumulated during a drier phase. Modern populations of *Mastacomys fuscus* require good vegetation cover and grasses in proximity to a watercourse (Happold, 2008; Woinarski et al., 2014). The modern course of the Bell River is less than 1 km west of the caves, and the larger Macquarie River is a little over 4 km to the north-east (Figure 2.3). The Macquarie River remained active through drier periods (Hesse et al., 2018), and the Bell River may well have too, and these would have facilitated suitable habitat for *M. fuscus*. Some species of owls are known to have home-ranges in the order of 6–12 km² (Kavanagh,

2002a), thus both watercourses would be within the hunting range of owls utilising Cathedral Cave. Even so, the reason behind such a prominent abundance peak remains unclear, but it seems probable that *M. fuscus* was relatively more abundant on the landscape during this drier period. The decline of *Pseudomys australis* after 65.8 ka ago (Figure 5.7f) is consistent with its modern associations with semi-arid and arid habitats (Watts and Aslin, 1981; Medlin, 2008). Other taxa known from open arid and semi-arid habitats, including *Notomys* sp. indet. (Figure 5.7c), *Dasyuroides byrnei* (Figure 5.7a) and *Lagorchestes leporides* (Figure 5.8c), appear intermittently through mid MIS 4 in low abundances, but have their highest MIS 4 abundances in sublayer 14c. *Osphranter rufus*, an inhabitant of open arid and semi-arid habitats (Croft and Clancy, 2008), appears in sublayer 14c (Figure 5.8a), thus also indicating drier conditions 65.8 ka ago.

Relative abundance trends for large mammals differ in some regards to those of their smaller counterparts. Similarly, large forest and woodland mammals, including *Thylacinus cynocephalus*, *Potorous tridactylus*, *Dasyurus maculatus* and *Macropus giganteus* (Figure 5.8b) are more abundant during mid MIS 4 than elsewhere in the excavation, and show a similar increase in combined relative abundance after 14c (Figure 5.10c). However, this group exhibits neither a strict increase through mid MIS 4 (followed by a decline in sublayer 13b), nor a similar decline in sublayer 13a, as seen in the small forest and woodland mammals (Figure 5.10a; 5.10c). There is no increase in the abundance of large arid and semi-arid mammals in sublayer 13b (Figure 5.10d), thus the decline of large forest and woodland mammals does not appear to indicate intermittent periods of increasing aridity through layer 13. Instead, it correlates with an increase in the abundance of more generalist taxa (e.g., *Tachyglossus aculeatus*, Figure 5.8a) and taxa with less informative or lesser known habitat preferences (e.g., *Dasyurus geoffroii* / *viverrinus*, Figure 5.8e; *Congruus kitcheneri* and *Baringa* sp. nov. 1, Figure 5.9).

Fossils of *Congruus kitcheneri* and *Baringa* sp. nov. 1 have previously been collected together from sites where a semi-arid habitat has been inferred (Prideaux et al., 2007b; Prideaux et al., 2010), but the ecology and distribution of these two species remain poorly established (G. Prideaux, pers comms). Being present in the Binjang region might imply that both species occupied a broader range of habitats. The majority of the megafauna species so far identified in Cathedral Cave have open forest and woodland associations, but some,

including *Procoptodon goliah*, *Sthenurus andersoni*, *S. atlas* and *Thylacoleo carnifex*, have distributions that include semi-arid regions (Appendix D Table 7.16).

During mid MIS 4, the region included treed habitats as shown by the abundance of arboreal and semi-arboreal taxa (Figure 5.10e), including *Conilurus albipes* (Figure 5.7c), *Petaurus breviceps* (Figure 5.7e), *Cercartetus nanus*, *Phascogale tapoatafa*, *Acrobates pygmaeus* (Figure 5.7f), *Baringa* sp. nov. 1, and *Congruus kitcheneri* (Figure 5.9). The habitat preferences of some of these taxa provide an insight into local vegetation types. *Acrobates pygmaeus*, present in layer 13, prefers tall eucalypt forests (Isaac et al., 2014; Harris, 2015). *Cercartetus nanus* is strongly associated with *Banksia* (Turner, 1985), a genus of large heath plants that does not feature strongly in remnant local vegetation today (Taylor et al., 2015). Eucalypt tall open forests can include *Banksia* and are restricted to regions with rainfall of 500–2000 mm per year (Table 5.3), thus placing a lower rainfall bound of 500 mm per year in the later portion of mid MIS 4.

Our fossil data suggests that during mid MIS 4, the vegetation around the caves was composed of open eucalypt forest and open eucalypt woodland, with heath and grassy understorey and riparian habitats occurring along the Bell and Macquarie Rivers. During the MIS 4 glacial peak, these environments were more open, and probably included tussock grassland as indicated by the increase in the numbers and population of open habitat taxa (Figure 5.6). These habitats all sit within an annual rainfall band of 200–2000, although most have an upper rainfall bound of 450–800 mm (Table 5.3). These vegetation structures resemble those which persists today within a 60 km radius of the Wellington Caves, including eucalypt woodlands with grassy or shrubby understorey, tussock grasslands, and mallee woodland with tussock grass understorey to the north (Department of the Department of Environment, 2012).

Table 5.3. Modern and prehistoric vegetation groups for the Binjang region during the late Pleistocene, based on the National Vegetation Information System (NVIS) Version 4.2 (<http://www.environment.gov.au/land/native-vegetation/national-vegetation-information-system/data-products>).

Major vegetation group	Major Vegetation Subgroups	Annual rainfall (mm)	Notes
3. Eucalypt open forests	4. Eucalyptus open forests with a shrubby understorey 5. Eucalyptus open forests with a grassy understorey 60. Eucalyptus tall open forests	500 - 2000	Includes <i>Banksia</i>
5. Eucalypt woodlands	8. Eucalyptus woodlands with a shrubby understorey 9. Eucalyptus woodlands with a tussock grass understorey 10. Eucalyptus woodlands with a hummock grass understorey 59. Eucalyptus woodlands with ferns, herbs, sedges, rushes or wet tussock grasslands 65. Eucalyptus woodlands with a chenopod or samphire understorey	200 - 800	Includes <i>Acacia</i> understorey
11. Eucalypt open woodlands	18. Eucalyptus low open woodlands with hummock grass 19. Eucalyptus low open woodlands with tussock grass 47. Eucalyptus open woodlands with shrubby understorey 48. Eucalyptus open woodlands with a grassy understorey 53. Eucalyptus low open woodlands with a shrubby understorey 56. Eucalyptus (+/-) low open woodlands with a chenopod or samphire understorey	200 - 450	Co-dominants can include <i>Acacia</i>
14. Mallee woodlands and shrublands	12. Mallee with hummock grass 29. Mallee with a dense shrubby understorey 55. Mallee with an open shrubby understorey 61. Mallee with a tussock grass understorey	200 – 500	
19. Tussock grasslands	34. Mitchell grass (<i>Astrebla</i>) tussock grasslands 35. Blue grass (<i>Dicanthium</i>) and tall bunch grass (<i>Vitiveria</i> syn: <i>Chrysopogon</i>) tussock grasslands 36. Temperate tussock grasslands 37. Other tussock grasslands	400 - 1000	
21. Other grasslands, herblands, sedgelands and rushlands	38. Wet tussock grassland with herbs, sedges or rushes, herblands or ferns 41. Saline or brackish sedgelands or grasslands 63. Sedgelands, rushes or reeds 64. Other grasslands		Associated with locally moist conditions created by high rainfall, near-surface groundwater and seepage or run-on from catchments

5.6.2.2 MIS 4–MIS 3 transition

Layer 12 accumulated 61.2–56.5 ka ago, during the transition between MIS 4 and MIS 3 (Figure 3.15). In a continental context, the transition represents a shift from colder, drier MIS 4 to warmer, wetter climatic conditions during MIS 3. Records of aeolian dust flux, terrestrial vegetation types, sea surface temperatures and foraminiferal assemblages from offshore South Australia had returned to or approached pre-MIS 4 levels (De Deckker et al., 2019). Central Australia remained relatively wet, as shown by high lake levels in the Willandra Lakes and high point-potential evapotranspiration (Miller and Fogel, 2016). In contrast to these records, fluvial discharge from the Darling River catchment (captured in core MD03-2607) decreased after 59 ka ago and disappeared by 57.3 ka ago (Bayon et al., 2017; De Deckker et al., 2019). Accordingly, effective rainfall was lower in the Darling River catchments, potentially including the Macquarie-Bogan catchment area in which the caves are located (for catchment map, see Herron et al., 2002, Fig 1.).

The Cathedral Cave fossil assemblage shows a continuation of the decline of temperate zone taxa that had commenced in sublayer 13a alongside an increase in taxa associated with the arid and semi-arid zones (Figure 5.6). These trajectories point to progressively drier conditions through the MIS 4–MIS 3 transition, although the sediment record shows at least one period of increased rainfall during this time with the formation of a flowstone (layer 11) band within the sequence sometime between 56.5–50 ka ago (Chapter 3). Some variable climatic conditions must have occurred within a trend of increasing aridity across the MIS 4–MIS 3 transition in Binjang. Species richness and diversity were high during the transition, despite some restructuring at both an assemblage and population level (Figure 5.4). Thus, the mammal community reshaped itself to meet its changing environment without suffering a loss of richness or diversity. This pattern contrasts with other studies that have revealed declining biodiversity indices during community restructuring (Grayson, 1998; Barnosky et al., 2004b; Blois et al., 2010; Macken et al., 2012; Lopes et al., 2013). However, species richness is also affected by habitat heterogeneity (Hadly and Barnosky, 2009). High species richness could reflect the presence of a mosaic habitats in proximity to the caves. Evenness is high as the assemblage is no longer dominated by a small number of taxa, including *Pseudomys novaehollandiae*, *P. australis* and *P. gracilicaudatus* (Figure 5.7c). Few fossil localities provide a well-dated record of faunal change through the MIS 4–MIS 3 transition. Tight Entrance Cave in Western Australia is one such locality and in contrast to this study, shows stable species richness until around 49 ka ago (Prideaux et al., 2010).

The relative abundance of open forest and woodland taxa reduced through the MIS 4–MIS 3 transition (Figure 5.10a, 54c). The decrease is driven primarily by taxa that lie at the more mesic end of the habitat scale, e.g., *Pseudomys novaehollandiae*, *Rattus* sp. cf. *R. lutreolus* and *Antechinus flavipes* continue to decline in abundance in layer 12 (Figure 5.7a, 51b). *Pseudomys gracilicaudatus*, a species often found in sympatry with *Rattus lutreolus* in heathland, dense wet heath and swamps (Haering and Fox, 1995; Fox, 2008b), is conspicuous in its absence after a relative abundance peak in sublayer 13a (Figure 5.7b). Together, the decline of these two taxa may indicate a decrease in riparian habitats.

The reduced relative abundance of arboreal taxa during the MIS 4–MIS 3 transition (Figure 5.10e) is consistent with vegetation change driven by lower precipitation. Of the tree dependent taxa, only *Conilurus albipes* (Figure 5.7b), *Petaurus breviceps* (Figure 5.7e), and *Congruus kitcheneri* (Figure 5.9) are present. Reduced precipitation in the Macquarie–Barwon catchment would facilitate a decrease in high precipitation habitats first, i.e., eucalypt open forests (Table 5.3), and an increase in woodland vegetation types requiring less available moisture. The absence of *Acrobates pygmaeus* from layer 13 points to a reduction in its preferred tall eucalypts (Isaac et al., 2014; Harris, 2015). *Petaurus breviceps* is broadly distributed through temperate, subtropical and tropical forest and woodland habitats today, where it feeds on gum from *Acacia* trees (Rowston et al., 2002). *Acacia*, a genus of flowering shrubs or trees, is common in woodland or shrubland communities where conditions become too dry for eucalypts (Groves, 1999). Terrestrial taxa add to this picture. *Onychogalea frenata*, also associated with *Acacia* (Evans and Gordon, 2008), makes its first appearance in layer 12 (Figure 5.8c). *Notamacropus dorsalis*, which is known to inhabit open forest with thick *Acacia* in the southern part of its modern distribution (Johnson, 2008b), also increases in abundance. *Acacia* probably formed a component of local vegetation structures at this time (Table 5.3).

There is little change over the transition in the combined abundance of arid and semi-arid mammals compared to sublayer 13a (Figure 5.10b, 54d). *Pseudomys australis* commences a minor increase in abundance as conditions became drier through the MIS 4–MIS 3 transition (Figure 5.10f). Several taxa associated with open, or grassland habitats show increases in layer 12. This includes *Aepyprymnus rufescens*, *Perameles gunnii* / *nasuta* and *Notamacropus agilis* (Figure 5.7d; Figure 5.8d). *Perameles gunnii* has more open habitat preferences than *P. nasuta* (Appendix D Table 7.16), therefore, additional work to separate

the craniodental remains of these two species could reveal an ecological signal. Of the two megafaunal species that appear in layer 12, the Pleistocene distribution of *Congruus kitcheneri* has been inadequately mapped, while *Simosthenurus pales* was widely distributed across southern, inland and eastern Australia (Prideaux, 2004; Figure 5.9, Appendix D Table 7.16).

The Cathedral Cave mammal community underwent some restructuring in response to the drier conditions initiated at the MIS 4–MIS 3 transition. Twenty-seven taxonomic units that are present during mid MIS 4 (including three unresolved morphospecies) do not appear in the assemblage during the transition (Table 5.2). It is too simplistic to point to this as high faunal turnover. All layers and sublayers are under-sampled, especially layer 12 (Figure 5.3). Turnover between stratigraphic partitions is generally high, i.e., a total of 55 taxonomic units appear in layers 14–13, but each sublayer contains a subset of just 36–25 of these (Table 5.2). Thus, not every stratigraphic partition has captured the full range of available taxa and additional sampling would increase the number of rare taxa shared between these layers and provide a more robust understanding of species turnover between stratigraphic units.

5.6.2.3 Early–mid MIS 3

Layers 10 and 9 accumulated 50.6–43.2 ka ago (Figure 3.15). Global palaeoclimate records show increasing variability through MIS 3 (Greenland Ice-core Project Members, 1993; Augustin et al., 2004; Huber et al., 2006; Jouzel et al., 2007), and spatial variability is evident in the Australian record for 49–40 ka ago (Kemp et al., 2019). Emu eggshell from central Australia demonstrates a shift to more arid vegetation types after 50 ka ago and decreasing lake levels from 43 ka ago (Cohen et al., 2015). Monsoon influenced regions underwent rapid drying from 48 ka ago (Kemp et al., 2019), as did Kati Thanda-Lake Eyre in central Australia (Cohen et al., 2015) and Willandra Lakes in north-west NSW (Bowler et al., 2012; De Deckker et al., 2020). Wetlands along the east coast of Australia also became drier at this time (Cadd et al., 2018; Kemp et al., 2019; Kemp et al., 2020). Closer to the caves, palaeochannels in the lower reaches of the Macquarie River became smaller during MIS 3 (Hesse et al., 2018). The chronology for this reduction is vague, but purportedly occurred sometime between 54 and 34 ka ago. In its reduced state, the 34 ka ago palaeochannel was 125 m wide, compared to the 25 m wide modern Macquarie River (Hesse et al., 2018). Thus, precipitation and temperature-driven runoff had decreased, but the river remained a substantial watercourse. Layer 10 is comprised mostly of coarse silts and fine sands

interpreted as the result of a drier, windier climate delivering more aeolian dust to the site (Figure 3.8). This record contrasts to the record from offshore South Australia that showed reduced aeolian dust flux (De Deckker et al., 2019).

Reorganisation of the community is manifested as increased relative abundances of species that inhabit the arid and semi-arid zones alongside declines in temperate zone taxa (Figure 5.6). Species richness continues to decline sharply at the bottom of layer 10, reaching levels lower than those apparent at 65.8 ka ago (Figure 5.4). This curve is closely mimicked by the biodiversity indices that show reduced diversity and evenness of the assemblage through layer 10, although these do not quite reach the same lows as sublayer 14a (Figure 5.4). Despite this, faunal turnover is not marked, with just ten species that were present in older sediments not appearing in layers 10–9; six of these had their last appearance prior to layer 12 (Table 5.2). In layer 9, species richness, diversity and evenness reflect some modest recovery (Figure 5.4).

In contrast to mid MIS 4, MIS 3 saw significant restructuring occurring between taxa from disparate ecological regions and the addition or increase of several arid and semi-arid zone specialists to the community (Table 5.2). Restructuring is particularly evident among the murines. Aridity adapted *Pseudomys australis* and *Notomys* sp. indet. (Figure 5.7c, 5.1f) show substantial increases. *Pseudomys desertor* (Figure 5.7c) makes its sole appearance in layer 10. This species is known mostly from spinifex hummock grasslands through the arid and semi-arid zones (Read et al., 1999) though it has been recorded in savannah woodland, shrubland and grassland habitats in Queensland (Kutt et al., 2004). The ecology of *P. gouldii*, that is also present in layer 10, (Figure 5.7a) is poorly known due to its extinction in the mid-1800s but most fossil and live specimens were collected from the arid and semi-arid zones (Woinarski et al., 2014). There is a corresponding reduction or loss of some of the less xeric elements of the murine assemblage e.g., *P. novaehollandiae* and *Rattus* sp. cf. *R. lutreolus* (Figure 5.7b).

Among the marsupials, two arid or semi-arid zone species appear exclusively in layer 10. *Macrotis lagotis* (Figure 5.8a) is known primarily from dry, open habitats that include grassland, dune fields, hummock grassland and *Acacia* shrubland (Johnson, 2008a). Late Pleistocene specimens of *Procoptodon goliah* (Figure 5.9) have been collected from locations considered to have been arid or semi-arid during their deposition (Prideaux et al., 2009). *Chaeropus ecaudatus* makes its first appearance in layer 10 (Figure 5.8a). Another poorly

known species due to its extinction after colonisation, *C. ecaudatus* is associated with semi-arid shrubland habitats (Travouillon et al., 2019). The arid and semi-arid zone species *Dasyuroides byrnei* appears intermittently through older sediments but is notably more abundant in layer 10 (Figure 5.7a). *Osphranter rufus* is also present in layer 10 (Figure 5.8a); it only otherwise occurs in sublayer 14c. Supporting a reduction in treed environments, arboreal and semi-arboreal taxa are present but are less abundant than during the MIS 4–MIS 3 transition (Figure 5.10e).

The most parsimonious explanation for this change is a shift in climatic conditions that were favourable to taxa with drier habitat requirements. Nonetheless, there is currently a paucity of terrestrial palaeoenvironmental records with direct relevance to the region that would provide an independent proxy for comparison. The difference in response to mid MIS 4, regarding the species with more xeric requirements, is surprising when considering the comparatively higher magnitude of the MIS 4 glacial peak (De Deckker et al., 2019). Being in proximity to the semi-arid zone boundary (Figure 2.1), restructuring at the taxonomic level may be a feature of Binjang mammal assemblages, with the ecosystem shifting along the ecotone between temperate and semi-arid biomes as climatic conditions change. Still, proximity does not explain why similar restructuring in the species composition of the assemblage was not evident during the MIS 4 glacial peak. Perhaps this conforms to findings at Naracoorte, where the mammals did not always follow consistent trends through comparable climatic changes (Prideaux et al., 2007a; Macken et al., 2012).

Also, worth noting in sublayer 10a is the sole appearance of *Wallabia bicolor* (Figure 5.8a). It is often considered an inhabitant of higher rainfall forests with dense understorey (Merchant, 2008b; Di Stefano et al., 2009) and has been used as such in palaeoecological reconstructions (Fraser and Wells, 2006). Recent range expansions of *W. bicolor* into dry and open environments tell that its association with more mesic habitats might describe an anthropogenically driven range contraction rather than its fundamental niche (Cooke, 2020).

In layer 9, small forest and woodland mammals show a slight decrease from sublayer 10a but are more abundant than in sublayers 10b and 10c (Figure 5.10a). Larger woodland mammals show a minor increase in their combined abundance since sublayer 10a (Figure 5.10c).

Arboreal taxa increase from sublayer 10a but are on par with the numbers present during the rest of layer 10 (Figure 5.10e). *Pseudomys australis* shows little change (Figure 5.10f). Thus, layer 9 likely represents a continuation of overall drier conditions that were on par with those

that occurred earlier in MIS 3. Layer 9 comprises of interbedded flowstones (Chapter 3), therefore, conditions above ground were intermittently wet enough to initiate infiltration of meteoric waters into the cave. The remainder of MIS 3, including the lead up to glacial MIS 2, is absent from the Cathedral Cave record due the accumulation hiatus between 43.2–5.8 ka ago (Figure 3.15).

5.6.2.4 MIS 1

Layers 8–1 accumulated between 5.81 and 0.8 ka ago. Across Australia, palaeoclimatic records show rainfall increased between 9 and 6 ka ago, followed by a period of rainfall variability and droughts (Williams et al., 2009; Petherick et al., 2013). Sediment cores from Little Llangothlin Lagoon, 400 km north-east of Wellington Caves, show conditions became drier after 6 ka ago (Woodward et al., 2014). The lower Macquarie River palaeochannels underwent a further reduction in size at 5.5 ka ago as river discharge fell (Hesse et al., 2018).

Despite the loss of the megafaunal taxa after MIS 3 (Figure 5.9), the mammal assemblage had returned to high levels of species richness and diversity by the mid to late Holocene (Figure 5.4). Although the number of taxa associated with temperate, and tropical associated taxa display a small increase alongside a small reduction in arid and semi-arid zone taxa, the distribution of these groups comes close to matching that of sublayer 14c (Figure 5.6). At a population level, increases are observed in the combined relative abundances of forest, woodland and arboreal mammals (Figure 5.10a, 5.10c, 5.10e). The most substantial increase is seen in the large forest and woodland mammals (Figure 5.10d), driven in part by a large increase in the abundance of *Aepyprymnus rufescens* (Figure 5.8d). This species remained common enough in the region to be considered a pest species by agriculturalists who hunted it to local extinction in the early 20th century (Short, 1998).

5.6.3 Megafaunal extinction implications

Of the eleven extinct megafaunal taxa identified within this study, seven appear in sediments that accumulated during MIS 3 (Figure 5.9). Poor sample sizes recovered from layers 12 and 9 might account for the appearance of just two taxa in these layers (Figure 5.3). This is a plausible cause for the low diversity of megafauna in layer 12, as layers 10 and 13 have a higher diversity and are better sampled (Figure 5.3; Figure 5.4). Taking the data at face value, the loss of megafaunal taxa between layers 10 and 9 suggests that the majority of these species disappeared from Binjang sometime between 50–45 ka ago. A handful persisted until at least 43.2 ka ago.

This pattern is consistent with the 51.2–39.8 ka ago extinction window proposed for human mediated extinction (Roberts et al., 2001) and also with records from south-west WA and Naracoorte Caves (Pate et al., 2002; Jankowski et al., 2016). The pattern is not consistent with extinction following sustained drying of the Murray–Darling Basin that occurred following 45 ka ago (Hocknull et al., 2020) as at Binjang, a shift to a drier environment appears to have occurred earlier. It does not follow the high faunal turnover revealed at sites above, or close to, the Tropic of Capricorn (Hocknull, 2005; Hocknull et al., 2007; Hocknull et al., 2020). Nor does it fit with a simultaneous extinction of Australia’s megafauna 42 ka ago, leading up to the Laschamps Excursion (Cooper et al., 2021). When viewed in the context of the disappearance of four taxa after layer 13, the successive loss could be fitted to staggered extinction model that is often promoted by advocates of a climate driven extinction event (e.g., Wroe and Field, 2006; Price et al., 2011; Wroe et al., 2013; Hocknull et al., 2020). In absence of an independent palaeoenvironmental proxy, or indeed any useful regional records, the only evidence that points to climatic changes in Binjang within MIS 3 is the Cathedral Cave fossil assemblage itself.

It should be said here that a pattern of staggered extinction does not have to be exclusively driven by climate and could also fit a human harvesting model where prey choice and accessibility could see susceptible species succumbing first. Indeed, some key characters of the assemblage trends do not fit with a climate extinction model. First, the majority of the extinct megafaunal taxa at Cathedral Cave have open woodland habitat preferences that are concordant to the majority of other taxa identified in the assemblage (Appendix D Table 7.16). The majority of these taxa, that are not megafaunal, remain present throughout the excavation, with many remaining extant until European colonisation (Burbidge et al., 2009; Taylor et al., 2015). Taxa that are abundant through MIS 4 and disappear sometime around the transition into MIS 3 include some of the more mesic adapted members of the assemblage i.e., *Pseudomys oralis* and *P. gracilicaudatus* (Appendix D Table 7.16). None of the megafauna identified here are known to have especially mesic associations and several, including *Thylacoleo carnifex*, *Sthenurus andersoni*, *S. atlas* and *Procoptodon goliath*, were also distributed through the semi-arid zone (Prideaux, 2004; Prideaux et al., 2007b; Prideaux et al., 2009). These arid-adapted taxa should not have been disproportionately affected by a drying phase at Wellington. It is true that in modern terrestrial mammals, body size is an important indicator of response to rapid climate change (McCain and King, 2014), yet not all of Binjang’s large mammals became extinct.

If it is assumed that these larger animals were impacted by a climatic disturbance similar to their small-bodied counterparts, then it could be expected that likewise, they would respond with fluctuations in numbers, some replacement with more xeric taxa, and faunal turnover would be low. However, this is not what the record reveals. A climate-driven loss of the megafaunal taxa in Binjang during MIS 3 is at odds with our other faunal data that shows the region maintained the majority of its small to medium sized, temperate zone taxa, as well as retaining a suite of macropodids (Figure 5.7; Figure 5.8). Work is already underway to establish a fossil-pollen based vegetation record from sediment samples taken during the FU excavation. This record will be critical to further investigation of the scale of environmental change in Binjang, and to provide an independent proxy against which to test extinction scenarios against.

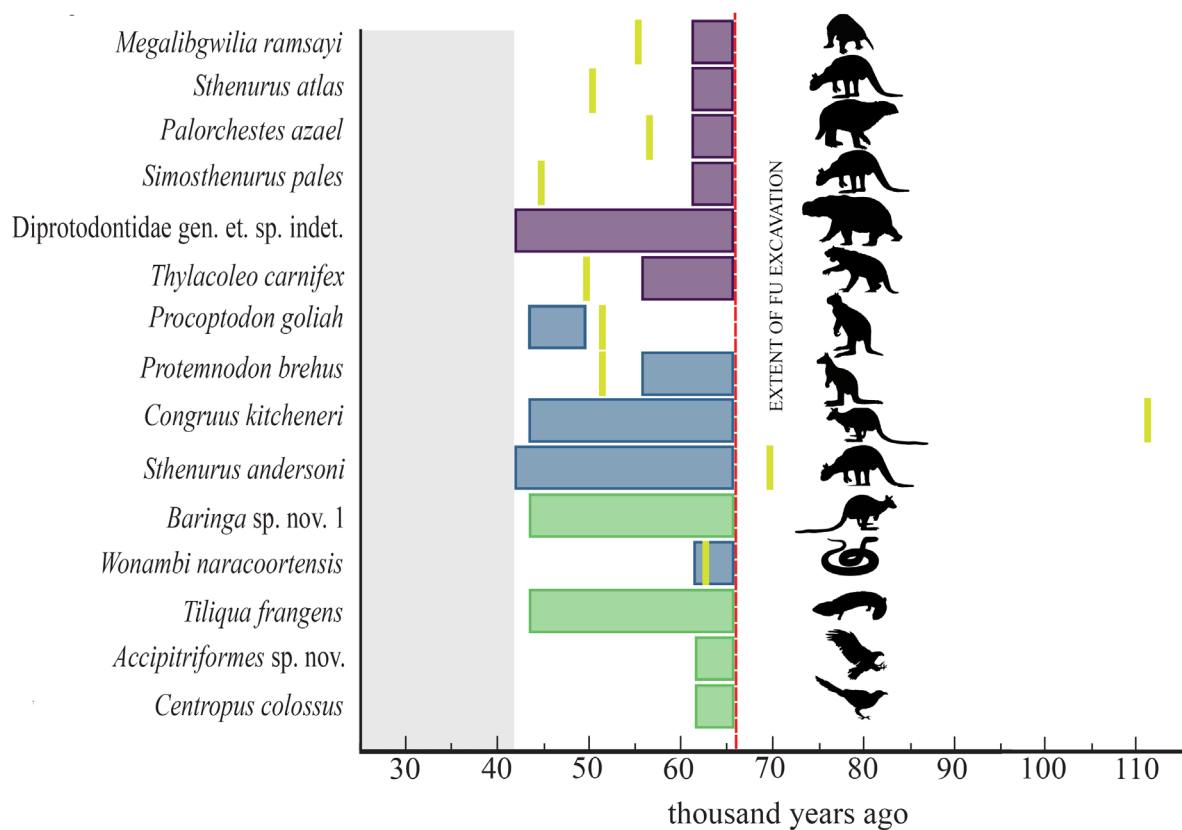


Figure 5.11. Megafauna of Cathedral Cave and other non-mammalian taxa of interest. Purple bars are taxa that appear in Cathedral Cave within their known temporal distribution. Blue bars represent taxa that appear in Cathedral Cave after their last known reliably dated occurrence outside of Cathedral Cave. Age range is based on the age-range of layers from which each taxon has been identified in. Green bars are taxa that have no prior ages. Yellow bars represent youngest fossil occurrence of each taxa, with ages taken from A* and A rated dates in the FosSahul 2.0 database (Peters et al., 2019). No youngest occurrence date is given for Diprotodontidae gen. et. sp. indet. Red line shows the current oldest extent of the FU excavation. Grey shading represents the start of the 37 ka hiatus in Cathedral Cave.

Cathedral Cave yields ages for five megafaunal taxa that are more recent than the youngest reliably dated remains of these species (Figure 5.11) that are listed in the database FosSahul 2.0 (Peters et al., 2019) and use the quality criteria established by Rodríguez-Rey et al. (2015). For some of the megafauna, the Cathedral Cave record extends their temporal range, showing that these taxa did indeed overlap with humans. *Procoptodon goliah* and *Protemnodon brehus* were present at Wellington between 50.6 and 44.7 ka ago. The youngest reliable ages for both these taxa previously are 52 ka ago at Lake Victoria (Roberts et al., 2001). *Sthenurus andersoni* was present at Wellington until at least 45.1–43.2 ka ago, whereas its previous youngest reliably dated occurrence was 70 ka ago in the Grant Hall deposit of Victoria Fossil Cave, Naracoorte (Macken et al., 2012). The youngest dated remains of *Congruus kitcheneri* are 112 ka from Tight Entrance Cave in Western Australia (Prideaux et al., 2010). The Cathedral Cave record extends this to 50.6–44.7 ka. *Baringa* sp. nov. 1 is brought forward from an estimated 400–200 ka ago in the Thylacoleo Caves, Western Australia (Prideaux et al., 2007b), to 50.6–44.7 ka ago. *Palorchestes azael* fossils aged 56 ka are known from Scotchtown Cave in Tasmania, but its youngest reliably dated mainland occurrence, outside of Cathedral Cave, is 257 ka, at Naracoorte (Prideaux et al., 2007a; Turney et al., 2008). The youngest record for *Thylacoleo carnifex* is 50 ka, at Black Creek Swamp on Kangaroo Island (Grün et al., 2008). Cathedral Cave could represent its youngest reliably dated occurrence as its remains were retrieved from a depth that is estimated to be 48.8 ka in layer 10 (Appendix C Table 7.9).

Among the non-mammal taxa, the youngest reliably dated remains of the extinct matdsoiid snake *Wonambi naracoortensis* hail from Mammoth Cave in Western Australia, where it has been dated at 63 ka (Roberts et al., 2001). It is present in Cathedral Cave between 65.8–61.8 ka ago. For *Baringa* sp. indet, and the non-mammalian taxa, *Tiliqua frangens*, *Accipitriformes* sp. nov. and *Centropus colossus*, Cathedral Cave represents their first, and currently only, dated occurrence (Figure 5.11). These examples underline the large gaps that persist in Australia's fossil record and caution that extinction timelines, currently used to model extinction causes, are far from adequate.

As discussed earlier, there is no established chronology of human arrival in the Binjang region, although a minimum date of 46 ka ago might be extrapolated from the Willandra Lakes record, some 560 km west of Wellington Caves (Bowler et al., 2003; Bowler et al., 2012). Thus, it is entirely possible that humans were present in Binjang during MIS 3, and if

so, were undoubtedly harvesting the region's resources and modifying the landscape. No evidence of human impacts has been identified in this study, however, finding archaeological evidence was not an expectation. The new chronology for Cathedral Cave presented in this study, places the Binjang megafauna into an overlap with human occupation of western NSW (Bowler et al., 2003; Westaway et al., 2017). Thus, the impacts of human harvesting, or landscape modifications, cannot be ruled out.

5.7 Conclusion

The Cathedral Cave fossil assemblage provides a record of late Pleistocene mammals at a resolution that is unmatched by other localities in Australia. This record reveals that late Pleistocene mammal community in Binjang was primarily, but not exclusively, composed of open forest and woodland taxa that are typical of the temperate climate zone of Australia. The assemblage also contains a smaller portion of taxa that are associated with the arid or semi-arid climate zones. The relative proportions of these groups underwent subtle fluctuations in response to changing environmental conditions during MIS 4. Biodiversity indices show that the richness, diversity, and evenness of the community were lower at around 65.8 ka ago than during the rest of MIS 4. This corresponds to cold, dry conditions that occurred during MIS 4 and peaked at 65 ka ago. The changing indices reveal that the diversity of the mammal community was reduced during the colder drier period but increased through MIS 4. During MIS 3, the community underwent a second, and greater, phase of restructuring. The temperate component of the small–medium members of assemblage remained dominant through this period. The majority of these smaller-bodied taxa responded by altering their relative abundance and only a small number of species, mostly with more mesic associations, became absent. These were replaced by taxa with xeric associations, indicating that Binjang had become drier between 50.6–44.7 ka ago. The second phase of restructuring occurred in the absence of palaeoenvironmental records that show a trend toward more arid conditions in central-eastern Australia across this time.

Megafaunal trends do not follow those of the smaller bodied mammals, with the majority of the megafaunal taxa having disappeared from the Cathedral Cave fossil record by 45 ka ago. A small number, including aridity adapted species, persisted at least until 43.2 ka ago. This pattern is consistent with other fossil localities from south and south-west Australia and not with those indicated for sites that lie above, or closer to, the Tropic of Capricorn. The Cathedral Cave fossil record extends the temporal range of at least nine megafaunal taxa,

placing more species into a potential overlap with humans. For four of these taxa, this represents their first, and only, dated occurrence. These findings exemplify the incomplete state of Australia's fossil record and show that extinction timelines that are currently used to model extinction causes, are far from sufficient.

Highlighted in this study is the different responses of the mammal community during MIS 4 and MIS 3, with little faunal turnover occurring at the middle of MIS 4, when conditions were glacial. During MIS 3, this response was elevated, although there are no palaeoenvironmental records that could give further insight into the local environment at the time. However, only a few of the small-medium mammals did not survive locally into the Holocene, which is in stark contrast to the megafaunal taxa. A climate-driven loss of these larger animals in Binjang during MIS 3 does not fit with the faunal trends shown by the smaller-bodied mammals, or with palaeoclimate records.

6 Chapter 6: General discussion and overview

6.1 Introduction and aims

The overarching aim addressed in this project was to investigate how the mammalian fauna of central-eastern Australia responded to late Pleistocene environmental change. This aim was achieved by:

1. Planning and executing a palaeontological excavation in Cathedral Cave (Chapter 2).
2. Interpreting the stratigraphy and depositional history of the Cathedral Cave deposit using sedimentary and geochemical data (Chapter 3).
3. Testing and updating the preceding chronology for Cathedral Cave with a new series of ages, obtained via radiocarbon dating and optically stimulated luminescence dating (Chapter 3).
4. Determining the species composition of the fossil assemblage (Chapter 4).
5. Interpreting changes in the composition of the faunal assemblage in relation to the depositional history and revised chronology of the deposit, and in the context of other published palaeoenvironmental and fauna records (Chapter 5).
6. Considering contemporary conservation implications of the Cathedral Cave fossil record (Chapter 6).

In this chapter, I: 1) discuss the key findings of the preceding chapters, in which aims 1–5 have been addressed; 2) report on the final aim, to examine the contemporary conservation implications of this study; 3) consider significant finds among the non-mammalian taxa; and 4) show how this study has progressed our knowledge and make suggestions for future directions.

6.2 The chronology and sedimentology of Cathedral Cave

Earlier attempts to use radiocarbon dating in Cathedral Cave indicated that the sediments had accumulated through late MIS 3 – 1, incorporating the glacial of MIS 2 (Dawson and Augee, 1997). This scenario suggested that megafaunal taxa had persisted in Binjang until at least 17 ka ago. The timing is not congruent with our current understanding of megafaunal extinctions across Australia (Roberts et al., 2001; Prideaux et al., 2010; Jankowski et al., 2016; Hocknull et al., 2020), underlining the need to revisit the chronology.

From the outset of this project, re-examining the chronology was a key aim, alongside gaining a more complete picture of the sedimentology and therewith any reworking or transport that might have occurred. By combining sedimentology, geochemistry, taphonomy, radiocarbon and OSL dating, a clearer picture from inside the cave emerged (Figure 3.15). This picture is detailed in Chapter 3. At 4.2 m deep, the fossiliferous sediments were aged 65.8 ka. At shallower depths, the sediments had accumulated mostly sequentially through time until 43.2 ka ago, when the cave roof entrance closed, and deposition paused for the next 37.4 ka. This contrasts with the earlier radiocarbon chronology that placed the deposit at 14.3 ka at around 5 m deep and did not detect a depositional hiatus. Instead of being primarily a LGM assemblage *sensu* Dawson and Augee (1997), accumulation had been active in the lead up to, and through the megafauna extinction window. What is remarkable is that aside from the Holocene layers, the cave has captured nearly 23 ka in a sequence of the deposit that spans around 4 m deep. If a constant sedimentation rate is assumed, this equates to nearly 6 ka per metre; a resolution that is unmatched among other Australian fossil sites.

Reconstructing the depositional environment of the Cathedral Cave deposit was a critical step in understanding the timeline and context of the fossils used in the palaeoecological analysis that forms part of this thesis. The work clearly establishes the significance of the infill deposit of Cathedral Cave, allowing it to be robustly anchored on the timeline of Australian palaeontology. It is revealed to be one of just a small number of Australian localities, and the sole example in central-eastern Australia, that provides a faunal record of the lead up to and through the megafaunal extinction interval.

6.3 The fossil fauna of Cathedral Cave

The systematic palaeontology of Cathedral Cave is detailed in Chapter 4. Gaining a clear image of the species composition of the assemblage was critical to the aims of this project, allowing accurate characterisation of the fauna by ecological and physical traits, e.g., habitat type and body-size. Earlier work in Cathedral Cave had identified a potential 53 species of mammals, although many of these had been identified to genus level only, and the small mammals had received limited attention (Dun, 1893; Flannery and Szalay, 1982; Blanford, 1985; Hodge, 1991; Dawson and Augee, 1997). The earlier collections were not suited to reanalysis as material from individual spits had been pooled and the collection was no longer complete. During the Flinders University excavation, at least 66 species of mammals were collected and identified, bringing the total number of mammals so far identified from

Cathedral Cave to 69 species (Table 5.2). Cathedral Cave is now known to hold the richest late Pleistocene mammal assemblage in Australia. Eleven of the mammals collected by the FU excavation are extinct megafaunal species. Identifications were assigned to over 21,000 individual specimens during the course of this project, thereby compiling a large and important collection of late Pleistocene vertebrates. Several non-mammalian taxa were also identified. These are included in Appendix D Table 7.13, but several of interest are discussed in more detail here.

Among the reptile fossils are vertebrae belonging to the extinct megafaunal madtsoiid snake *Wonambi naracoortensis*. *Wonambi* fossils are not numerous in the other fossil sites at Wellington and have vague provenance (Scanlon, 1995). The FU collection represents, the first *Wonambi* fossils collected from Wellington Caves with detailed provenance and places this taxon on the landscape in Binjang during mid to late MIS 4. Also of interest, are numerous fossil bones from a large shingleback skink, *Tiliqua frangens*, collected during the excavation. Fossils from this taxon have been redescribed as part of Kailah Thorn's PhD study on fossil skinks (Thorn, 2019), and has involved reassessment of two enigmatic fossils collected from heaps of sediment removed from the cave infill deposits of Wellington Caves during tourism development, hitherto thought to be Pliocene aged (Hutchinson and Scanlon, 2009; Čerňanský and Hutchinson, 2013). These new examples show that *T. frangens* was part of the Binjang fauna 65.8–44.7 ka ago, thus the first two fossils of this species collected earlier from the spoil heaps had probably come from Pleistocene sediments rather than Pliocene.

The excavation has yielded significant bird fossils. A right carpometacarpus belonging to an undescribed large species of Accipitriformes is being studied and described as part of Ellen Mather's PhD study on Australian fossil birds of this order. The carpometacarpus is the first fossil from this species to be placed within a dated chronology. Likewise, a left humerus of the giant cuckoo *Centropus colossus* is the first dated remains of the taxon to extend its temporal distribution into the late Pleistocene. *Centropus colossus* is only otherwise known from Green Waterhole Cave in south-east South Australia (Shute et al., 2016). The radius of an extinct megapode, *Latagallina naracoortensis*, has been provisionally identified by Trevor Worthy and I from bulk unidentified material from phase 1 sediments of the UNSW excavation.

6.4 Tracking mammalian faunal change

Chapter 5 addresses the overarching aim of this project, investigating how the late Pleistocene fauna in central-eastern Australia responded to changes in its environment. The work in this chapter is focused on using the fossil assemblage from Cathedral Cave to interpret changes in the composition of the faunal assemblage and uses the chronology and depositional framework (Chapter 3), alongside the palaeontological systematics (Chapter 4), to explore faunal change through the 4.2 m deep stratified sediments. Although other palaeoecological studies have looked at Australian late Quaternary fossil assemblages (e.g., Hocknull et al., 2007; Prideaux et al., 2007b; Prideaux et al., 2007a; Prideaux et al., 2010; Macken et al., 2012; McDowell, 2013; Macken and Reed, 2014; Hocknull et al., 2020), this study is unique. None of these other studies report faunal assemblages that match the temporal resolution or faunal diversity of Cathedral Cave, none were able to track megafaunal persistence through time alongside such a high diversity and abundance of smaller-bodied taxa into the megafaunal extinction window, and none are from central-eastern Australia.

Changes in taxonomic restructuring, species richness, diversity, evenness and relative abundances, reveal that the late Pleistocene mammal community of Binjang was typical of a temperate open forest and woodland community with xeric elements becoming more abundant during colder and drier periods (Figure 5.6). This community did not undergo major restructuring during MIS 4, but faunal turnover and loss was higher during MIS 3, with losses mostly confined to megafaunal taxa. Only a few of the more mesic of the small bodied species did not persist into the Holocene. The discordant trends between megafaunal and smaller bodied taxa may indicate that these faunal size classes were subjected to different drivers, or that the same driver affected both unequally. A model for this is seen in western USA where climate change impacted small mammals at lower trophic levels whereas anthropogenic impacts were seen first in the larger mammals occupying higher trophic levels (Barnosky et al., 2004b). However, large gaps remain in our understanding of how modern faunal communities, let alone palaeocommunities, respond to environmental change.

Biodiversity indices of richness, evenness and diversity were more reduced during MIS 3 than MIS 4 (Figure 5.4). There was a subtle increase in the number of taxa associated with xeric habitats but more significant was that the majority of the small–medium mammals displayed changes in their relative abundances. Turnover for non-megafaunal taxa was higher

in Binjang than at Naracoorte Caves (Macken and Reed, 2014) but less than that from sites above or near the Tropic of Capricorn (Hocknull, 2005; Hocknull et al., 2007), which lack the resolution available in Cathedral Cave and the more southern sites.

The changes in the assemblage composition and relative abundances of the Binjang mammals during MIS 3 are not associated with changes detected in palaeoenvironmental records that are directly relevant to the Binjang region (e.g., Cohen et al., 2015; Kemp et al., 2019). However, the assemblage composition suggests that regional conditions became drier over the transition between MIS 4 – MIS 3 (Figure 5.10), with these conditions continuing through to at least mid MIS 3. This in itself is an interesting finding and establishing local palaeoclimate records will be a key step in further elucidating these trends. The latter part of MIS 3 (after 43.2 ka ago) is missing from the Cathedral Cave record, precluding the ability to track how the community responded following the reduction in biodiversity and faunal turnover evident during late to mid MIS 3. Although the nature of the faunal turnover indicates a drier environment, MIS 3 also represents the probable commencement of anthropogenic impacts. Both climatic and anthropogenic factors may have driven environmental change in Binjang.

6.4.1 Megafaunal trends

This work provides new insight for megafaunal taxa. Of the eleven extinct megafaunal taxa that appear in the excavation, most of these disappeared from Binjang sometime between 50 and 45 ka ago. A small number persisted until at least 43.2 ka ago (Figure 5.9, Figure 5.11). This timeline fits well with that indicated for human mediated extinction (Roberts et al., 2001), especially records from south-west WA and Naracoorte Caves (Pate et al., 2002; Jankowski et al., 2016) and contrasts with that found above the Tropic of Capricorn where increasing aridity is the inferred extinction cause (Hocknull et al., 2020). As stated earlier, the loss of the Cathedral Cave megafauna does not fit well with major climatic changes indicated in palaeoclimate records and the only indicator of a drier environment in Binjang during MIS 3 is relatively subtle changes in the composition of the fossil assemblage itself. A climate driven extinction model does not explain the discrepancies between the megafaunal taxa and their smaller bodied counterparts, with most of the latter persisting locally into the Holocene. Investigating sediments deeper than those currently excavated will be key to understanding how the cold, dry middle of MIS 4 shaped the mammal community and the extent to which it was able to recover — in terms of richness and biodiversity — prior to the environmental

changes of MIS 3. The Cathedral Cave deposit does not contain cultural artefacts or bones modified in the manner expected of human harvesting, however, given the cave morphology, it is unlikely that the main chamber would have been used as a shelter by people. This means that the cave is not expected to provide direct evidence of human interactions with megafauna. The region is devoid of known Pleistocene aged archaeological sites that might confirm the date of human occupation in it, but people had reached Warraty Rock Shelter in the arid interior of southern Australia by 49 ka (Hamm et al., 2016; Figure 5.1) and were inhabiting the semi-arid Willandra Lakes region by 46 ka ago (Bowler et al., 2003; Bowler et al., 2012; Figure 5.1). It is therefore likely that there was a temporal overlap between humans and megafauna in Binjang.

For five megafaunal taxa identified during this study, their occurrence in Cathedral Cave is now their youngest reliably dated occurrence in Australia (Figure 5.11). For *Procoptodon goliah* and *Protemnodon brehus*, this work extends their temporal range some 2–6 ka from their hitherto youngest occurrence at Lake Victoria 52 ka ago (Roberts et al., 2001). *Sthenurus andersoni* is shown to have persisted nearly 30 ka longer than previously known (Macken et al., 2012). The temporal range of *Congruus kitcheneri* has been extended more recently by over 50 ka (Prideaux et al., 2010) and for *Baringa* sp. nov. 1, this extension is estimated to be in the range of 350–150 ka (Prideaux et al., 2007b). For *Baringa* sp. nov. and the non-mammalian taxa, *Tiliqua frangens*, Accipitriformes sp. nov. and *Centropus colossus*, this work provides their first, and currently only, tightly dated occurrence. For many of Australia's megafaunal taxa, the timing of their demise remains uncertain. This work brings more clarity to extinction timelines and brings an increasing number of megafaunal taxa into an overlap with human occupation of Australia. The extended temporal range of *Baringa* sp. nov. is an example that illustrates the large gaps that remain in Australia's fossil record, and it is unlikely to be the only instance. The findings of this study clearly show that current extinction chronologies being used to infer extinction causes are inadequate.

6.5 Conservation implications

Vertebrate fossil assemblages are valuable for elucidating ecosystem structures and interactions, as well as being a proxy for climatic and habitat conditions (Macken et al., 2012; McDowell, 2014). However, in Australia, few fossil localities are known that contain the necessary faunal and temporal resolution for detailed palaeoecological time-series analyses. As well as this, more often than not, the lens of late Quaternary palaeontology is focused on

the charismatic extinct megafaunal taxa rather than the palaeoecologically informative smaller bodied taxa. Predictably, the palaeoecological record in Australia remains understudied. However, it has never been more important and relevant than now to look to the past to increase our understanding of how our biota responds to changing environments.

6.5.1 Small mammal resilience to environmental change

The increasing biodiversity of the Binjang mammal community following the glacial conditions at 65 ka ago indicate that this community was able to recover and persist through climate cycling (Figure 5.4). Diminished biodiversity, such as that which followed European colonisation, reduces the capacity of ecosystems to respond and adapt (Wittebolle et al., 2009; Blois et al., 2010). If a healthy landscape, functioning ecosystems and biodiversity are seen as providing protection to the effects of environmental change, then our fragmented contemporary landscapes with their depauperate faunas have lost much of this buffer and are increasingly vulnerable. This study finds agreeance with earlier work finding that small mammal faunas remained relatively unchanged through the late Quaternary (Prideaux et al., 2007a; Macken et al., 2012; McDowell, 2013), however, it is dangerous to assume that this stability can still be expected of our now diminished faunas existing in anthropogenically modified landscapes.

6.5.2 Pre-European Mammalian baseline

The MIS 1 record from Cathedral Cave is most useful as an indicator of the mammal species likely present in Binjang at the time that it was colonised by Europeans. Holocene fossil assemblages are proving valuable for conservation management by establishing faunal baselines, elucidating patterns of extinction, and identifying candidate species for reintroductions (McDowell, 2014; Fusco et al., 2016). As European colonisers, and their introduced animals, spread across Australia after 1788, the landscape and its ecosystems were radically changed (Woinarski et al., 2015a). In many regions, change transpired before the systematic surveying of flora and fauna, thus leaving the original pre-colonisation fauna poorly documented (Fusco et al., 2017b). Agriculturalisation was rapid around Wellington, with pastoral occupation commenced in the Macquarie Valley by 1825 (Perry, 1955; Taylor et al., 2015). By 1840, much of the land adjoining its rivers was occupied by squatters. Grazing and cereal cropping was widespread in the area by the 1860s, resulting in clearing and degradation of the natural environment. Later, the local fauna was further decimated by

government bounties and wildlife drives that were aimed at protecting crops (Taylor et al., 2015).

The Dubbo Field Naturalist & Conservation Society lists 29 non-flying native mammals as having been present locally after European colonisation, including seven that no longer occur there (Taylor et al., 2015). The remains of all but two of the 29, *Ornithorhynchus anatinus*, and *Petaurus norfolcensis*, have been identified in the sediments of Cathedral Cave (Table 5.2). This assemblage also provides Holocene records for a number of taxa additional to those reported by the Dubbo Field Naturalist & Conservation Society. These are *Chaeropus ecaudatus*, *Isodon obesulus*, *Perameles gunnii/nasuta*, *Bettongia lesueur*, *Potorous tridactylus*, *Notamacropus dorsalis*, *Notamacropus parma*, *Onychogalea lunata*, *Mastacomys fuscus*, *Notomys* sp. 1., *Pseudomys australis*, *Pseudomys desertor*, *Pseudomys gouldii*, *Pseudomys gracilicaudatus*, *Rattus fuscipes* and *Rattus* sp. cf. *tunneyi*; all were possibly present in Binjang at the time that Europeans arrived (Table 5.2). If so, then at least 23 non-flying mammal species were lost to the region during the Holocene. Evidently, the effects of European colonisation have been far more severe here than previously thought. The revised list of pre-colonisation mammals for the region provides a new faunal baseline that may be of use to conservation initiatives seeking to restore the regional native fauna and for studies seeking to better understand the region's ecosystems.

6.5.3 Implications for a vulnerable native rodent

The Cathedral Cave record offers an insight into the biogeography of the rodent *Pseudomys oralis* (Hastings River Mouse). This species no longer inhabits the region today, being found only in fragmented populations in north-east NSW and far south-east QLD (Pyke and Read, 2002; Bilney et al., 2010; Woinarski et al., 2015b). The fossil record reveals its former distribution was much wider. Between 17 and 0.15 ka, the species inhabited a range that included eastern Victoria to south-east Queensland. The species underwent a large range contraction and is now listed as vulnerable to extinction by the IUCN but is considered Endangered under the Environment Protection and Biodiversity Conservation Act 1999. The species is rare overall in the Cathedral Cave assemblage, but its record there shows that its late Pleistocene range was even broader and may suggest that it has been contracting since at least MIS 4 (Figure 5.7b). This could suggest that *P. oralis* is stenotopic, or at least particularly sensitive to changes driven by drying conditions. It has been suggested that *P. oralis* may be adapted to stable environments, and therefore more vulnerable to change

(Townley, 2000). This hypothesis has been challenged in studies examining the impacts of logging disturbance on this species (Meek et al., 2003; Law et al., 2016), but the question of increased vulnerability to climate change remains. This may have implications for conservation planning for this species.

6.6 Future directions

During this project, several new avenues for future research were identified. As detailed earlier in this thesis, the palaeontological archives of the Wellington Caves are remarkably underexploited given the potential and significance of this location. The geology and stratigraphy of the Wellington Caves has been the subject of published and unpublished studies that largely looked at the exposed beds in the Phosphate Mine (Frank, 1971; Osborne, 1982; Hodge, 1991; Dawson and Augee, 1997; Osborne, 1997; Nipperess, 2002; Bell, 2004). Many key questions remain unresolved, including the origin and depositional history of the infill sediments and the bones they contain (Osborne, 2001). All the fossil sites (excluding Cathedral Cave) have only vague biochronological dates (Dawson, 1985; Dawson, 1995; Nipperess, 2002; Bell, 2004). Species assemblages reported from Big Sink, the Phosphate Mine complex and Mitchell Cave require updating and revision in line with modern taxonomy. The overall picture for Wellington Caves contains major gaps in our knowledge of its fauna, stratigraphy, taphonomy and chronology. There is little synthesis of how the age and the complex stratigraphy relate between sites in the Wellington Caves. Many words could be written here on the ample opportunity and need for further research across this cave system, but instead, this section is focused on that which directly relates to Cathedral Cave and the general palaeoecological research theme.

6.6.1 Extending the record

The Cathedral Cave record detailed here presently ends at 65.8 ka and appears to capture faunal response to an increase in warmer, wetter conditions that followed the colder, drier climate of mid MIS 4. Tracking the assemblage further back in time will allow insight into how the faunal community responded through the environmental changes of multiple marine isotope stages. Of particular interest is whether or not the community was characterised by a similar level of biodiversity and richness prior to mid MIS 4 as in layer 12, and if the composition of the assemblage was altered. This may elucidate whether mammal communities underwent progressive reshaping during climatic variability, such as that experienced during the late Pleistocene. This will enable testing of hypotheses related to

legacy effects of ongoing climate cycles and variability (e.g., Wroe and Field, 2006; Price et al., 2011; Wroe et al., 2013; Hocknull et al., 2020). The excavation has already been deepened by 0.8 m, with the unprocessed sediments currently in storage at Flinders University awaiting further work. If the age by depth relationship remains consistent, then this will extend the record back to the start of MIS 4. OSL and sedimentary samples have been collected for this section and are being analysed by Lee Arnold (University of Adelaide). The FU excavation has reached a depth of 5 m into the 10.5 m deep sediment floor of Cathedral Cave (Ramsay, 1882). This depth of sediment provides ample opportunity to expand the record deeper and further back in time.

The 37 ka hiatus between late MIS 3 to mid MIS 1 is an untimely interruption to the Cathedral Cave record, however, a nearby cave may provide an opportunity to bridge some of this gap. Douglas Cave is located on private land about 30 km from the Wellington Caves. Two pits have been excavated in different locations within the cave, and show that accumulation commenced 29.2 – 24.1 ka ago (Frank, 1969). The presence of large extant kangaroo species and absence of extinct megafaunal species in the deposit (Gorter, 1977) confirms that the sediments probably accumulated subsequent to the extinction interval. The highly informative small fauna from the excavation has been only partially explored. Applying modern, improved dating methods to this cave would refine the temporal span. Re-examination of existing material from Douglas Cave that is held in the National Mineral & Fossil Collection at Geoscience Australia, perhaps supplemented by further collections from the cave, will extend the faunal and palaeoecological record for Binjang.

6.6.2 Future approaches

The lack of useful regional palaeoenvironmental records for Binjang and surrounds leaves a vital question unresolved — that of the nature and scale of environmental changes during MIS 3. This gap in knowledge is clearly established in Chapter 5. An integrated approach that combines faunal data with sediment-related proxies may better elucidate the scale and type of environmental change that occurred in Binjang, as well as its impacts and legacy. This type of approach has been used successfully at Hall's Cave, Texas, and includes analysis of: faunal assemblages (Toomey, 1993; Toomey et al., 1993); species interactions (Smith et al., 2016); $\delta^{13}\text{C}$ and $\delta^{15}\text{N}$ isotopes of bone collagen and changes in body size (Tomé et al., 2020); pollen, phytoliths, spores and magnetic susceptibility (Ellwood and Gose, 2006; Cordova and Johnson, 2019). Additional complementary approaches that could be applied at Cathedral

Cave include dental microwear to establish diet (Arman et al., 2019), $\delta^{18}\text{O}$ records from speleothems to determine hydroclimate (Markowska et al., 2020), and sediment micromorphology to better understand depositional conditions and in-cave transport and movement (Smith et al., 2020). Given the exceptional resolution offered by Cathedral Cave, applying a multiple-evidence approach would maximise the interrogative potential of the cave's palaeoenvironmental archives. Such an integrated approach has not yet been undertaken in an Australian palaeoecological context.

Pollen has been recovered from the cave's sediments and analysis of these samples is expected to provide a useful vegetation record, the first of its kind for this region. This record will be critical to further investigation of environmental change in Binjang, and to provide an independent proxy against which faunal change can be mapped.

6.6.3 Unresolved and cryptic taxa

During the course of this project, several taxa were not able to be confidently identified to species level. The unresolved rodent morphotypes are present in mostly singular occurrences, but if identified, may still provide palaeoecological information given that many rodent species have well-defined environmental envelopes. Further work on the unresolved species pairs *Perameles gunnii* / *nasuta* and *Dasyurus geoffroii* / *viverrinus* in the assemblage is likely to tease out further ecological signals due to their abundance in the deposit and differing ecological traits. For example, *D. geoffroii* has more xeric habitat preferences than *D. viverrinus* (Appendix D Table 7.16). Characters noted for specimens referred to *Vombatus* sp. cf. *V. ursinus* in this assemblage cast doubt on the elevation of *Vombatus mitchellii* to full species level (contra Louys, 2015). Taxonomic revision of late Pleistocene *Vombatus* material may be warranted.

6.6.4 The non-mammalian fossil fauna

The non-mammalian fossil fauna holds great potential for further taxonomic and palaeoecological investigations. As detailed earlier in this chapter, several interesting specimens are currently under investigation. The fossil anurans in the assemblage were to form part of this thesis, but this work was halted due to the passing of collaborator Professor Michael Tyler. As yet, there have been no Australian studies focused on tracking fossil herpetofauna through a single deposit, and only a single example of a high-resolution palaeoecological study using birds (Shute, 2019). The fossil herpetofauna and bird sample

from the cave is not as rich as the mammal sample but includes enough material to carry out palaeoecological studies with these groups.

6.7 Revisiting Australia's palaeoecological record

What is evident from this study is that there is a need for more large-scale excavations and projects that can capture a reasonable representation of the true biodiversity of faunal communities and how these communities have changed through time. A large limiting factor to the Australian late Quaternary palaeoecological record is the paucity of known suitable fossil sites. It is obvious that we need to broaden our searching and locate more candidate sites, especially in underrepresented regions, and certainly, what palaeontologist does not dream of coming across a hitherto unknown treasure trove of fossils. However, until new localities are uncovered, this study has shown the clear merit in revisiting and rethinking existing known locations using refined methodology and approaches such as those used in this study. Considering not just the fossils, but the sediments and nature of the infill deposits, enabled a deeper understanding of the depositional environment than is normally achieved in a palaeoecological analysis. Only a small number of Australian fossiliferous cave deposits have undergone a comparable interrogation of their sediments (e.g., Macken et al., 2011; McDowell et al., 2013). The Taxonomic Habitat Index (THI) considers the diversity of habitats preferred by taxonomic units in a fossil assemblage, independent of their relative abundance (Evans et al., 1981). Despite its demonstrated usefulness elsewhere (e.g., Andrews, 1990; Aaris-Sbrensen, 1995; Matthews et al., 2005), this study is the first instance of THI being applied to an Australian palaeoecological context. Developing a database of THI habitat values assigned to Australian native animals would be of great use in applying this method to other assemblages.

One location that may benefit from revisiting or rethinking is McEachern's Cave in south-west Victoria. Some of the more immediately interesting aspects of its fauna have been studied (Hope and Wilkinson, 1982; Harris and Goldingay, 2005), but a palaeoecological analysis has not been attempted. A substantial collection from McEachern's Cave is retained by Museums Victoria. Corra-Lynn Cave on the Yorke Peninsula of South Australia contains multiple fossil bearing sites of late Quaternary age (Summary of State Heritage Place: 22798, South Australian Heritage Council, 2014). Collections from Corra-Lynn Cave have been mostly opportunistic, but a systematic approach could yield assemblages suited to palaeoecological analyses. Opportunistic collections from caves in the Cape Range in

Western Australia hint at the potential for a deeper palaeoecological analyses with a unique north-west perspective (Baynes and Jones, 1983). Assemblages from sites such as these have the potential to contribute to Australia's presently deficient palaeoecological record.

6.8 Conclusions

This study opens an unprecedented window into a late Pleistocene mammal community, through a critical period that saw the Australian fauna permanently changed. This work presents a new chronology for Cathedral Cave, which along with a deeper understanding gained of the conditions of accumulation, has given a robust backdrop against which the faunal assemblage can be interpreted. The exceptional nature of this deposit reveals how the mammal community of Binjang responded to a changing environment over the last 65.8 ka and clearly shows that current extinction chronologies being used to infer megafaunal extinction causes are inadequate. No other study in Australia has been able to capture such a high-resolution record of faunal change. One can only imagine the untapped potential that is waiting in the 5 m of sediments lying below the current extent of the excavation.


7 Appendices

7.1 Appendix A: Supplementary to Chapter 2

7.1.1 Origin of the disturbed sediments

The top layer of sediment in the floor of Cathedral Cave is not *in situ*, as demonstrated by the collection of anthropogenic artefacts in the top layer (Dawson and Augee, 1997). The stratigraphic column (Figure 3.15) shows the disturbed layer truncating *in situ* layers. Levelling of the cave floor must have occurred between August 1901 when the Wellington Times reports a dog falling in to a 32 foot deep rocky bottomed pit near the base of the Altar (1901), and before 1939 when Richard Dehm described a flat and reworked floor (M. Augee pers coms). It probably occurred during the Great Depression (1930s) as a former work for the dole participant recalled laying boards over the stairs of Cathedral Cave and wheelbarrowing loads of red soil into the cave from outside (M. Augee pers coms). The disturbed sediments are widely held to be sediments that were removed from the Phosphate Mine during mining. However, it is also likely that the cave floor has undergone disturbance at multiple times in the past, during development and fossicking activities. Thus, it would be unwise to assume a single provenance for the disturbed sediments.

7.1.2 Engineering schematics


Flinders
UNIVERSITY



FLINDERS UNIVERSITY SCHOOL
OF BIOLOGICAL SCIENCES

**WELLINGTON CAVES
PALEANTOLOGY DIG SHORING
DESIGN**

DRAWING SCHEDULE

23733-S00	- STRUCTURAL ENGINEERING COVER SHEET
23733-S01	- GENERAL NOTES & SPECIFICATIONS
23733-S02	- ELEVATION & PLAN
23733-S03	- DETAIL & SECTION
23733-S04	- TIMBER LID FRAME PLAN & SECTION

ISSUED FOR CONSTRUCTION

 barnson DESIGN.PLAN.MANAGE	Office Location: GABA, Mulka Park & Gullaroo CONTRACT No: 23733-S00 www.barnson.com.au	 NATA NATIONAL ASSOCIATION OF TECHNICAL DRAWING INSTITUTES	Client: FLINDERS UNIVERSITY SCHOOL OF BIOLOGICAL SCIENCES PALEANTOLOGY Project: FLINDERS PALEANTOLOGY WELLINGTON CAVES DIG SHORING	Drawing Title: COVER SHEET	Design By: JWA Checked By: EAH	Rev Date: 11/01/2023 Amendment: 1: ISSUE FOR CONSTRUCTION & REVISIONS	Drawings Number: 23733-S00	Revision: 0
----------------------------------------------------------------------------------------------------------------------	----------------------------------------------------------------------------------------------------	-----------------------------------------------------------------------------------------------------------------------------------------------------------	------------------------------------------------------------------------------------------------------------------------------------------	-------------------------------	-----------------------------------------	--------------------------------------------------------------------------------	-------------------------------	----------------

SUPER STRUCTURE LOADING NOTES

- ALL LOADS ARE ACCORDING TO AS1170
- DEAD LOADS:
 - A) SELF WEIGHT OF STEEL WORK STRUCTURE
 - B) TIMBER LID FRAMING ABOVE = 0.3 kPa
- LIVE LOADS:
 - A) 2.5 kPa ROOF ACCESS FLOOR LOADING TO AS1170.1-2002
 - B) 5.0 kPa SOIL SURCHARGE LOADING.
 - C) EARTH & GROUND WATER LOADING.
 - A) NATURAL CLAY, $\gamma = 19\text{kN/m}^3$ TO 6m.
 - B) WATER TABLE AT 2.5m BELOW CAVE SURFACE.
 - C) SANDY CLAY FROM 6m TO 10m, $\gamma = 20\text{kN/m}^3$

GEOTECHNICAL NOTES

- NO GEOTECHNICAL INVESTIGATION HAS BEEN UNDERTAKEN. THE FOLLOWING CONDITIONS SHALL BE INVESTIGATED AND CONFIRMED DURING EXCAVATION WORKS. SITE SOIL CONDITIONS IN THE BOTTOM OF THE CAVE HAVE BEEN DETERMINED FROM A HISTORICAL DIG CARRIED OUT BY THE UNIVERSITY OF NSW IN 1980 AND PAPER BY DAWSON & AUGEE DATED 1997. SOIL CONDITIONS ENCOUNTERED BY DAWSON & AUGEE INCLUDE MAINLY HEAVY RED SILTY CLAY WITH UP TO 300mm DIAMETER LIMESTONE BOULDERS, GRAVEL AND RIVER PEBBLES TO 5.5m DEEP AND SANDY RED CLAY WITH GRAVELS AND LIMESTONE TO 7.5m DEEP WHERE THE EXCAVATION TERMINATED. NO GROUND WATER WAS ENCOUNTERED DURING EXCAVATION.
- THE FOLLOWING DESIGN PARAMETERS ARE BASED ON THE ABOVE SOIL PROFILE AND SHALL BE CONFIRMED THROUGH SAMPLING AND TESTING OF SOIL AS THE DIG PROGRESSES. FACTORED ULTIMATE BEARING CAPACITIES Q_u : AS NOTED, SHALL BE CONFIRMED ON SITE:
 - A) 0 TO 2.5m, $\phi_{Qu} \geq 150$ kPa
 - B) 2.5m TO 10m, $\phi_{Qu} \geq 250$ kPa

3. WATER TABLE

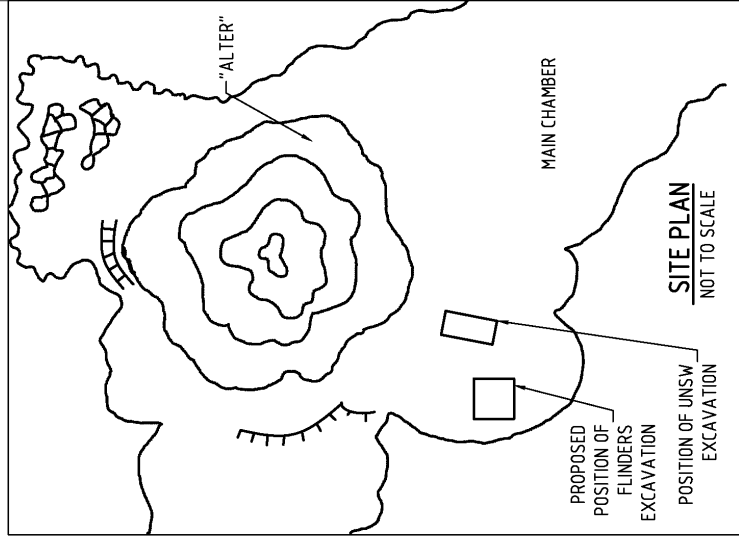
THE WATER TABLE WAS NOT ENCOUNTERED DURING THE DIG IN 1980. RECORDS SHOW THAT THE WATER TABLE IS AFFECTED BY THE BELL RIVER WATER LEVELS DURING TIMES OF FLOOD WITH THE HIGHEST LEVEL BEING RECORDED DURING THE 1956 FLOOD. THE WATER TABLE LEVEL REACHED 2.5m BENEATH THE CAVE FLOOR.

STRUCTURAL STEELWORK NOTES

- ALL WORKMANSHIP AND MATERIALS SHALL BE IN ACCORDANCE WITH AS4100-1998.
- BOLTS NOT DESIGNATED SHALL BE GRADE 8.8/S BOLTS TO AS1252-1996, TIGHTENED TO A SNUG TIGHT FIT. BOLTS DESIGNATED 8.8/TF AND 8.8/TB SHALL BE HIGH STRENGTH STEEL BOLTS TO AS1252-1996, FULLY TENSIONED IN ACCORDANCE WITH AS4100-1998.
- WELDING SHALL BE PERFORMED BY AN EXPERIENCED OPERATOR IN ACCORDANCE WITH AS1554-2011.
- ALL WELDS SHALL BE GP (GENERAL PURPOSE) IN ACCORDANCE WITH AS1554-2011, USING NOMINAL TENSILE STRENGTH $f_u w = 430\text{MPa}$ OR HIGHER TO AS4100-1998 UNLESS NOTED OTHERWISE.
- STEEL WORK CONNECTIONS SHALL BE IN ACCORDANCE WITH THE FOLLOWING MINIMUM REQUIREMENTS UNLESS NOTED OTHERWISE.
 - A) ALL WELDS SHALL BE 6mm CONTINUOUS FILLET WELD ALL AROUND.
 - B) ALL BOLTS SHALL BE M20-8.8/S BOLTS, WITH A MINIMUM OF 2 BOLTS PER CONNECTION.
 - C) ALL GUSSET AND CLEAT PLATES SHALL BE 10mm THICK.
- THE ENDS OF ALL TUBULAR MEMBERS ARE TO BE SEALED WITH NOMINAL THICKNESS PLATES AND CONTINUOUS FILLET WELDED UNLESS OTHERWISE SHOWN. SUBSTITUTIONS FOR STEEL SECTIONS SHOWN ON DRAWINGS SHALL NOT BE MADE WITHOUT APPROVAL OF THE ENGINEER.
- AFTER PLUMBING AND LEVELING OF COLUMNS AND MULLIONS, INSTALL A PAD OF NON SHRINK GROUT BETWEEN THE TOP OF THE FOOTING AND THE UNDERSIDE OF THE PLATE AND STRIKE OFF THE GROUT AT 45°.
- CAMBER TO BE AS NOTED ON THE DRAWINGS.
- UNLESS OTHERWISE SPECIFIED ALL STEELWORK SHALL BE PROVIDED WITH CORROSION PROTECTION TO SUIT THE ENVIRONMENT AS PER AS2312-2014, OR HOT DIPPED GALVANISED HDG320 TO AS4680-2006.
- MEMBERS ENCASED IN CONCRETE, FIRE SPRAYED OR HSTF BOLTED CONNECTIONS MUST NOT BE PAINTED.
- CONCRETE ENCASED STEELWORK SHALL BE WRAPPED WITH SL62 MESH, UNLESS NOTED OTHERWISE.

STRUCTURAL STEELWORK NOTES CONT'D

- THE CONTRACTOR SHALL PROVIDE AND LEAVE IN PLACE UNTIL PERMANENT BRACING ELEMENTS ARE CONSTRUCTED SUCH TEMPORARY BRACING AS IS NECESSARY TO STABILISE THE STRUCTURE DURING ERECTION.
- BEFORE FABRICATION IS COMMENCED THE CONTRACTOR SHALL SUBMIT COPIES OF THE SHOP DRAWINGS TO THE ENGINEER AND CLIENT FOR REVIEW. REVIEW DOES NOT INCLUDE CHECKING OF DIMENSIONS.



ISSUED FOR CONSTRUCTION

Design or Check	Drawn	Rev	Date	Amendment	Classification
	CA				
Drawing Sheet:	0 to 00000 ISSUED FOR CONSTRUCTION				7/03/2016
Author:	To be checked by the engineer before issue and by the contractor before construction. All dimensions are in millimetres unless otherwise stated.				23733-901
Checked:					0

Client:	FILINDERS UNIVERSITY SCHOOL OF BIOLOGICAL SCIENCES PALEONTOLOGY
Project:	FILINDERS PALEONTOLOGY
Drawing Title:	GENERAL NOTES & SPECIFICATIONS
Project:	FILINDERS PALEONTOLOGY
Drawing Title:	WELLINGTON CAVES DIG SHORING DESIGN



 Approved Contractor
 License Number: 13050

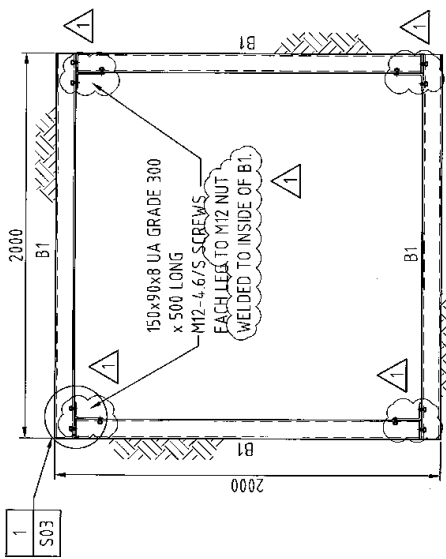


 Registered Professional Engineer
 License Number: 13050

Offices: Liverpool, Cessnock, Newcastle, Brisbane & Bathurst
 Contact: Lisa
 Email: info@barnson.com.au
 Website: www.barnson.com.au



barnson
DESIGN · PLAN · MANAGE



PLAN
SCALE = 1:20

MEMBER SCHEDULE		
LOCATION MARK	SIZE	COMMENT
(1)	100x2.0 SHS	B1 GRADE 450
(2)	100x2.0 SHS	B2 GRADE 450
(3)	100x3.0 SHS	B3 GRADE 450
(4)	100x4.0 SHS	B4 GRADE 450

- CONSTRUCTION SEQUENCE**
- 1) EXCAVATE FIRST 1200 WITHOUT SHORING.
 - 2) INSTALL TOP 1200 OF SHORING.
 - 3) EXCAVATE ONE SIDE AT A TIME 100 BELOW SHORING.
 - 4) INSTALL STEEL SHORING AND BOLTS.
 - 5) REPEAT STEPS 3 & 4 UNTIL 5 LEVELS CONSTRUCTED.
 - 6) INSTALL CORNER BRACKET AND BOLTS.
 - 7) REPEAT STEPS 3 TO 6.

ISSUED FOR CONSTRUCTION



Office Location:
Dunedin, New Zealand
Contact Us:
C. 0800 222 222
W. www.barnson.com.nz



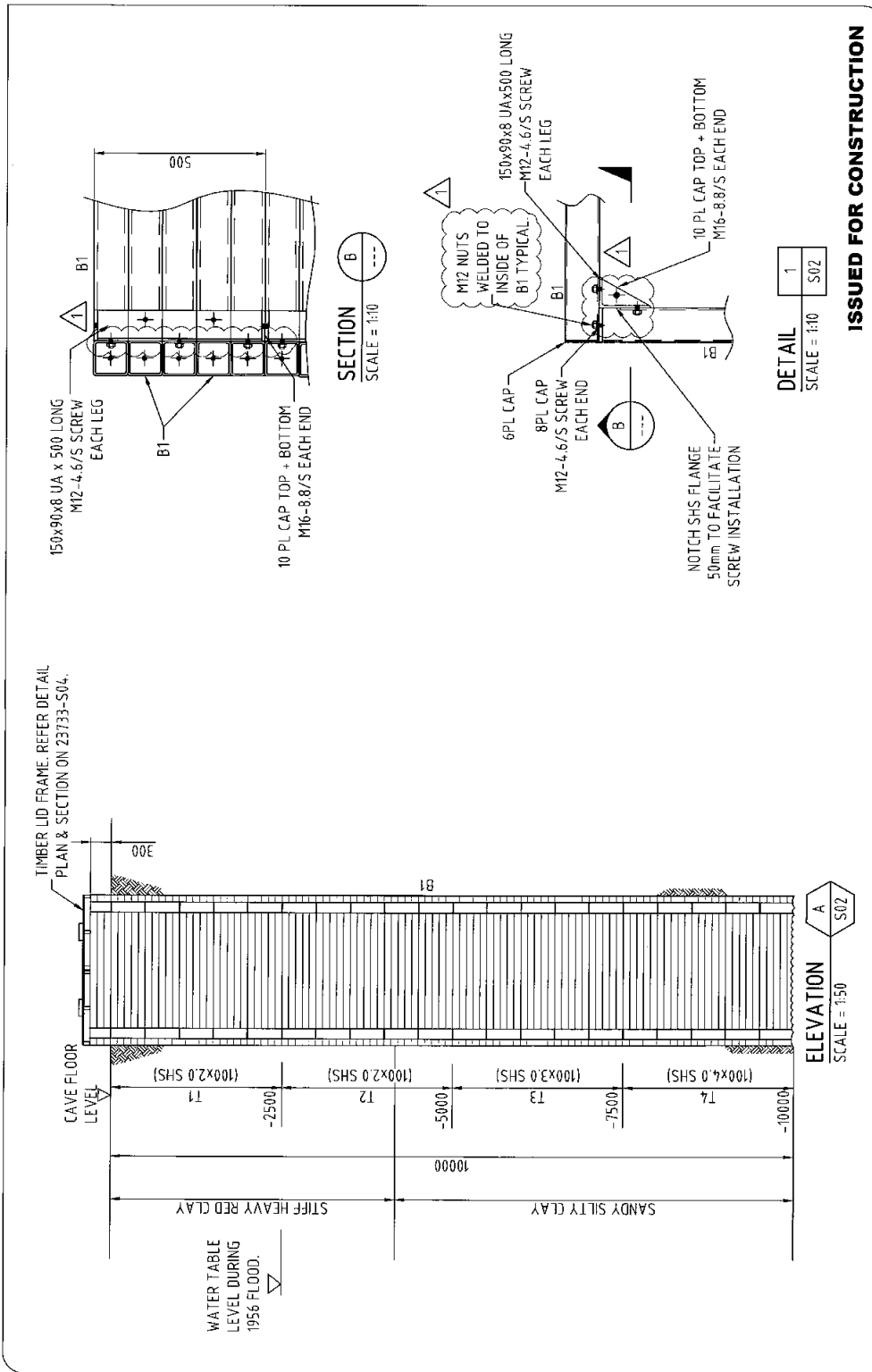
Client: FUMERS UNIVERSITY SCHOOL OF GEOLOGICAL SCIENCES/PALONTOLOGY
Project: FUMERS
Wellington, New Zealand

Drawing Title:
ELEVATION & PLAN

Design By: GA
Check: GA
Drawing Sheet:
All Sheets Used

Rev Desc Amendment:
1 200216 REVISIONS ISSUED
2 030216 ISSUED FOR CONSTRUCTION
3 030216 ISSUED FOR PERMIT
4 030216 ISSUED FOR PERMIT

Author: *[Signature]*
Drawing Number: 237833-S02
Revision: 1



barnson
DESIGN, PLAN, MANAGE

Office Located: Goolwa, Victoria, France & Lithuania
Contact Us: 11114 1300 057
 1300 057 1300 057
 www.barnson.com.au
 www.barnson.com.au

Client: FLINDERS UNIVERSITY SCHOOL OF BIOLOGICAL SCIENCES PALEONTOLOGY
Project: FLINDERS PALEONTOLOGY
 WELLINGTONS DIG SHORING

NATA
 NATIONAL ASSOCIATION OF TECHNICAL DRAWING INSTITUTIONS
 2015-2018

Rev. Date | **Amendment**

1	2018/01/16	M2 NUTS WELDED TO INSIDE OF B1 TYPICAL
A	03/02/16	ISSUED FOR APPROVAL

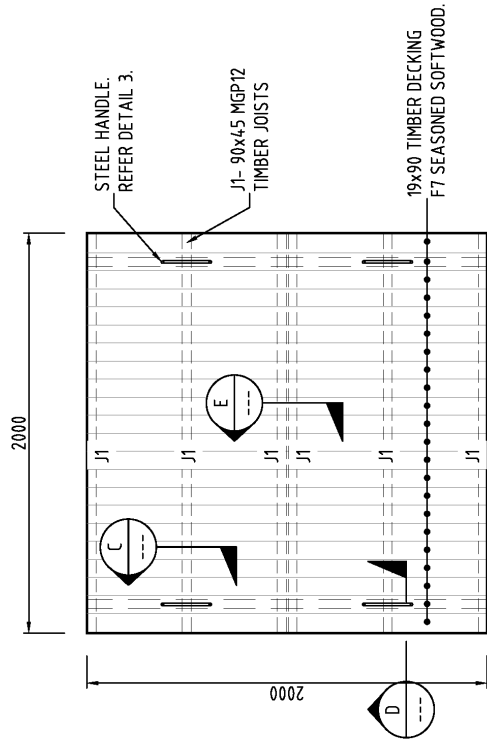
Design | **Drawn** | **Check** | **QA**

Designing Sheet | **Number** | **Revision**

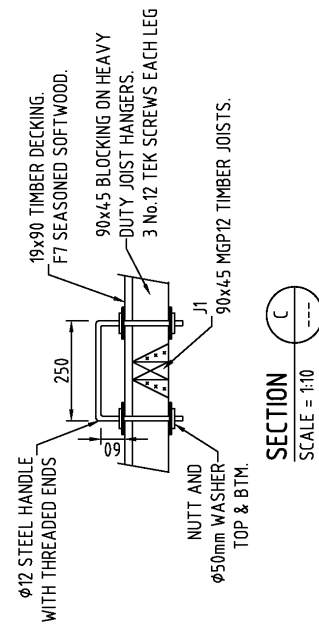
23733-S03 | 1

23/4/16

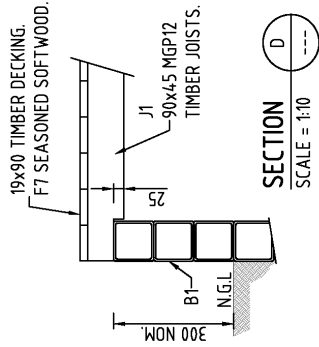
- STRUCTURAL TIMBER NOTES**
1. ALL WORKMANSHIP AND MATERIALS SHALL BE IN ACCORDANCE WITH AS1720-2010.
 2. ALL TIMBER CONNECTIONS TO BE IN ACCORDANCE WITH AS1720 UNLESS NOTED OTHERWISE.
 3. ALL PROPRIETARY CONNECTORS AND FIXINGS ARE TO BE INSTALLED IN ACCORDANCE WITH MANUFACTURERS SPECIFICATIONS.
 4. TIMBER MEMBERS SHALL HAVE THE FOLLOWING PROPERTIES U.N.O.:
 - A) SPECIES = SEASONED SOFTWOOD
 - B) STRESS GRADE = MGP12 & F7 AS SPECIFIED.
 5. MAXIMUM UNDERSIZE FOR ALL TIMBER MEMBERS SHALL BE AS FOLLOWS:
 - A) SEASONED PINE & OTHER SEASONED SOFTWOODS =0mm
 6. ALL TIMBER JOINTS ARE TO BE FREE OF DEFECTS.
 7. ALL NAILS, BOLTS AND SCREWS SHALL BE GALVANISED UNLESS APPROVED OTHERWISE BY THE SITE SUPERINTENDENT.



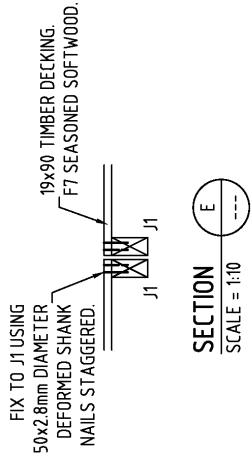
TIMBER LID FRAME PLAN
SCALE = 1:20



SECTION C
SCALE = 1:10



SECTION D
SCALE = 1:10



SECTION E
SCALE = 1:10

ISSUED FOR CONSTRUCTION

barntson
DESIGN . PLAN . MANAGE

Offices Located
Dunedin, Auckland, Parkville & Brisbane
Company Ltd
t: +64 (0)3 338 8879
e: barntson@barntson.com.au
w: www.barntson.com.au

Client: FLINDERS UNIVERSITY SCHOOL OF BIOLOGICAL SCIENCES PALEANTOLOGY
Project: FLINDERS PALEANTOLOGY
WELLINGTON CAVES DIG SHORING

Drawing Title:
TIMBER LID FRAME PLAN & SECTION

Design by: [Signature]
Check: [Signature]
Drawing Sheet: [Signature]
As Issued to: [Signature]

Rev Date: 7/03/2016
Amendment: [Signature]
A: 02/2016 ISSUED FOR CONSTRUCTION
A: 02/2016 ISSUED FOR APPROVAL

Identification:
Drawing Number: 23733-S04
Revision: 0

7.2 Appendix B: Supplementary to Chapter 3

Table 7.1. Radiocarbon dates obtained from charcoal from sediments excavated from the floor of Cathedral Cave, Wellington Caves during the UNSW excavation. * denotes pooled samples. Depth represents depth in UNSW excavation below present cave floor after (Dawson and Augee, 1997)

Sample #	Spit#	Depth (m)	Age (yrs BP)	Pooled
SUA 2097	6	1.6	2950 ± 80	
SUA 2098	14	2.7	2590 ± 80	
ANU 4480	39	5.1	14300 ± 730	*
ANU 4479	40	5.2	21400 ± 700	*
ANU 44+78	44	5.8	11900 ± 790	*
ANU 5323	46	6.1	21350 ± 1700	
ANU 5324	47	6.2	28000 ± 1100	*
ANU 5325	49	6.4	23700 ± 1400	
ANU 5326	50	6.5	26800 ± 1100	*
ANU 5327	51	6.6	33800 ± 2000	
ANU 5328	52	6.7	32500 ± 2100	

Table 7.2. Pearson's correlation coefficient (*r*) for XRF analysis. Significant results are shown in red.

	Na ₂ O	MgO	Al ₂ O ₃	SiO ₂	P ₂ O ₅	SO ₃	K ₂ O	CaO	TiO ₂	MnO	Fe ₂ O ₃	LOI	Quartz	Calcite
Na ₂ O		0.84	-0.52	-0.56	0.96	0.82	-0.40	0.08	-0.63	0.06	-0.49	0.50	-0.15	-0.32
MgO	0.84		-0.07	-0.12	0.87	0.63	0.02	-0.33	-0.21	-0.04	-0.08	0.04	0.26	-0.64
Al ₂ O ₃	-0.52	-0.07		0.91	-0.38	-0.44	0.93	-0.83	0.95	-0.21	0.90	-0.85	0.76	-0.58
SiO ₂	-0.56	-0.12	0.91		-0.43	-0.56	0.77	-0.80	0.96	-0.08	0.94	-0.95	0.80	-0.53
P ₂ O ₅	0.96	0.87	-0.38	-0.43		0.66	-0.26	-0.03	-0.51	0.12	-0.34	0.36	-0.06	-0.41
SO ₃	0.82	0.63	-0.44	-0.56	0.66		-0.33	0.05	-0.54	-0.26	-0.52	0.55	-0.10	-0.28
K ₂ O	-0.40	0.02	0.93	0.77	-0.26	-0.33		-0.81	0.80	-0.33	0.74	-0.70	0.70	-0.61
CaO	0.08	-0.33	-0.83	-0.80	-0.03	0.05	-0.81		-0.76	0.23	-0.76	0.68	-0.89	0.92
TiO ₂	-0.63	-0.21	0.95	0.96	-0.51	-0.54	0.80	-0.76		-0.10	0.94	-0.90	0.76	-0.48
MnO	0.06	-0.04	-0.21	-0.08	0.12	-0.26	-0.33	0.23	-0.10		0.16	-0.04	-0.13	0.24
Fe ₂ O ₃	-0.49	-0.08	0.90	0.94	-0.34	-0.52	0.74	-0.76	0.94	0.16		-0.93	0.76	-0.51
LOI	0.50	0.04	-0.85	-0.95	0.36	0.55	-0.70	0.68	-0.90	-0.04	-0.93		-0.74	0.44
Quartz	-0.15	0.26	0.76	0.80	-0.06	-0.10	0.70	-0.89	0.76	-0.13	0.76	-0.74		-0.79
Calcite	-0.32	-0.64	-0.58	-0.53	-0.41	-0.28	-0.61	0.92	-0.48	0.24	-0.51	0.44	-0.79	

Table 7.3. XRD analysis of %wt of crystalline structures in the Cathedral Cave sediments.

Field #	Layer	Quartz	Albite	Albite, -Ca, low, An16	Albite, -Ca, low, An28	Labradorite	Orthoclase	Microcline	Calcite	%wt												
										Aragonite	High Mag Calcite	Hematite	Kaolinite	Chlorite	Illite	Illite- smectite	Ankerite	Siderite	Gypsum	Goethite	Muscovite	
CC16-S3	1	42.7	1.0				0.0	0.7				6.7	8.1	0.4	6.1	5.4	0.3	2.7	15.7	0.4	9.9	
CC16-S4	2	50.7	5.2				1.2	0.6				3.3	4.4	1.6	6.6	6.6	0.5	1.5	9.5	1.5	6.8	
CC16-S9	2b	52.5	6.3				2.8	0.8				4.0	3.9	1.4	8.3	4.7	0.4	3.5	1.7	2.1	7.7	
CC16-S5	3	56.7	3.9				0.0	0.2				3.0	4.0	0.0	8.5	3.5	1.6	1.7	12.8	1.3	2.8	
CC16-S6	4	58.7	3.9				0.0	0.0				3.5	5.8	0.5	10.0	4.1	0.8	1.0	1.7	1.9	8.2	
CC16-S7	5	41.5	4.7				3.9	28.4				2.8	3.0	0.8	5.0	0.6	0.3	2.5	2.0	1.4	3.1	
CC16-S10	8	54.1	5.5				0.0	0.2				3.9	6.4	1.2	8.2	4.6	0.4	1.8	2.4	2.1	9.1	
CC16-S8	9	44.7	3.0				4.3	31.0				1.9	2.6	0.0	4.2	0.5	0.0	0.8	0.3	0.7	6.0	
CC16-S11	9	55.0	2.3				0.0	6.4				2.7	5.4	1.6	7.9	4.2	0.0	0.9	1.7	2.6	9.2	
CC 16-S23a	9	53.3	0	5.7	0.9	0	0	3.8	13.9	0	0	3.2	5.0	3.0	11.1							
CC 16-S20	10	64.5	0	6.7	0	0	0	3.4	1.2	0	0	4.0	5.8	2.6	12.0							
CC 16-S28	10	63.8	0	4.6	0	0.4	0	5.4	0.5	0	0.3	4.1	5.5	2.2	13.2							
CC 16-S34	10	53.4	1.3	3.5	0	0	0	13.4	0	0	0.9	5.3	5.9	2.6	13.6							
CC 17-S2	12	59.7	1.8	3.9	0	0	0	8.7	5.4	0	0.2	3.3	4.9	1.7	10.4							
CC 17-S4	12	57.0	0	3.7	1.3	0	0	7.5	7.8	0	0.4	4.4	3.8	3.9	10.1							
CC 17-S6	13	52.5	0	1.5	1.1	0	0	2.0	24.4	0	0	2.7	3.6	0.9	11.2							
CC 17-S10	13	24.2	0	0	0	2.7	6.4	0	50.1	1.6	1.9	1.8	3.4	1.2	6.7							
CC 17-SB	14	45.8	0	1.5	0	0.4	0	2.7	30.4	0.1	0	2.7	4.4	1.4	10.7							
CC 17-S12	14	62.8	0	7.0	1.6	0	0	7.5	0	0	0.5	3.9	4.0	2.4	10.3							
CC 17-S15	14	54.7	1.8	6.9	0	0	0	12.7	4.3	0	0	3.7	3.9	2.1	9.9							
	Average:	52.4	2.0	4.1	0.4	0.3	0.9	6.1	10.3	0.2	0.4	3.5	4.7	1.6	9.2	3.8	0.5	1.8	5.3	1.6	7.0	

Table 7.4. XRF analysis of the elemental composition of the Cathedral Cave sediments, given as parts per million (ppm).

Field #	Layer	Cl	Cu	Zn	Ga	Ge	As	Se	Br	Rb	Sr	Y	Zr	Nb	Sn	Ba	La	Ce	Hf	Hg	Pb	Th	U
ppm																							
CC16-S3	1	588	173	864	12	2	45	3	16	69	211	36	159	9	5	205	31	22	<1	3	35	10.5	3.5
CC16-S4	2	332	83	388	12	2	29	2	21	70	105	38	265	10	7	234	49	84	6	1	19	7.4	1.4
CC16-S9	2b	525	96	493	14	3	41	1	15	77	140	43	289	12	3	288	11	<4	6	1	23	9.7	2
CC16-S5	3	579	70	309	13	3	39	2	6	70	139	39	260	12	4	256	31	19	7	1	22	9.1	2.4
CC16-S6	4	316	66	222	16	3	49	1	4	88	142	46	298	14	4	385	28	146	7	2	27	11.7	2.4
CC16-S7	5	503	49	248	9	2	54	1	5	55	160	35	254	9	<3	331	17	<4	4	3	19	7.2	2.6
CC16-S10	8	282	65	255	16	3	47	1	4	85	140	47	305	14	2	313	<4	68	7	1	26	11.2	3.1
CC16-S8	9	305	39	110	10	<1	23	<1	3	56	109	31	320	11	<3	172	39	75	5	3	16	7.5	2.1
CC16-S11	9	386	51	154	16	1	39	<1	2	83	124	42	314	14	7	314	55	141	6	2	24	10.7	3.6
CC 16-S23a	9	185	43	134	15	3	41	<1	3	79	114	39	293	14	11	672	nr	nr	6	1	22	10.4	2.8
CC 16-S20	10	201	56	180	17	2	51	<1	2	90	131	50	307	15	14	1026	nr	nr	7	1	27	12.2	4.3
CC 16-S28	10	135	55	160	17	2	60	<1	1	93	127	55	328	16	12	858	nr	nr	8	1	30	12.6	3
CC 16-S34	10	161	87	272	16	3	52	<1	3	88	143	55	331	15	15	755	nr	nr	8	1	29	12.5	2.8
CC 17-S2	12	229	70	273	15	1	45	<1	1	81	141	49	329	14	13	872	nr	nr	8	3	26	11.6	6
CC 17-S4	12	224	65	226	15	2	47	<1	1	83	131	52	350	14	11	872	nr	nr	8	2	27	11.6	3.3
CC 17-S6	13	180	58	177	15	1	55	<1	1	76	121	44	307	12	13	723	nr	nr	5	4	23	9.8	3.8
CC 17-S10	13	128	38	123	10	2	62	<1	3	61	116	31	215	9	4	551	nr	nr	4	3	17	7	3.4
CC 17-SB	14	236	46	136	12	2	74	<1	2	74	124	38	284	12	8	655	nr	nr	6	1	21	9.6	4.2
CC 17-S12	14	334	85	380	14	3	44	<1	10	80	146	42	298	12	15	821	nr	nr	6	1	22	10.2	2.5
CC 17-S15	14	246	61	188	15	1	40	<1	3	79	132	43	318	14	16	645	nr	nr	8	1	24	10.6	3
Average:		304	68	265	14	2	47	2	5	77	135	43	291	13	9	547	33	79	6	2	24	10	3

Table 7.5. Eigenvalues for Principal Components Analysis in Figure 3.12b.

PC	Eigenvalue	Percentage of Variance	Cumulative
1	7.00182	53.86%	53.86%
2	3.84272	29.56%	83.42%
3	1.24116	9.55%	92.97%
4	0.35177	2.71%	95.67%
5	0.211	1.62%	97.30%
6	0.13698	1.05%	98.35%
7	0.1191	0.92%	99.27%
8	0.0493	0.38%	99.65%
9	0.02639	0.20%	99.85%
10	0.01214	0.09%	99.94%
11	0.00409	0.03%	99.97%
12	0.00253	0.02%	99.99%
13	9.95E-04	0.01%	100.00%

Table 7.6. Bone samples from the 1982-86 UNSW excavation submitted for AMS radiocarbon dating at ANSTO as part of this project. Spits follow those designated by Dawson and Augee (1997) and depths relate to the lower boundary of those spits.

Sample #	Spit	Depth (m)	Sample #	Spit	Depth (m)	Sample #	Spit	Depth (m)
1	10	2	5	10	2	16	10	2
2	12	2.2	7	13	2.3	8	13	2.3
3	15	2.5	9	15	2.5	10	17	2.7
4	19	3	11	19	3	12	17	2.7
13	23	3.4	14	23	3.4	15	25	3.7

Table 7.7. Charcoal samples from the FU excavation submitted for AMS radiocarbon dating at the University of Waikato.

Laboratory sample #	Collector sample #	Weight (g)	Layer	Quad	Depth (cm)
WK3563	CCW-B-CHCH1a	0.3	2	B	183-188
WK43564	CCW-B-CHC2	0.24	7	B	246-251

Table 7.8. Charcoal samples submitted for AMS radiocarbon dating at ANSTO.

Sample #	Layer	Quad	Depth (cm)	Sample #	Layer	Quad	Depth (cm)
OZW071	12	I	430-435	OZW078	10	II	400-405
OZW072	13	I	495-500	OZW079	10	II	415-420
OZW073	14F	I	530	OZW081	13	II	505-510
OZW074	14F	I	530-540	OZW083	14F	II	570
OZW075	14F	I	570	OZW084	12	IV	450-455
OZW077	10	II	380-385	OZW085	13	IV	530

7.2.1 Rbacon settings for Bayesian age-depth model

9 #d.min, 425 #d.max, 1 #d.by, 0 #depths.file, #slump, 67 67 #acc.mean, 1.5 1.5 #acc.shape, 0.7 #mem.mean, 4 #mem.strength, NA #boundary, 86.5 #hiatus.depths, 37400 #hiatus.max, 37400 #hiatus.max, 0 #BCAD, #cc – radiocarbon dates were pre-calibrated using the SHCal13 calibration curve prior to use in the model, cm #depth.unit, 0 #normal, 3 #t.a, 4 #t.b, 0 #delta.R, 0 #d.STD, 0.95 #prob, yr #age.unit

7.2.2 Bayesian age depth models

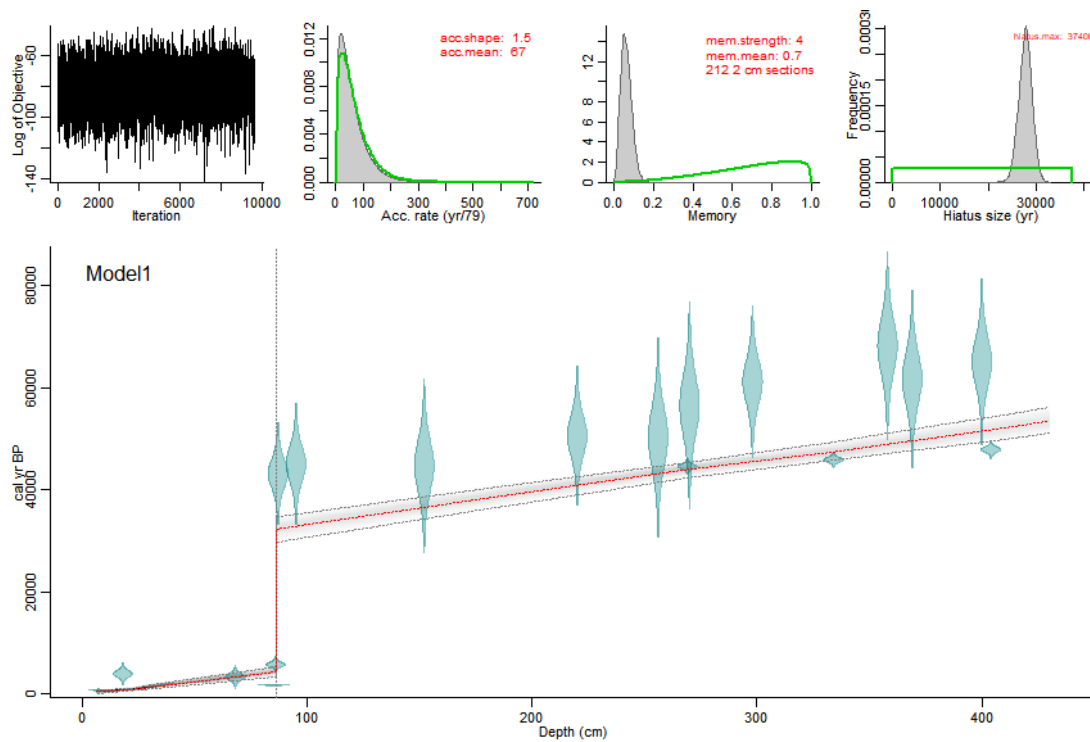


Figure 7.1. Bayesian age-depth model (Model1) for 425 cm of the Cathedral Cave deposit using fourteen OSL dates and five AMS radiocarbon dates.

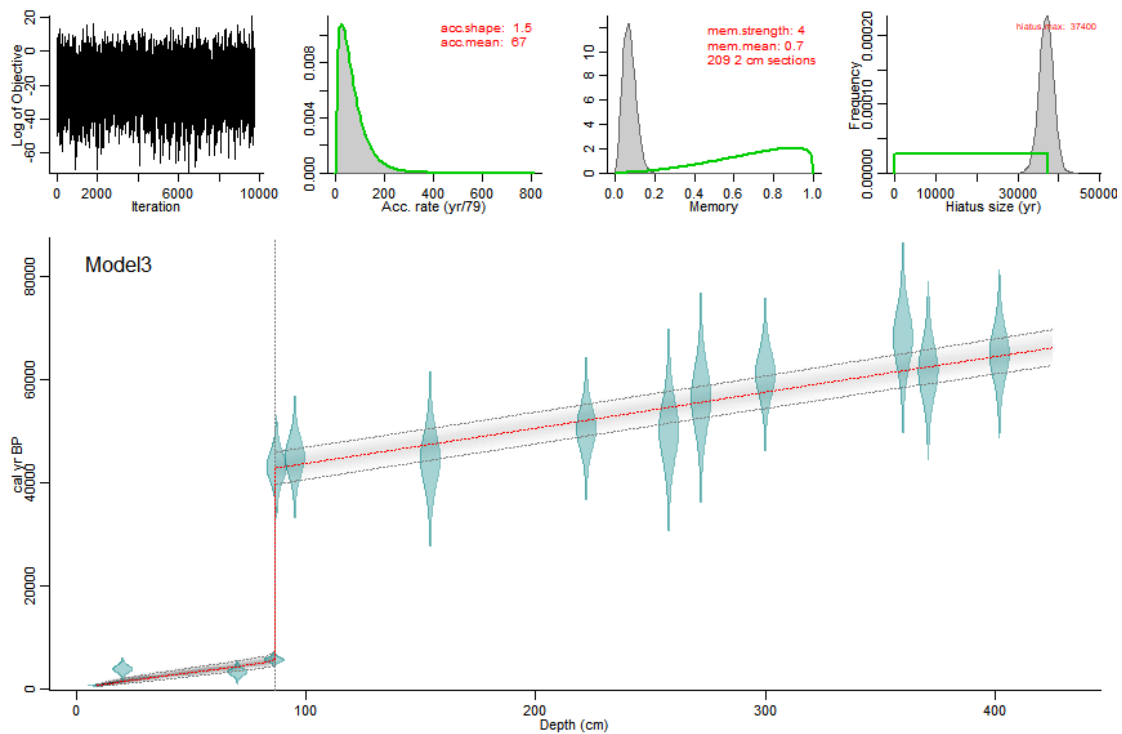


Figure 7.2. Bayesian age-depth model (Model3) for 425 cm of the Cathedral Cave deposit using all 14 OSL ages, excluding all radiocarbon ages.

Table 7.9. Bayesian age-depth modelled ages. Showing depth by cm, minimum age, maximum age, median age (\tilde{x}) and mean age (\bar{x}). Excavation commences at 14 c

depth (cm)	min	max	\tilde{x}	\bar{x}	depth (cm)	min	max	\tilde{x}	\bar{x}	depth (cm)	min	max	\tilde{x}	\bar{x}	depth (cm)	min	max	\tilde{x}	\bar{x}
9	196	791	576	553	113	41467	47795	44628	44648	219	48826	55036	51906	51915	325	56082	62481	59317	59308
10	241	815	601	581	114	41540	47853	44701	44716	220	48899	55099	51982	51983	326	56150	62550	59379	59377
11	278	844	628	609	115	41607	47929	44765	44785	221	48976	55167	52049	52052	327	56218	62635	59449	59446
12	318	867	654	637	116	41684	47988	44827	44852	222	49032	55242	52116	52120	328	56284	62695	59521	59515
13	354	895	681	665	117	41754	48058	44900	44920	223	49092	55307	52186	52189	329	56346	62768	59587	59584
14	410	918	706	694	118	41835	48124	44973	44988	224	49164	55379	52252	52258	330	56426	62841	59661	59652
15	454	948	732	722	119	41898	48175	45041	45055	225	49224	55441	52321	52327	331	56497	62908	59737	59721
16	503	970	756	751	120	41960	48252	45099	45124	226	49296	55531	52392	52399	332	56570	62972	59804	59790
17	542	1001	782	779	121	42010	48312	45170	45193	227	49361	55606	52460	52470	333	56618	63052	59873	59859
18	603	1024	805	807	122	42084	48385	45236	45261	228	49465	55655	52534	52542	334	56705	63098	59936	59929
19	642	1056	831	835	123	42151	48470	45308	45329	229	49543	55733	52609	52613	335	56763	63176	60010	59998
20	707	1079	852	862	124	42211	48544	45373	45397	230	49621	55805	52676	52683	336	56828	63228	60084	60068
21	748	1105	878	889	125	42292	48611	45439	45465	231	49676	55873	52748	52753	337	56895	63336	60150	60138
22	807	1141	909	925	126	42369	48682	45509	45533	232	49758	55947	52814	52823	338	56972	63410	60221	60208
23	833	1189	946	961	127	42431	48763	45569	45602	233	49812	56025	52879	52893	339	57038	63467	60294	60277
24	869	1253	1000	1015	128	42519	48819	45646	45669	234	49903	56080	52954	52962	340	57091	63540	60361	60346
25	889	1365	1047	1068	129	42585	48899	45714	45737	235	49960	56146	53025	53031	341	57141	63604	60426	60414
26	922	1429	1101	1121	130	42656	48960	45772	45805	236	50035	56245	53092	53101	342	57216	63670	60491	60482
27	941	1526	1153	1174	131	42730	49049	45840	45873	237	50098	56317	53165	53171	343	57291	63752	60563	60550
28	984	1590	1206	1227	132	42811	49105	45907	45940	238	50163	56390	53232	53240	344	57369	63821	60629	60619
29	1006	1680	1259	1280	133	42870	49171	45978	46007	239	50215	56457	53310	53309	345	57444	63903	60707	60687
30	1047	1737	1314	1333	134	42948	49223	46039	46074	240	50284	56521	53373	53378	346	57513	63977	60775	60757
31	1074	1819	1365	1386	135	43005	49295	46106	46140	241	50374	56603	53440	53447	347	57575	64066	60849	60827
32	1115	1879	1419	1440	136	43072	49368	46177	46208	242	50432	56667	53513	53517	348	57662	64137	60922	60896
33	1144	1950	1475	1493	137	43145	49436	46253	46276	243	50513	56741	53578	53588	349	57713	64193	60988	60966
34	1188	2013	1527	1546	138	43194	49491	46322	46344	244	50579	56812	53640	53656	350	57780	64263	61051	61035

depth (cm)	min	max	\bar{X}	\bar{X}	depth (cm)	min	max	\bar{X}	\bar{X}	depth (cm)	min	max	\bar{X}	\bar{X}	depth (cm)	min	max	\bar{X}	\bar{X}
35	1224	2090	1581	1599	139	43273	49569	46392	46413	245	50640	56885	53708	53723	351	57855	64329	61123	61103
36	1268	2152	1632	1652	140	43335	49636	46463	46482	246	50697	56945	53770	53791	352	57923	64368	61190	61173
37	1301	2228	1685	1704	141	43418	49713	46533	46551	247	50764	57008	53844	53859	353	58015	64438	61259	61242
38	1341	2288	1738	1758	142	43506	49800	46602	46620	248	50849	57086	53915	53930	354	58073	64508	61329	61311
39	1374	2362	1793	1813	143	43575	49854	46674	46689	249	50924	57149	53984	54001	355	58148	64572	61395	61379
40	1419	2424	1849	1866	144	43635	49917	46741	46756	250	51006	57211	54058	54069	356	58210	64641	61455	61447
41	1452	2504	1902	1919	145	43685	49985	46810	46824	251	51049	57289	54125	54138	357	58270	64705	61522	61515
42	1494	2559	1953	1973	146	43765	50059	46885	46892	252	51113	57341	54196	54208	358	58334	64779	61592	61583
43	1533	2628	2007	2028	147	43840	50115	46945	46961	253	51189	57405	54263	54277	359	58389	64837	61656	61651
44	1582	2682	2062	2081	148	43902	50176	47016	47029	254	51252	57483	54333	54347	360	58445	64911	61726	61719
45	1614	2761	2113	2134	149	43968	50252	47081	47097	255	51314	57547	54401	54417	361	58498	64994	61794	61787
46	1669	2818	2167	2186	150	44033	50324	47146	47166	256	51409	57600	54467	54486	362	58576	65030	61862	61855
47	1710	2884	2219	2238	151	44107	50372	47213	47235	257	51469	57662	54539	54555	363	58648	65102	61935	61924
48	1757	2940	2277	2291	152	44181	50446	47289	47304	258	51532	57728	54607	54625	364	58713	65179	62001	61993
49	1789	3000	2329	2344	153	44254	50522	47351	47374	259	51576	57792	54673	54694	365	58774	65269	62074	62061
50	1841	3058	2384	2398	154	44328	50595	47422	47443	260	51658	57866	54742	54765	366	58842	65329	62135	62129
51	1872	3130	2435	2451	155	44421	50667	47493	47513	261	51718	57944	54815	54835	367	58892	65388	62204	62198
52	1918	3199	2488	2504	156	44466	50717	47560	47581	262	51796	58035	54883	54907	368	58948	65464	62274	62265
53	1954	3271	2542	2558	157	44534	50783	47625	47649	263	51868	58088	54954	54978	369	59038	65514	62345	62331
54	2002	3332	2597	2612	158	44615	50869	47691	47720	264	51922	58146	55026	55047	370	59101	65599	62413	62399
55	2046	3407	2652	2667	159	44682	50940	47761	47790	265	51989	58218	55097	55116	371	59150	65678	62481	62468
56	2100	3459	2705	2719	160	44753	51018	47836	47859	266	52054	58301	55169	55187	372	59238	65735	62550	62536
57	2136	3524	2757	2772	161	44826	51081	47906	47928	267	52127	58376	55239	55258	373	59301	65814	62615	62604
58	2189	3572	2812	2825	162	44890	51137	47970	47996	268	52201	58444	55311	55329	374	59366	65874	62673	62674
59	2226	3632	2865	2878	163	44956	51231	48040	48065	269	52276	58507	55389	55399	375	59431	65945	62743	62743
60	2284	3693	2918	2932	164	45036	51309	48111	48133	270	52336	58589	55458	55470	376	59486	66011	62814	62811
61	2324	3761	2970	2986	165	45110	51367	48181	48201	271	52394	58653	55535	55541	377	59554	66101	62880	62879
62	2369	3817	3026	3039	166	45181	51450	48247	48271	272	52476	58718	55608	55611	378	59627	66165	62942	62947
63	2414	3886	3077	3092	167	45259	51518	48311	48341	273	52541	58782	55669	55682	379	59679	66221	63010	63014

depth (cm)	min	max	\bar{X}	\bar{X}	depth (cm)	min	max	\bar{X}	\bar{X}	depth (cm)	min	max	\bar{X}	\bar{X}	depth (cm)	min	max	\bar{X}	\bar{X}
64	2463	3931	3131	3146	168	45318	51574	48384	48409	274	52609	58858	55750	55753	380	59741	66292	63081	63082
65	2499	4004	3187	3199	169	45377	51664	48449	48477	275	52687	58951	55817	55824	381	59808	66386	63153	63150
66	2549	4056	3240	3254	170	45454	51724	48524	48546	276	52751	59026	55885	55896	382	59874	66459	63227	63219
67	2589	4119	3293	3308	171	45530	51774	48598	48615	277	52808	59097	55957	55967	383	59936	66533	63292	63287
68	2636	4173	3346	3361	172	45603	51850	48663	48683	278	52870	59157	56025	56037	384	60021	66595	63360	63355
69	2676	4247	3399	3415	173	45676	51927	48730	48752	279	52957	59231	56097	56106	385	60091	66674	63430	63423
70	2713	4305	3455	3468	174	45749	51996	48796	48820	280	53017	59290	56165	56176	386	60147	66732	63496	63491
71	2755	4375	3507	3522	175	45809	52072	48860	48889	281	53091	59356	56236	56246	387	60208	66791	63563	63558
72	2807	4439	3563	3577	176	45886	52147	48931	48957	282	53152	59426	56304	56316	388	60296	66845	63628	63626
73	2848	4511	3614	3632	177	45955	52214	48996	49025	283	53219	59489	56380	56385	389	60359	66910	63699	63693
74	2895	4574	3671	3687	178	46016	52271	49073	49094	284	53264	59567	56443	56455	390	60420	66985	63766	63762
75	2931	4643	3722	3741	179	46064	52353	49146	49163	285	53340	59671	56515	56525	391	60483	67061	63835	63830
76	2983	4704	3777	3796	180	46151	52410	49213	49232	286	53435	59750	56579	56595	392	60539	67135	63905	63897
77	3021	4786	3831	3851	181	46229	52474	49275	49301	287	53517	59822	56650	56665	393	60613	67194	63974	63965
78	3072	4844	3888	3906	182	46311	52538	49344	49369	288	53581	59896	56717	56736	394	60662	67266	64038	64032
79	3111	4922	3939	3961	183	46389	52599	49413	49438	289	53638	59980	56786	56808	395	60724	67345	64097	64100
80	3159	4984	3995	4016	184	46461	52661	49481	49507	290	53722	60039	56855	56877	396	60796	67435	64164	64166
81	3195	5048	4050	4070	185	46504	52716	49551	49575	291	53791	60123	56925	56947	397	60871	67501	64226	64233
82	3236	5116	4105	4125	186	46574	52773	49616	49645	292	53865	60179	56998	57017	398	60944	67584	64294	64303
83	3282	5186	4159	4180	187	46634	52843	49682	49714	293	53926	60233	57072	57087	399	61020	67650	64367	64372
84	3394	5343	4295	4316	188	46708	52905	49756	49784	294	53983	60291	57141	57156	400	61081	67735	64436	64440
85	3489	5552	4428	4452	189	46797	52991	49831	49853	295	54047	60349	57213	57226	401	61141	67808	64507	64509
86	3573	5772	4555	4588	190	46859	53075	49902	49924	296	54134	60410	57288	57297	402	61195	67877	64572	64576
86.5	3609	5896	4620	4656	191	46921	53153	49972	49994	297	54199	60486	57359	57368	403	61250	67948	64639	64644
86.5	39641	45987	42840	42832	192	47010	53232	50041	50062	298	54277	60571	57435	57438	404	61316	68021	64710	64713
87	39682	46009	42872	42866	193	47102	53293	50116	50130	299	54360	60657	57508	57509	405	61400	68121	64776	64782
88	39752	46067	42940	42935	194	47183	53357	50179	50199	300	54420	60714	57575	57578	406	61465	68195	64844	64851
89	39821	46147	43009	43003	195	47237	53429	50248	50268	301	54490	60782	57639	57648	407	61538	68260	64902	64920
90	39897	46229	43080	43072	196	47294	53502	50319	50336	302	54558	60850	57709	57717	408	61582	68323	64973	64988

depth (cm)	min	max	\bar{X}	\bar{X}	depth (cm)	min	max	\bar{X}	\bar{X}	depth (cm)	min	max	\bar{X}	\bar{X}	depth (cm)	min	max	\bar{X}	\bar{X}
91	39958	46286	43152	43141	197	47367	53577	50392	50404	303	54627	60925	57776	57786	409	61651	68384	65053	65056
92	40027	46341	43215	43211	198	47435	53636	50459	50472	304	54686	60986	57849	57855	410	61722	68457	65121	65125
93	40115	46406	43281	43281	199	47485	53687	50526	50540	305	54746	61044	57921	57924	411	61789	68548	65191	65193
94	40176	46470	43353	43348	200	47539	53759	50590	50609	306	54829	61116	57988	57993	412	61857	68613	65264	65261
95	40234	46534	43413	43415	201	47605	53819	50663	50678	307	54885	61190	58062	58062	413	61920	68682	65339	65330
96	40306	46592	43481	43483	202	47698	53878	50726	50746	308	54963	61279	58131	58131	414	61968	68739	65402	65397
97	40378	46673	43552	43551	203	47761	53954	50792	50814	309	55025	61361	58202	58201	415	62042	68818	65466	65465
98	40442	46739	43617	43620	204	47824	54031	50862	50881	310	55094	61431	58272	58270	416	62114	68893	65531	65534
99	40509	46835	43687	43688	205	47870	54092	50929	50949	311	55146	61494	58340	58338	417	62170	68992	65605	65603
100	40585	46894	43760	43757	206	47941	54161	50998	51017	312	55211	61565	58416	58408	418	62234	69058	65677	65671
101	40656	46952	43824	43826	207	48023	54215	51072	51085	313	55282	61636	58482	58478	419	62292	69132	65753	65740
102	40725	47032	43893	43894	208	48082	54284	51135	51154	314	55345	61701	58556	58548	420	62351	69192	65818	65809
103	40792	47111	43956	43962	209	48142	54367	51203	51222	315	55435	61758	58618	58618	421	62427	69255	65886	65877
104	40874	47173	44024	44030	210	48230	54424	51269	51291	316	55488	61844	58688	58687	422	62486	69319	65953	65947
105	40933	47236	44083	44097	211	48321	54492	51348	51359	317	55543	61915	58765	58757	423	62559	69403	66019	66016
106	40997	47297	44153	44167	212	48381	54551	51415	51428	318	55617	61956	58832	58826	424	62633	69474	66089	66083
107	41067	47378	44225	44236	213	48442	54615	51491	51497	319	55678	62031	58897	58894	425	62692	69555	66152	66150
108	41129	47436	44298	44305	214	48512	54676	51551	51566	320	55761	62108	58959	58963	426	62750	69621	66228	66218
109	41189	47503	44360	44373	215	48569	54751	51615	51636	321	55832	62178	59032	59031	427	62838	69674	66292	66287
110	41274	47565	44428	44442	216	48623	54821	51689	51706	322	55913	62260	59100	59100	428	62892	69749	66352	66355
111	41335	47631	44497	44511	217	48702	54886	51761	51776	323	55966	62312	59168	59170	429	62954	69832	66420	66424
112	41406	47710	44560	44579	218	48763	54952	51830	51845	324	56017	62391	59241	59239	430	63007	69908	66490	66491

7.2.3 Sedimentology data

Table 7.10. Reassignment of sedimentary layers that were detailed in field notebooks.

Former layer	Revised layer	Observations
7	2b	subsequently recognised as an intrusive fill originating from layer 2.
6 & 9	9	both part of the same interbedded dirty flowstone
8b	10	uppermost occurrence of layer 10
10bc	10	initially distinguished solely on a textural change
13F	13	cemented section of layer 13
14F	14	cemented section of layer 14
15	-	localised intrusive section of mixed sediments entering pit via north-west corner of QI. Not included in this analysis.

Table 7.11 Sediment samples used for grain size analysis including starting weight, weight of <1 mm fraction, Munsell colour determinations and dry weight after HCl treatment.

Sample #	Layer	Starting weight (g)	Depth (cm)	>1mm weight (g)	Munsell colour	Dry weight after HCl treatment (g)
CC16-S3	1	3.88	n/a	0.42	7.5YR 4/4 brown	2.25
CC16-S4	2	5.04	n/a	0.27	7.5YR 3/3 dark brown	3.87
CC16-S12	2b	7.31	58	0.51	7.5YR 4/4 brown	5.9
CC16-S9	2b	6.67	n/a	0.67	7.5YR 4/4 brown	4.87
CC16-S5	3	6.03	n/a	1.04	7.5YR 7/4 pink	2.67
CC16-S6	4	7.65	n/a	0.61	5YR 4/4 reddish brown	6.42
CC16-S7	5	7.58	n/a	1.07	5YR 4/4 reddish brown	5.25
CC16-S10	8	6.28	n/a	0.59	5YR 4/6 yellowish red	4.83
CC16-S8	9	5.26	n/a	0.29	5YR 5/8 yellowish red	4.37
CC16-S11	9	7.64	n/a	0.49	5YR 4.6 yellowish red	6.49
CC16-S23a	9	9.55	73	0.2	5YR 4.6 yellowish red	8.02
CC16-S20	10	3.35	138	0.08	5YR 5/6 Yellowish red	2.93
CC16-S28	10	20.73	143	0.63	5YR 5/6 yellowish red	19.61
CC16-S34	10	22.88	232	1.48	5YR 5/6 yellowish red	21.09
CC17-S2	12	11.3	268	1.02	5YR 4/6 yellowish red	8.57
CC17-S4	12	13.18	288	0.89	5YR 4/6 yellowish red	11.25
CC17-S6	13	15.13	308	3.43	2.5YR 4/6 dark red	7.93
CC17-S10	13	24.56	348	8.71	2.5YR 4/6 dark red	9.45
CC17-SB	14	5.73	~360	0.27	5YR 4/4 reddish brown	4.77
CC17-S12	14	15.98	378	3.55	5YR 5/6 yellowish red	8.9
CC17-S15	14	15.68	408	3.28	5YR 5/6 yellowish red	7.94

7.3 Appendix C: Supplementary to Chapter 4

Table 7.12. Comparative specimens. Prefixes; AM, Australian Museum; FUR, Flinders University Palaeontology; M, SA Museum Mammal collection; NVM, Museums Victoria; SAM, SA Museum Palaeontology; WAM, Western Australian Museum.

Taxa	Specimen number
<i>Megalibgwilia ramsayi</i>	AM F10948, AM F86749, AM F51453
<i>Zaglossus bruijnii</i>	AM M34012, AM M47975
<i>Zaglossus bartoni</i>	AM M8263
<i>Zaglossus</i> sp.	AM F.78589
<i>Tachyglossus aculeatus</i>	FUR007
<i>Dasyurus geoffroii</i>	M3067 M3066 M79
<i>Dasyurus viverrinus</i>	M7213 M7214 M6313 M7220 M7216
<i>Dasyurus hallucatus</i>	M3251, M7229, AM M8097, AM M9097, AM 26350
<i>Dasyurus maculatus</i>	M2085, M7212, M10989, M27408, M7210
<i>Antechinus flavipes</i>	M7509, M7516, M7512
<i>Antechinus agilis</i>	M23166
<i>Antechinus swainsonii</i>	M15075, M9696
<i>Antechinus stuartii</i>	M23734
<i>Antechinomys laniger</i>	M22633
<i>Dasyuroides byrnei</i>	M1014, M13909
<i>Planigale gilesi</i>	M19907or M17907
<i>Dasycercus cristicauda</i>	M1349
<i>Phascogale tapoatafa</i>	M8593, AM 37229
<i>Sminthopsis murina</i>	M27304, M13929
<i>Perameles eremana</i>	AM P440
<i>Perameles myosurus</i>	AM P437
<i>Cercartetus nanus</i>	M18249, M7373.
<i>Petaurus breviceps</i>	M8262, M4621, M7309, M7313, FUR026
<i>Pseudocheirus peregrinus</i>	M21441, M21440, M9540
<i>Cercartetus concinnus</i>	M2606, M9209
<i>Cercartetus lepidus</i>	M9925, M11637
<i>Petaurus australis</i>	M1700, M2237, M2745, M2747, M2237
<i>Petaurus norfolcensis</i>	M7304, M7305
<i>Pseudocheirus archeri</i>	M45
<i>Pseudocheirus. herbertensis</i>	M43
<i>Petauroides volans</i>	M4712, M3277
<i>Pseudomys australis</i>	M43424, M43426, M43427
<i>Pseudomys delicatulus</i>	M5686, P41
<i>Pseudomys gracilicaudatus</i>	M4209, M13672, NMV P201893
<i>Pseudomys desortor</i>	M9549, M9548, M8204, M9550
<i>Pseudomys fumeus</i>	M15191
<i>Pseudomys higginsi</i>	NMV P162491.1
<i>Pseudomys oralis</i>	AM M34538
<i>Notomys mitchellii</i>	M13701

Taxa	Specimen number
<i>Notomys longicaudatus</i>	M2420, M2435
<i>Notomys fuscus</i>	M1367
<i>Notomys alexis</i>	M3136
<i>Thylacoleo carnifex</i>	SAM P21108, SAM P18263, SAM P28392, SAM P28863, SAM P28960, SAM P12784, WAM 02.6.1 LH.157

Layer:	1-8																															
	Spit #	2	3	4	5	6	7	8	9	10	11	12	13	14	15	16	17	18	19	20	21	22	23	24	25	26	27	28	29	30	31	
<i>Notamacropus parma</i>	0	0	0	0	0	0	0	0	0	0	0	0	0	0	0	0	0	0	0	0	0	0	0	0	0	0	0	0	1	0	0	
<i>Notamacropus parryi</i>	0	0	0	0	0	0	0	0	0	0	0	0	0	0	0	0	0	0	0	0	0	0	0	0	0	0	0	0	0	0	0	
<i>Notamacropus</i> sp. indet.	0	0	0	0	0	0	0	0	0	0	1	0	0	0	0	0	0	0	0	0	0	0	0	0	0	0	0	0	0	0	0	
<i>Notomys</i> sp. indet.	0	0	0	0	0	1	0	0	0	0	1	0	0	0	0	1	0	0	0	0	1	0	0	0	0	0	0	1	1	1	2	
<i>Onychogalea frenata</i>	0	0	0	0	0	0	0	0	0	0	1	0	0	1	0	0	0	0	0	0	0	0	0	0	0	0	0	0	0	0	0	
<i>Onychogalea lunata</i>	0	0	0	0	0	0	0	0	0	0	0	0	0	0	0	0	0	0	0	0	0	0	0	0	0	0	0	0	0	0	0	
<i>Osphranter robustus</i>	0	0	0	0	0	0	0	0	0	0	0	0	0	0	0	0	0	0	0	0	0	0	0	0	0	0	0	0	0	0	0	
cf. <i>Osphranter robustus</i>	0	0	0	0	0	0	0	0	0	0	0	0	0	0	0	0	0	0	0	0	0	0	0	0	0	0	0	0	0	0	0	
<i>Osphranter rufus</i>	0	0	0	0	0	0	0	0	0	0	0	0	0	0	0	0	0	0	0	0	0	0	0	0	0	0	0	0	0	0	0	
<i>Palorchestes azael</i>	0	0	0	0	0	0	0	0	0	0	0	0	0	0	0	0	0	0	0	0	0	0	0	0	0	0	0	0	0	0	0	
<i>Perameles gunnii nasuta</i>	1	0	0	0	0	0	0	0	0	1	1	1	0	0	0	0	0	1	0	1	0	1	0	0	0	1	1	1	1	1		
<i>Petaurus breviceps</i>	0	0	0	0	0	0	0	0	0	0	1	0	0	0	0	0	0	0	0	0	0	0	0	0	0	0	0	0	0	0	0	
<i>Petaurus</i> sp. cf. <i>breviceps</i>	0	0	0	0	0	0	0	0	0	0	0	0	0	0	0	0	0	0	0	0	0	0	0	0	0	0	0	0	0	0	0	
<i>Petrogale</i> sp. indet.	0	0	0	0	0	0	0	0	0	0	0	0	0	0	0	0	0	0	0	0	0	0	0	0	0	0	0	0	0	0	0	
<i>Phascogale tapoatafa</i>	0	0	0	0	0	0	0	0	0	0	0	0	0	0	0	0	0	0	0	0	0	0	0	0	0	0	0	0	0	0	0	
<i>Phascogale</i> sp. cf. <i>tapoatafa</i>	0	0	0	0	0	0	0	0	0	0	0	0	0	0	0	0	0	0	0	0	0	0	0	0	0	0	0	0	0	0	0	
<i>Potorous tridactylus</i>	0	0	1	0	0	0	0	0	0	0	0	1	0	0	0	0	0	1	0	0	0	0	0	0	0	0	1	0	0	1	0	
<i>Potoroinae</i> sp. indet.	0	0	0	0	0	0	0	0	0	0	0	0	0	0	0	0	0	0	0	0	0	0	0	0	0	0	0	0	0	0	0	
<i>Procoptodon goliah</i>	0	0	0	0	0	0	0	0	0	0	0	0	0	0	0	0	0	0	0	0	0	0	0	0	0	0	0	0	0	1	0	
<i>Protomnodon brehus</i>	0	0	0	0	0	0	0	0	0	0	0	0	0	0	0	0	0	0	0	0	0	0	0	0	0	0	0	0	0	0	0	
<i>Protomnodon</i> sp. cf. <i>brehus</i>	0	0	0	0	0	0	0	0	0	0	0	0	0	0	0	0	0	0	0	0	0	0	0	0	0	0	0	0	0	0	0	
<i>Protomnodon</i> sp. indet.	0	0	0	0	0	0	0	0	0	0	0	0	0	0	0	0	0	0	0	0	0	0	0	0	0	0	0	0	0	0	0	
cf. <i>Protomnodon</i> sp. indet.	0	0	0	0	0	0	0	0	0	0	0	0	0	0	0	0	0	0	0	0	0	0	0	0	0	0	0	0	0	0	0	
<i>Pseudocheirus peregrinus</i>	0	0	0	0	0	0	0	0	0	0	1	0	0	0	0	0	0	0	0	0	0	0	0	0	0	0	0	0	0	0	0	
<i>Pseudomys australis</i>	0	1	0	0	0	1	1	1	0	1	7	7	7	7	0	2	0	1	0	0	2	1	3	2	1	2	2	5	5	2		
<i>Pseudomys desertor</i>	0	0	0	0	0	0	0	0	0	0	0	0	0	1	0	0	0	0	0	0	0	0	0	0	0	0	0	0	0	0	0	
<i>Pseudomys</i> sp. cf. <i>desertor</i>	0	0	0	0	0	0	0	0	0	0	0	0	0	0	0	0	0	0	0	0	0	0	0	0	0	0	0	0	1	0	0	
cf. <i>Pseudomys fumeus</i>	0	0	0	0	0	0	0	0	0	0	0	0	0	0	0	0	0	0	0	0	0	0	0	0	0	0	0	0	0	0	0	
cf. <i>Pseudomys gouldii</i>	0	0	0	0	0	0	0	0	0	0	0	0	0	0	0	0	0	0	0	0	0	0	0	0	0	0	0	0	0	0	0	
<i>Pseudomys gouldii</i>	0	0	0	0	0	0	1	0	0	0	0	0	0	0	0	0	0	0	0	0	0	0	0	0	0	0	0	0	0	0	0	
<i>Pseudomys gracilicaudatus</i>	0	0	0	0	0	0	0	0	0	0	1	1	0	0	0	1	0	0	0	0	0	0	0	0	0	0	0	0	0	0	0	0
cf. <i>Pseudomys gracilicaudatus</i>	0	0	0	0	0	0	0	0	0	0	0	0	0	0	0	0	0	0	0	0	0	0	0	0	0	0	0	0	0	0	0	
<i>Pseudomys</i> sp. cf. <i>gracilicaudatus</i>	0	0	0	0	0	0	0	0	0	0	0	0	0	0	0	0	0	0	0	0	0	0	0	0	0	0	0	0	0	0	0	
<i>Pseudomys novaehollandiae</i>	0	0	0	0	1	0	0	0	0	0	1	1	1	0	0	1	0	0	0	1	0	1	0	0	0	0	0	0	0	0	0	
<i>Pseudomys oralis</i>	0	0	0	0	0	0	0	0	0	0	0	0	0	0	0	0	0	0	0	0	0	0	0	0	0	0	0	0	0	0	0	
<i>Pseudomys</i> sp. cf. <i>oralis</i>	0	0	0	0	0	0	0	0	0	0	0	1	0	0	0	0	0	0	0	0	0	0	0	0	0	0	0	0	0	0	0	
<i>Rattus fuscipes</i>	0	0	0	0	0	0	0	0	0	0	0	0	1	0	0	0	0	0	0	0	0	0	0	0	0	0	0	0	0	0	0	
<i>Rattus</i> sp. cf. <i>tunneyi</i>	2	0	0	0	0	0	0	0	0	0	1	1	0	1	1	0	0	1	0	0	0	0	0	0	0	0	0	0	0	0	0	
<i>Rattus</i> sp. cf. <i>lutreolus</i>	0	0	0	0	0	0	0	0	0	0	0	0	0	0	0	0	0	0	0	0	0	0	0	0	0	0	0	0	0	0	0	
<i>Rattus</i> sp. indet.	0	0	0	0	2	0	0	0	0	0	0	0	0	0	0	0	0	0	0	0	0	0	0	0	0	0	0	0	1	0	0	
<i>Sarcophilus lanarius</i>	0	0	0	0	0	0	0	0	0	0	0	0	0	0	0	0	0	0	0	0	0	0	0	0	0	0	0	0	0	0	0	
<i>Simosthenurus pales</i>	0	0	0	0	0	0	0	0	0	0	0	0	0	0	0	0	0	0	0	0	0	0	0	0	0	0	0	0	0	0	0	
<i>Sminthopsis crassicaudata</i>	0	0	0	0	0	0	0	0	0	0	0	0	0	0	1	0	0	0	0	0	0	0	0	0	0	0	0	0	1	1	0	

Layer:	1-8																															
	Spit #	2	3	4	5	6	7	8	9	10	11	12	13	14	15	16	17	18	19	20	21	22	23	24	25	26	27	28	29	30	31	
<i>Sminthopsis</i> sp. cf. <i>crassicaudata</i>	0	0	0	0	0	0	0	0	0	0	0	0	0	0	0	0	0	0	0	0	0	0	0	0	0	0	0	0	0	0	0	0
cf. <i>Sminthopsis crassicaudata</i>	0	0	0	0	0	0	0	0	0	0	0	0	0	0	0	0	0	0	0	0	0	0	0	0	0	0	0	0	0	0	0	0
<i>Sminthopsis murina</i>	0	0	1	0	0	0	0	0	0	0	0	0	0	0	0	0	0	0	0	0	0	0	0	0	0	0	0	0	0	0	1	0
<i>Sminthopsis</i> sp. cf. <i>murina</i>	0	0	0	0	0	0	0	0	0	0	0	0	0	0	0	0	0	0	0	0	0	0	0	0	0	0	0	0	0	0	0	0
<i>Sminthopsis</i> sp. indet.	0	0	0	0	0	0	0	0	0	0	0	0	0	0	0	0	0	0	0	0	0	0	0	0	0	0	0	0	0	0	0	0
<i>Sthenurinae</i> sp. indet.	0	0	0	0	0	0	0	0	0	0	0	0	0	0	0	0	0	0	0	0	0	0	0	0	0	0	0	0	0	0	0	0
<i>Sthenurus andersoni</i>	0	0	0	0	0	0	0	0	0	0	0	0	0	0	0	0	0	0	0	0	0	0	0	0	0	0	0	0	0	0	0	0
<i>Sthenurus atlas</i>	0	0	0	0	0	0	0	0	0	0	0	0	0	0	0	0	0	0	0	0	0	0	0	0	0	0	0	0	0	0	0	0
<i>Tachyglossus aculeatus</i>	0	0	0	0	0	0	0	0	0	0	0	0	0	0	0	0	0	0	0	0	0	0	0	0	0	0	0	0	0	0	0	0
<i>Thylacinus cynocephalus</i>	0	0	0	0	0	0	0	0	0	0	0	0	0	0	0	0	0	0	0	0	0	0	0	0	0	0	0	0	0	0	0	0
<i>Thylacinus Sarcophilus</i> sp. indet.	0	0	0	0	0	0	0	0	0	0	0	0	0	0	0	0	0	0	0	0	0	0	0	0	0	0	0	0	0	0	0	0
<i>Thylacoleo carnifex</i>	0	0	0	0	0	0	0	0	0	0	0	0	0	0	0	0	0	0	0	0	0	0	0	0	0	0	0	0	0	0	0	0
<i>Trichosurus</i> sp. cf. <i>vulpecula</i>	0	0	0	0	0	0	0	0	0	0	0	0	0	0	0	0	0	0	0	0	0	0	0	0	0	0	0	0	0	0	0	0
<i>Trichosurus vulpecula</i>	1	1	0	0	0	0	0	1	0	0	0	0	0	0	1	0	0	0	0	0	0	0	0	0	0	0	0	1	0	2	1	0
Vombatidae sp. indet.	0	0	0	0	0	0	0	0	0	0	0	0	0	0	0	0	0	0	0	0	0	0	0	0	0	0	0	0	0	0	0	0
<i>Vombatus ursinus</i>	0	0	0	0	0	0	0	0	0	1	0	0	0	0	0	0	0	0	0	0	0	0	0	0	1	0	0	0	1	0	0	0
<i>Wallabia bicolor</i>	0	0	0	0	0	0	0	0	0	0	0	0	0	0	0	0	0	0	0	0	0	0	0	0	0	0	0	0	0	0	0	0
Accipitriformes sp. indet.	0	0	0	0	0	0	0	0	0	0	0	0	0	0	0	0	0	0	0	0	0	0	0	0	0	0	0	0	0	0	0	0
<i>Aquila audax</i>	0	0	0	0	0	0	0	0	0	0	0	0	0	0	0	0	0	0	0	0	0	0	0	0	0	0	0	0	0	0	0	0
Aves sp. indet.	1	0	0	1	1	1	0	1	1	1	0	1	1	1	1	1	0	1	0	0	0	1	0	0	1	0	1	0	1	0	1	1
<i>Centropus</i> sp. cf. <i>colossus</i>	0	0	0	0	0	0	0	0	0	0	0	0	0	0	0	0	0	0	0	0	0	0	0	0	0	0	0	0	0	0	0	0
<i>Coturnix pectoralis</i>	0	0	0	0	0	0	0	0	0	0	0	0	0	0	0	0	0	0	0	0	0	0	0	0	0	0	0	0	0	0	0	0
<i>Coturnix</i> sp. indet.	0	0	0	0	0	0	0	0	0	0	0	0	0	0	0	0	0	0	0	0	0	0	0	0	0	0	0	0	0	0	0	0
<i>Dromaius novaehollandiae</i>	0	0	0	0	0	0	0	0	0	0	0	0	0	0	0	0	0	0	0	0	0	0	0	0	0	0	0	0	0	0	0	0
<i>Menura novaehollandiae</i>	0	0	0	0	0	0	0	0	0	0	0	0	0	0	0	0	0	0	0	0	0	0	0	0	0	0	0	0	0	0	0	0
cf. <i>Menura novaehollandiae</i>	0	0	0	0	0	0	0	0	0	0	0	0	0	0	0	0	0	0	0	0	0	0	0	0	0	0	0	0	0	0	0	0
Passeriformes sp. indet.	0	0	0	0	0	0	0	0	0	0	0	0	0	0	0	0	0	0	0	0	0	0	0	0	0	0	0	0	0	1	0	0
<i>Tyto</i> sp. indet.	0	0	0	0	0	0	0	0	0	0	0	0	0	0	0	0	0	0	0	0	0	0	0	0	0	0	0	0	0	0	0	0
<i>Tyto</i> sp. cf. <i>novaehollandiae</i>	0	0	0	0	0	0	0	0	0	0	0	0	0	0	0	0	0	0	0	0	0	0	0	0	0	0	0	0	0	0	0	0
Agamidae sp. indet.	0	0	0	0	0	1	1	0	0	0	0	0	0	0	0	0	0	0	0	0	0	0	0	0	0	0	0	0	0	0	0	0
cf. Agamidae sp. indet.	0	0	0	0	0	0	0	0	0	0	0	0	0	0	0	0	0	0	0	0	0	0	0	0	0	0	0	0	0	0	0	0
<i>Egernia cunninghami</i>	0	0	0	0	0	0	0	0	0	0	0	0	0	0	0	0	0	0	0	0	0	0	0	0	0	0	0	0	0	0	0	0
<i>Egernia</i> sp. cf. <i>cunninghami</i>	0	0	0	0	0	0	0	0	0	0	0	0	0	0	0	0	0	0	0	0	0	0	0	0	0	0	0	0	0	0	0	0
<i>Egernia frangens</i>	0	0	0	0	0	0	0	0	0	0	0	0	0	0	0	0	0	0	0	0	0	0	0	0	0	0	0	0	0	0	0	0
<i>Egernia</i> sp. cf. <i>rugosa</i>	0	0	0	0	0	0	0	0	0	0	0	0	0	0	0	0	0	0	0	0	0	0	0	0	0	0	0	0	0	0	0	0
<i>Egernia striolata</i>	0	0	0	0	0	0	0	0	0	0	0	0	0	0	0	0	0	0	0	0	0	0	0	0	0	0	0	0	0	0	0	0
<i>Egernia</i> sp. indet.	0	0	0	0	0	0	0	0	0	0	0	0	0	0	0	0	0	0	0	0	0	0	0	0	0	0	0	0	0	0	0	0
cf. <i>Egernia</i> sp. indet.	0	0	0	0	0	0	0	0	0	0	0	0	0	0	0	0	0	0	0	0	0	0	0	0	0	0	0	0	0	0	0	0
<i>Egernia Liopholis</i> sp. indet.	0	0	0	0	0	0	0	0	0	0	1	0	0	0	0	0	0	0	0	0	0	0	0	0	0	0	0	0	0	0	0	0
Elapidae sp. indet.	1	0	0	0	0	0	0	1	0	0	0	0	1	1	0	0	1	0	0	0	0	0	0	0	0	0	0	0	0	0	0	0
Gekkonidae sp. indet.	0	0	0	0	0	0	0	0	0	0	0	1	2	0	1	0	0	1	0	0	0	0	0	0	0	0	0	0	0	0	0	0
<i>Liopholis inornata</i>	0	0	0	0	0	0	0	0	0	0	0	0	0	0	0	0	0	0	0	0	0	0	0	0	0	0	0	0	0	0	0	0
<i>Liopholis</i> sp. indet.	0	0	0	0	0	0	0	0	0	0	0	0	0	0	0	0	0	0	0	0	0	0	0	0	0	0	0	0	0	0	0	0

	Layer:		1-8																														
	Spit #		2	3	4	5	6	7	8	9	10	11	12	13	14	15	16	17	18	19	20	21	22	23	24	25	26	27	28	29	30	31	
<i>Liopholis whitii</i>			0	0	0	0	0	0	0	0	0	0	0	0	0	0	0	0	0	0	0	0	0	0	0	0	0	0	0	0	0	0	0
<i>Morelia</i> sp. indet.			0	0	0	0	0	0	0	0	0	0	0	0	0	0	0	0	0	0	0	0	0	0	0	0	0	0	0	0	1	0	0
Pythonidae sp. indet.			0	0	0	0	0	0	0	1	0	0	0	1	0	0	0	0	0	0	0	0	0	0	0	0	0	0	0	0	0	0	0
Scincidae sp. indet.			0	0	0	0	0	0	0	0	0	0	0	1	0	0	0	0	1	0	0	0	0	0	0	0	0	0	0	0	0	0	0
Sphenomorphinae sp. indet.			0	0	0	0	0	0	0	0	0	0	0	0	0	0	0	0	0	0	0	0	0	0	0	0	0	0	0	0	0	0	0
Sphenomorphus sp. indet.			0	0	0	0	0	0	0	0	0	0	0	0	0	0	0	0	0	0	0	0	0	0	0	0	0	0	0	0	0	0	0
cf. Sphenomorphus sp. indet.			0	0	0	0	0	0	0	0	0	0	0	0	0	0	0	0	0	0	0	0	0	0	0	0	0	0	0	0	0	0	0
<i>Tiliqua frangens</i>			0	0	0	0	0	0	0	1	0	0	1	0	0	0	0	0	0	0	0	0	0	0	0	0	0	0	0	0	1	0	0
Varanidae sp. indet.			0	0	0	0	0	0	0	0	0	0	0	0	0	0	0	0	0	0	0	0	0	0	0	0	0	0	0	0	0	0	0
Varanus sp. indet.			0	0	0	0	0	0	0	0	0	0	0	0	0	1	0	0	0	0	0	0	0	0	0	0	0	0	0	0	0	0	0
<i>Varanus varius</i>			0	0	0	0	0	0	0	0	0	0	0	0	0	0	0	0	0	0	0	0	0	0	0	0	0	0	0	0	0	0	0
<i>Wonambi naracoortensis</i>			0	0	0	0	0	0	0	0	0	0	0	0	0	0	0	0	0	0	0	0	0	0	0	0	0	0	0	0	0	0	0
Anura sp. indet.			1	1	1	1	1	1	1	1	0	1	0	2	1	1	0	0	0	1	0	0	0	0	0	0	0	0	0	0	1	1	1
<i>Crinia</i> sp. indet.			0	0	0	0	0	0	0	0	0	0	0	0	0	0	0	1	0	0	0	0	0	0	0	0	0	0	0	0	0	0	0
<i>Limnodynastes tasmaniensis</i>			0	0	0	0	0	0	0	0	0	1	0	0	0	1	0	0	0	0	0	0	0	0	0	0	0	0	0	0	0	0	0
<i>Litoria rubella</i>			0	0	0	0	0	0	0	0	0	1	0	0	0	0	0	0	0	0	0	0	0	0	0	0	0	0	0	0	0	0	0
Fish			0	1	0	0	0	0	0	0	0	0	0	0	0	0	0	0	0	0	0	0	0	0	0	0	0	0	0	0	0	0	

	Layer:		1-8																	9							10a						
	Spit #		32	33	34	35	36	37	38	39	40	41	42	43	44	45	46	47	48	49	50	52	53	54	55	56	57	58	59	60	61	62	
<i>Acrobates pygmaeus</i>			0	0	0	0	0	0	0	0	0	0	0	0	0	0	0	0	0	0	0	0	0	0	0	0	0	0	0	0	0	0	0
<i>Aepyrymnus rufescens</i>			1	0	0	0	0	0	0	0	0	0	0	0	0	0	0	0	0	0	0	0	0	0	0	0	0	0	0	0	0	0	0
<i>Antechinus flavipes</i>			0	0	0	0	0	0	0	0	0	0	0	0	0	0	0	0	0	0	0	0	0	0	0	1	0	0	0	0	0	0	
<i>Baringa</i> sp. nov. 1			0	0	0	0	0	0	0	0	0	0	0	0	0	0	0	0	0	0	0	0	0	0	0	0	0	0	0	0	0	0	
<i>Bettongia gaimardi</i>			0	0	0	0	0	0	0	0	0	0	0	0	0	0	0	0	0	0	0	0	0	0	0	0	0	0	0	0	0	0	0
<i>Bettongia lesueur</i>			0	0	1	1	0	0	0	0	0	0	0	0	0	0	0	0	0	1	0	0	0	0	0	0	0	1	0	0	0	0	
<i>Bettongia</i> sp. indet.			0	0	0	0	0	0	0	0	0	0	0	0	0	0	0	0	0	0	1	0	0	0	0	0	0	0	0	0	0	0	
<i>Cercartetus nanus</i>			0	0	0	0	0	0	0	0	0	0	0	0	0	0	0	0	0	0	0	0	0	0	0	0	0	0	0	0	0	0	0
<i>Chaeropus ecaudatus</i>			0	0	0	0	0	0	0	0	0	0	0	0	0	0	0	0	0	0	0	0	0	0	0	0	0	0	0	0	0	0	0
<i>Congruus kitcheneri</i>			0	0	0	0	0	0	0	0	0	0	0	0	0	0	0	0	0	0	0	0	0	0	0	0	0	0	0	0	0	0	0
<i>Conilurus albipes</i>			0	0	0	0	0	0	0	1	0	1	0	1	0	0	0	0	0	1	0	0	0	0	0	0	0	0	0	0	0	0	0
cf. <i>Dasyuroides byrnei</i>			0	0	0	0	0	0	0	0	0	0	0	0	0	0	0	0	1	1	0	0	0	0	0	0	0	0	0	0	0	0	0
Dasyuridae indet. sp. 3			0	0	0	0	0	0	0	0	0	0	0	0	0	0	0	0	0	0	0	0	0	0	0	0	0	0	0	0	0	0	0
Dasyuridae indet. sp. 4			0	0	0	0	0	0	0	0	0	0	0	0	0	0	0	0	0	0	0	0	0	0	0	0	0	0	0	0	0	0	0
<i>Dasyurus geoffroii viverrinus</i>			0	1	0	0	0	0	0	1	0	0	0	1	0	1	1	1	1	1	1	0	0	0	0	1	3	2	3	1	0	0	
<i>Dasyurus maculatus</i>			0	0	0	0	0	0	0	0	0	0	0	0	0	0	0	0	0	0	0	0	0	0	0	0	0	0	0	0	0	0	0
Diprotodontidae gen. et. sp. indet.			0	0	0	0	0	0	0	0	1	0	0	0	0	0	0	0	0	0	0	0	0	0	0	0	0	0	0	0	0	0	0
<i>Hydromys chrysogaster</i>			0	0	0	0	0	0	0	0	0	0	0	0	0	0	0	0	0	0	0	0	0	0	0	0	0	0	0	0	0	0	0
<i>Isodon obesulus</i>			0	0	0	1	1	0	0	1	0	0	0	1	1	0	1	0	1	0	0	0	0	0	0	1	1	1	1	0	1	1	
<i>Lagorchestes leporides</i>			0	0	0	0	0	0	0	1	0	0	0	0	0	0	0	0	0	0	0	0	0	0	0	0	2	0	0	0	0	0	
<i>Macroderma gigas</i>			0	0	0	0	0	0	0	0	0	0	0	0	0	0	0	0	0	0	0	0	0	0	0	0	0	0	0	0	0	0	0
<i>Macropus giganteus</i>			0	0	0	0	0	0	0	0	0	0	0	0	0	0	0	0	0	0	0	0	0	0	0	0	0	0	0	1	0	0	0
<i>Macropus</i> sp. indet.			0	0	0	0	0	0	0	0	0	0	0	0	0	0	0	0	0	0	0	0	0	0	0	0	0	0	0	0	0	0	0

	Layer:		1-8							9													10a									
	Spit #	32	33	34	35	36	37	38	39	40	41	42	43	44	45	46	47	48	49	50	52	53	54	55	56	57	58	59	60	61	62	
<i>Macrotis lagotis</i>		0	0	0	0	0	0	0	0	0	0	0	0	0	0	0	0	0	0	0	0	0	0	0	0	0	0	0	0	0	0	
<i>Mastacomys fuscus</i>		0	0	0	0	0	0	0	0	0	0	0	0	0	0	0	0	0	0	0	0	0	0	0	0	1	1	1	1	0	0	0
<i>Megalibgwilia ramsayi</i>		0	0	0	0	0	0	0	0	0	0	0	0	0	0	0	0	0	0	0	0	0	0	0	0	0	0	0	0	0	0	
<i>Microchiroptera sp. indet.</i>		0	0	0	0	0	0	0	0	1	0	0	0	1	0	0	1	0	1	0	0	0	0	0	0	0	0	0	1	0	1	
Murinae sp. 1		0	0	0	0	0	0	0	0	0	0	0	0	0	0	0	0	0	0	0	0	0	0	0	0	0	0	0	0	0	0	
Murinae sp. 2		0	0	0	0	0	0	0	0	0	0	0	0	0	0	0	0	0	0	0	0	0	0	0	0	0	0	0	0	0	0	
Murinae sp. 3		0	0	0	0	0	0	0	0	0	0	0	0	0	0	0	0	0	0	0	0	0	0	0	0	0	0	0	0	0	0	
Murinae sp. 4		0	0	0	0	0	0	0	0	0	0	0	0	0	0	0	0	0	0	0	0	0	0	0	0	0	0	0	0	0	0	
Murinae sp. 5		0	0	0	0	0	0	0	0	0	0	0	0	0	0	0	0	0	0	0	0	0	0	0	0	0	0	0	0	0	0	
Murinae sp. 6		0	0	0	0	0	0	0	0	0	0	0	0	0	0	0	0	0	0	0	0	0	0	0	0	0	0	0	0	0	0	
Murinae sp. 7		0	0	0	0	0	0	0	0	0	0	0	0	0	0	0	0	0	0	0	0	0	0	0	0	0	0	0	0	0	0	
<i>Notamacropus agilis</i>		0	0	0	0	0	0	0	0	0	0	0	0	0	0	0	0	0	0	0	0	0	0	0	0	0	0	0	0	0	0	
<i>Notamacropus dorsalis</i>		0	0	0	0	0	0	0	0	0	0	0	0	0	0	0	0	0	0	0	0	0	0	0	0	0	0	0	0	0	0	
<i>Notamacropus sp. cf. dorsalis</i>		0	0	0	0	0	0	0	0	0	0	0	0	0	0	0	0	0	0	0	0	0	0	0	0	0	0	0	0	0	0	
<i>Notamacropus parma</i>		0	0	0	0	1	0	0	0	0	0	0	0	0	0	0	0	0	0	0	0	0	0	0	0	0	0	0	0	0	0	
<i>Notamacropus parryi</i>		0	0	0	0	0	0	0	0	0	0	0	0	0	0	0	0	0	0	0	0	0	0	0	0	0	0	0	0	0	0	
<i>Notamacropus sp. indet.</i>		0	0	0	0	0	0	0	0	0	0	0	0	0	0	0	0	0	0	0	0	0	0	0	0	0	0	0	0	0	0	
<i>Notomys sp. indet.</i>		1	1	0	1	1	0	0	0	2	0	1	0	1	0	1	0	1	4	1	1	0	0	0	0	8	3	2	0	1	0	1
<i>Onychogalea frenata</i>		0	0	0	0	1	0	0	0	0	0	0	0	1	0	0	0	0	0	0	0	0	0	0	0	0	0	0	0	0	0	
<i>Onychogalea lunata</i>		0	0	0	1	0	0	0	0	0	0	0	0	0	0	0	0	0	0	0	0	0	0	0	0	0	0	0	0	0	0	
<i>Osphranter robustus</i>		0	0	0	0	0	0	0	0	0	0	0	0	0	0	0	0	0	0	0	0	0	0	0	0	0	0	0	0	0	0	
cf. <i>Osphranter robustus</i>		0	0	0	0	0	0	0	0	0	0	0	0	0	0	0	0	0	0	0	0	0	0	0	0	0	0	0	0	0	0	
<i>Osphranter rufus</i>		0	0	0	0	0	0	0	0	0	0	0	0	0	0	0	0	0	0	1	0	0	0	0	0	0	0	0	0	0	0	
<i>Palorchestes azael</i>		0	0	0	0	0	0	0	0	0	0	0	0	0	0	0	0	0	0	0	0	0	0	0	0	0	0	0	0	0	0	
<i>Perameles gunnii nasuta</i>		1	0	1	1	0	0	1	1	1	0	1	1	1	1	1	1	1	1	0	1	0	0	1	1	1	1	1	0	1	1	
<i>Petaurus breviceps</i>		0	0	0	0	0	0	0	0	0	0	0	0	0	0	0	0	0	0	1	0	0	0	0	0	0	0	0	0	0	0	
<i>Petaurus sp. cf. breviceps</i>		0	0	0	0	0	0	0	0	0	0	0	0	0	0	0	0	0	0	0	0	0	0	0	0	0	0	0	0	0	0	
<i>Petrogale sp. indet.</i>		0	0	0	0	0	0	0	0	0	0	0	0	0	0	0	0	0	0	0	0	0	0	0	0	0	0	0	0	0	0	
<i>Phascogale tapoatafa</i>		0	0	0	0	0	0	0	0	0	0	0	0	0	0	0	0	0	0	0	0	0	0	0	0	0	0	0	0	0	0	
<i>Phascogale sp. cf. tapoatafa</i>		0	0	0	0	0	0	0	0	0	0	0	0	0	0	0	0	0	0	0	0	0	0	0	0	0	0	0	0	0	0	
<i>Potorous tridactylus</i>		0	0	0	0	0	0	0	0	0	0	0	0	0	0	0	0	0	0	0	0	0	0	0	0	0	0	0	0	0	1	
Potoroinae sp. indet.		0	0	0	0	0	0	0	0	0	0	0	0	0	0	0	0	0	0	0	0	0	0	0	0	0	0	0	0	0	0	
<i>Procoptodon goliah</i>		0	0	0	0	0	0	0	0	0	0	0	0	0	0	0	0	0	0	0	0	0	0	0	0	0	0	0	0	0	0	
<i>Protomnodon brehus</i>		0	0	0	0	0	0	0	0	0	0	0	0	0	0	0	0	0	0	0	0	0	0	0	0	0	0	0	0	0	0	
<i>Protomnodon sp. cf. brehus</i>		0	0	0	0	0	0	0	0	0	0	0	0	0	0	0	0	0	0	0	0	0	0	0	0	0	0	0	0	0	0	
<i>Protomnodon sp. indet.</i>		0	0	0	0	0	0	0	0	0	0	0	0	0	0	0	0	0	0	0	0	0	0	0	0	0	0	0	0	0	0	
cf. <i>Protomnodon sp. indet.</i>		0	0	0	0	0	0	0	0	0	0	0	0	0	0	0	0	0	0	0	0	0	0	0	0	0	0	0	0	0	0	
<i>Pseudocheirus peregrinus</i>		0	0	0	0	0	0	0	0	0	0	0	0	0	0	0	0	0	0	0	0	0	0	0	0	0	0	0	0	0	0	
<i>Pseudomys australis</i>		2	2	4	6	3	1	0	2	7	0	6	1	4	1	9	7	10	45	9	5	1	6	1	20	33	24	10	7	0	13	
<i>Pseudomys desertor</i>		0	0	1	1	1	0	0	0	1	0	0	0	1	0	1	0	0	2	2	0	0	0	0	0	4	2	1	0	1	1	
<i>Pseudomys sp. cf. desertor</i>		0	0	0	0	0	0	0	0	0	0	0	0	0	0	0	0	0	0	0	0	0	0	0	0	0	0	0	0	0	0	
cf. <i>Pseudomys fumeus</i>		0	0	0	0	0	0	0	0	0	0	0	0	0	0	0	0	0	0	0	0	0	0	0	0	0	0	0	0	0	0	
cf. <i>Pseudomys gouldii</i>		0	0	0	0	0	0	0	0	0	0	0	0	0	0	0	0	0	0	0	0	0	0	0	0	0	0	0	0	0	0	

	Layer:		1-8							9															10a						
	Spit #	32	33	34	35	36	37	38	39	40	41	42	43	44	45	46	47	48	49	50	52	53	54	55	56	57	58	59	60	61	62
<i>Pseudomys gouldii</i>	0	0	0	0	0	0	0	0	0	0	0	0	0	0	0	0	0	0	0	0	0	0	0	0	0	0	0	0	0	0	0
<i>Pseudomys gracilicaudatus</i>	0	0	0	0	0	0	0	0	0	0	0	0	0	0	0	0	0	0	0	0	0	0	0	0	0	0	0	0	0	0	0
cf. <i>Pseudomys gracilicaudatus</i>	0	0	0	0	0	0	0	0	0	0	0	0	0	0	0	0	0	0	0	0	0	0	0	0	0	0	0	0	0	0	0
<i>Pseudomys sp. cf. gracilicaudatus</i>	0	0	0	0	0	0	0	0	0	0	0	0	0	0	0	0	0	0	0	0	0	0	0	0	0	0	0	0	0	0	0
<i>Pseudomys novaehollandiae</i>	0	0	1	0	0	0	0	0	1	0	0	0	0	0	0	0	0	1	0	0	0	1	0	1	2	1	0	1	0	1	
<i>Pseudomys oralis</i>	0	0	0	0	0	0	0	0	0	0	0	0	0	0	0	0	0	0	0	0	0	0	0	0	0	0	0	0	0	0	
<i>Pseudomys sp. cf. oralis</i>	0	0	0	0	0	0	0	0	0	0	0	0	0	0	0	0	0	0	0	0	0	0	0	0	0	0	0	0	0	0	
<i>Rattus fuscipes</i>	0	0	0	0	0	0	0	0	0	0	0	0	0	0	0	0	0	0	0	0	0	0	0	0	0	0	0	0	0	0	
<i>Rattus sp. cf. tunneyi</i>	0	0	0	0	0	0	0	0	0	0	0	0	0	0	0	0	0	0	0	0	0	0	0	0	0	0	0	0	0	0	
<i>Rattus sp. cf. lutreolus</i>	0	0	0	0	0	0	0	0	0	0	0	0	0	0	0	0	0	0	0	0	0	0	0	0	0	0	0	0	0	0	
<i>Rattus sp. indet.</i>	0	0	0	1	0	0	0	0	0	0	0	0	0	0	0	0	0	0	1	0	0	0	0	0	0	0	0	0	0	0	
<i>Sarcophilus lanarius</i>	0	0	0	0	0	0	0	0	0	0	0	0	0	0	0	0	0	0	0	0	0	0	0	0	0	0	0	0	0	0	
<i>Simosthenurus pales</i>	0	0	0	0	0	0	0	0	0	0	0	0	0	0	0	0	0	0	0	0	0	0	0	0	0	0	0	0	0	0	
<i>Sminthopsis crassicaudata</i>	0	0	0	0	0	0	0	0	0	0	0	0	0	1	1	0	1	0	0	0	1	0	1	1	1	0	0	0	0	0	
<i>Sminthopsis sp. cf. crassicaudata</i>	0	0	0	0	0	0	0	0	0	0	0	0	0	0	0	0	0	0	0	0	0	0	0	0	0	0	0	0	0	0	
cf. <i>Sminthopsis crassicaudata</i>	0	0	0	0	0	0	0	0	0	0	0	0	0	0	0	0	0	0	0	0	0	0	0	0	0	0	0	0	0	0	
<i>Sminthopsis murina</i>	0	0	0	0	0	0	0	1	0	0	0	0	0	0	0	0	0	1	0	0	0	0	0	1	1	1	0	0	0	0	
<i>Sminthopsis sp. cf. murina</i>	0	0	0	1	0	0	0	0	0	0	0	0	0	0	0	0	0	0	1	0	0	0	0	0	0	0	0	0	0	0	
<i>Sminthopsis sp. indet.</i>	0	0	0	0	0	0	0	0	0	1	0	0	0	0	0	0	0	0	0	0	1	0	0	0	0	0	0	0	0	0	
<i>Sthenurinae sp. indet.</i>	0	0	0	0	0	0	0	0	0	0	0	0	0	0	0	0	0	0	0	0	0	0	0	0	0	0	0	0	0	0	
<i>Sthenurus andersoni</i>	0	0	0	0	0	0	0	0	0	0	0	0	0	0	0	0	0	0	1	0	0	0	0	0	0	0	0	0	0	0	
<i>Sthenurus atlas</i>	0	0	0	0	0	0	0	0	0	0	0	0	0	0	0	0	0	0	0	0	0	0	0	0	0	0	0	0	0	0	
<i>Tachyglossus aculeatus</i>	0	0	0	0	0	0	0	0	0	0	0	0	0	0	0	0	0	0	0	0	0	0	0	0	0	0	0	0	0	0	
<i>Thylacinus cynocephalus</i>	0	0	0	0	0	0	0	0	0	0	0	0	0	0	0	0	0	0	0	0	0	0	0	0	0	0	0	0	0	0	
<i>Thylacinus Sarcophilus sp. indet.</i>	0	0	0	0	0	0	0	0	0	0	0	0	0	0	0	0	0	0	0	0	0	0	0	0	0	0	0	0	0	0	
<i>Thylacoleo carnifex</i>	0	0	0	0	0	0	0	0	0	0	0	0	0	0	0	0	0	0	0	0	0	0	0	0	0	0	0	0	0	0	
<i>Trichosurus sp. cf. vulpecula</i>	0	0	0	0	0	0	0	0	0	0	0	0	0	0	0	0	0	0	0	0	0	0	0	0	0	0	0	0	0	0	
<i>Trichosurus vulpecula</i>	0	0	0	1	0	0	0	0	0	0	0	0	0	0	0	0	0	1	0	0	0	0	0	0	0	0	0	0	0	0	
Vombatidae sp. indet.	0	0	0	0	0	0	0	0	0	0	0	0	0	0	0	0	0	0	0	0	0	0	0	0	0	0	0	0	0	0	
<i>Vombatus ursinus</i>	0	0	0	0	0	0	0	0	0	0	0	0	0	1	0	0	0	0	0	1	0	0	0	0	0	0	0	0	0	0	
<i>Wallabia bicolor</i>	0	0	0	0	0	0	0	0	0	0	0	0	0	0	0	0	0	0	0	0	0	0	0	0	0	0	0	0	0	0	
Accipitriformes sp. indet.	0	0	0	0	0	0	0	0	0	0	0	0	0	0	0	0	0	0	0	0	0	0	0	0	0	0	0	0	0	0	
<i>Aquila audax</i>	0	0	0	0	0	0	0	0	0	0	0	0	0	0	0	0	0	0	0	0	0	0	0	0	0	0	0	0	0	0	
Aves sp. indet.	0	0	1	0	1	0	0	0	0	0	1	1	1	1	1	1	1	1	1	0	1	1	1	0	0	1	1	1	1	1	
<i>Centropus sp. cf. colossus</i>	0	0	0	0	0	0	0	0	0	0	0	0	0	0	0	0	0	0	0	0	0	0	0	0	0	0	0	0	0	0	
<i>Coturnix pectoralis</i>	0	0	0	0	0	0	0	0	1	0	0	0	0	0	0	0	0	0	0	0	0	0	0	0	0	0	0	0	0	0	
<i>Coturnix sp. indet.</i>	0	0	0	0	0	0	0	0	0	0	0	0	0	0	0	0	0	0	0	1	0	0	0	0	0	0	0	0	0	0	
<i>Dromaius novaehollandiae</i>	0	0	0	1	0	0	0	0	0	0	0	0	0	0	0	0	0	0	0	0	0	0	0	0	0	0	0	0	0	0	
<i>Menura novaehollandiae</i>	0	0	0	0	0	0	0	0	0	0	0	0	0	0	0	0	0	0	0	0	0	0	0	0	0	0	0	0	0	0	
cf. <i>Menura novaehollandiae</i>	0	0	0	0	0	0	0	0	0	0	0	0	0	0	0	0	0	0	0	0	0	0	0	0	0	0	0	0	0	0	
Passeriformes sp. indet.	0	0	0	0	0	0	0	0	0	0	0	0	0	0	0	0	0	0	0	0	0	0	0	0	0	0	0	0	0	0	
<i>Tyto sp. indet.</i>	0	0	0	0	0	0	0	0	0	0	0	0	0	0	0	0	0	0	0	0	0	0	0	0	0	0	0	0	0	0	
<i>Tyto sp. cf. novaehollandiae</i>	0	0	0	0	0	0	0	0	0	0	0	0	0	0	0	0	0	0	0	0	0	0	0	0	0	0	0	0	0	0	

	Layer:		1-8							9														10a							
	Spit #	32	33	34	35	36	37	38	39	40	41	42	43	44	45	46	47	48	49	50	52	53	54	55	56	57	58	59	60	61	62
Agamidae sp. indet.		0	0	0	0	0	0	0	0	0	0	0	0	0	0	0	0	0	0	0	0	0	0	0	0	0	0	0	0	1	0
cf. Agamidae sp. indet.		0	0	0	0	0	0	0	0	0	0	0	0	0	0	0	0	0	0	0	0	0	0	0	0	0	0	0	0	0	0
<i>Egernia cunninghami</i>		0	0	0	0	0	0	0	0	0	0	0	0	0	0	0	0	0	0	0	0	0	0	0	0	0	0	0	0	0	0
<i>Egernia</i> sp. cf. <i>cunninghami</i>		0	0	0	0	0	0	0	0	0	0	0	0	0	0	0	0	0	0	0	0	0	0	0	0	0	0	0	0	0	0
<i>Egernia frangens</i>		0	0	0	0	0	0	0	0	0	0	0	0	0	0	0	0	0	0	0	0	0	0	0	0	0	0	0	0	0	0
<i>Egernia</i> sp. cf. <i>rugosa</i>		0	0	0	0	0	0	0	0	0	0	0	0	0	0	0	0	0	0	0	0	0	0	0	0	0	0	0	0	0	0
<i>Egernia striolata</i>		0	0	0	0	0	0	0	0	0	0	0	0	0	0	0	0	0	0	0	0	0	0	0	0	0	0	0	0	0	0
<i>Egernia</i> sp. indet.		0	0	0	0	0	0	0	0	0	0	0	0	0	0	0	0	0	0	0	0	0	1	0	0	0	0	0	0	0	0
cf. <i>Egernia</i> sp. indet.		0	0	0	0	0	0	0	0	0	0	0	0	0	0	0	0	0	0	0	0	0	0	0	0	0	0	0	0	0	0
<i>Egernia Liopholis</i> sp. indet.		0	0	0	0	0	0	0	0	0	0	0	0	0	0	0	0	0	0	0	0	0	0	0	0	0	0	0	0	0	0
Elapidae sp. indet.		0	0	0	0	0	0	0	0	1	0	0	0	0	0	0	0	0	0	0	1	0	0	0	0	0	0	0	0	0	0
Gekkonidae sp. indet.		0	0	0	0	0	0	0	2	0	0	0	0	0	0	0	1	0	0	0	0	0	0	0	0	0	0	0	0	0	0
<i>Liopholis inornata</i>		0	0	0	0	0	0	0	0	0	0	0	0	0	0	0	0	0	0	0	0	0	0	0	0	0	0	0	0	0	0
<i>Liopholis</i> sp. indet.		0	0	0	0	0	0	0	1	0	0	0	0	0	0	0	1	0	0	0	0	0	0	0	0	0	0	0	0	0	0
<i>Liopholis whittii</i>		0	0	0	0	0	0	0	0	0	0	0	0	0	0	0	0	0	0	0	0	0	0	0	0	0	0	0	0	0	0
<i>Morelia</i> sp. indet.		0	0	0	0	0	0	0	0	0	0	0	0	0	0	0	0	0	0	0	0	0	0	0	0	0	0	0	0	0	0
Pythonidae sp. indet.		0	0	0	0	0	0	0	0	0	0	0	0	0	0	0	0	0	0	0	0	0	0	0	0	0	0	0	0	0	0
Scincidae sp. indet.		0	0	0	0	0	0	0	0	0	0	0	0	0	0	0	0	0	0	0	0	0	0	1	0	0	0	0	0	0	0
Sphenomorphinae sp. indet.		0	0	0	0	0	0	0	0	0	0	0	0	0	0	0	0	0	0	0	0	0	0	0	0	0	0	0	0	0	0
Sphenomorphus sp. indet.		0	0	0	0	0	0	0	0	0	0	0	0	0	0	0	0	0	0	0	0	0	0	0	0	0	0	0	0	0	0
cf. Sphenomorphus sp. indet.		0	0	0	0	0	0	0	0	0	0	0	0	0	0	0	0	0	0	0	0	0	0	0	0	0	0	0	0	0	0
<i>Tiliqua frangens</i>		0	0	0	0	0	0	0	0	0	0	0	0	0	0	0	0	0	0	0	0	0	0	0	0	0	0	0	0	0	0
Varanidae sp. indet.		0	0	0	0	0	0	0	0	0	0	0	0	0	0	0	0	0	0	0	0	0	0	0	0	0	0	0	0	0	0
<i>Varanus</i> sp. indet.		0	0	0	0	0	0	0	0	0	0	0	0	0	0	0	0	0	0	0	0	0	0	0	0	0	0	0	0	0	0
<i>Varanus varius</i>		0	0	0	0	0	0	0	0	0	0	0	0	0	0	0	0	0	0	0	0	0	0	0	0	0	0	0	0	0	0
<i>Wonambi naracoortensis</i>		0	0	0	0	0	0	0	0	0	0	0	0	0	0	0	0	0	0	0	0	0	0	0	0	0	0	0	0	0	0
Anura sp. indet.		0	0	1	0	0	0	0	0	0	0	1	0	0	0	0	0	0	0	0	0	0	0	0	0	0	0	0	1	0	0
<i>Crinia</i> sp. indet.		0	0	0	1	0	0	0	0	0	0	0	0	0	0	0	0	0	0	0	0	0	0	0	0	0	0	0	0	0	0
<i>Limnodynastes tasmaniensis</i>		0	0	0	0	0	0	0	0	0	0	0	0	0	0	0	0	0	0	0	0	0	0	0	0	0	0	0	0	0	0
<i>Litoria rubella</i>		0	0	0	0	0	0	0	0	0	0	0	0	0	0	0	0	0	0	0	0	0	0	0	0	0	0	0	0	0	0
Fish		0	0	0	0	0	0	0	0	0	0	0	0	0	0	0	0	0	0	0	0	0	0	0	0	0	0	0	0	0	0

	Layer	10a					10b				10c			10d							12										
	Spit #	63	64	65	66	67	68	69	70	71	72	73	74	75	76	77	78	79	80	81	82	83	84	85	86	87	88	89	90	91	92
<i>Acrobates pygmaeus</i>		0	0	0	0	0	0	0	0	0	0	0	0	0	0	0	0	0	0	0	0	0	0	0	0	0	0	0	0	0	0
<i>Aepyprymnus rufescens</i>		1	0	1	0	1	1	0	0	1	1	1	1	0	1	0	1	1	1	1	1	0	1	0	1	1	1	1	1	1	2
<i>Antechinus flavipes</i>		1	0	0	0	2	1	1	0	0	1	0	0	0	1	0	0	0	1	0	0	0	0	0	0	0	0	0	0	0	0
<i>Baringa</i> sp. nov. 1		0	0	0	0	0	0	0	0	1	0	0	0	0	0	0	0	0	0	1	0	0	0	0	0	0	0	0	0	0	0
<i>Bettongia gaimardi</i>		0	0	0	0	0	0	0	0	0	0	1	1	0	0	0	0	0	0	0	0	0	0	0	0	0	0	0	0	0	0
<i>Bettongia lesueur</i>		0	0	1	1	1	1	1	1	1	1	1	1	2	2	0	0	0	0	1	0	0	0	0	1	0	0	0	0	0	0
<i>Bettongia</i> sp. indet.		0	0	0	0	0	0	0	0	0	0	0	0	0	0	0	0	0	0	0	0	0	0	0	0	0	0	0	1	0	0
<i>Cercartetus nanus</i>		0	0	0	0	0	0	0	0	0	1	1	0	0	0	0	0	0	0	0	0	0	0	0	0	0	0	0	0	0	0
<i>Chaeropus ecaudatus</i>		0	0	0	0	1	0	1	0	1	2	1	1	0	0	1	0	1	0	0	0	0	0	0	0	0	0	0	0	0	0

	Layer Spit #	10a					10b				10c				10d										12						
		63	64	65	66	67	68	69	70	71	72	73	74	75	76	77	78	79	80	81	82	83	84	85	86	87	88	89	90	91	92
<i>Congruus kitcheneri</i>		0	0	0	0	0	0	1	0	0	0	1	1	0	0	0	0	0	0	0	0	0	0	0	0	0	0	0	0	1	0
<i>Conilurus albipes</i>		0	1	0	0	1	1	0	1	3	2	1	2	0	3	1	1	1	1	0	0	0	0	0	1	0	0	0	0	1	1
<i>cf. Dasyuroides byrnei</i>		0	0	0	0	0	0	0	1	1	1	1	1	1	1	0	0	0	0	1	0	0	0	0	0	0	0	0	0	0	0
Dasyuridae indet. sp. 3		0	0	0	0	0	0	0	0	0	0	0	0	0	0	0	0	0	0	0	0	0	0	0	0	0	0	0	0	0	0
Dasyuridae indet. sp. 4		0	0	0	0	0	0	0	0	0	0	0	0	0	0	0	0	0	0	0	0	0	0	0	0	0	0	0	0	0	0
<i>Dasyurus geoffroii viverrinus</i>		1	1	1	6	11	4	4	2	9	6	8	6	1	2	0	2	1	1	1	1	1	0	0	1	1	0	1	1	0	1
<i>Dasyurus maculatus</i>		0	0	0	0	0	0	0	0	0	0	0	0	0	0	0	0	0	0	0	0	0	0	0	0	0	0	0	0	0	0
Diprotodontidae gen. et. sp. indet.		0	0	0	0	0	0	0	0	0	0	0	0	0	0	0	0	0	0	0	0	0	0	0	0	0	0	0	0	0	0
<i>Hydromys chrysogaster</i>		0	0	0	0	0	0	0	0	0	0	1	0	0	0	0	0	0	0	0	0	0	0	0	0	0	0	0	0	0	0
<i>Isoodon obesulus</i>		1	1	1	2	1	1	1	1	1	1	2	1	1	1	0	1	1	1	0	1	0	0	1	1	0	0	0	1	0	1
<i>Lagorchestes leporides</i>		0	0	0	0	0	0	0	0	0	0	0	1	0	0	0	0	0	0	0	0	0	0	0	0	0	0	0	0	0	0
<i>Macroderma gigas</i>		0	0	0	0	0	0	0	0	0	0	0	0	0	0	0	0	0	0	0	0	0	0	0	0	0	0	0	0	0	0
<i>Macropus giganteus</i>		0	0	0	0	0	0	0	1	0	0	1	1	0	1	0	1	0	1	0	0	0	0	0	1	0	0	0	0	0	2
<i>Macropus sp. indet.</i>		0	0	0	0	0	0	0	0	0	0	0	0	0	0	0	0	0	0	0	0	0	0	0	0	0	0	0	0	0	0
<i>Macrotis lagotis</i>		0	0	0	0	0	0	0	0	0	0	1	1	0	1	0	0	0	0	0	0	0	0	0	0	0	0	0	0	0	0
<i>Mastacomys fuscus</i>		0	0	0	3	1	4	2	1	3	1	0	1	0	1	0	0	0	0	0	0	0	0	0	0	0	0	0	0	0	0
<i>Megalibgwilia ramsayi</i>		0	0	0	0	0	0	0	0	0	0	0	0	0	0	0	0	0	0	0	0	0	0	0	0	0	0	0	0	0	0
<i>Microchiroptera sp. indet.</i>		0	0	0	0	0	0	1	0	1	1	1	1	0	1	0	0	1	1	0	1	0	0	0	1	0	1	1	1	1	0
Murinae sp. 1		0	0	1	0	0	0	0	1	0	0	0	0	0	0	0	0	0	0	0	0	0	0	0	0	0	0	0	0	0	0
Murinae sp. 2		0	0	0	0	0	0	0	0	0	0	0	0	1	0	0	0	0	0	0	0	0	0	0	0	0	0	0	0	0	0
Murinae sp. 3		0	0	0	0	0	0	0	0	0	0	0	0	0	0	0	0	0	0	0	0	0	0	0	0	0	0	0	0	0	0
Murinae sp. 4		0	0	0	1	0	0	0	0	0	0	0	0	0	0	0	0	0	0	0	0	0	0	0	0	0	0	0	0	0	0
Murinae sp. 5		0	0	0	0	0	0	0	0	0	0	0	0	0	0	0	0	0	0	0	0	0	0	0	0	0	0	0	0	0	0
Murinae sp. 6		0	0	0	0	1	0	0	0	0	0	0	0	0	0	0	0	0	0	0	0	0	0	0	0	0	0	0	0	0	0
Murinae sp. 7		0	0	0	0	0	0	0	0	0	0	0	0	0	0	0	0	0	0	0	0	0	0	0	0	0	0	0	0	0	0
<i>Notamacropus agilis</i>		1	0	0	0	0	0	0	0	0	0	0	0	1	0	0	0	1	0	0	1	0	0	0	1	0	0	1	0	1	1
<i>Notamacropus dorsalis</i>		0	0	0	0	0	0	0	0	0	0	0	0	1	1	0	0	0	0	1	0	0	0	0	0	0	0	0	0	1	1
<i>Notamacropus sp. cf. dorsalis</i>		0	0	0	0	0	0	0	0	0	0	0	0	0	0	0	0	0	0	0	0	0	0	0	0	0	0	0	0	0	0
<i>Notamacropus parma</i>		0	0	0	0	0	0	0	1	0	1	1	0	1	0	1	1	1	1	1	0	0	0	1	0	1	1	1	1	1	1
<i>Notamacropus parryi</i>		0	0	0	0	0	0	0	0	0	0	0	0	0	0	1	0	0	0	0	0	0	0	0	0	0	0	1	0	0	0
<i>Notamacropus sp. indet.</i>		0	0	0	0	0	0	0	0	1	0	0	0	0	0	0	0	0	0	0	0	0	0	0	0	0	0	0	0	0	0
<i>Notomys sp. indet.</i>		2	0	0	2	2	5	8	8	24	14	23	18	4	6	0	3	3	2	0	1	0	0	1	0	0	0	0	0	1	1
<i>Onychogalea frenata</i>		0	0	0	0	0	0	1	0	1	0	0	1	0	0	0	0	0	0	0	0	0	0	1	0	0	1	0	0	0	0
<i>Onychogalea lunata</i>		0	0	1	0	0	0	0	0	0	1	0	0	0	0	0	0	0	0	0	0	0	0	0	0	0	0	0	0	0	0
<i>Osphranter robustus</i>		0	0	0	0	0	0	0	0	0	0	0	1	0	1	0	0	0	0	0	0	0	0	0	0	0	0	1	0	1	0
<i>cf. Osphranter robustus</i>		0	0	0	0	0	0	0	0	0	0	0	0	0	0	0	0	0	0	0	0	0	0	0	0	0	0	0	0	0	0
<i>Osphranter rufus</i>		0	0	0	0	0	0	0	0	0	0	0	0	0	0	0	0	0	0	0	0	0	0	0	0	0	0	0	0	0	0
<i>Palorchestes azael</i>		0	0	0	0	0	0	0	0	0	0	0	0	0	0	0	0	0	0	0	0	0	0	0	0	0	0	0	0	0	0
<i>Perameles gunnii nasuta</i>		1	1	1	2	2	1	0	1	1	1	1	1	1	1	1	2	1	1	1	1	0	0	1	1	0	1	1	1	1	1
<i>Petaurus breviceps</i>		0	0	0	0	0	0	1	0	2	1	1	0	0	0	0	1	0	1	0	1	0	0	1	0	0	0	0	0	0	1
<i>Petaurus sp. cf. breviceps</i>		0	0	0	0	1	0	0	0	0	0	0	0	0	0	0	0	0	0	0	0	0	0	0	0	0	0	0	0	0	0
<i>Petrogale sp. indet.</i>		0	0	0	0	0	0	0	0	0	0	0	0	0	0	0	0	0	0	0	0	0	0	0	0	0	0	0	0	0	0
<i>Phascogale tapoatafa</i>		0	0	0	0	0	0	0	0	0	0	0	0	0	0	0	0	0	0	0	0	0	0	0	0	0	0	0	0	0	0

	Layer	10a					10b				10c				10d								12								
	Spit #	63	64	65	66	67	68	69	70	71	72	73	74	75	76	77	78	79	80	81	82	83	84	85	86	87	88	89	90	91	92
<i>Vombatus ursinus</i>		0	0	0	0	0	0	0	0	0	0	1	0	0	0	0	0	1	0	0	0	0	0	0	0	0	0	0	1	0	0
<i>Wallabia bicolor</i>		0	0	0	0	0	0	0	0	0	0	0	0	0	0	0	1	0	0	1	0	0	0	0	0	0	0	0	0	0	0
<i>Accipitriformes</i> sp. indet.		0	0	0	0	0	0	0	0	0	0	0	0	0	0	0	0	0	0	0	0	0	0	0	0	0	0	0	0	0	0
<i>Aquila audax</i>		0	0	0	0	0	0	0	0	0	0	0	0	0	0	0	0	0	0	0	0	0	0	0	0	0	0	0	0	0	0
<i>Aves</i> sp. indet.		1	1	1	2	1	1	1	1	1	1	1	1	1	1	1	1	1	0	1	0	0	0	0	0	1	1	1	1	1	1
<i>Centropus</i> sp. cf. <i>colossus</i>		0	0	0	0	0	0	0	0	0	0	0	0	0	0	0	0	0	0	0	0	0	0	0	0	0	0	0	0	0	0
<i>Coturnix pectoralis</i>		0	0	0	0	0	0	0	0	0	0	0	0	0	0	0	0	0	0	0	0	0	0	0	0	0	0	0	0	0	0
<i>Coturnix</i> sp. indet.		0	0	0	0	0	0	0	0	0	0	0	0	0	0	0	0	0	0	0	0	0	0	0	0	0	0	0	0	0	0
<i>Dromaius novaehollandiae</i>		0	0	0	0	0	0	0	0	0	0	0	0	0	0	0	0	0	0	0	0	0	0	0	0	0	0	0	0	0	0
<i>Menura novaehollandiae</i>		0	0	0	0	0	0	0	0	0	0	0	0	0	0	0	0	0	0	0	0	0	0	0	0	0	0	0	0	0	0
cf. <i>Menura novaehollandiae</i>		0	0	0	0	0	0	0	0	0	0	0	0	0	0	0	0	0	0	0	0	0	0	0	0	0	0	0	0	0	0
<i>Passeriformes</i> sp. indet.		0	0	0	0	0	0	0	0	0	0	0	0	0	0	0	0	0	0	0	0	0	0	0	0	0	0	0	0	0	0
<i>Tyto</i> sp. indet.		0	0	0	0	0	0	0	0	0	0	0	0	0	0	0	0	0	0	0	0	0	0	0	0	0	0	0	0	0	0
<i>Tyto</i> sp. cf. <i>novaehollandiae</i>		0	0	0	0	0	0	0	0	0	0	0	0	0	0	0	0	0	0	0	0	0	0	0	0	0	0	0	0	0	0
<i>Agamidae</i> sp. indet.		0	0	0	1	1	0	0	0	2	1	0	0	0	0	0	1	0	1	1	0	0	0	0	0	0	0	1	1	0	0
cf. <i>Agamidae</i> sp. indet.		0	0	0	0	0	0	0	0	0	0	0	0	0	0	0	0	0	0	0	0	0	0	0	0	0	0	0	0	0	0
<i>Egernia cunninghami</i>		0	0	0	0	1	0	0	0	0	0	0	0	0	0	0	0	0	0	0	0	0	0	0	0	0	0	0	0	0	0
<i>Egernia</i> sp. cf. <i>cunninghami</i>		0	0	0	0	0	0	0	0	1	0	1	1	0	0	0	0	0	0	0	0	0	0	0	0	0	0	0	0	0	1
<i>Egernia frangens</i>		0	0	0	0	0	0	0	0	0	0	0	0	0	0	0	0	0	0	0	0	0	0	0	1	0	0	0	0	0	0
<i>Egernia</i> sp. cf. <i>rugosa</i>		0	0	0	0	0	0	0	0	0	1	0	0	0	0	0	0	0	0	0	0	0	0	0	0	0	0	0	0	0	0
<i>Egernia striolata</i>		0	0	0	0	0	0	0	0	0	0	0	0	0	0	0	0	0	0	0	0	0	0	0	0	0	0	0	0	0	0
<i>Egernia</i> sp. indet.		0	0	0	0	1	0	0	0	0	0	0	0	0	0	0	0	0	0	0	0	0	0	0	0	0	0	0	1	0	0
cf. <i>Egernia</i> sp. indet.		0	0	0	0	0	1	0	0	0	0	0	0	0	0	1	0	0	0	0	0	0	0	0	0	0	0	0	0	1	0
<i>Egernia Liopholis</i> sp. indet.		0	0	0	0	0	0	0	0	0	0	0	0	0	0	0	0	0	0	0	0	0	0	0	0	0	0	0	0	0	0
<i>Elapidae</i> sp. indet.		0	0	0	0	0	0	0	0	0	0	1	1	0	0	0	1	0	0	0	0	0	0	0	1	0	1	1	1	0	0
<i>Gekkonidae</i> sp. indet.		0	0	0	0	0	0	0	0	0	0	0	0	0	0	1	0	1	0	0	0	0	0	0	0	0	0	0	0	0	0
<i>Liopholis inornata</i>		0	0	0	0	1	0	0	0	0	0	0	0	0	0	0	0	0	0	0	0	0	0	0	0	0	0	0	0	0	0
<i>Liopholis</i> sp. indet.		0	0	0	0	1	0	0	0	0	0	1	1	0	0	0	0	0	0	0	0	0	0	0	1	0	0	1	0	0	0
<i>Liopholis whittii</i>		0	0	0	0	0	0	0	2	0	0	0	0	0	0	1	0	0	0	0	0	0	0	0	0	0	0	0	0	0	0
<i>Morelia</i> sp. indet.		0	0	0	0	0	0	0	0	0	0	0	0	0	0	0	0	0	0	0	0	0	0	0	0	0	0	0	0	0	0
<i>Pythonidae</i> sp. indet.		0	0	0	0	0	0	0	0	0	0	0	0	0	0	0	0	0	0	0	0	0	0	0	0	0	0	0	0	0	0
<i>Scincidae</i> sp. indet.		0	0	1	0	0	0	0	0	0	0	0	0	1	0	0	0	0	0	0	0	0	0	0	0	0	0	0	0	0	0
<i>Sphenomorphinae</i> sp. indet.		0	0	0	0	0	0	0	0	0	0	0	0	0	0	0	0	0	0	0	0	0	0	0	0	0	2	0	0	0	0
<i>Sphenomorphus</i> sp. indet.		0	0	0	0	0	0	0	0	0	0	0	0	0	0	0	1	0	0	0	0	0	0	0	0	0	0	0	0	0	0
cf. <i>Sphenomorphus</i> sp. indet.		0	0	0	0	0	0	0	0	0	1	0	0	0	0	0	0	0	0	0	0	0	0	0	0	0	0	0	0	0	0
<i>Tiliqua frangens</i>		1	0	0	0	0	0	0	0	1	0	0	0	0	0	1	0	1	0	0	0	0	0	0	0	1	1	0	0	0	1
<i>Varanidae</i> sp. indet.		0	0	0	0	0	0	0	0	0	0	0	1	0	0	0	0	0	0	0	0	0	0	0	0	0	0	0	0	0	0
<i>Varanus</i> sp. indet.		0	0	0	1	0	0	0	1	0	0	0	0	1	1	0	0	0	0	0	0	0	0	0	0	0	0	0	0	0	1
<i>Varanus varius</i>		0	0	0	0	0	0	0	0	0	0	0	0	0	0	0	0	0	0	0	0	0	0	0	0	0	0	0	0	0	0
<i>Wonambi naracoortensis</i>		0	0	0	0	0	0	0	0	0	0	0	0	0	0	0	0	0	0	0	0	0	0	0	0	0	0	0	0	0	0
<i>Anura</i> sp. indet.		0	0	0	0	0	1	0	0	0	0	0	0	0	1	2	2	1	0	1	0	0	0	0	1	1	1	0	0	0	0
<i>Crinia</i> sp. indet.		0	0	0	0	0	0	0	0	0	0	0	0	0	0	0	0	0	0	0	0	0	0	0	0	0	0	0	0	0	0
<i>Limnodynastes tasmaniensis</i>		0	0	0	0	0	0	0	0	0	0	0	0	0	0	0	0	0	0	0	0	0	0	0	0	0	0	0	0	0	0

	Layer	10a					10b				10c			10d								12									
	Spit #	63	64	65	66	67	68	69	70	71	72	73	74	75	76	77	78	79	80	81	82	83	84	85	86	87	88	89	90	91	92
<i>Litoria rubella</i>		0	0	0	0	0	0	0	0	0	0	0	0	0	0	0	0	0	0	0	0	0	0	0	0	0	0	0	0	0	0
Fish		0	0	0	0	0	0	0	0	0	0	0	1	0	0	0	0	0	0	0	0	0	0	0	0	0	0	0	0	0	0
	Layer	12			13a							13b		13c							14a			14b							
	Spit #	93	94	95	96	97	98	99	100	101	102	103	104	105	106	107	108	109	110	111	112	113	114	115	116	117	118	119	120		
<i>Acrobates pygmaeus</i>		0	0	0	0	0	0	1	0	0	0	0	0	2	0	0	1	0	0	0	0	0	0	0	0	0	0	0			
<i>Aepyprymnus rufescens</i>		1	1	1	0	0	0	1	1	1	0	1	0	0	1	0	0	0	0	0	0	0	0	0	1	0	0	0			
<i>Antechinus flavipes</i>		0	1	0	0	0	2	0	0	1	0	3	4	3	6	0	1	6	0	5	2	0	0	0	7	4	0	0			
<i>Baringa</i> sp. nov. 1		0	0	0	0	0	0	0	0	0	0	0	0	0	0	0	0	0	1	0	0	0	0	0	0	0	0	0			
<i>Bettongia gaimardi</i>		0	1	0	0	0	0	2	0	0	0	0	0	0	0	0	1	0	0	0	0	0	0	0	0	0	0	0			
<i>Bettongia lesueur</i>		0	0	0	0	0	0	0	0	0	0	0	0	1	0	0	0	0	0	0	0	0	0	0	0	0	0	0			
<i>Bettongia</i> sp. indet.		0	0	0	0	0	0	0	0	0	0	0	0	0	0	0	0	0	0	0	0	0	0	0	0	0	0	0			
<i>Cercartetus nanus</i>		0	0	0	0	0	0	0	0	0	0	1	0	0	1	0	0	1	0	0	0	0	0	0	0	1	0	1	0		
<i>Chaeropus ecaudatus</i>		0	0	0	0	0	0	0	0	0	0	0	0	0	0	0	0	0	0	0	0	0	0	0	0	0	0	0	0		
<i>Congruus kitcheneri</i>		0	1	0	0	0	0	1	0	0	0	0	0	0	0	0	0	0	0	1	0	0	1	0	0	0	0	0	1		
<i>Conilurus albipes</i>		1	1	0	0	1	0	2	3	2	1	4	3	3	11	0	1	5	1	10	1	0	3	1	9	8	0	1	30		
cf. <i>Dasyuroides byrnei</i>		0	0	0	0	0	0	0	0	0	0	0	0	0	0	0	0	1	0	0	0	0	0	0	1	0	0	0	0		
Dasyuridae indet. sp. 3		0	0	0	0	0	0	0	0	0	0	0	0	0	0	0	0	0	0	0	0	0	1	0	0	0	0	0	0		
Dasyuridae indet. sp. 4		0	0	1	0	0	0	0	0	0	0	0	0	0	0	0	0	0	0	0	0	0	0	0	0	0	0	0	0		
<i>Dasyurus geoffroii viverrinus</i>		1	1	0	0	0	0	0	1	1	0	1	2	1	2	0	1	1	0	2	1	0	1	0	4	4	0	1	5		
<i>Dasyurus maculatus</i>		0	0	0	0	0	0	0	0	0	0	0	0	1	0	0	0	0	0	0	0	0	0	0	0	0	0	0	2		
Diprotodontidae gen. et. sp. indet.		0	0	0	0	0	0	0	0	0	0	0	0	0	0	0	0	0	0	0	0	0	0	0	0	0	0	0	1		
<i>Hydromys chrysogaster</i>		0	0	0	0	0	0	0	0	0	0	0	0	0	0	1	0	0	0	0	0	0	0	0	0	0	0	0	0		
<i>Isoodon obesulus</i>		1	0	1	0	0	1	1	1	2	1	1	2	2	2	0	1	2	0	6	0	0	1	1	9	6	0	1	10		
<i>Lagorchestes leporides</i>		1	0	0	0	0	1	0	0	0	0	0	0	0	0	0	0	0	0	0	0	0	0	0	0	0	0	0	0		
<i>Macroderma gigas</i>		0	0	0	0	0	0	0	0	0	0	0	0	0	0	0	0	0	0	0	0	0	0	0	0	0	0	0	0		
<i>Macropus giganteus</i>		1	0	1	0	1	1	1	1	2	0	1	1	0	0	0	0	0	0	0	0	0	0	0	3	1	1	1	5		
<i>Macropus</i> sp. indet.		0	0	0	0	0	0	0	0	0	0	0	0	0	0	1	0	0	0	0	0	0	0	0	0	0	0	0	0		
<i>Macrotis lagotis</i>		0	0	0	0	0	0	0	0	0	0	0	0	0	0	0	0	0	0	0	0	0	0	0	0	0	0	0	0		
<i>Mastacomys fuscus</i>		0	0	0	0	0	0	0	0	1	0	0	0	0	0	0	0	0	0	0	0	0	2	0	0	1	0	0	4		
<i>Megalibgwilia ramsayi</i>		0	0	0	0	0	0	0	0	0	0	0	0	0	0	0	0	0	0	0	0	0	0	0	0	0	0	0	1		
<i>Microchiroptera</i> sp. indet.		0	1	1	0	0	1	1	1	0	0	0	1	0	2	0	0	1	1	2	1	0	0	2	2	0	1	8			
Murinae sp. 1		0	0	0	0	0	0	0	0	0	0	0	0	0	0	0	0	0	0	0	0	0	0	0	0	0	0	0	0		
Murinae sp. 2		0	0	0	0	0	0	0	0	0	0	0	0	0	0	0	0	0	0	0	0	0	0	0	0	0	0	0	0		
Murinae sp. 3		0	0	0	0	0	0	0	0	0	0	0	0	0	0	0	0	0	0	0	0	0	0	0	0	0	0	0	0		
Murinae sp. 4		0	0	0	0	0	0	0	0	0	0	0	0	0	0	0	0	0	0	0	0	0	0	0	0	0	0	0	0		
Murinae sp. 5		0	0	0	0	0	0	0	0	0	0	0	0	1	0	0	0	0	0	0	0	0	0	0	0	0	0	0	0		
Murinae sp. 6		0	0	0	0	0	0	0	0	0	0	0	0	0	0	0	0	0	0	0	0	0	0	0	0	0	0	0	0		
Murinae sp. 7		0	0	0	0	0	0	0	0	0	0	0	0	0	0	0	0	0	0	0	0	0	1	0	0	0	0	0	0		
<i>Notamacropus agilis</i>		0	0	0	0	0	1	0	0	1	0	0	1	0	0	0	0	0	0	0	0	0	0	0	0	0	0	0	2		
<i>Notamacropus dorsalis</i>		2	1	0	0	0	0	0	0	1	0	1	0	0	0	0	0	0	0	0	0	0	0	0	0	0	0	0	1		
<i>Notamacropus</i> sp. cf. <i>dorsalis</i>		0	0	0	0	0	0	0	0	0	0	0	0	0	0	0	0	0	0	0	0	0	0	0	1	0	0	0	0		
<i>Notamacropus parma</i>		1	1	1	0	0	0	1	2	1	1	0	1	0	1	1	0	0	0	0	0	1	0	0	0	0	0	0	1		

	Layer	12			13a							13b		13c							14a			14b					
	Spit #	93	94	95	96	97	98	99	100	101	102	103	104	105	106	107	108	109	110	111	112	113	114	115	116	117	118	119	120
<i>Notamacropus parryi</i>		0	0	0	0	0	0	0	0	0	0	0	0	0	0	0	1	0	0	0	0	0	0	0	0	0	0	1	
<i>Notamacropus</i> sp. indet.		0	0	0	0	0	0	0	0	0	0	0	0	0	0	0	0	0	0	0	0	0	0	0	0	0	0	0	
<i>Notomys</i> sp. indet.		1	0	0	1	0	0	0	0	0	0	0	0	0	0	0	0	0	0	0	0	1	0	1	0	0	0	0	
<i>Onychogalea frenata</i>		0	0	0	0	0	0	0	0	0	0	0	0	0	0	0	0	0	0	0	0	0	0	0	0	0	0	0	
<i>Onychogalea lunata</i>		0	0	0	0	0	0	0	0	0	0	0	0	0	0	0	0	0	0	0	0	0	0	0	0	0	0	0	
<i>Osphranter robustus</i>		0	0	0	0	0	0	0	1	0	0	0	0	0	0	0	0	0	0	0	0	0	0	1	0	0	1	2	
cf. <i>Osphranter robustus</i>		0	0	0	0	0	0	0	0	0	0	0	0	0	0	0	0	0	1	0	0	0	0	0	0	0	0	0	
<i>Osphranter rufus</i>		0	0	0	0	0	0	0	0	0	0	0	0	0	0	0	0	0	0	0	0	0	0	0	0	0	0	0	
<i>Palorchestes azael</i>		0	0	0	0	0	0	0	0	0	0	0	0	0	0	0	0	0	0	0	0	0	0	0	0	0	0	0	
<i>Perameles gunnii nasuta</i>		0	1	0	0	1	1	2	2	1	2	1	2	2	6	0	1	2	1	4	1	0	3	1	10	8	0	1	12
<i>Petaurus breviceps</i>		0	0	0	0	0	1	1	1	0	1	1	1	0	2	0	0	2	0	1	1	0	1	0	2	2	0	3	
<i>Petaurus</i> sp. cf. <i>breviceps</i>		0	0	0	0	0	0	0	0	0	0	0	0	0	0	0	0	0	0	0	0	0	0	0	0	0	0	0	
<i>Petrogale</i> sp. indet.		0	0	0	0	0	0	1	0	0	0	0	0	0	0	0	0	0	0	0	0	0	0	0	0	0	0	0	
<i>Phascogale tapoatafa</i>		0	0	0	0	0	0	0	0	0	1	0	0	0	0	0	0	0	0	0	0	0	0	0	0	0	0	0	
<i>Phascogale</i> sp. cf. <i>tapoatafa</i>		0	0	0	0	0	0	1	0	0	0	0	0	1	1	0	0	0	1	1	0	0	0	1	1	0	1	0	
<i>Potorous tridactylus</i>		0	0	0	0	0	0	0	0	0	0	0	0	0	0	0	0	0	0	0	0	0	0	0	0	0	0	0	
Potoroinae sp. indet.		1	0	0	0	0	0	1	0	0	0	0	1	0	1	0	0	1	0	0	0	0	0	1	1	0	1	1	
<i>Procoptodon goliath</i>		0	0	0	0	0	0	0	0	0	1	1	0	0	0	0	0	0	0	0	0	0	0	1	0	0	0	1	
<i>Protemnodon brehus</i>		4	3	3	0	2	2	6	8	6	6	16	13	13	59	2	7	24	2	39	5	1	16	1	134	87	0	10	274
<i>Protemnodon</i> sp. cf. <i>brehus</i>		0	0	0	0	0	0	0	0	0	0	0	0	0	0	0	0	0	0	0	0	0	0	0	0	0	0	0	
<i>Protemnodon</i> sp. indet.		0	0	0	0	0	0	0	0	0	0	0	0	0	0	0	0	0	0	0	0	0	0	0	0	0	0	0	
cf. <i>Protemnodon</i> sp. indet.		0	0	0	0	0	0	0	0	0	0	0	0	0	0	0	0	0	0	0	0	0	0	0	0	0	0	0	
<i>Pseudocheirus peregrinus</i>		0	0	0	0	0	0	0	0	0	0	0	0	0	0	0	0	0	0	0	0	0	0	0	0	0	0	0	
<i>Pseudomys australis</i>		0	0	0	0	0	0	0	0	0	0	0	0	0	0	0	0	0	0	0	0	0	0	0	0	0	0	0	
<i>Pseudomys desertor</i>		0	0	0	0	0	3	2	1	4	1	5	4	3	10	0	1	5	1	7	2	0	2	0	10	11	0	1	18
<i>Pseudomys</i> sp. cf. <i>desertor</i>		0	0	0	0	0	0	0	0	0	0	0	0	0	0	0	0	0	0	0	0	0	0	0	0	0	0	0	
cf. <i>Pseudomys fumeus</i>		0	1	0	0	0	0	0	0	0	0	0	0	0	0	0	0	0	0	0	0	0	0	0	0	0	0	0	
cf. <i>Pseudomys gouldii</i>		0	0	0	0	1	2	2	3	4	2	7	10	10	26	0	5	9	1	15	3	0	4	1	37	15	0	2	28
<i>Pseudomys gouldii</i>		0	0	0	0	0	0	0	0	0	0	0	0	2	0	0	0	0	1	0	0	1	0	4	1	0	0	3	
<i>Pseudomys gracilicaudatus</i>		0	0	0	0	0	0	0	0	0	0	0	0	0	0	0	0	0	0	0	0	0	0	0	0	0	0	0	
cf. <i>Pseudomys gracilicaudatus</i>		0	0	0	0	0	0	0	0	0	0	0	0	0	0	0	0	0	0	0	0	0	0	0	0	0	0	0	
<i>Pseudomys</i> sp. cf. <i>gracilicaudatus</i>		0	0	0	0	0	0	1	1	0	0	1	0	0	0	1	0	0	1	0	0	0	0	0	0	0	0	0	
<i>Pseudomys novaehollandiae</i>		0	0	0	0	1	0	0	0	0	0	0	0	0	0	0	0	0	0	0	0	0	0	0	0	0	0	0	
<i>Pseudomys oralis</i>		0	0	0	0	0	0	0	0	1	0	0	0	0	0	0	0	0	0	0	0	0	0	0	0	0	0	0	
<i>Pseudomys</i> sp. cf. <i>oralis</i>		0	1	0	0	0	0	0	0	0	0	0	0	0	0	0	0	0	0	0	0	0	0	0	0	0	0	1	
<i>Rattus fuscipes</i>		0	0	0	0	0	0	0	0	0	0	0	0	0	0	0	0	0	0	0	0	0	0	0	0	0	0	0	
<i>Rattus</i> sp. cf. <i>tunneyi</i>		0	0	0	0	0	0	0	0	0	2	0	0	0	0	0	0	0	0	0	0	0	0	0	0	0	0	0	
<i>Rattus</i> sp. cf. <i>lutreolus</i>		0	0	0	0	0	0	1	1	2	0	0	0	3	2	0	0	2	0	2	0	0	2	0	4	3	0	13	
<i>Rattus</i> sp. indet.		0	0	0	0	0	0	0	0	0	0	3	0	0	0	0	0	0	0	0	0	0	0	0	0	0	0	1	0
<i>Sarcophilus lanarius</i>		0	0	0	0	0	0	0	0	0	0	0	0	0	0	0	0	0	0	0	0	0	0	0	0	0	0	0	0
<i>Simosthenurus pales</i>		0	0	0	0	1	0	0	0	0	0	0	0	0	0	0	0	0	0	0	0	0	0	0	0	0	0	0	
<i>Sminthopsis crassicaudata</i>		0	0	0	0	0	0	1	1	0	1	2	1	2	0	0	0	0	1	0	0	0	0	1	2	0	0	0	

	Layer	12			13a							13b		13c							14a			14b				
	Spit #	93	94	95	96	97	98	99	100	101	102	103	104	105	106	107	108	109	110	111	112	113	114	115	116	117	118	119
<i>Sminthopsis</i> sp. cf. <i>crassicaudata</i>		0	0	0	0	0	0	0	0	0	0	0	0	0	0	0	1	0	0	0	0	0	0	0	0	0	0	0
cf. <i>Sminthopsis crassicaudata</i>		0	0	0	0	0	0	0	0	0	0	0	0	0	0	0	0	0	0	0	0	0	0	0	0	0	1	0
<i>Sminthopsis murina</i>		0	0	0	0	0	0	1	0	0	1	0	1	5	0	2	3	2	1	1	0	0	0	7	2	0	0	9
<i>Sminthopsis</i> sp. cf. <i>murina</i>		0	0	0	0	0	0	0	0	0	0	1	0	0	0	0	0	0	0	0	0	0	1	0	0	0	0	0
<i>Sminthopsis</i> sp. indet.		0	1	0	0	0	0	0	0	0	0	0	0	0	0	0	0	0	0	0	0	0	0	0	0	0	0	0
<i>Sthenurinae</i> sp. indet.		0	0	0	0	0	0	0	0	0	0	0	0	0	0	0	0	0	0	0	0	0	1	0	0	0	0	0
<i>Sthenurus andersoni</i>		0	0	0	0	0	1	0	0	0	0	0	0	0	0	0	0	0	0	0	0	0	0	0	0	0	0	0
<i>Sthenurus atlas</i>		0	0	0	0	0	0	0	0	0	0	0	0	0	0	0	0	0	0	0	0	0	0	0	0	0	0	0
<i>Tachyglossus aculeatus</i>		0	0	0	0	0	0	0	0	0	0	0	0	0	0	1	0	0	0	0	0	0	0	0	0	0	0	0
<i>Thylacinus cynocephalus</i>		0	0	0	0	0	0	0	0	0	0	0	0	0	0	0	0	0	0	0	0	0	1	1	0	1	0	0
<i>Thylacinus Sarcophilus</i> sp. indet.		0	0	0	0	0	0	0	0	0	0	0	0	0	0	0	0	0	0	0	0	0	0	0	0	0	0	1
<i>Thylacoleo carnifex</i>		0	0	0	0	0	0	0	0	0	0	0	0	0	0	0	0	0	0	0	0	0	0	0	0	0	0	0
<i>Trichosurus</i> sp. cf. <i>vulpecula</i>		0	0	0	0	0	0	0	0	0	0	0	0	0	0	0	0	0	0	0	0	0	0	0	0	0	0	0
<i>Trichosurus vulpecula</i>		0	0	0	0	0	0	0	0	0	0	0	0	0	0	1	1	0	0	0	0	0	0	0	0	0	0	0
Vombatidae sp. indet.		0	0	0	0	0	0	0	0	0	0	0	0	0	0	0	0	0	0	0	0	0	0	0	0	0	0	0
<i>Vombatus ursinus</i>		0	0	0	1	0	0	1	0	1	0	1	1	1	0	0	1	0	0	0	0	0	0	0	0	0	0	1
<i>Wallabia bicolor</i>		0	0	0	0	0	0	0	0	0	0	0	0	0	0	0	0	0	0	0	0	0	0	0	0	0	0	0
Accipitriformes sp. indet.		0	0	0	0	0	0	0	0	0	0	0	1	0	0	0	0	0	0	0	0	0	0	0	0	0	0	0
<i>Aquila audax</i>		0	0	0	0	0	0	0	0	0	0	0	0	0	0	0	0	0	0	0	0	0	0	0	0	0	0	0
Aves sp. indet.		1	0	0	1	0	1	1	1	0	1	0	0	1	1	1	0	0	1	0	1	1	1	0	1	0	0	0
<i>Centropus</i> sp. cf. <i>colossus</i>		0	0	0	0	0	0	0	0	0	0	0	0	0	0	0	0	0	0	0	0	0	0	0	0	0	0	0
<i>Coturnix pectoralis</i>		0	0	0	0	0	0	0	0	0	0	0	0	0	0	0	0	0	0	0	0	0	0	0	0	0	0	0
<i>Coturnix</i> sp. indet.		0	0	0	0	0	0	0	0	0	0	0	1	0	0	0	0	0	0	0	0	0	0	0	0	0	0	0
<i>Dromaius novaehollandiae</i>		0	0	0	0	0	0	0	1	0	0	0	0	0	0	0	0	0	0	0	0	0	0	0	0	0	0	0
<i>Menura novaehollandiae</i>		0	0	0	0	0	0	0	0	0	0	0	0	0	0	0	0	0	1	0	0	0	0	1	0	0	0	1
cf. <i>Menura novaehollandiae</i>		0	0	0	0	0	0	0	0	0	0	0	1	0	0	0	0	0	0	0	0	0	0	0	0	0	0	0
Passeriformes sp. indet.		0	0	0	0	0	0	0	0	0	0	0	0	0	0	0	0	0	1	0	0	0	0	0	0	0	0	0
<i>Tyto</i> sp. indet.		0	0	0	0	0	0	0	0	0	0	0	0	0	0	0	0	0	0	0	0	0	0	0	0	0	0	0
<i>Tyto</i> sp. cf. <i>novaehollandiae</i>		0	0	0	0	0	0	0	0	0	0	0	0	0	0	0	0	0	0	0	0	0	0	0	0	0	0	0
Agamidae sp. indet.		0	2	0	0	1	0	1	0	0	0	0	0	0	0	0	0	0	0	0	0	0	0	0	0	0	0	0
cf. Agamidae sp. indet.		0	0	0	0	0	0	0	0	0	0	0	1	0	0	0	0	0	0	0	0	0	0	0	0	0	0	0
<i>Egernia cunninghami</i>		0	0	0	0	0	0	0	0	0	0	0	0	0	0	0	0	0	0	0	0	0	0	0	0	0	0	0
<i>Egernia</i> sp. cf. <i>cunninghami</i>		0	0	0	0	0	0	0	0	0	0	0	1	0	0	0	0	0	0	0	0	0	0	1	0	0	0	0
<i>Egernia frangens</i>		0	0	0	0	0	0	0	0	0	0	0	0	0	0	0	0	0	0	0	0	0	0	0	0	0	0	0
<i>Egernia</i> sp. cf. <i>rugosa</i>		0	0	0	0	0	0	1	0	0	0	0	0	0	0	0	0	0	0	0	0	0	0	0	0	0	0	0
<i>Egernia striolata</i>		0	1	0	0	0	0	0	0	0	0	0	0	0	0	0	0	0	0	0	0	0	0	0	0	0	0	0
<i>Egernia</i> sp. indet.		0	0	0	0	0	0	0	0	0	0	1	0	0	0	1	0	0	0	0	0	1	0	0	0	0	0	0
cf. <i>Egernia</i> sp. indet.		0	0	0	0	0	0	0	0	0	0	0	0	0	0	0	0	0	0	0	0	0	0	0	0	0	0	0
<i>Egernia Liopholis</i> sp. indet.		0	0	0	0	0	0	0	0	0	0	0	0	0	0	0	0	0	0	0	0	0	0	0	0	0	0	0
Elapidae sp. indet.		1	1	1	0	1	0	1	2	1	1	0	0	1	0	0	1	0	0	0	0	0	2	1	0	1	1	1
Gekkonidae sp. indet.		0	0	0	0	1	0	0	0	0	0	0	0	0	0	0	0	0	0	0	0	0	0	0	0	0	0	0
<i>Liopholis inornata</i>		0	0	0	0	0	0	1	0	0	1	0	0	0	0	0	0	0	0	0	0	0	0	0	0	0	0	0

	Layer	12			13a							13b		13c							14a			14b					
	Spit #	93	94	95	96	97	98	99	100	101	102	103	104	105	106	107	108	109	110	111	112	113	114	115	116	117	118	119	120
<i>Liopholis</i> sp. indet.		0	2	0	0	1	0	0	0	0	0	0	0	0	0	0	0	0	0	0	0	0	0	0	1	0	0	0	0
<i>Liopholis whitii</i>		0	0	0	0	0	0	0	0	0	0	0	0	0	0	0	0	0	0	0	0	0	0	0	0	0	0	1	0
<i>Morelia</i> sp. indet.		0	0	0	0	0	0	0	0	0	0	0	0	0	0	0	0	0	0	0	0	0	0	0	0	0	0	0	0
Pythonidae sp. indet.		0	0	0	0	0	0	0	0	0	0	0	0	0	0	0	0	0	0	0	0	0	0	0	0	0	0	0	0
Scincidae sp. indet.		0	0	0	0	0	0	0	0	0	0	0	0	0	0	0	0	0	0	0	0	0	0	0	0	0	0	0	0
Sphenomorphinae sp. indet.		0	0	0	0	0	0	0	0	0	0	0	0	0	0	0	0	0	0	0	0	0	0	0	0	0	0	0	0
Sphenomorphus sp. indet.		0	0	0	0	0	0	0	0	0	0	0	0	0	0	0	0	0	0	0	0	0	0	0	0	0	0	0	0
cf. Sphenomorphus sp. indet.		0	0	0	0	0	0	0	0	0	0	0	0	0	0	0	0	0	0	0	0	0	0	0	0	0	0	0	0
<i>Tiliqua frangens</i>		0	0	0	0	1	0	0	0	0	0	1	0	0	1	0	0	0	0	1	0	0	0	0	1	1	0	1	1
Varanidae sp. indet.		0	0	0	0	0	0	0	0	1	0	0	0	0	0	0	0	0	0	0	0	0	0	0	0	0	0	0	0
<i>Varanus</i> sp. indet.		0	0	0	0	0	0	1	0	0	0	0	1	0	1	0	1	0	0	1	0	0	0	0	2	1	0	0	1
<i>Varanus varius</i>		0	0	0	0	0	1	0	1	0	0	1	0	1	0	0	0	0	0	0	0	0	0	0	0	0	0	0	0
<i>Wonambi naracoortensis</i>		0	0	0	0	0	0	0	0	0	0	0	0	0	0	0	0	0	0	0	0	0	1	0	2	0	0	1	0
Anura sp. indet.		1	1	0	1	1	0	1	1	0	0	0	0	0	0	0	0	0	0	1	0	0	0	0	0	0	0	0	0
<i>Crinia</i> sp. indet.		0	0	0	0	0	0	0	0	0	0	0	0	0	0	0	0	0	0	0	0	0	0	0	0	0	0	0	0
<i>Limnodynastes tasmaniensis</i>		0	0	0	0	0	0	0	0	0	0	0	0	0	0	0	0	0	0	0	0	0	0	0	0	0	0	0	0
<i>Litoria rubella</i>		0	0	0	0	0	0	0	0	0	0	0	0	0	0	0	0	0	0	0	0	0	0	0	0	0	0	0	0
Fish		0	0	0	0	0	0	0	0	0	0	0	0	0	0	0	0	0	0	0	0	0	0	0	0	0	0	0	0

	Layer	14c			NI	14c			NI	14c			NI		
	Spit #	121	122	123	124	121	122	123	124	121	122	123	124		
<i>Acrobates pygmaeus</i>		0	0	0	0	<i>Palorchestes azael</i>	0	1	0	1	<i>Trichosurus vulpecula</i>	0	0	0	0
<i>Aepyrymnus rufescens</i>		0	0	2	0	<i>Perameles gunnii nasuta</i>	7	5	1	0	Vombatidae sp. indet.	0	0	0	0
<i>Antechinus flavipes</i>		3	2	0	0	<i>Petaurus breviceps</i>	0	0	0	0	<i>Vombatus ursinus</i>	0	0	0	0
<i>Baringa</i> sp. nov. 1		0	0	0	0	<i>Petaurus</i> sp. cf. <i>breviceps</i>	0	0	0	0	<i>Wallabia bicolor</i>	0	0	0	0
<i>Bettongia gaimardi</i>		0	0	0	0	<i>Petrogale</i> sp. indet.	0	0	0	0	Accipitriformes sp. indet.	0	0	0	0
<i>Bettongia lesueur</i>		0	0	0	0	<i>Phascogale tapoatafa</i>	0	0	0	0	<i>Aquila audax</i>	0	0	0	1
<i>Bettongia</i> sp. indet.		0	0	0	0	<i>Phascogale</i> sp. cf. <i>tapoatafa</i>	0	0	0	0	Aves sp. indet.	1	1	1	0
<i>Cercartetus nanus</i>		0	0	0	0	<i>Potorous tridactylus</i>	0	0	0	0	<i>Centropus</i> sp. cf. <i>colossus</i>	0	0	0	1
<i>Chaeropus ecaudatus</i>		0	0	0	0	Potoroinae sp. indet.	1	1	1	0	<i>Coturnix pectoralis</i>	0	0	0	0
<i>Congruus kitcheneri</i>		1	0	0	0	<i>Procoptodon goliah</i>	0	1	0	0	<i>Coturnix</i> sp. indet.	0	0	0	0
<i>Conilurus albipes</i>		9	8	4	0	<i>Protomnodon brehus</i>	197	151	0	1	<i>Dromaius novaehollandiae</i>	0	0	0	0
cf. <i>Dasyuroides byrnei</i>		1	0	1	0	<i>Protomnodon</i> sp. cf. <i>brehus</i>	0	0	0	0	<i>Menura novaehollandiae</i>	0	0	0	0
Dasyuridae indet. sp. 3		0	0	0	0	<i>Protomnodon</i> sp. indet.	0	0	0	0	cf. <i>Menura novaehollandiae</i>	0	0	0	0
Dasyuridae indet. sp. 4		0	0	0	0	cf. <i>Protomnodon</i> sp. indet.	0	0	0	0	Passeriformes sp. indet.	0	0	0	0
<i>Dasyurus geoffroii viverrinus</i>		3	3	1	0	<i>Pseudocheirus peregrinus</i>	0	0	0	0	<i>Tyto</i> sp. indet.	0	0	0	1
<i>Dasyurus maculatus</i>		1	0	1	0	<i>Pseudomys australis</i>	0	0	64	0	<i>Tyto</i> sp. cf. <i>novaehollandiae</i>	0	0	0	1
Diprotodontidae gen. et. sp. indet.		1	0	0	0	<i>Pseudomys desertor</i>	2	2	0	0	Agamidae sp. indet.	0	0	0	0
<i>Hydromys chrysogaster</i>		0	0	0	0	<i>Pseudomys</i> sp. cf. <i>desertor</i>	0	0	0	0	cf. Agamidae sp. indet.	0	0	0	0
<i>Isoodon obesulus</i>		1	1	1	0	cf. <i>Pseudomys fumeus</i>	0	0	0	0	<i>Egernia cunninghami</i>	0	0	0	0
<i>Lagorchestes leporides</i>		1	0	0	0	cf. <i>Pseudomys gouldii</i>	9	7	0	0	<i>Egernia</i> sp. cf. <i>cunninghami</i>	0	0	0	0
<i>Macroderma gigas</i>		0	0	0	0	<i>Pseudomys gouldii</i>	0	0	0	0	<i>Egernia frangens</i>	0	0	0	0
<i>Macropus giganteus</i>		1	1	0	1	<i>Pseudomys gracilicaudatus</i>	0	0	1	0	<i>Egernia</i> sp. cf. <i>rugosa</i>	0	0	0	0

	Layer Spit #	14c			NI		14c			NI		14c			NI
		121	122	123	124		121	122	123	124		121	122	123	124
<i>Macropus</i> sp. indet.		0	0	0	0	<i>cf. Pseudomys gracilicaudatus</i>	0	0	0	0	<i>Egernia striolata</i>	0	0	0	0
<i>Macrotis lagotis</i>		0	0	0	0	<i>Pseudomys</i> sp. cf. <i>gracilicaudatus</i>	0	0	0	0	<i>Egernia</i> sp. indet.	0	0	0	0
<i>Mastacomys fuscus</i>		6	6	1	0	<i>Pseudomys novaehollandiae</i>	0	0	3	0	cf. <i>Egernia</i> sp. indet.	0	0	0	0
<i>Megalibgwilia ramsayi</i>		1	0	0	0	<i>Pseudomys oralis</i>	0	1	0	0	<i>Egernia Liopholis</i> sp. indet.	0	0	0	0
<i>Microchiroptera</i> sp. indet.		2	2	1	0	<i>Pseudomys</i> sp. cf. <i>oralis</i>	0	0	0	0	Elapidae sp. indet.	0	1	0	0
Murinae sp. 1		0	0	0	0	<i>Rattus fuscipes</i>	0	0	0	0	Gekkonidae sp. indet.	0	0	0	0
Murinae sp. 2		0	0	0	0	<i>Rattus</i> sp. cf. <i>tunneyi</i>	1	0	0	0	<i>Liopholis inornata</i>	0	0	0	0
Murinae sp. 3		0	0	0	0	<i>Rattus</i> sp. cf. <i>lutreolus</i>	2	2	2	0	<i>Liopholis</i> sp. indet.	0	0	0	0
Murinae sp. 4		0	0	0	0	<i>Rattus</i> sp. indet.	0	0	0	1	<i>Liopholis whittii</i>	0	0	0	0
Murinae sp. 5		0	0	0	0	<i>Sarcophilus lanarius</i>	1	0	0	0	<i>Morelia</i> sp. indet.	0	0	0	0
Murinae sp. 6		0	0	0	0	<i>Simosthenurus pales</i>	0	0	0	0	Pythonidae sp. indet.	0	0	0	0
Murinae sp. 7		0	0	0	0	<i>Sminthopsis crassicaudata</i>	1	0	0	0	Scincidae sp. indet.	0	0	1	0
<i>Notamacropus agilis</i>		1	1	0	1	<i>Sminthopsis</i> sp. cf. <i>crassicaudata</i>	0	0	0	0	Sphenomorphinae sp. indet.	0	0	0	0
<i>Notamacropus dorsalis</i>		0	1	0	0	cf. <i>Sminthopsis crassicaudata</i>	0	0	0	0	Sphenomorphus sp. indet.	0	0	0	0
<i>Notamacropus</i> sp. cf. <i>dorsalis</i>		0	0	1	1	<i>Sminthopsis murina</i>	1	0	1	0	cf. Sphenomorphus sp. indet.	0	0	0	0
<i>Notamacropus parma</i>		1	1	0	0	<i>Sminthopsis</i> sp. cf. <i>murina</i>	0	0	0	0	<i>Tiliqua frangens</i>	0	1	0	1
<i>Notamacropus parryi</i>		0	0	0	0	<i>Sminthopsis</i> sp. indet.	0	0	0	0	Varanidae sp. indet.	0	0	0	0
<i>Notamacropus</i> sp. indet.		0	0	0	0	Sthenurinae sp. indet.	0	0	0	0	<i>Varanus</i> sp. indet.	0	1	0	0
<i>Notomys</i> sp. indet.		1	0	1	0	<i>Sthenurus andersoni</i>	0	1	0	0	<i>Varanus varius</i>	0	0	1	0
<i>Onychogalea frenata</i>		0	0	0	0	<i>Sthenurus atlas</i>	1	0	0	0	<i>Wonambi naracoortensis</i>	0	0	0	0
<i>Onychogalea lunata</i>		0	0	0	0	<i>Tachyglossus aculeatus</i>	0	0	0	0	Anura sp. indet.	1	0	0	0
<i>Osphranter robustus</i>		1	1	0	0	<i>Thylacinus cynocephalus</i>	1	0	0	0	<i>Crinia</i> sp. indet.	0	0	0	0
cf. <i>Osphranter robustus</i>		0	0	0	0	<i>Thylacinus Sarcophilus</i> sp. indet.	0	0	0	0	<i>Limnodynastes tasmaniensis</i>	0	0	0	0
<i>Osphranter rufus</i>		1	0	0	0	<i>Thylacoleo carnifex</i>	1	0	0	1	<i>Litoria rubella</i>	0	0	0	0
						<i>Trichosurus</i> sp. cf. <i>vulpecula</i>	0	0	1	0	Fish	0	0	0	0

Table 7.14 Spit concatenation. * indicates that only key specimens from this sample have been included. Spit 125 is only partially processed. Samples not included are listed at the bottom of the table as “NI”.

Spit		Quad-Layer-Depth		Spit		Quad-Layer-Depth	
1	B-1-181-183			63	B-10-295-300	E-10-295-300	A-10-295-300
2	B-2-183-188			64	B-10-300-305		
3	E-2-187-192	B-2-188-193		65	B-10-305-310	E-10-305-310	A-10-305-310
4	E-2-192-200			66	B-10-310-315	E-10-310-315	
5	E-2-200-205			67	B-10-315-320	E-10-315-320	A-10-315-320
6	E-2-205-210			68	E-10-320-325	B-10-320-325	A-10-320-325
7	E-2b-230-235			69	E-10-325-330	B-10-325-330	A-10-325-330
8	B-2b-236-241	A-2b-236-241	E-2b-235-240	70	E-10-330-335	B-10-330-335	A-10-330-335
9	A-2b-241-246	E-2b-240-245	E-2b-240-245	71	B-10-335-340	E-10-335-340	A-10-335-340
10	E-2b-245-250			72	B-10-340-345	E-10-340-345	A-10-340-345
11	A-2b-245-265 WC			73	B-10-345-350	E-10-345-350	
12	A-2b-247-252	B-2b-246-251	A-2b-246-261	74	E-10-350-355	B-10-350-355	
13	A-2b-252-257	B-2b-251-256		75	E-10-355-360	II-10-355-360	
14	A-2b-257-262			76	II-10-360-365	E-10-360-365	II-10-360-365
15	A-2b-265-270			77	II-10-365-370	E-10-365-370	
16	A-2b-270-275			78	II-10-370-375	E-10-370-375	
17	A-2b-275-280			79	II-10-375-380		
18	A-2b-280-285			80	II-10-380-385		
19	A-2b-285-290			81	II-10-385-390		
20	B-3-195-198.5			82	II-10-390-395		
21	B-4-195-200			83	II-10-395-400	I-10-395-400	
22	B-4-200-205			84	II-10-400-405		

Spit		Quad-Layer-Depth		Spit		Quad-Layer-Depth		
23	B-4-205-210			85	II-10-405-410			
24	E-4-210-215			86	II-12-410-415			
25	B-4-210-220			87	II-12-415-420			
26	E-4-215-220			88	II-12-420-425			
27	B-5-210-215			89	II-12-425-430			
28	A-8-248-253	A-8-251-256	E-8-250-255	90	II-12-430-435			
29	B-8-256-261	E-8-255-260	A-8-256-261	91	II-12-435-440			
30	A-8-258-264	E-8-260-265	A-8-261-266	B-8-261-266	92	II-12-440-445		
31	B-8-266-269	E-8-265-270	A-8-264-269	93	II-12-445-450			
32	E-8-270-275	B-8-269-274		94	II-12-450-455			
33	A-8-270-280			95	II-12-455-460			
34	B-8-274-279	B-8-275-280	E-8-275-280	96	II-13-455-460			
35	B-8-279-284	A-8-275-285	B-8-279-284	97	II-13-460-465			
36	B-8-284-289			98	II-13-465-470	I-13-465-470		
37	E-8-290-295			99	II-13-470-475	III-13-470-475		
38	B-8-295-300			100	II-13-475-480	I-13-475-480		
39	B-8-305-310			101	II-13-480-485	I-13-480-485		
40	E-9-230-235	E-9-235-240	B-9-SFR	A-9-SFR	102	II-13-480-495		
41	A-9-280-295			103	II-13-485-490	III-13-485-490		
42	B-9-220-225			104	II-13-490-495	I-13-490-495		
43	A-9-230-235			105	II-13-495-500			
44	E-9-250-255	B-9-251-256		106	II-13-500-505	I-13-500-505		
45	E-9-255-260			107	II-13-500-510			
46	E-9-260-265	B-9-261-266	A-9-258-264	B-9-260-265	108	II-13-500-515	IV-13-500-515	III-13-500-515

Spit						Quad-Layer-Depth						
47	E-9-265-270	A-9-264-269	B-9-266-269	A-9-265-270		109	II-13-505-510	I-13-505-510	III-13-505-510			
48	A-9-269-274	E-9-270-275	B-9-269-274			110	II-13-505-515					
49	E-9-275-280	B-9-275-280	E-9-275-280	A-9-274-279	A-9-275-280	111	II-13-505-520	I-13-505-520				
50	B-9-280-285	E-9-280-285	A-9-279-284			112	II-13-510-520	I-13-510-520				
51	A-9-280-295					113	II-13-515-520					
52	E-9-285-290	A-9-284-289	A-9-285-290			114	II-13-520-525	I-13-520-525				
53	A-9-289-294	E-9-290-295				115	II-13-525-530	IV-13-520-530				
54	A-9-295-300					116	II-14-9.2.17	II-14-515-520	I-14-513	II-14-10.2.17	I-14-9.2.17	
55	A-9-300-305					117	II-14-520-525					
56	B-10-220-225					118	II-14-515-530					
57	E-10-225-230					119	II-14-525-530	I-14-525-530	II-14-530-535	I-14-530-535		
58	E-10-230-235					120	II-14-535-540+	I-14-535-540+	I-14-535-540	II-14-535-540	I-14-535-540	III-14-555-560
59	E-10-235-240					121	II-14-560-565	IV-14-560-565	I-14-560-565+			
60	B-10-280-285	E-10-280-285				122	II-14-570-575+	II-14-570-575				
61	B-10-285-290					123	II-14-575-580	I-14-575-580	III-14-575-580			
62	E-10-290-295	B-10-290-295										
124	II-14-580-585	IV-14-585-590	I-14-620-625	I-14-615-620	I-14-635-640	I-14-635-640	IV-14-635-640	I-14-625-630	II-14-610-615	I-14-630-635	II-14-610-615	I-14-620-625
NI	I-13F-510-515	I-14F-530-540	I-14F-595-600	IV-14F-590-595	III-10-415	B-BT-215-220	B-BT-305-310	B-BT-315-320	A-BT-320-330	A-BT-330-335	C-2b-270-275	

Table 7.15, Partitioning logic for layers 10, 13 and 14 showing 5, 4, 3 and 2 clusters and the final layer partitioning used in this thesis based on achieving comparable sample sizes (n) within each layer.

layer 10					layer 13					layer 14						
partition (MNI)	spit #	n clusters				partition (n)	spit #	n clusters				partition (n)	spit #	n clusters		
		5	4	3	2			5	4	3	2			4	3	2
10a (496)	56	4	3	2	2	13a (233)	96	5	3	2	2	14a (413)	116	5	2	1
	57	2	1	2	2		97	3	2	1	2		117	5	2	1
	58	2	1	2	2		98	3	2	2	2		118	3	3	2
	59	2	3	2	2		99	3	2	2	2	14b (476)	119	4	2	1
	60	2	3	2	2		100	3	2	3	2		120	2	2	1
	61	1	4	3	1		101	3	2	2	2	14c (547)	121	1	4	1
	62	2	1	2	2		102	3	2	3	2		122	1	4	1
	63	3	3	1	1		103	3	2	3	2		123	1	1	1
	64	3	4	1	1		104	3	2	3	2					
	65	3	3	1	1		13b (218)	105	3	2	3	2				
66	2	1	2	2	106	3		2	3	2						
67	5	1	2	2	107	1		1	3	1						
10b (612)	68	5	1	2	2	13c (245)	108	2	2	3	2					
	69	5	1	2	2		109	3	2	3	2					
	70	2	1	2	2		110	4	2	2	2					
	71	5	1	2	2		111	3	2	3	2					
10c (555)	72	2	1	2	2	112	3	2	3	2						
	73	4	3	2	2	113	1	1	3	1						
	74	5	1	2	2	114	3	2	3	2						
	75	4	3	2	2	115	3	4	2	2						
10d (341)	76	2	1	2	2											
	77	5	1	2	2											
	78	2	3	2	2											
	79	4	3	1	2											
	80	4	3	1	2											
	81	3	4	1	1											
	82	3	4	1	1											
	83	3	3	1	1											
	84	1	2	3	1											
	85	3	4	1	1											

Table 7.16. Ecological table for the Cathedral Cave fauna. Diet; I = insectivore, C = carnivore, O = omnivore, H = herbivore, G = granivore, F = frugivore, Fo = foliovore, Fu = fungivore, E = exudivore. Behaviour; T = terrestrial, A = arboreal, S = scansorial, V = volant., Aq = aquatic. Conservation status; LC = least concern, EX = extinct, NT = near threatened, VU = vulnerable. Local status; P = present, EX = locally extinct, D = declined, SD = severely declined, ? = unknown.

species	Bodyweight (kg)	Ecology	Diet	Behaviour	Cons. status	Local status	References
Tachyglossidae							
<i>Tachyglossus aculeatus</i>	2 - 7	Found in most habitats of Australia.	I	T	LC	P	Augee (2008); Burbidge et al. (2009)
<i>Megalibgwilia ramsayi</i>	est. 10 - 12 kg	Mostly temperate distribution.	I	T	EX	EX	Johnson (2006); Peters et al. (2019)
Dasyuridae							
<i>Dasyurus geoffroii</i>	0.615 - 2.185	Forest, shrub, and desert, except in the south-east coast and top end where is now found in sclerophyll forest or drier woodland, heath and mallee shrubland.	C	T	NT	EX	Serena and Soderquist (2008); Woinarski et al. (2014)
<i>Dasyurus viverrinus</i>	0.700 - 1.9	Broad habitats, but preference for open forest and woodland, open grasslands, and alpine heaths.	C	T	EN	EX	Jones (2008a); Woinarski et al. (2014)
<i>Dasyurus maculatus</i>	0.8 - 2.5	Broad range of habitats, including rainforest, wet and dry sclerophyll forest, coastal heathland, scrub and dunes, woodland, heathy woodland, swamp forest, mangroves, on beaches and sometimes in grassland or pastoral areas adjacent to forested areas.	C	T	NT	SD	Belcher et al. (2008); Department of Environment Land Water and Planning (2016)
<i>Sarcophilus laniarius</i>	5 - 14	Open dry eucalyptus forests, grassy woodlands, coastal scrub.	C	T	EN (EX on mainland)	EX	Jones (2008b)
<i>Antechinus flavipes</i>	0.021 - 0.079	Dry arid scrubland, sclerophyll forest, coastal heath, swamps and woodland, far north tropical vine forest. Positively correlated with tree density, hollow bearing trees, ground cover and leaf litter.	I	T	LC	D	Crowther (2008); (Kelly and Bennett, 2008)
<i>Phascogale tapoatafa</i>	0.106 - 0.311	Dry sclerophyll forests and woodlands, open forest with sparse groundcover, but uses habitats ranging from mallee to rainforest.	C	A	NT	SD	Soderquist and Rhind (2008)
<i>Phascogale calura</i>	0.093 - 0.122	Forest, woodland, prefers Wandoo and sheoak woodlands.	C	A		EX	Bradley et al. (2008)
<i>Sminthopsis crassicaudata</i>	0.011 - 0.02	Open country, including open woodland, low shrublands of saltbush and bluebush, tussock and spinifex grasslands on clay or sandy soils, gibber plain.	C	T	LC	D	Morton and Dickman (2008)
<i>Sminthopsis murina</i>	0.010 - 0.028	Woodland, open forest and heathland and transitional habitat at edge of tropical moist forests.	C	T	LC	D	Fox (2008a)
<i>Dasyuroides byrnei</i>	0.07 - 0.18	Gibber plains and grasslands.	I	T	VU	EX	Lim (2008)
Thylacinidae							
<i>Thylacinus cynocephalus</i>	13 - 35 kg	Open forest and woodland.	C	T	EX	EX	Mooney and Rounsevell (2008)
Chaeropodidae							
<i>Chaeropus ecaudatus</i>	est. 0.2	Semi-arid shrubland.	H	T	EX	EX	Johnson and Burbidge (2008); Travouillon et al. (2019)
Peramelidae							

species	Bodyweight (kg)	Ecology	Diet	Behaviour	Cons. status	Local status	References
<i>Isoodon obesulus</i>	0.4 - 1.85	Forest woodland shrub and heath communities. Prefers dense vegetation.	O	T	LC	EX	Paull (2008)
<i>Perameles gunnii</i>	Av. 0.75 (Vic), 1 (Tas)	Perennial tussock grasslands and grassy woodlands particularly along watercourses.	O	T	VU	EX	Seebeck (1979); Brown (1989); Dufty (1994); Seebeck and Menkhorst (2008)
<i>Perameles nasuta</i>	0.52 - 1.33	Heath and forest habitats close to grassy open feeding sites.	O	T	LC	SD	Dickman and Stodart (2008)
Thylacomyidae							
<i>Macrotis lagotis</i>	0.8 - 2.5	Grassland, dune fields, hummock spinifex grassland and acacia shrubland.	O	T	VU	EX	Johnson (2008a)
Vombatidae							
<i>Vombatus ursinus</i>	2.2 - 2.9	Temperate forested areas, sclerophyll forest, coastal scrub and heathland.	H	T	LC	D	McIlroy (2008)
Diprotodontidae							
Diprotodontidae gen. et sp. indet.	-	-	H	T	EX	EX	-
Palorchestidae							
<i>Palorchestes azael</i>	791 - 1413	Forested environments	H	T	EX	EX	Richards et al. (2019)
Thylacoleonidae							
<i>Thylacoleo carnifex</i>	130	Dry, open forest habitat	C	T	EX	EX	Wroe et al. (1999)
Burramyidae							
<i>Cercartetus nanus</i>	15 - 43 g average 24.	Shrubby understorey of rainforest, sclerophyll forest, shrubland, heathland and woodland. Strongly associated with banksia.	E	A	LC	D	Ward and Turner (2008); Harris et al. (2014); (Isaac et al., 2014)
Petauridae							
<i>Petaurus breviceps</i>	0.095 - 0.160	Wet or dry sclerophyll forest and acacia scrub. Preferring habitats with eucalypt and acacia species. Requires many stems in the canopy and dense mid-upper canopy cover to allow efficient movement.	E	A, V	LC	D	Jackson (2000); Suckling (2008); (Isaac et al., 2014)
Pseudocheiridae							
<i>Pseudocheirus peregrinus</i>	0.7 - 0.9	Preference for forests of dense brush, particularly eucalyptus forests.	Fo	A	LC	D	How et al. (1984); Smith and Lee (1984)
Acrobatidae							
<i>Acrobates pygmaeus</i>	0.010 – 0.015	Open and closed forests and woodlands of eastern Australia, especially tall eucalyptus forest.	E	A, V	LC	D	Ward and Woodside (2008); (Isaac et al., 2014); Harris (2015)
Phalangeridae							
<i>Trichosurus vulpecula</i>	1.2 - 4.5	Broad but prefers dry eucalypt forests and woodlands	Fo, O	A	LC	D	Kerle and How (2008)
Potoroidae							
<i>Aepyprymnus rufescens</i>	1.9 - 3.0	Open forest woodlands. Sparse, grassy, tussock grass understorey. Shelters in dense tall grasses.	H	T	LC	EX	Dennis and Johnson (2008)

species	Bodyweight (kg)	Ecology	Diet	Behaviour	Cons. status	Local status	References
<i>Bettongia gaimardi</i>	1.2 - 2.25	Open forest with grassy understorey.	Fu	T	NT	EX	Rose and Johnson (2008)
<i>Bettongia lesueur</i>	0.68 - 1.28	Dry, open, fire-prone forests with grassy or heath understorey.	Fu	T	NT	EX	Burbidge and Short (2008)
<i>Potorous tridactylus</i>	0.66 - 1.64	Dry and wet sclerophyll forests, coastal heath, dense groundcover.	O	T	NT	EX	Johnston (2008)
Macropodidae							
<i>Sthenurus andersoni</i>	50	Browser, open habitats? Most widely distributed Sthenurine, through the south, includes temperate and semi-arid distributions	H	T	EX	EX	Johnson (2006)
<i>Sthenurus atlas</i>	150	Browser, includes temperate and semi-arid distributions	H	T	EX	EX	Johnson (2006)
<i>Simosthenurus pales</i>	150	Browser, temperate woodlands, and open forests	H	T	EX	EX	Johnson (2006); Prideaux (2004)
<i>Procoptodon goliah</i>	250	Browser, known from arid to semi-arid sites.	H	T	EX	EX	Prideaux et al. (2009)
<i>Congruus kitcheneri</i>	est. 60	Semi-arid woodland, savanna	H	S? A?	EX	EX	G. Prideaux, pers comms.
<i>Protemnodon brehus</i>	100-111	Open woodland?	H	T	EX	EX	Prideaux (2004); Helgen et al. (2006)
<i>Baringa</i> sp. nov. 1	est. 40	Semi-arid woodland, savanna.	H	S? A?	EX	EX	G. Prideaux, pers comms.
<i>Lagorchestes leporides</i>	2.5	Data deficient. Open plains and grassland.	H	T	EX	EX	Gould and Dixon (1983); Johnson et al. (1989)
<i>Macropus giganteus/titan/ferragus</i>	17 - 72 (<i>M. giganteus</i>)	Sclerophyll forest, woodlands (including mallee scrub), shrubland and heathlands.	H	T	LC	P	Coulson (2008)
<i>Notamacropus agilis</i>	9 - 27	Open woodland and grassland habitat.	H	T	LC	EX	Merchant (2008a)
<i>Notamacropus dorsalis</i>	5.2 - 21	Southern range - forest with dense shrub layer, rainforest margins, brigalow scrub, open forest with thick Acacia or other shrub understorey and lantana thickets. Northern range - dry vine thickets, rubber vine thickets, and open forest or woodland with a shrub understorey.	H	T	LC	EX	Johnson (2008b)
<i>Notamacropus parma</i>	3.2 - 5.	Wet and dry forests in rainforests but wet sclerophyll forest with thick shrubby understorey associated with grassy patches. Occasionally dry sclerophyll forest.	H	T	NT	EX	Maynes (2008); Woinarski et al. (2015b)
<i>Notamacropus parryi</i>	7 - 26	Open forest and grassy understorey, dry savanna.	H	T	LC	EX	Johnson (2008c)
<i>Onychogalea frenata</i>	4 - 8	Tall acacia shrubland and grassy woodland.	H	T	VU	EX	Evans and Gordon (2008)
<i>Onychogalea lunata</i>	est. 3.5	Data deficient. Woodland, thick scrub and dense thickets, open woodland. Open timbered country.	H	T	EX	EX	Burbidge (2008)
<i>Petrogale</i> sp. <i>indet.</i>	4.9 - 10.9	Rocky habitat, foraging habitat includes forest and woodland with a grassy understorey. Ecology based on <i>P. penicillata</i> as a likely candidate for the Wellington species.	H	T	VU	SD	Eldridge and Close (2008)
<i>Wallabia bicolor</i>	10.3 - 20.5	Dense vegetation, in forests, woodlands and heath, Brigalow scrub is a preferred habitat	H	T	LC	P	Merchant (2008b)
<i>Osphranter robustus/altus</i>	6.25 - 60 kg	Broad.	H	T	LC	P	Clancy and Croft (2008)
<i>Osphranter rufus</i>	7.45 - 14	Prefers open habitats, arid and semi-arid.	H	T	LC	P	Croft and Clancy (2008)

Muridae

species	Bodyweight (kg)	Ecology	Diet	Behaviour	Cons. status	Local status	References
<i>Conilurus albipes</i>	est. 0.2	Open eucalypt forest.	?	T,S?	EX	EX	Dixon (2008a); Woinarski et al. (2015b)
<i>Hydromys chrysogaster</i>	0.34 – 1.27	Watercourses. Needs free water.	C	Aq	LC	P	
<i>Mastacomys fuscus</i>	0.019 – 0.145	Preferred habitats include alpine and subalpine heathlands, grassland adjacent to boulder outcrops, swamps, sedgeland, coastal grassy or shrubby dunes, occasionally forests with grassy understorey. Requires available cover, grasses, and proximity to watercourses.	H	T	NT	EX	Happold (2008); Woinarski et al. (2015b)
<i>Notomys</i> sp. 1	<0.1	<i>N. mitchellii</i> - mallee/eucalypt woodland with sandy soils and dune fields. <i>N. longicaudatus</i> - acacia and eucalypt woodlands, hummock grassland and low shrubland. <i>N. fuscus</i> - dune fields. <i>N. cervinus</i> - harsh gibber plains and alluvial flats.	G	T	Varies for species	EX	Woinarski et al. (2015b)
<i>Pseudomys australis</i>	0.030 – 0.065	Gibber plains, cracking clay depressions in arid and semi-arid regions, grasslands, dunes, stony swales. Also, river flats, grasslands sand ridges and lowland shrubs.	H	T	VU	EX	Watts and Aslin (1981); Medlin (2008)
<i>Pseudomys desertor</i>	0.011 – 0.035	Most records from sand dune or sand plain spinifex habitats but has been found in savannah woodland, shrubland and grassland. Requires dense groundcover of hummock or tussock grasses, sedges or shrubs. Also known from samphire, chenopod and nitrebush shrublands.	O	T	LC	EX	Kutt et al. (2004); Kerle et al. (2008)
cf. <i>Pseudomys fumeus</i>	0.038 – 0.09	Coastal heath, dry ridgeline forest, sub-alpine heath, occasionally wetter gullies.	O	T	VU	EX	Menkhorst and Seebeck (1981); Ford (2008)
<i>Pseudomys gouldii</i>	est. 0.05	John Gould recorded <i>P. gouldii</i> on the "...plains and sand hills of the interior."	T	T	EX	EX	Dixon (2008b)
<i>Pseudomys gracilicaudatus</i>	0.045 – 0.118	Open woodlands and open dry sclerophyll forests in grassy understorey. Tall open wet sclerophyll forest with grassy round layers, often on ridgetops. Heathland dense wet heath and swampy areas usually shared with <i>Rattus lutreolus</i> .	T	T	LC	EX	Fox (2008b)
<i>Pseudomys novaehollandiae</i>	0.012 – 0.029	Heathlands, woodlands, open forest, paperbark swamps, sandy, loamy and rocky soils.	O	T	VU	EX	Kemper and Wilson (2008)
<i>Pseudomys oralis</i>	0.08 – 0.1	Small, frequently rocky areas in open wet or dry sclerophyll forest and woodlands with native grass, sedge, rush fern or heath understorey.	O	T	VU	EX	Townley (2008); Woinarski et al. (2015b)
<i>Rattus fuscipes</i>	0.04 – 0.225	Dense undergrowth of shrubs and ferns, subalpine woodland, coastal scrub, coastal heath, eucalypt forest and tropical moist forest.	O	T	LC	EX	Lunney (2008b)
<i>Rattus</i> sp. cf. <i>lutreolus</i>	0.05 – 0.2	Dense heath, grass, or sedge.	O	T	LC	EX	Lunney (2008a)
<i>Rattus</i> sp. cf. <i>tunneyi</i>	0.041 – 0.085	Tall grasslands often associated with seasonal waterways.	O	T	LC	EX	Aplin et al. (2008)
Chiroptera							
<i>Macroderma gigas</i>	0.14 – 0.165	Diverse, from lush rainforests of north QLD to arid Pilbara.	C	V	VU	EX	Richards et al. (2008)
<i>Microchiroptera</i> spp. inc.	<i>C.g.</i> 0.008 – 0.018	<i>C. gouldii</i> – distributed across most of Australia, except northern Cape York Peninsula and the Nullarbor Plain, in a variety of habitats. <i>R. megaphylus</i> – east coast distribution, forages in rainforest, eucalypt open forest and woodland, rarely moves outside stands of vegetation when foraging or commuting. <i>M. oriana</i> – temperate, subtropical and tropical distribution.	I	V	<i>R. m.</i> – LC <i>M. shreibersii</i> – VU <i>M. australis</i> - LC	<i>R. m.</i> – P <i>M. sp.</i> – P	Dixon and Lumsden (2008); Hoye and Hall (2008a, 2008b); Pavey and Young (2008),
<i>Chalinolobus gouldii</i> ,	<i>R.m.</i> 0.007 – 0.013						
<i>Rhinolophus megaphylus</i> ,	<i>M. spp.</i> 0.005 – 0.02						
<i>Miniopterus oriana</i>							

Table 7.17. Weighted habitat scores for Taxonomic Habitat Index, for arid, semi-arid, temperate, sub-tropical and tropical biomes across layers and sublayers.

	biome score					Present in layer												
	arid	semi-arid	temperate	sub-tropical	tropical	1-8	9	10a	10b	10c	10d	12	13a	13b	13c	14a	14b	14c
<i>Tachyglossus aculeatus</i>	0.2	0.2	0.2	0.2	0.2							X			X			
<i>cf. Dasyuroides byrnei</i>	0.5	0.5	0	0	0		X		X	X	X				X	X		X
<i>Dasyurus geoffroii/viverrinus</i>	0.2	0.25	0.5	0.05		X	X	X	X	X	X	X	X	X	X	X	X	X
<i>Dasyurus maculatus</i>	0	0.1	0.8	0.1	0									X			X	X
<i>Sarcophilus lanianus</i>	0	0	1	0	0				X									X
<i>Antechinus flavipes</i>	0	0.15	0.6	0.15	0.1	X		X	X	X	X	X	X	X	X	X	X	X
<i>Phascogale tapoatafa</i>	0	0.05	0.8	0.1	0.05				X	X			X	X	X	X	X	
<i>Sminthopsis crassicaudata</i>	0.35	0.35	0.15	0.15	0	X	X	X	X	X	X	X	X	X	X	X		X
<i>Sminthopsis murina</i>	0	0.25	0.25	0.45	0.05	X	X	X	X	X	X	X	X	X	X	X	X	X
<i>Thylacinus cynocephalus</i>	0	0	0.8	0.2	0							X				X	X	X
<i>Chaeropus ecaudatus</i>	0.1	0.8	0.1	0	0	X		X	X	X	X							
<i>Isoodon obesulus</i>	0	0.02	0.9	0.04	0.04	X	X	X	X	X	X	X	X	X	X	X	X	X
<i>Perameles gunni/nasuta</i>	0	0	0.7	0.3	0	X	X	X	X	X	X	X	X	X	X	X	X	X
<i>Macrotis lagotis</i>	0.2	0.3	0.4	0.1	0					X	X							
<i>Vombatus ursinus</i>	0	0.2	0.75	0.05	0	X	X			X	X	X	X	X	X		X	
<i>Palorchestes azael</i>	0	0	0.5	0.5	0													X
<i>Thylacoleo carnifex</i>	0	0.4	0.6	0	0					X								X
<i>Cercartetus nanus</i>	0	0.05	0.9	0.05	0					X	X		X	X	X	X		
<i>Petaurus breviceps</i>	0	0.1	0.6	0.2	0.1	X	X		X	X	X	X	X	X	X	X	X	
<i>Pseudocheirus peregrinus</i>	0	0.05	0.5	0.4	0.05	X			X				X			X	X	X
<i>Acrobates pygmaeus</i>	0.05	0.1	0.7	0.1	0.05								X	X	X			
<i>Trichosurus vulpecula</i>	0.1	0.2	0.4	0.2	0.1	X	X		X		X				X			X
<i>Aepyprymnus rufescens</i>	0	0.05	0.4	0.4	0.15	X		X	X	X	X	X	X	X		X	X	
<i>Bettongia gaimardi</i>	0	0	0.9	0.1	0					X		X	X		X			
<i>Bettongia lesueur</i>	0.4	0.4	0.2	0	0	X	X	X	X	X	X			X				
<i>Potorous tridactylus</i>	0	0	0.8	0.2	0	X		X		X	X	X	X	X	X	X	X	X
<i>Sthenurus andersoni</i>	0.1	0.4	0.5	0	0		X	X					X					X
<i>Sthenurus atlas</i>	0.1	0.4	0.5	0	0													X
<i>Simosthenurus pales</i>	0.1	0.4	0.5	0	0							X	X					

	biome score					Present in layer												
	arid	semi-arid	temperate	sub-tropical	tropical	1-8	9	10a	10b	10c	10d	12	13a	13b	13c	14a	14b	14c
<i>Procoptodon goliah</i>	0	0.5	0.5	0	0	X					X							
<i>Congruus kitcheneri</i>	0	1	0	0	0				X	X		X	X		X		X	X
<i>Protemnodon brehus</i>	0	0	1	0	0				X				X		X			
<i>Baringa</i> sp. nov. 1	0	1	0	0	0				X		X				X			
<i>Petrogale</i> sp. indet.	0	0.1	0.5	0.2	0.2								X					
<i>Lagorchestes leporides</i>	0.05	0.5	0.4	0.05	0	X	X	X		X		X	X					X
<i>Macropus giganteus/titan/ferragus</i>	0.05	0.2	0.4	0.25	0.1	X		X	X	X	X	X	X			X	X	X
<i>Notamacropus agilis</i>		0.2	0.25	0.25	0.3			X			X	X	X				X	X
<i>Notamacropus dorsalis</i>	0	0.2	0.3	0.5	0	X					X	X	X				X	X
<i>Notamacropus parma</i>	0	0	0.8	0.2	0	X			X	X	X	X	X	X	X		X	X
<i>Notamacropus parryi</i>	0	0.1	0.3	0.5	0.1						X	X			X		X	
<i>Onychogalea frenata</i>	0.1	0.3	0.3	0.3	0	X	X		X	X	X	X						
<i>Onychogalea lunata</i>	0	0.4	0.4	0.2	0	X		X		X								
<i>Wallabia bicolor</i>	0	0.15	0.5	0.3	0.05						X							
<i>Osphranter robustus/altus</i>	0.2	0.2	0.2	0.2	0.2					X	X	X	X			X	X	X
<i>Osphranter rufus</i>	0.4	0.3	0.2	0.05	0.05		X											X
<i>Conilurus albipes</i>	0.05	0.15	0.8	0	0	X	X	X	X	X	X	X	X	X	X	X	X	X
<i>Hydromys chrysogaster</i>	0.05	0.2	0.5	0.2	0.05					X					X			
<i>Mastacomys fuscus</i>	0	0	1	0	0	X		X	X	X	X		X		X	X	X	X
<i>Notomys</i> sp.	0.5	0.3	0.2	0	0	X	X	X	X	X	X	X	X		X	X		X
<i>Pseudomys australis</i>	0.4	0.4	0.2	0	0	X	X	X	X	X	X	X	X	X	X	X	X	X
<i>Pseudomys desertor</i>	0.45	0.45	0.05	0.05	0	X	X	X	X	X	X							
cf. <i>Pseudomys fumeus</i>	0	0	1	0	0			X										
<i>Pseudomys gouldii</i>	0.4	0.3	0.3	0	0	X			X									
<i>Pseudomys gracilicaudatus</i>	0	0	0.4	0.4	0.2	X	X	X	X	X	X		X	X	X	X	X	X
<i>Pseudomys novaehollandiae</i>	0	0	0.9	0.1	0	X	X	X	X	X	X	X	X	X	X	X	X	X
<i>Pseudomys oralis</i>	0	0	0.7	0.3	0									X	X	X	X	
<i>Rattus fuscipes</i>	0	0.05	0.8	0.1	0.05	X												

	biome score					Present in layer												
	arid	semi-arid	temperate	sub-tropical	tropical	1-8	9	10a	10b	10c	10d	12	13a	13b	13c	14a	14b	14c
<i>Rattus</i> sp. cf. <i>lutreolus</i>	0	0.05	0.85	0.1	0							X	X	X	X	X	X	X
<i>Rattus</i> sp. cf. <i>tunneyi</i>	0.05	0.05	0.2	0.35	0.35	X			X				X					X
					# species	31	19	23	28	33	32	28	34	22	30	24	28	34

Table 7.18 Cumulative habitat score and Taxonomic Habitat Index generated from biome scores for the Cathedral Cave fauna present in each layer

cumulative habitat score					
Layer	arid	semi-arid	temperate	sub-tropical	tropical
1-8	3.2	6.62	14.85	5.04	1.29
9	3.6	5.07	8	1.99	0.34
10a	2.65	5.57	10.8	2.54	0.74
10b	3.65	7.32	12.35	3.59	1.09
10c	3.6	7.97	16.8	3.79	0.84
10d	3.6	7.77	14.45	4.89	1.29
12	2.25	5.62	14	4.79	1.34
13a	2.1	5.77	18.85	5.34	1.94
13b	1.45	2.67	13.7	3.44	0.74
13c	2.4	5.62	16.8	4.14	1.04
14a	2.25	3.12	13.55	4.04	1.04
14b	0.9	3.72	16.1	5.84	1.44
14c	3.05	6.62	17.2	5.59	1.54
total habitat index					
1-8	0.10	0.21	0.48	0.16	0.04
9	0.19	0.27	0.42	0.10	0.02
10a	0.12	0.24	0.49	0.12	0.03
10b	0.13	0.26	0.44	0.13	0.04
10c	0.11	0.24	0.51	0.11	0.03
10d	0.11	0.24	0.45	0.15	0.04
12	0.08	0.20	0.50	0.17	0.05
13a	0.06	0.17	0.55	0.16	0.06
13b	0.07	0.12	0.62	0.16	0.03
13c	0.08	0.19	0.56	0.14	0.03
14a	0.09	0.13	0.56	0.17	0.04
14b	0.03	0.13	0.58	0.21	0.05
14c	0.09	0.19	0.51	0.16	0.05

Table 7.19. Data used for biodiversity curves showing species richness (S), expected species richness by rarefaction (E), Minimum Number of Individuals (MNI), Simpson 1-D, Shannon (H') and Equitability (J) for mammalian taxa across layers and sublayers. E was standardised by rarefaction normalised to the smallest sample of 119 from layer 12.

Layer/Sublayer	S	E	MNI	1-D	H'	J
1_8	35	26	269	0.88	2.76	0.78
9	21	17	181	0.61	1.69	0.56
10a	26	14	496	0.56	1.55	0.47
10b	30	14	612	0.49	1.38	0.41
10c	34	15	555	0.53	1.48	0.42
10d	33	21	341	0.67	2.01	0.57
10	51	16	3669	0.54	1.57	0.40
12	30	28	119	0.92	2.93	0.86
13a	35	26	233	0.89	2.80	0.79
13b	28	20	218	0.81	2.28	0.68
13c	31	21	245	0.83	2.39	0.70
13	47	23	1120	0.85	2.60	0.68
14a	25	16	413	0.69	1.87	0.58
14b	31	17	476	0.63	1.80	0.52
14c	36	15	547	0.43	1.29	0.36
14	44	16	2325	0.61	1.76	0.47

8 References

- Aaris-Sbrensen, K. 1995. Palaeoecology of a Late Weichselian vertebrate fauna from Nørre Lyngby, Denmark. *Boreas* 24:355-365.
- Adams, B., and Á. Ringer. 2004. New C14 dates for the Hungarian early Upper Palaeolithic. *Current Anthropology* 45:541-551.
- Adams, S. J., M. C. McDowell, and G. J. Prideaux. 2016. Understanding accumulation bias in the ecological interpretation of archaeological and paleontological sites on Kangaroo Island, South Australia. *Journal of Archaeological Science: Reports* 7:715-729.
- Aitken, M. J. 1985. Thermoluminescence dating. US Edition. Academic Press, Orlando, United States.
- Aitken, M. J. 1998. Introduction to optical dating: the dating of Quaternary sediments by the use of photon-stimulated luminescence. Oxford University Press, New York, United States.
- Akçakaya, H. R., E. L. Bennett, T. M. Brooks, M. K. Grace, A. Heath, S. Hedges, C. Hilton-Taylor, M. Hoffmann, D. A. Keith, and B. Long. 2018. Quantifying species recovery and conservation success to develop an IUCN Green List of Species. *Conservation Biology* 32:1128-1138.
- Anderson, C. 1926. The Wellington Caves. *Australian Museum Magazine* 2:367-374.
- Anderson, C. 1929. Palaeontological notes no. 1. *Macropus titan* Owen and *Thylacoleo carnifex* Owen. *Records of the Australian Museum* 17:35-49.
- Andrews, P. 1990. Owls, caves and fossils: Predation, preservation and accumulation of small mammal bones in caves, with an analysis of the Pleistocene cave faunas from Westbury-sub-Mendip, Somerset, UK. University of Chicago Press.
- Andrews, P., and E. Nesbit-Evans. 1983. Small mammal bone accumulations produced by mammalian carnivores. *Paleobiology* 9:289-307.
- Anon. 1901. A Lucky Dog. *Wellington Times* 5th August:2.
- Aplin, K., R. W. Braithwaite, and P. R. Baverstock. 2008. Pale Field-rat, *Rattus tunneyi*; pp. 698-699 in S. van Dyck and R. Strahan (eds.), *The Mammals of Australia*. Reed New Holland, Australia.
- Aplin, K. P., S. G. Rhind, J. Ten Have, and R. T. Chesser. 2015. Taxonomic revision of *Phascogale tapoatafa* (Meyer, 1793)(Dasyuridae; Marsupialia), including descriptions of two new subspecies and confirmation of *P. pirata* Thomas, 1904 as a 'Top End' endemic. *Zootaxa* 4055:1-73.
- Araujo, B. B. A., L. G. R. Oliveira-Santos, M. S. Lima-Ribeiro, J. A. F. Diniz-Filho, and F. A. S. Fernandez. 2017. Bigger kill than chill: The uneven roles of humans and climate on late Quaternary megafaunal extinctions. *Quaternary International* 431:216-222.
- Archer, M. 1974. Apparent association of bone and charcoal of different origin and age in cave deposits. *Memoirs of the Queensland Museum* 17:37-48.
- Archer, M. 1976. The dasyurid dentition and its relationships to that of didelphids, thylacinids, borhyaenids (Marsupicarnivora) and peramelids (Peramelina: Marsupialia). *Australian Journal of Zoology* 24:1-34.
- Archer, M. 1981. Results of the Archbold expeditions. No. 104. Systematic revision of the marsupial dasyurid genus *Sminthopsis* Thomas. *Bulletin of the American Museum of Natural History* 168:61-224.
- Archer, M. 1984. The Australian marsupial radiation; pp. in M. Archer and G. Clayton (eds.), *Vertebrate zoogeography and evolution in Australasia*. Hesperian Press, Marrickville New South Wales.

- Archer, M., and S. Hand. 1984. Background to the search for Australia's oldest mammals. Vertebrate zoogeography and evolution in Australasia (M. Archer and G. Clayton, eds.). Hesperian Press, Carlisle, Western Australia 1203:517-565.
- Archer, M., K. Black, and K. Nettle. 1997. Giant ringtail possums (Marsupialia, Pseudocheiridae) and giant koalas (Phascolarctidae) from the late Cainozoic of Australia. Proceedings of the Linnean Society of New South Wales 117:3-16.
- Archer, M., H. Godthelp, S. Hand, and D. Megirian. 1989. Fossil mammals of Riversleigh, northwestern Queensland: preliminary overview of biostratigraphy, correlation and environmental change. Australian Zoologist 25:29-66.
- Archer, M., H. Bates, S. J. Hand, T. Evans, L. Broome, B. McAllan, F. Geiser, S. Jackson, T. Myers, A. Gillespie, C. Palmer, T. Hawke, and A. M. Horn. 2019. The *Burrarmys* Project: A conservationist's reach should exceed history's grasp, or what is the fossil record for? Philosophical Transactions of the Royal Society B: Biological Sciences 374:20190221.
- Arman, S. D., and G. J. Prideaux. 2016. Behaviour of the Pleistocene marsupial lion deduced from claw marks in a southwestern Australian cave. Scientific Reports 6:21372.
- Arman, S. D., T. A. Prowse, A. M. Couzens, P. S. Ungar, and G. J. Prideaux. 2019. Incorporating intraspecific variation into dental microwear texture analysis. Journal of the Royal Society Interface 16:20180957.
- Arnold, L. J., and R. G. Roberts. 2009. Stochastic modelling of multi-grain equivalent dose (De) distributions: Implications for OSL dating of sediment mixtures. Quaternary Geochronology 4:204-230.
- Arnold, L. J., M. Demuro, and M. N. Ruiz. 2012a. Empirical insights into multi-grain averaging effects from 'pseudo' single-grain OSL measurements. Radiation Measurements 47:652-658.
- Arnold, L. J., R. G. Roberts, R. F. Galbraith, and S. B. DeLong. 2009. A revised burial dose estimation procedure for optical dating of young and modern-age sediments. Quaternary Geochronology 4:306-325.
- Arnold, L. J., M. Duval, C. Falguères, J. J. Bahain, and M. Demuro. 2012b. Portable gamma spectrometry with cerium-doped lanthanum bromide scintillators: Suitability assessments for luminescence and electron spin resonance dating applications. Radiation Measurements 47:6-18.
- Arnold, L. J., M. Demuro, M. Navazo, A. Benito-Calvo, and A. Pérez-González. 2013. OSL dating of the Middle Palaeolithic Hotel California site, Sierra de Atapuerca, north-central Spain. Boreas 42:285-305.
- Arnold, L. J., M. C. McDowell, G. J. Prideaux, M. Demuro, and N. A. Spooner. 2019. Chronological assessments of Pleistocene megafaunal deposits at Kelly Hill Cave, Kangaroo Island, South Australia. Australian Quaternary Science Review in prep.
- Arnold, L. J., M. Duval, M. Demuro, N. A. Spooner, M. Santonja, and A. Pérez-González. 2016. OSL dating of individual quartz 'supergrains' from the Ancient Middle Palaeolithic site of Cuesta de la Bajada, Spain. Quaternary Geochronology 36:78-101.
- Augee, M. 1997. Dedication to Professor Richard Dehm. Proceedings of the Linnean Society of New South Wales 117:2.
- Augee, M., R. Dehm, and L. Dawson. 1986. The Munich Collection of Wellington Cave Fossil Marsupials. Australian Zoologist 22:3-6.
- Augee, M. L. 2008. Short-beaked echidna, *Tachyglossus aculeatus*; pp. 37-39 in S. van Dyck and R. Strahan (eds.), The Mammals of Australia. Reed New Holland, Australia.
- Augustin, L., C. Barbante, P. R. Barnes, J. M. Barnola, M. Bigler, E. Castellano, O. Cattani, J. Chappellaz, D. Dahl-Jensen, and B. Delmonte. 2004. Eight glacial cycles from an Antarctic ice core. Nature 429:623-628.

- Ayliffe, L. K., and H. Veeh. 1988. Uranium-series dating of speleothems and bones from Victoria Cave, Naracoorte, South Australia. *Chemical Geology: Isotope Geoscience section* 72:211-234.
- Ayliffe, L. K., G. J. Prideaux, M. I. Bird, R. Grün, R. G. Roberts, G. A. Gully, R. Jones, L. K. Fifield, and R. G. Cresswell. 2008. Age constraints on Pleistocene megafauna at Tight Entrance Cave in southwestern Australia. *Quaternary Science Reviews* 27:1784-1788.
- Ayliffe, L. K., A. Baynes, T. F. Flannery, R. Jones, G. M. Laslett, J. M. Olley, G. J. Prideaux, R. G. Roberts, B. L. Smith, M. A. Smith, and H. Yoshida. 2001. New ages for the last Australian megafauna: Continent-wide extinction about 46,000 years ago. *Science* 292:1888.
- Backwell, L. R., A. H. Parkinson, E. M. Roberts, F. d'Errico, and J.-B. Huchet. 2012. Criteria for identifying bone modification by termites in the fossil record. *Palaeogeography, Palaeoclimatology, Palaeoecology* 337-338:72-87.
- Baho, D. L., C. R. Allen, A. S. Garmestani, H. B. Fried-Petersen, S. E. Renes, L. H. Gunderson, and D. G. Angeler. 2017. A quantitative framework for assessing ecological resilience. *Ecology and Society* 22:1-17.
- Baird, R. 1991. The taphonomy of late Quaternary cave localities yielding vertebrate remains in Australia; pp. 267-310 in P. Vickers-Rich, J. M. Monaghan, R. F. Baird, and T. H. Rich (eds.), *Vertebrate Palaeontology of Australasia*. Pioneer Design Studio in cooperation with the Monash University Publication Committee, Melbourne.
- Baker, A., T. Mutton, E. Mason, and E. Gray. 2015. A taxonomic assessment of the Australian dusky *Antechinus* complex: a new species, the Tasman peninsula dusky *Antechinus* (*Antechinus vandycki* sp. nov.) and an elevation to species of the mainland dusky antechinus (*Antechinus swainsonii mimetes* (Thomas)). *Memoirs of the Queensland Museum—Nature* 59:75-126.
- Baker, A., C. N. Jex, H. Rutledge, M. Woltering, A. J. Blyth, M. S. Andersen, M. O. Cuthbert, C. E. Marjo, M. Markowska, and G. C. Rau. 2016. An irrigation experiment to compare soil, water and speleothem tetraether membrane lipid distributions. *Organic geochemistry* 94:12-20.
- Baker, A. M., and S. Van Dyck. 2013. Taxonomy and redescription of the Yellow-footed *Antechinus*, *Antechinus flavipes* (Waterhouse) (Marsupialia: Dasyuridae). *Zootaxa* 3649:1-62.
- Balakrishnan, M., and C. J. Yapp. 2004. Flux balance models for the oxygen and carbon isotope compositions of land snail shells. *Geochimica et Cosmochimica Acta* 68:2007-2024.
- Bar-Yosef, O., and A. Belfer-Cohen. 2001. From Africa to Eurasia — early dispersals. *Quaternary International* 75:19-28.
- Barnosky, A. D. 2008. Megafauna biomass tradeoff as a driver of Quaternary and future extinctions. *Proceedings of the National Academy of Sciences* 105:11543.
- Barnosky, A. D., and E. L. Lindsey. 2010. Timing of Quaternary megafaunal extinction in South America in relation to human arrival and climate change. *Quaternary International* 217:10-29.
- Barnosky, A. D., P. L. Koch, R. S. Feranec, S. L. Wing, and A. B. Shabel. 2004a. Assessing the Causes of Late Pleistocene Extinctions on the Continents. *Science* 306:70-75.
- Barnosky, A. D., C. J. Bell, S. D. Emslie, H. T. Goodwin, J. I. Mead, C. A. Repenning, E. Scott, and A. B. Shabel. 2004b. Exceptional record of mid-Pleistocene vertebrates helps differentiate climatic from anthropogenic ecosystem perturbations. *Proceedings of the National Academy of Sciences of the United States of America* 101:9297-9302.

- Barrows, T. T., J. O. Stone, L. K. Fifield, and R. G. Cresswell. 2001. Late Pleistocene glaciation of the Kosciuszko Massif, Snowy Mountains, Australia. *Quaternary Research* 55:179-189.
- Baynes, A., and B. Jones. 1983. The mammals of Cape Range peninsula, north-western Australia. *Records of the Western Australian Museum* 45:207-225.
- Bayon, G., P. De Deckker, J. W. Magee, Y. Germain, S. Bermell, K. Tachikawa, and M. D. Norman. 2017. Extensive wet episodes in Late Glacial Australia resulting from high-latitude forcings. *Scientific Reports* 7:44054.
- Becerra-Valdivia, L., R. Leal-Cervantes, R. Wood, and T. Higham. 2020. Challenges in sample processing within radiocarbon dating and their impact in ^{14}C -dates-as-data studies. *Journal of Archaeological Science* 113:105043.
- Behrensmeyer, A. K. 1978. Taphonomic and ecologic information from bone weathering. *Paleobiology* 4:150-162.
- Beisner, B. E., D. T. Haydon, and K. Cuddington. 2003. Alternative stable states in ecology. *Frontiers in Ecology and the Environment* 1:376-382.
- Belcher, C., S. Burnett, and M. E. Jones. 2008. Spotted-tailed Quoll, *Dasyurus maculatus*; pp. 60-62 in S. van Dyck and R. Strahan (eds.), *The Mammals of Australia*. Reed New Holland, Australia.
- Bell, P. R. 2004. Mammal Bones and Talus Cones: Palaeontology, Stratigraphy and Geochronology of Phosphate Mine East, Wellington Caves, NSW. Unpublished Honours thesis. Centre for Ecostratigraphy and Palaeobiology, Macquarie University, NSW, Australia.
- Bender, E. A., T. J. Case, and M. E. Gilpin. 1984. Perturbation Experiments in Community Ecology: Theory and Practice. *Ecology* 65:1-13.
- Bereiter, B., D. Lüthi, M. Siegrist, S. Schüpbach, T. F. Stocker, and H. Fischer. 2012. Mode change of millennial CO_2 variability during the last glacial cycle associated with a bipolar marine carbon seesaw. *Proceedings of the National Academy of Sciences* 109:9755-9760.
- Berto, C., J. M. López-García, and E. Luzi. 2019. Changes in the Late Pleistocene small-mammal distribution in the Italian Peninsula. *Quaternary Science Reviews* 225:106019.
- Bickford, S., P. Gell, and G. J. Hancock. 2008. Wetland and terrestrial vegetation change since European settlement on the Fleurieu Peninsula, South Australia. *The Holocene* 18:425-436.
- Bilney, R. J. 2012. A reassessment of the predator responsible for Wakefield's 'Native Cat den' sub-fossil deposits in the Buchan district: Sooty Owl, not Eastern Quoll. *The Victorian Naturalist* 129:138-143.
- Bilney, R. J., R. Cooke, and J. G. White. 2010. Underestimated and severe: Small mammal decline from the forests of south-eastern Australia since European settlement, as revealed by a top-order predator. *Biological Conservation* 143:52-59.
- Bird, M. I., L. B. Hutley, M. J. Lawes, J. Lloyd, J. G. Luly, P. V. Ridd, R. G. Roberts, S. Ulm, and C. M. Wurster. 2013. Humans, megafauna and environmental change in tropical Australia. *Journal of Quaternary Science* 28:439-452.
- Birks, H. J. B. 2012. Ecological palaeoecology and conservation biology: Controversies, challenges, and compromises. *International Journal of Biodiversity Science, Ecosystem Services & Management* 8:292-304.
- Birks, H. J. B. 2019. Paleoeology; pp. 494-504 in B. Fath (ed.), *Encyclopedia of Ecology* Second Edition. Elsevier, Oxford.
- Birks, H. J. B., and H. H. Birks. 1980. *Quaternary palaeoecology*. Edward Arnold (Publishers) Limited, London.

- Blaauw, M., and J. A. Christen. 2011. Flexible paleoclimate age-depth models using an autoregressive gamma process. *Bayesian Analysis* 6:457-474.
- Blaauw, M., and A. Christen. 2018. rbacon: Age-depth modelling using Bayesian statistics: R package version 2.3.4.
- Black, M., S. Mooney, and H. Martin. 2006. A >43,000-year vegetation and fire history from Lake Baraba, New South Wales, Australia. *Quaternary Science Reviews* 25:3003-3016.
- Blanford, S. 1985. The fossil rodents of Wellington Caves: a murid montage. Unpublished Honours thesis. University of New South Wales.
- Bliege Bird, R., D. W. Bird, B. F. Coddling, C. H. Parker, and J. H. Jones. 2008. The “fire stick farming” hypothesis: Australian Aboriginal foraging strategies, biodiversity, and anthropogenic fire mosaics. *Proceedings of the National Academy of Sciences* 105:14796-14801.
- Blois, J. L., and E. A. Hadley. 2009. Mammalian response to Cenozoic climatic change. *Annual Review of Earth and Planetary Sciences* 37:181-208.
- Blois, J. L., J. L. McGuire, and E. A. Hadly. 2010. Small mammal diversity loss in response to late-Pleistocene climatic change. *Nature* 465:771-774.
- Blott, S. J., and K. Pye. 2001. GRADISTAT: a grain size distribution and statistics package for the analysis of unconsolidated sediments. *Earth Surface Processes and Landforms* 26:1237-1248.
- Blunier, T., and E. J. Brook. 2001. Timing of millennial-scale climate change in Antarctica and Greenland during the last glacial period. *Science* 291:109-112.
- Blunier, T., J. Chappellaz, J. Schwander, A. Dällenbach, B. Stauffer, T. F. Stocker, D. Raynaud, J. Jouzel, H. B. Clausen, C. U. Hammer, and S. J. Johnsen. 1998. Asynchrony of Antarctic and Greenland climate change during the last glacial period. *Nature* 394:739.
- Boles, W. 1999. Avian prey of the Australian ghost bat *Macroderma gigas* (Microchiroptera: Megadermatidae): prey characteristics and damage from predation. *Australian Zoologist* 31:82-91.
- Bøtter-Jensen, L., and V. Mejdahl. 1988. Assessment of beta dose-rate using a GM multicounter system. *International Journal of Radiation Applications and Instrumentation. Part D. Nuclear Tracks and Radiation Measurements* 14:187-191.
- Bowler, J. M., R. Gillespie, H. Johnston, and K. Sporadic. 2012. Wind v water: glacial maximum records from the Willandra Lakes; pp. 271-296 in S. G. H. B. David (ed.), *Peopled landscapes: archaeological and biogeographic approaches to landscapes*. ANU ePress, Canberra ACT.
- Bowler, J. M., H. Johnston, J. M. Olley, J. R. Prescott, R. G. Roberts, W. Shawcross, and N. A. Spooner. 2003. New ages for human occupation and climatic change at Lake Mungo, Australia. *Nature* 421:837-840.
- Bowman, D. M. J. S. 1998. The impact of Aboriginal landscape burning on the Australian biota. *New Phytologist* 140:385-410.
- Bradley, A. J., W. K. Foster, and D. A. Taggart. 2008. Red-tailed Phascogale, *Phascogale calura*; pp. 101-102 in S. van Dyck and R. Strahan (eds.), *The Mammals of Australia*. Reed New Holland, Australia.
- Bradshaw, C. J. A., C. N. Johnson, J. Llewelyn, V. Weisbecker, G. Strona, and F. Saltré. 2021. Relative demographic susceptibility does not explain the extinction chronology of Sahul’s megafauna. *eLife* 10:e63870.
- Brennan, B. 2003. Beta doses to spherical grains. *Radiation Measurements* 37:299-303.
- Broecker, W. S. 1998. Paleoocean circulation during the last deglaciation: A bipolar seesaw? *Paleoceanography* 13:119-121.

- Bronk Ramsey, C. 2008. Radiocarbon dating: revolutions in understanding. *Archaeometry* 50:249-275.
- Bronk Ramsey, C. 2009. Bayesian analysis of radiocarbon dates. *Radiocarbon* 51:337-360.
- Bronk Ramsey, C. 2013. OxCal 4.2.
- Brook, B. W., and C. N. Johnson. 2006. Selective hunting of juveniles as a cause of the imperceptible overkill of the Australian Pleistocene megafauna. *Alcheringa* 30:39-48.
- Brook, B. W., D. M. J. S. Bowman, D. A. Burney, T. F. Flannery, M. K. Gagan, R. Gillespie, C. N. Johnson, P. Kershaw, J. W. Magee, P. S. Martin, G. H. Miller, B. Peiser, and R. G. Roberts. 2007. Would the Australian megafauna have become extinct if humans had never colonised the continent? Comments on "A review of the evidence for a human role in the extinction of Australian megafauna and an alternative explanation" by S. Wroe and J. Field. *Quaternary Science Reviews* 26:560-564.
- Brown, P. R. 1989. Management Plan for the Conservation of the Eastern Barred Bandicoot, *Perameles gunnii*, in Victoria: A Report to the Department of Conservation, Forests, and Lands, Victoria and the World Wildlife Fund Australia. Department of Conservation, Forests, and Lands, Arthur Rylah Institute for Environmental Research.
- Brown, S. P., and R. T. Wells. 2000. A middle Pleistocene vertebrate fossil assemblage from Cathedral Cave, Naracoorte, South Australia. *Transactions of the Royal Society of South Australia* 124:91-104.
- Brown, T. A., D. E. Nelson, J. S. Vogel, and J. R. Southon. 1988. Improved collagen extraction by modified Longin method. *Radiocarbon* 30:171-177.
- Buckland, W. 1824. *Reliquiae Diluvianae; or, Observations on the organic remains contained in caves, fissures, and diluvial gravel, and on other geological phenomena, attesting the action of an universal Deluge.* John Murray, London.
- Burbidge, A. A. 2008. Crescent nailtail Wallaby, *Onychogalea lunata*; pp. 357-359 in S. van Dyck and R. Strahan (eds.), *The Mammals of Australia*. Reed New Holland, Australia.
- Burbidge, A. A., and J. C. Short. 2008. Burrowing Bettong, *Bettongia lesueur*; pp. 288-290 in S. van Dyck and R. Strahan (eds.), *The Mammals of Australia*. Reed New Holland, Australia.
- Burbidge, A. A., N. L. McKenzie, K. E. C. Brennan, J. C. Z. Woinarski, C. R. Dickman, A. Baynes, G. Gordon, P. W. Menkhorst, and A. C. Robinson. 2009. Conservation status and biogeography of Australia's terrestrial mammals. *Australian Journal of Zoology* 56:411-422.
- Bureau of Meteorology. 2018. Australian Climate Observations Reference Network - Surface Air Temperature Version 2, <http://www.bom.gov.au/climate/data/acorn-sat/>.
- Burney, D. A., and T. F. Flannery. 2005. Fifty millennia of catastrophic extinctions after human contact. *Trends in Ecology & Evolution* 20:395-401.
- Byrne, M. 2008. Evidence for multiple refugia at different time scales during Pleistocene climatic oscillations in southern Australia inferred from phylogeography. *Quaternary Science Reviews* 27:2576-2585.
- Cadd, H. R., J. Tibby, C. Barr, J. Tyler, L. Unger, M. J. Leng, J. C. Marshall, G. McGregor, R. Lewis, L. J. Arnold, T. Lewis, and J. Baldock. 2018. Development of a southern hemisphere subtropical wetland (Welsby Lagoon, south-east Queensland, Australia) through the last glacial cycle. *Quaternary Science Reviews* 202:53-65.
- Cai, Y., Z. An, H. Cheng, R. L. Edwards, M. J. Kelly, W. Liu, X. Wang, and C.-C. Shen. 2006. High-resolution absolute-dated Indian Monsoon record between 53 and 36 ka from Xiaobailong Cave, southwestern China. *Geology* 34:621-624.
- Calder, W. J., and B. Shuman. 2019. Detecting past changes in vegetation resilience in the context of a changing climate. *Biology Letters* 15:20180768.

- Camens, A. B., and S. P. Carey. 2013. Contemporaneous trace and body fossils from a late Pleistocene lakebed in Victoria, Australia, allow assessment of bias in the fossil record. *Plos One* 8:e52957.
- Cardillo, M., G. M. Mace, K. E. Jones, J. Bielby, O. R. P. Bininda-Emonds, W. Sechrest, C. D. L. Orme, and A. Purvis. 2005. Multiple causes of high extinction risk in large mammal species. *Science* 309:1239-1241.
- Cawson, J., G. Sheridan, H. Smith, and P. Lane. 2012. Surface runoff and erosion after prescribed burning and the effect of different fire regimes in forests and shrublands: a review. *International Journal of Wildland Fire* 21:857-872.
- Čerňanský, A., and M. N. Hutchinson. 2013. A new large fossil species of *Tiliqua* (Squamata; Scincidae) from the Pliocene of the Wellington Caves (New South Wales, Australia). *Alcheringa* 37:131-136.
- Chase, B. M., L. Scott, M. E. Meadows, G. Gil-Romera, A. Boom, A. S. Carr, P. J. Reimer, L. Truc, V. Valsecchi, and L. J. Quick. 2012. Rock hyrax middens: A palaeoenvironmental archive for southern African drylands. *Quaternary Science Reviews* 56:107-125.
- Chen, I.-C., J. K. Hill, R. Ohlemüller, D. B. Roy, and C. D. Thomas. 2011. Rapid range shifts of species associated with high levels of climate warming. *Science* 333:1024-1026.
- Christensen, J., and A. Olhoff. 2019. Lessons from a decade of emissions gap assessments; United Nations Environment Programme, Nairobi.
- Clancy, T. F., and D. B. Croft. 2008. Common Wallaroo, *Macropus robustus*; pp. 346-348 in S. van Dyck and R. Strahan (eds.), *The Mammals of Australia*. Reed New Holland, Australia.
- Clark, P. U., and A. C. Mix. 2002. Ice sheets and sea level of the Last Glacial Maximum. *Quaternary Science Reviews* 21:1-7.
- Clark, P. U., A. S. Dyke, J. D. Shakun, A. E. Carlson, J. Clark, B. Wohlfarth, J. X. Mitrovica, S. W. Hostetler, and A. M. McCabe. 2009. The Last Glacial Maximum. *Science* 325:710-714.
- Clarkson, C., Z. Jacobs, B. Marwick, R. Fullagar, L. Wallis, M. Smith, R. G. Roberts, E. Hayes, K. Lowe, X. Carah, S. A. Florin, J. McNeil, D. Cox, L. J. Arnold, Q. Hua, J. Huntley, H. E. A. Brand, T. Manne, A. Fairbairn, J. Shulmeister, L. Lyle, M. Salinas, M. Page, K. Connell, G. Park, K. Norman, T. Murphy, and C. Pardoe. 2017. Human occupation of northern Australia by 65,000 years ago. *Nature* 547:306.
- Clements, C. F., and A. Ozgul. 2018. Indicators of transitions in biological systems. *Ecology Letters* 21:905-919.
- Cohen, T., G. Nanson, J. D. Jansen, B. Jones, Z. Jacobs, J. Larsen, J.-H. May, P. Treble, D. Price, and A. Smith. 2012. Late Quaternary mega-lakes fed by the northern and southern river systems of central Australia: Varying moisture sources and increased continental aridity. *Palaeogeography, Palaeoclimatology, Palaeoecology* 356:89-108.
- Cohen, T. J., J. D. Jansen, L. A. Gliganic, J. R. Larsen, G. C. Nanson, J.-H. May, B. G. Jones, and D. M. Price. 2015. Hydrological transformation coincided with megafaunal extinction in central Australia. *Geology* 43:195-198.
- Colditz, M. 1942. The physiography of the Wellington district, NSW. *Journal and Proceedings of the Royal Society of New South Wales* 76:235-251.
- Connell, J. H. 1978. Diversity in tropical rain forests and coral reefs. *Science* 199:1302-1310.
- Cooke, B. D. 2020. Swamp wallaby (*Wallabia bicolor*) distribution has dramatically increased following sustained biological control of rabbits. *Australian Mammalogy* 42:321-328.

- Cooper, A., C. Turney, K. A. Hughen, B. W. Brook, H. G. McDonald, and C. J. A. Bradshaw. 2015. Abrupt warming events drove Late Pleistocene Holarctic megafaunal turnover. *Science* 349:602-606.
- Cooper, A., C. S. M. Turney, J. Palmer, A. Hogg, M. McGlone, J. Wilmshurst, A. M. Lorrey, T. J. Heaton, J. M. Russell, K. McCracken, J. G. Anet, E. Rozanov, M. Friedel, I. Suter, T. Peter, R. Muscheler, F. Adolphi, A. Dosseto, J. T. Faith, P. Fenwick, C. J. Fogwill, K. Hughen, M. Lipson, J. Liu, N. Nowaczyk, E. Rainsley, C. Bronk Ramsey, P. Sebastianelli, Y. Souilmi, J. Stevenson, Z. Thomas, R. Tobler, and R. Zech. 2021. A global environmental crisis 42,000 years ago. *Science* 371:811-818.
- Cordova, C. E., and W. C. Johnson. 2019. An 18 ka to present pollen- and phytolith-based vegetation reconstruction from Hall's Cave, south-central Texas, USA. *Quaternary Research* 92:497-518.
- Correll, R. A., T. A. Prowse, and G. J. Prideaux. 2016. Lean-season primary productivity and heat dissipation as key drivers of geographic body-size variation in a widespread marsupial. *Ecography* 39:77-86.
- Coulson, G. 2008. Eastern Grey Kangaroo, *Macropus giganteus*; pp. 335-338 in S. van Dyck and R. Strahan (eds.), *The Mammals of Australia*. Reed New Holland, Australia.
- Cramb, J., and S. Hocknull. 2010. New Quaternary records of *Conilurus* (Rodentia: Muridae) from eastern and northern Australia with the description of a new species. *Zootaxa* 2634:41-56.
- Croft, D. B., and T. F. Clancy. 2008. Red Kangaroo, *Macropus rufus*; pp. 352-354 in S. van Dyck and R. Strahan (eds.), *The Mammals of Australia*. Reed New Holland, Australia.
- Crowley, B. E. 2010. A refined chronology of prehistoric Madagascar and the demise of the megafauna. *Quaternary Science Reviews* 29:2591-2603.
- Crowther, M. S. 2008. Yellow-footed Antechinus, *Antechinus flavipes*; pp. 86-88 in S. van Dyck and R. Strahan (eds.), *The Mammals of Australia*. Reed New Holland, Australia.
- Cupper, M. L., and J. Duncan. 2006. Last glacial megafaunal death assemblage and early human occupation at Lake Menindee, southeastern Australia. *Quaternary Research* 66:332-341.
- Curnoe, D., J.-x. Zhao, M. Aubert, M. Fan, Y. Wu, A. Baker, G. H. Mei, X.-f. Sun, R. Mendoza, L. Adler, S. Ma, L. Kinsey, and X. Ji. 2019. Implications of multi-modal age distributions in Pleistocene cave deposits: A case study of Maludong palaeoanthropological locality, southern China. *Journal of Archaeological Science: Reports* 25:388-399.
- Cuthbert, M. O., A. Baker, C. N. Jex, P. W. Graham, P. C. Treble, M. S. Andersen, and R. Ian Acworth. 2014a. Drip water isotopes in semi-arid karst: Implications for speleothem paleoclimatology. *Earth and Planetary Science Letters* 395:194-204.
- Cuthbert, M. O., G. Rau, M. Andersen, H. Roshan, H. Rutledge, C. Marjo, M. Markowska, C. Jex, P. Graham, and G. Mariethoz. 2014b. Evaporative cooling of speleothem drip water. *Scientific Reports* 4:5162.
- Darrénougué, N., P. De Deckker, K. E. Fitzsimmons, M. D. Norman, L. Reed, S. van der Kaars, and S. Fallon. 2009. A late Pleistocene record of aeolian sedimentation in Blanche Cave, Naracoorte, South Australia. *Quaternary Science Reviews* 28:2600-2615.
- David, B., L. J. Arnold, J.-J. Delannoy, J. Fresløv, C. Urwin, F. Petchey, M. C. McDowell, R. Mullett, G. Land, and J. Mialanes. 2021. Late survival of megafauna refuted for Cloggs Cave, SE Australia: Implications for the Australian Late Pleistocene megafauna extinction debate. *Quaternary Science Reviews* 253:106781.

- Davies, A. L., R. Streeter, I. T. Lawson, K. H. Roucoux, and W. Hiles. 2018. The application of resilience concepts in palaeoecology. *The Holocene* 28:1523-1534.
- Davis, M. B., R. G. Shaw, and J. R. Etterson. 2005. Evolutionary responses to changing climate. *Ecology* 86:1704-1714.
- Dawson, L. 1982a. Marsupial Fossils from Wellington Caves, New South Wales. Unpublished PhD thesis. University of New South Wales.
- Dawson, L. 1982b. Taxonomic status of fossil devils (*Sarcophilus*, Dasyuridae, Marsupialia) from late Quaternary eastern Australia localities; pp. 517-525 in M. Archer (ed.), *Carnivorous Marsupials*. Surrey Beatty & Sons Pty Ltd, Chipping Norton.
- Dawson, L. 1983. The taxonomic status of small fossil wombats (Vombatidae: Marsupialia) from Quaternary deposits, and of related modern wombats. *Proceedings of the Linnean Society of New South Wales* 107:1-123.
- Dawson, L. 1985. Marsupial fossils from Wellington Caves, New South Wales; the historic and scientific significance of the collections in the Australian Museum, Sydney. *Records of the Australian Museum* 37:55-69.
- Dawson, L. 1995. Biostratigraphy and biochronology of sediments from the Bone Cave, Wellington Caves, NSW, based on vertebrate fossil remains; in Quaternary Symposium The Linnean Society of New South Wales, , Wellington Caves, New South Wales.
- Dawson, L. 1999. Wellington Caves new life for dormant system. *Riversleigh Notes*. Newsletter of the Riversleigh Society November:2-4.
- Dawson, L. 2000. The power of the paradigm. The more things change the more they stay the same. *Riversleigh Notes*. Newsletter of the Riversleigh Society December:2-4.
- Dawson, L., and T. Flannery. 1985. Taxonomic and phylogenetic status of living and fossil kangaroos and wallabies of the genus *Macropus* Shaw (Macropodidae: Marsupialia), with a new subgeneric name for the larger wallabies. *Australian Journal of Zoology* 33:473-498.
- Dawson, L., and M. Augee. 1997. The late Quaternary sediments and fossil vertebrate fauna from Cathedral Cave, Wellington Caves, New South Wales. *Proceedings of the Linnean Society of New South Wales* 117:51-78.
- Dawson, L., J. Muirhead, and S. Wroe. 1999. The Big Sink local fauna: A lower Pliocene mammalian fauna from the Wellington Caves complex, Wellington, New South Wales. *Records of the Western Australian Museum Supplement* 57:265-290.
- De Deckker, P., S. van der Kaars, M. K. Macphail, and G. S. Hope. 2018a. Land-sea correlations in the Australian region: 460 ka of changes recorded in a deep-sea core offshore Tasmania. Part 1: The pollen record. *Australian Journal of Earth Sciences*:1-15.
- De Deckker, P., T. T. Barrows, J. B. W. Stuut, S. van der Kaars, M. A. Ayress, J. Rogers, and G. Chaproniere. 2018b. Land-sea correlations in the Australian region: 460 ka of changes recorded in a deep-sea core offshore Tasmania. Part 2: The marine compared with the terrestrial record. *Australian Journal of Earth Sciences*:1-20.
- De Deckker, P., L. J. Arnold, S. van der Kaars, G. Bayon, J.-B. W. Stuut, K. Perner, R. Lopes dos Santos, R. Uemura, and M. Demuro. 2019. Marine Isotope Stage 4 in Australasia: A full glacial culminating 65,000 years ago – Global connections and implications for human dispersal. *Quaternary Science Reviews* 204:187-207.
- De Deckker, P., M. Moros, K. Perner, T. Blanz, L. Wacker, R. Schneider, T. T. Barrows, T. O’Loingsigh, and E. Jansen. 2020. Climatic evolution in the Australian region over the last 94 ka - spanning human occupancy - and unveiling the Last Glacial Maximum. *Quaternary Science Reviews* 249:106593.

- Dehm, R., and J. Schroder. 1941. Auf dem spuren vorzeitlicher Beuteltiere in Australien. *Vereoeffentlichungen der Gesellschaft der Freunde und Foerderer der Universitat Munchen* 8:15-24.
- DeNiro, M. J., and S. Weiner. 1988. Chemical, enzymatic and spectroscopic characterization of "collagen" and other organic fractions from prehistoric bones. *Geochimica et Cosmochimica Acta* 52:2197-2206.
- Dennis, A. J., and P. M. Johnson. 2008. Rufous Bettong, *Aepyprymnus rufescens*; pp. 285-286 in S. van Dyck and R. Strahan (eds.), *The Mammals of Australia*. Reed New Holland, Australia.
- Department of Environment. 2012. Australia - Present Major Vegetation Subgroups - NVIS 4.1 (Albers 100m analysis product). Bioregional Assessment Source Dataset., Department of the Environment, Canberra.
- Department of Environment Land Water and Planning. 2016. National Recovery Plan for the Spotted-tailed Quoll *Dasyurus maculatus*, Department of Environment Land Water and Planning, Canberra.
- Deviese, T., D. Comeskey, J. McCullagh, C. Bronk Ramsey, and T. Higham. 2018. New protocol for compound-specific radiocarbon analysis of archaeological bones. *Rapid Communications in Mass Spectrometry* 32:373-379.
- Di Stefano, C., V. Ferro, and S. Mirabile. 2010. Comparison between grain-size analyses using laser diffraction and sedimentation methods. *Biosystems Engineering* 106:205-215.
- Di Stefano, J., A. York, M. Swan, A. Greenfield, and G. Coulson. 2009. Habitat selection by the swamp wallaby (*Wallabia bicolor*) in relation to diel period, food and shelter. *Austral Ecology* 34:143-155.
- Díaz, S., J. Settele, E. Brondízio, H. Ngo, M. Guèze, J. Agard, A. Arneth, P. Balvanera, K. Brauman, and S. Butchart. 2020. Summary for policymakers of the global assessment report on biodiversity and ecosystem services of the Intergovernmental Science-Policy Platform on Biodiversity and Ecosystem Services.
- Dice, L. R. 1945. Minimum intensities of illumination under which owls can find dead prey by sight. *The American Naturalist* 79:385-416.
- Dickman, C. R., and E. Stodart. 2008. Long-nosed Bandicoot, *Perameles nasuta*; pp. 189-190 in S. van Dyck and R. Strahan (eds.), *The Mammals of Australia*. Reed New Holland, Australia.
- Dirzo, R., H. S. Young, M. Galetti, G. Ceballos, N. J. Isaac, and B. Collen. 2014. Defaunation in the Anthropocene. *Science* 345:401-406.
- Dixon, J. 2008a. White-footed Rabbit-rat, *Conilurus albipes*; pp. 578-579 in S. van Dyck and R. Strahan (eds.), *The Mammals of Australia*. Reed New Holland, Sydney.
- Dixon, J. M. 2008b. Gould's Mouse, *Pseudomys gouldii*; pp. 632-633 in S. van Dyck and R. Strahan (eds.), *The Mammals of Australia*. Reed New Holland, Australia.
- Dixon, J. M., and L. F. Lumsden. 2008. Gould's Wattleed Bat, *Chalinolobus gouldii*; pp. 533-534 in S. van Dyck and R. Strahan (eds.), *The Mammals of Australia*. Reed New Holland, Australia.
- Dobson, G. 1875. Conspectus of the suborders, families, and genera of Chiroptera arranged according to their natural affinities. *Annals and Magazine of Natural History* 4:345-357.
- Dodson, P., and D. Wexlar. 1979. Taphonomic investigations of owl pellets. *Paleobiology* 5:275-284.
- Dortch, J., M. Cupper, R. Grün, B. Harpley, K. Lee, and J. Field. 2016. The timing and cause of megafauna mass deaths at Lancefield Swamp, south-eastern Australia. *Quaternary Science Reviews* 145:161-182.

- Dowdy, A. J., H. Ye, A. Pepler, M. Thatcher, S. L. Osbrough, J. P. Evans, G. Di Virgilio, and N. McCarthy. 2019. Future changes in extreme weather and pyroconvection risk factors for Australian wildfires. *Scientific Reports* 9:1-11.
- Dowle, M., A. Srinivasan, J. Gorecki, M. Chirico, P. Stetsenko, T. Short, S. Lianoglou, E. Antonyan, M. Bonsch, and H. Parsonage. 2019. Package 'data.table'. Extension of 'data.frame'. .
- Dragovich, D., and R. Morris. 2002. Fire intensity, slopewash and bio-transfer of sediment in eucalypt forest, Australia. *Earth Surface Processes and Landforms* 27:1309-1319.
- Dufty, A. C. 1994. Habitat and spatial requirements of the eastern barred bandicoot (*Perameles gunnii*) at Hamilton, Victoria. *Wildlife Research* 21:459-471.
- Dugan, K. G. 1980: Darwin and *Diprotodon*: The Wellington Caves fossils and the law of succession. *Proceedings of the Linnean Society of New South Wales*, 1980.
- Dun, W. 1893. On palatal remains of *Palorchestes azael*, Owen, from the Wellington Caves bone deposit. *Records of the Geological Survey of New South Wales* 3:120-124.
- Dunkley, J. R. 2016. The 1830 Cave Diaries of Thomas Livingstone Mitchell. *Helictite* 42:21-37.
- Earle, A. 1826. Mosman's Cave, Wellington Valley, New South Wales, No. 1; National Library of Australia. nla.obj-134499531, Rex Nan Kivell Collection NK/1241.
- Eldridge, M. D. B., and R. L. Close. 2008. Brush-tailed Rock-wallaby, *Petrogale penicillata*; pp. 382-384 in S. van Dyck and R. Strahan (eds.), *The Mammals of Australia*. Reed New Holland, Australia.
- Ellwood, B. B., and W. A. Gose. 2006. Heinrich H1 and 8200 yr BP climate events recorded in Hall's Cave, Texas. *Geology* 34:753-756.
- Elmqvist, T., C. Folke, M. Nyström, G. Peterson, J. Bengtsson, B. Walker, and J. Norberg. 2003. Response diversity, ecosystem change, and resilience. *Frontiers in Ecology and the Environment* 1:488-494.
- Epica Community Members, C. Barbante, J. M. Barnola, S. Becagli, J. Beer, M. Bigler, C. Boutron, T. Blunier, E. Castellano, O. Cattani, J. Chappellaz, D. Dahl-Jensen, M. Debret, B. Delmonte, D. Dick, S. Falourd, S. Faria, U. Federer, H. Fischer, J. Freitag, A. Frenzel, D. Fritzsche, F. Fundel, P. Gabrielli, V. Gaspari, R. Gersonde, W. Graf, D. Grigoriev, I. Hamann, M. Hansson, G. Hoffmann, M. A. Hutterli, P. Huybrechts, E. Isaksson, S. Johnsen, J. Jouzel, M. Kaczmarek, T. Karlin, P. Kaufmann, S. Kipfstuhl, M. Kohno, F. Lambert, A. Lambrecht, A. Lambrecht, A. Landais, G. Lawer, M. Leuenberger, G. Littot, L. Loulergue, D. Lüthi, V. Maggi, F. Marino, V. Masson-Delmotte, H. Meyer, H. Miller, R. Mulvaney, B. Narcisi, J. Oerlemans, H. Oerter, F. Parrenin, J. R. Petit, G. Raisbeck, D. Raynaud, R. Röthlisberger, U. Ruth, O. Rybak, M. Severi, J. Schmitt, J. Schwander, U. Siegenthaler, M. L. Siggaard-Andersen, R. Spahni, J. P. Steffensen, B. Stenni, T. F. Stocker, J. L. Tison, R. Traversi, R. Udisti, F. Valero-Delgado, M. R. van den Broeke, R. S. W. van de Wal, D. Wagenbach, A. Wegner, K. Weiler, F. Wilhelms, J. G. Winther, and E. Wolff. 2006. One-to-one coupling of glacial climate variability in Greenland and Antarctica. *Nature* 444:195.
- Evans, E. M. N., J. A. H. Van Couvering, and P. Andrews. 1981. Palaeoecology of Miocene sites in Western Kenya. *Journal of Human Evolution* 10:99-116.
- Evans, M., and G. Gordon. 2008. Bridled Nailtail Wallaby, *Onychogalea fraenata*; pp. 355-356 in S. van Dyck and R. Strahan (eds.), *The Mammals of Australia*. Reed New Holland, Australia.
- Faith, J. T. 2014. Late Pleistocene and Holocene mammal extinctions on continental Africa. *Earth-Science Reviews* 128:105-121.

- Falk, D. A., and C. I. Millar. 2016. The Influence of Climate Variability and Change on the Science and Practice of Restoration Ecology; pp. 484-513 in M. A. Palmer, J. B. Zedler, and D. A. Falk (eds.), *Foundations of Restoration Ecology*. Island Press/Center for Resource Economics, Washington, DC.
- Falk, D. A., A. C. Watts, and A. E. Thode. 2019. Scaling Ecological Resilience. *Frontiers in Ecology and Evolution* 7.
- Fernández-García, M., J. M. López-García, and C. Lorenzo. 2016. Palaeoecological implications of rodents as proxies for the Late Pleistocene–Holocene environmental and climatic changes in northeastern Iberia. *Comptes Rendus Palevol* 15:707-719.
- Fernandez-Jalvo, Y., and P. Andrews. 1992. Small mammal taphonomy of Gran Dolina, Atapuerca (Burgos), Spain. *Journal of Archaeological Science* 19:407-428.
- Fernández-Jalvo, Y., and P. Andrews. 2003. Experimental effects of water abrasion on bone fragments. *Journal of taphonomy* 1:147-163.
- Fernández, M. H. 2006. Rodent paleofaunas as indicators of climatic change in Europe during the last 125,000 years. *Quaternary Research* 65:308-323.
- Field, J., M. Fillios, and S. Wroe. 2008. Chronological overlap between humans and megafauna in Sahul (Pleistocene Australia–New Guinea): A review of the evidence. *Earth-Science Reviews* 89:97-115.
- Fillios, M., J. Field, and B. Charles. 2010. Investigating human and megafauna co-occurrence in Australian prehistory: Mode and causality in fossil accumulations at Cuddie Springs. *Quaternary International* 211:123-143.
- Fillios, M., M. S. Crowther, and M. Letnic. 2012. The impact of the dingo on the thylacine in Holocene Australia. *World Archaeology* 44:118-134.
- Finch, M., and L. Freedman. 1988. Functional morphology of the limbs of *Thylacoleo carnifex* Owen (Thylacoleonidae, Marsupialia). *Australian Journal of Zoology* 36:251-272.
- Fink, D., M. Hotchkis, Q. Hua, G. Jacobsen, A. M. Smith, U. Zoppi, D. Child, C. Mifsud, H. van der Gaast, and A. Williams. 2004. The ANTARES AMS facility at ANSTO. *Nuclear Instruments and Methods in Physics Research Section B: Beam Interactions with Materials and Atoms* 223:109-115.
- Fischer, M. 1997. Speleothem chronology and its implications for biochronology, Wellington Caves, New South Wales; in *Conference on Australasian Vertebrate Evolution Palaeontology & Systematics*, Perth, Western Australia.
- Flannery, T. 1990. Pleistocene faunal loss: Implications of the aftershock for Australia's past and future. *Archaeology in Oceania* 25:45-55.
- Flannery, T. 1994. *The future eaters: an ecological history of the Australasian lands and people*. Reed, Melbourne.
- Flannery, T., and F. Szalay. 1982. *Bohra paulae*, a new giant fossil tree-kangaroo (Marsupialia: Macropodidae) from New South Wales, Australia. *Australian Mammalogy* 5:83-94.
- Folk, R. L., and W. C. Ward. 1957. Brazos River bar [Texas]; a study in the significance of grain size parameters. *Journal of Sedimentary Research* 27:3-26.
- Forbes, M. S., and E. A. Bestland. 2006. Guano-derived deposits within the sandy cave fills of Naracoorte, South Australia. *Alcheringa* 30:129-146.
- Forbes, M. S., E. A. Bestland, R. T. Wells, and E. S. Krull. 2007. Palaeoenvironmental reconstruction of the Late Pleistocene to Early Holocene Robertson Cave sedimentary deposit, Naracoorte, South Australia. *Australian Journal of Earth Sciences* 54:541-559.
- Ford, F. 2008. Smokey Mouse, *Pseudomys fumeus*; pp. 629-630 in S. van Dyck and R. Strahan (eds.), *The Mammals of Australia*. Reed New Holland, Australia.

- Fordham, D. A., S. T. Jackson, S. C. Brown, B. Huntley, B. W. Brook, D. Dahl-Jensen, M. T. P. Gilbert, B. L. Otto-Bliesner, A. Svensson, S. Theodoridis, J. M. Wilmshurst, J. C. Buettel, E. Canteri, M. McDowell, L. Orlando, J. Pilowsky, C. Rahbek, and D. Nogues-Bravo. 2020. Using paleo-archives to safeguard biodiversity under climate change. *Science* 369:eabc5654.
- Foster, W. 1936. Colonel Sir Thomas Mitchell, DCL, and fossil mammalian research. *Journal and Proceedings of the Royal Historical Society* 22:433-443.
- Fox, B. J. 2008a. Common Dunnart, *Sminthopsis murina*; pp. 153-154 in S. van Dyck and R. Strahan (eds.), *The Mammals of Australia*. Reed New Holland, Australia.
- Fox, B. J. 2008b. Eastern Chestnut Mouse, *Pseudomys gracilicaudatus*; pp. 634-635 in S. van Dyck and R. Strahan (eds.), *The Mammals of Australia*. Reed New Holland, Australia.
- Francis, G. 1973. Evolution of the Wellington Caves landscape. *Helictite* 11:79-91.
- Frank, R. 1969. The clastic sediments of Douglas Cave, Stuart Town. New South Wales: *Helictite* 7:3-13.
- Frank, R. 1971. The clastic sediments of the Wellington Caves. New South Wales. *Helictite* 9:3-26.
- Fraser, R. A., and R. T. Wells. 2006. Palaeontological excavation and taphonomic investigation of the late Pleistocene fossil deposit in Grant Hall, Victoria Fossil Cave, Naracoorte, South Australia. *Alcheringa* 30:147-161.
- Freeman, P. W. 1998. Form, function, and evolution in skulls and teeth of bats; pp. 140-156 in T. H. Kunz and P. A. Racey (eds.), *Bat Biology and Conservation*. Smithsonian Institution Press, Washington DC.
- Froyd, C. A., and K. J. Willis. 2008. Emerging issues in biodiversity and conservation management: The need for a palaeoecological perspective. *Quaternary Science Reviews* 27:1723-1732.
- Fusco, D. A. 2014. The biodiversity of the Holocene terrestrial mammal faunas of the Murray Mallee, South Australia. Unpublished Honours thesis. Flinders University of South Australia.
- Fusco, D. A., M. C. McDowell, and G. J. Prideaux. 2016. Late Holocene mammal fauna from southern Australia reveals rapid species declines post-European settlement: implications for conservation biology. *The Holocene* 26:699-708.
- Fusco, D. A., M. C. McDowell, G. Medlin, and G. J. Prideaux. 2017a. Fossils reveal late Holocene diversity and post-European decline of the terrestrial mammals of the Murray–Darling Depression. *Wildlife Research* 44:60-71.
- Fusco, D. A., M. C. McDowell, G. Medlin, and G. J. Prideaux. 2017b. Fossil insights in to the peri-European diversity and decline of terrestrial mammals from Australia’s Murray Darling Depression. *International Mammal Congress, Perth, Australia, 2017b*.
- Galbraith, R. F., R. G. Roberts, G. M. Laslett, H. Yoshida, and J. M. Olley. 1999. Optical dating of single and multiple grains of quartz from Jinmium rock shelter, northern Australia: Part I, experimental design and statistical models. *Archaeometry* 41:339-364.
- Galetti, M., M. Moleón, P. Jordano, M. M. Pires, P. R. Guimarães Jr., T. Pape, E. Nichols, D. Hansen, J. M. Olesen, M. Munk, J. S. de Mattos, A. H. Schweiger, N. Owen-Smith, C. N. Johnson, R. J. Marquis, and J.-C. Svenning. 2018. Ecological and evolutionary legacy of megafauna extinctions. *Biological Reviews* 93:845-862.
- Garnier, S. 2018. viridis: Default Color Maps from “matplotlib”. R package version 0.5. 1. 2018.

- Gienapp, P., C. Teplitsky, J. S. Alho, J. A. Mills, and J. Merilä. 2008. Climate change and evolution: disentangling environmental and genetic responses. *Molecular Ecology* 17:167-178.
- Gingele, F. X., P. De Deckker, and C.-D. Hillenbrand. 2004. Late Quaternary terrigenous sediments from the Murray Canyons area, offshore South Australia and their implications for sea level change, palaeoclimate and palaeodrainage of the Murray–Darling Basin. *Marine Geology* 212:183-197.
- Glasby, T. M., and A. Underwood. 1996. Sampling to differentiate between pulse and press perturbations. *Environmental Monitoring and Assessment* 42:241-252.
- Goede, A., and J. L. Bada. 1985. Electron spin resonance dating of Quaternary bone material from Tasmanian caves—A comparison with ages determined by aspartic acid racemization and C14. *Australian Journal of Earth Sciences* 32:155-162.
- Gorter, J. D. 1977. Fossil marsupials from the Douglas Cave, near Stuart Town, New South Wales. *Journal and Proceedings of the Royal Society of New South Wales* 110:139-145.
- Gotelli, N. J., and R. K. Colwell. 2001. Quantifying biodiversity: procedures and pitfalls in the measurement and comparison of species richness. *Ecology Letters* 4:379-391.
- Gould, J., and J. M. Dixon. 1983. *The Mammals of Australia: Incorporating the 3 Original Volumes*. Macmillan Company of Australia.
- Grace, M., H. R. Akçakaya, E. Bennett, C. Hilton-Taylor, B. Long, E. J. Milner-Gulland, R. Young, and M. Hoffmann. 2019. Using historical and palaeoecological data to inform ambitious species recovery targets. *Philosophical Transactions of the Royal Society B: Biological Sciences* 374:20190297.
- Graham, R. W., E. L. Lundelius, M. A. Graham, E. K. Schroeder, R. S. Toomey, E. Anderson, A. D. Barnosky, J. A. Burns, C. S. Churcher, D. K. Grayson, R. D. Guthrie, C. R. Harington, G. T. Jefferson, L. D. Martin, H. G. McDonald, R. E. Morlan, H. A. Semken, S. D. Webb, L. Werdelin, and M. C. Wilson. 1996. Spatial response of mammals to late Quaternary environmental fluctuations. *Science* 272:1601-1606.
- Grant, K. M., E. J. Rohling, M. Bar-Matthews, A. Ayalon, M. Medina-Elizalde, C. B. Ramsey, C. Satow, and A. P. Roberts. 2012. Rapid coupling between ice volume and polar temperature over the past 150,000 years. *Nature* 491:744-747.
- Grayson, D. K. 1998. Moisture history and small mammal community richness during the latest Pleistocene and Holocene, northern Bonneville Basin, Utah. *Quaternary Research* 49:330-334.
- Grealy, A., M. McDowell, C. Retallick, M. Bunce, and D. Peacock. 2020. Novel mitochondrial haplotype of spotted-tailed quoll (*Dasyurus maculatus*) present on Kangaroo Island (South Australia) prior to extirpation. *The Holocene* 30:136-144.
- Greenland Ice-core Project Members. 1993. Climate instability during the last interglacial period recorded in the GRIP ice core. *Nature* 364:203.
- Griffiths, A. D., and B. W. Brook. 2014. Effect of fire on small mammals: a systematic review. *International Journal of Wildland Fire* 23:1034-1043.
- Groves, R. H. 1999. Present vegetation types; pp. 369-401 in A. E. Orchard (ed.), *Flora of Australia* ABR/CSIRO, Melbourne Australia.
- Grün, R., R. Wells, S. Eggins, N. Spooner, M. Aubert, L. Brown, and E. Rhodes. 2008. Electron spin resonance dating of South Australian megafauna sites. *Australian Journal of Earth Sciences* 55:917-935.
- Guérin, G., N. Mercier, and G. Adamiec. 2011. Dose-rate conversion factors: update. *Ancient TL* 29:5-8.

- Gunderson, L. H., and L. Pritchard. 2012. Resilience and the behavior of large-scale systems, Volume 60. Island Press, Washington, DC.
- Gunn, J. 2004. Encyclopedia of caves and karst science. Taylor & Francis, New York.
- Gynther, I., N. Waller, and L. K.-P. Leung. 2016. Confirmation of the extinction of the Bramble Cay melomys *Melomys Rubicola* on Bramble Cay, Torres Strait: Results and conclusions from a comprehensive survey in August-September 2015. Unpublished report to the Department of Environment and Heritage Protection, Queensland Government, Brisbane.
- Hadly, E. A., and A. D. Barnosky. 2009. Vertebrate fossils and the future of conservation biology. *The Palaeontological Society Papers* 15:39-59.
- Haering, R., and B. J. Fox. 1995. Habitat utilization patterns of sympatric populations of *Pseudomys gracilicaudatus* and *Rattus lutreolus* in coastal heathland: A multivariate analysis. *Australian Journal of Ecology* 20:427-441.
- Halpern, C. B. 1988. Early Successional Pathways and the Resistance and Resilience of Forest Communities. *Ecology* 69:1703-1715.
- Hamm, G., P. Mitchell, L. J. Arnold, G. J. Prideaux, D. Questiaux, N. A. Spooner, V. A. Levchenko, E. C. Foley, T. H. Worthy, B. Stephenson, V. Coulthard, C. Coulthard, S. Wilton, and D. Johnston. 2016. Cultural innovation and megafauna interaction in the early settlement of arid Australia. *Nature* 539:280-283.
- Hammer, Ø., D. A. Harper, and P. D. Ryan. 2001. PAST: Paleontological statistics software package for education and data analysis. *Palaeontologia electronica* 4:9.
- Haouchar, D., J. Haile, M. C. McDowell, D. C. Murray, N. E. White, R. J. N. Allcock, M. J. Phillips, G. J. Prideaux, and M. Bunce. 2014. Thorough assessment of DNA preservation from fossil bone and sediments excavated from a late Pleistocene–Holocene cave deposit on Kangaroo Island, South Australia. *Quaternary Science Reviews* 84:56-64.
- Happold, D. C. D. 2008. Broad-toothed Rat, *Mastacomys fuscus*; pp. 589-590 in S. van Dyck and R. Strahan (eds.), *The Mammals of Australia*. Reed New Holland, Australia.
- Harle, K. J. 1997. Late Quaternary vegetation and climate change in southeastern Australia: palynological evidence from marine core E55-6. *Palaeogeography, Palaeoclimatology, Palaeoecology* 131:465-483.
- Harris, J. M. 2015. *Acrobates pygmaeus* (Diprotodontia: Acrobatidae). *Mammalian Species* 47:32-44.
- Harris, J. M., and R. L. Goldingay. 2005. The distribution of fossil and sub-fossil records of the eastern pygmy-possum *Cercartetus nanus* in Victoria. *Victorian Naturalist* 122:160-170.
- Harris, J. M., R. L. Goldingay, and L. O. Brooks. 2014. Population ecology of the eastern pygmy-possum (*Cercartetus nanus*) in a montane woodland in southern New South Wales. *Australian Mammalogy* 36:212-218.
- Heiri, O., A. F. Lotter, and G. Lemcke. 2001. Loss on ignition as a method for estimating organic and carbonate content in sediments: reproducibility and comparability of results. *Journal of Paleolimnology* 25:101-110.
- Helgen, K. M., R. P. Miguez, J. L. Kohen, and L. E. Helgen. 2012. Twentieth century occurrence of the long-beaked echidna *Zaglossus bruijnii* in the Kimberley region of Australia. *ZooKeys* 255:103-132.
- Helgen, K. M., R. T. Wells, B. P. Kear, W. R. Gerdtz, and T. F. Flannery. 2006. Ecological and evolutionary significance of sizes of giant extinct kangaroos. *Australian Journal of Zoology* 54:293-303.

- Herron, N., R. Davis, and R. Jones. 2002. The effects of large-scale afforestation and climate change on water allocation in the Macquarie River catchment, NSW, Australia. *Journal of Environmental Management* 65:369-381.
- Hesse, P. P., and G. H. McTainsh. 2003. Australian dust deposits: Modern processes and the Quaternary record. *Quaternary Science Reviews* 22:2007-2035.
- Hesse, P. P., J. W. Magee, and S. van der Kaars. 2004. Late Quaternary climates of the Australian arid zone: A review. *Quaternary International* 118–119:87-102.
- Hesse, P. P., L. Dawson, K. Tomkins, and F. Townsend. 1999. Geomorphic constraints on the evolution of the Wellington Caves. *Conference on Australasian Vertebrate Evolution Palaeontology & Systematics*:10-12.
- Hesse, P. P., R. Williams, T. J. Ralph, Z. T. Larkin, K. A. Fryirs, K. E. Westaway, and D. Yonge. 2018. Dramatic reduction in size of the lowland Macquarie River in response to Late Quaternary climate-driven hydrologic change. *Quaternary Research* 90:360-379.
- Higham, T. 2011. European Middle and Upper Palaeolithic radiocarbon dates are often older than they look: problems with previous dates and some remedies. *Antiquity* 85:235-249.
- Higham, T. F., R. Jacobi, and C. B. Ramsey. 2006. AMS radiocarbon dating of ancient bone using ultrafiltration. *Radiocarbon* 48:179.
- Higham, T. F. G., H. Barton, C. S. M. Turney, G. Barker, C. B. Ramsey, and F. Brock. 2009. Radiocarbon dating of charcoal from tropical sequences: results from the Niah Great Cave, Sarawak, and their broader implications. *Journal of Quaternary Science* 24:189-197.
- Hill, M. O., C. A. Harrower, and C. D. Preston. 2013. Spherical k-means clustering is good for interpreting multivariate species occurrence data. *Methods in Ecology and Evolution* 4:542-551.
- Hiscock, P. 2007. *Archaeology of ancient Australia*. Routledge, New York.
- Hocking, T. D. 2020. *directlabels: Direct labels for multicolor plots*. <https://cran.r-project.org/web/packages/directlabels/>.
- Hocknull, S. A. 2005. Ecological succession during the late Cainozoic of central eastern Queensland: Extinction of a diverse rainforest community. *Memoirs of the Queensland Museum* 51:39-122.
- Hocknull, S. A., J.-x. Zhao, Y.-x. Feng, and G. E. Webb. 2007. Responses of Quaternary rainforest vertebrates to climate change in Australia. *Earth and Planetary Science Letters* 264:317-331.
- Hocknull, S. A., R. Lewis, L. J. Arnold, T. Pietsch, R. Joannes-Boyau, G. J. Price, P. Moss, R. Wood, A. Dosseto, J. Louys, J. Olley, and R. A. Lawrence. 2020. Extinction of eastern Sahul megafauna coincides with sustained environmental deterioration. *Nature Communications* 11:2250.
- Hodge, G. 1991. Faunal and sedimentological study of Cathedral Cave: The late Pleistocene picture. Unpublished Honours thesis. University of New South Wales.
- Hoegh-Guldberg, O., P. Mumby, A. Hooten, R. Steneck, P. Greenfield, E. Gomez, C. Harvell, P. Sale, A. Edwards, and K. Caldeira. 2007. Coral reefs under rapid climate change and ocean acidification. *Science* 318:1737-1742.
- Hoffmann, A. A., P. D. Rymer, M. Byrne, K. X. Ruthrof, J. Whinam, M. McGeoch, D. M. Bergstrom, G. R. Guerin, B. Sparrow, L. Joseph, S. J. Hill, N. R. Andrew, J. Camac, N. Bell, M. Riegler, J. L. Gardner, and S. E. Williams. 2019. Impacts of recent climate change on terrestrial flora and fauna: Some emerging Australian examples. *Austral Ecology* 44:3-27.

- Hogg, A. G., Q. Hua, P. G. Blackwell, M. Niu, C. E. Buck, T. P. Guilderson, T. J. Heaton, J. G. Palmer, P. J. Reimer, and R. W. Reimer. 2013. SHCal13 Southern Hemisphere calibration, 0–50,000 cal yr BP. *Radiocarbon* 55:1889-1903.
- Holdaway, R. N., and C. Jacomb. 2000. Rapid Extinction of the Moas (Aves: Dinornithiformes): Model, Test, and Implications. *Science* 287:2250-2254.
- Holdaway, R. N., M. E. Allentoft, C. Jacomb, C. L. Oskam, N. R. Beavan, and M. Bunce. 2014. An extremely low-density human population exterminated New Zealand moa. *Nature Communications* 5:5436.
- Holling, C. S. 1973. Resilience and stability of ecological systems. *Annual review of ecology and systematics* 4:1-23.
- Holling, C. S. 1996. Engineering resilience versus ecological resilience.; pp. 32-44 in P. C. Schulze (ed.), *Engineering within ecological constraints*. National Academy Press, Washington, DC.
- Holt, R. D. 2009. Bringing the Hutchinsonian niche into the 21st century: Ecological and evolutionary perspectives. *Proceedings of the National Academy of Sciences* 106:19659-19665.
- Hope, J., and H. Wilkinson. 1982. *Warendja wakefieldi*, a new genus of wombat (Marsupialia, Vombatidae) from Pleistocene sediments in McEacherns Cave, western Victoria.
- How, R., J. Barnett, A. Bradley, W. Humphreys, and R. Martin. 1984. The population biology of *Pseudocheirus peregrinus* in a *Leptospermum laevigatum* thicket. *Possums and gliders*:261-268.
- Hoye, G. A., and L. S. Hall. 2008a. Eastern Bent-Winged Bat, *Miniopterus schreibersii oceanensis*; pp. 507-508 in S. van Dyck and R. Strahan (eds.), *The Mammals of Australia*. Reed New Holland, Australia.
- Hoye, G. A., and L. S. Hall. 2008b. Little Bent-winged Bat, *Miniopterus australis*; pp. 503-504 in S. van Dyck and R. Strahan (eds.), *The Mammals of Australia*. Reed New Holland, Australia.
- Huber, C., M. Leuenberger, R. Spahni, J. Flückiger, J. Schwander, T. F. Stocker, S. Johnsen, A. Landais, and J. Jouzel. 2006. Isotope calibrated Greenland temperature record over Marine Isotope Stage 3 and its relation to CH₄. *Earth and Planetary Science Letters* 243:504-519.
- Hughes, L. 2000. Biological consequences of global warming: Is the signal already apparent? *Trends in Ecology & Evolution* 15:56-61.
- Hughes, T. P., J. T. Kerry, M. Álvarez-Noriega, J. G. Álvarez-Romero, K. D. Anderson, A. H. Baird, R. C. Babcock, M. Beger, D. R. Bellwood, and R. Berkelmans. 2017. Global warming and recurrent mass bleaching of corals. *Nature* 543:373-377.
- Hutchinson, G. E. 1950. The biogeochemistry of vertebrate excretion (cave guano); pp. 381-461 in G. E. Hutchinson (ed.), *Survey of contemporary knowledge of biogeochemistry* 3. *Bulletin of the American Museum of Natural History*.
- Hutchinson, M. N., and J. D. Scanlon. 2009. New and Unusual Plio-Pleistocene Lizard (Reptilia: Scincidae) from Wellington Caves, New South Wales, Australia. *Journal of Herpetology* 43:139-147.
- Hutton, J. 1788. X. Theory of the earth; or an investigation of the laws observable in the composition, dissolution, and restoration of land upon the globe. *Earth and Environmental Science Transactions of The Royal Society of Edinburgh* 1:209-304.
- Isaac, B., J. White, D. Lerodiaconou, and R. Cooke. 2014. Simplification of arboreal marsupial assemblages in response to increasing urbanization. *Plos One* 9:e91049.

- Itambi, A., T. Von Dobeneck, S. Mulitza, T. Bickert, and D. Heslop. 2009. Millennial-scale northwest African droughts related to Heinrich events and Dansgaard-Oeschger cycles: Evidence in marine sediments from offshore Senegal. *Paleoceanography* 24.
- Ives, A. R., and S. R. Carpenter. 2007. Stability and diversity of ecosystems. *Science* 317:58-62.
- Jackson, S., and C. Groves. 2015. *Taxonomy of Australian Mammals*. CSIRO Publishing, Victoria, Australia.
- Jackson, S. M. 2000. Habitat relationships of the mahogany glider, *Petaurus gracilis*, and the sugar glider, *Petaurus breviceps*. *Wildlife Research* 27:39-48.
- Jacobs, Z., G. A. Duller, A. G. Wintle, and C. S. Henshilwood. 2006. Extending the chronology of deposits at Blombos Cave, South Africa, back to 140 ka using optical dating of single and multiple grains of quartz. *Journal of Human Evolution* 51:255-273.
- Jankowski, N. R., G. A. Gully, Z. Jacobs, R. G. Roberts, and G. J. Prideaux. 2016. A late Quaternary vertebrate deposit in Kudjal Yolghah Cave, south-western Australia: Refining regional late Pleistocene extinctions. *Journal of Quaternary Science* 31:538-550.
- Jarvie, S., T. H. Worthy, F. Saltré, R. P. Scofield, P. J. Seddon, and A. Cree. 2021. Using Holocene fossils to model the future: Distribution of climate suitability for tuatara, the last rhynchocephalian. *Journal of Biogeography* Early Access <https://doi.org/10.1111/jbi.14092>.
- Jerzolimski, A., and C. A. Peres. 2003. Bringing home the biggest bacon: a cross-site analysis of the structure of hunter-kill profiles in Neotropical forests. *Biological Conservation* 111:415-425.
- Jex, C. N., G. Mariethoz, A. Baker, P. Graham, M. S. Andersen, I. Acworth, N. Edwards, and C. Azcurra. 2012. Spatially dense drip hydrological monitoring and infiltration behaviour at the Wellington Caves, South East Australia. *International Journal of Speleology* 41:14.
- Johnsen, S. J., W. Dansgaard, H. B. Clausen, and C. C. Langway jun. 1972. Oxygen isotope profiles through the Antarctic and Greenland ice sheets. *Nature* 235:429.
- Johnson, C. N. 2002. Determinants of loss of mammal species during the Late Quaternary 'megafauna' extinctions: Life history and ecology, but not body size. *Proceedings of the Royal Society of London. Series B: Biological Sciences* 269:2221-2227.
- Johnson, C. N. 2005. What can the data on late survival of Australian megafauna tell us about the cause of their extinction? *Quaternary Science Reviews* 24:2167-2172.
- Johnson, C. N. 2006. *Australia's mammal extinctions: A 50000 year history*. Cambridge University Press.
- Johnson, C. N., and S. Wroe. 2003. Causes of extinction of vertebrates during the Holocene of mainland Australia: arrival of the dingo, or human impact? *The Holocene* 13:941-948.
- Johnson, K., A. A. Burbidge, and N. McKenzie. 1989. Australian Macropodoidea: status, causes of decline and future research and management. *Kangaroos, wallabies and rat-kangaroos* 2:641-657.
- Johnson, K. A. 2008a. Bilby, *Macrotis lagotis*; pp. 191-193 in S. van Dyck and R. Strahan (eds.), *The Mammals of Australia*. Reed New Holland, Australia.
- Johnson, K. A., and A. A. Burbidge. 2008. Pig-footed Bandicoot, *Chaeropus ecaudatus*; pp. 172-173 in S. van Dyck and R. Strahan (eds.), *The Mammals of Australia*. Reed New Holland, Australia.

- Johnson, P. M. 2008b. Black-striped Wallaby, *Macropus dorsalis*; pp. 329-330 in S. van Dyck and R. Strahan (eds.), *The Mammals of Australia*. Reed New Holland, Australia.
- Johnson, P. M. 2008c. Whiptail Wallaby, *Macropus parryi*; pp. 343-345 in S. van Dyck and R. Strahan (eds.), *The Mammals of Australia*. Reed New Holland, Australia.
- Johnston, P. G. 2008. Long-nosed Potoroo, *Potorous tridactylus*; pp. 302-304 in S. van Dyck and R. Strahan (eds.), *The Mammals of Australia*. Reed New Holland, Australia.
- Jones, B. 2009. Cave pearls—the integrated product of abiogenic and biogenic processes. *Journal of Sedimentary Research* 79:689-710.
- Jones, M. E. 2008a. Eastern Quoll, *Dasyurus viverrinus*; pp. 62-64 in S. van Dyck and R. Strahan (eds.), *The Mammals of Australia*. Reed New Holland, Australia.
- Jones, M. E. 2008b. Tasmanian Devil, *Sarcophilus harrisii*; pp. 78-80 in S. van Dyck and R. Strahan (eds.), *The Mammals of Australia*. Reed New Holland, Australia.
- Jouzel, J., V. Masson-Delmotte, O. Cattani, G. Dreyfus, S. Falourd, G. Hoffmann, B. Minster, J. Nouet, J. M. Barnola, J. Chappellaz, H. Fischer, J. C. Gallet, S. Johnsen, M. Leuenberger, L. Loulergue, D. Luethi, H. Oerter, F. Parrenin, G. Raisbeck, D. Raynaud, A. Schilt, J. Schwander, E. Selmo, R. Souchez, R. Spahni, B. Stauffer, J. P. Steffensen, B. Stenni, T. F. Stocker, J. L. Tison, M. Werner, and E. W. Wolff. 2007. Orbital and millennial antarctic climate variability over the past 800,000 years. *Science* 317:793-796.
- Kassambara, A. 2020. gpubr: 'ggplot2' Based Publication Ready Plots.: <https://cran.r-project.org/web/packages/ggpubr/>.
- Kavanagh, R. P. 2002a. Conservation and management of large forest owls in southeastern Australia; pp. 201-219 in I. Newton, R. Kavanagh, J. Olsen, and I. Taylor (eds.), *Ecology and Conservation of Owls*. CSIRO Publishing, Collingwood Victoria.
- Kavanagh, R. P. 2002b. Comparative diets of the powerful owl (*Ninox strenua*), sooty owl (*Tyto tenebricosa*) and masked owl (*Tyto novaehollandiae*) in southeastern Australia; pp. 175-191 in I. Newton, R. Kavanagh, J. Olsen, and I. Taylor (eds.), *Ecology and Conservation of Owls*. CSIRO Publishing, Collingwood, Victoria.
- Kawagata, S. 2001. Tasman Front shifts and associated paleoceanographic changes during the last 250,000 years: Foraminiferal evidence from the Lord Howe Rise. *Marine Micropaleontology* 41:167-191.
- Kawamura, H., A. Holbourn, and W. Kuhnt. 2006. Climate variability and land–ocean interactions in the Indo Pacific Warm Pool: A 460-ka palynological and organic geochemical record from the Timor Sea. *Marine Micropaleontology* 59:1-14.
- Kelly, L. T., and A. Bennett. 2008. Habitat requirements of the yellow-footed antechinus (*Antechinus flavipes*) in box-ironbark forest, Victoria, Australia. *Wildlife Research* 35:128-133.
- Kemp, C. W., J. Tibby, L. J. Arnold, and C. Barr. 2019. Australian hydroclimate during Marine Isotope Stage 3: A synthesis and review. *Quaternary Science Reviews* 204:94-104.
- Kemp, C. W., J. Tibby, L. J. Arnold, C. Barr, P. S. Gadd, J. C. Marshall, G. B. McGregor, and G. E. Jacobsen. 2020. Climates of the last three interglacials in subtropical eastern Australia inferred from wetland sediment geochemistry. *Palaeogeography, Palaeoclimatology, Palaeoecology* 538:109463.
- Kemper, C. M., and B. A. Wilson. 2008. New Holland Mouse, *Pseudomys novaehollandiae*; pp. 643-644 in S. van Dyck and R. Strahan (eds.), *The Mammals of Australia*. Reed New Holland, Australia.
- Kent, M., and P. Coker. 1992. *Vegetation description and analysis: A practical approach*. 1992. Ann Arbor, MI. CRC Press.

- Kerle, J. A., and R. A. How. 2008. Common Brushtail Possum, *Trichosurus vulpecula*; pp. 275-276 in S. van Dyck and R. Strahan (eds.), *The Mammals of Australia*. Reed New Holland, Australia.
- Kerle, J. A., A. S. Kutt, and J. L. Read. 2008. Desert Mouse, *Pseudomys desertor*; pp. 625-626 in S. van Dyck and R. Strahan (eds.), *The Mammals of Australia*. Reed New Holland, Australia.
- Kershaw, A. P. 1995. Environmental change in greater Australia. *Antiquity* 69:656-675.
- Kershaw, A. P., D. Bulman, and J. R. Busby. 1994. An examination of modern and pre-European settlement pollen samples from southeastern Australia—assessment of their application to quantitative reconstruction of past vegetation and climate. *Review of Palaeobotany and Palynology* 82:83-96.
- Kershaw, A. P., J. S. Clark, A. M. Gill, and D. M. D’Costa. 2002. A history of fire in Australia; pp. 3-25 in R. A. Bradstock, J. E. Williams, and A. M. Gill (eds.), *Flammable Australia: the fire regimes and biodiversity of a continent*. Cambridge University Press, Cambridge UK.
- Kershaw, P., P. Moss, and S. Van Der Kaars. 2003. Causes and consequences of long-term climatic variability on the Australian continent. *Freshwater Biology* 48:1274-1283.
- Keshavarzi, M., A. Baker, B. F. J. Kelly, and M. S. Andersen. 2017. River–groundwater connectivity in a karst system, Wellington, New South Wales, Australia. *Hydrogeology Journal* 25:557-574.
- Kidwell, S. M. 2015. Biology in the Anthropocene: Challenges and insights from young fossil records. *Proceedings of the National Academy of Sciences* 112:4922-4929.
- Kiernan, K., S. E. Lauritzen, and N. Duhig. 2001. Glaciation and cave sediment aggradation around the margins of the Mt Field Plateau, Tasmania. *Australian Journal of Earth Sciences* 48:251-263.
- Koch, P. L., and A. D. Barnosky. 2006. Late Quaternary extinctions: State of the debate. *Annual Review of Ecology, Evolution, and Systematics* 37:215-250.
- Kohen, J. L. 1995. *Aboriginal environmental impacts*. University of New South Wales Press, Sydney, New South Wales.
- Kos, A. M. 2001. Stratigraphy, sedimentary development and palaeoenvironmental context of a naturally accumulated pitfall cave deposit from southeastern Australia. *Australian Journal of Earth Sciences* 48:621-632.
- Kos, A. M. 2003a. Pre-burial taphonomic characterisation of a vertebrate assemblage from a pitfall cave fossil deposit in southeastern Australia. *Journal of Archaeological Science* 30:769-779.
- Kos, A. M. 2003b. Characterisation of post-depositional taphonomic processes in the accumulation of mammals in a pitfall cave deposit from southeastern Australia. *Journal of Archaeological Science* 30:781-796.
- Kreffft, G. 1882. *Exploration of the caves and rivers of New South Wales; Notes and Proceedings*. Legislative Assembly of New South Wales Session 5.
- Krishna, K., and M. N. Murty. 1999. Genetic K-means algorithm. *IEEE Transactions on Systems, Man, and Cybernetics, Part B (Cybernetics)* 29:433-439.
- Kulzer, E., J. Nelson, J. McKean, and F. Moehres. 1984. Prey-catching behaviour and echolocation in the Australian ghost bat, *Macroderma gigas* (Microchiroptera: Megadermatidae). *Australian Mammalogy* 7:37-50.
- Kusmer, K. D. 1990. Taphonomy of owl pellet deposition. *Journal of Paleontology* 64:629-637.
- Kutt, A. S., N. Y. Thurgate, and D. S. Hannah. 2004. Distribution and habitat of the desert mouse (*Pseudomys desertor*) in Queensland. *Wildlife Research* 31:129-142.

- Lake, P. S. 2000. Disturbance, patchiness, and diversity in streams. *Journal of the North American Benthological Society* 19:573-592.
- Lake, P. S. 2013. Resistance, Resilience and Restoration. *Ecological Management & Restoration* 14:20-24.
- Lane, E., and A. Richards. 1963. The discovery, exploration and scientific investigation of the Wellington Caves. *Helictite* 2:1-53.
- Lang, J. D. 1830. Interesting discovery. *Sydney Gazette and New South Wales Advertiser* 25th May:3.
- Lang, J. D. 1831. Account of the Discovery of Bone Caves in Wellington Valley. *Edinburgh New Philosophical Journal* 10:364-68.
- Law, B., T. Brassil, and L. Gonsalves. 2016. Recent decline of an endangered, endemic rodent: does exclusion of disturbance play a role for Hastings River mouse (*Pseudomys oralis*)? *Wildlife Research* 43:482-491.
- Lee, M. K., Y. I. Lee, H. S. Lim, J. I. Lee, J. H. Choi, and H. I. Yoon. 2011. Comparison of radiocarbon and OSL dating methods for a Late Quaternary sediment core from Lake Ulaan, Mongolia. *Journal of Paleolimnology* 45:127-135.
- Liang, Y., Y. Wang, Q. Wang, J. Wu, Q. Shao, Z. Zhang, S. Yang, X. Kong, and R. L. Edwards. 2019. East Asian summer monsoon climates and cave hydrological cycles over Dansgaard-Oeschger events 14 to 11 revealed by a new stalagmite record from Hulu Cave. *Quaternary Research* 92:725-737.
- Lim, T. L. 2008. Kowari, *Dasyuroides byrnei*; pp. 52-54 in S. van Dyck and R. Strahan (eds.), *The Mammals of Australia*. Reed New Holland, Australia.
- Lisiecki, L. E., and M. E. Raymo. 2005. A Pliocene-Pleistocene stack of 57 globally distributed benthic $\delta^{18}O$ records. *Paleoceanography* 20:PA1003.
- Lone, M. A., S. M. Ahmad, N. C. Dung, C.-C. Shen, W. Raza, and A. Kumar. 2014. Speleothem based 1000-year high resolution record of Indian monsoon variability during the last deglaciation. *Palaeogeography, Palaeoclimatology, Palaeoecology* 395:1-8.
- Long, J. A. 2002. *Prehistoric mammals of Australia and New Guinea: one hundred million years of evolution*. John Hopkins University Press, Baltimore, Maryland.
- Longin, R. 1971. New Method of Collagen Extraction for Radiocarbon Dating. *Nature* 230:241-242.
- Lopes, R. P., A. M. Ribeiro, S. R. Dillenburg, and C. L. Schultz. 2013. Late middle to late Pleistocene paleoecology and paleoenvironments in the coastal plain of Rio Grande do Sul State, Southern Brazil, from stable isotopes in fossils of *Toxodon* and *Stegomastodon*. *Palaeogeography, Palaeoclimatology, Palaeoecology* 369:385-394.
- López-García, J. M., H.-A. Blain, J. I. Morales, C. Lorenzo, S. Bañuls-Cardona, and G. Cuenca-Bescós. 2013. Small-mammal diversity in Spain during the late Pleistocene to early Holocene: Climate, landscape, and human impact. *Geology* 41:267-270.
- López, G. I. 2017. Grain Size Analysis; pp. 341-348 in A. S. Gilbert (ed.), *Encyclopedia of Geoarchaeology*. Springer Netherlands, Dordrecht.
- Louys, J. 2012. Paleontology in Ecology and Conservation: An Introduction; pp. 1-7 in J. Louys (ed.), *Paleontology in Ecology and Conservation*. Springer Berlin Heidelberg.
- Louys, J. 2015. Wombats (*Vombatidae*: Marsupialia) from the Pliocene Chinchilla Sand, southeast Queensland, Australia. *Alcheringa* 39:394-406.
- Louys, J., and P. Roberts. 2020. Environmental drivers of megafauna and hominin extinction in Southeast Asia. *Nature* 586:402-406.
- Louys, J., D. Curnoe, and H. Tong. 2007. Characteristics of Pleistocene megafauna extinctions in Southeast Asia. *Palaeogeography, Palaeoclimatology, Palaeoecology* 243:152-173.

- Louys, J., L. C. Bishop, and D. M. Wilkinson. 2009a. Opening dialogue between the recent and the long ago. *Nature* 462:847-847.
- Louys, J., K. J. Travouillon, M. Bassarova, and H. Tong. 2009b. The use of protected natural areas in palaeoecological analyses: Assumptions, limitations and application. *Journal of Archaeological Science* 36:2274-2288.
- Lowe, J. J., and M. J. Walker. 2014. Lithological evidence; pp. 93-179, *Reconstructing quaternary environments*. Routledge.
- Luckett, W. P. 1993. An ontogenetic assessment of dental homologies in therian mammals; pp. 182-204 in F. Szalay, M. Novacek, and M. McKenna (eds.), *Mammal Phylogeny*. Springer, New York.
- Lunney, D. 2008a. Swamp Rat, *Rattus lutreolus*; pp. 690-692 in S. van Dyck and R. Strahan (eds.), *The Mammals of Australia*. Reed New Holland, Australia.
- Lunney, D. 2008b. Bush Rat, *Rattus fuscipes*; pp. 685-687 in S. van Dyck and R. Strahan (eds.), *The Mammals of Australia*. Reed New Holland, Australia.
- Lyell, C. 1830. *Principles of geology*, Volume 1. John Murray, London.
- Lyman, R. L. 1994. *Vertebrate taphonomy*. Cambridge University Press, Cambridge.
- Lyman, R. L. 2017. Paleoenvironmental reconstruction from faunal remains: Ecological basics and analytical assumptions. *Journal of Archaeological Research* 25:315-371.
- Macken, A. C., and E. H. Reed. 2014. Postglacial reorganization of a small-mammal paleocommunity in southern Australia reveals thresholds of change. *Ecological Monographs* 84:563-577.
- Macken, A. C., G. J. Prideaux, and E. H. Reed. 2012. Variation and pattern in the responses of mammal faunas to Late Pleistocene climatic change in southeastern South Australia. *Journal of Quaternary Science* 27:415-424.
- Macken, A. C., M. C. McDowell, D. N. Bartholomeusz, and E. H. Reed. 2013. Chronology and stratigraphy of the Wet Cave vertebrate fossil deposit, Naracoorte, and relationship to paleoclimatic conditions of the Last Glacial Cycle in south-eastern Australia. *Australian Journal of Earth Sciences* 60:271-281.
- Macken, A. C., N. R. Jankowski, G. J. Price, E. A. Bestland, E. H. Reed, G. J. Prideaux, and R. G. Roberts. 2011. Application of sedimentary and chronological analyses to refine the depositional context of a Late Pleistocene vertebrate deposit, Naracoorte, South Australia. *Quaternary Science Reviews* 30:2690-2702.
- Magurran, A. E. 1988. *Ecological diversity and its measurement*, Volume 168. Princeton University Press, Princeton.
- Mahoney, J. 1977. Skull characters and relationships of *Notomys mordax* Thomas (Rodentia: Muridae), a poorly known Queensland hopping-mouse. *Australian Journal of Zoology* 25:749-754.
- Malhi, Y., C. E. Doughty, M. Galetti, F. A. Smith, J.-C. Svenning, and J. W. Terborgh. 2016. Megafauna and ecosystem function from the Pleistocene to the Anthropocene. *Proceedings of the National Academy of Sciences* 113:838-846.
- Markowska, M., M. O. Cuthbert, A. Baker, P. C. Treble, M. S. Andersen, L. Adler, A. Griffiths, and S. Frisia. 2020. Modern speleothem oxygen isotope hydroclimate records in water-limited SE Australia. *Geochimica et Cosmochimica Acta* 270:431-448.
- Markowska, M., A. Baker, M. S. Andersen, C. N. Jex, M. O. Cuthbert, G. C. Rau, P. W. Graham, H. Rutledge, G. Mariethoz, and C. E. Marjo. 2016. Semi-arid zone caves: Evaporation and hydrological controls on $\delta^{18}\text{O}$ drip water composition and implications for speleothem paleoclimate reconstructions. *Quaternary Science Reviews* 131:285-301.

- Marshall, F., and T. Pilgram. 1993. NISP vs. MNI in quantification of body-part representation. *American Antiquity* 58:261-269.
- Martin, G. R. 1986. Sensory capacities and the nocturnal habit of owls (Strigiformes). *Ibis* 128:266-277.
- Martinez, S. 2010. Palaeoecology of the Mount Etna bat fauna, coastal eastern Queensland. Unpublished PhD thesis. Faculty of Science and Technology, Queensland University of Technology.
- Mathes, G. H., J. van Dijk, W. Kiessling, and M. J. Steinbauer. 2021. Extinction risk controlled by interaction of long-term and short-term climate change. *Nature Ecology & Evolution* 5:304-310.
- Matthews, T., C. Denys, and J. E. Parkington. 2005. The palaeoecology of the micromammals from the late middle Pleistocene site of Hoedjiespunt 1 (Cape Province, South Africa). *Journal of Human Evolution* 49:432-451.
- Mayer, E. L., A. Hubbe, J. Botha-Brink, A. M. Ribeiro, P. M. Haddad-Martim, and W. Neves. 2020. Diagenetic changes on bone histology of Quaternary mammals from a tropical cave deposit in southeastern Brazil. *Palaeogeography, Palaeoclimatology, Palaeoecology* 537:109372.
- Maynes, G. 2008. Parma Wallaby, *Macropus parma*; pp. 341-343 in S. van Dyck and R. Strahan (eds.), *The Mammals of Australia*. Reed New Holland, Australia.
- McCain, C. M., and S. R. B. King. 2014. Body size and activity times mediate mammalian responses to climate change. *Global Change Biology* 20:1760-1769.
- McCarroll, J., F. M. Chambers, J. C. Webb, and T. Thom. 2017. Application of palaeoecology for peatland conservation at Mossdale Moor, UK. *Quaternary International* 432:39-47.
- McClymont, E. L., S. M. Sostdian, A. Rosell-Melé, and Y. Rosenthal. 2013. Pleistocene sea-surface temperature evolution: Early cooling, delayed glacial intensification, and implications for the mid-Pleistocene climate transition. *Earth-Science Reviews* 123:173-193.
- McDermott, F. 2004. Palaeo-climate reconstruction from stable isotope variations in speleothems: a review. *Quaternary Science Reviews* 23:901-918.
- McDonough, L., C. Iverach, S. Beckmann, M. Manefield, G. Rau, A. Baker, and B. Kelly. 2016. Spatial variability of cave-air carbon dioxide and methane concentrations and isotopic compositions in a semi-arid karst environment. *Environmental Earth Sciences* 75:700.
- McDowell, M. C. 2002. The analysis of Late Quaternary fossil mammal faunas from Robertson Cave (5U17, 18, 19) & Wet Cave (5U10, 11) in the Naracoorte World Heritage Area, South Australia. Unpublished Masters thesis. School of Biological Sciences, Flinders University of South Australia.
- McDowell, M. C. 2013. Late Quaternary faunal responses to environmental change and isolation on a large Australian land-bridge island. Unpublished PhD Thesis. School of Biological Sciences, Flinders University of South Australia.
- McDowell, M. C. 2014. Holocene vertebrate fossils aid the management and restoration of Australian ecosystems. *Ecological Management & Restoration* 15:58-63.
- McDowell, M. C., and G. C. Medlin. 2010. Natural Resource Management implications of the pre-European non-volant mammal fauna of the southern tip of Eyre Peninsula, South Australia. *Australian Mammalogy* 32:87-93.
- McDowell, M. C., A. Baynes, G. C. Medlin, and G. J. Prideaux. 2012. The impact of European colonization on the late-Holocene non-volant mammals of Yorke Peninsula, South Australia. *The Holocene* 22:1441-1450.

- McDowell, M. C., E. A. Bestland, F. Bertuch, L. K. Ayliffe, J. C. Hellstrom, G. E. Jacobsen, and G. J. Prideaux. 2013. Chronology, stratigraphy and palaeoenvironmental interpretation of a Late Pleistocene to mid-Holocene cave accumulation on Kangaroo Island, South Australia. *Boreas* 42:974-994.
- McIlroy, J. C. 2008. Common Wombat, *Vombatus ursinus*; pp. 206-208 in S. van Dyck and R. Strahan (eds.), *The Mammals of Australia*. Reed New Holland, Australia.
- McNabb, E. G. 2002. Notes on the diet and observations of the Southern Boobook *Ninox novaeseelandiae* in southern Victoria; pp. 192-198 in I. Newton, R. Kavanagh, J. Olsen, and I. Taylor (eds.), *Ecology and Conservation of Owls*. CSIRO Publishing, Collingwood, Australia.
- Medina, M. E., N. A. De Santi, D. E. Rivero, D. H. Verzi, and E. P. Tonni. 2020. Fossorial rodents and applied zooarchaeology to ecosystem conservation in Sierras of Córdoba, Argentina. *Austral Ecology* 46:139-147.
- Medlin, G. C. 2008. Plains Mouse, *Pseudomys australis*; pp. 617-618 in S. van Dyck and R. Strahan (eds.), *Mammals of Australia*.
- Meek, P., K. McCray, and B. Cann. 2003. New records of Hastings River mouse *Pseudomys oralis* from State Forest of New South Wales pre-logging surveys. *Australian Mammalogy* 25:101-105.
- Mejdahl, V. 1979. Thermoluminescence dating: beta-dose attenuation in quartz grains. *Archaeometry* 21:61-72.
- Mejdahl, V. 1987. Internal radioactivity in quartz and feldspar grains. *Ancient TL* 5:10-17.
- Menkhorst, P., and J. Seebeck. 1981. The status, habitat and distribution of *Pseudomys fumeus* Brazenor (Rodentia: Muridae). *Australian Wildlife Research* 8:87-98.
- Menu, H., and J. B. Popelard. 1987. Utilisation des caractères dentaires pour la détermination des Vespertilioninès de l'ouest européen. *Le Rhinolophe*. Muséum d'Histoire Naturelle de Genève 4:1-88.
- Merchant, J. C. 2008a. Agile Wallaby, *Macropus agilis*; pp. 323-324 in S. van Dyck and R. Strahan (eds.), *The Mammals of Australia*. Reed New Holland, Australia.
- Merchant, J. C. 2008b. Swamp Wallaby, *Wallabia bicolor*; pp. 404-406 in S. van Dyck and R. Strahan (eds.), *The Mammals of Australia*. Reed New Holland, Australia.
- Merrilees, D. 1967. Cranial and mandibular characters of modern mainland Wombats (Marsupialia Vombatidae) from a palaeontological viewpoint and their bearing on the fossils called *Phascolomys parvus* by Owen (1872). *15*:399-418.
- Metcalf, J. L., C. Turney, R. Barnett, F. Martin, S. C. Bray, J. T. Vilstrup, L. Orlando, R. Salas-Gismondi, D. Loponte, M. Medina, M. De Nigris, T. Civalero, P. M. Fernández, A. Gasco, V. Duran, K. L. Seymour, C. Otaola, A. Gil, R. Paunero, F. J. Prevosti, C. J. A. Bradshaw, J. C. Wheeler, L. Borrero, J. J. Austin, and A. Cooper. 2016. Synergistic roles of climate warming and human occupation in Patagonian megafaunal extinctions during the Last Deglaciation. *Science advances* 2:e1501682.
- Miller, G., J. Magee, M. Smith, N. Spooner, A. Baynes, S. Lehman, M. Fogel, H. Johnston, D. Williams, and P. Clark. 2016. Human predation contributed to the extinction of the Australian megafaunal bird *Genyornis newtoni* ~ 47 ka. *Nature Communications* 7:1-7.
- Miller, G. H., and M. L. Fogel. 2016. Calibrating $\delta^{18}O$ in *Dromaius novaehollandiae* (emu) eggshell calcite as a paleo-aridity proxy for the Quaternary of Australia. *Geochimica et Cosmochimica Acta* 193:1-13.
- Miller, G. H., M. L. Fogel, J. W. Magee, M. K. Gagan, S. J. Clarke, and B. J. Johnson. 2005. Ecosystem collapse in Pleistocene Australia and a human role in megafaunal extinction. *Science* 309:287-290.

- Miller, K. G., J. V. Browning, W. J. Schmelz, R. E. Kopp, G. S. Mountain, and J. D. Wright. 2020. Cenozoic sea-level and cryospheric evolution from deep-sea geochemical and continental margin records. *Science advances* 6:eaaz1346.
- Mitchell, T. 1838. *Three Expeditions in the interior of eastern Australia: with descriptions of the recently explored region of Australia Felix, and of the present colony of New South Wales*. T & W Boone London.
- Mooney, N., and D. E. Rounsevell. 2008. Thylacine, *Thylacinus cynocephalus*; pp. 167-168 in S. van Dyck and R. Strahan (eds.), *The Mammals of Australia*. Reed New Holland, Australia.
- Mooney, S. D., S. P. Harrison, P. Bartlein, and J. Stevenson. 2012. The prehistory of fire in Australasia; pp. 3-25 in R. A. Bradstock, A. M. Gill, and R. J. Williams (eds.), *Flammable Australia: Fire regimes, biodiversity and ecosystems in a changing world*. CSIRO, Collingwood, Victoria, Australia.
- Morel, A. C., and S. Nogu . 2019. Combining Contemporary and Paleoecological Perspectives for Estimating Forest Resilience. *Frontiers in Forests and Global Change* 2:1-17.
- Moriarty, K. C., M. T. McCulloch, R. T. Wells, and M. C. McDowell. 2000. Mid-Pleistocene cave fills, megafaunal remains and climate change at Naracoorte, South Australia: towards a predictive model using U-Th dating of speleothems. *Palaeogeography, Palaeoclimatology, Palaeoecology* 159:113-143.
- Morton, S. R., and C. R. Dickman. 2008. Fat-tailed Dunnart, *Sminthopsis crassicaudata*; pp. 132-133 in S. van Dyck and R. Strahan (eds.), *The Mammals of Australia*. Reed New Holland, Australia.
- Mosblech, N. A. S., M. B. Bush, and R. van Woesik. 2011. On metapopulations and microrefugia: Palaeoecological insights. *Journal of Biogeography* 38:419-429.
- Moulds, T. 2004. Review of Australian cave guano ecosystems with a checklist of guano invertebrates. *Proceedings of the Linnean Society of New South Wales* 125:1-42.
- Munsell, C. 1994. *Munsell soil color charts, 1994 revised edition*. Macbeth Division of Kollmorgen Instruments Corporation, New Windsor, NY.
- Murray, A. S., and A. G. Wintle. 2000. Luminescence dating of quartz using an improved single-aliquot regenerative-dose protocol. *Radiation Measurements* 32:57-73.
- Murray, D. C., J. Haile, J. Dortch, N. E. White, D. Haouchar, M. I. Bellgard, R. J. Allcock, G. J. Prideaux, and M. Bunce. 2013. Scrapheap Challenge: A novel bulk-bone metabarcoding method to investigate ancient DNA in faunal assemblages. *Scientific Reports* 3:1-8.
- Murray, D. C., S. G. Pearson, R. Fullagar, B. M. Chase, J. Houston, J. Atchison, N. E. White, M. I. Bellgard, E. Clarke, and M. Macphail. 2012. High-throughput sequencing of ancient plant and mammal DNA preserved in herbivore middens. *Quaternary Science Reviews* 58:135-145.
- Murray, P. 1978. Late Cenozoic monotreme anteaters. *Australian Zoologist* 20:29-55.
- Musgrave, R. J., and J. A. Webb. 2007. Palaeomagnetic Analysis Of Sediments In The Buchan Caves, Southeastern Australia, Provides A Pre-Late Pleistocene Date For Landscape And Climate Evolution; pp. 47-69 in I. D. Sasowsky and J. Mylroie (eds.), *Studies of Cave Sediments: Physical and Chemical Records of Paleoclimate*. Springer Netherlands, Dordrecht.
- Musser, G. G. 1981. The giant rat of Flores and its relatives east of Borneo and Bali. *Bulletin of the American Museum of Natural History* 169:67-176.
- Navarro, C., J. Carri n, M. Munuera, and A. Prieto. 2001. Cave surface pollen and the palynological potential of karstic cave sediments in palaeoecology. *Review of Palaeobotany and Palynology* 117:245-265.

- Newton, A. C. 2016. Biodiversity Risks of Adopting Resilience as a Policy Goal. *Conservation Letters* 9:369-376.
- Nguyen, J. M., S. J. Hand, and M. Archer. 2016. The late Cenozoic passerine avifauna from Rackham's Roost Site, Riversleigh, Australia. *Records of the Australian Museum* 68:201-230.
- Nipperess, D. 2002. The Koppa's Pool local fauna, an early pliocene fossil vertebrate assemblage from the Wellington Caves complex, Australia. Unpublished Honours thesis. Centre for Ecostratigraphy and Palaeobiology.
- Nogués-Bravo, D., J. Rodríguez, J. Hortal, P. Batra, and M. B. Araújo. 2008. Climate change, humans, and the extinction of the woolly mammoth. *PLoS biology* 6:e79.
- Nogués-Bravo, D., F. Rodríguez-Sánchez, L. Orsini, E. de Boer, R. Jansson, H. Morlon, D. A. Fordham, and S. T. Jackson. 2018. Cracking the code of biodiversity responses to past climate change. *Trends in Ecology & Evolution* 33:765-776.
- O'Connell, J. F., J. Allen, M. A. J. Williams, A. N. Williams, C. S. M. Turney, N. A. Spooner, J. Kamminga, G. Brown, and A. Cooper. 2018. When did *Homo sapiens* first reach Southeast Asia and Sahul? *Proceedings of the National Academy of Sciences* 115:8482-8490.
- Oksanen, J., F. Blanchet, M. Friendly, R. Kindt, P. Legendre, D. Mcglinn, P. Minchin, R. O'Hara, G. Simpson, P. Solymos, E. Szoecs, and H. Wagner. 2019. *Vegan: community ecology package*. Version 2.5-7.: <https://cran.r-project.org/web/packages/vegan/>.
- Osborne, R. 1982. Cainozoic stratigraphy at Wellington Caves, New South Wales. *Proceedings of the Linnean Society of New South Wales* 107:129-145.
- Osborne, R. 1984. Lateral facies changes, unconformities and stratigraphic reversals: Their significance for cave sediment stratigraphy. *Cave science* 11:175-184.
- Osborne, R. 1997. Rehabilitation of the Wellington Caves phosphate mine: Implications for Cainozoic stratigraphy. *Proceedings of the Linnean Society of New South Wales* 117:175-180.
- Osborne, R. 2001. Karst geology of Wellington Caves: A review. *Helictite* 37:3-12.
- Osborne, R. 2003. Geoheritage and Cave Furnishing Heritage Inventory of Cathedral Cave, Wellington Caves, NSW. Unpublished report to Wellington Council.
- Osborne, R. 2007. Cathedral Cave, Wellington Caves, New South Wales, Australia. A multiphase, non-fluvial cave. *Earth Surface Processes and Landforms* 32:2075-2103.
- Osborne, R. 2010. Rethinking eastern Australian caves. *Geological Society, London, Special Publications* 346:289-308.
- Owen, R. 1872. On the fossil mammals of Australia. Part VI. Genus *Phascolomys* Geoffroy. *Philosophical Transactions of the Royal Society of London* 162:173-196.
- Parmesan, C. 2006. Ecological and evolutionary responses to recent climate change. *Annual Review of Ecology, Evolution, and Systematics* 37:637-669.
- Parmesan, C., and G. Yohe. 2003. A globally coherent fingerprint of climate change impacts across natural systems. *Nature* 421:37-42.
- Pate, D., M. C. McDowell, R. T. Wells, and S. M. Smith. 2002. Last recorded evidence for megafauna at Wet Cave, Naracoorte, South Australia 45,000 years ago. *Australian Archaeology* 54:53-55.
- Paull, D. J. 2008. Southern Brown Bandicoot, *Isoodon obesulus*; pp. 180-182 in S. van Dyck and R. Strahan (eds.), *The Mammals of Australia*. Reed New Holland, Australia.
- Pavey, C., and R. A. Young. 2008. Eastern Horseshoe Bat, *Rhinolophus megaphyllus*; pp. 451-453 in S. van Dyck and R. Strahan (eds.), *The Mammals of Australia*. Reed New Holland, Australia.

- Pawley, S. M., R. M. Bailey, J. Rose, B. S. Moorlock, R. J. Hamblin, S. J. Booth, and J. R. Lee. 2008. Age limits on Middle Pleistocene glacial sediments from OSL dating, north Norfolk, UK. *Quaternary Science Reviews* 27:1363-1377.
- Pearson, R. G. 2006. Climate change and the migration capacity of species. *Trends in Ecology & Evolution* 21:111-113.
- Pecl, G. T., M. B. Araújo, J. D. Bell, J. Blanchard, T. C. Bonebrake, I.-C. Chen, T. D. Clark, R. K. Colwell, F. Danielsen, B. Evengård, L. Falconi, S. Ferrier, S. Frusher, R. A. Garcia, R. B. Griffis, A. J. Hobday, C. Janion-Scheepers, M. A. Jarzyna, S. Jennings, J. Lenoir, H. I. Linnetved, V. Y. Martin, P. C. McCormack, J. McDonald, N. J. Mitchell, T. Mustonen, J. M. Pandolfi, N. Pettorelli, E. Popova, S. A. Robinson, B. R. Scheffers, J. D. Shaw, C. J. B. Sorte, J. M. Strugnell, J. M. Sunday, M.-N. Tuanmu, A. Vergés, C. Villanueva, T. Wernberg, E. Wapstra, and S. E. Williams. 2017. Biodiversity redistribution under climate change: Impacts on ecosystems and human well-being. *Science* 355:eaai9214.
- Perry, G. L. W., A. B. Wheeler, J. R. Wood, and J. M. Wilmshurst. 2014. A high-precision chronology for the rapid extinction of New Zealand moa (Aves, Dinornithiformes). *Quaternary Science Reviews* 105:126-135.
- Perry, T. 1955. The spread of rural settlement in New South Wales, 1788–1826. *Australian Historical Studies* 6:377-395.
- Peters, K. J., F. Saltré, T. Friedrich, Z. Jacobs, R. Wood, M. McDowell, S. Ulm, and C. J. Bradshaw. 2019. FosSahul 2.0, an updated database for the Late Quaternary fossil records of Sahul. *Scientific Data* 6:1-7.
- Petherick, L., H. Bostock, T. Cohen, K. Fitzsimmons, J. Tibby, M.-S. Fletcher, P. Moss, J. Reeves, S. Mooney, and T. Barrows. 2013. Climatic records over the past 30 ka from temperate Australia—a synthesis from the Oz-INTIMATE workgroup. *Quaternary Science Reviews* 74:58-77.
- Petit, J.-R., J. Jouzel, D. Raynaud, N. I. Barkov, J.-M. Barnola, I. Basile, M. Bender, J. Chappellaz, M. Davis, and G. Delaygue. 1999. Climate and atmospheric history of the past 420,000 years from the Vostok ice core, Antarctica. *Nature* 399:429-436.
- Pielou, E. C. 1966. The measurement of diversity in different types of biological collections. *Journal of theoretical biology* 13:131-144.
- Pimm, S. L. 1994. Biodiversity and the balance of nature; pp. 347-359, *Biodiversity and ecosystem function*. Springer.
- Piñero, P., and J. Agustí. 2020. Rodents from Botardo-D and the Miocene-Pliocene transition in the Guadix-Baza Basin (Granada, Spain). *Palaeobiodiversity and Palaeoenvironments* 100:903-920.
- Pino, M., A. M. Abarzúa, G. Astorga, A. Martel-Cea, N. Cossio-Montecinos, R. X. Navarro, M. P. Lira, R. Labarca, M. A. LeCompte, and V. Adedeji. 2019. Sedimentary record from Patagonia, southern Chile supports cosmic-impact triggering of biomass burning, climate change, and megafaunal extinctions at 12.8 ka. *Scientific Reports* 9:1-27.
- Pokines, J. T., K. Faillace, J. Berger, D. Pirtle, M. Sharpe, A. Curtis, K. Lombardi, and J. Admans. 2018. The effects of repeated wet-dry cycles as a component of bone weathering. *Journal of Archaeological Science: Reports* 17:433-441.
- Powers, M. C. 1953. A new roundness scale for sedimentary particles. *Journal of Sedimentary Research* 23:117-119.
- Prescott, G. W., D. R. Williams, A. Balmford, R. E. Green, and A. Manica. 2012. Quantitative global analysis of the role of climate and people in explaining late Quaternary megafaunal extinctions. *Proceedings of the National Academy of Sciences* 109:4527-4531.

- Prescott, J. R., and J. T. Hutton. 1994. Cosmic ray contributions to dose rates for luminescence and ESR dating: large depths and long-term time variations. *Radiation Measurements* 23:497-500.
- Price, G. 2002. *Perameles sobbei* sp. nov. (Marsupialia, Peramelidae), a Pleistocene bandicoot from the Darling Downs, south-eastern Queensland. *Memoirs of the Queensland Museum* 48:193-197.
- Price, G., and G. Webb. 2006. Late Pleistocene sedimentology, taphonomy and megafauna extinction on the Darling Downs, southeastern Queensland. *Australian Journal of Earth Sciences* 53:947-970.
- Price, G. J. 2004. Fossil bandicoots (Marsupialia, Peramelidae) and environmental change during the Pleistocene on the Darling Downs, southeastern Queensland, Australia. *Journal of Systematic Palaeontology* 2:347-356.
- Price, G. J. 2012. Plio-Pleistocene climate and faunal change in central eastern Australia. *Episodes* 35:160-165.
- Price, G. J., J.-x. Zhao, Y.-x. Feng, and S. A. Hocknull. 2009. New U/Th ages for Pleistocene megafauna deposits of southeastern Queensland, Australia. *Journal of Asian Earth Sciences* 34:190-197.
- Price, G. J., J. Louys, G. K. Smith, and J. Cramb. 2019. Shifting faunal baselines through the Quaternary revealed by cave fossils of eastern Australia. *PeerJ* 6:e6099.
- Price, G. J., G. E. Webb, J.-x. Zhao, Y.-x. Feng, A. S. Murray, B. N. Cooke, S. A. Hocknull, and I. H. Sobbe. 2011. Dating megafaunal extinction on the Pleistocene Darling Downs, eastern Australia: The promise and pitfalls of dating as a test of extinction hypotheses. *Quaternary Science Reviews* 30:899-914.
- Prideaux, G. 2004. Systematics and evolution of the sthenurine kangaroos, Volume 146. University of California Press.
- Prideaux, G. J. 2007. Mid-Pleistocene vertebrate records: Australia; pp. 1517-1537 in S. A. Elias (ed.), *Encyclopedia of Quaternary Science*. Elsevier, Oxford, UK.
- Prideaux, G. J., and N. M. Warburton. 2010. An osteology-based appraisal of the phylogeny and evolution of kangaroos and wallabies (Macropodidae: Marsupialia). *Zoological Journal of the Linnean Society* 159:954-987.
- Prideaux, G. J., R. G. Roberts, D. Megirian, K. E. Westaway, J. C. Hellstrom, and J. M. Olley. 2007a. Mammalian responses to Pleistocene climate change in southeastern Australia. *Geology* 35:33-36.
- Prideaux, G. J., L. K. Ayliffe, L. R. G. DeSantis, B. W. Schubert, P. F. Murray, M. K. Gagan, and T. E. Cerling. 2009. Extinction implications of a chenopod browse diet for a giant Pleistocene kangaroo. *Proceedings of the National Academy of Sciences* 106:11646-11650.
- Prideaux, G. J., J. A. Long, L. K. Ayliffe, J. C. Hellstrom, B. Pillans, W. E. Boles, M. N. Hutchinson, R. G. Roberts, M. L. Cupper, and L. J. Arnold. 2007b. An arid-adapted middle Pleistocene vertebrate fauna from south-central Australia. *Nature* 445:422-425.
- Prideaux, G. J., G. A. Gully, A. M. C. Couzens, L. K. Ayliffe, N. R. Jankowski, Z. Jacobs, R. G. Roberts, J. C. Hellstrom, M. K. Gagan, and L. M. Hatcher. 2010. Timing and dynamics of Late Pleistocene mammal extinctions in southwestern Australia. *Proceedings of the National Academy of Sciences* 107:22157-22162.
- Pushkina, D., and P. Raia. 2008. Human influence on distribution and extinctions of the late Pleistocene Eurasian megafauna. *Journal of Human Evolution* 54:769-782.
- Pyke, G., and D. Read. 2002. Hastings River mouse *Pseudomys oralis*: a biological review. *Australian Mammalogy* 24:151-176.

- Ramsay, E. P. 1882. Curator's report on the exploration of caves. 31st December 1881; pp., Exploration of the Caves and Rivers of New South Wales. Notes and Proceedings. Legislative Assembly of New South Wales Session 5, New South Wales.
- Rau, G. C., M. O. Cuthbert, M. S. Andersen, A. Baker, H. Rutledge, M. Markowska, H. Roshan, C. E. Marjo, P. W. Graham, and R. I. Acworth. 2015. Controls on cave drip water temperature and implications for speleothem-based paleoclimate reconstructions. *Quaternary Science Reviews* 127:19-36.
- Read, J., P. Copley, and P. Bird. 1999. The distribution, ecology and current status of *Pseudomys desertor* in South Australia. *Wildlife Research* 26:453-462.
- Reed, E., and S. Bourne. 2000. Pleistocene fossil vertebrate sites of the South East region of South Australia. *Transactions of the Royal Society of South Australia* 124:61-90.
- Reed, E. H. 2006. In situ taphonomic investigation of Pleistocene large mammal bone deposits from the Ossuaries, Victoria Fossil Cave, Naracoorte, South Australia. *Helictite* 39:5-15.
- Reed, E. H., and S. J. Bourne. 2009. Pleistocene Fossil vertebrate Sites of the South East Region of South Australia II. *Transactions of the Royal Society of South Australia* 133:30-40.
- Rees-Jones, J. 1995. Optical dating of young sediments using fine-grain quartz. *Ancient TL* 13:9-14.
- Rees-Jones, J., and M. Tite. 1997. Optical dating results for British archaeological sediments. *Archaeometry* 39:177-187.
- Retallack, G. J. 1990. *Soils of the past: An introduction to paleopedology*. Unwin Hyman Inc, London.
- Richards, G. C., S. Hand, K. N. Armstrong, and L. S. Hall. 2008. Ghost Bat, *Macroderma gigas*; pp. 449-450 in S. van Dyck and R. Strahan (eds.), *The Mammals of Australia*. Reed New Holland, Australia.
- Richards, H. L., R. T. Wells, A. R. Evans, E. M. Fitzgerald, and J. W. Adams. 2019. The extraordinary osteology and functional morphology of the limbs in Palorchestidae, a family of strange extinct marsupial giants. *Plos One* 14:e0221824.
- Roberts, R. G. 2014. A pardon for the Dingo. *Science* 343:142-143.
- Roberts, R. G., T. F. Flannery, L. K. Ayliffe, H. Yoshida, J. M. Olley, G. J. Prideaux, G. M. Laslett, A. Baynes, M. A. Smith, R. Jones, and B. L. Smith. 2001. New ages for the last Australian megafauna: Continent-wide extinction about 46,000 years ago. *Science* 292:1888-1892.
- Rodríguez-Rey, M., S. Herrando-Pérez, R. Gillespie, Z. Jacobs, F. Saltré, B. W. Brook, G. J. Prideaux, R. G. Roberts, A. Cooper, and J. Alroy. 2015. Criteria for assessing the quality of Middle Pleistocene to Holocene vertebrate fossil ages. *Quaternary Geochronology* 30:69-79.
- Rodríguez-Rey, M., S. Herrando-Pérez, B. W. Brook, F. Saltré, J. Alroy, N. Beeton, M. I. Bird, A. Cooper, R. Gillespie, Z. Jacobs, C. N. Johnson, G. H. Miller, G. J. Prideaux, R. G. Roberts, C. S. M. Turney, and C. J. A. Bradshaw. 2016. A comprehensive database of quality-rated fossil ages for Sahul's Quaternary vertebrates. *Scientific Data* 3:160053.
- Rose, R. W., and K. A. Johnson. 2008. Tasmanian Bettong, *Bettongia gaimardi*; pp. 287-288 in S. van Dyck and R. Strahan (eds.), *The Mammals of Australia*. Reed New Holland, Australia.
- Rowe, R. J., and R. C. Terry. 2014. Small mammal responses to environmental change: integrating past and present dynamics. *Journal of Mammalogy* 95:1157-1174.

- Rowston, C., C. P. Catterall, and C. Hurst. 2002. Habitat preferences of squirrel gliders, *Petaurus norfolcensis*, in the fragmented landscape of southeast Queensland. *Forest Ecology and Management* 164:197-209.
- Royer, A., S. Montuire, S. Legendre, E. Discamps, M. Jeannet, and C. Lécuyer. 2016. Investigating the influence of climate changes on rodent communities at a regional-scale (MIS 1-3, Southwestern France). *Plos One* 11:e0145600.
- Rull, V. 2010. Ecology and palaeoecology: Two approaches, one objective. *Open Ecology Journal* 3:1-5.
- Rull, V. 2014. Time continuum and true long-term ecology: From theory to practice. *Frontiers in Ecology and Evolution* 2:1-7.
- Rutledge, H., A. Baker, C. E. Marjo, M. S. Andersen, P. W. Graham, M. O. Cuthbert, G. C. Rau, H. Roshan, M. Markowska, and G. Mariethoz. 2014. Dripwater organic matter and trace element geochemistry in a semi-arid karst environment: Implications for speleothem paleoclimatology. *Geochimica et Cosmochimica Acta* 135:217-230.
- Saltré, F., J. Chadoeuf, K. J. Peters, M. C. McDowell, T. Friedrich, A. Timmermann, S. Ulm, and C. J. A. Bradshaw. 2019. Climate-human interaction associated with southeast Australian megafauna extinction patterns. *Nature Communications* 10:5311.
- Saltré, F., M. Rodríguez-Rey, B. W. Brook, C. N. Johnson, C. S. Turney, J. Alroy, A. Cooper, N. Beeton, M. I. Bird, and D. A. Fordham. 2016. Climate change not to blame for late Quaternary megafauna extinctions in Australia. *Nature Communications* 7:10511.
- Sandom, C., S. Faurby, B. Sandel, and J.-C. Svenning. 2014. Global late Quaternary megafauna extinctions linked to humans, not climate change. *Proceedings of the Royal Society B: Biological Sciences* 281:20133254.
- Scanlon, J. D. 1995: First records from Wellington Caves, New South Wales, of the extinct madtsoiid snake *Wonambi naracoortensis* Smith, 1976. *Proceedings of the Linnean Society of New South Wales*, 1995.
- Schloss, C. A., T. A. Nuñez, and J. J. Lawler. 2012. Dispersal will limit ability of mammals to track climate change in the Western Hemisphere. *Proceedings of the National Academy of Sciences* 109:8606-8611.
- Seddon, A. W., A. W. Mackay, A. G. Baker, H. J. B. Birks, E. Breman, C. E. Buck, E. C. Ellis, C. A. Froyd, J. L. Gill, and L. Gillson. 2014. Looking forward through the past: Identification of 50 priority research questions in palaeoecology. *Journal of Ecology* 102:256-267.
- Seebeck, J. 1979. Status of the barred bandicoot, *Perameles gunnii*, in Victoria: With a note on husbandry of a captive colony. *Wildlife Research* 6:255-264.
- Seebeck, J. H., and P. W. Menkhorst. 2008. Eastern Barred Bandicoot, *Perameles gunnii*; pp. 187-188 in S. van Dyck and R. Strahan (eds.), *The Mammals of Australia*. Reed New Holland, Australia.
- Serena, M., and T. R. Soderquist. 2008. Western Quoll, *Dasyurus geoffroii*; pp. 54-56 in S. van Dyck and R. Strahan (eds.), *The Mammals of Australia*. Reed New Holland, Australia.
- Shannon, C. E. 1948. A mathematical theory of communication. *The Bell System Technical Journal* 27:379-423, 623-656.
- Shaw, G. 1792. *The Naturalist's miscellany, or coloured figures of natural objects; drawn and described immediately from nature*, Volume 3. Nodder, RP, London.
- Short, J. 1998. The extinction of rat-kangaroos (Marsupialia: Potoroidae) in New South Wales, Australia. *Biological Conservation* 86:365-377.
- Short, J., and A. Hide. 2012. Distribution and status of the Red-tailed Phascogale (*Phascogale calura*). *Australian Mammalogy* 34:88-99.

- Shute, E. 2019. Early and Middle Pleistocene non-passerine bird fossils from the Thylacoleo Caves, Nullarbor Plain. Unpublished PhD thesis. College of Science and Engineering, Flinders University of South Australia.
- Shute, E., G. J. Prideaux, and T. H. Worthy. 2016. Three terrestrial Pleistocene coucals (*Centropus*: Cuculidae) from southern Australia: Biogeographical and ecological significance. *Zoological Journal of the Linnean Society* 177:964-1002.
- Signor, P. W., J. H. Lipps, L. Silver, and P. Schultz. 1982. Sampling bias, gradual extinction patterns, and catastrophes in the fossil record. Geological implications of impacts of large asteroids and comets on the Earth 190:291-296.
- Simpson, E. H. 1949. Measurement of diversity. *Nature* 163:688.
- Singh, G., A. P. Kershaw, and R. Clark. 1981. Quaternary vegetation and fire history in Australia; pp. 23-54 in A. Gill and R. Groves (eds.), *Fire and the Australian Biota*. Australian Academy of Science, Canberra.
- Smith, A., and A. Lee. 1984. The evolution of strategies for survival and reproduction in possums and gliders. *Possums and gliders*:17-33.
- Smith, F. A., C. P. Tome, E. A. Elliott Smith, S. K. Lyons, S. D. Newsome, and T. W. Stafford. 2016. Unraveling the consequences of the terminal Pleistocene megafauna extinction on mammal community assembly. *Ecography* 39:223-239.
- Smith, H. E., M. W. Morley, and J. Louys. 2020. Taphonomic Analyses of Cave Breccia in Southeast Asia: A Review and Future Directions. *Open Quaternary* 6:13.
- Soderquist, T. R., and S. G. Rhind. 2008. Brush-tailed Phascogale, *Phascogale tapoatafa*; pp. 105-107 in S. van Dyck and R. Strahan (eds.), *The Mammals of Australia*. Reed New Holland, Australia.
- Spanbauer, T. L., C. R. Allen, D. G. Angeler, T. Eason, S. C. Fritz, A. S. Garmestani, K. L. Nash, J. R. Stone, C. A. Stow, and S. M. Sundstrom. 2016. Body size distributions signal a regime shift in a lake ecosystem. *Proceedings of the Royal Society B: Biological Sciences* 283:20160249.
- Springer, M. S., E. C. Teeling, O. Madsen, M. J. Stanhope, and W. W. de Jong. 2001. Integrated fossil and molecular data reconstruct bat echolocation. *Proceedings of the National Academy of Sciences* 98:6241-6246.
- Staff, G. M., and E. N. Powell. 1988. The paleoecological significance of diversity: The effect of time averaging and differential preservation on macroinvertebrate species richness in death assemblages. *Palaeogeography, Palaeoclimatology, Palaeoecology* 63:73-89.
- Steig, E. J., and R. B. Alley. 2002. Phase relationships between Antarctic and Greenland climate records. *Annals of Glaciology* 35:451-456.
- Stenni, B., V. Masson-Delmotte, E. Selmo, H. Oerter, H. Meyer, R. Röthlisberger, J. Jouzel, O. Cattani, S. Falourd, H. Fischer, G. Hoffmann, P. Iacumin, S. J. Johnsen, B. Minster, and R. Udisti. 2010. The deuterium excess records of EPICA Dome C and Dronning Maud Land ice cores (East Antarctica). *Quaternary Science Reviews* 29:146-159.
- Stern, H., G. De Hoedt, and J. Ernst. 2000. Objective classification of Australian climates. *Australian Meteorological Magazine* 49:87-96.
- Strusz, D. 1965. A note on the stratigraphy of the Devonian Garra Beds of New South Wales. *Journal and Proceedings of the Royal Society of New South Wales* 98:85-90.
- Stuart, A. J., and A. M. Lister. 2012. Extinction chronology of the woolly rhinoceros *Coelodonta antiquitatis* in the context of late Quaternary megafaunal extinctions in northern Eurasia. *Quaternary Science Reviews* 51:1-17.
- Suckling, G. G. 2008. Sugar Glider, *Petaurus breviceps*; pp. 230-232 in S. van Dyck and R. Strahan (eds.), *The Mammals of Australia*. Reed New Holland, Australia.

- Taylor, R., D. Shelly, T. Hosking, J. Hosking, S. Lewer, D. Geering, and D. Coote. 2015. Plants and animals of the Dubbo region. 2nd Edition. Dubbo Field Naturalist and Conservation Society, Dubbo.
- Terry, R. C. 2010. On raptors and rodents: testing the ecological fidelity and spatiotemporal resolution of cave death assemblages. *Paleobiology* 36:137-160.
- Thomas, C. D., A. Cameron, R. E. Green, M. Bakkenes, L. J. Beaumont, Y. C. Collingham, B. F. Erasmus, M. F. De Siqueira, A. Grainger, and L. Hannah. 2004. Extinction risk from climate change. *Nature* 427:145-148.
- Thorn, K. M. 2019. Integrating fossils, morphology and molecules to understand the diversification of egeriine skinks. Unpublished PhD thesis. College of Science and Engineering, Flinders University of South Australia.
- Tomé, C. P., E. A. Elliott Smith, S. K. Lyons, S. D. Newsome, and F. A. Smith. 2020. Changes in the diet and body size of a small herbivorous mammal (hispid cotton rat, *Sigmodon hispidus*) following the late Pleistocene megafauna extinction. *Ecography* 43:604-619.
- Toomey, R. S. 1993. Late Pleistocene and Holocene faunal and environmental changes at Hall's Cave, Kerr County, Texas. Unpublished PhD thesis.
- Toomey, R. S., M. D. Blum, and S. Valastro Jr. 1993. Late Quaternary climates and environments of the Edwards Plateau, Texas. *Global and planetary change* 7:299-320.
- Townley, S. 2000. The ecology of the Hastings River Mouse *Pseudomys oralis* (Rodentia: Muridae) in northeastern New South Wales and southeastern Queensland. Unpublished PhD thesis. Southern Cross University.
- Townley, S. 2008. Hastings River Mouse, *Pseudomys oralis*; pp. 646-647 in S. van Dyck and R. Strahan (eds.), *The Mammals of Australia*. Reed New Holland, Australia.
- Travouillon, K. J. 2016. Oldest fossil remains of the enigmatic pig-footed bandicoot show rapid herbivorous evolution. *Royal Society Open Science* 3:160089.
- Travouillon, K. J., B. F. Simoes, R. P. Miguez, S. Brace, P. Brewer, D. Stemmer, G. J. Price, J. Cramb, and J. Louys. 2019. Hidden in plain sight: reassessment of the pig-footed bandicoot, *Chaeropus ecaudatus* (Peramelemorphia, Chaeropodidae), with a description of a new species from central Australia, and use of the fossil record to trace its past distribution. *Zootaxa* 4566:1-69.
- Trueman, C. N. G., J. H. Field, J. Dortch, B. Charles, and S. Wroe. 2005. Prolonged coexistence of humans and megafauna in Pleistocene Australia. *Proceedings of the National Academy of Sciences of the United States of America* 102:8381-8385.
- Turner, V. 1985. The ecology of the eastern pygmy-possum, *Cercartetus nanus*, and its association with Banksia. Monash University, Department of Zoology.
- Turney, C. S., M. I. Bird, L. K. Fifield, R. G. Roberts, M. Smith, C. E. Dortch, R. Grün, E. Lawson, L. K. Ayliffe, and G. H. Miller. 2001a. Early human occupation at Devil's Lair, southwestern Australia 50,000 years ago. *Quaternary Research* 55:3-13.
- Turney, C. S., T. F. Flannery, R. G. Roberts, C. Reid, L. K. Fifield, T. F. Higham, Z. Jacobs, N. Kemp, E. A. Colhoun, and R. M. Kalin. 2008. Late-surviving megafauna in Tasmania, Australia, implicate human involvement in their extinction. *Proceedings of the National Academy of Sciences* 105:12150-12153.
- Turney, C. S. M., M. I. Bird, and R. G. Roberts. 2001b. Elemental $\delta^{13}\text{C}$ at Allen's Cave, Nullarbor Plain, Australia: assessing post-depositional disturbance and reconstructing past environments. *Journal of Quaternary Science* 16:779-784.
- Turney, C. S. M., A. P. Kershaw, S. C. Clemens, N. Branch, P. T. Moss, and L. Keith Fifield. 2004. Millennial and orbital variations of El Niño/Southern Oscillation and high-latitude climate in the last glacial period. *Nature* 428:306.

- Van Der Kaars, S., G. H. Miller, C. S. Turney, E. J. Cook, D. Nürnberg, J. Schönfeld, A. P. Kershaw, and S. J. Lehman. 2017. Humans rather than climate the primary cause of Pleistocene megafaunal extinction in Australia. *Nature Communications* 8:14142.
- Van Dyck, S. 1982a. The relationships of *Antechinus stuartii* and *A. flavipes* (Dasyuridae, Marsupialia) with special reference to Queensland; pp. 723-766 in M. Archer (ed.), *Carnivorous Marsupials*. Surrey Beatty & Sons Pty Ltd, Chipping Norton.
- Van Dyck, S. 1982b. *Antechinus puteus* (Marsupialia, Dasyuridae), a new fossil species from the Texas Caves, southeastern Queensland. *Australian Mammalogy* 5:59-68.
- Van Dyck, S. 1987. The bronze quoll, *Dasyurus spartacus* (Marsupialia: Dasyuridae), a new species from the savannahs of Papua New Guinea. *Australian Mammalogy* 11:145-156.
- Van Klinken, G. J. 1999. Bone Collagen Quality Indicators for Palaeodietary and Radiocarbon Measurements. *Journal of Archaeological Science* 26:687-695.
- Vegas-Vilarrúbia, T., V. Rull, E. Montoya, and E. Safont. 2011. Quaternary palaeoecology and nature conservation: a general review with examples from the neotropics. *Quaternary Science Reviews* 30:2361-2388.
- Voorhies, M. R. 1969. Taphonomy and population dynamics of an early Pliocene vertebrate fauna, Knox County, Nebraska, Volume 1. University of Wyoming Laramie.
- Waikato University, R. D. L. 2017. AMS Processing Technical Report (Unpublished) Waikato University, Waikato, New Zealand.
- Wang, Y. J., H. Cheng, R. L. Edwards, Z. S. An, J. Y. Wu, C.-C. Shen, and J. A. Dorale. 2001. A high-resolution absolute-dated late Pleistocene monsoon record from Hulu Cave, China. *294:2345-2348*.
- Warburton, N. M., and G. J. Prideaux. 2021. The skeleton of *Congruus kitcheneri*, a semiarboreal kangaroo from the Pleistocene of southern Australia. *Royal Society Open Science* 8:202216.
- Ward, S. J., and V. Turner. 2008. Eastern Pygmy-Possum, *Cercartetus nanus*; pp. 219-221 in S. van Dyck and R. Strahan (eds.), *The Mammals of Australia*. Reed New Holland, Australia.
- Ward, S. J., and D. P. Woodside. 2008. Feathertail Glider, *Acrobates pygmaeus*; pp. 261-264 in S. van Dyck and R. Strahan (eds.), *The Mammals of Australia*. Reed New Holland, Australia.
- Watts, C. H., and H. J. Aslin. 1981. *The rodents of Australia*. Angus & Robertson, Sydney.
- Wells, R. T., K. Moriarty, and D. Williams. 1984. The fossil vertebrate deposits of Victoria Fossil Cave Naracoorte: an introduction to the geology and fauna. *The Australian Zoologist* 21:305-333.
- Westaway, M. C., J. Olley, and R. Grün. 2017. At least 17,000 years of coexistence: Modern humans and megafauna at the Willandra Lakes, South-Eastern Australia. *Quaternary Science Reviews* 157:206-211.
- Westaway, M. C., G. Price, T. Miscamble, J. McDonald, J. Cramb, J. Ringma, R. Grün, D. Jones, and M. Collard. 2019. A palaeontological perspective on the proposal to reintroduce Tasmanian devils to mainland Australia to suppress invasive predators. *Biological Conservation* 232:187-193.
- White, L. C., F. Saltré, C. J. A. Bradshaw, and J. J. Austin. 2018. High-quality fossil dates support a synchronous, Late Holocene extinction of devils and thylacines in mainland Australia. *Biology Letters* 14.
- Whittaker, R. H. 1972. Evolution and measurement of species diversity. *TAXON* 21:213-251.
- Wickham, H. 2007. Reshaping data with the reshape package. *Journal of statistical software* 21:1-20.

- Wickham, H. 2016. *ggplot2: elegant graphics for data analysis*. Springer International Publishing, Cham, Switzerland.
- Wickham, H., M. Averick, J. Bryan, W. Chang, L. McGowan, R. François, G. Grolemund, A. Hayes, L. Henry, and J. Hester. 2019. Welcome to the Tidyverse. *Journal of Open Source Software* 4:1686.
- Williams, A. N., P. Veth, W. Steffen, S. Ulm, C. S. Turney, J. M. Reeves, S. J. Phipps, and M. Smith. 2015. A continental narrative: Human settlement patterns and Australian climate change over the last 35,000 years. *Quaternary Science Reviews* 123:91-112.
- Williams, M., E. Cook, S. van der Kaars, T. Barrows, J. Shulmeister, and P. Kershaw. 2009. Glacial and deglacial climatic patterns in Australia and surrounding regions from 35 000 to 10 000 years ago reconstructed from terrestrial and near-shore proxy data. *Quaternary Science Reviews* 28:2398-2419.
- Willis, K., R. Bailey, S. Bhagwat, and H. Birks. 2010. Biodiversity baselines, thresholds and resilience: testing predictions and assumptions using palaeoecological data. *Trends in Ecology & Evolution* 25:583-591.
- Wittebolle, L., M. Marzorati, L. Clement, A. Balloi, D. Daffonchio, K. Heylen, P. De Vos, W. Verstraete, and N. Boon. 2009. Initial community evenness favours functionality under selective stress. *Nature* 458:623-626.
- Woinarski, J., A. Burbidge, and P. Harrison. 2014. *Action Plan for Australian Mammals 2012*. CSIRO Publishing, Collingwood, Victoria.
- Woinarski, J. C., A. A. Burbidge, and P. L. Harrison. 2015a. Ongoing unraveling of a continental fauna: Decline and extinction of Australian mammals since European settlement. *Proceedings of the National Academy of Sciences* 112:4531-4540.
- Woinarski, J. C., A. A. Burbidge, and P. L. Harrison. 2015b. A review of the conservation status of Australian mammals. *THERYA* 6:155-166.
- Woinarski, J. C. Z., M. F. Braby, A. A. Burbidge, D. Coates, S. T. Garnett, R. J. Fensham, S. M. Legge, N. L. McKenzie, J. L. Silcock, and B. P. Murphy. 2019. Reading the black book: The number, timing, distribution and causes of listed extinctions in Australia. *Biological Conservation* 239:108261.
- Wolfe, A. L., and J. M. Broughton. 2021. More on overkill, the associational critique, and the North American megafaunal record: A reply to Grayson et al. (2021). *Journal of Archaeological Science* 128:105313.
- Wolff, E. W., J. Chappellaz, T. Blunier, S. O. Rasmussen, and A. Svensson. 2010. Millennial-scale variability during the last glacial: The ice core record. *Quaternary Science Reviews* 29:2828-2838.
- Wood, R. E., K. Douka, P. Boscato, P. Haesaerts, A. Sinitsyn, and T. F. G. Higham. 2012. Testing the ABOx-SC method: Dating known-age charcoals associated with the Campanian Ignimbrite. *Quaternary Geochronology* 9:16-26.
- Woods, J. T. 1958. The extinct marsupial genus *Palorchestes* Owen. *Memoirs of the Queensland Museum* 13:177-193.
- Woodward, C., J. Shulmeister, D. Bell, R. Haworth, G. Jacobsen, and A. Zawadzki. 2014. A Holocene record of climate and hydrological changes from Little Llangothlin Lagoon, south eastern Australia. *The Holocene* 24:1665-1674.
- Worthy, T. H. 2001. A fossil vertebrate fauna accumulated by laughing owls (*Sceloglaux albifacies*) on the Goulard Downs, northwest Nelson, South Island. *Notornis* 48:223-233.
- Wroe, S., and B. Mackness. 1998. Revision of the Pliocene dasyurid, *Dasyurus dunmalli* (Dasyuridae: Marsupialia). *Memoirs of the Queensland Museum* 42:605-612.

- Wroe, S., and J. Field. 2006. A review of the evidence for a human role in the extinction of Australian megafauna and an alternative interpretation. *Quaternary Science Reviews* 25:2692-2703.
- Wroe, S., T. J. Myers, R. T. Wells, and A. Gillespie. 1999. Estimating the weight of the Pleistocene marsupial lion, *Thylacoleo carnifex* (Thylacoleonidae:Marsupialia): implications for the ecomorphology of a marsupial super-predator and hypotheses of impoverishment of Australian marsupial carnivore faunas. *Australian Journal of Zoology* 47:489-498.
- Wroe, S., J. Field, R. Fullagar, and L. S. Jermin. 2004. Megafaunal extinction in the late Quaternary and the global overkill hypothesis. *Alcheringa* 28:291-331.
- Wroe, S., J. H. Field, M. Archer, D. K. Grayson, G. J. Price, J. Louys, J. T. Faith, G. E. Webb, I. Davidson, and S. D. Mooney. 2013. Climate change frames debate over the extinction of megafauna in Sahul (Pleistocene Australia-New Guinea). *Proceedings of the National Academy of Sciences* 110:8777-8781.
- Xia, Q., J.-x. Zhao, and K. D. Collerson. 2001. Early–Mid Holocene climatic variations in Tasmania, Australia: Multi-proxy records in a stalagmite from Lynds Cave. *Earth and Planetary Science Letters* 194:177-187.
- Yokoyama, Y., K. Lambeck, P. De Deckker, P. Johnston, and L. K. Fifield. 2000. Timing of the Last Glacial Maximum from observed sea-level minima. *Nature* 406:713.
- Zhou, X., J. Yang, S. Wang, G. Xiao, K. Zhao, Y. Zheng, H. Shen, and X. Li. 2018. Vegetation change and evolutionary response of large mammal fauna during the Mid-Pleistocene Transition in temperate northern East Asia. *Palaeogeography, Palaeoclimatology, Palaeoecology* 505:287-294.